Summer 2019

Investigation of Energy-Related Wastewater Impacts on Disinfection By-Product Formation in Drinking Water

Hannah K. Liberatore

INVESTIGATION OF ENERGY-RELATED WASTEWATER IMPACTS ON DISINFECTION BY-PRODUCT FORMATION IN DRINKING WATER

by

Hannah K. Liberatore

Bachelor of Science
University of North Carolina at Wilmington, 2013

Submitted in Partial Fulfillment of the Requirements

For the Degree of Doctor of Philosophy in

Chemistry

College of Arts and Sciences

University of South Carolina

2019

Accepted by:

Susan D. Richardson, Major Professor

S. Michael Angel, Committee Member

Linda S. Shimizu, Committee Member

Geoff Scott, Committee Member

Cheryl L. Addy, Vice Provost and Dean of the Graduate School

DEDICATION

This dissertation is dedicated to every mentor, instructor, teacher, and friend that helped me to where I am today. To my family, thank you for your unwavering support. To Grandma Kay, thank you for molding me into the person I am today, for giving me your “fire” and teaching me not to let any obstacle extinguish it.

ACKNOWLEDGEMENTS

Most of all, I would like to thank Dr. Susan Richardson for all of the time, thought, care, and faith that she invested in me over the last five years. I am truly honored to be one of the first graduate students to come out of such an amazing mentor's lab. I am beyond grateful for the support that you and Andy have given me.

Thank you to all of my current and past lab mates, especially: Dr. Amy Cuthbertson, Josh Allen, Danielle Westerman, Caroline Granger, Dallas Abraham, Dr. Susana Kimura, and Kristin Cochran. I couldn't have done this without you all.

I am extremely grateful for my Ph.D. committee members, Drs. Mike Angel, Linda Shimizu, and Geoff Scott. Thank you for the knowledge you've shared and guidance you've given me.

I have been blessed to have the opportunity to work with a variety of collaborators in my research. Thank you all, especially: Drs. Mark Strynar and James McCord, Dr. Kelly Good, Drs. Michael Plewa and Elizabeth Wagner, Dr. David DeMarini, Dr. Amy McKenna, Dr. Richard Liberatore (brother *and* collaborator), Dr. Jeanne VanBriesen, Dave Burnett, Dr. Leslie Cizmas, and Keith McLeroy.

I would also like to acknowledge the Department of Education's GAANN program for funding during my first and second years, as well as the National Science Foundation for supplemental funding that awarded me the opportunity to intern at the U.S. EPA.

ABSTRACT

Elevated bromide and iodide in drinking water sources contribute to the formation of toxic brominated and iodinated disinfection by-products (DBPs) during drinking water treatment. Energy extraction and utilization processes, including hydraulic fracturing (HF) and coal-fired power plants (CFPPs), produce wastewaters with bromide/iodide levels on the order of tens to thousands of mg/L. These wastes have the potential to impact drinking water sources through both intentional (e.g., direct discharge) and accidental (e.g., basin overflow, spill) release pathways. This research focuses on a combination of quantitative and non-targeted approaches to assess DBP formation impacts from HF and CFPP wastewaters, with complementary toxicity studies contributed by collaborators.

The HF studies reported here are the first non-targeted investigations of the formation of DBPs from both geogenic (phenolics) and anthropogenic (surfactant) organic DBP-precursors. In both cases, high-resolution mass spectrometry (MS) was crucial to the identification of never-before-reported DBPs. Fifty-six iodo-phenolics were identified, comprising three homologous series of iodinated phenolics, including two new classes of DBPs: iodocresols and iodoxylenols. Many of these newly-identified DBPs were cytotoxic in mammalian cell assays. In addition, over 300 new sulfur-containing DBPs were identified in gas-extraction wastewaters. These originated from a mixture of isomers of olefin sulfonate (dodecene sulfonate) surfactant, a common fracking fluid additive. Brominated, iodinated, and chlorinated sulfonate-based DBPs were identified,

as well as halogenated di-S-species, derived from surfactant impurities. Chlorine and chloramine disinfection of these gas wastewaters increased cytotoxicity by several orders of magnitude, with chloraminated water being the most toxic.

We also conducted the first *experimental* investigation of the impacts of CFPP wastewater on resulting DBP formation from chlorination *and* chloramination. It is the most comprehensive quantification of DBPs from CFPP impact, as well as the first to assess CFPP impact on iodide and iodo-DBP formation. The presence of CFPP waste significantly enhanced the formation of brominated and iodinated DBPs, as well as calculated cyto- and geno-toxicity, under both disinfection conditions. While chloramination resulted in lower overall DBP formation, higher levels of iodo-DBPs, including highly toxic iodinated haloacetamides, formed with CFPP impact.

Speciation and toxicity associated with formation of these CFPP and HF waste-derived DBPs is important for energy waste-impacted drinking water treatment plants that may consider switching from chlorination to chloramination, which will effectively control regulated DBPs, but could result in higher-toxicity drinking water.

TABLE OF CONTENTS

Dedication iii

Acknowledgements iv

Abstract v

List of Tables ix

List of Figures xi

List of Abbreviations xiv

Chapter 1: Introduction 1

Chapter 2: Identification and Comparative Mammalian Cell Cytotoxicity of New Iodo-Phenolic Disinfection By-Products in Chloraminated Oil and Gas Wastewaters 7

2.0 Abstract 8

2.1 Introduction 8

2.2 Materials and Methods 10

2.3 Results and Discussion 13

2.4 Tables and Figures 18

Chapter 3: Potential Impacts of Hydraulic Fracturing on Drinking Water: High-Resolution Mass Spectrometry Identification of >300 Novel Surfactant-Derived S-DBPs 22

3.0 Abstract 23

3.1 Introduction 24

3.2 Materials and Methods 26

3.3 Results and Discussion 31

3.4 Tables and Figures 44

Chapter 4: Are Coal-Fired Power Plants a Threat to Downstream Drinking Water? The Impact of Bromide and Iodide on Emerging Disinfection By-Products 51

4.0 Abstract 52

4.1 Introduction 53

4.2 Materials and Methods 55

4.3 Results and Discussion 60

4.4 Tables and Figures 70

Chapter 5: Conclusions and Future Work 74

5.1 Hydraulic Fracturing-Impacted Waters 74

5.2 Coal-Fired Power Plant-Impacted Waters 76

References 78

Appendix A: Reprint and Adaptation Permissions 86

Appendix B: *Supporting Information for* Identification and Comparative Mammalian Cell Cytotoxicity of New Iodo-Phenolic Disinfection By-Products in Chloraminated Oil and Gas Wastewaters 95

Appendix C: *Supporting Information for* Potential Impacts of Hydraulic Fracturing on Drinking Water: High-Resolution Mass Spectrometry Identification of >300 Novel Surfactant-Derived S-DBPs 112

Appendix D: *Supporting Information for* Are Coal-Fired Power Plants a Threat to Downstream Drinking Water? The Impact of Bromide and Iodide on Emerging Disinfection By-Products 126

Appendix E: Publications 141

E.1 List of Manuscripts 141

E.2 Published Manuscript Reprints 144

LIST OF TABLES

Table 1.1 Halo-Organic Disinfection By-Products Regulated by the U.S. Environmental Protection Agency 5

Table 1.2 Semiquantitative Assessment of the Sinks of Iodine During Disinfection: Influence of Disinfectant 6

Table 2.1 Sample Characteristics of Barnett and McAllen Produced Waters 18

Table 2.2 Molecular Formulas, Observed and Theoretical Accurate Masses, and Isomer Identification Information for Iodo-Phenols, -Methylphenols, and -Dimethylphenols Identified 19

Table 3.1. Precursor Compounds in Raw Feed Samples and C_{12} Olefin Sulfonate "Standard" 44

Table 4.1 Sample Characteristics for Samples Used in Disinfection Experiments 71

Table B.1. GC-MS Instrument Parameters 98

Table B.2. Iodinated Phenolics Identified in Barnett and McAllen Chloraminated Waters 99

Table B.3 Brominated and Chlorinated Iodo-Phenolics Identified in Chloraminated McAllen MF Water Samples 101

Table B.4 Cresol (Methylphenol) and Xylenol (Dimethylphenol) Precursor Study: 72 h Chloramination Conditions 102

Table B.5 Chinese Hamster Ovary (CHO) Cell Chronic Cytotoxicity Analyses of Iodo-Phenolics 102

Table C.1 LC Parameters for LC-QTOF MS - All Ions Analyses 112

Table C.2 QTOF Parameters for LC-QTOF MS - All Ions Analyses 113

T able C.3 LC Parameters for Orbitrap MS Analyses 114

Table C.4 Orbitrap MS Parameters for High Resolution MS^1 Analyses 114

Table C.5 Orbitrap MS Parameters for MS^3 Analyses 115

Table C.6 DBPs Identified by Class in Disinfected Surfactant Mixture and Gas Wastewater.....116

Table C.7 LC_{50} and CTI Values for Waters.....118

Table D.1. Analytes, Vendors, Calibration Range, and Ions Monitored for DBPs Quantified 127

Table D.2 Sample Characteristics from 2017 and 2018 Samplings 131

Table D.3 GC-MS Methods for (1) Bromo-Trihalo-HANs and –HAMs and (2) Other DBPs ("Main List") 132

Table D.4 Individual DBP Formation (µg/L, average ± SE) from Chlorination (HOCl) and Chloramination (NH_2Cl) with and without Coal-Fired Power Plant Wastewater "Impact".....133

Table D.5 Sample t-test Results for the Impact of Coal-Fired Power Plant Wastewater (CFPP WW) on DBP Formation During Chlor(am)ination.....135

Table D.6 Individual DBP and Class Sum Formation (nM, Average ± SE) from Chlorination (HOCl) and Chloramination (NH_2Cl) with and without Coal-Fired Power Plant Wastewater "Impact" 137

LIST OF FIGURES

Figure 1.1. Preferential formation of brominated DBPs in bromide-rich chlorinated drinking water 5

Figure 1.2 Fate of iodide in chlorine and chloramine disinfection of drinking water 6

Figure 2.1 Iodo-phenolic DBPs identified in chloraminated Barnett nanofiltered (NF) ...20

Figure 2.2 CHO cytotoxicity concentration-response curves for 2-iodophenol, 4-iodophenol, 2,4,6-triiodophenol, and 4-iodo-2-methylphenol 21

Figure 3.1 LC-QTOF extracted ion chromatograms (XICs) of two brominated S-containing DBPs.....45

Figure 3.2 Extracted ion chromatograms and ESI(-) mass spectra showing molecular ions ($[M-H]^-$) for C_{12} olefin sulfonates and resulting halohydrin DBPs in undisinfected, chlorinated, and chloraminated RF samples.....46

Figure 3.3 Extracted ion chromatogram (XIC) comparisons of DBPs and their suspected precursors in gas extraction wastewater to the commercial olefin sulfonate surfactant mixture.....47

Figure 3.4 Extracted ion chromatograms (XICs) and molecular ions, including doubly-charged $[M-2H]^{2-}$ where applicable, for olefin disulfonate precursor and its major halogenated DBPs formed during disinfection of RF and C_{12} olefin sulfonate commercial product 48

Figure 3.5 Dose-response curves for cytotoxicity of undisinfected, chlorinated (HOCl), and chloraminated (NH_2Cl) field blank, pretreated, and raw feed samples.....49

Figure 3.6 Total organic halogen concentrations (left y-axis; ± SE [n = 2]) and cytotoxicity index values (right y-axis) for field blank (FB), pretreated (PT), and raw feed (RF) undisinfected, chlorinated (HOCl), and chloraminated (NH_2Cl) reactors 50

Figure 4.1 Bromide and iodide concentrations measured in 2017 and 2018 grab samples from the coal-fired power plant (CFPP) discharge, impacted river, and tributaries to the impacted river.....70

Figure 4.2 DBP concentrations by class and total organic halogen measurements in disinfected settled water with and without simulated CFPP wastewater impact....72

Figure 4.3 Portion of total organic halogen (TOX) accounted for by the 50 quantified DBPs and percentage of TOX that is unknown....73

Figure 4.4 Calculated CHO cell cytotoxicity and genotoxicity by DBP class and halogen species profile....73

Figure B.1 Membrane-filtration process of produced water samples....103

Figure B.2 Library search result for unknown with molecular ion of m/z 360....104

Figure B.3 Isomeric confirmation of 2-iodophenol via retention time and mass spectral matching....105

Figure B.4 Mass spectra of confirmed iodophenol, iodocresol (iodomethylphenol), and iodoxylenol (iododimethylphenol) isomers identified in Barnett NF and McAllen MF chloraminated waters....106

Figure B.5 Mass spectra of iodocresols (iodomethylphenols) and iodoxylenols (iododimethyl-phenols) identified in Barnett NF and McAllen MF chloraminated waters....107

Figure B.6 Example mass spectral interpretation of diiodomethylphenol....108

Figure B.7 Iodo-phenolics identified in chloraminated McAllen MF samples....109

Figure B.8 Mass spectra of tentatively identified chlorinated and brominated iodo-phenols and iodocresols in McAllen MF chloraminated water....110

Figure B.9 Detection of phenol, methylphenol (cresol), and dimethylphenol (xylenol) in non-disinfected samples....111

Figure B.10 Chinese hamster ovary (CHO) cell cytotoxicity index (CTI) values, $(LC_{50})^{-1}(10^3)$, of 2-iodophenol, 4-iodophenol, 2,4,6-iodophenol, and 4-iodo -2-methylphenol....111

Figure C.1 LC-QTOF MS/MS product ion scan of precursor ion *m/z* 405.0046 ($C_{12}H_{22}Br_2S_2O_6^-$)....119

Figure C.2 LC-QTOF MS/MS product ion scan of precursor ion *m/z* 343.0583 ($C_{12}H_{24}BrSO_4^-$)....120

Figure C.3 FT-ICR MS scan of undisinfected, chlorinated, and chloraminated RF wastewater.....121

Figure C.4 FT-ICR MS^3 mass spectrum of $C_{12}H_{24}BrSO_4^-$ (*m/z* 343.05854) after loss of HBr (*m/z* 263.13230) 122

Figure C.5 Mass spectra of molecular ion ($[M-H]^-$) for the halohydrin sulfonate by-products and suspected olefin sulfonate precursor obtained from different high resolution systems.....123

Figure C.6 Extracted ion chromatograms (XICs) and molecular ions, including $[2M-H]^-$, for olefin sulfonate precursor and its major DBPs formed during disinfection.....124

Figure C.7 Mass spectrum of chlorinated RF at 2.90 min, highlighting faux halogen patterns that could have led to misidentification by unit-resolution analyses 125

Figure D.1 Impacted vs. unimpacted concentrations of DBPs by class sums and halogenation in chlorinated and chloraminated waters.....139

Figure D.2 Calculated CHO cell cytotoxicity and genotoxicity by DBP class and halogen species profile.....140

LIST OF ABBREVIATIONS

CFPP ..... Coal-fired power plant

DBP ..... Disinfection by-product

DWTP ..... Drinking water treatment plant

HAA5 ..... Regulated haloacetic acids

HALs ..... Haloacetaldehydes

HAMs ..... Haloacetamides

HANs ..... Haloacetonitriles

HKs ..... Haloketones

HNMs ..... Halonitromethanes

HF ..... Hydraulic fracturing

HOCl ..... Hypochlorous acid (aqueous chlorine disinfectant)

I-DBPs ..... Iodinated disinfection by-products

IP ..... Iodophenol

N-DBPs ..... Nitrogenous disinfection by-products

NH_2Cl ..... Monochloramine (preformed chloramine disinfectant)

S-DBPs ..... Sulfur-containing disinfection by-products

THMs ..... Trihalomethanes

THM4 ..... Regulated trihalomethanes

TOX ..... Total organic halogen

WW ..... Wastewater

CHAPTER 1
INTRODUCTION

Chlorine-based disinfectants react with dissolved organic matter (DOM) in source waters and produce chlorinated disinfection by-products (DBPs). In the presence of iodide and bromide, iodinated and brominated DBPs, which are much more toxic than their chlorinated analogues (I > Br >> Cl), can also be formed.[1–3] There are currently nine halo-organic DBPs, listed in Table 1.1, which are regulated at drinking water treatment plants (DWTPs) in the United States. Regulated DBPs consist of four bromo-/chloro-trihalomethanes, collectively referred to as "THM4" and five bromo- and chloro-acetic acids, known as "HAA5".[1,4] Currently, no iodinated DBPs are regulated, despite their enhanced toxicity over their chloro- and bromo- analogues, and their tendency to form under different conditions than Br- and Cl-DBPs (i.e., chloramination vs. chlorination).

Chlorination is the most common disinfection process in the U.S., which can be performed with the use of chlorine gas (Cl_2) or the use of hypochlorous acid/hypochlorite ($HOCl/OCl^-$). Chloramination – which can be carried out by chlorination followed by addition of ammonia to form NH_2Cl (monochloramine), or by the addition of preformed NH_2Cl – is becoming increasingly popular as an alternative to chlorination. This is due to formation of much lower levels of regulated DBPs with chloramine disinfection.[1–3,5] Both chlorination and chloramination are known to yield halogenated DBPs, as these are chlorine-based oxidants. When bromide and iodide are abundant, the disinfectant

oxidizes these halides, which in turn react with organic matter and form brominated and iodinated DBPs.[1–3,6–9]

Abundant bromide poses an issue for water disinfection because HOCl oxidizes bromide to HOBr/OBr^-, with little reversal.[8] HOBr is much more reactive than HOCl, reacting with organic matter at a faster rate, at least one order of magnitude faster. This favors the formation of bromo-DBPs over chloro-DBPs.[9] Formation of more bromo-DBPs will increase the overall toxicity of drinking water.[3] Bromine is a heavier atom than chlorine (79.9 g/mol vs. 35.5 g/mol), which increases the challenge faced by DWTPs to meet DBP regulations. THMs and HAAs are regulated not as individual DBPs, but as classes and are regulated according to mass concentration (µg/L), rather than on a molar basis.[4,10]

Iodinated DBP formation from iodide is favored in chloraminated systems, while only low levels form in chlorinated water.[1,2,7] This discrepancy is because HOCl will oxidize iodide to iodate (IO_3^-), which is non-toxic. Iodate is the major product with little to no reverse reaction, serving as a sink for iodide. However, in chloraminated water, oxidation of iodide beyond HOI/OI^- is a very slow reaction. The half-life of OI^- in water is much longer, allowing time for the reaction of OI^- with DOM to dominate over the oxidation of OI^-. I-DBPs become the sink for iodide in chloraminated water, with little formation of iodate, shown in Table 1.2 and Figure 1.2.[2,7,11] Because no iodo-DBPs are regulated, DWTPs seeking to lower their levels of regulated DBPs may unknowingly increase the toxicity of their water by switching to chloramination.[3,6,12]

This research investigates the formation of toxic bromo- and iodo-DBPs resulting from chlorination and chloramination (collectively, "chlor(am)ination") disinfection of

water, with a primary focus on the impact of energy-related wastewater inputs. This investigation includes comprehensive identification of both known and newly-discovered DBPs. Identification and quantification are complemented by the contributions of collaborators, who evaluate the genotoxicity, cytotoxicity, and risks of human and ecological health effects associated with the formation of these DBPs.

The research in Chapters 2-4 investigates the effects of high-bromide and -iodide wastewaters from energy extraction and utilization processes on DBP formation. Fossil fuel (i.e., oil, gas, coal) extraction and utilization processes can lead to the introduction of elevated bromide and iodide levels to drinking water sources.[10,13–20] These waters have significantly higher concentrations of Br^- and I^- than natural waters. Hydraulic fracturing (HF) activities release salt brines trapped deep within shale formations, while the use of bromide-rich coals (or addition of bromide salts) at coal-fired power plants (CFPPs) is favorable to reduce atmospheric mercury emissions.[13,15,18–20] Bromide levels in waters from coal-fired power plants are comparable to that of seawater (up to hundreds of mg/L), and hydraulic fracturing produced and flowback waters have been reported with halide levels on the order of hundreds to thousands of mg/L bromide and tens of mg/L iodide.[10,14,16,17,21–23]

Bromide levels in CFPP wastewaters typically range from 10-100 mg/L, and downstream drinking water sources have been reported to contain hundreds of µg/L bromide from CFPP discharge. While bromide itself may not pose health risks to communities, its presence in drinking water sources leads to the formation of higher-toxicity brominated DBPs during the disinfection process. Several studies have previously reported elevated bromide levels and enhanced formation of regulated DBPs

(THM4 and HAA5) at CFPP waste-impacted drinking water treatment plants.[15,17–20] In these situations, the enhanced formation of brominated analogues can lead to regulation violations. Chlorine-disinfecting plants that struggle with bromide/Br-DBPs may switch to chloramine-disinfection to regain compliance with THM and HAA regulations. Iodide levels in coal-related waste and/or impacted surface waters have not been the focus of previous studies, though iodide is known to co-occur with bromide in coal. In addition to elevated bromo-DBPs, CFPP wastewater discharged to drinking water sources has the potential to form highly toxic iodinated DBPs. Since iodinated DBPs form preferentially with chloramine disinfection, CFPP-impacted drinking water treatment plants that implement chloramination practices may unknowingly increase the finished drinking water toxicity, despite lower levels of Br-THMs and HAAs.

Parker et al. reported bromide values for flowback waters from Pennsylvania's Marcellus Shale as high as 693 mg/L and iodide as high as 5.6 mg/L.[16] With the large volume of wastewater produced from hydraulic fracturing activities, drinking water sources have the potential to be impacted through a variety of pathways, including accidental spills, leakage from surface impoundments, leakage during injection, and illegal disposal.[14,16] Oil and gas wastewater is also sometimes released to surface waters after treatment at brine treatment facilities (a common practice in Pennsylvania). Brine treatment processes successfully remove other components of concern (e.g., heavy metals, total dissolved solids [TDS], and naturally occurring radioactive material [NORM]), but bromide and iodide are not removed, meaning that treated water is still high in Br^- and I^-.[14,16,21,22] For example, Harkness et al. reported levels ranging from 340-650 ppm Br^- and 11-29 ppm I^- in the effluents of three different Marcellus Shale brine

treatment facilities.[14] This halide-rich treated water mixes with source waters, which leads to the formation of bromo- and iodo-DBPs at downstream DWTPs.[13,16,17]

Table 1.1. Halo-Organic Disinfection By-Products Regulated by the U.S. Environmental Protection Agency

Class	Compounds	MCLG (µg/L)	MCL (µg/L)	Potential Health Effects from Long Term Exposure Above the MCL
THM4	Chloroform	70	80	Increased risk of cancer
	Bromodichloromethane	zero		
	Dibromochloromethane	60		
	Bromoform	zero		
HAA5	Chloroacetic acid	70	60	Liver, kidney, or central nervous system problems; increased risk of cancer
	Dichloroacetic acid	zero		
	Trichloroacetic acid	20		
	Bromoacetic acid	n/a		
	Dibromoacetic acid	n/a		

MCL = maximum contaminant level (regulation; highest acceptable concentration); MCLG = maximum contaminant level goal (unenforced; no anticipated health risk <MCLG)

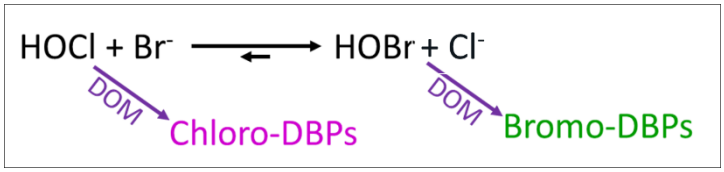

Figure 1.1. Preferential formation of brominated DBPs in bromide-rich chlorinated drinking water.

Table 1.2. Semiquantitative Assessment of the Sinks of Iodine During Disinfection: Influence of Disinfectant[7]*

Disinfectant	Products		
	Iodoform	Other I-THMs	Iodate
Chlorine	+	++	++
Chloramine	+++	++	-

**Table adapted from Bichsel and von Gunten 1999*

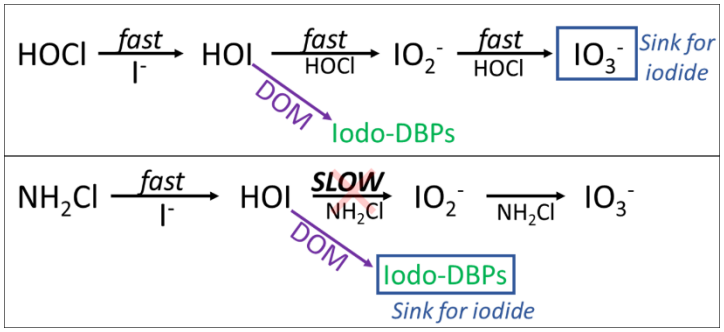

Figure 1.2. Fate of iodide in chlorine and chloramine disinfection of drinking water.[2]*
**Figure adapted from Richardson et al. 2008.*

CHAPTER 2
IDENTIFICATION AND COMPARATIVE MAMMALIAN CELL CYTOTOXICITY OF NEW IODO-PHENOLIC DISINFECTION BY-PRODUCTS IN CHLORAMINATED OIL AND GAS WASTEWATERS[*]

[*] Liberatore, H. K.; Plewa, M. J.; Wagner, E. D.; VanBriesen, J. M.; Burnett, D. B.; Cizmas, L. H.; Richardson, S. D. *Environ. Sci. Technol. Lett.* **2017**, *4*, 475-480.

2.0 ABSTRACT

Hydraulic fracturing wastewaters discharged to surface water have led to elevated bromide and iodide levels, as well as enhanced formation of brominated trihalomethanes, haloacetic acids, haloacetonitriles, and iodo-trihalomethanes at downstream drinking water treatment plants, in chlorinated effluent from wastewater treatment plants, and in controlled laboratory studies. This enhanced formation of brominated and iodinated disinfection by-products (DBPs) raises concerns regarding human health, because they are much more toxic than chlorinated DBPs. This study represents the first non-target, comprehensive analysis of iodinated DBPs formed in chloraminated produced waters associated with hydraulic fracturing of shale and conventional gas formation. Fifty-six iodo-phenolics were identified, comprising three homologous series of mono-, di-, and tri-iodinated phenols, along with two new classes of DBPs: iodomethylphenols and iododimethylphenols. Four iodo-phenolics (2-iodophenol, 4-iodophenol, 2,4,6-triiodophenol, and 4-iodo-2-methylphenol) were investigated for mammalian cell cytotoxicity. All were cytotoxic, especially 2,4,6-triiodophenol, which was more cytotoxic than all trihalomethanes and most haloacetic acids. In addition, geogenic organic compounds present in the oil and gas produced waters, including methylphenol and dimethylphenol, were found to be potential precursors to these iodo-DBPs.

2.1 INTRODUCTION

Oil and gas extraction processes employ large volumes of water, amended with chemicals and injected into wells at high pressure to facilitate withdrawal from shale or reservoirs. Water, carrying oil and gas as well as residual chemicals, returns to the wellhead as “produced water”. Produced water also contains high levels of geogenic

components from the formation, including total dissolved solids (TDS), naturally occurring radioactive material (NORM), organic material, and halides. Drinking water sources have the potential to be impacted by oil and gas wastewater through spills during storage or transportation, illegal disposal, or discharge from treatment facilities that do not fully remove contaminants. While conventional wastewater treatment removes the majority of TDS and NORM, dissolved organic matter and halides are not removed, and thus, can be released to surface waters.[10,14–17,21,22,24–29] Elevated levels of bromide and iodide are a concern, as their release into surface waters used as drinking water sources can lead to formation of brominated and iodinated disinfection by-products (DBPs) during drinking water treatment. Many of these DBPs are cytotoxic, genotoxic, mutagenic, or tumorigenic.[1–3,30–37] In general, iodinated DBPs are the most toxic, followed by brominated, with chlorinated DBPs the least toxic.[1–3,6,34,35,37]

To reduce regulated DBP levels, many drinking water plants have switched from chlorine to monochloramine for disinfection. While monochloramine reduces regulated trihalomethanes (THMs) and haloacetic acids (HAAs), it promotes the formation of more toxic unregulated DBPs, including iodinated and nitrogenous DBPs.[1–3,6,11,30,34–36,38–45] Recent studies showed that chloraminated water with elevated bromide and iodide levels produces water that is more cytotoxic and genotoxic than chlorinated water, due to enhanced formation of iodinated DBPs.[3,12]

Previous studies reported that oil and gas wastewater discharged to surface waters after partial treatment leads to elevated bromide and iodide concentrations in receiving streams and at downstream drinking water plants[14,17,26] and enhanced formation of brominated and iodinated DBPs upon disinfection. DBPs reported to-date from oil and

gas wastewater impacts include bromo- and iodo-THMs, bromo-HAAs, bromo-acetaldehydes, bromo-nitromethanes, and bromo-acetonitriles.[10,15,16,24] Due to the large amount of water required, as well as water scarcity issues, the oil and gas industry initiated treatment methods to minimize disposal and allow reuse of wastewater for further hydraulic fracturing or for agriculture.[46,47] These treatments include microfiltration and nanofiltration, which were the focus of our study. Raw (untreated) produced waters were also analyzed. In this study, we conducted the first comprehensive, non-target assessment of DBPs formed in chloraminated oil and gas produced water, as well as the first cytotoxicity analyses of the iodo-phenolic DBPs identified.

2.2 MATERIALS AND METHODS

Standards and Reagents. Reagents for disinfection reactions and chemical analyses were purchased from VWR International (Radnor, PA), Fisher Scientific (Fair Lawn, NJ), and Sigma-Aldrich (St. Louis, MO). Authentic standards for DBP confirmation were purchased from Sigma-Aldrich and Spectra Group Synthetics LLC (Millbury, OH). Detailed vendor information and solution preparation can be found in the Supporting Information (SI).

Sample Treatment and Characterization. Produced waters from a hydraulic fracturing well in the Barnett Shale (TX) and a gas reservoir in McAllen, TX were subjected to successive membrane-filtration treatments. Barnett Shale and McAllen produced waters were filtered successively to nanofiltration permeate (Barnett NF) and to microfiltration permeate (McAllen MF), respectively (Figure B.1), and were shipped on ice and stored at 4°C. Total organic carbon (TOC) analyses were performed using a Sievers InnovOx TOC Analyzer (GE Analytical Instruments, Boulder, CO); levels of

1.91 and 23.7 mg/L were measured in Barnett NF and McAllen MF, respectively. Halide measurements were performed using a Dionex ICS-1600 ion chromatograph with conductivity detection (Thermo Fisher Scientific, Waltham, MA); sample dilutions ranged from 10 to 10,000-fold. Concentrations of bromide and iodide in Barnett NF were 96.6 and 38.4 mg/L, respectively. In McAllen MF, bromide and iodide concentrations were 28.8 and 13.6 mg/L, respectively. Sample characteristics for these and raw produced waters are summarized in Table 2.1.

Disinfection and DBP Analysis. Disinfection reactions were performed in 60 mL amber bottles at room temperature (21 [± 2] °C). A 50 mL sample of each water was disinfected at pH 7 with 1 mg/L NH_2Cl per mg/L TOC for Barnett NF (1.91 mg/L) and 1 mg/L NH_2Cl per 3 mg/L TOC (7.80 mg/L) for McAllen MF. The McAllen MF was dosed at a lower ratio due to its extremely high TOC (23.7 mg/L). After 72 h reaction time, sample pH was adjusted with concentrated sulfuric acid to pH 1.4. Immediately after acidification, samples were liquid-liquid extracted three times with 15 mL dichloromethane, residual water was removed from extracts by passing through a column packed with sodium sulfate, and extracts were concentrated 50-fold to 1 mL. As a control, 50 mL of each non-disinfected water was extracted and analyzed. Additional experimental details regarding monochloramine preparation, sample pH, and chlorine dose are provided in the Supporting Information. Samples were analyzed by gas chromatography- mass spectrometry (GC-MS) with electron ionization. Unit resolution MS was used for initial comprehensive analysis, while high resolution (50,000) MS was used for the determination of molecular formulas. Detailed instrumentation and method parameters are provided in Table B.1.

Biological and Chemical Reagents, Chinese Hamster Ovary (CHO) Cells. CHO K1 cell line AS52, clone 11−4−8 was used.[48] The CHO cells were maintained in Hams F12 medium containing 5% fetal bovine serum (FBS), 1% L-glutamine, and 1% antibiotics (0.25 μg/mL amphotericin B, 100 μg/mL streptomycin sulfate, and 100 units/mL sodium penicillin G in 0.85% saline) at 37°C in a mammalian cell incubator with a humidified atmosphere of 5% CO_2.

CHO Cell Chronic Cytotoxicity Analyses. The CHO cell chronic cytotoxicity assay quantitatively measures the reduction in cell density as a function of the concentration of the individual iodo-phenolic compounds over 72 h. Details of the CHO cell cytotoxicity assay were published.[34,37] Each individual iodo-phenolic (1 M in dimethylsulfoxide (DMSO)) was diluted with F12 plus FBS cell culture medium, and in general 10 concentrations (with replicates) were analyzed in a 96-well microplate. After 72 h, the cell density expressed as the percentage of the concurrent negative control was recorded. These data were used to construct concentration-response curves.

Statistical Analysis. For individual iodophenols, one-way ANOVA tests were conducted to determine the lowest molar concentration that induced a statistically significant level of cytotoxicity as compared to their concurrent negative control ($P \leq 0.05$). To determine whether a statistically significant difference existed amongst different iodophenols, LC_{50} values (the concentration of each iodophenol that induced a cell density 50% of the negative control) were determined through regression analyses of each concentration–response curve. Using a bootstrap statistical approach the LC_{50} values were converted into mean cytotoxicity index values (CTI) = $(LC_{50}^{-1})(10^3)$ to allow for ANOVA statistical tests among the different compounds. The power of the test was

maintained at ≥0.8 at $\alpha = 0.05$. A detailed discussion of the statistical methods were published.[34]

2.3 RESULTS AND DISCUSSION

Bromide and Iodide. Previous studies of U.S. oil and gas wastewater report bromide levels ranging from tens to thousands of ppm and iodide ranging from 2 to 50 ppm.[14,49] Comparatively, McAllen MF halide levels were on the low end of these ranges (28.8 and 13.6 ppm for bromide and iodide, respectively), whereas Barnett NF levels were higher than McAllen, with 96.6 ppm bromide and 38.4 ppm iodide (Table 2.1).

Iodo-DBP Identification and Confirmation. A total of 56 iodinated DBPs were identified in the chloraminated produced waters. Thirty-seven of these contained only iodine. Extracted ion chromatograms of *m/z* 127 were used to target iodinated compounds in the GC-MS analyses. Each peak's mass spectrum was analyzed by manual inspection and library database searching the 2014 National Institute of Standards and Technology (NIST) library. NIST library matches were found for 2-iodophenol, 4-iodophenol, and 2,4,6-triiodophenol, with molecular ions ($M^{\bullet+}$) of *m/z* 220, 220, and 472, respectively. Peaks with $M^{\bullet+}$ *m/z* 234 resulted in high-similarity matches with iodomethylphenols, but also matched very closely with iodoanisoles, which have almost identical fragmentation patterns. Peaks with $M^{\bullet+}$ *m/z* 360 matched closest with diiodobenzoquinone (Figure B.2), but differences in fragmentation indicated that these were likely another type of diiodo-aromatic compound.

High-resolution mass spectrometry confirmed molecular formulas for all iodo-phenolics identified; all 30 iodine-containing DBPs were within three homologous series of mono-, di-, and tri-iodo-phenolics: iodophenols, iodomethylphenols (iodocresols), and

iododimethylphenols (iodoxylenols). Importantly, high resolution-MS also reinforced that the DBPs that showed a library match to diiodobenzoquinones were actually diiodomethylphenols (observed accurate mass of *m/z* 359.8505, molecular formula of $C_7H_6I_2O$) and not diiodobenzoquinones (theoretical *m/z* 359.8139, $C_6H_2I_2O_2$). Observed and formula-calculated theoretical exact masses are presented in Table 2.2.

Authentic standards of iodo-phenols, -methylphenols, and -dimethylphenols were analyzed to confirm their identities in the chloraminated treated produced waters. Mass spectra of standards were compared to those in the chloraminated water extracts to make presumptive compound identifications without isomeric confirmation, while mass spectral matches combined with retention time matches (Figure B.3), were used to confirm the exact isomer of each iodo-phenolic. A total of 11 isomer-specific structures were confirmed (Figure B.4): 2-iodophenol, 4-iodophenol, 2,6-diiodophenol, 2,4-diiodophenol, 2,4,6-triiodophenol, 2-iodo-4-methylphenol, 4-iodo-2-methylphenol, 2-iodo-4,5-dimethylphenol, 4-iodo-2,6-dimethylphenol, 4-iodo-2,5-dimethylphenol, and 4,6-diiodo-2,3-dimethylphenol. Further generic (non-isomer-specific) compound determinations (Figure B.5) were made for four more isomers of iodomethylphenol, six more isomers of iododimethylphenol, and eight more isomers of diiododimethylphenol. Standards were not available for diiodomethylphenols, triiodomethylphenols, or triiododimethylphenols, and thus, they were tentatively identified by manual spectral interpretation (Figure B.6) and high resolution-accurate mass MS (Table B.2). GC-MS chromatograms are shown in Figures 2.1 and B.7, with details regarding mass spectral interpretation provided in the Supporting Information.

In addition to the solely iodinated phenolics, 19 brominated and chlorinated phenolics were also tentatively identified using extracted ion chromatograms (extracting $M^{\bullet+}$ and predicted fragment ion *m/z*, based on iodo-phenolic mass spectra), accurate masses, and distinctive halogen patterns.[50] While the chloraminated Barnett NF sample did not show evidence of brominated or chlorinated components, the chloraminated McAllen MF sample yielded multiple isomers of mixed bromo-chloro-iodo-phenols and -methylphenols (Figure B.8, Table B.3).

None of these iodo-phenolics, nor any other iodinated compounds, were observed in either non-disinfected control. To our knowledge, this is the first report of iodomethylphenols and iododimethylphenols as DBPs. Though mono-, di-, and tri-iodo-phenols, -methylphenols, and -dimethylphenols were observed in both Barnett NF and McAllen MF chloraminated waters, the number of isomers varied between the two. More isomers of iodinated dimethylphenol were formed during chloramination of McAllen MF than Barnett NF. In addition, the predominant species formed (based on GC-MS abundances, Table B.2) varied between the two. While iodinated phenol species were most abundant in McAllen MF, iodinated methylphenols were the dominant DBPs formed in Barnett NF. It is possible that more species, including the bromoiodo- and chloroiodo-phenolics, were formed in McAllen MF than in Barnett NF due to much higher TOC:X^- ratios of McAllen MF. Given that the McAllen MF and Barnett NF are products of different processes and geological formations (gas from a conventional reservoir and oil from a shale formation, respectively), it is also likely that the precursors in each water vary, leading to different chloramination by-products.

Precursors of Iodo-Phenolics. We suspected that the precursors for iodo-phenol formation were phenol, methylphenols (cresols), dimethylphenols (xylenols), or other short-chain alkyl phenols, as these are common geogenic organics found in produced waters.[24,25,49,51,52] These have been previously reported in produced waters at concentrations as high as 20.2, 13.7, and 8.2 mg/L for phenol, total cresols, and total xylenols, respectively.[52] GC-MS analysis of the non-disinfected produced waters showed evidence of the presence of phenol, at least two isomers of methylphenol, and several isomers of dimethylphenol (Figure B.9). To further confirm these as potential precursors, controlled reactions were performed in purified water with 4-methylphenol and 2,6-dimethylphenol for 72 h, under the following conditions: (1) chloramination, (2) addition of iodide, and (3) addition of iodide and chloramination (Table B.4). Reactors spiked with iodide followed by chloramination resulted in 75% and 100% consumption of 4-methylphenol and 2,6-dimethylphenol, respectively, and the formation of three iodo-phenolic DBPs: 2-iodo-4-methylphenol and diiodomethylphenol from 4-methylphenol, as well as 4-iodo-2,6-dimethylphenol from 2,6-dimethylphenol. In chloraminated reactors without iodide, chlorinated analogues were observed, with only 15% of the starting 4-methylphenol and 30% of 2,6-dimethylphenol consumed. In reactors with iodide in the absence of disinfectant, no halogenated species were formed. The lack of trihalogenated species in any of the chloraminated reactors is not surprising, as further substitution of iodine or chlorine into the structure (>2 halogens for 4-methylphenol and >1 halogen for 2,6-dimethylphenol) is unfavorable due to ortho/para-directing of the hydroxy- and methyl-groups, as well as limited availability of positions on the ring. The high number of iodinated species (56) formed in the chloraminated produced water samples suggests

that multiple methylphenol/dimethylphenol isomers or other compounds containing cresol or xylenol groups may also serve as precursors for the iodomethylphenol and iododimethylphenol DBPs discovered. There is also the possibility that nonylphenol surfactants added to hydraulic fracturing fluids or other geogenic alkylphenols may be a source.[25,46,51,52]

Mammalian Cell Cytotoxicity of Iodo-Phenolics. The first compounds to be confirmed (2-iodophenol, 4-iodophenol, 2,4,6-triiodophenol, and 4-iodo-2-methylphenol) were investigated for chronic cytotoxicity with CHO cells. Cytotoxicity concentration-response curves are illustrated in Figure 2.2. The lowest cytotoxic concentration, LC_{50}, and cytotoxicity index values are presented in Table B.5 and Figure B.10. The descending order of cytotoxicity is 2,4,6-triiodophenol >> 4-iodo-2-methylphenol > 4-iodophenol >> 2-iodophenol, with LC_{50} values of 4.37×10^{-5}, 1.63×10^{-4}, 2.16×10^{-4}, and 6.01×10^{-4} M, respectively. 2,4,6-Triiodophenol was more cytotoxic than the THMs and HAAs with the exception of bromoacetic acid and iodoacetic acid.[34] A previous study demonstrated that 4-iodophenol and 2,4,6-triiodophenol were toxic to marine algae at 1-2 orders of magnitude lower concentrations than aliphatic halogenated DBPs, including iodoacetic acid.[53] In a developmental toxicity study, 2,4,6-triiodophenol was two orders of magnitude more toxic to polychaete embryos than iodoacetic acid.[54]

Implications for Drinking Water. Previous studies demonstrated enhanced formation of bromo- and iodo-THMs, bromo-HAAs, and bromoacetonitriles in chlorinated and chloraminated source waters impacted by oil and gas wastewater,[10,15,16] as well as the discharge of DBPs and phenolics into surface waters from facilities that treat produced water.[24] This study specifically investigated the hypothesis that organic

compounds in oil and gas wastewaters can act as precursors to halogenated organic DBPs. We discovered novel chloramine-mediated iodo-DBPs. In addition to the cytotoxicity in the present study, iodophenols and iodomethylphenols have extremely low taste and odor thresholds, and are often associated with medicinal-like and fecal-like odors.[55,56] Thus, these iodo-DBPs might contribute to foul-tasting drinking water, as well as pose a potential public health risk.

It is likely that in oil- and gas-impacted drinking water sources, iodo-phenolic DBPs could form at significant levels, particularly where chloramination is used. This is important to consider in circumstances where discharge of treated oil and gas wastewater may have led to THM and HAA levels that exceed EPA regulations, leading to utility decisions to switch to chloramination to improve compliance. While chloramination will significantly reduce regulated DBPs, it can lead to formation of more toxic unregulated iodo-DBPs, including these iodo-phenolics, when source waters are elevated in bromide and iodide. Furthermore, to protect drinking water in areas impacted by hydraulic fracturing waste, methods for removing bromide and iodide should be further investigated as pre-treatment options before release to surface waters.

2.4 TABLES AND FIGURES

Table 2.1. Sample Characteristics of Barnett and McAllen Produced Waters

Source	Barnett		McAllen	
	Raw Feed	Nanofiltered	Raw Feed	Microfiltered
TOC (mg C/L)	214 ± 11	1.91 ± 1.09	575[b]	23.7[b]
Cl^- (mg/L)	31,256 ± 1,332	24,058[b]	12,838 ± 20	12,422 ± 184[a]
Br^- (mg/L)	125 ± 7	96.6 ± 5.6	29.1 ± 0.1	28.8 ± 0.3[a]
I^- (mg/L)	53.5 ± 0.8[a]	38.4[b]	14.3 ± 0.1	13.6 ± 0.6

Reported as average ± standard error of 2 replicate measurements (n=2), except where otherwise specified
[a] Reported as average ± standard error of 3 replicate measurements (n=3); [b] Single measurement (n=1)

Table 2.2. Molecular Formulas, Observed and Theoretical Accurate Masses, and Isomer Identification Information for Iodo-Phenols, -Methylphenols, and -Dimethylphenols Identified

Compound	Formula	Observed Mass (Da)	Theoretical Mass (Da)	Isomers Observed Barnett NF	Isomers Observed McAllen MF	Isomers Confirmed [a]
Iodophenol	C_6H_5IO	219.9381	219.9380	2	2	2
Diiodophenol	$C_6H_4I_2O$	345.8348	345.8346	2	2	2
Triiodophenol	$C_6H_3I_3O$	471.7311	471.7313	1	1	1
Iodomethylphenol	C_7H_7IO	233.9536	233.9537	6	6	2
Diiodomethylphenol	$C_7H_6I_2O$	359.8505	359.8503	5	5	0
Triiodomethylphenol	$C_7H_5I_3O$	485.7468	485.7469	1	1	0
Iododimethylphenol	C_8H_9IO	247.9694	247.9693	7	9	3
Diiododimethylphenol	$C_8H_8I_2O$	373.8661	373.8659	6	9	1
Triiododimethylphenol	$C_8H_7I_3O$	499.7626	499.7626	2	2	0

[a] No standards were available for diiodomethylphenols, triiodomethylphenols, or triiododimethylphenols. These identifications are based on manual mass spectral interpretation and comparison to those confirmed.

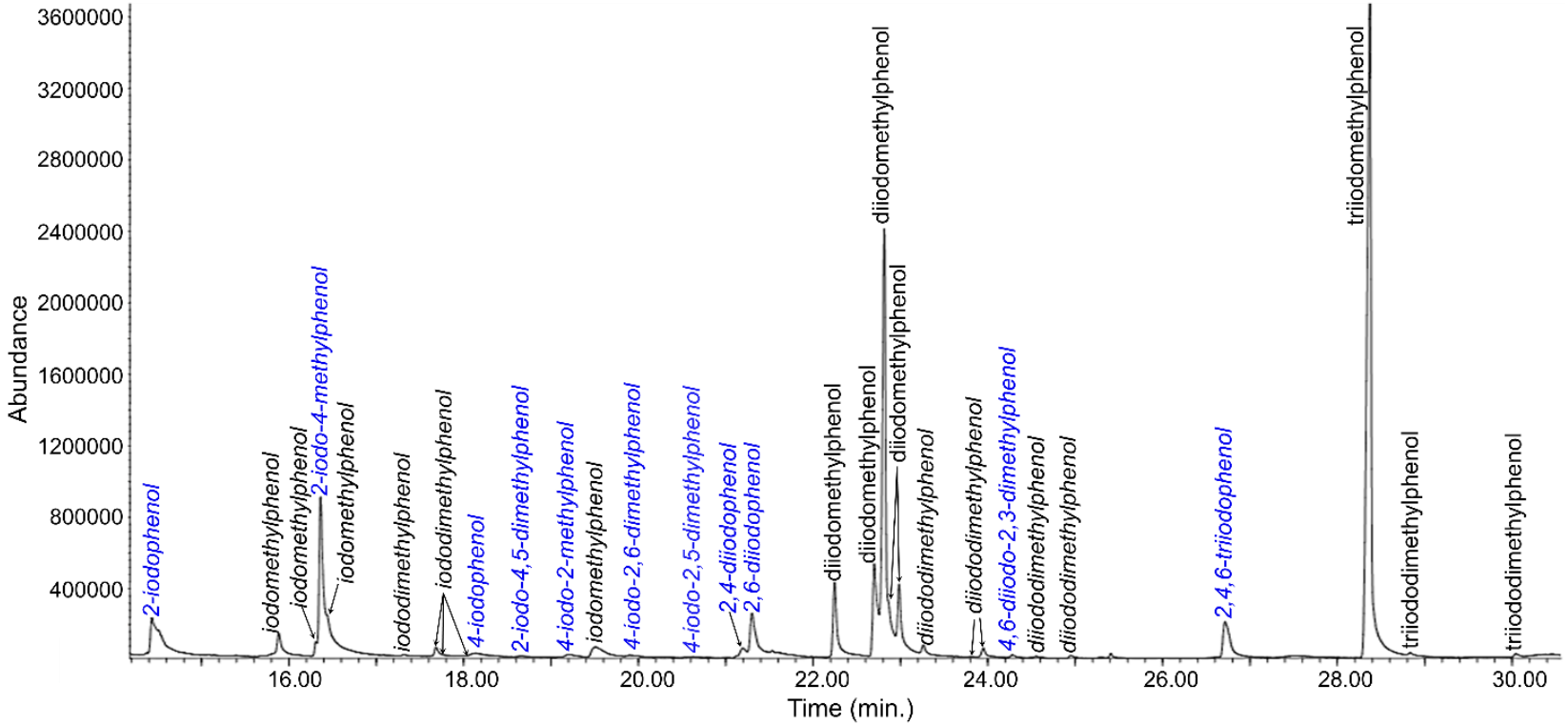

Figure 2.1. Iodo-phenolic DBPs identified in chloraminated Barnett nanofiltered (NF).[a,b]

[a] Italicized names correspond to components that have been mass spectrally confirmed against a standard

[b] Blue text indicates exact isomeric matches, determined via retention time confirmation

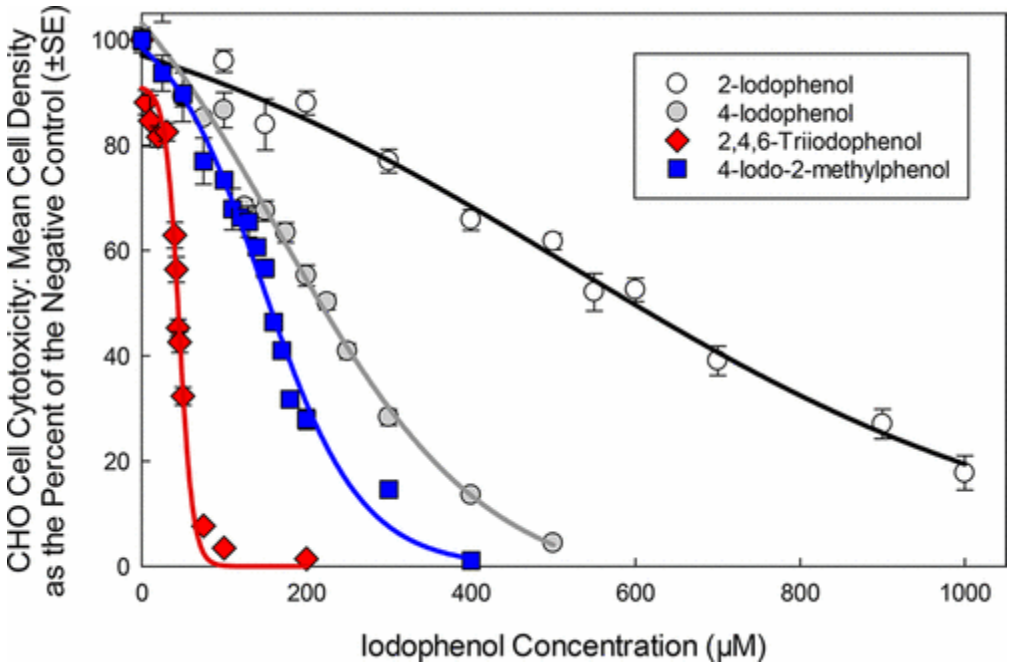

Figure 2.2. CHO cytotoxicity concentration-response curves for 2-iodophenol, 4-iodophenol, 2,4,6-triiodophenol, and 4-iodo-2-methylphenol.

CHAPTER 3
POTENTIAL IMPACTS OF HYDRAULIC FRACTURING ON DRINKING WATER: HIGH-RESOLUTION MASS SPECTROMETRY IDENTIFICATION OF NOVEL SURFACTANT-DERIVED S-DBPS[†]

[†] Liberatore, H. K.; Westerman, D. C.; Allen, J. M.; Plewa, M. J.; Wagner, E. D.; McKenna, A.; Weisbrod, C. R.; McCord, J. P.; Liberatore, R. J.; Richardson, S. D. To be submitted to *Environ. Sci. Technol.*

3.0 ABSTRACT

Studies have shown that hydraulic fracturing (HF) wastewaters introduced to surface water lead to elevated bromide and iodide levels, as well as enhanced formation of brominated and iodinated disinfection by-products (DBPs) at downstream drinking water treatment plants. In addition to geogenic components, like bromide and iodide, HF wastewaters contain high levels of chemical additives to optimize extraction activities. Among these additives are surfactants, which are used to increase fluid viscosity and enhance hydrocarbon extraction. At hundreds of mg/L, fluid additives, including surfactants, have the potential to serve as organic DBP precursors in HF wastewater (WW)-impacted drinking water sources.

This study reports the first identification of olefin sulfonate surfactant-derived DBPs, identified from disinfected gas-extraction WW. Over 300 sulfur-containing DBPs, with 43 unique molecular formulas, were found by non-targeted high-resolution mass spectrometry. In both chlorinated and chloraminated WW, these consisted of mostly brominated species, including bromohydrin sulfonates, dihalo-bromosufonates, and bromosultone sulfonates. Comparison to a commercially available C_{12} olefin sulfonate (dodecene sulfonate) surfactant mixture revealed that most of these DBPs originated from several isomers of dodecene sulfonate, while di-S-containing DBPs, like bromosultone sulfonate and bromohydrin disulfonate, originated from C_{12} olefin disulfonate species, which are common impurities in the production of olefin sulfonate. The most prominent DBPs, bromohydrin sulfonates, constituted approximately 10% of the total organic bromine in the chlor(am)inated WWs. Further, disinfection of the gas WW increased cytotoxicity by several orders of magnitude, with chloraminated water being the most

toxic. This finding is important to HF-impacted drinking water, as drinking water plants with high bromide source waters may switch to chloramination to meet DBP regulations.

3.1 INTRODUCTION

Hydraulic fracturing (HF) activities have become increasingly common, due to enhanced gas extraction from shale. Millions of liters of water are injected per well, and water that is injected returns to the surface, containing components released from the shale – like bromide and iodide. With the large volumes of wastewater being created, transported, and disposed of, there is concern for contamination of drinking water sources.[14,16] In most source waters, the major organic DBP precursor is natural organic matter (NOM), which is comprised of fulvic and humic acids.[1] However, disinfectants can also react with organic contaminants to form DBPs.[1,23,57] Hydraulic fracturing wastewaters tend to be very high in dissolved organic matter (DOM), contributed by both anthropogenic and geogenic constituents.[23,25]

HF fluids (and their wastewaters [WWs]) contain chemical additives to optimize the efficiency of shale fracturing and oil/gas extraction processes. Common additives include biocides, friction reducers, corrosion inhibitors, and surfactants, among others. While additives make up a small portion of the fracking fluid on a percentage basis (mostly sand and water; <1% additives), they are added at what are quite high levels (hundreds to thousands of parts-per-million [ppm; mg/L]) from an environmental contaminant perspective. There are thousands of chemicals used in the oil and gas industry, and different combinations are employed for different wells, determined by the optimum conditions for a given geological formation. Companies are often disinclined to

share proprietary chemical details; generally, chemicals that are disclosed are done so generically, without revealing exact mixture compositions.[58]

Surfactants constitute approximately 0.075% (750 mg/L) of the fluid injected during the fracking process.[58] At these high levels, after release to surface waters and mixing, surfactants still have the potential to exist at mg/L levels in impacted source waters. This is similar to typical NOM levels observed in surface waters. Surfactants present in oil and gas wastewater are not well characterized, as they are a broad class of chemicals with a variety of compositions (i.e., cationic, anionic, nonionic, and amphoteric), and exact chemical compositions are often unknown.[58] Most literature discussing non-targeted identification of HF WW surfactants have focused on nonionic ethoxylate-based surfactants.[58–60] To the best of our knowledge, the only class of surfactants that has been studied related to DBP formation are alkylphenol ethoxylates, studied after chlorination at municipal WW treatment plants (not related to HF).[61,62]

Previous HF DBP studies have primarily focused on quantifying select known brominated and iodinated DBPs formed from bromide and iodide contributed by HF waste in the presence of NOM after dilution with surface waters.[10,14–17,24,26] Though a previous study reported unintended halogenated by-products formed during the fracking process, likely from biocide or other oxidant fluid additives,[63] very little work has been conducted pertaining to the role of anthropogenic constituents (HF fluid additives, including surfactants) on DBP formation during drinking water disinfection. This study reports the first non-targeted identification of olefin sulfonate surfactant-derived DBPs, identified from disinfected gas-extraction wastewater (WW).

3.2 MATERIALS AND METHODS

Standards and Reagents. Sodium hypochlorite solution (NaOCl, 5.65-6%) was purchased from Fisher Scientific (Fair Lawn, NJ). Ammonium chloride (NH_4Cl) and sodium halide salts (i.e., NaCl, NaBr, and NaI) were obtained from Sigma-Aldrich (St. Louis, MO). Ethyl acetate and methanol were GC^2 grade from Burdick & Jackson (Muskegon, MI). Anhydrous dibasic potassium phosphate, hydrochloric acid, sulfuric acid, and sodium hydroxide were obtained from Fisher Scientific.

All inorganic reagents (i.e, halides, NaOCl, NH_4Cl, and buffer stock solutions) were prepared at least monthly in purified water (18 MΩ-cm^{-1}) from a Barnstead E-Pure system (Lake Balboa, CA). NaOCl reagent was standardized (λ_{max} = 292 nm, ε = 350 M^{-1} cm^{-1})[41] within a week prior to each disinfection experiment using a Molecular Devices SpectraMax M5 spectrophotometer (Sunnyvale, CA). Monochloramine reagent was prepared fresh with new solutions of NaOCl and NH_4Cl. Briefly, 100 mL of 0.05 M NH_4Cl was adjusted to pH 8.5 with 1 M NaOH. While stirring and maintaining pH between 8.4 and 8.7 with HCl and NaOH, 77 mL of 0.05 M NaOCl was added to the NH_4Cl solution, a few mL at a time, to satisfy a 1:1.3 NaOCl:NH_4Cl molar ratio. Resulting monochloramine concentration was determined spectrophotometrically (λ_{max} = 243 nm, ε = 461 M^{-1} cm^{-1})[41].

Sample Collection and Characterization. Produced water samples from a Texas gas-charged reservoir were collected headspace-free in 2 L high density polyethylene (HDPE) containers. Prior to two-day shipment on ice, a portion of the produced water was subjected to pretreatment methods that included bag filtration (20 µm) and gas/hydrocarbon removal. The two types of samples were thereafter deemed "pretreated (PT)" and "raw feed (RF)". HPLC grade water was shipped, unopened, to the sample

collection site, where it was transferred to HDPE bottles headspace-free and shipped alongside samples as a travel/field blank (FB).

Total organic carbon (TOC) analyses were performed using a Sievers InnovOx TOC Analyzer (GE Analytical Instruments, Boulder, CO). Prior to halide analysis, samples were 0.45-µm filtered through polyethersulfone membrane syringe filters (VWR International, City, State) that were pre-rinsed with a 10 mL wash of purified water to remove iodide interferent. Calibration standards for chloride (10-750 µg/L), bromide (1-750 µg/L), and iodide (10-750 µg/L) were prepared in purified water. Standards and filtered samples were analyzed by a Dionex 1600 ion chromatograph (IC) with conductivity detector (Sunnyvale, CA).

Simulated Disinfection Experiments. RF, PT, and FB waters were each mixed separately in purified water (10% sample + 90% purified water). Large-scale reactions (18 L for PT and RF; 21 L for FB) were performed in stoppered glass jugs, covered to minimize light exposure. Chlorination and chloramination reactions were performed for 24 and 72 h, respectively, with disinfectant doses to achieve a 1.0-2.0 mg/L chlorine residual at the end of the allotted reaction times. Each reactor was buffered at pH 7.5 with 10 mM phosphate. Controls of each sample, with no disinfectant applied, were analyzed in the same manner for comparison.

A portion of the reaction mixture was quenched with ascorbic acid (1.3:1 quench:chlorine, assuming a 2.5 mg/L residual) and analyzed directly by liquid chromatography (LC)-high resolution mass spectrometry (MS). A 250 mL aliquot of the quenched mixture was used for duplicate measurements of speciated total organic

halogen (TOX). The remainder of the water was extracted using XAD resins for high-concentration factor, high-sensitivity MS analyses. mammalian cell cytotoxicity studies.

Total Organic Halogen (TOX). Total organic chlorine, bromine, and iodine (TOCl, TOBr, TOI) were measured, in duplicate, according to a previously published method using a TOX analyzer (Mitsubishi Chemical Analytech, Chigasaki, Japan; Cosa Xentaur, Yaphank, NY, USA), followed by ion chromatography (IC).[64,65] For each replicate, approximately 50 mL of quenched, acidified (pH < 2) sample were passed through two activated carbon columns on the Mitsubishi TXA-04 adsorption unit to isolate organic components. Residual inorganic species were removed from the carbons with a 5 mL nitric acid wash (5 mg NO_3^-/mL).

The two carbons for each sample were placed into separate ceramic boats for combustion, though their combustion products were collected into the same tube during sorption. An autosampler (Mitsubishi ASC-240S) loaded boats containing carbons into the combustion unit (AQF-2100H). Carbons were pyrolyzed at 1000 °C for 4 min in the presence of oxygen and argon. Combustion products of halo-organic compounds (i.e., hydrogen halide gases [HCl, HBr, HI]) were collected in approximately 5 mL of 0.03% H_2O_2, with an additional 3 mL of H_2O_2 solution that were used to rinse the gas line from the furnace to the sorption unit (AU-250). TOCl, TOBr, and TOI were quantified as Cl^-, Br^-, and I^- using the IC halides method described above.

For accurate TOX determination, each of the lines on the adsorption unit were calibrated within two months of analysis to determine the exact volume of each, which ranged from 45-47 mL. In addition, test tubes used for sorption of hydrogen halide (HCl,

HBr, HI) gases were weighed empty and after the sorption process to gravimetrically determine the dilution factor associated with this step of the process.

XAD Resin Extraction. A previously published standard operating procedure[66–68] was modified and used to extract and concentrate the organic material and DBPs from the reactors. Briefly, 30 mL each of XAD-2 and DAX-8 resins (Sigma-Aldrich) were conditioned with successive rinses of water, 0.1 M HCl, and 0.1 M NaOH, as stated in the SOP. Samples were acidified, 2 L at a time, to pH 0-2 with concentrated sulfuric acid. Acidified samples were poured over the resins to waste. Adsorbed components of samples were eluted with 200 mL of ethyl acetate, which was dried with sodium sulfate and concentrated under nitrogen to 2 mL. A portion of this extract was solvent exchanged in methanol for high-sensitivity mass spectrometric analyses.

Biological and Chemical Reagents, Chinese Hamster Ovary (CHO) Cells. CHO K1 cell line AS52, clone 11−4−8 was used.[48] Cells were kept at 37 °C in a mammalian cell incubator with a humidified atmosphere of 5% CO_2, and were maintained in Hams F12 medium with 5% fetal bovine serum (FBS), 1% L-glutamine, and 1% antibiotics (0.25 μg/mL amphotericin B, 100 μg/mL streptomycin sulfate, and 100 units/mL sodium penicillin G in 0.85% saline)

CHO Cell Chronic Cytotoxicity Analyses. The majority (85%) of the ethyl acetate XAD extracts were used for cytotoxic evaluation in Chinese hamster ovary (CHO) cells based on a previously published method.[34,37] Each extract was solvent exchanged in dimethylsulfoxide (DMSO) and diluted with F12 plus FBS cell culture medium. A variety of concentration factors (CFs) were analyzed (with replicates) in a 96-well microplate. After 72 h of cell exposure to each sample (i.e., RF, PT, FB; disinfected

and raw), the cell density was recorded and used to construct concentration-response curves. LC_{50}, the CF which induced 50% cell density compared to a negative control, and cytotoxicity index value ($CTI = [LC_{50}]^{-1}[10^3]$) were determined from concentration-response curves. Both LC_{50} and CTI value are expressed in terms of the CF associated with induction of cytotoxic effects.

LC-MS and Ultrahigh-Resolution MS Analyses. For initial non-targeted DBP screening, an Agilent (Santa Clara, CA) liquid chromatograph (LC)-quadrupole-time-of-flight (Q-TOF) mass spectrometer (MS) was used. LC (1290 Infinity II UHPLC) and MS (6545 QTOF) parameters are provided in Appendix C Tables C.1 and C.2, respectively. Briefly, quenched water samples were diluted 10-fold, and 10 µL was injected onto a C18 column (2.1 mm x 150 mm x 2.7 µm). The LC method employed a gradient elution program with water and methanol (both with 0.1% formic acid), ramping from 5% to 95% methanol over a 12 min period. Negative electrospray ionization [ESI(-)] MS and MS/MS spectra were obtained simultaneously, allowing for correlation of precursor and product ions during data processing.[69]

For further DBP identification and structural elucidation, a 21T Fourier transform ion cyclotron resonance (FT-ICR) MS (National High Magnetic Field Laboratory, Tallahassee, FL) was used. High-sensitivity, ultra-high resolution (≥1,000,000) ESI(-) MS, MS/MS, and MS^3 analyses were performed. Prior to analysis, portions of the XAD ethyl acetate extracts (equivalent to approximately 2 L of aqueous sample) were solvent exchanged into 200 µL of methanol, followed by a 2-fold dilution before direct-infusion ICR analyses. Direct-infusion allowed for longer acquisition and, thus, higher sensitivity MS and MS^n analysis of whole-sample components. Ten-minute data-dependent

acquisition (DDA) methods were utilized in MS^n experiments, employing both abundance-based and hydrogen halide neutral loss (-HCl, -HBr, -HI) parameters to initiate MS^3 from MS/MS fragments.

Later analyses for isomer-specific MS, MS/MS, and MS^3 data were performed using an LC-Orbitrap Fusion Tribrid MS (Thermo Scientific, Waltham, MA). LC and MS parameters for both MS scan and MS^n analyses are outlined in Tables C.3–C.5. Briefly, 10 µL of quenched water samples was injected onto a C18 column (2.1 mm x 50 mm x 1.7 µm). A gradient elution program of (A) 95:5 water:acetonitrile (ACN) and (B) 95:5 ACN:water (both with 0.4 mM ammonium formate) ramped from 10% to 100 B over a 5 min period and held at 100% B for 3 min. Separate methods were used for the acquisition of high-resolution (120,000) MS scan data and targeted-mass MS^3 (30,000); details of each are provided in Tables C.4 and C.5, respectively.

3.3 RESULTS AND DISCUSSION

In this study, a variety of high resolution MS techniques were utilized to obtain as much valuable information about the compounds of interest as possible. LC-QTOF was used as an initial high-resolution (30,000 resolution) screening tool, using "All Ions MS/MS" data independent acquisition (DIA) to quickly acquire associated accurate-mass MS and MS/MS data.[69] While QTOF provided sufficient mass accuracy for formula assignments, fragmentation beyond MS/MS was necessary for structural elucidation of compounds. For this reason, 21T FT-ICR-MS was used to obtain high-sensitivity, ultrahigh-resolution (1,000,000 resolution) MS^3 data of concentrated XAD resin extracts. An Orbitrap Fusion Tribrid (30,000-120,000 resolution) instrument was later used for data-dependent MS^3 scans of selected MS/MS transitions (i.e., MS^1 and MS^2 ions fixed

while scanning MS^3) coupled to chromatography for isomer-specific information in aqueous samples.

Preliminary Identification of Two Br-S-DBPs by LC-QTOF. The "All Ions" DIA data files were processed in MassHunter Qual software using molecular feature extraction (small organic molecule) and molecular formula generation software tools. Molecular formula results were filtered by Br-containing, given that brominated DBPs are well-known to be the highest forming during disinfection of halide-rich waters.[8,9] Four major isomers of $C_{12}H_{24}BrSO_4^-$ and one isomer of $C_{12}H_{22}BrS_2O_6^-$ were observed. While previous studies have reported sulfur-containing DBPs,[57,68] this was the first identification these brominated sulfur-containing DBPs. MS/MS data (Figures C.1 and C.2) provided little structural information, aside from the existence of Br and S in the structures and product ions indicative of SO_4/SO_3.

In the undisinfected control, the presence of several isomers of $C_{12}H_{25}SO_4^-$ (m/z 265.1474) at high abundance seemed to be candidates for precursors to the $C_{12}H_{24}BrSO_4^-$ DBPs, as they differed by only the addition of a bromine. This is the molecular formula of lauryl sulfate, a widely used surfactant.[58,70] However, the structure of lauryl sulfate (i.e., linear, saturated, with no rings or double bonds) is not conducive to common halogenated DBP formation during chlor(am)ination. In addition, there was not a significant decline in abundance for the isomers of $C_{12}H_{25}SO_4^-$ after disinfection, indicating that this component was non-reactive with chlorine and monochloramine. Given that high-purity surfactants are not necessary for most industrial uses, we believed that an impurity (perhaps an unsaturated analogue) in industrial-grade lauryl sulfate could have served as the DBP precursor instead. As a result, we obtained industrial-grade

sodium lauryl sulfate and subjected it to chlorine disinfection in the presence of bromide. However, no significant differences in mixture components were observed for chlorinated vs. undisinfected, confirming that lauryl sulfate is not reactive with chlorine and that any unsaturated analogues present were not at high enough levels to be detected nor formed detectable levels of DBPs. It was, therefore, unlikely that lauryl sulfate products were involved in the formation of these DBPs.

FT-ICR Direct Infusion Ultrahigh Resolution MS and MS^3 of Extracts.

Further analysis by ultra-high resolution FT-ICR-MS direct infusion of XAD extracts (solvent exchanged in methanol) enabled the identification of lower abundance chloro- and iodo- analogs of these compounds, as well as simple, direct visual comparison of prominent spectral features between disinfected and undisinfected samples (Figure C.3). MS^3 experiments were necessary for structural elucidation, unveiling that these were not sulfates, but sulfonate compounds (likely halohydrin sulfonates). After MS/MS loss of HX, the major MS^3 transitions (Figure C.4) were variations of SO_3- and SO_2-containing fragments/losses, as well as the loss of carbon monoxide (-CO). This type of variation associated with SO_x losses and fragments is not uncommon for sulfonate compounds, as gas-phase rearrangements can occur during collision-induced dissociation.[71–74] High sensitivity provided by FT-ICR direct infusion analysis was crucial to the isolation and MS/MS (and MS^3) elucidation of the iodohydrin sulfonate and bromochlorosulfonate, which were not detected by QTOF-MS, and were of very low abundance during later LC-MS/MS analyses on the Orbitrap MS (Figures 3.2 and C.3). In addition to its sensitivity, FT-ICR's ultra-high resolution further confirmed the presence of sulfur through its ability to distinguish the two distinct A+2 peaks in the molecular ion (Figure C.5), resulting

from the natural abundance of heavy halogens (^{81}Br, ^{37}Cl) and sulfur (^{34}S). The difference between light and heavy atoms is 1.997954 for Br, 1.99705 for Cl, and 1.995796 for S, resulting in mass spectral features that are 0.002158 and 0.001254 Da apart for the bromohydrin and chlorohydrin, respectively – a difference of just 3 to 4 electrons' mass. FT-ICR's ultrahigh resolution could also distinguish between the ^{81}Br^{35}Cl and ^{79}Br^{37}Cl isotopes of the bromochlorosulfonate, a difference of just 2 electrons' mass.

In the undisinfected RF and PT samples, the major peaks present were *m/z* 247.13741 and 495.28217, corresponding to formulas of $C_{12}H_{23}SO_3^-$ and $C_{24}H_{47}S_2O_6^-$ (Figure C.3). These mass spectral components greatly decreased following disinfection with both chlorine and chloramine (Figure 3.2), indicating that these were transformed, likely to form the observed halohydrin- and dihalo-sulfonate DBPs.

Another commonly used surfactant in oil and gas extraction is olefin sulfonate.[70] The twelve-carbon variation of these surfactants (C_{12}-olefin sulfonate) possesses the same molecular formula of $C_{12}H_{23}SO_3^-$ and a theoretical $[M-H]^-$ of *m/z* 247.13734, a difference of just 0.07 mDa from the exact mass of the unknown compounds in the undisinfected RF and PT samples. At high concentrations, proton dimers ($[2M-H]^-$) of sulfonates can form in-source during electrospray ionization.[74] This phenomenon is responsible for the presence of the $C_{24}H_{47}S_2O_6^-$ (*m/z* 495.28217) spectral feature observed in the undisinfected samples.

Many commercial olefin sulfonate products also contain hydroxysulfonate compounds, formed as by-products during olefin sulfonate production.[75] These compounds are functional isomers of alkylsulfate compounds, having the same mass and

formula, but with a sulfonate (SO_3) and a hydroxy (OH) group in lieu of the sulfate (SO_4). This explains the abundant presence of *m/z* 265.14796 ($C_{12}H_{25}SO_4^-$) in the spectra of both the undisinfected and chlor(am)inated samples. This component was in fact, not lauryl sulfate, but several isomers of hydroxydodecane sulfonate.

DBP and Precursor Confirmation. For further high resolution MS, MS/MS, and MS^3 analyses with isomeric information, an LC-Orbitrap Fusion MS was used. Several isomers of dodecene sulfonate (C_{12} olefin sulfonate) found in the undisinfected samples were determined to be the likely precursors to these halohydrin sulfonate by-products. Figure 3.1 shows the formation of halohydrins only after disinfection, while the suspected precursor isomers were almost entirely consumed during disinfection, confirming our hypothesis.

A surfactant mixture of sodium dodecene sulfonate (20-30%) and hydroxydodecylsulfonate (20-30%) was acquired from Stepan Company (Northfield, IL). This commercial product was diluted (~50 ppm) in pH 7.2 phosphate-buffered purified water and subjected to 18 h chlorination (100 ppm as Cl_2) in the presence of bromide (10 ppm). Three suspected DBP-precursors were identified based on area counts (>1500) and percent consumed (≥50%) during disinfection in both RF and bromide-containing surfactant mixture samples (Table 3.1). Two of these compounds, $C_{12}H_{23}SO_3^-$ (olefin sulfonate) and $C_{12}H_{21}SO_3^-$ (diolefin sulfonate impurity) were suspected to be the precursors to the singly-sulfonated DBPs identified. With olefin sulfonate being the major component of both the RF and commercial surfactant, it is probable that the majority of the singly-sulfonated DBPs derived from the various isomers of $C_{12}H_{23}SO_3^-$.

A single compound, $C_{12}H_{23}S_2O_6^-$, was determined to be the sole precursor to all di-sulfur-containing DBPs found.

In addition to consumption of the suspected precursors, further evidence was provided in the formation of three of the same bromohydrin sulfonate isomers identified in the RF chlor(am)ination reactions, as well as many of the same $C_{12}H_{22}BrS_2O_6^-$ isomers (Figure 3.3). All six isomers of olefin sulfonate formed in-source proton-dimers, as did the isomers of the major halohydrin by-products. Different isomers possessed different $[M-H]^-$ to $[2M-H]^-$ ratios, which could be based on structural differences (e.g., branching vs. linear) or may be concentration-related.

During initial analyses, prior to obtaining the commercial surfactant mixture, we had overlooked the S_2O_6 precursor. We did not anticipate by-products or precursors that would doubly-charge, so the preliminary data processing workflow used on the LC-QTOF instrument did not incorporate the possibility of 2- charges in molecular formula assignments. While the singly-charged $[M-H]^-$ of *m/z* 327.0935 was detected at this stage in our investigation, it was at very low abundance (too low to indicate it might have formed the higher-abundance Br-DBPs). This is because the doubly-charged ions are favored during ionization, so the majority of these components' signals were present as an ion that the processing method did not associate as related to the compound. These doubly- charged $[M-2H]^{2-}$ ions are unmistakeable, given that their isotopic pattern is the same as the singly-charged, but with half the *m/z* difference between isotopes (e.g., 163.04332/163.54430 [^{13}C]/164.0486[^{34}S]), varying by approximately half of one Dalton between each isotope (Figure 3.4). This same S_2O_6 precursor went undetected by FT-

ICR, because an organic extract (not aqueous sample), which did not recover the doubly-charged precursor, was analyzed.

C12-Olefin Sulfonate-Derived DBP Speciation. Thermo Compound Discoverer software was used for non-targeted analytical comparisons between Orbitrap MS (120,000 resolution) data for raw, chlorinated, and chloraminated gas wastewaters and bromide-spiked surfactant mixture. Thousands of features were identified; results were filtered to include only those with assigned formulas containing "C_{12}", "S", and "O". With these three collective filters, 92 molecular formulas were identified for C_{12} sulfur oxide-containing components alone. From these, 43 formulas were determined to be DBPs, based on at least a doubling in signal from undisinfected to disinfected (indicating significant formation during disinfection) and a minimum abundance of 1500. Almost all of these had multiple isomers, with as many as 24 visible isomers (Table C.6). A total of 330 C_{12}-sulfonate DBPs were identified in chlorinated RF, 292 were identified in chloraminated RF, and 158 were present in the chlorinated olefin sulfonate mixture with bromide. Many DBPs shared the same isomeric distribution between samples, but others (e.g., $C_{12}H_{24}ClSO_4^-$) favored the formation of one or two specific isomers via chloramination that were much lower-abundance, sometimes not detected, in chlorinated samples.

The halohydrin sulfonates ($C_{12}H_{24}XSO_4^-$) were by far the most abundantly-formed DBPs in both chlorinated and chloraminated waters. While chlor(am)inated RF formed mostly bromohydrin sulfonates, the chlorinated Br-spiked surfactant mixture favored the formation of one chlorohydrin isomer over the other chloro- and bromo-hydrins. This is likely due to a difference between the surfactant to Br^- ratios of the gas

wastewater samples vs. the controlled reactions with the surfactant mixture, or due to failure to meet the chlorine demand in this proof-of-concept chlorination reaction setup for the surfactant mixture.

There was a vast difference observed for chlorohydrin by-products between disinfection types that was not observed for the analogous bromo- and iodohydrin DBPs. This is because the extremely high levels of bromide and iodide in the HF wastewaters drive bromo- and iodo-DBP formation much more so than the disinfectant type; however, the chlorine in chloro-DBPs is contributed by the chlorine or chloramine disinfectant itself, not dependent on chloride concentration.[7–9] For this reason, the difference in reactivity of chlorine vs. chloramine is demonstrated most by the chlorohydrin (and other chloro-DBPs) formation. In general, chloramine-disinfection tended to favor a few isomers, while chlorination tended to form similar (and higher) amounts of more isomers of the chloro-DBPs. For example, chloramination favored a single chlorohydrin species (3.8 min) over the others, which was 100-fold more abundant than in chlorinated water, while chlorine had a more equal distribution to form many other isomers. Unlike the gas wastewater, chlorinated Br-spiked surfactant mixture yielded many chlorohydrin isomers, but formed mostly a single isomer (3.5 min) that was different than that favored by chloramine disinfection. While not as extreme as chlorohydrin, there were slight differences in favoritism towards major bromohydrin species from the two disinfectants, as well as lower formation of the iodohydrin from chlorine than chloramine. Because of the tendency of iodide to form iodate in the presence of chlorine, this is not unexpected.

It was apparent that "disulfonate" (S_2O_6) by-products were no longer disulfonates; their characteristic double charge was no longer present post-disinfection. Unlike the

olefin disulfonate precursors, the two-sulfur-containing halo-DBPs were observed in the organic extracts analyzed by direct infusion FT-ICR, meaning they were effectively extracted from the aqueous phase, which would be extremely unlikely if both sulfonate groups were left intact. In addition, it was odd to observe DBPs that had the same number of ring/double bond equivalents (RDBE) as their precursor compound, as usually double bonds are eliminated in the halogen addition reactions of olefins.[76] Given that both the precursor ($C_{12}H_{23}S_2O_6^-$) and the halogenated S_2O_6 DBPs (e.g., $C_{12}H_{22}BrS_2O_6^-$) had the same RDBE of 1.5, this indicated that halogenation of the double bond initiated a reaction to form cyclic sulfur groups (sultones). Various isomers exist, likely due to differences in sultone ring size based on double bond placement in olefin disulfonate precursor isomers (Figure 3.4).[77] This conclusion was further supported by the large difference in retention time and chromatographic peak shape between the precursor (early-eluting with tailing) and Br-S_2O_6 by-product (later-eluting, sharp Gaussian peaks). In addition, another di-S DBP, a bromohydrin disulfonate ($C_{12}H_{24}BrS_2O_7^-$), was identified in the chlor(am)inated gas wastewater samples. As shown in Figure 3.4, this by-product was early-eluting with broad, tailing chromatography and possessed a prominent $[M-2H]^{2-}$, similar to the precursor compound.

Other, lower-abundance halogenated DBP series were also identified in chlor(am)inated gas wastewater samples and the chlorinated Br-spiked surfactant mixture (Table C.6, Figure C.6), including mono- and di-halogenated sulfonates formed from the same suspected olefin sulfonate precursors. A large variety of DBPs were formed that could have resulted from both the olefin sulfonate or from impurities, like di-olefin sulfonates, that resulted in multiply-unsaturated and/or oxidized by-products. For

example, DBPs of the generic formula $C_{12}H_{23-n}X_nSO_4^-$, including the monochlorinated species ($C_{12}H_{22}ClSO_4^-$), have the same RDBE as olefin sulfonate (1.5), indicating either halohydrination of di-olefin sulfonate (RDBE 2.5) to form halohydroxydodecene sulfonates or the formation of halo-carbonyl sulfonates from olefin sulfonate precursors. Both olefin and di-olefin sulfonates were completely consumed in chlor(am)ination of RF (Table 3.1), and several isomers of these DBPs were formed at higher abundance than the di-olefin precursor. This indicates that both species are likely precursors, with olefin sulfonate having a larger contribution than di-olefin sulfonate. The formation of dihalogenated variations of this same DBP class (e.g., $C_{12}H_{21}Cl_2SO_4^-$) support the idea of ketone and aldehyde formation, as it is common for multiple α-substitutions to occur, resulting in multiply-halogenated carbonyl compounds.[76]

In addition to halogenated DBPs, many non-halogenated products were observed post-disinfection, including higher degrees of unsaturation (i.e., more double bonds), as well as mono- and multi-hydroxy- and carbonyl-sulfonates (Table C.6). In general, chlorination and chloramination both resulted in these by-products, but tended to vary in which major isomers formed. Nitrogen-containing DBPs (both halogenated and non-halogenated) were also formed, but only in the chloraminated samples. N-DBPs with RDBE of 2.5 (e.g., $C_{12}H_{22}NSO_3^-$ and $C_{12}H_{22}NSO_4^-$) are likely nitriles or hetero-rings containing a double bond, while those with RDBE of 1.5 are likely amides, which can be formed through the hydrolysis of nitrile intermediates in disinfected water.[45,78]

Importance of High-Resolution MS. High resolution MS was crucial to the identification of DBPs in this mixture, given its extreme complexity. Figure C.7 shows a single LC-MS spectrum from the chlorinated RF sample that alone has several examples

where low resolution may have led to misidentification of components as halo-DBPs from the appearance of characteristic halogen isotope patterns. With the high level of co-elution and convolution that is present in these complex mixtures, in the absence of high-resolution, accurate mass capabilities, *m/z* series of A/A+2/A+4/A+6, like that of 313/315/317/319 shown in Figure C.5 could be mistaken for a tribromo-compound, based on its pattern. However, further decimal places reveal that, in fact, only two of these peaks belong to the same compound (315/317), which contains only one bromine. Similarly, the ions at *m/z* 261/263/265 could be indicative of a dibrominated compound, when in fact, each *m/z* belongs to a different compound.

There are thousands of chemicals used in HF, which vary from well to well based on geological conditions.[58] Complexity of mixtures and lack of proprietary chemical details make the identification of additives, much less DBPs resulting from these additives, extremely difficult. In the absence of information and high-quality standards, high-resolution MS (with MS^n information) is a crucial tool in the generic structural elucidation of unknowns. While specific isomers are unknown, new classes of DBPs can still be identified through high-resolution accurate mass analyses.

Cytotoxicity and TOX. The toxicity of both RF and PT gas wastewaters were greatly enhanced by chlor(am)ination. In fact, disinfected samples were so cytotoxic that they required dilution (concentration factor < 1) beyond their initial concentration (Figure 3.5, Table C.7). Chlorinated and chloraminated WWs were 14-fold and 26-fold more toxic than undisinfected controls for both PT and RF samples. Though chloraminated PT and RF wastewaters exhibited lower formation in overall total organic halogen (TOX), chloraminated waters were more cytotoxic than chlorinated waters (Figure 3.6). This is

likely due to the formation of higher toxicity iodinated and nitrogenous DBPs during chloramination.[1–3]

Based on olefin sulfonate's ion abundance in the surfactant mixture analyzed, it was estimated that the bromohydrin sulfonate DBPs constituted approximately 10% of the quantified total organic bromine (TOBr) in the chlor(am)inated HF wastewaters. Nothing is known about the toxicity of these newly identified sulfonate DBPs; it is unclear whether their formation contributes significantly to the observed increase in toxicity with disinfection. It is possible that the observed toxicity could be due to the formation of other DBPs not identified in this study. For example, a previous study of surfactant-based DBPs in WW, halogenated nonylphenol compounds, revealed that halo-nonylphenolics exhibited weaker estrogenicity than the parent surfactant.[61] To better understand the newly-identified sulfonate DBPs' contribution to toxicity, we plan to perform cytotoxicity assays for the C_{12} olefin sulfonate product ("standard") mixture with bromide and iodide under chlor(am)ination conditions similar to those used for RF and PT WWs. Comparison of chlor(am)inated standard sample toxicities to that of the undisinfected control, combined with non-targeted LC- and GC-high-resolution-MS and TOX analyses, will provide insight regarding these new DBPs' potential health risks.

Far more industries (e.g., personal care products, detergents) than just oil and gas extraction utilize these surfactants, meaning that these organic DBP precursors could enter drinking water sources through a variety of wastewater introduction pathways, including from municipal wastewater.[61,62,79,80] Depending on disinfected "standard" toxicity results, it may be important to continue to study these surfactants and how they degrade/transform in natural waters during drinking water treatment. While it is possible

that they could biodegrade[75,80,81] or be outcompeted by NOM to form DBPs in natural waters, it is also likely that their high concentrations could result in persistence long enough to form appreciable levels of these newly-identified DBPs.

3.4 TABLES AND FIGURES

Table 3.1. Precursor Compounds in Raw Feed Samples and C_{12} Olefin Sulfonate "Standard"

Primary Ion Formula, ion, m/z_{theo}	m/z_{obs}	**Secondary Ion** Formula, ion, m/z_{theo}	m/z_{obs}	**Retention Time (min)**	**Standard** % Consumed with HOCl	**RF Sample** % Consumed with HOCl	% Consumed with NH2Cl
$C_{12}H_{23}SO_3^-$ [M-H]$^-$ 247.13734	247.1372	**$C_{24}H_{47}S_2O_6^-$** [2M-H]$^-$ 495.28195	495.2821	3.38	94	100	99
	247.1372		495.2820	3.44	100	100	100
	247.1373		495.2822	3.51	96	90	94
	247.1373		495.2823	3.58	100	100	100
	247.1373		495.2822	3.62	90	100	100
	247.1374		495.2822	3.69	21	100	97
$C_{12}H_{22}S_2O_6^{2-}$ [M-2H]$^{2-}$ 163.04344	163.0435	**$C_{12}H_{23}S_2O_6^-$** [M-H]$^-$ 327.09415	327.0942	0.58	*not present*	100	100
	163.0434		327.0941	0.62	81	100	100
	163.0433		327.0940	0.76	16	100	100
	163.0433		327.0940	0.88	31	100	100
	163.0433		327.0940	0.97	-140	100	100
	163.0434		327.0941	1.05	46	100	100
	163.0434		327.0940	1.29	17	100	100
	163.0433		327.0940	1.48	21	100	100
$C_{12}H_{21}SO_3^-$ [M-H]$^-$ 245.12169	245.1216			3.11	*not present*	100	100
	245.1215			3.27	94	100	100
	245.1216			3.54	76	100	100
	245.1219			3.65	32	100	100

Note: Negative % consumption for a single isomer of $C_{12}H_{22}S_2O_6^{2-}$, as this specific isomer was *formed* in the standard, while other isomers were consumed.

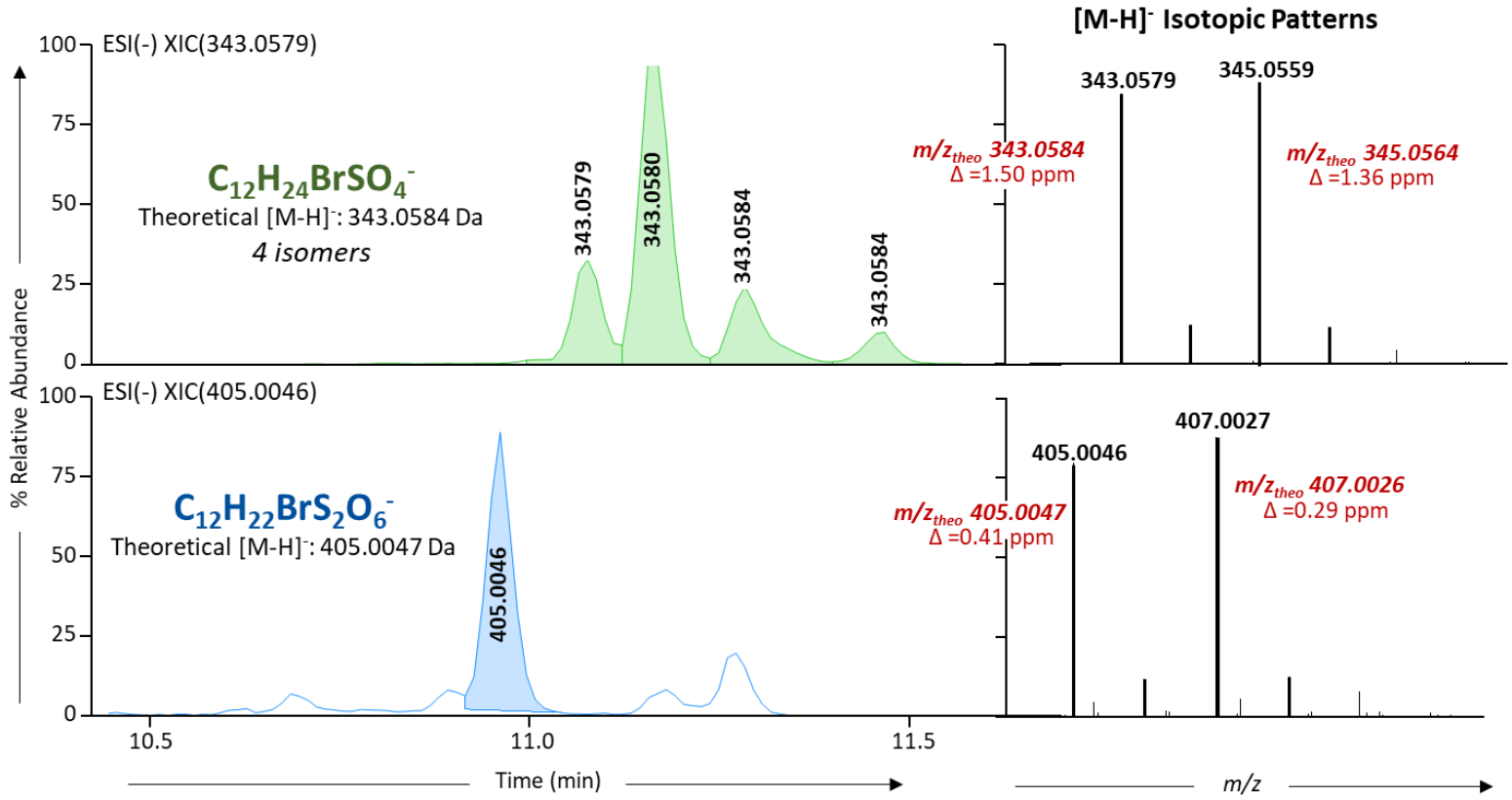

Figure 3.1. LC-QTOF extracted ion chromatograms (XICs) of two brominated S-containing DBPs.

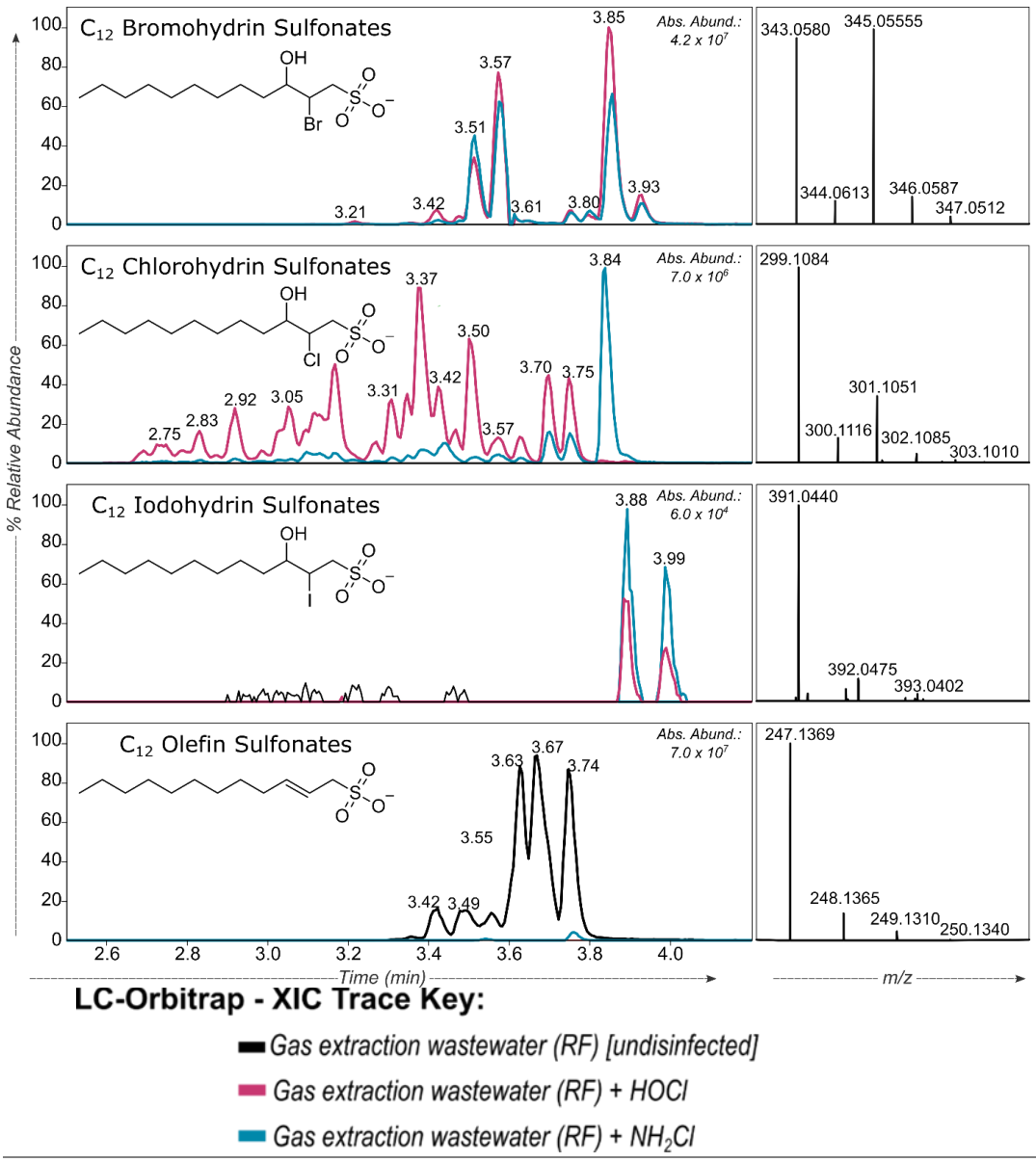

Figure 3.2. Extracted ion chromatograms and ESI(-) mass spectra showing molecular ions ($[M-H]^-$) for C_{12} olefin sulfonates and resulting halohydrin DBPs in undisinfected, chlorinated, and chloraminated RF samples.

Note: Structures shown as basic linear form based on alpha-olefin sulfonate. A multitude of isomeric possibilities exist in variety of branched/cyclic/double-bond location.

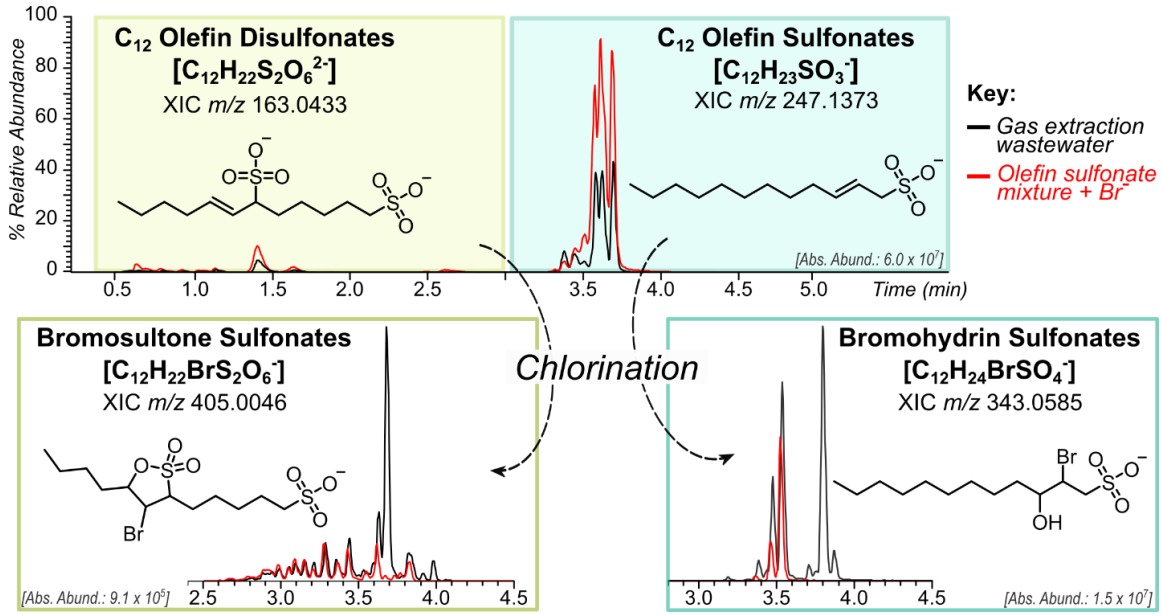

Figure 3.3. Extracted ion chromatogram (XIC) comparisons of DBPs and their suspected precursors in gas extraction wastewater to the commercial olefin sulfonate surfactant mixture. Top: olefin disulfonates (XIC *m/z* 163.0433) and sulfonates (*m/z* 247.1374) in undisinfected wastewater and surfactant mixture; Bottom: major chlorination by-products, bromosultone sulfonates (*m/z* 405.0046) and bromohydrin sulfonates (*m/z* 343.0585).

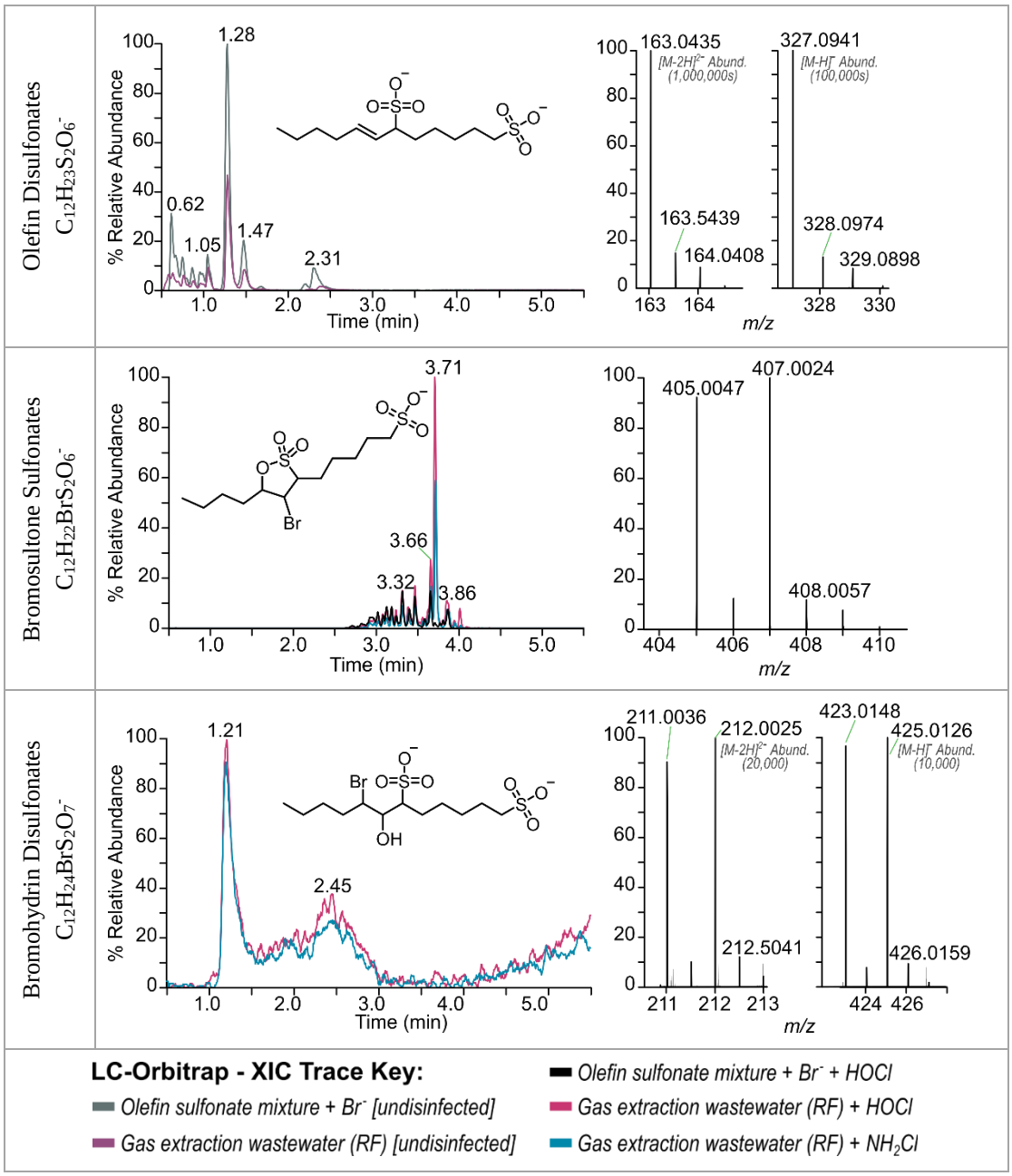

Figure 3.4. Extracted ion chromatograms (XICs) and molecular ions, including doubly-charged $[M-2H]^{2-}$ where applicable, for olefin disulfonate precursor and its major halogenated DBPs formed during disinfection of RF and C_{12} olefin sulfonate commercial product.

.

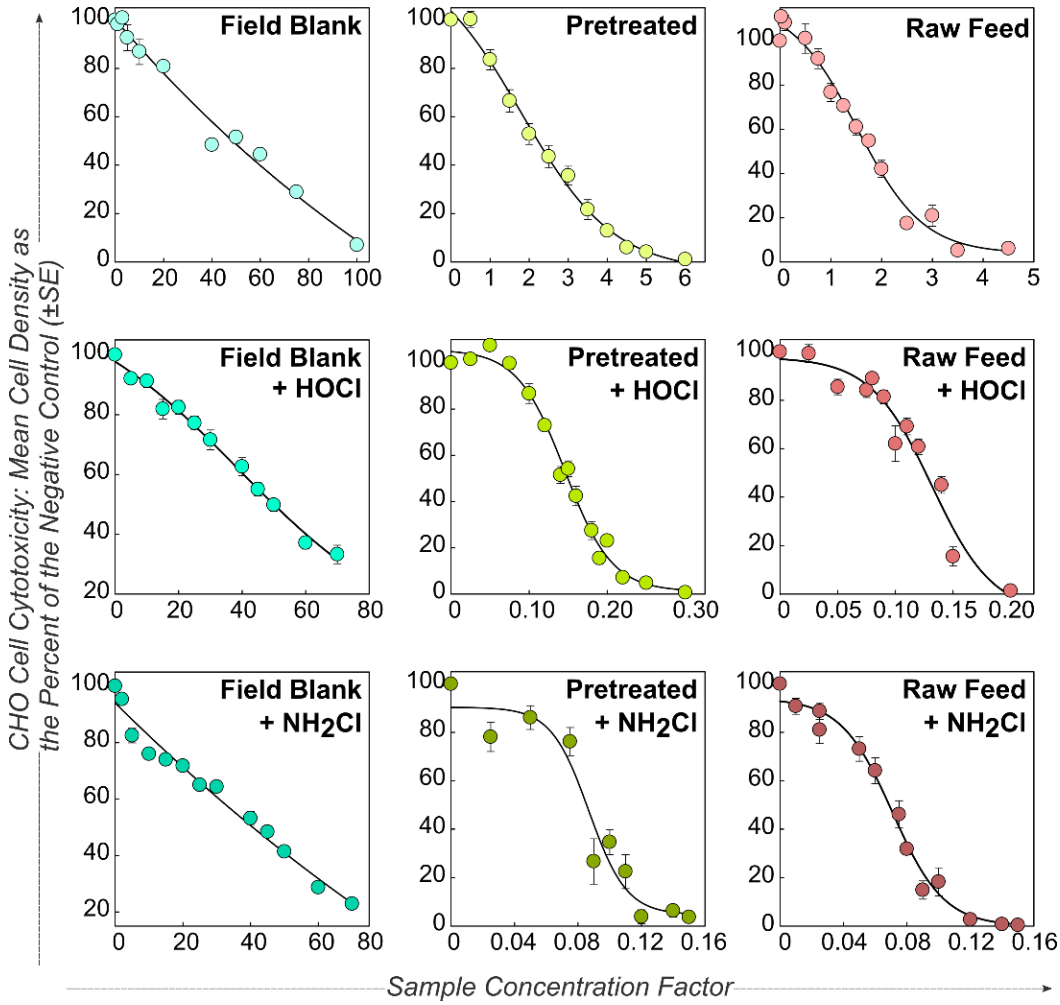

Figure 3.5. Dose-response curves for cytotoxicity of undisinfected, chlorinated (HOCl), and chloraminated (NH_2Cl) field blank, pretreated, and raw feed samples.

Notes: Concentration factors incorporate the 10-fold dilution performed and thus represent concentration factor of the *undiluted* sample. Concentration factors <1 indicate that samples required dilution, rather than further concentration, to induce quantifiable cytotoxic effects.

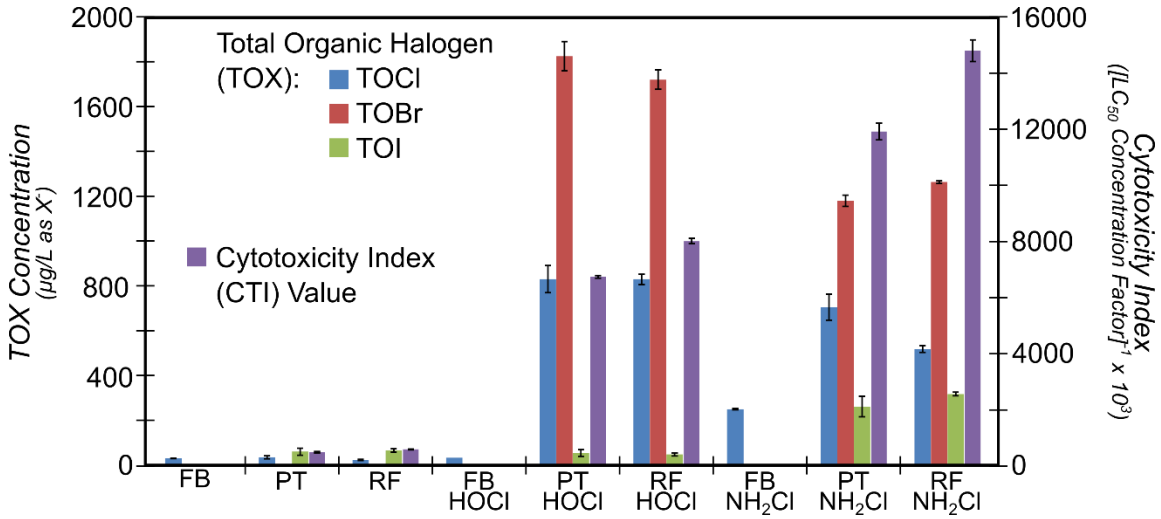

Figure 3.6. Total organic halogen concentrations (left y-axis; ± SE [n = 2]) and cytotoxicity index values (right y-axis) for field blank (FB), pretreated (PT), and raw feed (RF) undisinfected, chlorinated (HOCl), and chloraminated (NH_2Cl) reactors.

CHAPTER 4
ARE COAL-FIRED POWER PLANTS A THREAT TO DOWNSTREAM DRINKING WATER? THE IMPACT OF BROMIDE AND IODIDE ON EMERGING DISINFECTION BY-PRODUCTS[‡]

[‡] Liberatore, H. K.; Good, K. D.; Allen, J. M.; Cuthbertson, A. A.; Rich, D. C; Plewa, M. J.; Wagner, E. D.; Morgan, S. L.; VanBriesen, J. M.; Richardson, S. D.
To be submitted to *Environ. Sci. Technol. Lett.*

4.0 ABSTRACT

Coal-fired power plant (CFPP) wastewaters contain tens to hundreds of mg/L bromide and iodide, especially at plants that employ wet flue gas desulfurization (FGD). Release of these high-halide wastes to surface waters has impacted downstream drinking water quality, with elevated formation of brominated regulated disinfection by-products (DBPs) forcing drinking water treatment plants (DWTPs) out of compliance with EPA DBP regulations. Some plants that struggle with DBP regulations will switch their disinfection practice to use chloramine disinfection, which greatly lowers regulated DBPs, but enhances the formation of higher-toxicity iodo-DBPs in high-iodide waters.

This is the first study to *experimentally investigate* the impacts of CFPP wastewater on resulting drinking water DBP formation and toxicity from chlorination *and* chloramination. Under both disinfection conditions, the presence of CFPP waste significantly enhanced the formation of brominated and iodinated DBPs, while also increasing the total molar DBP concentration of all seven classes (THM4, iodo-THMs, haloacetaldehydes, haloketones, haloacetonitriles, haloacetamides, and halonitromethanes). In lieu of measured toxicity, estimated cyto- and geno-toxic contribution was calculated for each DBP quantified. In all disinfected waters (chlorine/chloramine; impacted/unimpacted), nitrogenous DBPs were the major forcing agents of calculated toxicity, with brominated nitriles contributing most to chlorinated waters, while iodinated amides drove chloraminated "impacted" water toxicity. With both disinfection types, CFPP impact significantly enhanced the calculated toxicity. Based on calculated values, chlorination resulted in higher toxicity from known DBPs. However, total organic halogen (TOX) analyses revealed that much less of the TOX resulting from chloramination is accounted for by quantified DBPs than chlorination. To truly compare

chlorination vs. chloramination health risk associated with CFPP wastewater impacts, whole-water toxicity data is necessary. Because no N- or I-DBPs are regulated, it is likely that a switch to chloramination may instill a false sense of security in CFPP-impacted communities' drinking water.

4.1 INTRODUCTION

As wet flue gas desulfurization (FGD) processes are becoming increasingly common at coal-fired power plants (CFPPs), the use of halide-rich coals, or refined coals with bromide-addition, has become favorable over other coal variations. Halides are beneficial to the reduction of mercury emissions during FGD, and the addition of halide salts to coal has been encouraged to aid in plant compliance with the Mercury and Air Toxics Standards (MATS).[13,18,19] In wet FGD processes, halogens that would normally be released to the atmosphere through the stack are captured in wastewater and discharged from the CFPP. This halide-rich water can be discharged to nearby surface waters from the flue gas operations, or comingled with other CFPP wastewaters (i.e., cooling water, etc.) and stored in basins. Wastewaters may be discharged directly or after some form of treatment, or even overflow from storage basins into nearby waters. In general, most CFPPs do not employ treatment processes that efficiently remove halides, as these are power-intensive and expensive to implement.[13,18]

In general, bromide levels in FGD wastewater range from 10-100 mg/L,[18] leading to elevated levels of bromide in surface waters. Iodide is less well-studied, but co-occurs with bromide naturally in coal. Discharge of halide-rich waste to waters poses a threat to drinking water quality downstream, in the formation of brominated and iodinated disinfection by-products (DBPs), which are much more toxic than their chlorinated

analogues.[3] Previous research has focused on the formation of regulated DBPs, haloacetic acids (HAA5) and trihalomethanes (THM4), in drinking water sources impacted by the presence of high-bromide CFPP discharge. With high-bromide waters, bromine-incorporation into DBP structures is enhanced.[82] Because HAAs and THMs are regulated on mass-concentration basis, higher bromine-incorporation makes it harder for plants to comply with DBP regulations. Commonly, chlorinating plants that fail to meet regulations, consider switching to chloramination.[5] Because iodide co-occurs in coal with bromide and chloramine disinfection favors the formation of iodinated DBPs, none of which are regulated, a switch to chloramine could lead to higher-toxicity finished drinking water despite much lower regulated DBP formation.

The purpose of this study originated in an area where a CFPP's coal ash basin overflowed into a nearby river for years, impacting two downstream drinking water treatment plants (DWTPs). Both DWTPs exceeded U.S. EPA limits for THM4 because of the elevated bromide levels and enhanced Br-THM formation when they disinfected with chlorine. To regain compliance, both plants changed their treatment processes; one switched to chloramination, while other continued to chlorinate with an aeration step before the distribution system to remove THMs. Based on this case, we investigated the impacts of CFPP wastewater on the same drinking water source disinfected by both chlorine and chloramine. This is the most comprehensive investigation of DBP species formed with CFPP wastewater impact, quantifying 50 DBPs, including THM4 as well as 46 priority emerging brominated and iodinated DBPs and total organic halogen (TOX). To the best of our knowledge, this is also the first report of CFPP impact on source water

iodide levels and the formation of iodinated and other unregulated DBPs in drinking water.

4.2 MATERIALS AND METHODS

Standards and Reagents. All DBP standards were obtained at the highest purity available from Sigma-Aldrich (St. Louis, MO), CanSyn Chem. Corp. (Toronto, ON, Canada), Aldlab Chemicals (Woburn, MA), or TCI America (Portland, OR). Individual, standard-specific vendor information has been published previously[65,67,83] and is available in the Supporting Information (Appendix D, Table D.1). Sodium hypochlorite solution (NaOCl, 5.65-6%) was purchased from Fisher Scientific (Fair Lawn, NJ). Ammonium chloride (NH_4Cl) and sodium halide salts (i.e., NaCl, NaBr, and NaI), as well as anhydrous granular sodium sulfate and methyl *tert*-butyl ether (MTBE) for extraction procedures were obtained from Sigma-Aldrich. Anhydrous dibasic potassium phosphate, hydrochloric acid, sulfuric acid, and sodium hydroxide were obtained from Fisher Scientific.

All inorganic reagents (i.e, halides, NaOCl, NH_4Cl, and buffer stock solutions) were prepared in purified water (18 MΩ-cm^{-1}) obtained from a Barnstead E-Pure system (Lake Balboa, CA). Halide and buffer solutions were prepared fresh monthly. NaOCl reagent was standardized (λ_{max} = 292 nm, ε = 350 M^{-1} cm^{-1})[41] using a Molecular Devices SpectraMax M5 spectrophotometer (Sunnyvale, CA) within a week prior to each disinfection experiment. Monochloramine reagent was prepared day-of with fresh solutions of NaOCl and NH_4Cl. Briefly, 100 mL of 0.05 M NH_4Cl was adjusted to pH 8.5 with 1 M NaOH. While continuously stirring and maintaining pH between 8.4 and 8.7 with 1 M solutions of HCl and NaOH, 77 mL of 0.05 M NaOCl was slowly added to the

NH_4Cl solution, to satisfy a 1:1.3 NaOCl:NH_4Cl molar ratio. Monochloramine concentration was determined spectrophotometrically (λ_{max}= 243 nm, ε = 461 M^{-1} cm^{-1})[41].

Sampling Collection and Characterization. An initial, small-volume (1 L) sampling was performed in August 2017 to conduct a halide survey of the area surrounding the coal-fired power plant (CFPP). Samples were taken from the suspected discharge point and the nearby river at bridge access points, including the intake locations of two drinking water treatment plants, A and B. Drinking water treatment plants (DWTPs) A and B were approximately 12 and 31 miles downstream of the CFPP, respectively. As controls, samples were also collected upstream of the suspected point of discharge, as well as from all major tributaries nearby (Table D.2).

Samples were stored at 4 °C in the dark between collection and reaction times. Prior to disinfection, waters were vacuum-filtered through 5.0 µm cellulose filters (Millipore, Sigma-Aldrich). Prior to sample characterization analyses, samples were 0.45-µm filtered through polyethersulfone membrane syringe filters (VWR International, Radnor, PA) that were pre-rinsed with a 10 mL wash of purified water to remove iodide interferent. Total organic carbon (TOC) and total nitrogen (TN) measurements were obtained on a Shimadzu TOC-L/TNM-L (Kyoto, Japan), running simultaneous ASTM methods D7573[84] and D8083[85] for non-purgeable organic carbon (NPOC) and TN, respectively. Calibration standards for chloride (10-750 µg/L), bromide (1-750 µg/L), and iodide (10-750 µg/L) were prepared in purified water. Standards and filtered samples were analyzed by a Dionex 1600 ion chromatograph (IC) with conductivity detector (Sunnyvale, CA).

Simulated Disinfection Experiments. Because 2018 samples showed no evidence of recent halide-discharge to the river, simulated experiments mixing source water and CFPP discharge were performed. To assess the impact of CFPP discharge on DBP formation from both chlorination and chloramination (collectively, "chlor(am)ination") in downstream drinking water, controlled laboratory reactions were performed. Settled water (coagulated, flocculated river water) collected from Plant B in the 2018 sampling, was used in chlor(am)ination reactions with and without the addition of discharge to simulate "impacted" versus "unimpacted" river conditions. For simulating impacted river conditions, the settled water was mixed with 3.8% of discharge sample from 2018 and additional sodium iodide (36 µg/L as I^-) to achieve the approximate concentrations of bromide and iodide (282 and 60.5 µg/L, respectively) observed at Plant A's intake during the 2017 sampling. The characteristics of these waters are shown in Table 4.1. As the unimpacted control, the same settled water (with no fortification) was also disinfected with chlorine and chloramine.

Chlorine demand test-reactions were performed on 20 mL aliquots, mimicking desired reaction conditions to achieve between 1.0-2.0 mg/L chlorine residual after 24 h reaction time. Based on these results, 4.0 and 5.0 mg/L as Cl_2 were used in disinfection reactions of "unimpacted" and "impacted" river water, respectively. Large-volume (18 L) reactions were conducted in stoppered glass jugs (covered to eliminate light exposure) for toxicity and speciated total organic halogen (TOX) analysis. Samples for quantitative analysis (100 mL) were reacted in triplicate in 125 mL amber bottles. Chlorination and chloramination reactions were performed at room temperature (23 ± 2 °C) for 24 and 72 h, respectively. All reactions were buffered with 1.0 mM phosphate at pH 7.5.

DBP Quantification Procedure. For DBP analyses, 100 mL chlorination reactions were quenched (molar ratio of 1.3:1 quench:residual Cl_2, based on an estimated maximum residual of 2 mg/L as Cl_2) with ammonium chloride. Chloramination reactions were not quenched. All extractions were performed within an hour of reaction end-time.

Due to interference/interaction of some DBP standards with others in water, two calibration sets were prepared and analyzed separately: (1) Brominated trihalo-nitromethanes (HNMs) and brominated trihalo-acetonitriles (HANs) and (2) trihalomethanes (THMs), iodinated THMs (I-THMs), trihalo-acetaldehydes (HALs), haloketones (HKs), other HANs, other HNMs, and haloacetamides (HAMs).[65,67,83] DBP standard mixes (10 ppm) were prepared fresh in methanol from concentrated individual standards. Mixes were spiked at varying volumes into 100 mL aliquots of purified water and extracted according to the same procedure as the samples. Samples were analyzed in triplicate for 50 priority DBPs. Additional information for DBPs is shown in Table D.1.

Samples and calibration points were extracted according to a previously published method.[65,67,83] Briefly, sample pH was adjusted to < 1.0 by the addition of 1 mL concentrated sulfuric acid to the 100 mL samples. Three successive liquid-liquid extractions with 5 mL MTBE (15 mL total) were performed, shaking for 15 min each time and allowing the organic and aqueous phases to settle for about 10 min before collecting the organic layer in a test tube. Prior to the first shake, 30 g of sodium sulfate was added for salting out of organics. MTBE extracts were passed through Pasteur pipettes packed with sodium sulfate to remove any residual water. Dried extracts were concentrated to 200 µL under a gentle stream of nitrogen, resulting in a 500-fold

concentration factor. Concentrated extracts were spiked with 1,2-dibromopropane internal standard prior to analysis.

Samples were analyzed by gas chromatography-mass spectrometry (GC-MS) using electron ionization on an Agilent 7890 GC coupled to a 5977A MS (Agilent Technologies, Santa Clara, CA). Selected ion monitoring was used for two characteristic ions for each analyte. Method specifications, including ions monitored and GC conditions, are provided in Tables D.1 and D.3

TOX Analysis. A 250 mL aliquot was removed from the large-scale (18 L) reactors and quenched with ascorbic acid (molar ratio of 1.3:1 quench:residual Cl_2, based on an estimated maximum residual of 2 mg/L as Cl_2). TOX analyses were conducted based on a previously published method.[64,65] Total organic chlorine, bromine, and iodine (TOCl, TOBr, TOI) were measured in duplicate using a TOX analyzer (Mitsubishi Chemical Analytech, Chigasaki, Japan; Cosa Xentaur, Yaphank, NY, USA), with ion chromatography (IC) detection. Each 50 mL replicate was acidified (pH < 2) and passed through two activated carbon columns on the Mitsubishi TXA-04 adsorption unit to extract organic compounds. Adsorbed inorganics were removed from the carbons with a 5 mL sodium nitrate wash (5 mg NO_3^-/mL).

The two carbons for each sample were placed into separate ceramic boats for combustion, though their combustion products were collected into the same tube during sorption. An autosampler (Mitsubishi ASC-240S) loaded boats containing carbons into the combustion unit (AQF-2100H). Carbons were combusted for 4 min at 1000 °C in the presence of oxygen and argon. Combustion products of halo-organic compounds (i.e., hydrogen halide gases [HCl, HBr, HI]) were collected in approximately 5 mL of 0.03%

aqueous H_2O_2, with an additional 3 mL from rinsing the gas line from the furnace to the sorption unit (AU-250). TOCl, TOBr, and TOI were quantified as Cl^-, Br^-, and I^- using the IC halides method described above.

For accurate TOX determination, each of the lines on the adsorption unit were calibrated within two months of analysis to determine the exact volume of each, which ranged from 45-47 mL. In addition, test tubes used for sorption of hydrogen halide (HCl, HBr, HI) gases were weighed empty and after the sorption process to gravimetrically determine the dilution factor associated with this step of the process.

4.3 RESULTS AND DISCUSSION

Bromide and Iodide. Concentrations of halides from both sampling events are shown in Figure 4.1, with sample sites depicted with respect to their distance from the discharge site. In 2017, elevated levels of bromide and iodide (as high as 362 and 75 µg/L, respectively) were observed in river samples downstream of the CFPP, especially when compared to background levels of nearby tributaries. At this time, halide concentrations were highest at the first downstream bridge-sampling location two miles after the CFPP and exhibited consistent decreases with distance downstream from the plant, with correlation coefficients (R^2) of 0.9673 and 0.9521 for bromide and iodide, respectively.

As shown in Figure 4.1, in the second sampling in 2018, non-elevated levels of halides (tens of ppb) were detected, with no indication of recent halide discharge to the nearby river. Construction of piping in the area indicated there may be some diversion of the coal ash pond, perhaps to another new storage area that has not overflown to the river. Supporting our observations and measurements, the CFPP's newsletter mentioned that

during 2017-2018, implementation of procedures to close their ash basins was taking place, including the use of new basins for managing water, use of water treatment technologies (e.g., reverse osmosis), and moving toward processes that manage dry coal ash.

During the initial 2017 sampling, water from near the intake of the first downstream drinking water treatment plant, Plant A, had iodide and bromide levels of 60.5 and 282 µg/L, respectively. To mimic this real-world impact to downstream drinking water, we used these halide concentrations in our laboratory disinfection experiments.

DBP Formation. Of the 50 DBPs monitored, a total of 41 were detected and quantified (Table D.4). Two sample t-tests ([1] HOCl vs. HOCl "Impacted" and [2] NH_2Cl vs. NH_2Cl "Impacted"; 95% confidence) were performed for each DBP to assess the impact of wastewater on formation during chlorination and chloramination treatment. These results are shown in Figure 4.2 and Table D.5. All differences in chlorine-DBP formation between "impacted" and "unimpacted" were statistically significant for every DBP measured, except for 1,3-dichloropropanone (13DCP). For chloramination, fewer DBPs exhibited statistically significant impacts on their formation due to the CFPP wastewater. These were comprised only of bromine- and iodine-containing DBPs; no solely-chlorinated DBP was significantly affected by the presence of wastewater when treated by chloramination. Though Figure D.1 makes it seem as though chlorinated ketones, 13DBP and 1,1,3,3-tetrachloropropanone (1133TeCP) increased with wastewater impact, while other Cl-DBPs decreased, variation between chloraminated sample replicates was too high to determine significance.

In chlorinated samples, experiments to mimic impacted river drinking water conditions from 2017 (3.8% CFPP wastewater + additional 36 µg/L iodide) resulted in predominantly brominated DBPs, while current (unimpacted river) conditions resulted in mostly chloro-DBP formation (Figures 4.2 and D.1). For example, the predominant THM species without wastewater impact was chloroform (trichloromethane; TCM), while bromodichloromethane (BDCM) and dibromochloromethane (DBCM) were the major species formed in chlorinated "impacted" water. TCM exhibited an almost 3-fold decrease in formation as a result of wastewater impact (from ~50 µg/L in "unimpacted" to 18 µg/L in "impacted"), while BDCM concentration doubled from 29 to ~46 µg/L, DBCM concentration increased more than 5-fold from 8 to ~41 µg/L, and bromoform (tribromomethane; TBM) formation increased almost 30-fold from 0.36 to 10 µg/L with wastewater impact. This enhanced formation of THMs, especially brominated THMs, with CFPP wastewater impact is the same issue that downstream DWTPs A and B experienced for years when the discharge was being released to the river with high halide levels. Prior to adjusting their treatment practices (Plant A added aeration; Plant B switched to chloramination), both plants had failed to meet total THM (TTHM) regulations because of this phenomenon.

This preference toward more highly brominated DBPs in "impacted" chlorinated water was also apparent in the other DBP classes, especially in HALs, HANs, and HAMs. Without wastewater, chlorination mostly favored fully chlorinated and bromochloro-DBPs (e.g., trichloroacetaldehyde [TCAL], bromochloro- and dichloro-acetonitriles [BCAN and DCAN], bromochloro- and dichloro-acetamides [BCAM and DCAM]), while chlorination of CFPP-wastewater "impacted" water resulted in higher

bromine-incorporation for all classes (e.g., bromodichloro- and dibromochloro-acetaldehydes [BDCAL and DBCAL], dibromoacetonitrile [DBAN], and dibromoacetamide [DBAM]).

In addition to shifts toward bromo-DBP formation, the molar concentration increased for entire DBP-classes and total DBP formation (Table D.6 and Figure D.1. There are two major reasons that this could be the case: (1) because bromide is quickly and favorably oxidized to reactive bromine species ($HOBr/OBr^-$), and brominated DBPs form much faster than chlorinated DBPs[8,9] and (2) the CFPP discharge may have also contributed organic DBP (i.e., DOM) precursors in addition to halides. Not unexpectedly, chloramination resulted in much lower overall DBP formation (30-fold lower for "unimpacted", 11-fold lower for "impacted"; Table D.6). This difference is mostly due to the greatly reduced formation of the four regulated THMs (THM4; TTHM) with chloramine, which accounted for 80-85% of the total molar sum of DBPs formed in chlorinated samples and only 6-14% in chloraminated samples. Despite lower total molar DBP formation, the presence/lack of wastewater played a much larger role on total DBP formation in chloramination than in chlorination. Wastewater increased total molar DBP formation in chlorinated samples by 10%, while DBP formation from chloramination was 230% higher in "impacted" than the "unimpacted" scenario. This may be due to the precursors contributed by the discharge being predisposed to preferentially react with chloramine over chlorine; however, it is more likely that this is due to more selective oxidation by chloramine.

All DBP classes increased in concentration (nM) with the addition of discharge waste for both chlorination and chloramination (Figure D.1 and Table D.6). Almost all

classes increased by the same amount (~10 nM) in chlorinated samples with wastewater impact, which is apparent in the slope of the classes graphed in Figure D.1 being almost parallel to y = x. THMs and HKs were the only exceptions, with increases of over 30 nM and just 0.7 nM, respectively. However, when class formations are compared based on the ratios of "impacted" versus "unimpacted", most class sums were enhanced less than 100% (i.e., wastewater less than doubled their formation). HANs were enhanced by 50%, HKs by 25%, HALs by 17%, and THMs by just 5%. I-THMs, having formed at < 3 nM in chlorinated water without wastewater impact, exhibited almost a tripling (increased by 190%) in concentration when the CFPP wastewater was present, while HNMs approximately doubled.

Higher variation was observed in the class formation enhancement in the presence of wastewater for DBPs resulting from chloramine-disinfection. Higher-forming DBP classes in the "unimpacted" water exhibited larger concentration increases from wastewater impact, as evidenced by the slope of DBP classes being much steeper than y = x (Figure D.1). The only exception to this was I-THMs, which increased in concentration by almost 30 nM. However, on an impacted/unimpacted ratio basis, most classes were enhanced by at least 100% (i.e., at least doubled with wastewater impact). HKs increased by 150%, HAMs by 140%, HANs and HNMs by 110%, and I-THMs by 1100%. Exceptions were THMs and HALs which only increased 30% and 60%, respectively.

Most classes formed at higher levels from chlorination, except for two: I-THMs and HKs. Though I-THMs formed at roughly the same levels with chlorination and chloramination in "unimpacted" water (2.8 vs. 2.6 µg/L, respectively), comprised mostly

of dichloroiodomethane (DCIM), I-THM formation with CFPP wastewater was 250% higher in chloraminated than in chlorinated waters (28.5 vs. 8.1 µg/L, respectively). In chloraminated "impacted" water, all six I-THMs formed at levels significantly higher than in chlorinated, especially the di- and tri-halo-iodinated THMs (DCIM 37% more, bromochloroiodomethane [BCIM] 197% more, dibromoiodomethane [DBIM] 395% more, chlorodiiodomethane [CDIM] 750% more, bromodiiodomethane [BDIM] 1944% more, and iodoform [triiodomethane; TIM] 274% more). This is not unexpected, as iodinated DBPs preferentially form with chloramine, while chlorine-disinfection forms lower levels due to over-oxidation of iodide to iodate.[7]

Some DBPs were only detected under specific conditions in these experiments based on presence of wastewater, as well as disinfectant type. TBNM, as well as the multiply-iodinated THMs (i.e., CDIM, BDIM, TIM), were only formed at detectable levels when there was simulated CFPP wastewater impact on the water samples. This was the case for both chlorination and chloramination, with the exception of BDIM, which formed at a low level (0.12 ppb) in "unimpacted" chloraminated water. Iodinated HAMs were only formed with simulated wastewater impact from chloramination, not chlorination. In addition, no trihalogenated HAMs or HANs were detected in any of the chloraminated reactors, while they were present in both "unimpacted" and "impacted" chlorinated samples. This could result from differences in formation pathways of these N-DBPs between chlorination and chloramination, with monochloramine (NH_2Cl) contributing nitrogen to N-DBPs, while chlorinatation N-DBPs originate more so from dissolved organic nitrogen (DON).[45]

Total Organic Halogen (TOX). Notable trends in speciated TOX were consistent with the DBPs quantified individually. Chlorinated waters exhibited higher formation of TOX than either chloraminated sample. With CFPP WW-impact, the shift toward higher bromine-incorporation into DBP structures is especially apparent in the chlorinated samples, with an observed decrease in TOCl and even larger increase in TOBr (Figure 4.2, bottom right). Although much lower levels formed, there was also an observed slight decrease in TOCl and simultaneous, larger increase in TOBr in chloraminated "impacted" vs. "unimpacted". Unsurprisingly, the only sample with detectable TOI (< 10 µg/L as I^-) was the impacted NH_2Cl.

In Figure 4.4, the sum of quantified DBP concentrations (as µg/L X^-) are shown alongside the quantified TOX. With quantification of just nine iodo-DBPs (six I-THMs + three I-HAMs), we accounted for 74% of TOI. However, much less of the TOBr and TOCl was accounted for. Quantified DBPs comprised much less of the TOCl and TOBr in chloraminated than in chlorinated samples, with less than 8% of TOCl and 20% of TOBr accounted for, respectively. On the other hand, over 50% of both TOCl and TOBr were accounted for in chlorinated, with TOCl actually less unknown than TOBr (64-68% vs. 50-52%).

Calculated Cytotoxicity and Genotoxicity. In the absence of toxicological measurements, the toxic contribution of each DBP quantified was estimated, similar to previous studies,[65,86,87] to determine the drivers of toxicity. Cytotoxicity and genotoxicity were calculated using DBP concentrations and literature values of individual DBPs' LC_{50} and 50% tail DNA (50% TDNA),[34] as such:

$$\text{calculated cytotoxicity} = [\text{DBP}] \times LC_{50}^{-1} \times 10^6 \quad (1)$$

$$\text{calculated genotoxicity} = [\text{DBP}] \times 50\%\text{TDNA}^{-1} \times 10^{6} \quad (2)$$

where DBP concentration, LC_{50}, and 50%TDNA are in molarity. A normalization factor of 10^6 leads to calculated toxicities in parts-per-million (ppm). Additivity of DBP toxicities was assumed to make inferences about DBP classes and total quantified DBPs' estimated contribution to water toxicity.

Based on the sum of quantified DBPs' toxicity (Figures 4.4 and D.2), the chlorinated (HOCl) water was calculated to be more toxic than chloraminated (NH_2Cl). HOCl was 9x more cytotoxic and 5x more genotoxic than NH_2Cl in the absence of WW ("unimpacted"). Under "impacted" reaction conditions, HOCl was only 2-3x more toxic than NH_2Cl. With CFPP impact, both chlorination and chloramination conditions resulted in higher calculated toxicity. The calculated toxicity was tripled by WW impact in chlorination, while chloramine-disinfection resulted in 11x and 5x enhancements over "unimpacted" in cytotoxicity and genotoxicity, respectively.

Of the DBPs quantified, haloacetonitriles (HANs) were the major driver of toxicity for both geno- and cytotoxicity in chlorinated samples, with and without CFPP impact (Figure 4.4). Under "unimpacted" conditions, bromochloroacetonitrile (BCAN) was the highest-contributing to cytotoxicity, while dibromoacetonitrile (DBAN) dominated when CFPP WW was present (Figure D.2). DBAN was also calculated to be the driver of genotoxicity with and without CFPP WW. In chloraminated waters, more of a difference was observed between cyto- and geno-toxic forcing agent species. While BCAN was the major driver of cytotoxicity in unimpacted NH_2Cl, halonitromethanes (HNMs), specifically trichoronitromethane (chloropicrin; TCNM), contributed most to genotoxicity (Figures 4.4 and D.2). In impacted NH_2Cl, haloacetamides (HAMs),

specifically diiodoacetamide (DIAM), were responsible for the enhanced cyto- and geno-toxicity observed.

In all cases, nitrogenous DBPs (N-DBPs) were the major drivers of toxicity for both chlorine and chloramine disinfection, which is consistent with the results of Cuthbertson et al.'s recent study of DWTPs.[65] As with all DBP classes studied, all classes of N-DBPs (HANs, HNMs, HAMs) increased with WW impact and favored formation of higher-toxicity brominated and iodinated species. While total DBP formation was reduced 11-fold, there was only a 3-fold reduction in N-DBPs with chloramination, consistent with the 2-3x lower cyto- and geno-toxicity observed for impacted NH_2Cl vs. HOCl. Calculated toxicity for chloraminated water was much lower than chlorinated, but based on TOX comparison to quantified DBP concentrations as X^- (Figure 4.3), it was obvious that higher proportions of unknown DBPs were formed during chloramination. Without measured toxicity data for the whole-water extracts, it is uncertain whether the unknown portion of the TOX contributes significantly to the toxicity of each water. Toxicity studies are ongoing, with collaborators currently assessing both geno- and cyto-toxicity of the whole-water extracts of NH_2Cl and HOCl "impacted" and "unimpacted" waters. Previous studies have shown that chlorination vs. chloramination of the same source water resulted in different trends depending on halide levels. In elevated-halide scenarios (500 µg/L Br^-; 100 µg/L I^-),[3,88] chloraminated water was more cyto- and geno-toxic than chlorinated water. In the absence of added halides, chlor(am)inated waters were much less toxic. When comparing disinfectants without added halides, chlorinated water was more cytotoxic, while chloramination resulted in higher genotoxicity.[3] Given

the similarity in halide levels, 282 µg/L Br^-; 60.5 µg/L I^- in "impacted", we anticipate similar toxicity results to those observed in these studies.

Despite reducing total DBP formation by an order of magnitude, the real-world scenario where a CFPP-impacted DWTP switches to chloramine from chlorine may not necessarily result in safer drinking water. In addition to the high levels of bromide that keep DWTPs from complying with DBP regulations, CFPP WW also contains high levels of iodide, which is more likely to form toxic iodinated DBPs with chloramination than with chlorination. The regulated DBPs in this study, THMs, accounted for a negligible amount of the calculated toxicity, despite being the highest-forming class by far. With no I- or N-DBPs regulated, DWTPs impacted by CFPP waste do not necessarily have access to useful information in deciding whether a change in disinfection practice is the best choice for their community's health.

4.4 TABLES AND FIGURES

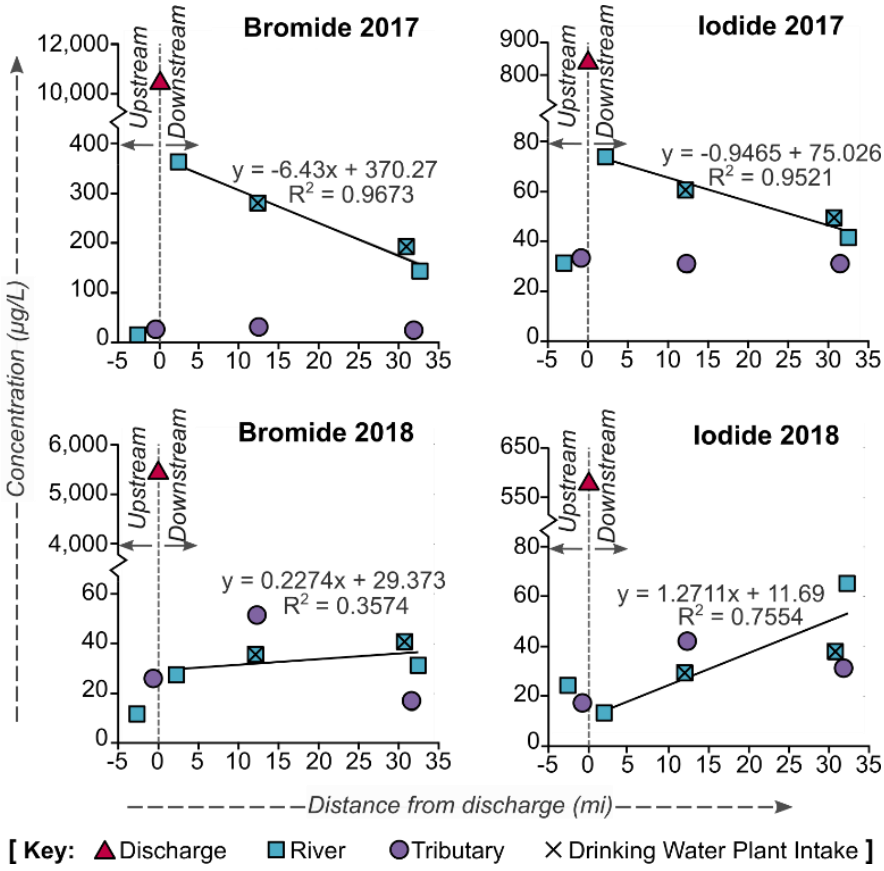

Figure 4.1. Bromide and iodide concentrations measured in 2017 and 2018 grab samples from the coal-fired power plant (CFPP) discharge, impacted river, and tributaries to the impacted river. Locations are plotted in distance (in miles) from the discharge site, where negative distances represent upstream samples and positive represent downstream. Linear regressions represent correlations between downstream river sample halide concentrations and distance downstream from the discharge site.

Table 4.1. Sample Characteristics for Samples Used in Disinfection Experiments

Parameter	2018 Plant B Settled Water	2018 Discharge	2017 Plant A Intake[b]
TOC[a] (mg/L as C)	1.30	3.21	1.43
TN (mg/L as N)	0.334	1.413	0.413
$SUVA_{254}$ (L/mg-m)	3.0	1.1	3.4
Bromide (µg/L)	56.6	5,436	282
Iodide (µg/L)	ND	578	60.5

[a] TOC was measured by non-purgeable organic carbon (NPOC) method; ND: not detected; [b] Discharge mixed at 3.8% in Plant B settled water with 36 µg/L of I^- added to mimic 2017 Plant A intake levels.

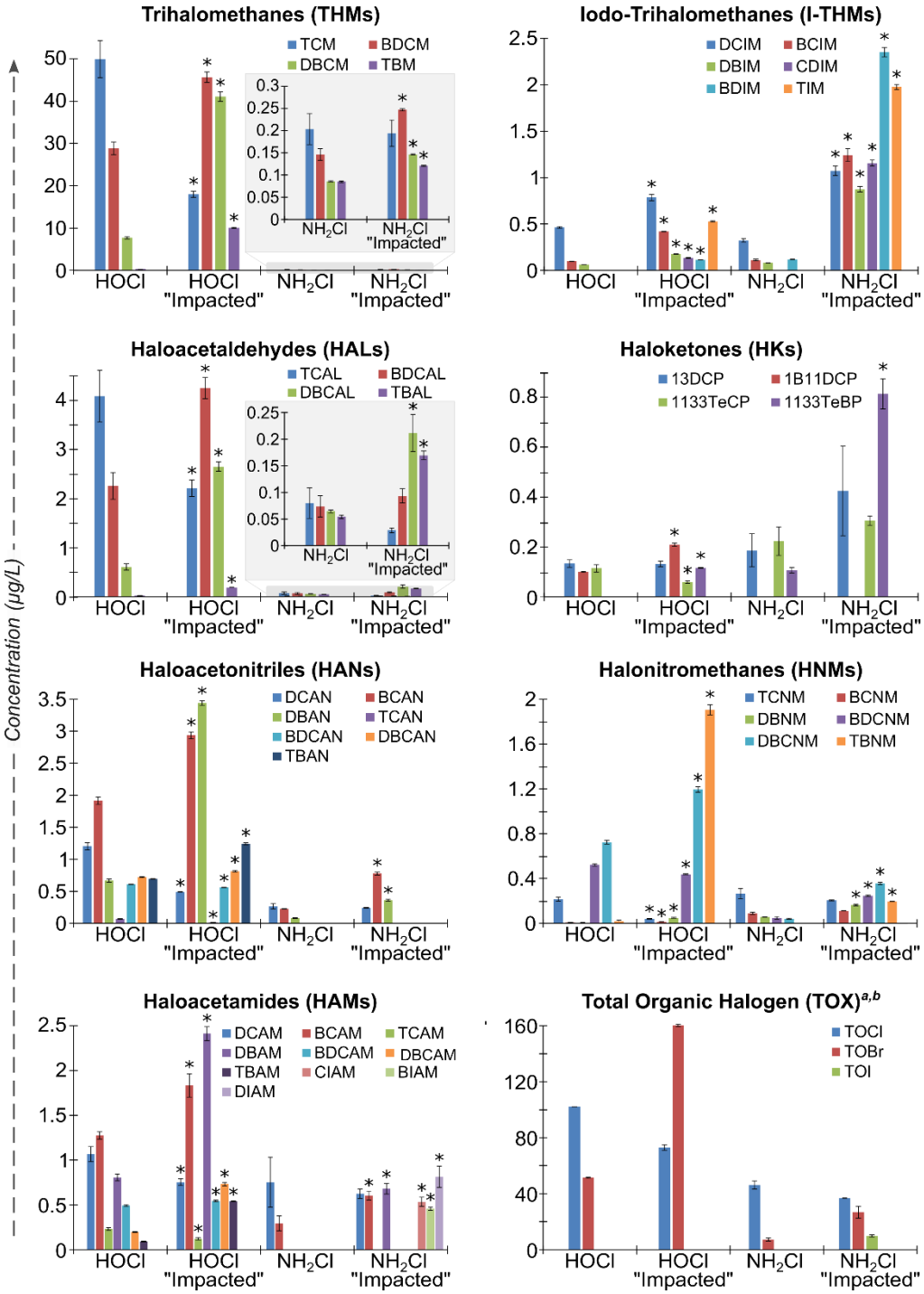

Figure 4.2. DBP concentrations by class and total organic halogen measurements in disinfected settled water with and without simulated CFPP wastewater impact (± standard error of 3 replicates).

* Indicates compounds that formed at significantly different levels with vs. without CFPP wastewater and I^- addition; [a] TOX measured in µg/L as X^- (i.e, TOCl in µg/L as Cl^-, TOBr in µg/L as Br^-, TOI in µg/L as I^-); [b] TOX only measured in duplicate, so lacks statistical power to make comparison; B = bromo; C = chloro; I = iodo; D = di; T = tri; Te = tetra; M = methane; AL = acetaldehyde; P = propanone; AN = acetonitrile; NM = nitromethane; AM = acetamide.

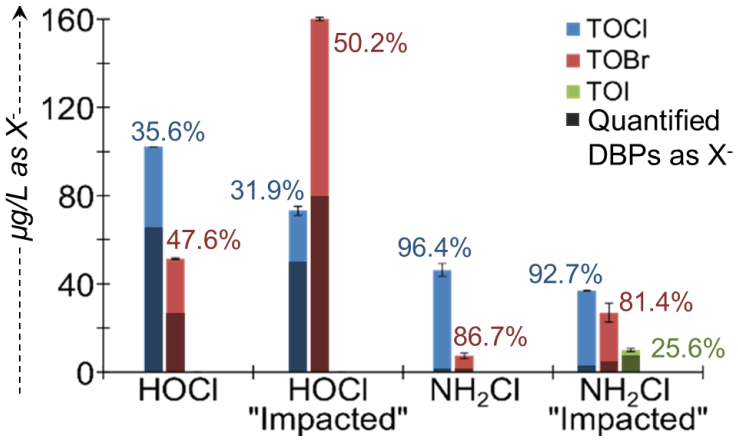

Figure 4.3. Portion of total organic halogen (TOX) accounted for by the 50 quantified DBPs (dark bar) and percentage of TOX that is unknown (labeled % over bars).

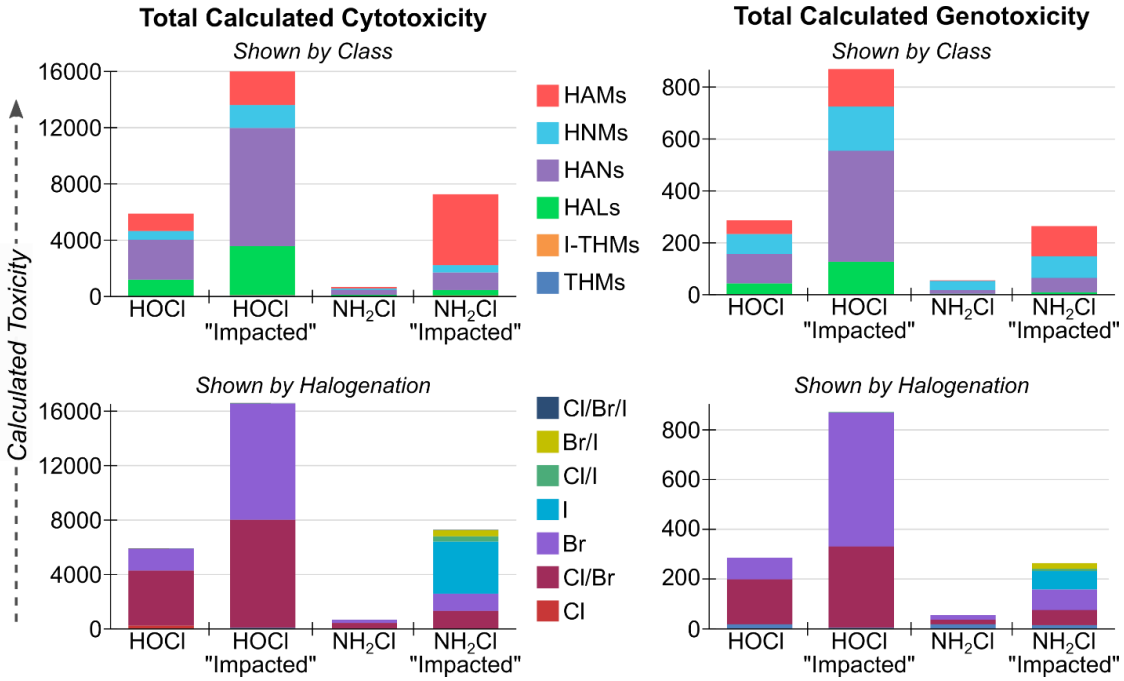

Figure 4.4. Calculated CHO cell cytotoxicity (left) and genotoxicity (right) by DBP class (top) and halogen species profile (bottom). Based on toxicity index values in Wagner and Plewa, 2017.[34]

Note: No toxicity data available for HKs or trihalo-Br-HANs; calculated cytotoxicity = $[DBP]x[LC_{50}]^{-1}x10^6$; calculated genotoxicity = $[DBP]x[50\%\ TDNA]x10^6$.

CHAPTER 5
CONCLUSIONS AND FUTURE WORK

5.1 HYDRAULIC FRACTURING-IMPACTED WATERS

The work presented in this dissertation focused on non-targeted analysis of DBPs formed solely from precursors present in oil and gas wastewaters (WWs). High levels of bromide and iodide, as well as both geogenic (phenolics) and anthropogenic (sulfonate surfactants) organic components led to the formation of never-before-reported DBPs upon chlorination and chloramination of WW.

Iodophenolics and Other Semivolatile DBPs. Standards of iodophenolic DBPs were obtained for confirmation and toxicity studies, with many of them being just as toxic as previously-known iodo-DBPs. Being of toxicological relevance, and having a good chance of forming even in the presence of natural organic matter (NOM), these classes of DBPs – iodophenols, iodocresols, and iodoxylenols – are important to quantify in HF-impacted source waters. A preliminary method for quantifying these iodophenolics by GC-MS/MS was developed based on the existing extraction method for other DBPs, but when applied to 10% HF waste samples (raw, chlorinated, and chloraminated), had very low recovery and varied between matrix disinfection types. Because of the matrices, development of this method will require standard addition techniques or further dilution prior to extraction. Similarly, our typical DBP suite will be assessed for matrix effects by comparison of internal calibration to standard addition methods. These other DBPs were preliminarily quantified, but the poor extraction efficiency of the iodophenolics leads us

to question whether other DBPs may also have had hindered extraction, resulting in lower measurements than actual sample concentrations.

Olefin Sulfonate-Derived DBPs. With over 300 new surfactant-based DBPs identified, it is difficult to assign structural identities, and none of these DBPs are available as standards for confirmation. In lieu of typical standard DBP confirmation practices, we plan to obtain individual-isomer standards of the precursors that are available and subject each to disinfection in the presence of bromide and iodide to compare to samples. Without individual, pure standards, it is impossible to assess each DBP's toxic potency, but whole-mixture determinations can be made for disinfected olefin sulfonate product, as well as individual disinfected standards. The toxicities of the olefin sulfonate product and individual precursor isomers (with and without disinfection) will aid in the assessment of potential health risks associated with these surfactant-DBPs, and better our understanding of their contribution to the high cytotoxicity of the chlor(am)inated gas-extraction WW.

Future Work. Future research in the Richardson group will include continued non-targeted analysis with collaborative toxicology, while also expanding the scope of the study to include DBP quantification. Mixing studies with surface water will be performed to assess real-world HF-impact on drinking water. As NOM is typically the major precursor to DBPs, it is important to understand whether NOM outcompetes the organic precursors identified in these HF WWs to form primarily known iodo- and bromo-DBPs, or if WW-contributed organics also play a significant role. It is important to assess the potential formation of these DBPs under conditions that would be realistic to a HF-impacted drinking water treatment plant's (DWTP) source water (i.e., low

percentage of WW mixed with surface water). The conduction of mixing studies that combine toxicological assessment with a full suite of DBP analyses, including (1) quantification of known DBPs, including the iodophenolics, (2) semi-targeted analysis of the recently identified surfactant-derived DBPs, (3) non-targeted analysis for unknown DBPs, and (4) total organic halogen (TOX) analyses for HF-impacted waters, will guide the way for future research in this area of study.

5.2 COAL-FIRED POWER PLANT-IMPACTED WATERS

DBP and TOX Quantification. This was the most extensive study of coal-fired power plant (CFPP) impact on DBP formation to-date. While most previous work has focused on bromide and regulated DBP levels at downstream drinking water treatment plants (DWTPs), we assessed the formation of 50 priority DBPs and TOX with and without CFPP impact. All seven DBP-class concentrations were enhanced by the presence of WW during both chlorination and chloramination, with observed shifts toward higher bromine- and iodine-incorporation.

In lieu of analytical cyto- and geno-toxicity measurements, we calculated the estimated toxic contribution from each of the DBPs measured to the disinfected waters' toxicity. Dibromoacetonitrile (DBAN) was determined to be the major driver of toxicity for chlorination (with and without CFPP WW), which approximately tripled the resulting "impacted" calculated toxicity compared to "unimpacted", while CFPP-impact enhanced chloraminated water cytotoxicity by an order of magnitude as a result of diiodoacetamide (DIAM) formation (Figure D.2). Calculated toxicity for chloraminated water was much lower than chlorinated, but based on TOX comparison to quantified DBP concentrations as X^-, it was obvious that higher levels of unknown DBPs were formed during

chloramination. It is unknown whether the unknown portion of the TOX contributes significantly to the toxicity of each water.

Future Work. Toxicologist collaborators at the University of Illinois are currently in the process of performing cyto- and geno-toxicity assays to compare the "impacted" vs. "unimpacted" chlor(am)inated waters. The measured water toxicities and calculated toxic contribution of individual DBPs will be compared to assess the potential importance of the unknown portion of TOX for each disinfection type. If much of the toxicity is unaccounted for by the quantified DBPs, non-targeted analysis will be an important future tool in this work to identify unknown DBPs. In addition, further work in the Richardson group will likely be conducted with drinking water samples from currently-impacted areas to gain understanding of real-world impacts, as the full water treatment process at a DWTP employs many more steps than in-laboratory disinfection.

REFERENCES

(1) Richardson, S. D.; Plewa, M. J.; Wagner, E. D.; Schoeny, R.; Demarini, D. M. Occurrence, Genotoxicity, and Carcinogenicity of Regulated and Emerging Disinfection by-Products in Drinking Water: A Review and Roadmap for Research. *Mutat. Res.* **2007**, *636*, 178–242.

(2) Richardson, S. D.; Fasano, F.; Ellington, J. J.; Crumley, F. G.; Buettner, K. M.; Evans, J. J.; Blount, B. C.; Silva, L. K.; Waite, T. J.; Luther, G. W.; et al. Occurrence and Mammalian Cell Toxicity of Iodinated Disinfection Byproducts in Drinking Water. *Environ. Sci. Technol.* **2008**, *42* (22), 8330–8338.

(3) Yang, Y.; Komaki, Y.; Kimura, S. Y.; Hu, H. Y.; Wagner, E. D.; Mariñas, B. J.; Plewa, M. J. Toxic Impact of Bromide and Iodide on Drinking Water Disinfected with Chlorine or Chloramines. *Environ. Sci. Technol.* **2014**, *48* (20), 12362–12369.

(4) Ground Water and Drinking Water: National Primary Drinking Water Regulations https://www.epa.gov/ground-water-and-drinking-water/national-primary-drinking-water-regulations.

(5) Seidel, C. J.; McGuire, M. J.; Summers, R. S.; Via, S. Have Utilities Switched to Chloramines? *J. Am. Water Works Assoc.* **2005**, *97*, 87–97.

(6) Plewa, M. J.; Wagner, E. D.; Richardson, S. D.; Thruston, A. D.; Woo, Y. T.; McKague, A. B. Chemical and Biological Characterization of Newly Discovered Iodoacid Drinking Water Disinfection Byproducts. *Environ. Sci. Technol.* **2004**, *38* (18), 4713–4722.

(7) Bichsel, Y.; Von Gunten, U. Oxidation of Iodide and Hypoiodous Acid in the Disinfection of Natural Waters. *Environ. Sci. Technol* **1999**, *33*, 4040–4045.

(8) Liu, Q.; Margerum, D. W. Equilibrium and Kinetics of Bromine Chloride Hydrolysis. *Environ. Sci. Technol* **2001**, *35*, 1127–1133.

(9) Westerhoff, P.; Chao, P.; Mash, H. Reactivity of Natural Organic Matter with Aqueous Chlorine and Bromine. *Water Res.* **2004**, *38*, 1502–1513.

(10) States, S.; Cyprych, G.; Stoner, M.; Wydra, F.; Kuchta, J.; Monnell, J.; Casson, L. Marcellus Shale Drilling and Brominated THMs in Pittsburgh, Pa., Drinking Water. *J. Am. Water Works Assoc.* **2013**, *105* (8), E432–E448.

(11) Bichsel, Y.; Von Gunten, U. Formation of Iodo-Trihalomethanes during Disinfection and Oxidation of Iodide-Containing Waters. *Environ. Sci. Technol.* **2000**, *34* (13), 2784–2791.

(12) Dong, S.; Nguyen, T. H.; Plewa, M. J. Comparative Mammalian Cell Cytotoxicity of Wastewater for Reuse after Chlorination, Chloramination, or Ozonation Disinfection with Elevated Bromide and Iodide. *J. Environ. Sci.* **2017**, *58*, 296–

301.

(13) VanBriesen, J. M. Potential Drinking Water Effects of Bromide Discharges from Coal-Fired Electric Power Plants. *Form. Comments Environ. Integr. Proj. al. Effl. Limitations Guidel. Stand. Steam Electr. Power Gener. Point Source Categ. Append. B Water Docket EPA-HQ-OW-2009-0819-4687* **2013**, 1–38.

(14) Harkness, J. S.; Dwyer, G. S.; Warner, N. R.; Parker, K. M.; Mitch, W. A.; Vengosh, A. Iodide, Bromide, and Ammonium in Hydraulic Fracturing and Oil and Gas Wastewaters: Environmental Implications. *Environ. Sci. Technol.* **2015**, *49* (3), 1955–1963.

(15) Wang, Y.; Small, M. J.; VanBriesen, J. M. Assessing the Risk Associated with Increasing Bromide in Drinking Water Sources in the Monongahela River, Pennsylvania. *J. Environ. Eng.* **2017**, *143* (3), 04016089.

(16) Parker, K. M.; Zeng, T.; Harkness, J.; Vengosh, A.; Mitch, W. A. Enhanced Formation of Disinfection Byproducts in Shale Gas Wastewater-Impacted Drinking Water Supplies. *Environ. Sci. Technol.* **2014**, *48* (19), 11161–11169.

(17) Wilson, J. M.; Van Briesen, J. M. Source Water Changes and Energy Extraction Activities in the Monongahela River, 2009-2012. *Environ. Sci. Technol.* **2013**, *47* (21), 12575–12582.

(18) Good, K. D.; Vanbriesen, J. M. Coal-Fired Power Plant Wet Flue Gas Desulfurization Bromide Discharges to U.S. Watersheds and Their Contributions to Drinking Water Sources. *Environ. Sci. Technol.* **2019**, *53* (1), 213–223.

(19) Good, K. D.; Vanbriesen, J. M. Power Plant Bromide Discharges and Downstream Drinking Water Systems in Pennsylvania. *Environ. Sci. Technol.* **2017**, *51* (20), 11829–11838.

(20) Good, K. D.; VanBriesen, J. M. Current and Potential Future Bromide Loads from Coal-Fired Power Plants in the Allegheny River Basin and Their Effects on Downstream Concentrations. *Environ. Sci. Technol.* **2016**, *50* (17), 9078–9088.

(21) Vengosh, A.; Jackson, R. B.; Warner, N.; Darrah, T. H.; Kondash, A. A Critical Review of the Risks to Water Resources from Unconventional Shale Gas Development and Hydraulic Fracturing in the United States. *Environ. Sci. Technol.* **2014**, *48* (15), 8334–8348.

(22) Warner, N. R.; Christie, C. A.; Jackson, R. B.; Vengosh, A. Impacts of Shale Gas Wastewater Disposal on Water Quality in Western Pennsylvania. *Environ. Sci. Technol.* **2013**, *47* (20), 11849–11857.

(23) Liberatore, H. K.; Plewa, M. J.; Wagner, E. D.; Vanbriesen, J. M.; Burnett, D. B.; Cizmas, L. H.; Richardson, S. D. Identification and Comparative Mammalian Cell Cytotoxicity of New Iodo-Phenolic Disinfection Byproducts in Chloraminated Oil and Gas Wastewaters. *Environ. Sci. Technol. Lett.* **2017**, *4* (11).

(24) Hladik, M. L.; Focazio, M. J.; Engle, M. Discharges of Produced Waters from Oil and Gas Extraction via Wastewater Treatment Plants Are Sources of Disinfection By-Products to Receiving Streams. *Sci. Total Environ.* **2014**, *466–467*, 1085–1083.

(25) Orem, W.; Tatu, C.; Varonka, M.; Lerch, H.; Bates, A.; Engle, M.; Crosby, L.; Mcintosh, J. Organic Substances in Produced and Formation Water from Unconventional Natural Gas Extraction in Coal and Shale. *Int. J. Coal Geol.* **2014**, *126*, 20–31.

(26) Burgos, W. D.; Castillo-Meza, L.; Tasker, T. L.; Geeza, T. J.; Drohan, P. J.; Liu, X.; Landis, J. D.; Blotevogel, J.; McLaughlin, M.; Borch, T.; et al. Watershed-Scale Impacts from Surface Water Disposal of Oil and Gas Wastewater in Western Pennsylvania. *Environ. Sci. Technol.* **2017**, *51*, 8851–8860.

(27) Rahm, B. G.; Riha, S. J. Evolving Shale Gas Management: Water Resource Risks, Impacts, and Lessons Learned. *Environ. Sci. Process. Impacts* **2014**, *16* (6), 1400–1412.

(28) Vidic, R. D.; Brantley, S. L.; Vandenbossche, J. M.; Yoxtheimer, D.; Abad, J. D. Impact of Shale Gas Development on Regional Water Quality. *Science* **2013**, *340* (6134), 1235009.

(29) Ferrar, K. J.; Michanowicz, D. R.; Christen, C. L.; Mulcahy, N.; Malone, S. L.; Sharma, R. K. Assessment of Effluent Contaminants from Three Facilities Discharging Marcellus Shale Wastewater to Surface Waters in Pennsylvania. *Environ. Sci. Technol.* **2013**, *47* (7), 3472–3481.

(30) Plewa, M. J.; Wagner, E. D.; Jazwierska, P.; Richardson, S. D.; Chen, P. H.; McKague, A. B. Halonitromethane Drinking Water Disinfection Byproducts: Chemical Characterization and Mammalian Cell Cytotoxicity and Genotoxicity. *Environ. Sci. Technol.* **2004**, *38* (1), 62–68.

(31) Wei, X.; Wang, S.; Zheng, W.; Wang, X.; Liu, X.; Jiang, S.; Pi, J.; Zheng, Y.; He, G.; Qu, W. Drinking Water Disinfection Byproduct Iodoacetic Acid Induces Tumorigenic Transformation of NIH3T3 Cells. *Environ. Sci. Technol.* **2013**, *47* (11), 5913–5920.

(32) Stalter, D.; O'Malley, E.; Von Gunten, U.; Escher, B. I. Fingerprinting the Reactive Toxicity Pathways of 50 Drinking Water Disinfection By-Products. *Water Res.* **2016**, *91*, 19–30.

(33) Harvey, J. B.; Hong, H.-H. L.; Bhusari, S.; Ton, T.-V.; Wang, Y.; Foley, J. F.; Peddada, S. D.; Hooth, M.; DeVito, M.; Nyska, A.; et al. F344/NTac Rats Chronically Exposed to Bromodichloroacetic Acid Develop Mammary Adenocarcinomas With Mixed Luminal/Basal Phenotype and *Tgfβ* Dysregulation. *Vet. Pathol.* **2016**, *53* (1), 170–181.

(34) Wagner, E. D.; Plewa, M. J. CHO Cell Cytotoxicity and Genotoxicity Analyses of Disinfection By-Products: An Updated Review. *J. Environ. Sci.* **2017**, *58*, 64–76.

(35) Plewa, M. J.; Muellner, M. G.; Richardson, S. D.; Fasano, F.; Buettner, K. M.; Woo, Y. T.; Mckague, A. B.; Wagner, E. D. Occurrence, Synthesis, and Mammalian Cell Cytotoxicity and Genotoxicity of Haloacetamides: An Emerging Class of Nitrogenous Drinking Water Disinfection Byproducts. *Environ. Sci. Technol.* **2008**, *42* (3), 955–961.

(36) Muellner, M. G.; Wagner, E. D.; Mccalla, K.; Richardson, S. D.; Woo, Y. T.; Plewa, M. J. Haloacetonitriles vs. Regulated Haloacetic Acids: Are Nitrogen-

Containing DBPs More Toxic? *Environ. Sci. Technol.* **2007**, *41* (2), 645–651.

(37) Plewa, M. J.; Wagner, E. D. Mammalian Cell Cytotoxicity and Genotoxicity of Disinfection By-Products. In *Water Research Foundation*; Denver, CO, 2009; p 134.

(38) Bond, T.; Huang, J.; Templeton, M. R.; Graham, N. Occurrence and Control of Nitrogenous Disinfection By-Products in Drinking Water - A Review. *Water Res.* **2011**, *45* (15), 4341–4354.

(39) Liu, S.; Li, Z.; Dong, H.; Goodman, B. A.; Qiang, Z. Formation of Iodo-Trihalomethanes, Iodo-Acetic Acids, and Iodo-Acetamides during Chloramination of Iodide-Containing Waters: Factors Influencing Formation and Reaction Pathways. *J. Hazard. Mater.* **2017**, *321*, 28–36.

(40) Diehl, A. C.; Speitel, G. E.; Symons, J. M.; Krasner, S. W.; Hwang, C. J.; Barrett, S. E. DBP Formation during Chloramination. *J. / Am. Water Work. Assoc.* **2000**, *92* (6), 76–90.

(41) Kimura, S. Y.; Komaki, Y.; Plewa, M. J.; Mariñas, B. J. Chloroacetonitrile and N,2-Dichloroacetamide Formation from the Reaction of Chloroacetaldehyde and Monochloramine in Water. *Environ. Sci. Technol.* **2013**, *47* (21), 12382–12390.

(42) Chu, W.; Gao, N.; Yin, D.; Krasner, S. W. Formation and Speciation of Nine Haloacetamides, an Emerging Class of Nitrogenous DBPs, during Chlorination or Chloramination. *J. Hazard. Mater.* **2013**, *260* (260), 806–812.

(43) Chu, W.; Gao, N.; Yin, D.; Krasner, S. W.; Templeton, M. R. Trace Determination of 13 Haloacetamides in Drinking Water Using Liquid Chromatography Triple Quadrupole Mass Spectrometry with Atmospheric Pressure Chemical Ionization. *J. Chromatogr. A* **2012**, *1235*, 178–181.

(44) Richardson, S. D.; Thruston, A. D.; Krasner, S. W.; Weinberg, H. S.; Miltner, R. J.; Schenck, K. M.; Narotsky, M. G.; McKague, A. B.; Simmons, J. E. Integrated Disinfection By-Products Mixtures Research: Comprehensive Characterization of Water Concentrates Prepared from Chlorinated and Ozonated/Postchlorinated Drinking Water. *J. Toxicol. Environ. Heal. Part A* **2008**, *71* (17), 1165–1186.

(45) Shah, A. D.; Mitch, W. A. Halonitroalkanes, Halonitriles, Haloamides, and N-Nitrosamines: A Critical Review of Nitrogenous Disinfection Byproduct Formation Pathways. *Environ. Sci. Technol* **2012**, *46*, 119–131.

(46) Gregory, K. B.; Vidic, R. D.; Dzombak, D. A. Water Management Challenges Associated with the Production of Shale Gas by Hydraulic Fracturing. *Elements* **2011**, *7* (3), 181–186.

(47) Maloney, K. O.; Yoxtheimer, D. A. Production and Disposal of Waste Materials from Gas and Oil Extraction from the Marcellus Shale Play in Pennsylvania. *Environ. Pract.* **2012**, *14* (04), 278–287.

(48) Wagner, E. D.; Rayburn, A. L.; Anderson, D.; Plewa, M. J. Analysis of Mutagens with Single Cell Gel Electrophoresis, Flow Cytometry, and Forward Mutation Assays in an Isolated Clone of Chinese Hamster Ovary Cells. *Environ. Mol. Mutagen.* **1998**, *32* (4), 360–368.

(49) Hayes, T. *Sampling and Analysis of Water Streams Associated with the Development of Marcellus Shale Gas*; Des Plaines, IL, 2009.

(50) McLafferty, F. W.; Tureček, F. *Interpretation of Mass Spectra*, 4th ed.; University Science Books: Sausalito, CA, 1993.

(51) Thomas, K. V.; Langford, K.; Petersen, K.; Smith, A. J.; Tollefsen, K. E. Effect-Directed Identification of Naphthenic Acids as Important in Vitro Xeno-Estrogens and Anti-Androgens in North Sea Offshore Produced Water Discharges. *Environ. Sci. Technol.* **2009**, *43* (21), 8066–8071.

(52) Boitsov, S.; Mjøs, S. A.; Meier, S. Identification of Estrogen-Like Alkylphenols in Produced Water from Offshore Oil Installations. *Mar. Environ. Res.* **2007**, *64* (5).

(53) Liu, J.; Zhang, X. Comparative Toxicity of New Halophenolic DBPs in Chlorinated Saline Wastewater Effluents against a Marine Alga: Halophenolic DBPs Are Generally More Toxic than Haloaliphatic Ones. *Water Res.* **2014**, *65*, 64–72.

(54) Yang, M.; Zhang, X. Comparative Developmental Toxicity of New Aromatic Halogenated DBPs in a Chlorinated Saline Sewage Effluent to the Marine Polychaete Platynereis Dumerilii. *Environ. Sci. Technol.* **2013**, *47* (19), 10868–10876.

(55) Strube, A.; Guth, H.; Buettner, A. Identification of a Medicinal Off-Flavour in Mineral Water. *Water Res.* **2009**, *43*, 5216–5224.

(56) Strube, A.; Buettner, A.; Czerny, M. Influence of Chemical Structure on Absolute Odour Thresholds and Odour Characteristics of Ortho- and Para-Halogenated Phenols and Cresols. *Flavour Fragr. J.* **2012**, *27* (4), 304–312.

(57) Richardson, S. D.; Ternes, T. A. Water Analysis: Emerging Contaminants and Current Issues. *Anal. Chem.* **2018**, *90* (1), 398–428.

(58) Ferrer, I.; Thurman, E. M. Chemical Constituents and Analytical Approaches for Hydraulic Fracturing Waters. *Trends Environ. Anal. Chem.* **2015**, *5*, 18–25.

(59) Sitterley, K. A.; Linden, K. G.; Ferrer, I.; Thurman, E. M. Identification of Proprietary Amino Ethoxylates in Hydraulic Fracturing Wastewater Using Liquid Chromatography/Time-of-Flight Mass Spectrometry with Solid-Phase Extraction. *Anal. Chem.* **2018**, *90* (18), 10927–10934.

(60) Thurman, E. M.; Ferrer, I.; Blotevogel, J.; Borch, T. Analysis of Hydraulic Fracturing Flowback and Produced Waters Using Accurate Mass: Identification of Ethoxylated Surfactants. *Anal. Chem.* **2014**, *86* (19), 9653–9661.

(61) García-Reyero, N.; Requena, V.; Petrovic, M.; Fischer, B.; Hansen, P. D.; Díaz, A.; Ventura, F.; Barceló, D.; Piña, B. Estrogenic Potential of Halogenated Derivatives of Nonylphenol Ethoxylates and Carboxylates. *Environ. Toxicol. Chem.* **2004**, *23* (3), 705–711.

(62) González, S.; Petrovic, M.; Barceló, D. Simultaneous Extraction and Fate of Linear Alkylbenzene Sulfonates, Coconut Diethanol Amides, Nonylphenol Ethoxylates and Their Degradation Products in Wastewater Treatment Plants, Receiving Coastal Waters and Sediments in the Catalonian Area (NE Spain). *J.*

Chromatogr. A **2004**, *1052*, 111–120.

(63) Hoelzer, K.; Sumner, A. J.; Karatum, O.; Nelson, R. K.; Drollette, B. D.; O'connor, M. P.; D'ambro, E. L.; Gordon, ⊥; Getzinger, J.; Ferguson, # P Lee; et al. Indications of Transformation Products from Hydraulic Fracturing Additives in Shale-Gas Wastewater. *Environ. Sci. Technol* **2016**, *50*, 8048.

(64) Y Kimura, S.; Zheng, W.; N Hipp, T.; M Allen, J.; D Richardson, S. Total Organic Halogen (TOX) in Human Urine: A Halogen-Specific Method for Human Exposure Studies. *J. Environ. Sci. (China)* **2017**, *58*, 285–295.

(65) Cuthbertson, A. A.; Kimura, S. Y.; Liberatore, H. K.; Summers, R. S.; Knappe, D. R. U.; Stanford, B. D.; Maness, J. C.; Mulhern, R. E.; Selbes, M.; Richardson, S. D. Does Granular Activated Carbon with Chlorination Produce Safer Drinking Water? From Disinfection Byproducts and Total Organic Halogen to Calculated Toxicity. *Environ. Sci. Technol.* **2019**, *53*, 5987–5999.

(66) Richardson, S. D. XAD Resin Extraction of Disinfection By-Products in Drinking Water: SOP – RSB-003.1 – Revision No. 1. U.S. Environmental Protection Agency: Athens, GA 2011.

(67) Allen, J. M.; Cuthbertson, A. A.; Liberatore, H. K.; Kimura, S. Y.; Mantha, A.; Edwards, M. A.; Richardson, S. D. Showering in Flint, MI: Is There a DBP Problem? *J. Environ. Sci.* **2017**, *58*, 271–284.

(68) Daiber, E. J.; DeMarini, D. M.; Ravuri, S. A.; Liberatore, H. K.; Cuthbertson, A. A.; Thompson-Klemish, A.; Byer, J. D.; Schmid, J. E.; Afifi, M. Z.; Blatchley, E. R.; et al. Progressive Increase in Disinfection Byproducts and Mutagenicity from Source to Tap to Swimming Pool and Spa Water: Impact of Human Inputs. *Environ. Sci. Technol.* **2016**, *50* (13), 6652–6662.

(69) Agilent Technologies. All Ions MS/MS: Targeted Screening and Quantitation Using Agilent TOF and Q-TOF LC/MS Systems https://www.agilent.com/cs/library/technicaloverviews/public/5991-2465EN.pdf.

(70) Negin, C.; Ali, S.; Xie, Q. Most Common Surfactants Employed in Chemical Enhanced Oil Recovery. *Petroleum* **2017**, *3* (2), 197–211.

(71) Binkley, R. W.; Flechtner, T. W.; Tevesz, M. J. S.; Winnik, W.; Zhong, B. Rearrangement of Aromatic Sulfonate Anions in the Gas Phase. *Org. Mass Spectrom.* **1993**, *28*, 769–772.

(72) Riva, M.; Tomaz, S.; Cui, T.; Lin, Y. H.; Perraudin, E.; Gold, A.; Stone, E. A.; Villenave, E.; Surratt, J. D. Evidence for an Unrecognized Secondary Anthropogenic Source of Organosulfates and Sulfonates: Gas-Phase Oxidation of Polycyclic Aromatic Hydrocarbons in the Presence of Sulfate Aerosol. *Environ. Sci. Technol.* **2015**, *49* (11), 6654–6664.

(73) Suter, M. J. F.; Riediker, S.; Giger, W. Selective Determination of Aromatic Sulfonates in Landfill Leachates and Groundwater Using Microbore Liquid Chromatography Coupled with Mass Spectrometry. *Anal. Chem.* **1999**, *71* (4), 897–904.

(74) Steckel, A.; Schlosser, G. An Organic Chemist's Guide to Electrospray Mass

Spectrometric Structure Elucidation. *Molecules* **2019**, *24* (3), 611.

(75) *Environmental and Human Safety of Major Surfactants Volume 1. Anionic Surfactants Part 4. Alpha Olefin Sulfonates Final Report To: The Soap and Detergent Association*; Cambridge, MA, 1993.

(76) John McMurray. *Organic Chemistry*, 7th ed.; Thomson Brooks/Cole: Belmont, CA, 2008.

(77) MOLBASE. 4-Bromooxathiolane 2,2-dioxide (Synthesis Route) www.molbase.com/en/synthesis_189756-6-moldata-1587719.html.

(78) Glezer, V.; Harris, B.; Tal, N.; Iosefzon, B.; Lev, O. Hydrolysis of Haloacetonitriles: Linear Free Energy Relationship. Kinetics and Products. *Water Res.* **1999**, *33* (8), 1938–1948.

(79) Petrovic, M.; Barceló, D.; Diaz, A.; Ventura, F. Low Nanogram per Liter Determination of Halogenated Nonylphenols, Nonylphenol Carboxylates, and Their Non-Halogenated Precursors in Water and Sludge by Liquid Chromatography Electrospray Tandem Mass Spectrometry. *J. Am. Soc. Mass Spectrom.* **2003**, *14* (5), 516–527.

(80) SURFACTANTS Types and Uses. **2002**, *2*.

(81) González, S.; Petrovic, M.; Barceló, D. Removal of a Broad Range of Surfactants from Municipal Wastewater--Comparison between Membrane Bioreactor and Conventional Activated Sludge Treatment. *Chemosphere* **2007**, *67*, 335–343.

(82) Cadwallader, A.; VanBriesen, J. M. Temporal and Spatial Changes in Bromine Incorporation into Drinking Water-Disinfection By-Products in Pennsylvania. *J. Environ. Eng.* **2019**, *145*, 04018147.

(83) Kimura, S. Y.; Cuthbertson, A. A.; Byer, J. D.; Richardson, S. D. The DBP Exposome: Development of a New Method to Simultaneously Quantify Priority Disinfection by-Products and Comprehensively Identify Unknowns. *Water Res.* **2019**, *148*, 324–333.

(84) ASTM D7573-18ae1, Standard Test Method for Total Carbon and Organic Carbon in Water by High Temperature Catalytic Combustion and Infrared Detection www.astm.org.

(85) ASTM D8083-16, Standard Test Method for Total Nitrogen, and Total Kjeldahl Nitrogen (TKN) by Calculation, in Water by High Temperature Catalytic Combustion and Chemiluminescence Detection www.astm.org.

(86) Plewa, M. J.; Wagner, E. D.; Richardson, S. D. TIC-Tox: A Preliminary Discussion on Identifying the Forcing Agents of DBP- Mediated Toxicity of Disinfected Water. *J. Environ. Sci.* **2017**, *58*, 208–216.

(87) Krasner, S. W.; Lee, T. C. F.; Westerhoff, P.; Fischer, N.; Hanigan, D.; Karanfil, T.; Beita-Sandi, W.; Taylor-Edmonds, L.; Andrews, R. C. Granular Activated Carbon Treatment May Result in Higher Predicted Genotoxicity in the Presence of Bromide. *Environ. Sci. Technol.* **2016**, *50*, 9583–9591.

(88) Dong, S.; Nguyen, T. H.; Plewa, M. J. Comparative Mammalian Cell Cytotoxicity of Wastewater with Elevated Bromide and Iodide after Chlorination,

Chloramination, or Ozonation. *J. Environ. Sci.* **2017**, *58*, 296–301.

(89) Weinberg, H. S.; Krasner, S. W.; Richardson, S. D.; Thruston, J. A. D. *The Occurrence of Disinfection By-Products (DBPs) of Health Concern in Drinking Water: Results of a Nationwide DBP Occurrence Study*. *EPA/600/R02/068*; Athens, GA, 2002.

APPENDIX A
REPRINT AND ADAPTATION PERMISSIONS

A.1 LIBERATORE ET AL. 2017

Adapted in Chapter 2 and reprinted in Appendix E with permission from:

Liberatore, H. K.; Plewa, M. J.; Wagner, E. D.; VanBriesen, J. M.; Burnett, D. B.; Cizmas, L. H.; Richardson, S. D. *Environ. Sci. Technol. Lett.* **2017**, *4*, 475-480.

Copyright Clearance Center RightsLink®

Home | Create Account | Help

ACS Publications
Most Trusted. Most Cited. Most Read.

Title: Identification and Comparative Mammalian Cell Cytotoxicity of New Iodo-Phenolic Disinfection Byproducts in Chloraminated Oil and Gas Wastewaters

Author: Hannah K. Liberatore, Michael J. Plewa, Elizabeth D. Wagner, et al

Publication: Environmental Science & Technology Letters

Publisher: American Chemical Society

Date: Nov 1, 2017

Copyright © 2017, American Chemical Society

LOGIN

If you're a copyright.com user, you can login to RightsLink using your copyright.com credentials.

Already a RightsLink user or want to learn more?

PERMISSION/LICENSE IS GRANTED FOR YOUR ORDER AT NO CHARGE

This type of permission/license, instead of the standard Terms & Conditions, is sent to you because no fee is being charged for your order. Please note the following:

- Permission is granted for your request in both print and electronic formats, and translations.
- If figures and/or tables were requested, they may be adapted or used in part.
- Please print this page for your records and send a copy of it to your publisher/graduate school.
- Appropriate credit for the requested material should be given as follows: "Reprinted (adapted) with permission from (COMPLETE REFERENCE CITATION). Copyright (YEAR) American Chemical Society." Insert appropriate information in place of the capitalized words.
- One-time permission is granted only for the use specified in your request. No additional uses are granted (such as derivative works or other editions). For any other uses, please submit a new request.

A.2 CUTHBERTSON ET AL. 2019

Reprinted in Appendix E with permission from:

Cuthbertson, A. A.; S. Y. Kimura; H. K. Liberatore; D. R. U. Knappe; B. Stanford; R. S. Summers; E. Dickenson; C. Maness; R. E. Mulhern; C. Glover; M. Selbes; S. D. Richardson. Does GAC Produce Safer Drinking Water? From DBPs and TOX to Calculated Toxicity. *Environ. Sci. Technol.* **2019**, *53*, 5987-5999

Copyright Clearance Center RightsLink®

Home | Create Account | Help

ACS Publications Most Trusted. Most Cited. Most Read.

Title:	Does Granular Activated Carbon with Chlorination Produce Safer Drinking Water? From Disinfection Byproducts and Total Organic Halogen to Calculated Toxicity
Author:	Amy A. Cuthbertson, Susana Y. Kimura, Hannah K. Liberatore, et al
Publication:	Environmental Science & Technology
Publisher:	American Chemical Society
Date:	May 1, 2019

Copyright © 2019, American Chemical Society

LOGIN

If you're a copyright.com user, you can login to RightsLink using your copyright.com credentials.

Already a RightsLink user or want to learn more?

PERMISSION/LICENSE IS GRANTED FOR YOUR ORDER AT NO CHARGE

This type of permission/license, instead of the standard Terms & Conditions, is sent to you because no fee is being charged for your order. Please note the following:

- Permission is granted for your request in both print and electronic formats, and translations.
- If figures and/or tables were requested, they may be adapted or used in part.
- Please print this page for your records and send a copy of it to your publisher/graduate school.
- Appropriate credit for the requested material should be given as follows: "Reprinted (adapted) with permission from (COMPLETE REFERENCE CITATION). Copyright (YEAR) American Chemical Society." Insert appropriate information in place of the capitalized words.
- One-time permission is granted only for the use specified in your request. No additional uses are granted (such as derivative works or other editions). For any other uses, please submit a new request.

A.3 DEHAVEN ET AL. 2019

Reprinted in Appendix E with permission from:

DeHaven, B. A.; H. K. Liberatore; A. Greer, S. D. Richardson; L. S. Shimizu. Probing the Formation of Reactive Oxygen Species by a Porous Self-Assembled Benzophenone bis-Urea Host. *ACS Omega* **2019**, *4*, 8290-8298. https://pubs.acs.org/doi/10.1021/acsomega.9b00831

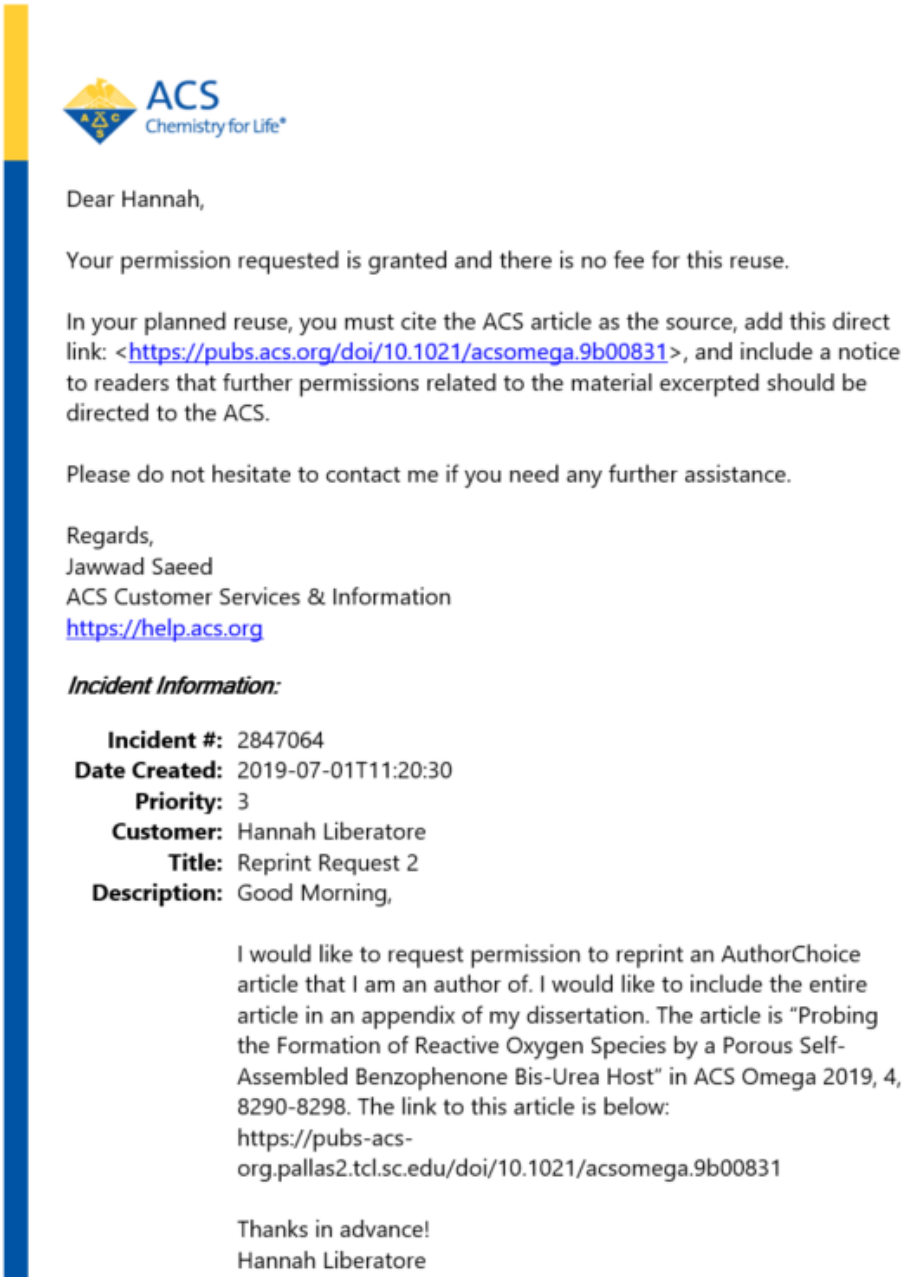

ACS Chemistry for Life®

Dear Hannah,

Your permission requested is granted and there is no fee for this reuse.

In your planned reuse, you must cite the ACS article as the source, add this direct link: <https://pubs.acs.org/doi/10.1021/acsomega.9b00831>, and include a notice to readers that further permissions related to the material excerpted should be directed to the ACS.

Please do not hesitate to contact me if you need any further assistance.

Regards,
Jawwad Saeed
ACS Customer Services & Information
https://help.acs.org

Incident Information:

Incident #: 2847064
Date Created: 2019-07-01T11:20:30
Priority: 3
Customer: Hannah Liberatore
Title: Reprint Request 2
Description: Good Morning,

I would like to request permission to reprint an AuthorChoice article that I am an author of. I would like to include the entire article in an appendix of my dissertation. The article is "Probing the Formation of Reactive Oxygen Species by a Porous Self-Assembled Benzophenone Bis-Urea Host" in ACS Omega 2019, 4, 8290-8298. The link to this article is below:
https://pubs-acs-org.pallas2.tcl.sc.edu/doi/10.1021/acsomega.9b00831

Thanks in advance!
Hannah Liberatore

A.4 YANG ET AL. 2019

Reprinted in Appendix E

Yang, M.; H. K. Liberatore; X. Zhang. Current Methods for Analyzing Drinking Water Disinfection Byproducts. *Curr. Opin. Environ. Sci. Health* **2019**, *7*, 98-107.

A.5 POSTIGO ET AL. 2018

Reprinted in Appendix E with permission from:

Postigo, C.; D. M. DeMarini; M. Armstrong; H. K. Liberatore; K. Lamann; S. Y. Kimura; A. A. Cuthbertson; S. H. Warren; S. D. Richardson; T. McDonald; Y. Sey; S. E. Duirk; J. E. Simmons. Chlorination of Source Water Containing Iodinated X-ray Contrast Media: Mutagenicity and Identification of New Iodinated Disinfection Byproducts. *Environ. Sci. Technol.* **2018**, *52*, 13047-13056.

Copyright Clearance Center RightsLink®

Home | Create Account | Help

ACS Publications
Most Trusted. Most Cited. Most Read.

Title:	Chlorination of Source Water Containing Iodinated X-ray Contrast Media: Mutagenicity and Identification of New Iodinated Disinfection Byproducts
Author:	Cristina Postigo, David M. DeMarini, Mikayla D. Armstrong, et al
Publication:	Environmental Science & Technology
Publisher:	American Chemical Society
Date:	Nov 1, 2018

Copyright © 2018, American Chemical Society

LOGIN

If you're a copyright.com user, you can login to RightsLink using your copyright.com credentials.

Already a RightsLink user or want to learn more?

PERMISSION/LICENSE IS GRANTED FOR YOUR ORDER AT NO CHARGE

This type of permission/license, instead of the standard Terms & Conditions, is sent to you because no fee is being charged for your order. Please note the following:

- Permission is granted for your request in both print and electronic formats, and translations.
- If figures and/or tables were requested, they may be adapted or used in part.
- Please print this page for your records and send a copy of it to your publisher/graduate school.
- Appropriate credit for the requested material should be given as follows: "Reprinted (adapted) with permission from (COMPLETE REFERENCE CITATION). Copyright (YEAR) American Chemical Society." Insert appropriate information in place of the capitalized words.
- One-time permission is granted only for the use specified in your request. No additional uses are granted (such as derivative works or other editions). For any other uses, please submit a new request.

A.6 ACKERSON ET AL. 2019

Reprinted in Appendix E

Ackerson, N. O. B.; A. H. Killinger; H. K. Liberatore; T. A. Ternes; M. J. Plewa; S. D. Richardson; S. E. Duirk. The Impact of Chlorine Exposure Time on Disinfection Byproduct Formation in the Presence of Iopamidol and Natural Organic Matter During Chloramination. *J. Env. Sci*. **2019**, *78*, 204-214.

A.7 ACKERSON ET AL. 2018

Reprinted in Appendix E

Ackerson, N. O. B.; E. J. Machek; A. H. Killinger; E. A. Crafton; P. Kumkum; H. K. Liberatore; M. J. Plewa; S. D. Richardson; T. A. Ternes; S. E. Duirk. Formation of DBPs and Halogen-Specific TOX in the Presence of Iopamidol and Chlorinated Oxidants. *Chemosphere* **2018**, *202*, 349-357.

A.8 ALLEN ET AL. 2017

Reprinted in Appendix E

Allen, J. M.; A. A. Cuthbertson; H. K. Liberatore; S. Y. Kimura; A. Mantha; M. A. Edwards; S. D. Richardson. Showering in Flint, MI: Is there a DBP problem? *J. Environ. Sci.* **2017**, *58*, 271-284.

A.9 DAIBER ET AL. 2016

Reprinted in Appendix E with permission from:

Daiber, E. J.; D. M. DeMarini; S. A. Ravuri; H. K. Liberatore; A. A. Cuthbertson; A. Thompson-Klemish; J. D. Byer; J. E. Schmid; M. Z. Afifi; E. R. Blatchley; S. D. Richardson. Progressive Increase in Disinfection Byproducts and Mutagenicity from Source to Tap to Swimming Pool and Spa Water: Impact of Human Inputs. *Environ. Sci. Technol.* **2016**, *50*, 6652-6662.
https://pubs.acs.org/doi/10.1021/acs.est.6b00808

Dear Hannah,

Please find below official response for the request 2847044.

Your permission requested is granted and there is no fee for this reuse.

In your planned reuse, you must cite the ACS article as the source, add this direct link: <https://pubs.acs.org/doi/10.1021/acs.est.6b00808>, and include a notice to readers that further permissions related to the material excerpted should be directed to the ACS.

Please do not hesitate to contact me if you need any further assistance.

Regards,
Jawwad Saeed
ACS Customer Services & Information
https://help.acs.org

Incident Information:

Incident #: 2847044
Date Created: 2019-07-01T11:13:02
Title: Reprint Request
Description: Good Morning,

I would like to request permission to reprint an Editors' Choice article that I am an author of. I would like to include the entire article in an appendix of my dissertation. The article is "Progressive Increase in Disinfection Byproducts and Mutagenicity from Source to Tap to Swimming Pool and Spa Water: Impact of Human Inputs" in Environ. Sci. Technol. 2016, 50, 6652-6662. The link to this article is below: https://pubs-acs-org.pallas2.tcl.sc.edu/doi/10.1021/acs.est.6b00808

Thanks in advance!
Hannah Liberatore

APPENDIX B
SUPPORTING INFORMATION FOR:
IDENTIFICATION AND COMPARATIVE MAMMALIAN CELL CYTOTOXICITY OF NEW IODO-PHENOLIC DISINFECTION BYPRODUCTS IN CHLORAMINATED OIL AND GAS WASTEWATERS

Reagents and Solution Preparation. All aqueous solutions were prepared in purified water (18 MΩ cm^{-1}) obtained from a Barnstead E-pure Milli-Q system. Honeywell Burdick & Jackson® GC^2-grade dichloromethane (Muskegon, MI) was used for extractions and preparation of iodophenolic standard solutions. Sodium hypochlorite solution (5.65-6.00%), potassium phosphate dibasic (≥98%), potassium phosphate monobasic (≥99%), and concentrated sulfuric acid (98%) were purchased from Fisher Scientific (Fair Lawn, NJ). Anhydrous sodium sulfate (≥99%), ammonium chloride (ReagentPlus®, ≥99.5%), sodium iodide (≥99.5%), 2-iodophenol (98%), 3-iodophenol (98%), 4-iodophenol (99%), 2,4,6-triiodophenol (97%), 4-iodo-2-methylphenol (97%), *p*-cresol (≥99%), and 2,6-xylenol (≥99%) were purchased from Sigma-Aldrich (St. Louis, MO). Other iodophenolic standards (98%) – 2,4-diiodophenol, 2,5-diiodophenol, 2,6-diiodophenol, 2-iodo-4-methylphenol, 2,3-dimethyl-4-iodophenol, 2,5-dimethyl-4-iodophenol, 2,6-dimethyl-4-iodophenol, 4,5-dimethyl-2-iodophenol, and 4,6-diiodo-2,3-xylenol – were purchased from Spectra Group Synthetics LLC (Millbury, OH). Iodophenolic standard stock solutions (~1,000 mg/L) were prepared by dissolving approximately 20 mg of each pure standard in 20 mL of dichloromethane. These

solutions were further diluted to approximately 10 mg/L for analysis by gas chromatography-mass spectrometry (GC-MS).

Monochloramine was freshly prepared according to a previously published procedure.[21] Briefly, hypochlorite solution was added slowly while stirring to a solution containing 10% molar excess ammonium chloride solution. Both solutions were maintained at pH 8.5 (±0.1) with phosphate buffer. Sodium hypochlorite stock solutions (λ_{max} = 292 nm, ε = 350 $M^{-1}cm^{-1}$) and resulting monochloramine (λ_{max} = 243 nm, ε = 461 $M^{-1}cm^{-1}$) solutions were standardized by UV-Vis absorbance using a Molecular Devices SpectraMax M5 spectrophotometer (Sunnyvale, CA). McAllen MF chloramination was performed in duplicate; due to very low volumes received (<200 mL), Barnett NF chloramination was not replicated.

An apparent incompatibility of phosphate buffer with the high salinity in produced water samples was observed, exhibiting a "crashing out" effect of a dissolved species, upon the addition of phosphate buffer to form an insoluble salt (likely barium phosphate). For this reason, chlorine demands of the samples were not experimentally determined, as colorimetric chlorine residual analyses use phosphate buffer, and reactors were not buffered during chloramination. Instead, a disinfectant dose of 1 mg/L NH_2Cl as Cl_2 per 1 mg/L TOC as C and 1:3 for McAllen MF due to high TOC (1.91 and 7.80 mg/L for Barnett NF and McAllen MF, respectively) and pH was adjusted to pH 7.0 at the beginning of the chloramination period and remained within ±1.2 pH units after 72 h. Chlorine doses applied in our study are similar to those applied at drinking water treatment plants in the U.S.[89]

Mass Spectral Interpretation. Mass spectra of all suspected iodinated compounds were extensively interpreted to determine potential structures (Figures B.5, B.6, and B.8). Particular attention was paid to spectral features indicative of the presence of iodine, including the iodine ion (I^+, *m/z* 127) and a neutral loss of iodine between fragments (Δ*m/z* of 127). The molecular ions of members in each homologous series increased successively by *m/z* 126 (+I, -H) from mono- to di- to tri-iodo-species. Mass spectra of diiodo- and triiodo-species contained the same fragments as monoiodo- and diiodo-species, shifted by the difference of one hydrogen. A difference of *m/z* 14 was observed between molecular ions of homologous series, indicating a structural difference of a methyl substituent (+CH_3, -H). Fragments of *m/z* 39 ($C_3H_3^+$) and 51 ($C_4H_3^+$) were present in every compound's mass spectrum, as well as fragments within *m/z* ranges 63-65 and 75-78, indicating that these were aromatic compounds.[40]

Brominated and chlorinated phenolics were also tentatively identified using extracted ion chromatograms, accurate masses, fragmentation patterns, and distinctive isotopic patterns of bromine and chlorine. For example, compounds that have one bromine will show patterns of a given *m/z* (M) and M+2, where the abundance of M+2 is 97% of M. Similarly, compounds with one chlorine will exhibit patterns where the abundance of M+2 is 32% of M. With increasing halogen substitution, the pattern changes due the probability of M+2 (as well as M+4, M+6, etc.) isotopes occurring.[40]

Table B.1. GC-MS Instrument Parameters

GC Parameters [a]	
Carrier Gas	Helium
Sample Volume	1.0 µL
Inlet Mode	Pulsed Splitless
Injection Port Temperature	250 °C
Capillary Column [b]	Rxi-5ms
Column Length	30 m
Inner Diameter	0.25 mm
Film Thickness	0.25 µm
Pressure	13.0 psi
Initial Flow	1.2 mL/min
Transfer Line Temperature	280 °C
Oven Program	
Initial Temperature; Hold Time	35 °C; 4 min
Temperature Ramp	9 °C/min
Final Temperature; Hold Time	280 °C; 20 min
MS Parameters [c]	
Ion Source	Electron Ionization
Source Temperature	200 °C
Electron Energy	70 eV
Quad Temperature	150 °C
Emission Current	35 µA
Solvent Delay	4 min
Scan Mode	Full Scan
Low Mass	33
High Mass	550

[a] Agilent 6890N (Santa Clara, CA) (low resolution analyses). Agilent 7890B (high resolution analyses). [b] Restek Corporation, Bellefonte, PA. [c] Agilent 5975 quadrupole mass spectrometer (low resolution analyses). LECO Pegasus GC-HRT time-of-flight mass spectrometer (St. Joseph, MI) (high resolution analyses)

Table B.2. Iodinated Phenolics Identified in Barnett and McAllen Chloraminated Waters [a]

Compound (Molecular Formula)	Theoretical *m/z*	Isomer	RT (min.)	Barnett NF NH2Cl		McAllen MF NH2Cl	
				Observed *m/z*	Abundance	Observed *m/z*	Abundance
Iodophenol (C6H5IO)	219.9380	2-IP	14.78	219.9382	8.96 × 104	219.9381	1.49 × 106
		4-IP	18.12	219.9382	5.71 × 103	219.9380	1.14 × 105
Diiodophenol (C6H4I2O)	345.8346	2,4-DiIP	21.05	345.8348	2.12 × 104	345.8347	1.47 × 105
		2,6-DiIP	21.13	345.8349	1.02 × 105	345.8349	2.36 × 105
Triiodophenol (C6H3I3O)	471.7313	2,4,6-TIP	26.20	471.7311	5.81 × 104	471.7315	1.59 × 105
Iodomethylphenol (C7H7IO)	233.9536	IMeP #1	16.16	233.9538	4.02 × 104	233.9537	5.82 × 104
		IMeP #2	16.60	233.9537	3.09 × 104	233.9537	4.67 × 103
		2-I-4-MeP	16.67	233.9539	3.15 × 105	233.9537	7.97 × 103
		IMeP #4	16.71	233.9538	8.19 × 104	233.9537	3.18 × 103
		4-I-2-MeP	19.24	233.9538	5.39 × 103	233.9537	1.71 × 104
		IMeP #6	19.56	233.9538	2.04 × 104	233.9538	1.57 × 104
Diiodomethylphenol (C7H6I2O)	359.8503	DiIMeP #1	22.09	359.8507	1.44 × 105	359.8507	1.20 × 105
		DiIMeP #2	22.57	359.8506	1.89 × 105	359.8505	3.55 × 104
		DiIMeP #3	22.64	359.8508	8.79 × 105	359.8503	1.20 × 104
		DiIMeP #4	22.67	359.8505	1.08 × 105	359.8504	9.49 × 103
		DiIMeP #5	22.73	359.8505	1.03 × 105	359.8507	6.81 × 103
Triiodomethylphenol (C7H5I3O)	485.7469	TriIMeP	27.77	485.7468	1.26 × 106	485.7471	8.69 × 104
Iododimethylphenol (C8H9IO)	247.9693	IDiMeP #1	17.46	247.9695	2.03 × 103	247.9694	1.96 × 103
		IDiMeP #2	17.83	247.9694	1.58 × 104	247.9696	4.24 × 103
		IDiMeP #3	17.99	247.9694	8.92 × 102	247.9695	8.06 × 102
		IDiMeP #4	18.11	-	-	247.9695	4.72 × 103
		IDiMeP #5	18.23	247.9696	3.92 × 103	247.9695	9.21 × 102
		2I45DiMeP	18.83	247.9696	1.45 × 103	247.9696	1.47 × 103

		4I26DiMeP	20.08	247.9696	2.16 × 103	247.9693	1.14 × 103
		4I25DiMeP	20.65	247.9697	1.58 × 103	247.9696	3.03 × 103
		IDiMeP #9	21.28	-	-	247.9691	2.92 × 102
Diiododimethylphenol (C8H8I2O)	373.8659	DiIDiMeP #1	23.03	373.8661	1.34 × 104	373.8661	4.97 × 103
		DiIDiMeP #2	23.32	-	-	373.8661	4.31 × 102
		DiIDiMeP #3	23.58	373.8658	9.62 × 102	373.8660	4.80 × 103
		DiIDiMeP #4	23.67	373.8661	1.57 × 104	373.8662	9.14 × 103
		DiIDiMeP #5	23.75	-	-	373.8661	1.99 × 103
		46DiI23Xy	23.98	373.8663	4.50 × 103	373.8662	4.30 × 103
		DiIDiMeP #7	24.04	-	-	373.8661	1.91 × 103
		DiIDiMeP #8	24.23	373.8662	2.17 × 103	373.8661	9.64 × 103
		DiIDiMeP #9	24.57	373.8662	4.23 × 103	373.8662	1.59 × 103
Triiododimethylphenol (C8H7I3O)	499.7626	TriIDiMeP #1	28.22	499.7626	3.67 × 103	499.7626	6.54 × 103
		TriIDiMeP #2	29.33	499.7627	5.05 × 103	499.7631	2.56 × 103

Table B.3. Brominated and Chlorinated Iodo-Phenolics Identified in Chloraminated McAllen MF Water Samples

Compound (Molecular Formula)	Theoretical *m/z*			RT (min.)	Observed *m/z*		
	$M^{\cdot+}$	$[M+2]^{\cdot+}$	$[M+4]^{\cdot+}$		$M^{\cdot+}$	$[M+2]^{\cdot+}$	$[M+4]^{\cdot+}$
Chloroiodophenol (C6H4ClIO)	253.8990	255.8961		17.8482	253.8992	255.8963	
				17.9922	253.8992	255.8964	
				18.1859	253.8992	255.8962	
Bromoiodophenol (C6H4BrIO)	297.8485	299.8465		19.1426	297.8486	299.8469	
				19.4117	297.8488	299.8468	
				19.4863	297.8486	299.8466	
Dichloroiodophenol (C6H3Cl2IO)	287.8600	289.8571	291.8543	20.4930	287.8603	289.8572	291.8539
				20.6133	287.8602	289.8570	291.8546
Bromochloroiodophenol (C6H3BrClIO)	331.8095	333.8073	335.8046	21.7365	331.8100	333.8080	335.8047
				21.8531	331.8097	333.8076	335.8049
Chlorodiiodophenol (C6H3ClI2O)	379.7956	381.7928		23.3800	379.7959	381.7928	
				23.5029	379.7959	381.7930	
Bromodiiodophenol (C6H3BrI2O)	423.7451	425.7431		24.6751	423.7453	425.7432	
Chloroiodomethylphenol (C7H6ClIO)	267.9146	269.9118		19.1178	267.9149	269.9121	
				19.7514	267.9151	269.9120	
Bromoiodomethylphenol (C7H6BrIO)	311.8641	313.8621		20.3748	311.8643	313.8624	
				30.4654	311.8641	313.8623	
				20.7575	311.8646	313.8630	
				20.9513	311.8647	313.8622	

Table B.4. Cresol (Methylphenol) and Xylenol (Dimethylphenol) Precursor Study: 72 h Chloramination Conditions

Reactor	Compound (10 mg/L)	I^-	NH_2Cl
1	4-Methylphenol	50 mg/L	10 mg/L
2	4-Methylphenol	50 mg/L	0 mg/L
3	4-Methylphenol	0 mg/L	10 mg/L
4	2,6-Dimethylphenol	50 mg/L	10 mg/L
5	2,6-Dimethylphenol	50 mg/L	0 mg/L
6	2,6-Dimethylphenol	0 mg/L	10 mg/L

Table B.5. Chinese Hamster Ovary (CHO) Cell Chronic Cytotoxicity Analyses of Iodo-Phenolics

Compound	**Lowest Cytotoxic Conc. (M)** [a]	**LC_{50} (M)** [b]	**r^2** [c]	**ANOVA Test** [d]
2-Iodophenol	1.50×10^{-4}	6.01×10^{-4}	0.98	$F_{12, 139} = 100.3$; $P < 0.001$
4-Iodophenol	5.00×10^{-5}	2.16×10^{-4}	0.98	$F_{13, 122} = 268.5$; $P < 0.001$
2,4,6-Triiodophenol	5.00×10^{-6}	4.37×10^{-5}	0.98	$F_{12, 119} = 442.6$; $P < 0.001$
4-Iodo-2-methylphenol	2.50×10^{-5}	1.63×10^{-4}	0.98	$F_{15, 120} = 226.3$; $P < 0.001$

[a] Lowest cytotoxic concentration was the lowest concentration (M) that induced a statistically significant reduction in cell density as compared to the negative control. [b] The LC_{50} value is the concentration of the water sample, determined from a regression analysis of the data, that induced a cell density of 50% as compared to the concurrent negative controls. [c] r^2 is the coefficient of determination for the regression analysis upon which the LC_{50} value was calculated. [d] The degrees of freedom for the between-groups and residual associated with the calculated *F*-test result and the resulting probability value.

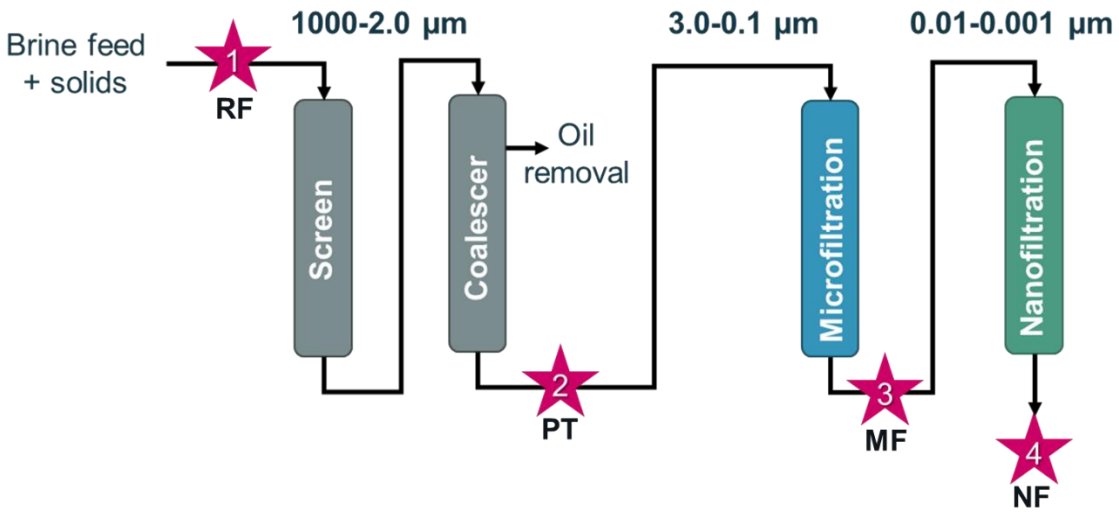

Figure B.1. Membrane-filtration process of produced water samples.[a]

[a] Stars indicate sampling points, where "RF" is raw feed, "PT" is pretreated, "MF" is microfiltration permeate, and "NF" is nanofiltration permeate.

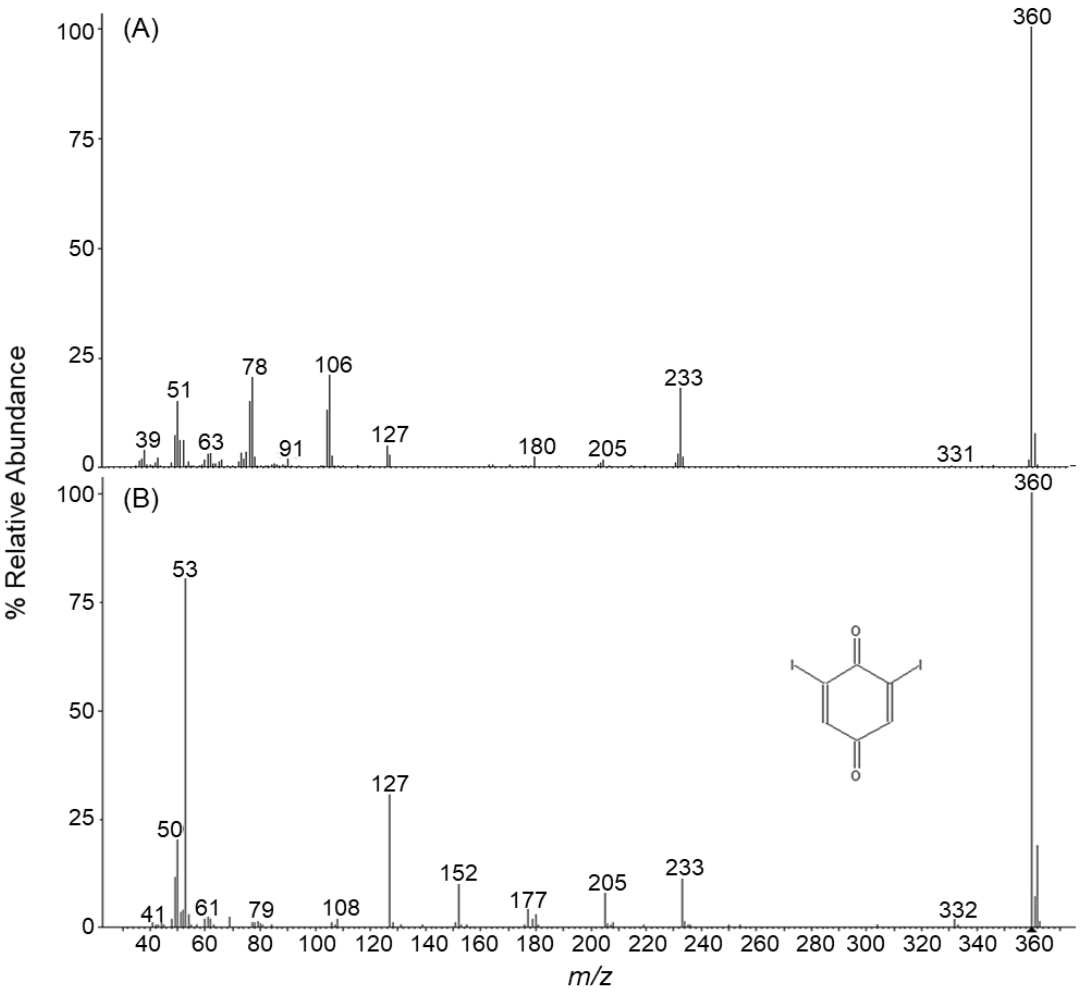

Figure B.2. Library search result for unknown with molecular ion of *m/z* 360. (A) Mass spectrum of unknown in chloraminated Barnett NF sample. (B) Closest NIST library match (63%) with 2,6-diiodo-*p*-benzoquinone.

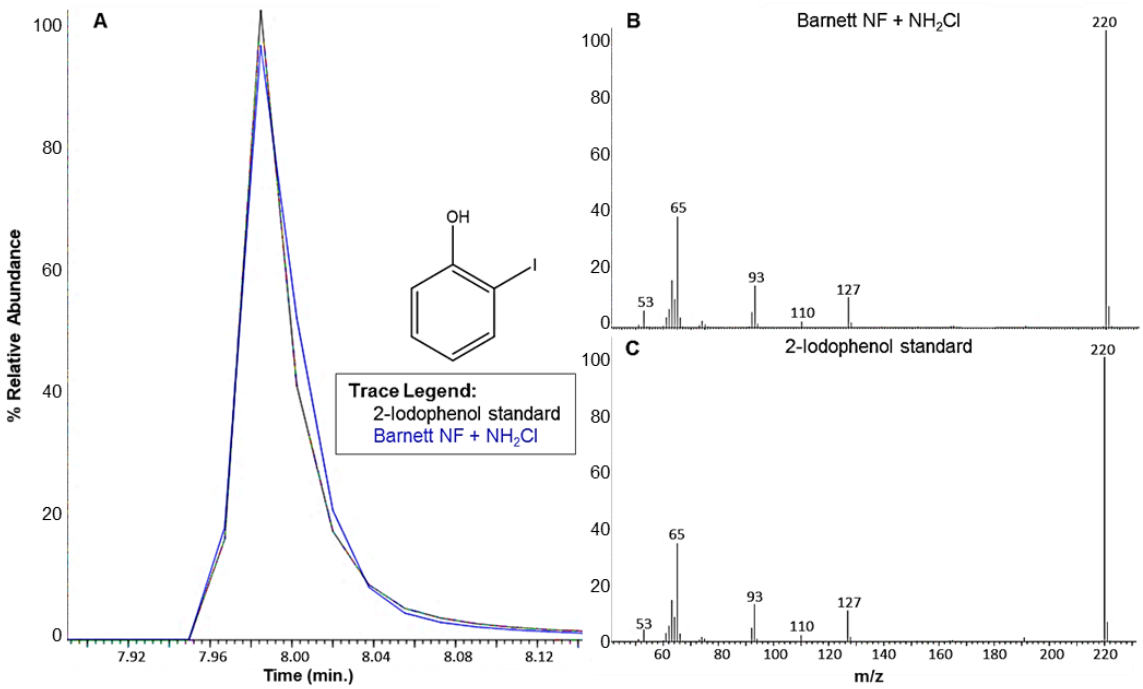

Figure B.3. Isomeric confirmation of 2-iodophenol via retention time (A) and mass spectral matching (B,C). Generic (non-isomer-specific) compound confirmations were determined by mass spectral matching of the sample component (B) and standard (C).

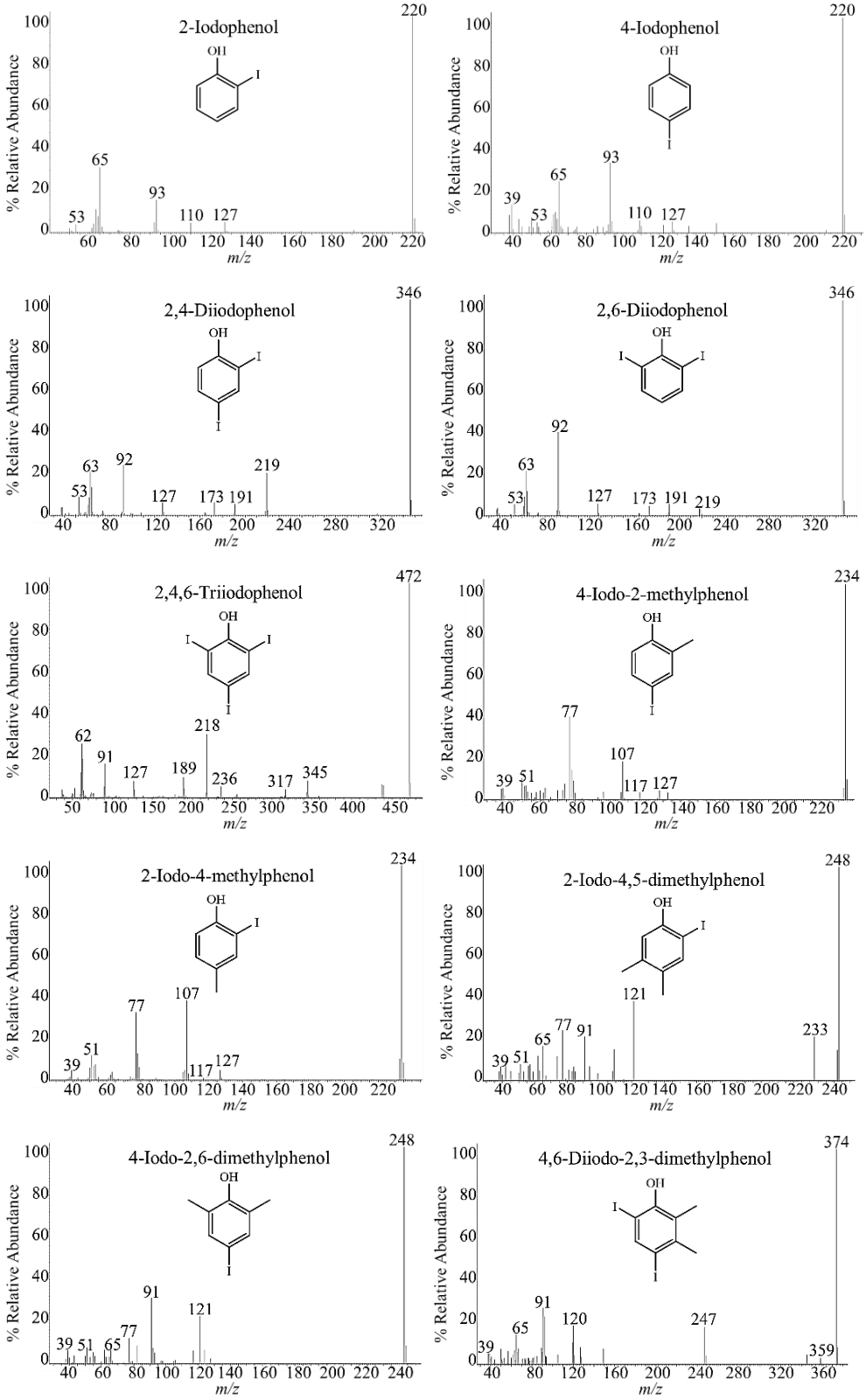

Figure B.4. Mass spectra of confirmed iodophenol, iodocresol (iodomethylphenol), and iodoxylenol (iododimethylphenol) isomers identified in Barnett NF and McAllen MF chloraminated waters.

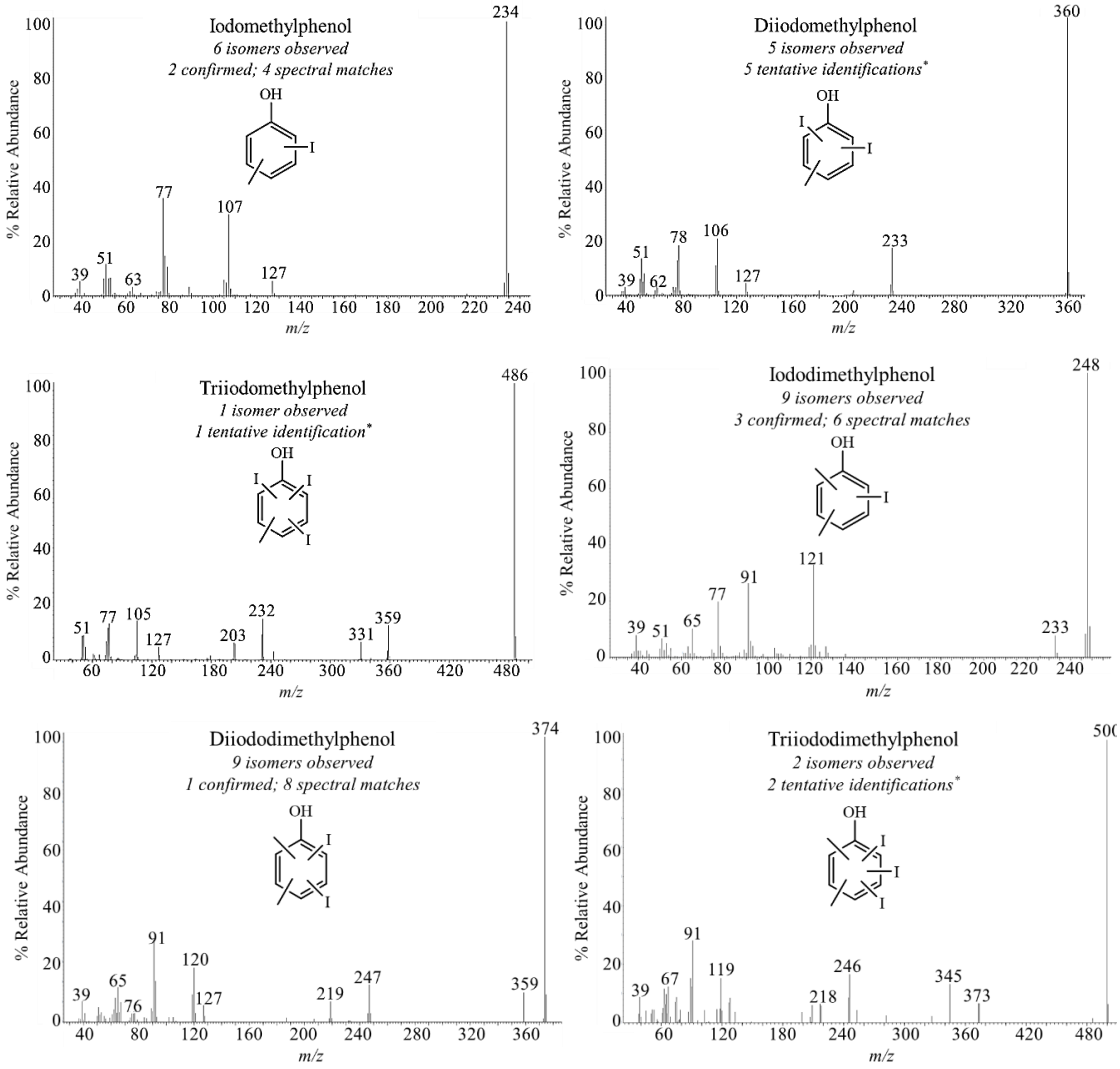

Figure B.5. Mass spectra of iodocresols (iodomethylphenols) and iodoxylenols (iododimethyl-phenols) identified in Barnett NF and McAllen MF chloraminated waters.
* Compounds without commercially available standards.

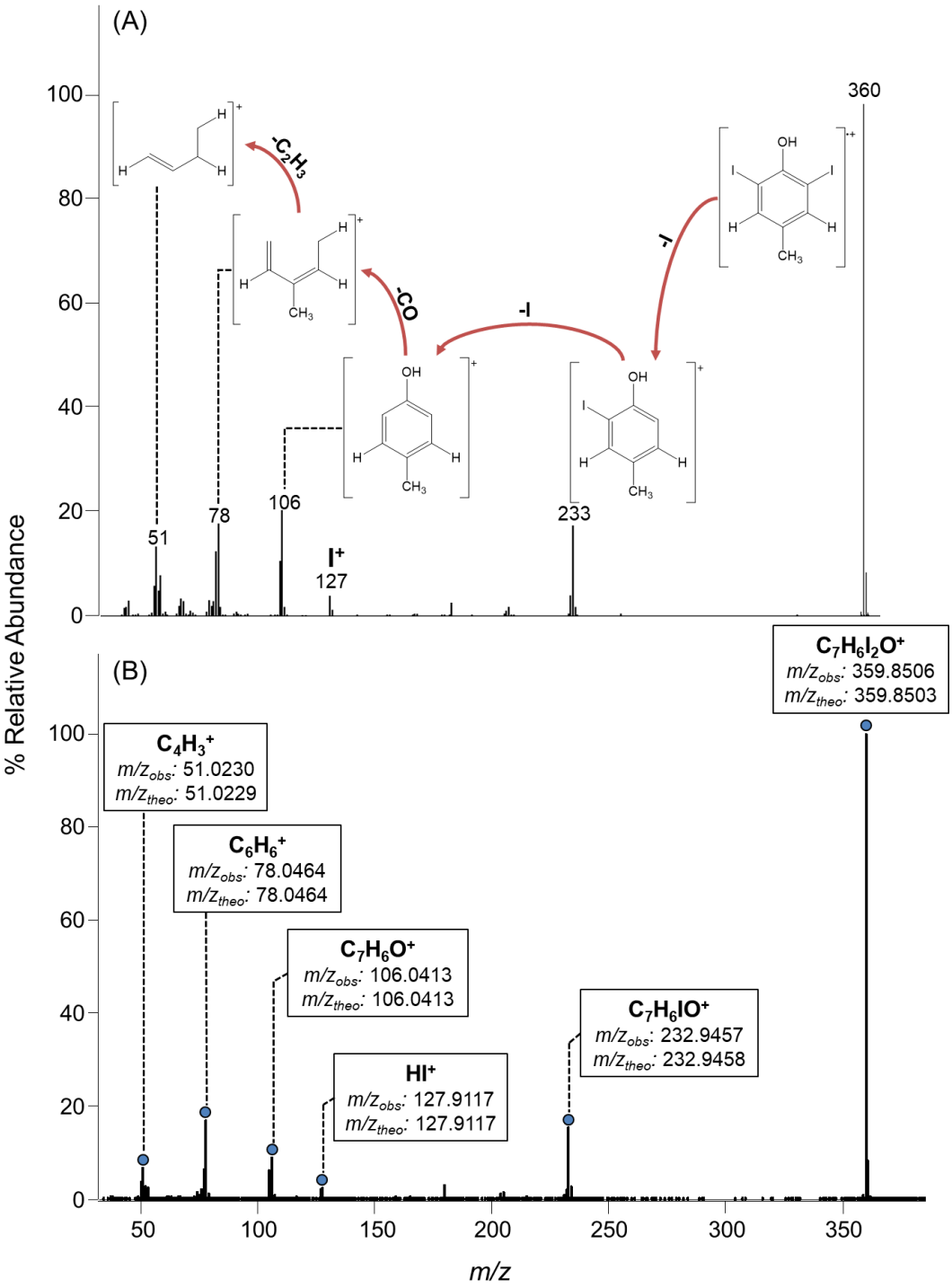

Figure B.6. Example mass spectral interpretation of diiodomethylphenol. (A) Unit resolution electron ionization mass spectrum depicting proposed structural fragmentation pathway. (B) High-resolution accurate mass spectrum depicting the calculated formula, observed mass (m/z_{obs}), and theoretical mass (m/z_{theo}) of each fragment.

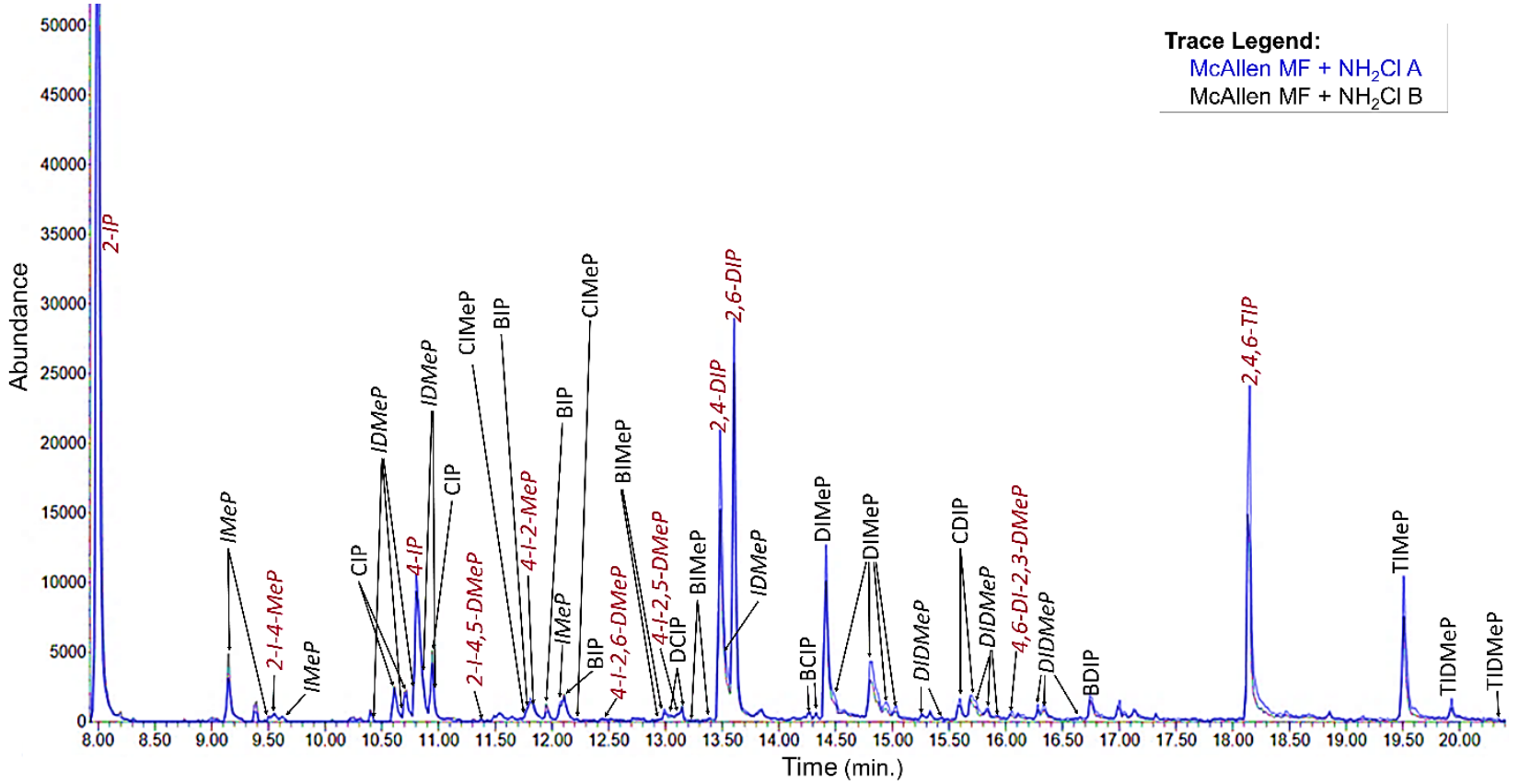

Figure B.7. Iodo-phenolics identified in chloraminated McAllen MF samples (replicates).[a]

[a] Key: Overlay of extracted ion chromatograms of *m/z* 127. Italicized labels indicate mass spectral matches with standard, red font indicates retention time match for specific isomer. IP: iodophenol; DIP: diiodophenol; TIP: triiodophenol; IMeP: iodomethylphenol; DIMeP: diiodomethylphenol; TIMeP: triiodomethylphenol; IDMeP: iododimethylphenol; DIDMeP: diiododimethylphenol; TIDMeP: triiododimethylphenol; CIP: chloroiodophenol; BIP: bromoiodophenol; DCIP: dichloroiodophenol; BCIP: bromochloroiodophenol; CDIP: chlorodiiodophenol; BDIP: bromodiiodophenol; CIMeP: chloroiodomethylphenol; BIMeP: bromoiodomethylphenol

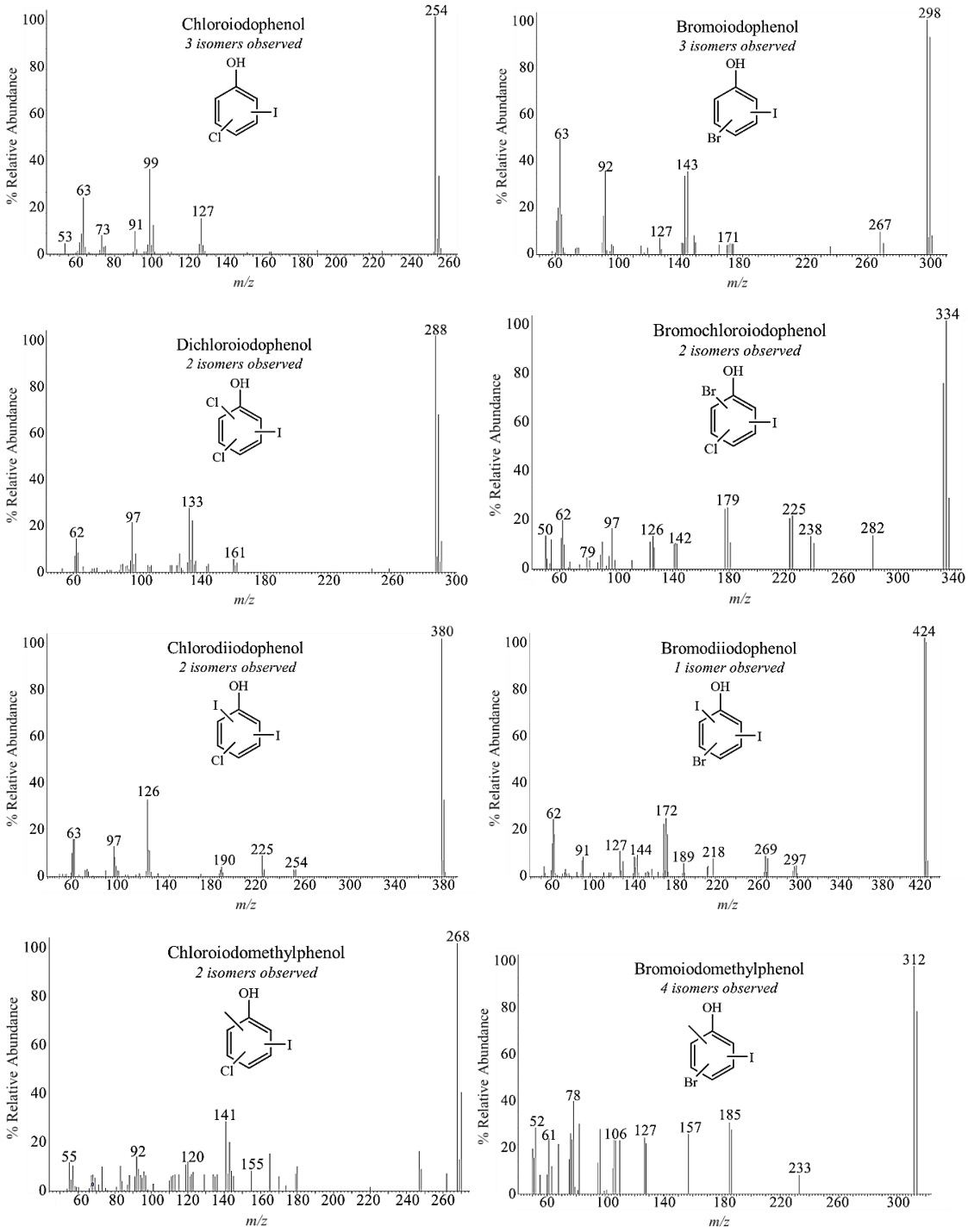

Figure B.8. Mass spectra of tentatively identified chlorinated and brominated iodophenols and iodocresols (iodomethylphenols) in McAllen MF chloraminated water.

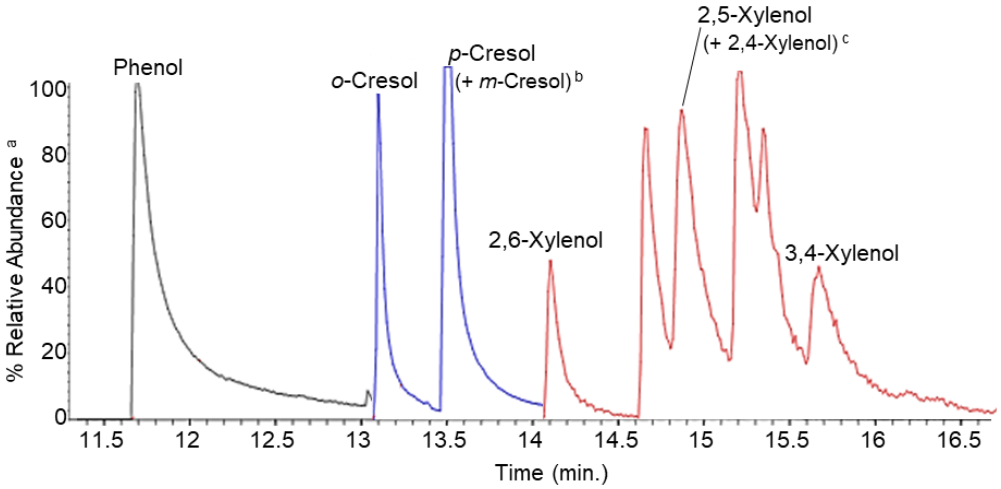

Figure B.9. Detection of phenol, methylphenol (cresol), and dimethylphenol (xylenol) in non-disinfected samples.

Key: [a] Percent relative abundance of extracted ion chromatograms of *m/z* 94 (phenol), *m/z* 108 (cresol), and *m/z* 122 (xylenol). [b] *p*- and *m*-Cresol were chromatographically unresolvable. The presence of *p*-cresol is supported by the formation of 2-iodo-4-methylphenol. Due to the many iodinated methylphenol (iodocresol) isomers formed and plateaued peak, it is likely that both isomers are present. [c] 2,5- and 2,4-xylenol were chromatographically unresolvable. The presence of 2,5-xylenol is supported by the formation of 4-iodo-2,5-dimethylphenol. Due to the many iodinated dimethylphenol (iodoxylenol) isomers, it is likely that both isomers are present.

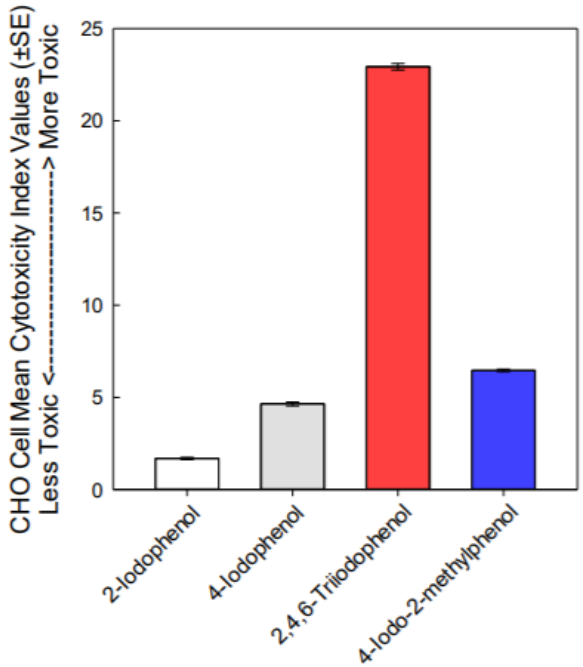

Figure B.10. Chinese hamster ovary (CHO) cell cytotoxicity index (CTI) values, $(LC_{50})^{-1}(10^3)$, of 2-iodophenol, 4-iodophenol, 2,4,6-iodophenol, and 4-iodo-2-methylphenol.

APPENDIX C

SUPPORTING INFORMATION FOR:

POTENTIAL IMPACTS OF HYDRAULIC FRACTURING ON DRINKING WATER: HIGH-RESOLUTION MASS SPECTROMETRY IDENTIFICATION OF >300 NOVEL SURFACTANT-DERIVED S-DBPS

Table C.1. LC Parameters for LC-QTOF MS - All Ions Analyses

Parameter	Value	
Instrument	1290 Infinity II UHPLC Binary Pump	
Mobile Phase	A) 0.1% formic acid in water B) 0.1% formic acid in methanol	
Gradient	Time (min)	%B
	0	5
	1	5
	10	95
	12	95
	12.1	5
Flow rate	0.5 mL/min	
Column	Agilent InfinityLab Poroshell C18 column (2.1 mm × 150 mm × 2.7 µm)	
Temperature	30 °C	
Injection Volume	10 µL	

Table C.2. QTOF Parameters for LC-QTOF MS - All Ions Analyses

Parameter	Value
Instrument	6545 QTOF LC-MS
MS1 mass range	100-3000 m/z
MS2 mass range	50-3000 m/z
MS1 acquisition rate	4.5 spectra/s
MS2 acquisition rate	1 spectra/s
Collision energy	30 eV
Dry gas temperature	300 °C
Drying gas flow rate	12 l/min
Sheath gas temperature	375 °C
Sheath gas flow rate	12 l/min
Nebulizer gas	35 psi
Skimmer voltage	40 V
Octopole RF	750 V
Fragmentor voltage	110 V
Capillary voltage	4 kV

Table C.3. LC Parameters for Orbitrap MS Analyses

Parameter	Value	
Instrument	Vanquish™ UHPLC	
Mobile Phase	A) 95:5 water:acetonitrile (0.4 mM ammonium formate) B) 95:5 acetonitrile:water (0.4 mM ammonium formate)	
Gradient	Time (min)	%B
	-3*	10
	0	10
	5	100
	8	100
Flow rate	0.3 mL/min	
Column	Waters Acquity UPLC© BEH C18 column (2.1 mm × 50 mm × 1.7 µm)	
Temperature	30 °C	
Injection Volume	10 µL	

*3 min equilibration time at starting conditions before sample injection

Table C.4. Orbitrap MS Parameters for High Resolution MS^1 Analyses

Ion Source		**MS1**	
Ion source type	H-ESI	Detector type	Orbitrap
Spray voltage	Static	Resolution	120,000
Negative ion (V)	2500	Mass range	Normal
Sheath gas (arb)	11	Scan range (m/z)	120-1000
Aux gas (arb)	2	RF Lens (%)	45
Sweep gas (arb)	1	AGC target	2.0e5
Ion transfer tube temp (°C)	300	Maximum injection time (ms)	54
Vaporizor temp (°C)	50	Microscans	1

Table C.5. Orbitrap MS Parameters for MS^3 Analyses

Ion Source	
Ion source type	H-ESI
Spray voltage	Static
Negative ion (V)	2500
Sheath gas (arb)	11
Aux gas (arb)	2
Sweep gas (arb)	1
Ion transfer tube temp (°C)	300
Vaporizor temp (°C)	50

MS1	
Detector type	Ion trap
Ion trap scan rate	Rapid
Mass range	Normal
Scan range (m/z)	120-1000
RF lens (%)	45
AGC target	1.0e4
Max. injection time (ms)	10
Microscans	1
Filters:	
Intensity threshold	2.0e5
Targeted list (m/z)	343.0585 247.1373 299.1043 391.0434 405.0044 263.1318 265.1476
Mass tolerance	± 25 ppm
# of data dependent scans	2

Data-dependent MS2	
Isolation mode	Quadrupole
Isolation window (m/z)	1.6
Activation type	HCD
HCD collision energies (%)	30, 45, 60
Detector type	Orbitrap
Scan range mode	Normal
Orbitrap resolution	30,000
First mass (m/z)	65
AGC target	1.0e4
Max. injection time (ms)	54
Microscans	1
Filters:	
Targeted exclusion (m/z)	75 ± 10 m/z
# of data dependent scans	4

Data-dependent MS3	
MS Isolation window (m/z)	2.5
MS2 Isolation window (m/z)	2
Activation type	HCD
HCD collision enegy (%)	30
Detector type	Orbitrap
Scan range mode	Normal
Orbitrap resolution	30,000
First mass (m/z)	65
AGC target	1.0e4
Max. injection time (ms)	54
Microscans	1

Table C.6. DBPs Identified by Class in Disinfected Surfactant Mixture and Gas Wastewater[a,b]

Class $[M-H]^-$ Ring/Double Bond Equivalence (RDBE)	$[M-H]^-$ Formula	Theoretical *m/z*	Dimer/ double charge	Number of Isomers: C_{12} Olefin Sulfonate + Br^- + HOCl	Number of Isomers: Raw Feed + HOCl	Number of Isomers: Raw Feed + NH_2Cl	Maximum Abundance	Highest Abundance Sample
$C_{12}H_{23-n}X_nSO_3^-$ 1.5 RDBE	$C_{12}H_{22}ClSO_3^-$	281.09837		6	1	2	42800	HOCl
	$C_{12}H_{22}BrSO_3^-$	325.04785		5	1	1	20400	HOCl
$C_{12}H_{25-n}X_nSO_3^-$ 0.5 RDBE	$C_{12}H_{23}Cl_2SO_3^-$	317.07504		3	6	4	88300	HOCl
	$C_{12}H_{23}Br_2SO_3^-$	406.97197*		6	1	0	4060	HOCl
	$C_{12}H_{23}BrClSO_3^-$	361.02453		4	5	3	64400	HOCl
$C_{12}H_{21-n}X_nSO_4^-$ 2.5 RDBE	$C_{12}H_{21}SO_4^-$	261.11660		6	12	7	268000	NH_2Cl
	$C_{12}H_{20}ClSO_4^-$	295.07763		0	3	3	67600	NH_2Cl
	$C_{12}H_{20}BrSO_4^-$	339.02712		0	12	8	16200	NH_2Cl
	$C_{12}H_{20}ISO_4^-$	387.01325		no I^-	4	3	25600	HOCl
$C_{12}H_{23-n}X_nSO_4^-$ 1.5 RDBE	$C_{12}H_{23}SO_4^-$***	263.13225	Dimer	14	14	12	2800000	HOCl
	$C_{12}H_{22}ClSO_4^-$	297.09328		9	17	13	282000	NH_2Cl
	$C_{12}H_{22}BrSO_4^-$	341.04277		8	11	11	321000	HOCl
	$C_{12}H_{22}ISO_4^-$	389.0289		no I^-	6	7	103000	HOCl
	$C_{12}H_{21}Cl_2SO_4^-$	331.05431		1	0	1	8940	NH_2Cl
	$C_{12}H_{21}Br_2SO_4^-$	420.95123*		0	4	4	11600	HOCl
$C_{12}H_{25-n}X_nSO_4^-$ 0.5 RDBE	$C_{12}H_{24}ClSO_4^-$	299.10893	Dimer	7	16	5	2390000	HOCl
	$C_{12}H_{24}BrSO_4^-$	343.05842	Dimer	3	6	7	13800000	HOCl
	$C_{12}H_{24}ISO_4^-$	391.04455		no I^-	2	2	14400	NH_2Cl
	$C_{12}H_{23}Cl_2SO_4^-$	333.06996		12	20	8	93700	NH_2Cl
	$C_{12}H_{23}Br_2SO_4^-$	422.96688*		0	7	7	426000	HOCl
	$C_{12}H_{23}BrClSO_4^-$	377.01944		0	15	13	61300	HOCl

(Table C.6 continued)

Class $[M-H]^-$ Ring/Double Bond Equivalence (RDBE)	$[M-H]^-$ Formula	Theoretical *m/z*	Dimer/ double charge	Number of Isomers: C_{12} Olefin Sulfonate + Br^- + HOCl	Number of Isomers: Raw Feed + HOCl	Number of Isomers: Raw Feed + NH_2Cl	Maximum Abundance	Highest Abundance Sample
$C_{12}H_{23-n}X_nSO_5^-$ 1.5 RDBE	$C_{12}H_{23}SO_5^-$	279.12717		14	20	18	439000	HOCl
	$C_{12}H_{22}ClSO_5^-$	313.08820		1	12	8	65900	NH_2Cl
	$C_{12}H_{22}BrSO_5^-$	357.03768		0	17	14	70300	HOCl
	$C_{12}H_{22}ISO_5^-$	405.02381		no I^-	7	5	21700	HOCl
	$C_{12}H_{21}BrClSO_5^-$	390.99871		0	2	2	14900	NH_2Cl
$C_{12}H_{25-n}X_nSO_5^-$ 0.5 RDBE	$C_{12}H_{25}SO_5^-$***	281.14282		13	15	19	1920000	HOCl
	$C_{12}H_{24}ClSO_5^-$	315.10385		7	24	21	85900	NH_2Cl
	$C_{12}H_{24}BrSO_5^-$	359.05333		5	22	18	309000	NH_2Cl
	$C_{12}H_{24}ISO_5^-$	407.03946		no I^-	8	7	8610	HOCl
$C_{12}H_{23-n}X_nS_2O_6^-$ 1.5 RDBE	$C_{12}H_{22}ClS_2O_6^-$	361.05518		17	11	5	128000	NH_2Cl
	$C_{12}H_{22}BrS_2O_6^-$	405.00467		17	14	15	706000	HOCl
$C_{12}H_{23-n}X_nS_2O_7^-$ 1.5 RDBE	$C_{12}H_{22}BrS_2O_7^-$	420.99958		0	13	13	23000	HOCl
$C_{12}H_{25-n}X_nS_2O_7^-$ 0.5 RDBE	$C_{12}H_{24}ClS_2O_7^-$	379.06575	Double charge	0	0	1	*1660***	*HOCl*
	$C_{12}H_{24}BrS_2O_7^-$	423.01523	Double charge	0	2	2	17500**	HOCl
$C_{12}H_{22-n}X_nNSO_3^-$ 2.5 RDBE	$C_{12}H_{22}NSO_3^-$	260.13259		0	0	8	130000	NH_2Cl
	$C_{12}H_{21}ClNSO_3^-$	294.09362		0	0	1	2100	NH_2Cl
$C_{12}H_{24-n}X_nNSO_3^-$ 1.5 RDBE	$C_{12}H_{24}NSO_3^-$	262.14824		0	0	1	4690	NH_2Cl
	$C_{12}H_{23}ClNSO_3^-$	296.10927		0	0	2	*1620*	*NH_2Cl*

(Table C.6 continued)

Class $[M-H]^-$ Ring/Double Bond Equivalence (RDBE)	$[M-H]^-$ Formula	Theoretical *m/z*	Dimer/ double charge	Number of Isomers: C_{12} Olefin Sulfonate + Br^- + HOCl	Number of Isomers: Raw Feed + HOCl	Number of Isomers: Raw Feed + NH_2Cl	Maximum Abundance	Highest Abundance Sample
$C_{12}H_{22-n}X_nNSO_4^-$ 2.5 RDBE	$C_{12}H_{22}NSO_4^-$	276.12750		0	0	3	28100	NH_2Cl
	$C_{12}H_{21}BrNSO_4^-$	354.03801		0	0	4	11500	NH_2Cl
	$C_{12}H_{21}ClNSO_4^-$	310.08853		0	0	1	3690	NH_2Cl
$C_{12}H_{24-n}X_nNSO_4^-$ 1.5 RDBE	$C_{12}H_{24}NSO_4^-$	278.14315		0	0	3	9470	NH_2Cl

[a] XIC, within 3 mmu of theoretical m/z above 2000 height; [b] Exhibited at least a doubling in signal from undisinfected; * A+2; **abundance from XIC of doubly charged molecular ion; not every isomer doubly-charges; *** some isomers existed in raw feed before disinfection, but most at least doubled post-disinfection.

Table C.7. LC_{50} and CTI Values for Waters

Sample	LC_{50} (concentration factor)	Cytotoxicity Index (CTI)
Field Blank	48.3 ± 1.5	20.9 ± 0.7
Raw Feed	1.77 ± 0.05	571 ± 17
Pretreated	2.13 ± 0.04	469 ± 27
HOCl Field Blank	49.7± 1.5	20.3 ± 0.7
HOCl Raw Feed	0.125 ± 0.002	8000 ± 97
HOCl Pretreated	0.149 ± 0.001	6725 ± 46
NH_2Cl Field Blank	40.2 ± 0.8	24.9 ± 0.5
NH_2Cl Raw Feed	0.068 ± 0.002	14788 ± 383
NH_2Cl Pretreated	0.085 ± 0.002	11906 ± 299

Notes: Concentration factors incorporate the 10-fold dilution performed and thus represent concentration factor of the *undiluted* sample. LC_{50} concentration factors <1 indicate that samples required dilution, rather than further concentration, to induce quantifiable cytotoxic effects.

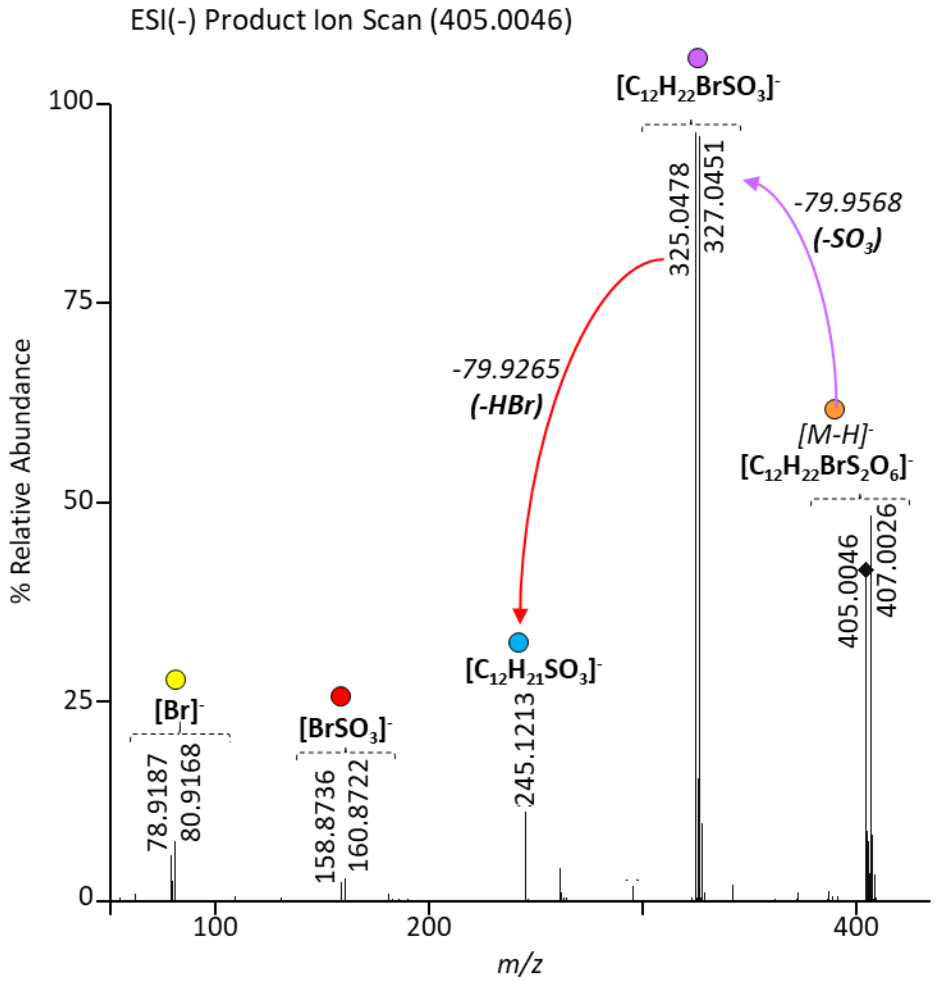

$C_{12}H_{22}BrS_2O_6^-$

Theoretical $[M-H]^-$: 405.0047 Da

m/z	m/z (Calc)	Formula & Ion Species	Diff (ppm)
78.9187	78.9189	[Br]-	2.53
80.9168	80.9169	[Br]-	1.24
158.8736	158.8752	[Br O3 S]-	9.84
160.8722	160.8732	[Br O3 S]-	6.22
245.1213	245.1217	[C12 H21 O3 S]-	1.50
325.0478	325.0479	[C12 H22 Br O3 S]-	0.19
327.0451	327.0458	[C12 H22 Br O3 S]-	2.35
328.0492	328.0490	[C12 H22 Br O3 S]-	-0.74
405.0046	405.0047	[C12 H22 Br O6 S2]-	0.24
407.0023	407.0026	[C12 H22 Br O6 S2]-	0.62

Loss Da (Obs)	Loss Da (Calc)	Loss Formula	Diff (ppm)
79.9568	79.9568	-SO3	0.18
79.9265	79.9262	-HBr	-4.22

Figure C.1. LC-QTOF MS/MS product ion scan of precursor ion *m/z* 405.0046 ($C_{12}H_{22}Br_2S_2O_6^-$).

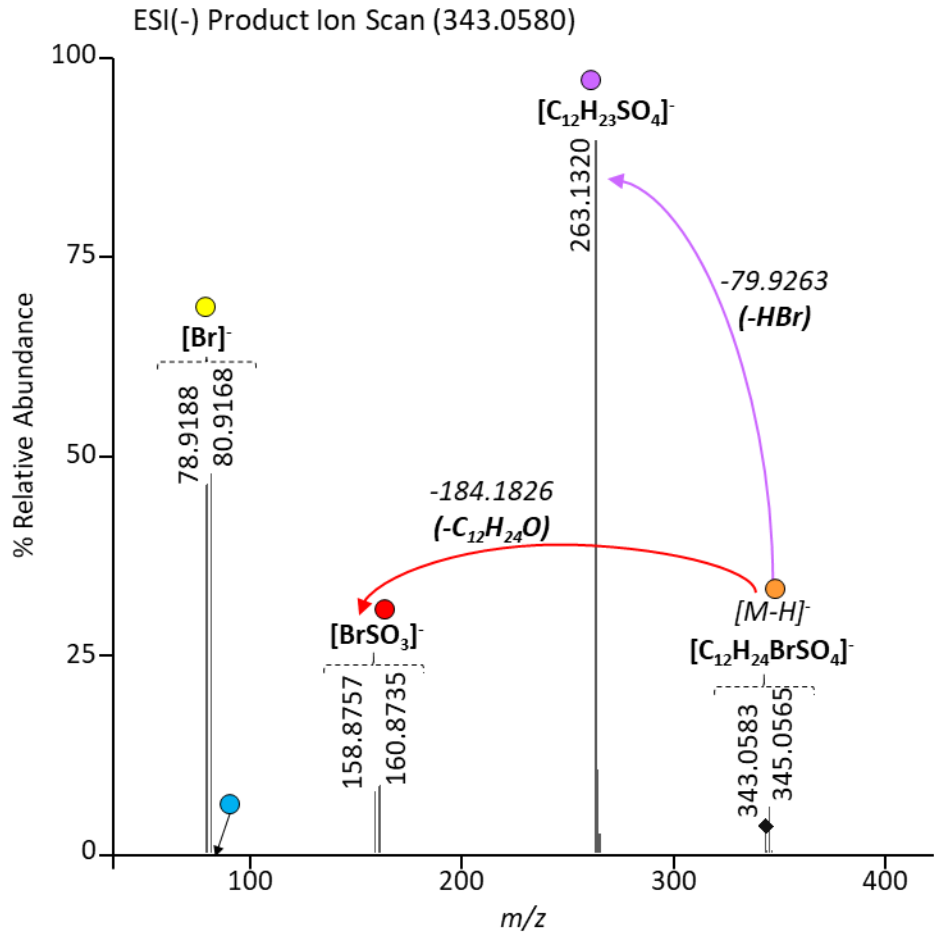

$C_{12}H_{24}BrSO_4^-$

Theoretical [M-H]⁻: 343.0584 Da

4 isomers

m/z (Obs)	m/z (Calc)	Formula & Ion Species	Diff (ppm)
78.9188	78.9189	[Br]-	1.27
80.9168	80.9169	[Br]-	1.24
80.9652	80.9652	[H O3 S]-	-0.43
158.8757	158.8757	[Br O3 S]-	0.08
160.8735	160.8736	[Br O3 S]-	0.55
263.1320	263.1323	[C12 H23 O4 S]-	0.89
264.1356	264.1355	[C12 H23 O4 S]-	-0.42
265.1309	265.1308	[C12 H23 O4 S]-	-0.40
343.0583	343.0584	[C12H24O4SBr]-	0.29
345.0565	345.0564	[C12H24O4SBr]-	-0.29

Loss Da (Obs)	Loss Da (Calc)	Loss Formula	Diff (ppm)
79.9263	79.9262	-HBr	-1.25
184.1826	184.1827	-C12H24O	0.54

Figure C.2. LC-QTOF MS/MS product ion scan of precursor ion *m/z* 343.0583 ($C_{12}H_{24}BrSO_4^-$).

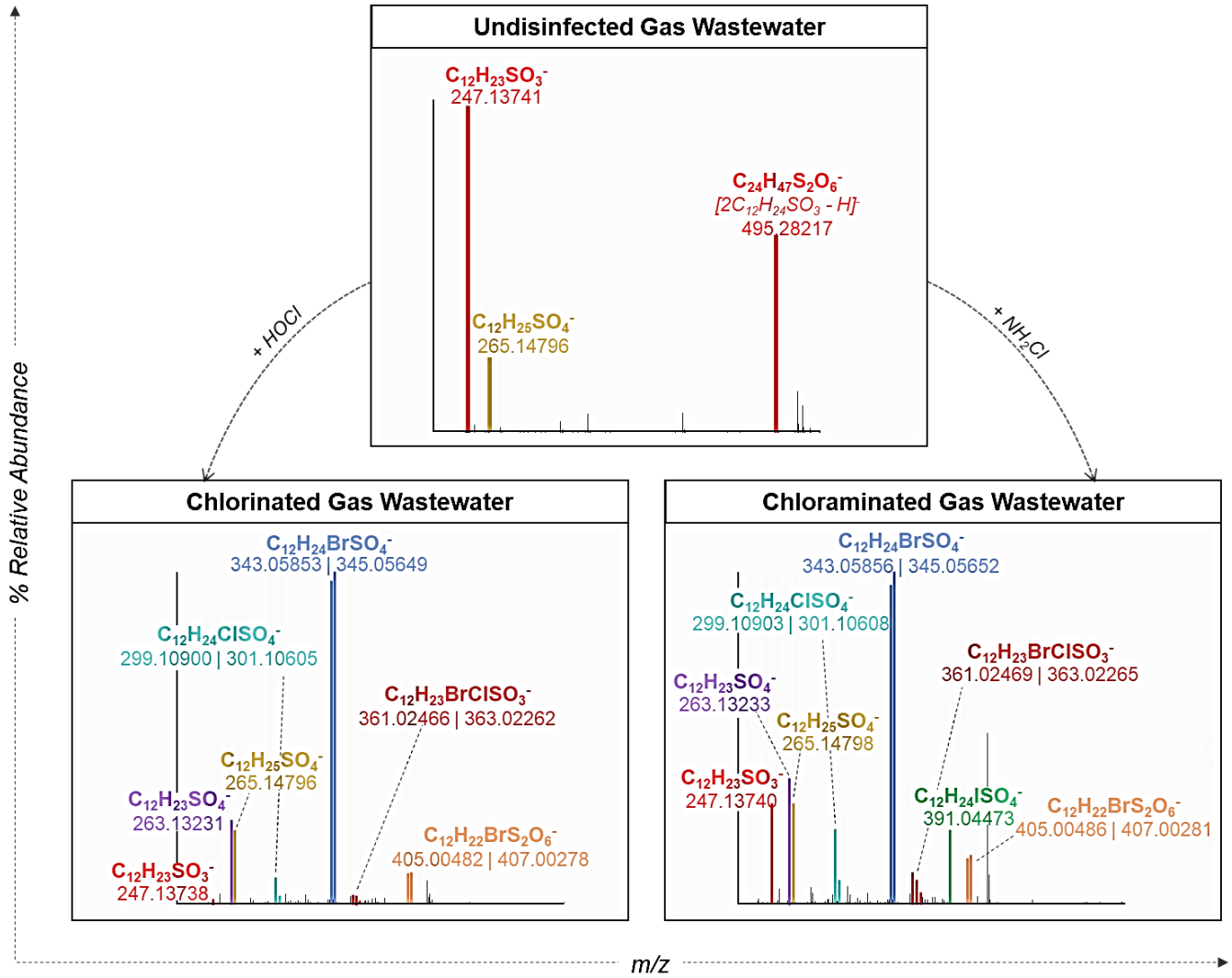

Figure C.3. FT-ICR MS scan of undisinfected (top), chlorinated (bottom left), and chloraminated (bottom right) RF wastewater.

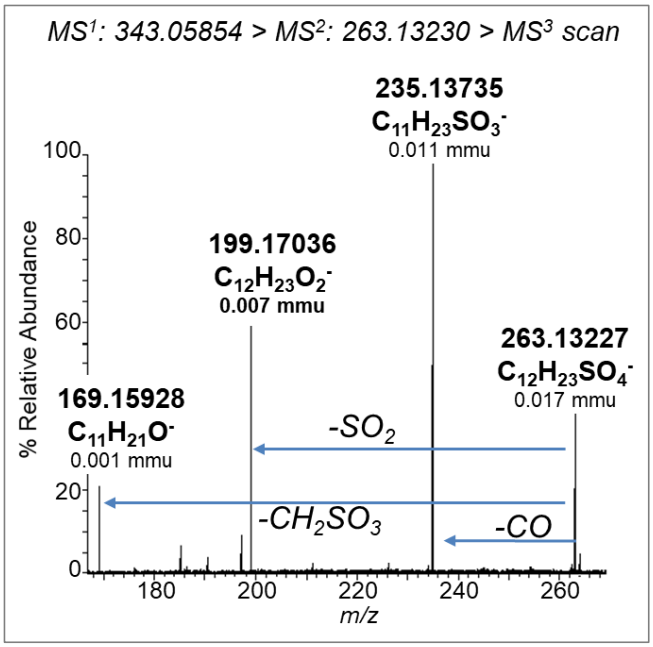

Figure C.4. FT-ICR MS^3 mass spectrum of $C_{12}H_{24}BrSO_4^-$ (*m/z* 343.05854) after loss of HBr (*m/z* 263.13230).

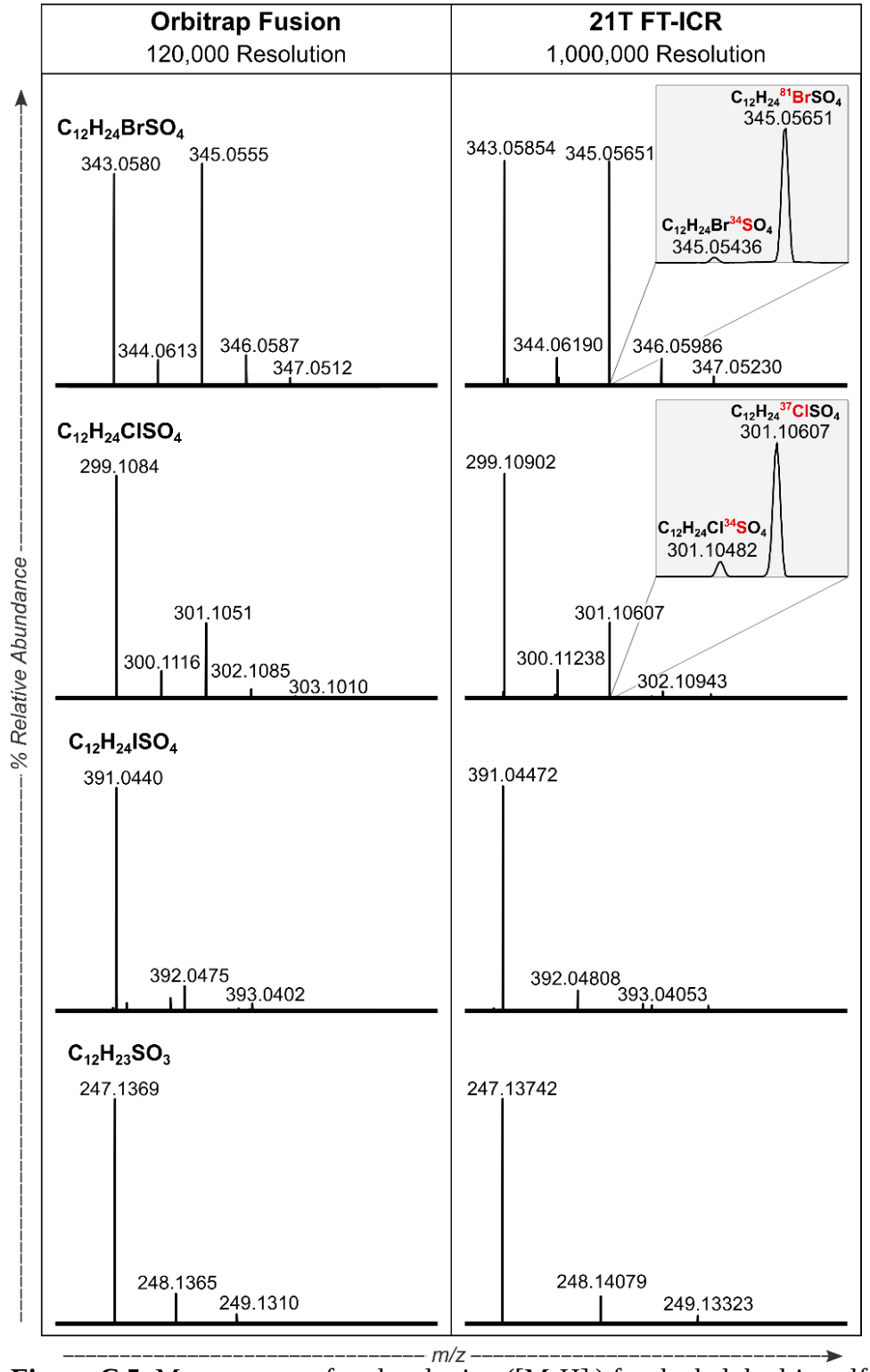

Figure C.5. Mass spectra of molecular ion ([M-H]$^-$) for the halohydrin sulfonate by-products and suspected olefin sulfonate precursor obtained from different high resolution systems.

Note: Insets depict a zoomed-in view of the A+2 m/z to show the resolved peaks pertaining to the heavy halogen vs. sulfur atoms.

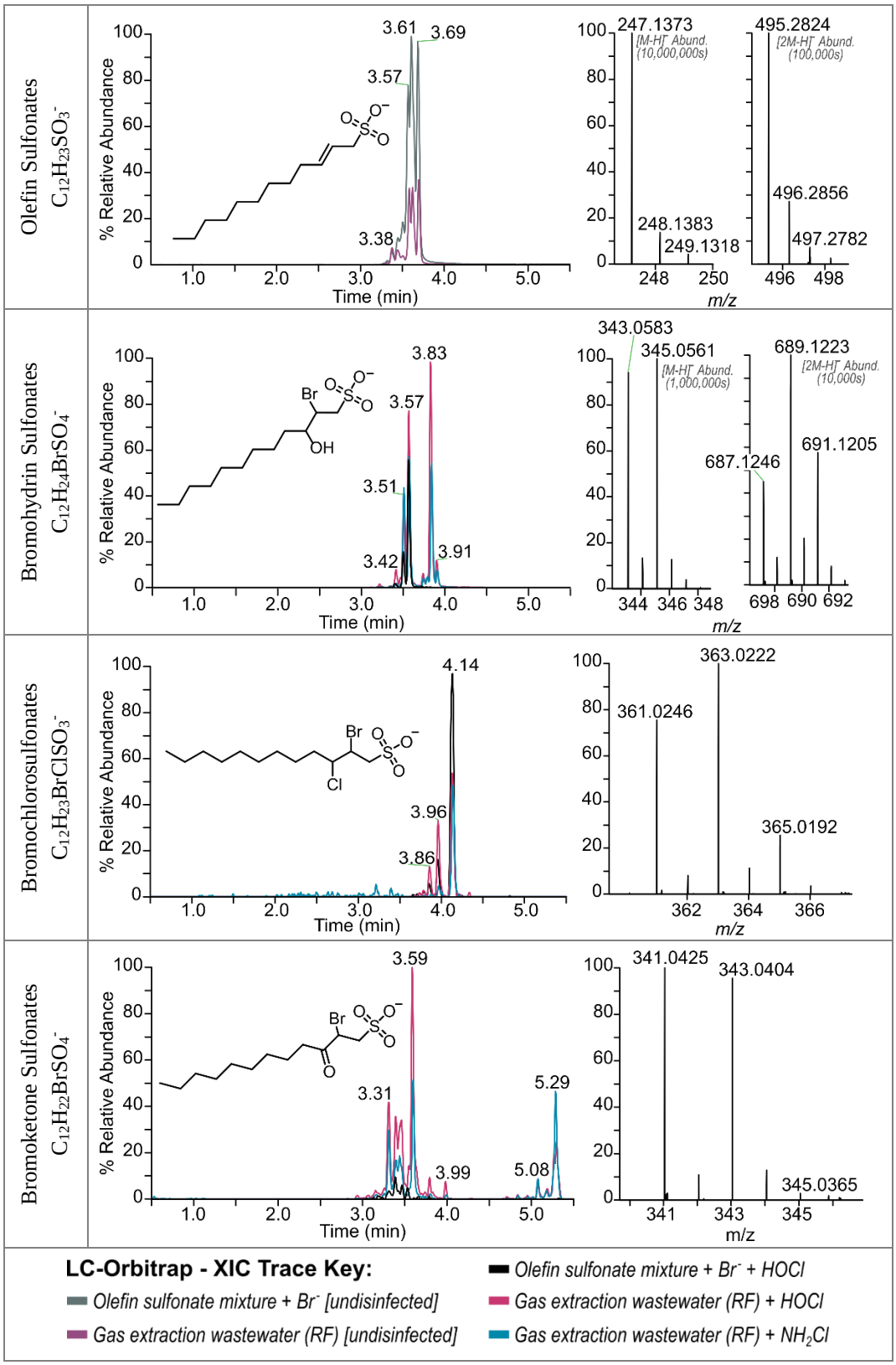

Figure C.6. Extracted ion chromatograms (XICs) and molecular ions, including $[2M-H]^-$, for olefin sulfonate precursor and its major DBPs formed during disinfection.

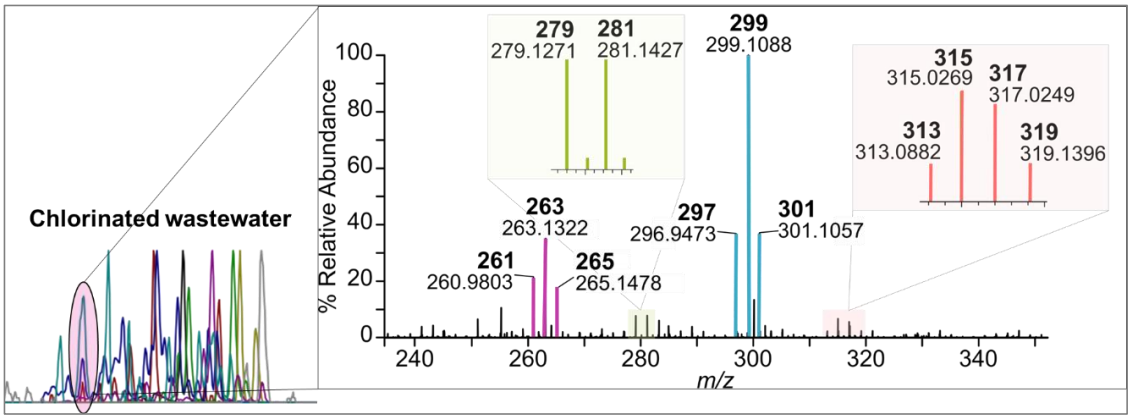

Figure C.7. Mass spectrum of chlorinated RF at 2.90 min, highlighting faux halogen patterns that could have led to misidentification by unit-resolution analyses.

APPENDIX D

SUPPORTING INFORMATION FOR:

ARE COAL-FIRED POWER PLANTS A THREAT TO DOWNSTREAM DRINKING WATER? THE IMPACT OF BROMIDE AND IODIDE ON EMERGING DISINFECTION BY-PRODUCTS

Table D.1. Analytes, Vendors, Calibration Range, and Ions Monitored for DBPs Quantified.

Class	DBP	Abbrev.	Vendor	RT (min)	Quant *m/z*	Qual *m/z*	Lowest cal. (ppb)
Internal Standard	1,2-Dibromopropane	12DBP	Sigma Aldrich	7.591	121	123	
Trihalomethanes (THMs)	Trichloromethane (Chloroform)	TCM	Sigma Aldrich	3.701	83	85	0.1
	Bromodichloromethane	BDCM	Sigma Aldrich	4.202	83	129	0.1
	Dibromochloromethane	DBCM	Sigma Aldrich	5.529	129	127	0.5
	Tribromomethane (Bromoform)	TBM	Sigma Aldrich	7.383	173	252	0.1
Iodo-Trihalomethanes (I-THMs)	Dichloroiodomethane	DCIM	CanSyn Chem. Corp.	5.993	83	126.9	0.05
	Bromochloroiodomethane	BCIM	CanSyn Chem. Corp.	7.942	128.9	126.9	0.025
	Dibromoiodomethane	DBIM	CanSyn Chem. Corp.	9.743	172.8	299.7	0.005
	Chlorodiiodomethane	CDIM	CanSyn Chem. Corp.	10.23	174.9	126.9	0.025
	Bromodiiodomethane	BDIM	CanSyn Chem. Corp.	11.958	218.8	220.8	0.025
	Triiodomethane (Iodoform)	TIM	Sigma Aldrich	13.885	266.8	393.7	0.025
Trihaloacetaldehydes (HALs)	Trichloroacetaldehyde (Chloral hydrate)	TCAL	Sigma Aldrich	5.125	82	110.9	0.0125
	Bromodichloroacetaldehyde	BDCAL	CanSyn Chem. Corp.	7.121	111	83, 163.8	0.0125
	Dibromochloroacetaldehyde	DBCAL	CanSyn Chem. Corp.	9.184	128.9	127.9	0.0125
	Tribromoacetaldehyde (Bromal hydrae)	TBAL	Sigma Aldrich	11.052	172.8	171.8	0.005

(Table D.1 continued)

Class	DBP	Abbrev.	Vendor	RT (min)	Quant *m/z*	Qual *m/z*	Lowest cal. (ppb)
Haloketones (HKs)	Chloropropanone	CP	Sigma Aldrich	6.521	92	43	0.25
	1,1-Dichloropropanone	11DCP	Sigma Aldrich	6.436	83	43	0.1
	1,3-Dichloropropanone	13DCP	CanSyn Chem. Corp.	10.832	77	49	0.025
	1,1-Dibromopropanone	11DBP	CanSyn Chem. Corp.	10.139	215.9	43	0.025
	1,1,1-Trichloropropanone	111TCP	Sigma Aldrich	8.618	43	125	0.1
	1,1,3-Trichloropropanone	113TCP	Sigma Aldrich	11.867	77	83	0.05
	1-Bromo-1,1-dichloropropanone	1B11DCP	CanSyn Chem. Corp.	10.745	125	43	0.0125
	1,1,3,3-Tetrachloropropanone	1133TeCP	CanSyn Chem. Corp.	12.749	83	85	0.0125
	1,1,3,3-Tetrabromopropanone	1133TeBP	Aldlab Chemicals	17.968	200.8	119.9	0.0125
Halonitromethanes (HNMs)	Dichloronitromethane	DCNM	CanSyn Chem. Corp.	6.599	83	85	0.0125
	Bromochloronitromethane	BCNM	CanSyn Chem. Corp.	8.631	129	127	0.0125
	Dibromonitromethane	DBNM	CanSyn Chem. Corp.	10.421	172.8	171	0.005
	Trichloronitromethane (Chloropicrin)	TCNM	Sigma Aldrich	6.55	116.9	119	0.005
	Bromodichloronitromethane	BDCNM	CanSyn Chem. Corp.	8.491	163	161	0.1
	Dibromochloronitromethane	DBCNM	CanSyn Chem. Corp.	10.559	206.8	209	0.1
	Tribromonitromethane (Bromopicrin)	TBNM	CanSyn Chem. Corp.	12.429	253	251	0.1

(Table D.1 continued)

Class	DBP	Abbrev.	Vendor	RT (min)	Quant *m/z*	Qual *m/z*	Lowest cal. (ppb)
Haloacetonitriles (HANs)	Chloroacetonitrile	CAN	Sigma Aldrich	6.011	75	48	1
	Bromoacetonitrile	BAN	Sigma Aldrich	8.17	118.9	120.9	1
	Iodoacetonitrile	IAN	Sigma Aldrich	10.824	167	126.9	0.0125
	Dichloroacetonitrile	DCAN	Sigma Aldrich	5.766	74	82	0.0125
	Bromochloroacetonitrile	BCAN	Sigma Aldrich	7.951	155	74	0.025
	Dibromoacetonitrile	DBAN	Sigma Aldrich	10.084	117.9	199	0.0125
	Trichloroacetonitrile	TCAN	Sigma Aldrich	4.434	108	110	0.0125
	Bromodichloroacetonitrile	BDCAN	CanSyn Chem. Corp.	6.115	154	108	0.1
	Dibromochloroacetonitrile	DBCAN	CanSyn Chem. Corp.	8.512	154	152	0.1
	Tribromoacetonitrile	TBAN	CanSyn Chem. Corp.	10.785	197.8	195.8	0.1

(Table D.1 continued)

Class	DBP	Abbrev.	Vendor	RT (min)	Quant *m/z*	Qual *m/z*	Lowest cal. (ppb)
Haloacetamides (HAMs)	Dichloroacetamide	DCAM	TCI America	13.893	44	127	0.1
	Bromochloroacetamide	BCAM	CanSyn Chem. Corp.	15.244	44	173	0.1
	Dibromoacetamide	DBAM	CanSyn Chem. Corp.	16.492	44	217	0.1
	Trichloroacetamide	TCAM	Sigma Aldrich	15.679	44	82	0.0125
	Bromodichloroacetamide	BDCAM	CanSyn Chem. Corp.	17.003	44	128	0.025
	Dibromochloroacetamide	DBCAM	CanSyn Chem. Corp.	18.246	44	128	0.05
	Tribromoacetamide	TBAM	CanSyn Chem. Corp.	19.428	44	295	0.025
	Chloroiodoacetamide	CIAM	CanSyn Chem. Corp.	16.997	92	219	0.25
	Bromoiodoacetamide	BIAM	CanSyn Chem. Corp.	18.143	136	138	0.25
	Diiodoacetamide	DIAM	CanSyn Chem. Corp.	19.782	184	311	0.1

Table D.2. Sample Characteristics from 2017 and 2018 Samplings

Sample	Year	Distance from discharge (mi)[a]	TOC[b] (mg/L as C)	TN (mg/L as N)	$SUVA_{254}$ (L/mg-m)	Bromide (µg/L)	Iodide (µg/L)
Upstream River	2017	-2.8	1.17	0.320	4.0	11.6	31.8
	2018		1.86	0.521	4.5	11.3	24.4
Upstream Tributary	2017	-0.6[c]	1.86	0.403	3.6	26.4	33.2
	2018		2.46	0.635	3.7	25.9	17.8
Discharge	2017	0.0	3.36	0.703	1.1	10,468	843
	2018		3.21	1.413	1.1	5,436	578
Downstream River 1	2017	2.1	1.41	0.411	3.5	362	74.8
	2018		2.01	0.538	3.9	27.5	13.3
Downstream River 2 (Plant A Intake)	2017	12.2	1.43	0.413	3.4	282	60.5
	2018		1.71	0.568	3.9	35.3	29.9
Downstream Tributary 1	2017	12.6[c]	1.07	0.374	4.7	29.6	29.9
	2018		1.21	0.307	4.4	51.4	41.2
Downstream River 3 (Plant B Intake)	2017	30.8	1.42	0.352	3.5	194	49.3
	2018		1.59	0.468	4.6	40.7	37.2
Downstream Tributary 2	2017	31.8[c]	1.39	0.50	3.1	20.6	31.1
	2018		1.40	0.276	3.6	15.8	31.1
Downstream River 4	2017	32.5	1.56	0.381	3.2	144	42.0
	2018		1.57	0.365	3.8	31.6	65.0
Plant B Settled[*]	2018	31.3	1.30	0.334	3.0	56.6	ND

[a]Negative distances represent samples upstream of the discharge site, while positive represent downstream; [b]TOC measured as non-purgeable organic carbon (NPOC); [c]Distance shown for tributaries is distance from the discharge site to the river's junction with the tributary; the upstream tributary was sampled from a bridge approximately 4.5 miles upstream of its junction with the river, while downstream tributaries were sampled within 0.8 miles upstream of their junction with the river; ND = not detected.

Table D.3. GC Methods for (1) Bromo-Trihalo-HANs and –HAMs and (2) Other DBPs ("Main List")

	Parameter	Br-Trihalo-N-DBPs (1)	Main List (2)
Inlet Program	Injection Mode, Volume	Splitless, 1 uL	Splitless, 1 uL
	Init. Temp., Hold Time	125, 13	250
	Temp. Ramp	720/min	n/a
	Final Temp., Hold Time	250, 5	250
Column Specs	Type	Rtx-200	Rtx-200
	Length	30	30
	Inner Diameter	250 um	250 um
	Film Thickness	0.25 um	0.25 um
Oven Program	Column Flow	1.3 mL/min	1.3
	Init. Temp., Hold Time	35, 5	35, 5
	Temp. Ramp 1	9/min	9/min
	Temp. 2, Hold Time	200, 0	220, 0
	Temp. Ramp 2	20/min	20/min
	Final Temp., Hold Time	250, 20	280, 20
MS Program	Transfer Line Temp.	225	290
	Source Temp.	200	200
	Electron Energy	70	70
	Quad Temp.	150	150

Table D.4. Individual DBP Formation (µg/L, average ± SE) from Chlorination (HOCl) and Chloramination (NH_2Cl) with and without Coal-Fired Power Plant Wastewater "Impact"[a]

Class	DBP	HOCl	HOCl "Impacted"	NH_2Cl	NH_2Cl "Impacted"
THMs	TCM	[49.961 ± 4.363]	18.014 ± 0.709	0.204 ± 0.035	0.194 ± 0.030
	BDCM	28.867 ± 1.488	[45.689 ± 1.255]	0.146 ± 0.013	0.247 ± 0.003
	DBCM	7.720 ± 0.295	[41.101 ± 1.139]	(0.086 ± 0.002)	0.146 ± 0.002
	TBM	0.365 ± 0.018	10.077 ± 0.145	(0.085 ± 0.002)	0.120 ± 0.001
I-THMs	DCIM	0.464 ± 0.009	0.786 ± 0.035	0.323 ± 0.019	1.074 ± 0.052
	BCIM	0.098 ± 0.003	0.419 ± 0.004	0.113 ± 0.009	1.243 ± 0.070
	DBIM	0.0618 ± 0.0004	0.177 ± 0.002	0.083 ± 0.001	0.876 ± 0.030
	CDIM	<0.025	0.136 ± 0.004	ND	1.156 ± 0.034
	BDIM	<0.025	0.115 ± 0.001	0.120 ± 0.003	2.351 ± 0.050
	TIM	<0.025	0.529 ± 0.004	ND	1.976 ± 0.027
HALs	TCAL	4.089 ± 0.526	2.213 ± 0.170	0.080 ± 0.029	0.029 ± 0.004
	BDCAL	2.262 ± 0.274	4.252 ± 0.214	0.074 ± 0.020	0.093 ± 0.013
	DBCAL	0.611 ± 0.065	2.653 ± 0.097	0.064 ± 0.003	0.212 ± 0.035
	TBAL	0.026 ± 0.001	0.195 ± 0.000	0.054 ± 0.003	0.169 ± 0.008
HKs	13DCP	0.134 ± 0.015	0.133 ± 0.012	0.187 ± 0.066	0.426 ± 0.180
	1B11DCP	0.101 ± 0.002	0.210 ± 0.007	<0.0125	ND
	1133TeCP	0.115 ± 0.015	0.060 ± 0.005	0.224 ± 0.057	0.307 ± 0.019
	1133TeBP	<0.0125	0.117 ± 0.002	0.107 ± 0.011	0.816 ± 0.061
HANs	DCAN	1.209 ± 0.058	0.492 ± 0.006	0.265 ± 0.040	0.243 ± 0.005
	BCAN	1.914 ± 0.057	2.936 ± 0.054	0.225 ± 0.005	0.777 ± 0.022
	DBAN	0.668 ± 0.028	3.442 ± 0.037	0.081 ± 0.004	0.359 ± 0.015
	TCAN	0.067 ± 0.006	0.014 ± 0.002	<0.0125	ND
	BDCAN	0.612 ± 0.002	0.560 ± 0.001	ND	ND
	DBCAN	0.720 ± 0.007	0.815 ± 0.009	ND	ND
	TBAN	0.692 ± 0.005	1.243 ± 0.017	<0.1	ND

(Table D.4 continued)

Class	DBP	HOCl	HOCl "Impacted"	NH_2Cl	NH_2Cl "Impacted"
HNMs	TCNM	0.215 ± 0.016	0.042 ± 0.002	0.267 ± 0.045	0.206 ± 0.004
	BCNM	0.009 ± 0.001	0.015 ± 0.001	0.091 ± 0.009	0.113 ± 0.001
	DBNM	0.007 ± 0.001	0.050 ± 0.004	0.057 ± 0.002	0.164 ± 0.007
	BDCNM	0.523 ± 0.010	0.438 ± 0.004	(0.049 ± 0.011)	0.247 ± 0.005
	DBCNM	0.726 ± 0.018	1.198 ± 0.025	(0.041 ± 0.005)	0.357 ± 0.009
	TBNM	<0.1	1.909 ± 0.045	ND	0.197 ± 0.001
HAMs	DCAM	1.032 ± 0.081	0.730 ± 0.035	0.729 ± 0.270	0.604 ± 0.050
	BCAM	1.235 ± 0.039	1.775 ± 0.127	0.283 ± 0.080	0.585 ± 0.048
	TCAM	0.224 ± 0.015	0.118 ± 0.012	<0.0125	ND
	DBAM	0.781 ± 0.036	2.335 ± 0.075	<0.1	0.658 ± 0.058
	BDCAM	0.477 ± 0.011	0.527 ± 0.008	<0.025	ND
	DBCAM	0.191 ± 0.006	0.708 ± 0.019	<0.05	ND
	TBAM	0.088 ± 0.004	0.525 ± 0.004	<0.025	ND
	CIAM	<0.25	ND	ND	0.518 ± 0.049
	BIAM	<0.25	ND	ND	0.443 ± 0.019
	DIAM	<0.1	ND	ND	0.788 ± 0.114

[a] [ ] = above highest calibration point, 30 µg/L; ( ) = below lowest calibration point for compound, 0.1 µg/L; ND = not detected

Table D.5. Sample t-test Results for the Impact of Coal-Fired Power Plant Wastewater (CFPP WW) on DBP Formation During Chlor(am)ination[a]

Class	DBP	Chlorination (HOCl)			Chloramination (NH_2Cl)		
		h	p	CFPP WW Impact on Formation	h	p	CFPP WW Impact on Formation
THMs	TCM	1	0.016	Decrease	0	0.840	n/a
	BDCM	1	<0.001	Increase	1	0.013	Increase
	DBCM	1	<0.001	Increase	1	<0.001	Increase
	TBM	1	<0.001	Increase	1	<0.001	Increase
I-THMs	DCIM	1	<0.001	Increase	1	<0.001	Increase
	BCIM	1	<0.001	Increase	1	0.003	Increase
	DBIM	1	<0.001	Increase	1	0.001	Increase
	CDIM	1	<0.001	Increase	1	<0.001	Increase
	BDIM	1	<0.001	Increase	1	<0.001	Increase
	TIM	1	<0.001	Increase	1	<0.001	Increase
HALs	TCAL	1	0.042	Decrease	0	0.100	n/a
	BDCAL	1	<0.001	Increase	0	0.230	n/a
	DBCAL	1	<0.001	Increase	1	0.018	Increase
	TBAL	1	<0.001	Increase	1	<0.001	Increase
HKs	13DCP	0	0.930	n/a	0	0.097	n/a
	1B11DCP	1	<0.001	Increase	n/a	n/a	n/a
	1133TeCP	1	0.003	Increase	0	0.076	n/a
	1133TeBP	1	<0.001	Increase	1	0.002	Increase
HANs	DCAN	1	0.006	Decrease	0	0.650	n/a
	BCAN	1	<0.001	Increase	1	0.001	Increase
	DBAN	1	<0.001	Increase	1	<0.001	Increase
	TCAN	1	<0.001	Decrease	n/a	n/a	n/a
	BDCAN	1	<0.001	Increase	n/a	n/a	n/a
	DBCAN	1	0.001	Increase	n/a	n/a	n/a
	TBAN	1	<0.001	Increase	n/a	n/a	n/a
HNMs	TCNM	1	0.008	Decrease	0	0.300	n/a
	BCNM	1	0.003	Increase	0	0.140	n/a
	DBNM	1	<0.001	Increase	1	<0.001	Increase
	BDCNM	1	0.002	Decrease	1	<0.001	Increase
	DBCNM	1	<0.001	Increase	1	<0.001	Increase
	TBNM	1	<0.001	Increase	1	<0.001	Increase

(Table D.5 continued)

Class	DBP	Chlorination (HOCl)			Chloramination (NH_2Cl)		
		h	p	CFPP WW Impact on Formation	h	p	CFPP WW Impact on Formation
HAMs	DCAM	1	0.004	Decrease	0	0.510	n/a
	BCAM	1	0.002	Increase	1	0.005	Increase
	TCAM	1	<0.001	Decrease	n/a	n/a	n/a
	DBAM	1	<0.001	Increase	1	<0.001	Increase
	BDCAM	1	0.003	Increase	n/a	n/a	n/a
	DBCAM	1	<0.001	Increase	n/a	n/a	n/a
	TBAM	1	<0.001	Increase	n/a	n/a	n/a
	CIAM	n/a	n/a	n/a	1	<0.001	Increase
	BIAM	n/a	n/a	n/a	1	<0.001	Increase
	DIAM	n/a	n/a	n/a	1	<0.001	Increase

[a] Two sample t-tests (95% confidence) for (1) HOCl vs. HOCl "Impacted" and (2) NH_2Cl vs. NH_2Cl "Impacted"; h = 0: no significant difference with/without wastewater; h = 1: significant difference; p-values ≤0.05 indicate a significant difference and p-values >0.05 indicate no significant difference at 95% confidence level

Table D.6. Individual DBP and Class Sum Formation (nM, Average ± SE) from Chlorination (HOCl) and Chloramination (NH_2Cl) with and without Coal-Fired Power Plant Wastewater "Impact"

Class	DBP	Molar Mass	HOCl	HOCl "Impacted"	NH_2Cl	NH_2Cl "Impacted"
THMs	TCM	119.38	418.51 ± 36.54	150.89 ± 5.94	1.71 ± 0.29	1.63 ± 0.25
	BDCM	163.83	176.20 ± 9.08	278.88 ± 7.66	0.89 ± 0.08	1.50 ± 0.02
	DBCM	208.28	37.07 ± 1.42	197.34 ± 5.47	0.41 ± 0.01	0.70 ± 0.01
	TBM	252.73	1.44 ± 0.07	39.87 ± 0.57	0.34 ± 0.01	0.48 ± 0.01
	∑THMs		*633.2 ± 37.7*	*667.0 ± 10.2*	*3.34 ± 0.30*	*4.31 ± 0.25*
I-THMs	DCIM	210.83	2.20 ± 0.04	3.73 ± 0.16	1.53 ± 0.09	5.09 ± 0.25
	BCIM	255.28	0.39 ± 0.01	1.64 ± 0.02	0.44 ± 0.04	4.87 ± 0.28
	DBIM	299.73	0.21 ± 0.00	0.59 ± 0.01	0.28 ± 0.00	2.92 ± 0.10
	CDIM	302.28	ND	0.45 ± 0.01	ND	3.83 ± 0.11
	BDIM	346.73	ND	0.33 ± 0.00	0.35 ± 0.01	6.78 ± 0.14
	TIM	393.73	ND	1.34 ± 0.01	ND	5.02 ± 0.07
	∑I-THMs		*2.79 ± 0.04*	*8.08 ± 0.17*	*2.60 ± 0.10*	*28.51 ± 0.40*
HALs	TCAL	147.39	27.74 ± 3.57	15.02 ± 1.15	0.54 ± 0.19	0.19 ± 0.03
	BDCAL	191.84	11.79 ± 1.43	22.17 ± 1.11	0.38 ± 0.10	0.49 ± 0.07
	DBCAL	236.29	2.59 ± 0.28	11.23 ± 0.41	0.27 ± 0.01	0.90 ± 0.15
	TBAL	280.74	0.09 ± 0.00	0.69 ± 0.00	0.19 ± 0.01	0.60 ± 0.03
	∑HALs		*42.21 ± 3.84*	*49.10 ± 1.60*	*1.39 ± 0.22*	*2.18 ± 0.08*
HKs	13DCP	126.97	1.06 ± 0.12	1.05 ± 0.09	1.47 ± 0.52	3.36 ± 1.41
	1B11DCP	205.87	0.49 ± 0.01	1.02 ± 0.03	ND	ND
	1133TeCP	195.86	0.59 ± 0.07	0.31 ± 0.02	1.14 ± 0.29	1.56 ± 0.10
	1133TeBP	373.66	ND	0.31 ± 0.01	0.29 ± 0.03	2.18 ± 0.16
	∑HKs		*2.14 ± 0.12*	*2.69 ± 0.10*	*2.90 ± 0.52*	*7.11 ± 1.41*

Table D.6 continued

Class	DBP	Molar Mass	HOCl	HOCl "Impacted"	NH_2Cl	NH_2Cl "Impacted"
HANs	DCAN	109.94	10.99 ± 0.53	4.48 ± 0.05	2.41 ± 0.36	2.21 ± 0.05
	BCAN	154.39	12.39 ± 0.37	19.02 ± 0.35	1.46 ± 0.03	5.04 ± 0.14
	DBAN	198.84	3.36 ± 0.14	17.31 ± 0.19	0.41 ± 0.02	1.81 ± 0.08
	TCAN	144.39	0.46 ± 0.04	0.10 ± 0.01	ND	ND
	BDCAN	188.84	3.24 ± 0.01	2.97 ± 0.00	ND	ND
	DBCAN	233.29	3.09 ± 0.03	3.49 ± 0.04	ND	ND
	TBAN	277.74	2.49 ± 0.02	4.47 ± 0.06	ND	ND
	∑HANs		*36.03 ± 0.66*	*51.84 ± 0.40*	*4.27 ± 0.36*	*9.05 ± 0.17*
HNMs	TCNM	164.38	1.31 ± 0.10	0.25 ± 0.01	1.62 ± 0.27	1.25 ± 0.02
	BCNM	174.38	0.05 ± 0.00	0.09 ± 0.00	0.52 ± 0.05	0.65 ± 0.01
	DBNM	218.83	0.03 ± 0.01	0.23 ± 0.02	0.26 ± 0.01	0.75 ± 0.03
	BDCNM	208.83	2.50 ± 0.05	2.10 ± 0.02	0.23 ± 0.05	1.18 ± 0.03
	DBCNM	253.28	2.86 ± 0.07	4.73 ± 0.10	0.16 ± 0.02	1.41 ± 0.04
	TBNM	297.73	ND	6.41 ± 0.15	ND	0.66 ± 0.00
	∑HNMs		*6.76 ± 0.11*	*13.81 ± 0.03*	*2.80 ± 0.28*	*5.91 ± 0.05*
HAMs	DCAM	127.96	8.07 ± 0.63	5.71 ± 0.28	5.70 ± 2.11	4.72 ± 0.39
	BCAM	172.41	7.16 ± 0.23	10.30 ± 0.74	1.64 ± 0.47	3.39 ± 0.28
	TCAM	162.40	1.38 ± 0.09	0.73 ± 0.08	ND	ND
	DBAM	216.86	3.60 ± 0.17	10.77 ± 0.34	ND	3.04 ± 0.27
	BDCAM	206.85	2.31 ± 0.05	2.55 ± 0.04	ND	ND
	DBCAM	251.30	0.76 ± 0.02	2.82 ± 0.08	ND	ND
	TBAM	295.76	0.30 ± 0.01	1.77 ± 0.01	ND	ND
	CIAM	219.41	ND	ND	ND	2.36 ± 0.22
	BIAM	263.86	ND	ND	ND	1.68 ± 0.07
	DIAM	310.86	ND	ND	ND	2.54 ± 0.37
	∑HAMs		*23.58 ± 0.70*	*34.64 ± 0.87*	*7.34 ± 2.16*	*17.73 ± 0.59*
All Classes	***∑DBPs***		***746.73 ± 37.86***	***827.14 ± 10.4***	***24.66 ± 2.30***	***74.79 ± 1.62***
	∑Unregulated		***113.50 ± 3.967***	***160.16 ± 1.88***	***21.31 ± 2.28***	***70.48 ± 1.60***

ND = not detected; *∑DBPs = ∑THMs + ∑I-THMs + ∑HALs + ∑HKs + ∑HANs + ∑HNMs + ∑HAMs; ∑Unregulated = ∑DBPs - ∑THMs*

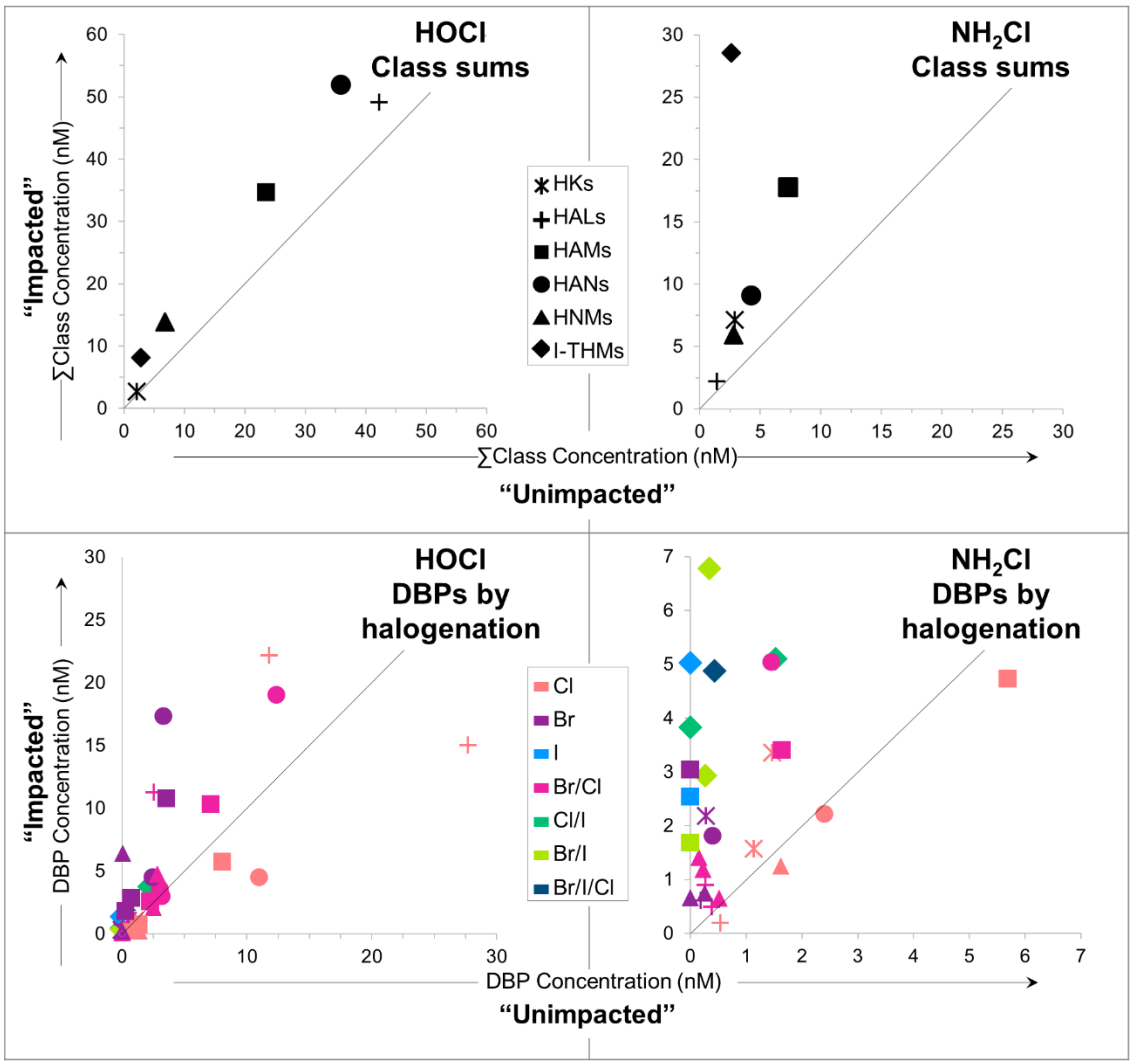

Figure D.1. Impacted vs. unimpacted concentrations of DBPs by class sums (top) and halogenation (bottom) in chlorinated and chloraminated waters.

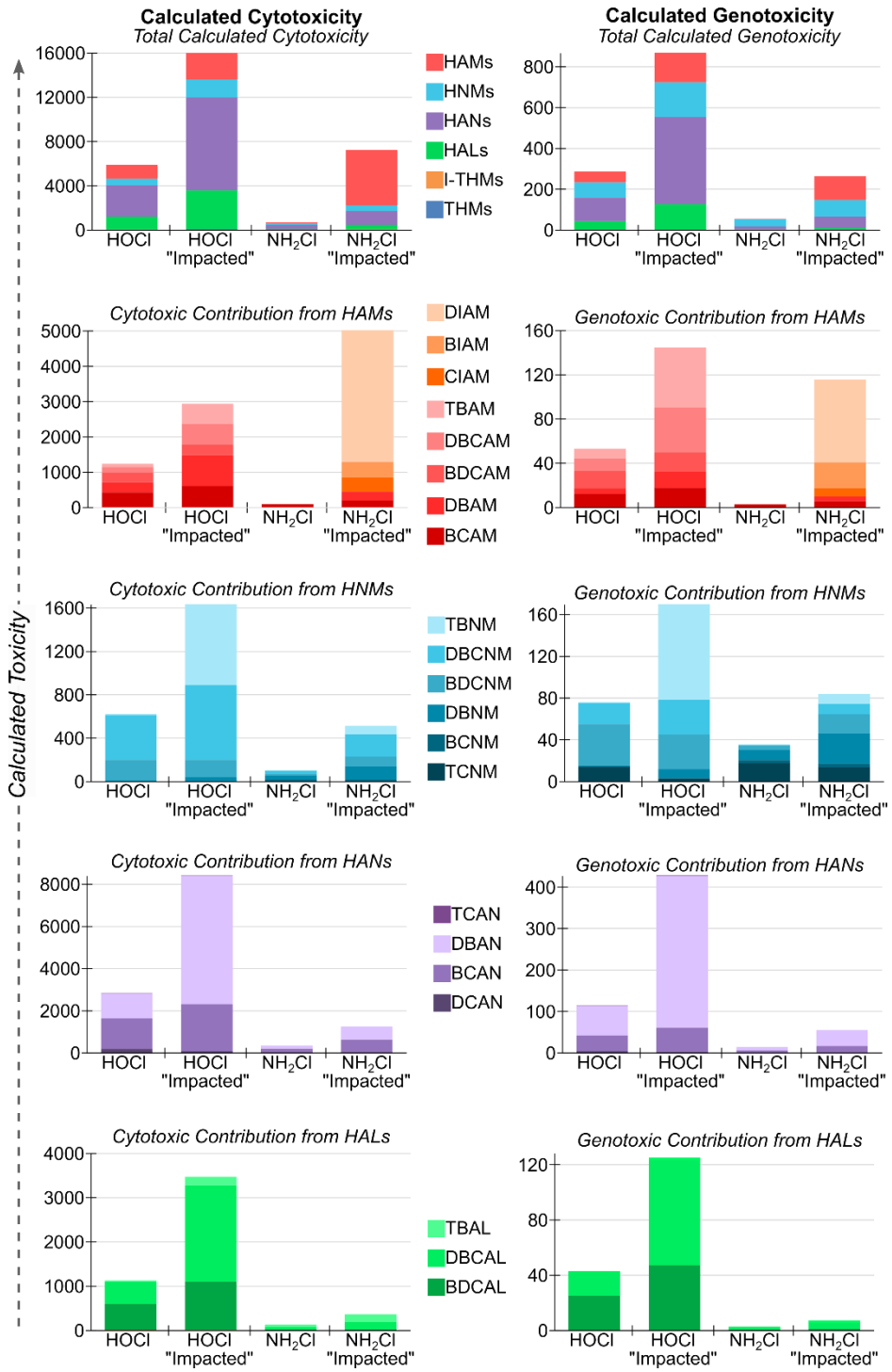

Figure D.2. Calculated CHO cell cytotoxicity (right) and genotoxicity (left) by DBP class (top) and halogen species profile (bottom). Based on toxicity values in Wagner and Plewa, 2017.[34]

Note: No toxicity data available for HKs or trihalo-Br-HANs; calculated cytotoxicity = $[DBP]x[LC_{50}]^{-1}x10^{6}$; calculated genotoxicity = $[DBP]x[50\%\ TDNA]x10^{6}$

APPENDIX E
PUBLICATIONS

E.1 LIST OF MANUSCRIPTS

Published Manuscripts

1. Liberatore, H. K.; M. J. Plewa; E. D. Wagner; J. M. VanBriesen; D. B. Burnett; L. H. Cizmas; S. D. Richardson. Identification and Comparative Mammalian Cell Cytotoxicity of New Iodo-Phenolic Disinfection By-Products in Chloraminated Oil and Gas Wastewaters. *Environ. Sci. Technol. Lett.* **2017**, *4*, 475-480.
2. Cuthbertson, A. A.; S. Y. Kimura; H. K. Liberatore; D. R. U. Knappe; B. Stanford; R. S. Summers; E. Dickenson; C. Maness; R. E. Mulhern; C. Glover; M. Selbes; S. D. Richardson. Does GAC Produce Safer Drinking Water? From DBPs and TOX to Calculated Toxicity. *Environ. Sci. Technol.* **2019**, *53*, 5987-5999.
3. DeHaven, B. A.; H. K. Liberatore; A. Greer, S. D. Richardson; L. S. Shimizu. Probing the Formation of Reactive Oxygen Species by a Porous Self-Assembled Benzophenone bis-Urea Host. *ACS Omega* **2019**, *4*, 8290-8298.
4. Yang, M.; H. K. Liberatore; X. Zhang. Current Methods for Analyzing Drinking Water Disinfection Byproducts. *Curr. Opin. Environ. Sci. Health* **2019**, *7*, 98-107.
5. Postigo, C.; D. M. DeMarini; M. Armstrong; H. K. Liberatore; K. Lamann; S. Y. Kimura; A. A. Cuthbertson; S. H. Warren; S. D. Richardson; T. McDonald; Y. Sey; S. E. Duirk; J. E. Simmons. Chlorination of Source Water Containing Iodinated X-ray Contrast Media: Mutagenicity and Identification of New Iodinated Disinfection Byproducts. *Environ. Sci. Technol.* **2018**, *52*, 13047-13056.
6. Ackerson, N. O. B.; A. H. Killinger; H. K. Liberatore; T. A. Ternes; M. J. Plewa; S. D. Richardson; S. E. Duirk. The Impact of Chlorine Exposure Time on Disinfection Byproduct Formation in the Presence of Iopamidol and Natural Organic Matter During Chloramination. *J. Env. Sci*. **2019**, *78*, 204-214.
7. Ackerson, N. O. B.; E. J. Machek; A. H. Killinger; E. A. Crafton; P. Kumkum; H. K. Liberatore; M. J. Plewa; S. D. Richardson; T. A. Ternes; S. E. Duirk. Formation of DBPs and Halogen-Specific TOX in the Presence of Iopamidol and Chlorinated Oxidants. *Chemosphere* **2018**, *202*, 349-357.

8. Allen, J. M.; A. A. Cuthbertson; H. K. Liberatore; S. Y. Kimura; A. Mantha; M. A. Edwards; S. D. Richardson. Showering in Flint, MI: Is there a DBP problem? *J. Environ. Sci.* **2017**, *58*, 271-284.
9. Daiber, E. J.; D. M. DeMarini; S. A. Ravuri; H. K. Liberatore; A. A. Cuthbertson; A. Thompson-Klemish; J. D. Byer; J. E. Schmid; M. Z. Afifi; E. R. Blatchley; S. D. Richardson. Progressive Increase in Disinfection Byproducts and Mutagenicity from Source to Tap to Swimming Pool and Spa Water: Impact of Human Inputs. *Environ. Sci. Technol.* **2016**, *50*, 6652-6662.

Manuscripts in Review

1. Verdugo E. M.; M. Gifford; C. Glover; A. A. Cuthbertson; R. Trenholm; S. Y. Kimura; H. K. Liberatore; S. D. Richardson; B. D. Stanford; R. S. Summers; E. Dickenson. Removal of Regulated and Unregulated Disinfection Byproducts and their Precursors from Treated Wastewater with Granular Activated Carbon: Impact of Pre-Ozonation and Pre-Chlorination. *Submitted to Water Research.*

Manuscripts in Preparation

1. Liberatore, H. K.; D. C. Westerman; J. M. Allen; A. M. McKenna; C. R. Weisbrod; J. P. McCord; R.J. Liberatore; S. D. Richardson. Potential Impacts of Hydraulic Fracturing on Drinking Water: High-Resolution Mass Spectrometry Identification of >300 Novel Surfactant-Derived S-Disinfection By-Products. *For submission to Environ. Sci. Technol.*
2. Liberatore, H. K.; C. O. Granger; A. A. Cuthbertson; S. D. Richardson. Formation of Nitrogenous Disinfection By-Products from Medical Imaging Compound Iopamidol. For submission to *Environ. Sci. Technol. Lett.*
3. Liberatore, H. K.; K. D. Good; J. M. Allen; A. A. Cuthbertson; D. C. Rich; M. J. Plewa; E. D. Wagner; J. M. VanBriesen; S. L. Morgan; S. D. Richardson. Are Coal-Fired Power Plants a Threat to Downstream Drinking Water? The Impact of Bromide and Iodide on Emerging Disinfection By-Products. *For submission to Environ. Sci. Technol. Lett.*
4. Liberatore, H. K.; D. Abraham; M. J. Plewa; E. D. Wagner; J. M. Allen; S. D. Richardson. Hydraulic Fracturing and Drinking Water: Quantification of Disinfection By-Products and Toxicological Impacts. *For submission to Environ. Sci. Technol.*
5. Cuthbertson, A. A.; H. K. Liberatore; S. Y. Kimura; S. D. Richardson. A Method for the Quantification of >60 Regulated and Priority Emerging Disinfection By-Products by GC-MS and GC-MS/MS. *For submission to Anal. Chem.*
6. Cuthbertson, A. A.; S. Y. Kimura; H. K. Liberatore; D. R. U. Knappe; B. Stanford; R. S. Summers; E. Dickenson; C. Maness; R. E. Mulhern; C. Glover; M. Selbes; S. D.

Richardson. GAC to BAC: Can It Make Chloraminated Drinking Water Safer? *For submission to Water Res.*

7. Ackerson, N. O. B.; M. J. Plewa; H. K. Liberatore; S. D. Richardson; T. A. Ternes; S. E. Duirk. Disinfection Byproducts and Halogen-Specific Total Organic Halogen Speciation in Chlorinated Source Waters – The Impact of Iopamidol and Bromide. *For submission to Sci. Total Environ.*
8. Liberatore, H. K.; E. J. Daiber; S. A. Ravuri; J. E. Schmid; S. D. Richardson; D. M. DeMarini. Extensive Analysis of DBPs and Mutagenicity in Swimming Pools and Spas. *For submission to Environ. Molec. Mutagen.*
9. Wendel, F. M.; C. Dietrich; C. Postigo; H. K. Liberatore; A. A. Cuthbertson; C. M. Joseph; M. J. Plewa; S. E. Duirk; S. D. Richardson; T. A. Ternes. Quantitative Analysis of Iopamidol Disinfection By-Products Formed in Purified and Natural Waters. *For submission to Environ. Sci. Technol.*
10. H. Dong; Lamann, K.; Nordhorn, I. D.; H. K. Liberatore; A. A. Cuthbertson; S. D. Richardson. QuEChERS-Based Method for the Determination of Iodinated Disinfection By-Products in Pasta Cooked with Chloraminated Tap Water Using Iodized Table Salt. *For submission to J. Agric. Food Chem.*

Environmental Science & Technology Letters

Letter

Cite This: Environ. Sci. Technol. Lett. 2017, 4, 475-480

pubs.acs.org/journal/estlcu

Identification and Comparative Mammalian Cell Cytotoxicity of New Iodo-Phenolic Disinfection Byproducts in Chloraminated Oil and Gas Wastewaters

Hannah K. Liberatore,[†] Michael J. Plewa,[‡,§] Elizabeth D. Wagner,[‡,§] Jeanne M. VanBriesen,[∥] David B. Burnett,[⊥] Leslie H. Cizmas,[#] and Susan D. Richardson*[,†]

[†]Department of Chemistry and Biochemistry, University of South Carolina, Columbia, South Carolina 29208, United States

[‡]Department of Crop Sciences, University of Illinois at Urbana-Champaign, Urbana, Illinois 61801, United States

[§]Safe Global Water Institute, University of Illinois at Urbana-Champaign, Urbana, Illinois 61801, United States

[∥]Department of Civil and Environmental Engineering, Carnegie Mellon University, Pittsburgh, Pennsylvania 15213, United States

[⊥]Department of Petroleum Engineering, Texas A&M University, College Station, Texas 77843, United States

[#]Department of Environmental and Occupational Health, School of Public Health, Texas A&M University, College Station, Texas 77843, United States

Supporting Information

ABSTRACT: Hydraulic fracturing wastewaters discharged to surface water have led to elevated bromide and iodide levels, as well as enhanced formation of brominated trihalomethanes, haloacetic acids, haloacetonitriles, and iodo-trihalomethanes at downstream drinking water treatment plants, in chlorinated effluent from wastewater treatment plants, and in controlled laboratory studies. This enhanced formation of brominated and iodinated disinfection byproducts (DBPs) raises concerns regarding human health, because they are much more toxic than chlorinated DBPs. This study represents the first nontarget, comprehensive analysis of iodinated DBPs formed in chloraminated produced waters associated with hydraulic fracturing of shale and conventional gas formations. Fifty-six iodo-phenolics were identified, comprising three homologous series of mono-, di-, and tri-iodinated phenols, along with two new classes of DBPs: iodomethylphenols and iododimethylphenols. Four iodo-phenolics (2-iodophenol, 4-iodophenol, 2,4,6-triiodophenol, and 4-iodo-2-methylphenol) were investigated for mammalian cell cytotoxicity. All were cytotoxic, especially 2,4,6-triiodophenol, which was more cytotoxic than all trihalomethanes and most haloacetic acids. In addition, geogenic organic compounds present in the oil and gas produced waters, including methylphenol and dimethylphenol, were found to be potential precursors to these iodo-DBPs.

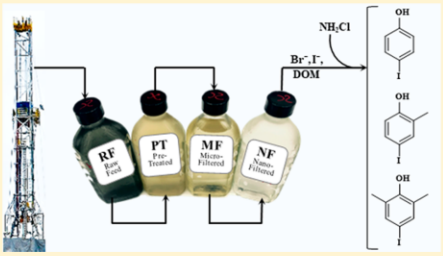

INTRODUCTION

Oil and gas extraction processes employ large volumes of water, amended with chemicals and injected into wells at high pressure to facilitate withdrawal from shale or reservoirs. Water, carrying oil and gas as well as residual chemicals, returns to the wellhead as "produced water". Produced water also contains high levels of geogenic components from the formation, including total dissolved solids (TDS), naturally occurring radioactive material (NORM), organic material, and halides. Drinking water sources have the potential to be impacted by oil and gas wastewater through spills during storage or transportation, illegal disposal, or discharge from treatment facilities that do not fully remove contaminants. While conventional wastewater treatment removes the majority of TDS and NORM, dissolved organic matter and halides are not removed and, thus, can be released to surface waters.[1−13] Elevated levels of bromide and iodide are a concern, as their release into surface waters used as drinking water sources can lead to formation of brominated and iodinated disinfection byproducts (DBPs) during drinking water treatment. Many of these DBPs are cytotoxic, genotoxic, mutagenic, or tumorigenic.[14−24] In general, iodinated DBPs are the most toxic, followed by brominated, with chlorinated DBPs being the least toxic.[15,18,19,21−23,25]

To reduce regulated DBP levels, many drinking water plants have switched from chlorine to monochloramine for disinfection. While monochloramine reduces regulated trihalo-

Received: October 18, 2017
Revised: October 30, 2017
Accepted: October 31, 2017
Published: October 31, 2017

DOI: 10.1021/acs.estlett.7b00468
Environ. Sci. Technol. Lett. 2017, 4, 475−480

Table 1. Sample Characteristics of Barnett and McAllen Produced Waters[a]

	Barnett		McAllen	
source	raw feed	nanofiltered	raw feed	microfiltered
TOC (mg of C/L)	214 ± 11	1.91 ± 1.09	575[c]	23.7[c]
Cl^- (mg/L)	31256 ± 1332	24058[c]	12838 ± 20	12422 ± 184[b]
Br^- (mg/L)	125 ± 7	96.6 ± 5.6	29.1 ± 0.1	28.8 ± 0.3[b]
I^- (mg/L)	53.5 ± 0.8[b]	38.4[c]	14.3 ± 0.1	13.6 ± 0.6

[a]Reported as the average ± the standard error of two replicate measurements (n = 2), except where otherwise specified. [b]Reported as the average ± the standard error of three replicate measurements (n = 3). [c]Single measurement (n = 1).

methanes (THMs) and haloacetic acids (HAAs), it promotes the formation of more toxic unregulated DBPs, including iodinated and nitrogenous DBPs.[15,18−22,24−34] Recent studies showed that chloraminated water with elevated bromide and iodide levels produces water that is more cytotoxic and genotoxic than chlorinated water, because of the enhanced formation of iodinated DBPs.[21,35]

Previous studies reported that oil and gas wastewater discharged to surface waters after partial treatment leads to elevated bromide and iodide concentrations in receiving streams and at downstream drinking water plants[1,3,13] and enhanced formation of brominated and iodinated DBPs upon disinfection. DBPs reported to date from oil and gas wastewater impacts include bromo- and iodo-THMs, bromo-HAAs, bromo-acetaldehydes, bromo-nitromethanes, and bromo-acetonitriles.[2,4,5,11] Because of the large amount of water required, as well as water scarcity issues, the oil and gas industry initiated treatment methods to minimize disposal and allow reuse of wastewater for further hydraulic fracturing or for agriculture.[36,37] These treatments include microfiltration and nanofiltration, which were the focus of our study. Raw (untreated) produced waters were also analyzed. In this study, we conducted the first comprehensive, nontarget assessment of DBPs formed in chloraminated oil and gas produced water, as well as the first cytotoxicity analyses of the iodo-phenolic DBPs identified.

MATERIALS AND METHODS

Standards and Reagents. Reagents for disinfection reactions and chemical analyses were purchased from VWR International (Radnor, PA), Fisher Scientific (Fair Lawn, NJ), and Sigma-Aldrich (St. Louis, MO). Authentic standards for DBP confirmation were purchased from Sigma-Aldrich and Spectra Group Synthetics LLC (Millbury, OH). Detailed vendor information and solution preparation can be found in the Supporting Information.

Sample Treatment and Characterization. Produced waters from a hydraulic fracturing well in the Barnett Shale (Texas) and a gas reservoir in McAllen, TX, were subjected to successive membrane filtration treatments. Barnett Shale and McAllen produced waters were filtered successively to nanofiltration permeate (Barnett NF) and to microfiltration permeate (McAllen MF), respectively (Figure S1), and were shipped on ice and stored at 4 °C. Total organic carbon (TOC) analyses were performed using a Sievers InnovOx TOC Analyzer (GE Analytical Instruments, Boulder, CO); levels of 1.91 and 23.7 mg/L were measured in Barnett NF and McAllen MF, respectively. Halide measurements were performed using a Dionex ICS-1600 ion chromatograph with conductivity detection (Thermo Fisher Scientific, Waltham, MA); sample dilutions ranged from 10- to 10000-fold. Concentrations of bromide and iodide in Barnett NF were 96.6 and 38.4 mg/L, respectively. In McAllen MF, bromide and iodide concentrations were 28.8 and 13.6 mg/L, respectively. Sample characteristics for these and raw produced waters are summarized in Table 1.

Disinfection and DBP Analysis. Disinfection reactions were performed in 60 mL amber bottles at room temperature (21 ± 2 °C). A 50 mL sample of each water was disinfected at pH 7 with 1 mg/L NH_2Cl per 1 mg/L TOC for Barnett NF (1.91 mg/L) and 1 mg/L NH_2Cl per 3 mg/L TOC (7.80 mg/L) for McAllen MF. The McAllen MF was dosed at a lower ratio because of its extremely high TOC (23.7 mg/L). After reaction for 72 h, the sample pH was adjusted with concentrated sulfuric acid to pH 1.4. Immediately after acidification, samples were liquid−liquid extracted three times with 15 mL of dichloromethane, residual water was removed from extracts by passing them through a column packed with sodium sulfate, and extracts were concentrated 50-fold to 1 mL. As a control, 50 mL of each nondisinfected water was extracted and analyzed. Additional experimental details regarding monochloramine preparation, sample pH, and chlorine dose are provided in the Supporting Information. Samples were analyzed by gas chromatography and mass spectrometry (GC−MS) with electron ionization. Unit-resolution MS was used for initial comprehensive analysis, while high-resolution (50000) MS was used for the determination of molecular formulas. Detailed instrumentation and method parameters are provided in Table S1.

Biological and Chemical Reagents and Chinese Hamster Ovary (CHO) Cells. CHO K1 cell line AS52, clone 11-4-8 was used.[38] The CHO cells were maintained in Hams F12 medium containing 5% fetal bovine serum (FBS), 1% L-glutamine, and 1% antibiotics (0.25 μg/mL amphotericin B, 100 μg/mL streptomycin sulfate, and 100 units/mL sodium penicillin G in 0.85% saline) at 37 °C in a mammalian cell incubator with a humidified atmosphere of 5% CO_2.

CHO Cell Chronic Cytotoxicity Analyses. The CHO cell chronic cytotoxicity assay quantitatively measures the decrease in cell density as a function of the concentration of the individual iodo-phenolic compounds over 72 h. Details of the CHO cell cytotoxicity assay were published previously.[18,23] Each individual iodo-phenolic [1 M in dimethyl sulfoxide (DMSO)] was diluted with F12 and FBS cell culture medium, and in general, 10 concentrations (with replicates) were analyzed in a 96-well microplate. After 72 h, the cell density expressed as the percentage of the concurrent negative control was recorded. These data were used to construct concentration−response curves.

Statistical Analysis. For individual iodophenols, one-way analysis of variance (ANOVA) tests were conducted to determine the lowest molar concentration that induced a statistically significant level of cytotoxicity as compared to their concurrent negative control ($P \leq 0.05$). To determine whether

DOI: 10.1021/acs.estlett.7b00468
Environ. Sci. Technol. Lett. 2017, 4, 475−480

Table 2. Molecular Formulas, Observed and Theoretical Accurate Masses, and Isomer Identification Information for Iodo-Phenols, -Methylphenols, and -Dimethylphenols Identified

compound	formula	observed mass (Da)	theoretical mass (Da)	no. of isomers observed in Barnett NF	no. of isomers observed in McAllen MF	no. of isomers confirmed[a]
iodophenol	C_6H_5IO	219.9381	219.9380	2	2	2
diiodophenol	$C_6H_4I_2O$	345.8348	345.8346	2	2	2
triiodophenol	$C_6H_3I_3O$	471.7311	471.7313	1	1	1
iodomethylphenol	C_7H_7IO	233.9536	233.9537	6	6	2
diiodomethylphenol	$C_7H_6I_2O$	359.8505	359.8503	5	5	0
triiodomethylphenol	$C_7H_5I_3O$	485.7468	485.7469	1	1	0
iododimethylphenol	C_8H_9IO	247.9694	247.9693	7	9	3
diiododimethylphenol	$C_8H_8I_2O$	373.8661	373.8659	6	9	1
triiododimethylphenol	$C_8H_7I_3O$	499.7626	499.7626	2	2	0

[a]No standards were available for diiodomethylphenols, triiodomethylphenols, or triiododimethylphenols. These identifications are based on manual mass spectral interpretation and comparison to those confirmed.

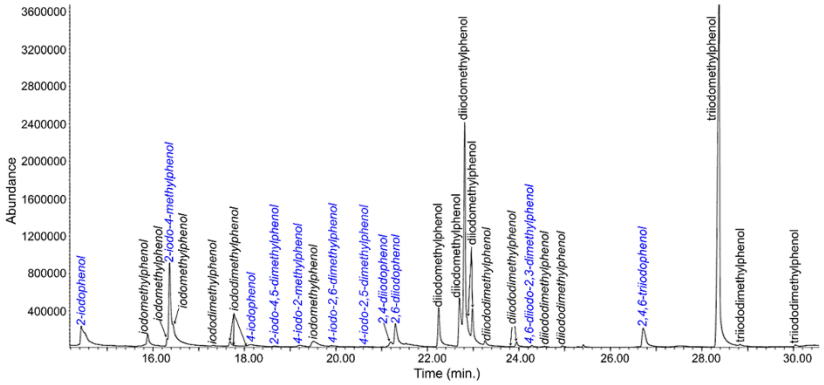

Figure 1. Iodo-phenolic DBPs identified in chloraminated Barnett nanofiltered (NF). Italicized names correspond to components that have been mass spectrally confirmed against a standard. Blue text indicates exact isomeric matches, determined via retention time confirmation.

a statistically significant difference existed among different iodophenols, LC_{50} values (the concentration of each iodophenol that induced a cell density that was 50% of the negative control) were determined through regression analyses of each concentration–response curve. Using a bootstrap statistical approach, the LC_{50} values were converted into mean cytotoxicity index (CTI) values ($CTI = 10^3 \times LC_{50}^{-1}$) to allow for ANOVA statistical tests among the different compounds. The power of the test was maintained at ≥0.8 at $\alpha = 0.05$. A detailed discussion of the statistical methods was published previously.[18]

■ RESULTS AND DISCUSSION

Bromide and Iodide. Previous studies of U.S. oil and gas wastewater report bromide levels ranging from tens to thousands of parts per million and iodide levels ranging from 2 to 50 ppm.[1,39] Comparatively, McAllen MF halide levels were on the low end of these ranges (28.8 and 13.6 ppm for bromide and iodide, respectively), whereas Barnett NF levels were higher than McAllen levels, with 96.6 ppm bromide and 38.4 ppm iodide (Table 1).

Iodo-DBP Identification and Confirmation. A total of 56 iodinated DBPs were identified in the chloraminated produced waters. Thirty-seven of these contained only iodine. Extracted ion chromatograms of m/z 127 were used to target iodinated compounds in the GC–MS analyses. Each peak's mass spectrum was analyzed by manual inspection and library database searching the 2014 National Institute of Standards and Technology (NIST) library. NIST library matches were found for 2-iodophenol, 4-iodophenol, and 2,4,6-triiodophenol, with molecular ions ($M^{\bullet+}$) of m/z 220, 220, and 472, respectively. Peaks with $M^{\bullet+}$ m/z 234 resulted in high-similarity matches with iodomethylphenols but also matched very closely with iodoanisoles, which have almost identical fragmentation patterns. Peaks with $M^{\bullet-}$ m/z 360 matched closest with diiodobenzoquinone (Figure S2), but differences in fragmentation indicated that these were likely another type of diiodo-aromatic compound.

High-resolution mass spectrometry confirmed molecular formulas for all iodo-phenolics identified; all 37 iodine-containing DBPs were within three homologous series of mono-, di-, and tri-iodo-phenolics: iodophenols, iodomethylphenols (iodocresols), and iododimethylphenols (iodoxylenols). Importantly, high-resolution MS also reinforced that the DBPs that showed a library match to diiodobenzoquinones were actually diiodomethylphenols (observed accurate mass of m/z 359.8505, molecular formula of $C_7H_6I_2O$) and not diiodobenzoquinones (theoretical m/z 359.8139, $C_6H_2I_2O_2$).

DOI: 10.1021/acs.estlett.7b00468
Environ. Sci. Technol. Lett. 2017, 4, 475−480

Observed and formula-calculated theoretical exact masses are listed in Table 2.

Authentic standards of iodo-phenols, -methylphenols, and -dimethylphenols were analyzed to confirm their identities in the chloraminated treated produced waters. Mass spectra of standards were compared to those in the chloraminated water extracts to make presumptive compound identifications without isomeric confirmation, while mass spectral matches combined with retention time matches (Figure S3) were used to confirm the exact isomer of each iodo-phenolic. A total of 11 isomer-specific structures were confirmed (Figure S4): 2-iodophenol, 4-iodophenol, 2,6-diiodophenol, 2,4-diiodophenol, 2,4,6-triiodophenol, 2-iodo-4-methylphenol, 4-iodo-2-methylphenol, 2-iodo-4,5-dimethylphenol, 4-iodo-2,6-dimethylphenol, 4-iodo-2,5-dimethylphenol, and 4,6-diiodo-2,3-dimethylphenol. Further generic (non-isomer-specific) compound determinations (Figure S5) were made for four more isomers of iodomethylphenol, six more isomers of iododimethylphenol, and eight more isomers of diiododimethylphenol. Standards were not available for diiodomethylphenols, triiodomethylphenols, or triiododimethylphenols, and thus, they were tentatively identified by manual spectral interpretation (Figure S6) and high-resolution accurate mass MS (Table S2). GC−MS chromatograms are shown in Figure 1 and Figure S7, with details regarding mass spectral interpretation provided in the Supporting Information.

In addition to the solely iodinated phenolics, 19 brominated and chlorinated phenolics were also tentatively identified using extracted ion chromatograms (extracting $M^{\bullet+}$ and predicted fragment ion m/z, based on iodo-phenolic mass spectra), accurate masses, and distinctive halogen patterns.[40] While the chloraminated Barnett NF sample did not show evidence of brominated or chlorinated components, the chloraminated McAllen MF sample yielded multiple isomers of mixed bromo-chloro-iodo-phenols and -methylphenols (Figure S8 and Table S3).

None of these iodo-phenolics, or any other iodinated compounds, were observed in either nondisinfected control. To the best of our knowledge, this is the first report of iodomethylphenols and iododimethylphenols as DBPs. Though mono-, di-, and tri-iodo-phenols, -methylphenols, and -dimethylphenols were observed in both Barnett NF and McAllen MF chloraminated waters, the number of isomers varied between the two. More isomers of iodinated dimethylphenol were formed during chloramination of McAllen MF than during chloramination of Barnett NF. In addition, the predominant species formed [based on GC−MS abundances (Table S2)] varied between the two. While iodinated phenol species were most abundant in McAllen MF, iodinated methylphenols were the dominant DBPs formed in Barnett NF. It is possible that more species, including the bromoiodo- and chloroiodo-phenolics, were formed in McAllen MF than in Barnett NF because of the much higher TOC:X^- ratios of McAllen MF. Given that the McAllen MF and Barnett NF are products of different processes and geological formations (gas from a conventional reservoir and oil from a shale formation, respectively), it is also likely that the precursors in each water vary, leading to different chloramination byproducts.

Precursors of Iodo-Phenolics. We suspected that the precursors for iodo-phenol formation were phenol, methylphenols (cresols), dimethylphenols (xylenols), or other short-chain alkyl phenols, as these are common geogenic organics found in produced waters.[11,12,39,41,42] These have been previously reported in produced waters at concentrations as high as 20.2, 13.7, and 8.2 mg/L for phenol, total cresols, and total xylenols, respectively.[42] GC−MS analysis of the non-disinfected produced waters showed evidence of the presence of phenol, at least two isomers of methylphenol, and several isomers of dimethylphenol (Figure S9). To further confirm these as potential precursors, controlled reactions were performed in purified water with 4-methylphenol and 2,6-dimethylphenol for 72 h, under the following conditions: (1) chloramination, (2) addition of iodide, and (3) addition of iodide and chloramination (Table S4). Reactors spiked with iodide followed by chloramination resulted in 75 and 100% consumption of 4-methylphenol and 2,6-dimethylphenol, respectively, and the formation of three iodo-phenolic DBPs: 2-iodo-4-methylphenol and diiodomethylphenol from 4-methylphenol, as well as 4-iodo-2,6-dimethylphenol from 2,6-dimethylphenol. In chloraminated reactors without iodide, chlorinated analogues were observed, with only 15% of the starting 4-methylphenol and 30% of 2,6-dimethylphenol consumed. In reactors with iodide in the absence of a disinfectant, no halogenated species were formed. The lack of trihalogenated species in any of the chloraminated reactors is not surprising, as further substitution of iodine or chlorine into the structure (more than two halogens for 4-methylphenol and more than one halogen for 2,6-dimethylphenol) is unfavorable due to ortho/para directing of the hydroxy and methyl groups, as well as the limited availability of positions on the ring. The high number of iodinated species (S6) formed in the chloraminated produced water samples suggests that multiple methylphenol/dimethylphenol isomers or other compounds containing cresol or xylenol groups may also serve as precursors for the iodomethylphenol and iododimethylphenol DBPs discovered. There is also the possibility that nonylphenol surfactants added to hydraulic fracturing fluids or other geogenic alkylphenols may be a source.[12,36,41,42]

Mammalian Cell Cytotoxicity of Iodo-Phenolics. The first compounds to be confirmed (2-iodophenol, 4-iodophenol, 2,4,6-triiodophenol, and 4-iodo-2-methylphenol) were investigated for chronic cytotoxicity with CHO cells. Cytotoxicity concentration−response curves are illustrated in Figure 2. The lowest cytotoxic concentration, LC_{50}, and cytotoxicity index values are presented in Table S5 and Figure S10. The cytotoxicities decrease in the following order: 2,4,6-triiodophe-

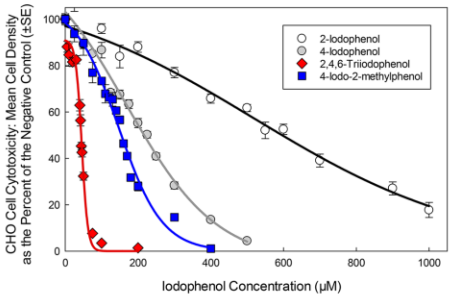

Figure 2. CHO cytotoxicity concentration−response curves for 2-iodophenol, 4-iodophenol, 2,4,6-triiodophenol, and 4-iodo-2-methylphenol.

DOI: 10.1021/acs.estlett.7b00468
Environ. Sci. Technol. Lett. 2017, 4, 475−480

nol ≫ 4-iodo-2-methylphenol > 4-iodophenol ≫ 2-iodophenol (LC_{50} values of 4.37×10^{-5}, 1.63×10^{-4}, 2.16×10^{-4}, and 6.01×10^{-4} M, respectively). 2,4,6-Triiodophenol was more cytotoxic than the THMs and HAAs, with the exception of bromoacetic acid and iodoacetic acid.[18] A previous study demonstrated that 4-iodophenol and 2,4,6-triiodophenol were toxic to marine algae at concentrations 1−2 orders of magnitude lower than those of aliphatic halogenated DBPs, including iodoacetic acid.[43] In a developmental toxicity study, 2,4,6-triiodophenol was 2 orders of magnitude more toxic to polychaete embryos than iodoacetic acid was.[44]

Implications for Drinking Water. Previous studies demonstrated enhanced formation of bromo- and iodo-THMs, bromo-HAAs, and bromoacetonitriles in chlorinated and chloraminated source waters impacted by oil and gas wastewater,[2,4,5] as well as the discharge of DBPs and phenolics into surface waters from facilities that treat produced water.[11] This study specifically investigated the hypothesis that organic compounds in oil and gas wastewaters can act as precursors to halogenated organic DBPs. We discovered novel chloramine-mediated iodo-DBPs. In addition to the cytotoxicity found in the study presented here, iodophenols and iodomethylphenols have extremely low taste and odor thresholds and are often associated with medicinal-like and fecal-like odors.[45,46] Thus, these iodo-DBPs might contribute to foul-tasting drinking water, as well as pose a potential public health risk.

It is likely that in oil- and gas-impacted drinking water sources, iodo-phenolic DBPs could form at significant levels, particularly in cases in which chloramination is used. This is important to consider in circumstances where discharge of treated oil and gas wastewater may have led to THM and HAA levels that exceed U.S. Environmental Protection Agency regulations, leading to decisions by utilities to switch to chloramination to improve compliance. While chloramination will significantly reduce the levels of regulated DBPs, it can lead to formation of more toxic unregulated iodo-DBPs, including these iodo-phenolics, when source waters have elevated levels of bromide and iodide. Furthermore, to protect drinking water in areas impacted by hydraulic fracturing waste, methods for removing bromide and iodide should be further investigated as pretreatment options before wastewater is released to surface waters.

■ ASSOCIATED CONTENT

Supporting Information

The Supporting Information is available free of charge on the ACS Publications website at DOI: 10.1021/acs.estlett.7b00468.

Additional information regarding experimental and instrumental details, compound identification, and cytotoxicity (PDF)

■ AUTHOR INFORMATION

Corresponding Author

*E-mail: richardson.susan@sc.edu. Phone: 803-777-6932.

ORCID

Hannah K. Liberatore: 0000-0001-7423-3251

Notes

The authors declare no competing financial interest.

■ ACKNOWLEDGMENTS

This research was supported by the National Science Foundation (Grant 1438625). H.K.L. acknowledges financial support from the Department of Education through GAANN Award P200A120075. The authors thank Keith McLeroy, Carl Vavra, and the Global Petroleum Research Institute for their assistance and knowledge, as well as Dr. Sandra Karcher for her oil rig photo.

■ REFERENCES

(1) Harkness, J. S.; Dwyer, G. S.; Warner, N. R.; Parker, K. M.; Mitch, W. A.; Vengosh, A. Iodide, Bromide, and Ammonium in Hydraulic Fracturing and Oil and Gas Wastewaters: Environmental Implications. *Environ. Sci. Technol.* **2015**, *49*, 1955−1963.

(2) Parker, K. M.; Zeng, T.; Harkness, J.; Vengosh, A.; Mitch, W. A. Enhanced Formation of Disinfection Byproducts in Shale Gas Wastewater-Impacted Drinking Water Supplies. *Environ. Sci. Technol.* **2014**, *48*, 11161−11169.

(3) Wilson, J. M.; Van Briesen, J. M. Source Water Changes and Energy Extraction Activities in the Monongahela River, 2009−2012. *Environ. Sci. Technol.* **2013**, *47*, 12575−12582.

(4) Wang, Y.; Small, M. J.; VanBriesen, J. M. Assessing the Risk Associated with Increasing Bromide in Drinking Water Sources in the Monongahela River, Pennsylvania. *J. Environ. Eng.* **2017**, *143*, 04016089.

(5) States, S.; Cyprych, G.; Stoner, M.; Wydra, F.; Kuchta, J.; Monnell, J.; Casson, L. Marcellus Shale Drilling and Brominated THMs in Pittsburgh, Pa., Drinking Water. *J. Am. Water Works Assoc.* **2013**, *105*, E432−E448.

(6) Vengosh, A.; Jackson, R. B.; Warner, N.; Darrah, T. H.; Kondash, A. A Critical Review of the Risks to Water Resources from Unconventional Shale Gas Development and Hydraulic Fracturing in the United States. *Environ. Sci. Technol.* **2014**, *48*, 8334−8348.

(7) Warner, N. R.; Christie, C. A.; Jackson, R. B.; Vengosh, A. Impacts of Shale Gas Wastewater Disposal on Water Quality in Western Pennsylvania. *Environ. Sci. Technol.* **2013**, *47*, 11849−11857.

(8) Rahm, B. G.; Riha, S. J. Evolving Shale Gas Management: Water Resource Risks, Impacts, and Lessons Learned. *Environ. Sci. Process. Impacts* **2014**, *16*, 1400−1412.

(9) Vidic, R. D.; Brantley, S. L.; Vandenbossche, J. M.; Yoxtheimer, D.; Abad, J. D. Impact of Shale Gas Development on Regional Water Quality. *Science* **2013**, *340*, 1235009.

(10) Ferrar, K. J.; Michanowicz, D. R.; Christen, C. L.; Mulcahy, N.; Malone, S. L.; Sharma, R. K. Assessment of Effluent Contaminants from Three Facilities Discharging Marcellus Shale Wastewater to Surface Waters in Pennsylvania. *Environ. Sci. Technol.* **2013**, *47*, 3472−3481.

(11) Hladik, M. L.; Focazio, M. J.; Engle, M. Discharges of Produced Waters from Oil and Gas Extraction via Wastewater Treatment Plants Are Sources of Disinfection By-Products to Receiving Streams. *Sci. Total Environ.* **2014**, *466*−*467*, 1085−1083.

(12) Orem, W.; Tatu, C.; Varonka, M.; Lerch, H.; Bates, A.; Engle, M.; Crosby, L.; Mcintosh, J. Organic Substances in Produced and Formation Water from Unconventional Natural Gas Extraction in Coal and Shale. *Int. J. Coal Geol.* **2014**, *126*, 20−31.

(13) Burgos, W. D.; Castillo-Meza, L.; Tasker, T. L.; Geeza, T. J.; Drohan, P. J.; Liu, X.; Landis, J. D.; Blotevogel, J.; McLaughlin, M.; Borch, T.; Warner, N. R. Watershed-Scale Impacts from Surface Water Disposal of Oil and Gas Wastewater in Western Pennsylvania. *Environ. Sci. Technol.* **2017**, *51*, 8851−8860.

(14) Wei, X.; Wang, S.; Zheng, W.; Wang, X.; Liu, X.; Jiang, S.; Pi, J.; Zheng, Y.; He, G.; Qu, W. Drinking Water Disinfection Byproduct Iodoacetic Acid Induces Tumorigenic Transformation of NIH3T3 Cells. *Environ. Sci. Technol.* **2013**, *47*, 5913−5920.

(15) Richardson, S. D.; Plewa, M. J.; Wagner, E. D.; Schoeny, R.; Demarini, D. M. Occurrence, Genotoxicity, and Carcinogenicity of Regulated and Emerging Disinfection By-Products in Drinking Water:

DOI: 10.1021/acs.estlett.7b00468
Environ. Sci. Technol. Lett. 2017, 4, 475−480

A Review and Roadmap for Research. *Mutat. Res., Rev. Mutat. Res.* **2007**, *636*, 178−242.
(16) Stalter, D.; O'Malley, E.; Von Gunten, U.; Escher, B. I. Fingerprinting the Reactive Toxicity Pathways of 50 Drinking Water Disinfection By-Products. *Water Res.* **2016**, *91*, 19−30.
(17) Harvey, J. B.; Hong, H.-H. L.; Bhusari, S.; Ton, T.-V.; Wang, Y.; Foley, J. F.; Peddada, S. D.; Hooth, M.; DeVito, M.; Nyska, A.; Pandiri, A. R.; Hoenerhoff, M. J. F344/NTac Rats Chronically Exposed to Bromodichloroacetic Acid Develop Mammary Adenocarcinomas With Mixed Luminal/Basal Phenotype and *Tgfβ* Dysregulation. *Vet. Pathol.* **2016**, *53*, 170−181.
(18) Wagner, E. D.; Plewa, M. J. CHO Cell Cytotoxicity and Genotoxicity Analyses of Disinfection By-Products: An Updated Review. *J. Environ. Sci.* **2017**, *58*, 64−76.
(19) Plewa, M. J.; Muellner, M. G.; Richardson, S. D.; Fasano, F.; Buettner, K. M.; Woo, Y. T.; Mckague, A. B.; Wagner, E. D. Occurrence, Synthesis, and Mammalian Cell Cytotoxicity and Genotoxicity of Haloacetamides: An Emerging Class of Nitrogenous Drinking Water Disinfection Byproducts. *Environ. Sci. Technol.* **2008**, *42*, 955−961.
(20) Muellner, M. G.; Wagner, E. D.; Mccalla, K.; Richardson, S. D.; Woo, Y. T.; Plewa, M. J. Haloacetonitriles vs. Regulated Haloacetic Acids: Are Nitrogen-Containing DBPs More Toxic? *Environ. Sci. Technol.* **2007**, *41*, 645−651.
(21) Yang, Y.; Komaki, Y.; Kimura, S. Y.; Hu, H. Y.; Wagner, E. D.; Mariñas, B. J.; Plewa, M. J. Toxic Impact of Bromide and Iodide on Drinking Water Disinfected with Chlorine or Chloramines. *Environ. Sci. Technol.* **2014**, *48*, 12362−12369.
(22) Richardson, S. D.; Fasano, F.; Ellington, J. J.; Crumley, F. G.; Buettner, K. M.; Evans, J. J.; Blount, B. C.; Silva, L. K.; Waite, T. J.; Luther, G. W.; McKague, A. B.; Miltner, R. J.; Wagner, E. D.; Plewa, M. J. Occurrence and Mammalian Cell Toxicity of Iodinated Disinfection Byproducts in Drinking Water. *Environ. Sci. Technol.* **2008**, *42*, 8330−8338.
(23) Plewa, M. J.; Wagner, E. D. *Mammalian Cell Cytotoxicity and Genotoxicity of Disinfection By-Products*; Water Research Foundation: Denver, 2009; p 134.
(24) Plewa, M. J.; Wagner, E. D.; Jazwierska, P.; Richardson, S. D.; Chen, P. H.; McKague, A. B. Halonitromethane Drinking Water Disinfection Byproducts: Chemical Characterization and Mammalian Cell Cytotoxicity and Genotoxicity. *Environ. Sci. Technol.* **2004**, *38*, 62−68.
(25) Plewa, M. J.; Wagner, E. D.; Richardson, S. D.; Thruston, A. D.; Woo, Y. T.; McKague, A. B. Chemical and Biological Characterization of Newly Discovered Iodoacid Drinking Water Disinfection By-products. *Environ. Sci. Technol.* **2004**, *38*, 4713−4722.
(26) Shah, A. D.; Mitch, W. A. Halonitroalkanes, Halonitriles, Haloamides, and N-Nitrosamines: A Critical Review of Nitrogenous Disinfection Byproduct Formation Pathways. *Environ. Sci. Technol.* **2012**, *46*, 119−131.
(27) Bichsel, Y.; Von Gunten, U. Formation of Iodo-Trihalomethanes during Disinfection and Oxidation of Iodide-Containing Waters. *Environ. Sci. Technol.* **2000**, *34*, 2784−2791.
(28) Bond, T.; Huang, J.; Templeton, M. R.; Graham, N. Occurrence and Control of Nitrogenous Disinfection By-Products in Drinking Water - A Review. *Water Res.* **2011**, *45*, 4341−4354.
(29) Liu, S.; Li, Z.; Dong, H.; Goodman, B. A.; Qiang, Z. Formation of Iodo-Trihalomethanes, Iodo-Acetic Acids, and Iodo-Acetamides during Chloramination of Iodide-Containing Waters: Factors Influencing Formation and Reaction Pathways. *J. Hazard. Mater.* **2017**, *321*, 28−36.
(30) Diehl, A. C.; Speitel, G. E.; Symons, J. M.; Krasner, S. W.; Hwang, C. J.; Barrett, S. E. DBP Formation during Chloramination. *J.—Am. Water Works Assoc.* **2000**, *92*, 76−90.
(31) Kimura, S. Y.; Komaki, Y.; Plewa, M. J.; Mariñas, B. J. Chloroacetonitrile and N,2-Dichloroacetamide Formation from the Reaction of Chloroacetaldehyde and Monochloramine in Water. *Environ. Sci. Technol.* **2013**, *47*, 12382−12390.
(32) Chu, W.; Gao, N.; Yin, D.; Krasner, S. W. Formation and Speciation of Nine Haloacetamides, an Emerging Class of Nitrogenous DBPs, during Chlorination or Chloramination. *J. Hazard. Mater.* **2013**, *260*, 806−812.
(33) Chu, W.; Gao, N.; Yin, D.; Krasner, S. W.; Templeton, M. R. Trace Determination of 13 Haloacetamides in Drinking Water Using Liquid Chromatography Triple Quadrupole Mass Spectrometry with Atmospheric Pressure Chemical Ionization. *J. Chromatogr. A* **2012**, *1235*, 178−181.
(34) Richardson, S. D.; Thruston, A. D.; Krasner, S. W.; Weinberg, H. S.; Miltner, R. J.; Schenck, K. M.; Narotsky, M. G.; McKague, A. B.; Simmons, J. E. Integrated Disinfection By-Products Mixtures Research: Comprehensive Characterization of Water Concentrates Prepared from Chlorinated and Ozonated/Postchlorinated Drinking Water. *J. Toxicol. Environ. Health, Part A* **2008**, *71*, 1165−1186.
(35) Dong, S.; Nguyen, T. H.; Plewa, M. J. Comparative Mammalian Cell Cytotoxicity of Wastewater for Reuse after Chlorination, Chloramination, or Ozonation Disinfection with Elevated Bromide and Iodide. *J. Environ. Sci.* **2017**, *58*, 296−301.
(36) Gregory, K. B.; Vidic, R. D.; Dzombak, D. A. Water Management Challenges Associated with the Production of Shale Gas by Hydraulic Fracturing. *Elements* **2011**, *7*, 181−186.
(37) Maloney, K. O.; Yoxtheimer, D. A. Production and Disposal of Waste Materials from Gas and Oil Extraction from the Marcellus Shale Play in Pennsylvania. *Environ. Pract.* **2012**, *14*, 278−287.
(38) Wagner, E. D.; Rayburn, A. L.; Anderson, D.; Plewa, M. J. Analysis of Mutagens with Single Cell Gel Electrophoresis, Flow Cytometry, and Forward Mutation Assays in an Isolated Clone of Chinese Hamster Ovary Cells. *Environ. Mol. Mutagen.* **1998**, *32*, 360−368.
(39) Hayes, T. Sampling and Analysis of Water Streams Associated with the Development of Marcellus Shale Gas. Technical Report; Marcellus Shale Coalition: Pittsburgh, PA, 2009.
(40) McLafferty, F. W.; Tureček, F. *Interpretation of Mass Spectra*, 4th ed.; University Science Books: Sausalito, CA, 1993.
(41) Thomas, K. V.; Langford, K.; Petersen, K.; Smith, A. J.; Tollefsen, K. E. Effect-Directed Identification of Naphthenic Acids as Important in Vitro Xeno-Estrogens and Anti-Androgens in North Sea Offshore Produced Water Discharges. *Environ. Sci. Technol.* **2009**, *43*, 8066−8071.
(42) Boitsov, S.; Mjøs, S. A.; Meier, S. Identification of Estrogen-Like Alkylphenols in Produced Water from Offshore Oil Installations. *Mar. Environ. Res.* **2007**, *64*, 651−665.
(43) Liu, J.; Zhang, X. Comparative Toxicity of New Halophenolic DBPs in Chlorinated Saline Wastewater Effluents against a Marine Alga: Halophenolic DBPs Are Generally More Toxic than Haloaliphatic Ones. *Water Res.* **2014**, *65*, 64−72.
(44) Yang, M.; Zhang, X. Comparative Developmental Toxicity of New Aromatic Halogenated DBPs in a Chlorinated Saline Sewage Effluent to the Marine Polychaete *Platynereis Dumerilii*. *Environ. Sci. Technol.* **2013**, *47*, 10868−10876.
(45) Strube, A.; Guth, H.; Buettner, A. Identification of a Medicinal off-Flavour in Mineral Water. *Water Res.* **2009**, *43*, 5216−5224.
(46) Strube, A.; Buettner, A.; Czerny, M. Influence of Chemical Structure on Absolute Odour Thresholds and Odour Characteristics of Ortho- and Para-Halogenated Phenols and Cresols. *Flavour Fragrance J.* **2012**, *27*, 304−312.

DOI: 10.1021/acs.estlett.7b00468
Environ. Sci. Technol. Lett. 2017, 4, 475−480

Environmental Science & Technology

Article

Cite This: Environ. Sci. Technol. 2019, 53, 5987−5999

pubs.acs.org/est

Does Granular Activated Carbon with Chlorination Produce Safer Drinking Water? From Disinfection Byproducts and Total Organic Halogen to Calculated Toxicity

Amy A. Cuthbertson,[†] Susana Y. Kimura,[†,‡] Hannah K. Liberatore,[†] R. Scott Summers,[§] Detlef R. U. Knappe,[∥] Benjamin D. Stanford,[⊥] J. Clark Maness,[∥] Riley E. Mulhern,[§] Meric Selbes,[#] and Susan D. Richardson*[,†]

[†]Department of Chemistry and Biochemistry, University of South Carolina, Columbia, South Carolina 29208, United States

[‡]Department of Chemistry, University of Calgary, 2500 University Drive, NW Calgary, Alberta T2N 1N4, Canada

[§]Department of Civil, Environmental and Architectural Engineering, University of Colorado, Boulder, Colorado 80309-0428, United States

[∥]Department of Civil, Construction, and Environmental Engineering, North Carolina State University, Campus Box 7908, Raleigh, North Carolina 27695-7908, United States

[⊥]Hazen and Sawyer, 143 S. Union Blvd., Suite 200, Lakewood, Colorado 80228, United States

[#]Hazen and Sawyer, 4035 Ridge Top Road, Suite 400, Fairfax, Virginia 22030, United States

Supporting Information

ABSTRACT: Granular activated carbon (GAC) adsorption is well-established for controlling regulated disinfection byproducts (DBPs), but its effectiveness for unregulated DBPs and DBP-associated toxicity is unclear. In this study, GAC treatment was evaluated at three full-scale chlorination drinking water treatment plants over different GAC service lives for controlling 61 unregulated DBPs, 9 regulated DBPs, and speciated total organic halogen (total organic chlorine, bromine, and iodine). The plants represented a range of impacts, including algal, agricultural, and industrial wastewater. This study represents the most extensive full-scale study of its kind and seeks to address the question of whether GAC can make drinking water safer from a DBP perspective. Overall, GAC was effective for removing DBP precursors and reducing DBP formation and total organic halogen, even after >22 000 bed volumes of treated water. GAC also effectively removed preformed DBPs at plants using prechlorination, including highly toxic iodoacetic acids and haloacetonitriles. However, 7 DBPs (mostly brominated and nitrogenous) increased in formation after GAC treatment. In one plant, an increase in tribromonitromethane had significant impacts on calculated cytotoxicity, which only had 7−17% reduction following GAC. While these DBPs are highly toxic, the total calculated cytotoxicity and genotoxicity for the GAC treated waters for the other two plants was reduced 32−83% (across young−middle−old GAC). Overall, calculated toxicity was reduced post-GAC, with preoxidation allowing further reductions.

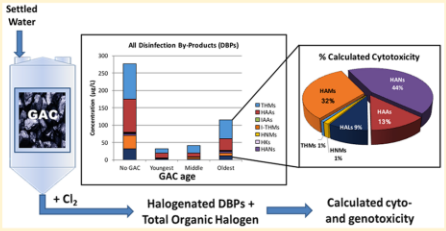

INTRODUCTION

Drinking water disinfection is vital for prevention of waterborne illness. Since its introduction in the U.S. in the early 1900s, disinfection is reported to have contributed significantly to an estimated 29-year increase in life expectancy.[1] An unintended consequence of disinfection is the formation of disinfection byproducts (DBPs), which have been associated with adverse health effects, including bladder cancer, colon cancer, miscarriage, and birth defects.[2−10] In the U.S., regulations are enforced for four trihalomethanes (THMs), five haloacetic acids (HAAs), bromate, and chlorite under the Stage 2 Disinfectants and DBP Rule.[11] Several recent studies indicate that, while THMs and HAAs are the dominant DBPs formed upon chlorination, they are not necessarily drivers of toxicity associated with DBP formation.[12−14]

DBPs are formed by the reaction of disinfectants with natural organic matter (NOM), bromide, and iodide.[6,15] Many NOM fractions can react to form THMs and HAAs, while phenolic NOM structures have been shown to form haloacetaldehydes (Table S1).[16] Free and combined amino acids, aldehydes, and aromatic NOM have been shown to form

Received: January 2, 2019
Revised: April 13, 2019
Accepted: April 30, 2019
Published: April 30, 2019

DOI: 10.1021/acs.est.9b00023
Environ. Sci. Technol. 2019, 53, 5987−5999

Table 1. Water Quality Parameters for Plants 1−3

plant		impacts on source water	preoxidant	GAC operation	bed volumes treated by GAC	TOC (mg/L as C)	UV_{254} (cm^{-1})	SUVA (L/mg·m)	TN (mg/L as N)	Br^- (μg/L)	I^- (μg/L)
1		algae	chlorine dioxide, chlorine	post-filter adsorber (seasonal partial treatment)	GAC inf.	1.5	0.018	1.2	0.13	9	<5
					5600	0.5	0.003	0.64	0.07	13	<5
					12 600	0.8	0.007	0.8	0.09	14	<5
					22 400	1.1	0.01	0.9	0.11	15	<5
2		industrial wastewater, agricultural	$KMnO_4$, chlorine	post-filter adsorber	GAC inf.	2.1	0.037	1.8			
					3000	0.3	0.007	1.0			
					8700	0.6	0.006	1.0			
					22 000	1.2	0.020	1.7			
3	(first sampling)	minimal	$KMnO_4$	filter adsorber	GAC inf.	2.0	0.037	1.8	0.19	<5	<5
					9200	1.4	0.022	1.6	0.14	<5	<5
	(second sampling)				GAC inf.	2.0	0.046	2.3		<5	<5
					3400	0.7	0.015	2.0		<5	<5
					3800	0.8	0.017	2.0		<5	<5

haloacetamides and haloacetonitriles.[17−19] The presence of inorganic nitrogen, such as ammonia, nitrite, and nitrate, can play a role in the formation of nitrogenous DBPs (N-DBPs),[20] which are generally more toxic than DBPs without nitrogen,[21−24] yet no N-DBPs are currently regulated. Extensive studies have shown that iodo-DBPs, which are also not regulated, are typically more toxic than brominated DBPs (Br-DBPs), which are much more toxic than chlorinated analogues.[25−28] Table S1 summarizes precursors associated with each DBP class measured in this study.

The use of granular activated carbon (GAC) is well-established for controlling THMs and HAAs because it can effectively remove NOM fractions that serve as their precursors.[13,29−31] Studies indicate that some N-DBP precursors are not as readily removed using GAC.[13,32] GAC columns are biologically active, even if the influent contains a disinfectant, as GAC will reduce the disinfectant at the top of the GAC column, allowing biomass to grow in the rest of the bed.[33] Thus, in addition to adsorption of DBP precursors, biodegradation plays a role in GAC treatment.[33]

Many drinking water plants use preoxidation (e.g., prechlorination), which may result in the formation of DBPs within the treatment system. We refer to these as "preformed" DBPs; they can be removed by GAC or, with additional disinfection, can act as precursor material for the formation of other DBPs.[17,18] One potential benefit of preoxidation is transformation of NOM into intermediate aromatic halogenated DBPs, which may be more easily removed by GAC than larger precursor molecules.[34]

GAC preferentially removes dissolved organic carbon (DOC) over dissolved organic nitrogen (DON), and it does not remove bromide.[31,35,36] Therefore, the DON/DOC and Br^-/DOC ratios increase across GAC adsorbers, which may result in increased formation of N- and Br-DBPs, due to increased competition of HOBr.[13,31,35,36] Higher Br^-/DOC ratios cause a shift in halogen speciation to more brominated THMs, and some brominated THM concentrations can be higher after GAC treatment.[35,36] A shift from dichloroacetonitrile to dibromoacetonitrile has also been reported in a bench-scale GAC study.[13] Shifts in halogen speciation to more cytotoxic and genotoxic brominated DBPs must be evaluated for possible adverse health implications.

Given concerns about potential increased formation of Br- and N-DBPs, it is important to ask: Do GAC treated waters have lower associated toxicity than waters not treated with GAC? One way to address this is the "TIC-Tox" approach, which multiplies molar concentrations of individual DBPs by their corresponding cytotoxicity and genotoxicity index values.[14] Other previously published studies have used this approach in modeling toxicity of DBP mixtures[14,37,38] and have shown increases in calculated genotoxicity following GAC.[13] This approach can also be used to assess which DBPs are toxicity drivers, regulated or otherwise.

The goal of our study was to assess the effectiveness of full-scale GAC treatment at chlorination plants for controlling: (1) human exposure to a wide range of 70 regulated and unregulated DBPs, as well as speciated total organic halogen (TOCl, TOBr, TOI), and (2) the calculated toxicity associated with these DBPs. Both removal of preformed DBPs and control of DBPs under conditions that represent the utilities' distribution systems, i.e., simulated distribution system (SDS) conditions, were assessed. Using each plant's SDS conditions allows for the study of more realistic DBP concentrations and, therefore, exposure to real populations within those systems. Water samples were collected at three full-scale chlorination plants in the U.S., with DBP control evaluated across GAC service life (e.g., youngest, middle-aged, and oldest GAC). At each plant, the same influent water was used across three different aged filters on the same type of carbon, allowing for the comparison of filter age with the same DBP/DBP precursor composition. Because source water quality can impact the types of DBPs that form, plants were carefully chosen to represent a wide range of impacts, including algal, agricultural, and industrial wastewater impacts. This study was limited to three full-scale chlorine plants due to the extensive analysis required. Formation of 70 DBPs, including haloacetonitriles (HANs), haloacetamides (HAMs), halonitromethanes (HNMs), haloacetaldehydes (HALs), haloketones (HKs), iodinated acetic acids (IAAs), iodinated trihalomethanes (I-THMs), THMs, and HAAs, was studied during full-scale prechlorination (preformed DBPs) at two plants and in bench-scale SDS tests at all three plants. This is the most extensive list of DBPs studied across GAC filter lifetimes. TOCl, TOBr, and TOI were also measured and compared to

DOI: 10.1021/acs.est.9b00023
Environ. Sci. Technol. 2019, 53, 5987−5999

the total measured DBP concentrations, with the balance representing *unknown* DBPs. This is the first study that evaluated total organic halogen (TOX) across GAC lifetimes in full-scale plants. Preformed DBPs were evaluated before and after GAC treatment, providing information on their adsorbability and/or biodegradability, which is unknown for many emerging DBPs. Cytotoxicity and genotoxicity were calculated using the TIC-Tox method across GAC lifetime.[14] Most importantly, this study seeks to address whether DBP concentrations correlate with calculated toxicity and which DBPs are the driving forces of toxicity across GAC age.

MATERIALS AND METHODS

Sampling of Drinking Water Treatment Plants. Three full-scale drinking water plants were sampled; for each plant, three GAC service lives were evaluated, which was quantified in terms of throughput in bed volumes (BV; i.e., the volume of water treated relative to the GAC bed volume) and was different for each plant to reflect early, middle, and late stages of GAC operation. Operating characteristics and source water quality parameters for each plant and water sample are summarized in Table 1. Total organic carbon (TOC), absorbance at 254 nm (UV_{254}), specific ultraviolet absorbance (SUVA), bromide, iodide, and total nitrogen (TN) were quantified as surrogates for DBP precursors (Table 1). All plants used one or more preoxidants prior to GAC treatment (chlorine dioxide and chlorine in Plant 1, $KMnO_4$ and chlorine in Plant 2, $KMnO_4$ in Plant 3) and relied on chlorine as the primary disinfectant post-GAC and as the secondary disinfectant throughout the distribution system. Information regarding sampling dates, flow rates, empty bed contact times (EBCT), GAC type, and DOC breakthrough is found in Table S2. Due to the real-world nature of this study, the activated carbons were slightly different at the different plants studied, but they were consistent within each plant, allowing the impact of carbon age and the impact of GAC vs no GAC to be evaluated at each plant. Schematic diagrams of each plant are found in Figures S1−S3. All plants operated GAC contactors in a staged parallel mode and blended the effluents. GAC influents and effluents at different service times were collected. Plant 3 was sampled on two occasions: in the first event, samples were taken after treating 9200 BV of water; the second event occurred after GAC was replaced in two contactors.

Chlorination of Samples. For each sample, water was analyzed for preformed DBPs, and SDS testing was carried out according to protocols set by each plant (Text S1). Chlorine residual concentrations and contact times were equivalent to each plant's longest water age in the distribution system (3−7 days). For example, Plant 1 was pH adjusted with borate buffer to 8.0 and spiked with 1.0 to 4.0 mg/L to achieve a chlorine residual of approximately 1.0 mg Cl_2/L after 24 h of reaction.

Samples were collected in duplicate in two, 1 L bottles, one containing ascorbic acid and one containing ammonium chloride (quenching agents; chlorine to quencher molar ratio of 1:1.3 based on an assumed maximum potential residual chlorine concentration of 5 mg/L as Cl_2), and adjusted to pH 3.5−4 with 1 M H_2SO_4. Samples were shipped cold overnight and extracted the same day as received or stored at 4 °C and extracted within 2 days. Quantified DBPs were stable over this storage time.[39−41] Further details are provided in Text S2.

Chemicals and Reagents. Analytical standards for unregulated DBPs (Table S3) were purchased or custom-synthesized at the highest purity available (CanSyn Chem. Corp., Toronto, Ontario; Sigma-Aldrich, St. Louis, MO; Aldlab Chemicals, Boston, MA; TCI America, Boston, MA). Organic solvents were of the highest purity. Acetonitrile, methyl *tert*-butyl ether (MTBE), methanol, hexane, and pure water were purchased from Sigma-Aldrich (St. Louis, MO) and Fisher Scientific (Pittsburgh, PA).

Analytical Methods. *Background Water Quality and Regulated DBPs.* Water quality parameters (residual chlorine, DOC, UV_{254}, SUVA, TN, ammonia, nitrite, nitrate, bromide, and iodide) were measured using methods described in Table S4. THMs and HAAs were measured using EPA Methods 551.1 and 552.3, respectively.[42,43]

Unregulated DBPs. Three extraction methods and two derivatization methods were required to analyze 57 unregulated DBPs.[41] For HANs, HKs, I-THMs, HNMs, and tri-HALs, a single liquid−liquid extraction (LLE) with 100 mL of sample, 2 mL of MTBE, and 30 g of sodium sulfate was conducted for samples quenched with ascorbic acid (Text S3.1). For HAMs, IAAs, and a subset of compounds (bromodichloronitromethane, dibromochloronitromethane, tribromonitromethane, and tribromoacetonitrile), 100 mL was pH adjusted with H_2SO_4 to pH < 2, followed by multiple LLEs (×3) conducted with 5 mL of MTBE and 30 g of sodium sulfate (samples quenched with ammonium chloride), followed by concentrating under nitrogen (Text S3.2). Final extracts were spiked with 1,2-dibromopropane internal standard and analyzed using gas chromatography (GC)-mass spectrometry (MS) with electron ionization (EI) and selected ion monitoring (SIM) (7890 GC, 5977A mass spectrometer, Agilent Technologies, Santa Clara, CA) with a Rtx-200 column (30m × 0.25 mm × 0.25 μm film thickness; Restek Corporation, Bellefonte, PA). A portion of the extract was removed for IAA analysis, which required diazomethane derivatization (Text S3.3),[41,44] followed by GC-EI-MS/MS analysis (TRACE GC Ultra, Quantum GC MS/MS, Thermo Scientific, Waltham, MA). Mono- and dihaloacetaldehydes were analyzed using *O*-(2,3,4,5,6-pentafluorobenzyl) hydroxylamine (PFBHA) derivatization followed by LLE and GC-EI-MS analysis[45] (Text S3.4). The summed mass concentration of all regulated and unregulated DBPS was termed as "DBP sum".

Minimum reporting limits (MRLs) for most compounds in this study were 0.10 μg/L, excluding IAAs, chloroacetamide (CAM), bromoacetamide (BAM), and iodoacetamide (IAM), which had reporting limits of 0.025, 0.75, 5.0, and 0.75 μg/L, respectively. CAM, BAM, and IAM were not detected in this study.

Total Organic Halogen. TOCl, TOBr, and TOI were determined using a TOX analyzer (Mitsubishi Chemical Analytech, Chigasaki, Japan; Cosa Xentaur, Yaphank, USA)[37,46−48] (Text S4). Briefly, acidified samples (pH < 2) were adsorbed on activated carbon, washed with nitric acid, and combusted at 1000 °C in the presence of oxygen and argon as a carrier gas. Combusted gases were collected in a fresh aqueous solution containing 0.03% H_2O_2, which was analyzed for chloride using a Dionex 1600 ion chromatograph (Dionex, Sunnyvale, CA).[37,46−48] An inductively coupled plasma (ICP)-mass spectrometer (Finnigan ELEMENT XR, Thermo Electron Corporation) was used for trace-level bromide and iodide analysis.[48,49]

Contributions of DBP Classes to TOX and Toxicity. The contribution of each DBP class to TOX was calculated by first multiplying the molar concentration of each compound pertaining to a specific DBP class by its corresponding number

DOI: 10.1021/acs.est.9b00023
Environ. Sci. Technol. 2019, 53, 5987−5999

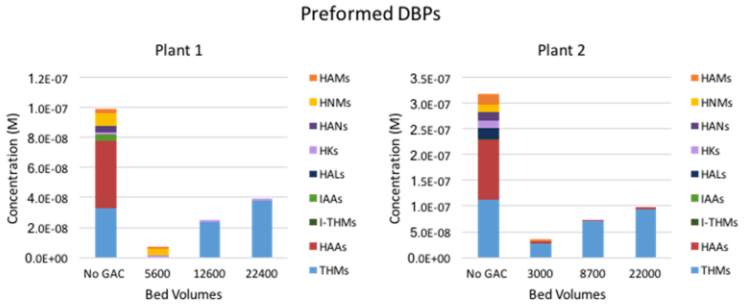

Figure 1. Effectiveness of GAC to control preformed DBPs formed during preoxidation using chlorine over a range of GAC service times in bed volumes (grouped by class). TCM and BDCM are dominant breakthrough compounds at Plant 1. TCM and DBCM are the dominant breakthrough compounds at Plant 2.

of halogens (i.e., 1−4 halogen atoms). Then, these values were added and divided by the sum molar concentration of TOCl, TOBr, and TOI. For example, the percent contribution of haloacetonitriles to TOCl ($\%HAN_{TOCl}$) and the percent contribution of haloacetonitriles to TOX ($\%HAN_{TOX}$) are defined as

$$\%HAN_{TOCl} = \frac{\sum b[CH_aCl_bBr_cI_dCN]}{[TOCl]} \times 100\% \quad (1)$$

$$\%HAN_{TOX} = \frac{\sum (b + c + d)[CH_aCl_bBr_cI_dCN]}{[TOCl] + [TOBr] + [TOI]} \times 100\% \quad (2)$$

where a is the number of hydrogens and b, c, and d are the number of chlorine, bromine, and iodine atoms for each individual HAN. Similar equations were used for other DBP classes.

Toxicity associated with DBPs in each sample was based on the "TIC-Tox" method.[14] In brief, molar concentrations of each DBP were multiplied by their corresponding cyto- or genotoxicity index values for Chinese hamster ovary cells (CHO) and summed together[14,50] (eqs 3 and 4).

$$\text{total calculated water cytotoxicity} = \sum ([DBP] \times LC_{50}^{-1} \times 10^6) \quad (3)$$

$$\text{total calculated water genotoxicity} = \sum ([DBP] \times 50\%\ TDNA^{-1} \times 10^6) \quad (4)$$

where [DBP] is the molar concentration of each DBP, the cytotoxicity index is the inverse of the lethal concentration at 50% (LC_{50}) in M, the genotoxicity index is the inverse of the 50% tail DNA (50% TDNA) measurement in M, and 10^6 is a normalization factor.

RESULTS AND DISCUSSION

Overview. We evaluated the effectiveness of GAC for the removal of (1) DBPs that formed via prechlorination and (2) DBP precursors. The former is important because many drinking water utilities add chlorine for iron and manganese control to filters that precede GAC adsorbers. Thus, it is common that these influents contain DBPs. Two of the three drinking water utilities evaluated used prechlorination, providing an opportunity to conduct a comprehensive evaluation of the effectiveness of GAC treatment for removal of preformed DBPs. Removal of DBP precursors is also critically important because many utilities use chlorine to meet disinfection requirements for GAC-treated water and to maintain a disinfectant residual in the distribution system. Chlorinated GAC influent water simulates DBP levels expected at the consumers' tap in the absence of GAC treatment, and chlorinated GAC effluent samples permit an evaluation of DBP precursor (and preformed DBP) removal and thus effectiveness for controlling DBPs expected at the consumers' tap. This study provided an opportunity to assess realistic exposure concentrations for each plant. The following sections are organized as follows: First, a general discussion of DBP formation at the three plants is presented; second, GAC effectiveness for the control of preformed DBPs is presented; third, DBP precursor control by GAC is discussed by presenting results from SDS tests; fourth, GAC effectiveness for reducing cyto- and genotoxicity, as calculated from measured DBP levels, is discussed.

DBP Formation at the Three Full-Scale Plants. As expected, Plants 1, 2, and 3, which have different impacts to their source waters (Table 1), exhibited different DBP formation (Tables S6, S8, S9, and S11). Plant 2, which has agricultural and industrial impacts (indicated by discharge permits upstream of the plant), formed higher levels of N-DBPs, such as HAMs, HANs, and HNMs (Table S8). Water impacted by agriculture and industry often results in increased levels of inorganic and organic nitrogen in source waters, which can form increased N-DBP levels.[51−54] Plant 1, with algal impacts, formed moderate levels of trihalonitromethanes (Table S6), consistent with previous studies that have shown formation of trichloronitromethane from algae, while it is unknown whether a bloom was occurring during sampling.[55−59] Plant 3 has minimally impacted source water (and low concentrations of bromide and iodide) and produced mostly chlorinated DBPs. Forty-six DBPs (of 70 measured) were detected among all three plants, two of which were only preformed (1,1-dibromopropanone, 1,1-dichloropropanone).

Behavior of Preformed DBPs in GAC Contactors. As a result of prechlorination (and potentially prechlorine dioxide treatment), Plants 1 and 2 had measurable preformed DBPs, most of which were completely removed by GAC over the

DOI: 10.1021/acs.est.9b00023
Environ. Sci. Technol. 2019, 53, 5987−5999

Figure 2. Effectiveness of GAC treatment for controlling regulated and unregulated DBPs (nM) and calculated cytotoxicity and genotoxicity (unitless) for Plants 1, 2, and 3. "No GAC" represents the level of DBPs that would be expected at the consumers' tap following simulated distribution system (SDS) chlorination in the absence of GAC treatment. Subsequent columns represent the effectiveness of GAC for DBP control following SDS chlorination over a range of GAC service times, indicated by the number of bed volumes (BV) treated. For Plant 3, (1) and (2) indicate the first and second sampling, respectively.

evaluated service times (Figure 1). Thirteen preformed DBPs, including HAMs, HANs, HKs, HNMs, IAAs, THMs, and HAAs (Table S5), were measured in Plant 1 GAC influent; eight were completely removed. The total molar concentration of measured preformed DBPs at Plant 1 accounted for approximately 1−10% of TOCl, 2−30% of TOBr, and 0−11% of TOI. At Plant 2, 36 preformed DBPs, including HALs, HAMs, HANs, HKs, HNMs, I-THMs, THMs, and HAAs (Table S7), were measured in the GAC influent; 30 were completely removed. The total molar concentration of measured preformed DBPs at Plant 2 accounted for 26−85% of TOCl, 25−78% of TOBr, and 0−100% of TOI. Both adsorption and biodegradation can contribute to DBP removal by GAC. Previous studies modeled adsorption breakthrough

DOI: 10.1021/acs.est.9b00023
Environ. Sci. Technol. 2019, 53, 5987−5999

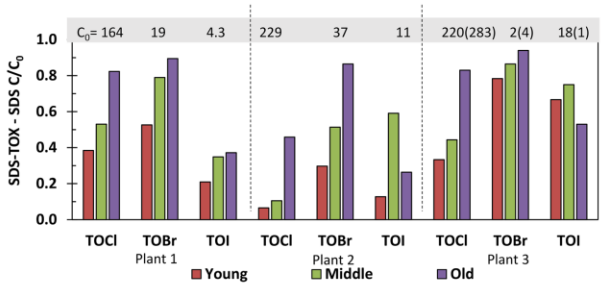

Figure 3. SDS total organic halogen (TOCl, TOBr, TOI) breakthrough for Plants 1, 2, and 3 with influent SDS. C_0 values (μg/L) from Plant 3 second sampling are shown in parentheses. Plant specific bed volumes are found in Table 1. C_0 is the GAC influent concentration.

using the pH-dependent octanol−water partition coefficient (logD).[60] Lower logD values indicate higher hydrophilic character and, in general, lower adsorbability to GAC. DBPs measured in this study have logD values ranging from −3.70 to 3.66 (Table S3). Molecular weight, polarizability, and charged surface interactions are also important factors impacting GAC adsorption.[30] Because GAC columns are biologically active, correlations between GAC adsorption removal and logD values may underpredict removal of biodegradable DBPs in biologically active GAC. For example, IAAs have negative logD values, suggesting they are poorly adsorbable, but preformed IAAs were removed 100% at both Plants 1 and 2 (Figure 1), indicating that they may be biodegradable, as are many other haloacetic acids.[61] DBPs that were completely removed covered the entire range of logD values studied, which suggests that both biodegradation and adsorption contributed to their removal. *The effectiveness of GAC treatment for the removal of most of the DBPs evaluated in this study has not been reported in the literature, including removal for the highly toxic IAAs, I-THMs, and iodinated HAMs.*

Five preformed DBPs were detected in Plant 1 GAC effluent: bromochloroacetamide, 1-bromo-1,1-dichloropropanone, bromodichloronitromethane, and two THMs (trichloromethane, bromodichloromethane) (Table S5). Seven preformed DBPs were detected in Plant 2 GAC effluent: two HAMs (bromochloroacetamide, bromoiodoacetamide), two THMs (trichloromethane, dibromochloromethane), and three HAAs (trichloroacetic acid, bromodichloroacetic acid, and dibromochloroacetic acid) (Table S7). In Plant 1, 1-bromo-1,1-dichloropropanone (logD 1.21) yielded complete breakthrough at early GAC service times (Table S5). At both plants, bromochloroacetamide (logD 0.35, 0.4 μg/L) and, at Plant 1, bromodichloronitromethane (logD 2.63, 0.8 μg/L) broke through early (5600 BV) but were not present in the effluent at later times. This behavior is indicative of biological removal, as older GAC columns tend to have higher biological activity.[33] Trichloromethane (logD 1.94) at both plants, bromodichloromethane (logD 2.04) at Plant 1, and dibromochloromethane (logD 2.21) at Plant 2 displayed classic breakthrough behavior; i.e., adsorptive removal of THMs became less effective with increasing GAC service life, consistent with previous studies.[62,63] Interestingly, in Plant 2, bromoiodoacetamide was not detected in the GAC influent but was present in the GAC effluent at two of the three GAC service times (1.3 and 1.1 μg/L). This could be due to a surface-catalyzed reaction with chlorine (chlorine was present in the GAC influent). Previous studies have shown that GAC can act as an effective catalyst in the oxidation and reduction of micropollutants where oxygen, nitrogen, and available functional groups on the surface of GAC play an important role.[64] These types of reactions may also cause the reductive dehalogenation of a trihaloamide and subsequent formation of bromoiodoacetamide. More research is needed to understand these possible reactions. Haloamides may also from form the hydrolysis of haloacetonitriles (Table S1).

The normalized breakthrough behavior of TOCl, TOBr, TOI, and the total DBP sum is shown in Figures S4 and S5 for preformed DBPs at Plants 1 and 2, respectively. GAC was effective in removing >50% of TOCl, TOBr, and the total DBP sum over the studied throughput range of 22 000 bed volumes (>10 months of GAC service life at Plant 2).

Impact of GAC on Simulated Distribution System DBPs. GAC effectively controlled SDS-DBPs at all three chlorination plants (Figures 2 and S6). The DBP sum decreased after treatment, with control ranging from 49% to 83% at Plant 1, 58% to 88% at Plant 2, and 19% to 67% at Plant 3, decreasing with service time. These combined results correlate with TOC removal (Figures S7−S9), and similar correlations were obtained with UV_{254} (Table 1). When accounting for molar concentrations, the total measured SDS Cl-DBPs accounted for 15−40%, 53−100%, and 50−57% of the TOCl at Plants 1, 2, and 3, respectively. The total measured SDS Br-DBPs accounted for 45−52%, 73−100%, and 38−58% of the TOBr at Plants 1, 2, and 3, respectively. Total measured I-DBPs only accounted for 3−10%, 0−4%, and <1% of the TOI at Plants 1, 2, and 3, respectively. TOCl, TOBr, and TOI were also lower after GAC treatment at all three plants (Figures 3 and S10−S13) for the duration of GAC service times. At Plants 1 and 2, TOI was the most effectively controlled TOX parameter, while TOBr was the most poorly controlled at all three plants. Bromide, iodide, TOBr, and TOI measurements were taken for the prechlorinated GAC influent water and not the raw water. TOBr and TOI exceeded bromide and iodide concentrations of GAC influent in some cases, which we believe is caused by preoxidation conversion to HOBr and HOI, which would not be detected by ion chromatography methods used to measure bromide and iodide. Another possible explanation is that brominated and iodinated contaminants, such as brominated flame retardants or iodinated X-ray contrast media, may have been present in

DOI: 10.1021/acs.est.9b00023
Environ. Sci. Technol. 2019, 53, 5987−5999

the raw source waters and contributed to the TOBr and TOI levels observed.[65−67] As expected, DBP control was most effective at the youngest GAC service life and decreased with increasing service life (Figures 2 and S6). However, GAC adsorbers at the longest service life still controlled overall SDS-DBP values (TOX and DBP sum concentrations) when compared to using no GAC.

DBPs Not Well Controlled by GAC. While SDS concentrations of 28 of the 44 DBPs detected were effectively controlled by GAC, ten DBPs were unaffected; i.e, the concentrations were not significantly different between GAC influent and effluent (two-tailed *t* test, 1 degree of freedom (d.f.), 95% confidence interval (CI)) (Table 2). In addition, the SDS concentrations of seven DBPs were *higher* in the GAC effluent (one-tailed *t* test, 1 d.f., 95% CI): tribromoacetonitrile, 1,1,1-trichloropropanone, tribromonitromethane, trichloronitromethane, bromodichloronitromethane, dibromochloromethane, and tribromomethane (Table 2). For example, tribromoacetonitrile increased in formation following GAC treatment at Plant 2 from below detection (MRL of 0.1 μg/L) to 0.7 μg/L (Table S8). Twelve of these 16 DBPs were brominated, and the lack of control or increase in Br-DBPs after GAC is consistent with earlier studies that showed increases in regulated brominated THMs,[35,36,68] as well as recent work showing an increase in dibromoacetonitrile.[32,13] Increased Br-DBP formation is partially explained by an increased Br^-/TOC ratio, as TOC is removed by GAC while Br^- is not, allowing increased competition of HOBr.[35,36] TOBr/TOC ratios in SDS samples increased by 155−207% from 17.5 μg/L at Plant 2 and increased 144−205% from 0.9 and 1.9 μg/L at Plant 3, respectively, as a result of GAC treatment (Table S12), but TOBr was still controlled overall by GAC, even after treating 22 000 BV of water (Plants 1 and 2, Figure 3). One compound was unchanged in one plant and higher in another plant (1,1,1-trichloropropanone).

N-DBP precursors were not well removed, as HANs, HNMs, and HAMs either increased in formation or remained unchanged. For example, tribromonitromethane increased in formation following GAC treatment at Plant 1 from below detection (MRL of 0.1 μg/L) to 1.9 μg/L (Figure 4). This significant increase, like bromoiodoacetamide, may be due to desorption or surface catalyzed reactions. A previous study showed formation of nitrosamines from GAC catalyzed oxidation of amines.[64] Another study showed that GAC can activate nitrite, which can nitrosate amines, in turn forming nitromethanes.[69] As GAC filters age, biofilms develop and can shed precursors for N-DBPs.[70] Future research is needed to understand the formation of other N-DBPs within GAC. Nine N-DBPs including bromochloroacetamide, dibromoacetamide, dichloroacetamide, tribromoacetonitrile, bromochloroacetonitrile, dibromoacetonitrile, trichloronitromethane, tribromoni-

Table 2. DBPs That Were Not Significantly Reduced by GAC or Increased after the Use of GAC

class	DBP	change after GAC	location
HAL	bromodichloroacetaldehyde	no change	Plant 2
HAM	bromochloroacetamide	no change	Plant 1
HAM	dibromoacetamide	no change	Plant 2
HAM	dichloroacetamide	no change	Plant 1
HAN	tribromoacetonitrile	increased	Plant 2
HAN	bromochloroacetonitrile	no change	Plant 1, Plant 3[b]
HAN	dibromoacetonitrile	no change	Plant 1, Plant 2
HK	1,1,1-trichloropropanone	increased	Plant 2, Plant 3[a]
HK	1,1,1-trichloropropanone	no change	Plant 3[b]
HK	1,1,3,3-tetrachloropropanone	no change	Plant 3[b]
HNM	tribromonitromethane	increased	Plant 1
HNM	trichloronitromethane	increased	Plant 3[a]
HNM	bromodichloronitromethane	increased	Plant 3[a]
THM	dibromochloromethane	increased	Plant 2
THM	tribromomethane	increased	Plant 2
THM	bromodichloromethane	no change	Plant 3[a,b]
HAA	bromoacetic acid	no change	Plant 2

[a]First sampling. [b]Second sampling.

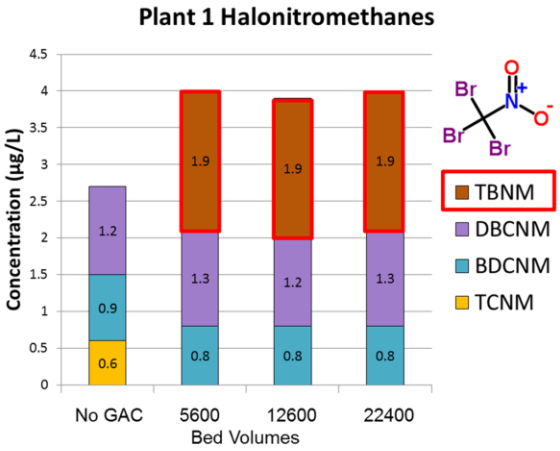

Figure 4. Plant 1 halonitromethanes before and after GAC following SDS procedures.

DOI: 10.1021/acs.est.9b00023
Environ. Sci. Technol. 2019, 53, 5987−5999

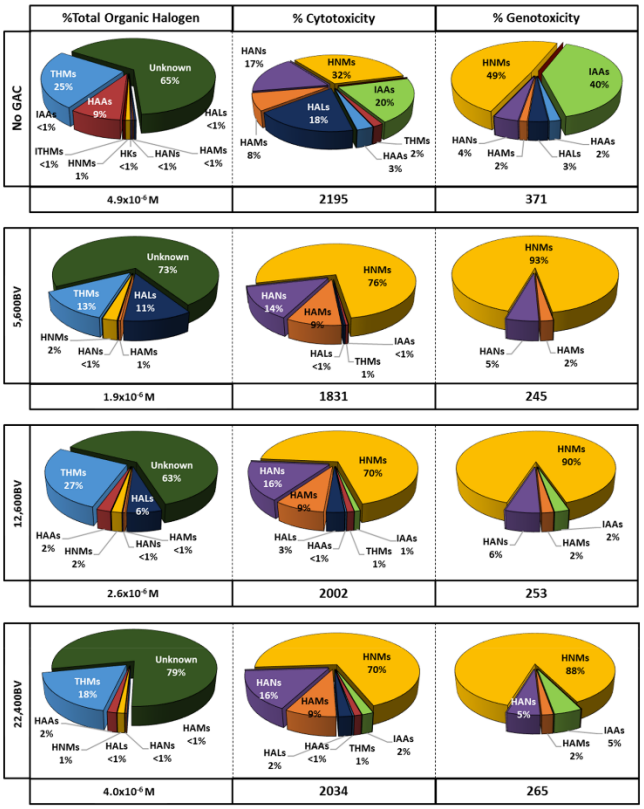

Figure 5. Effectiveness of GAC treatment at Plant 1 for SDS-TOX, cytotoxicity, and genotoxicity: % total organic halogen (in molarity), % calculated cytotoxicity, and % calculated genotoxicity for each DBP class. Total toxicity = $\Sigma([\text{DBP}] \times (C_{1/2})^{-1} \times 10^6)$. Note that there are no data on cytotoxicity or genotoxicity in the literature for haloketones or tribromoacetonitrile.

tromethane, and bromodichloronitromethane (Tables 2, S5, and S6) were either poorly controlled or increased following GAC treatment, consistent with two recent studies that investigated HANs[13,32] and one HNM.[32]

Preformed vs SDS-DBPs. At Plant 1, 11 of the 23 SDS-DBPs formed in the GAC influent were also prefomed DBPs (formed by prechlorination and prechlorine dioxide), and at Plant 2, 29 of the preformed DBPs (formed by prechlorination) were among the 35 SDS-DBPs. Thus, only 12 and 6 DBPs, respectively, were in the SDS samples that were not in the preformed samples at Plants 1 and 2. At both plants, some of the unregulated DBPs (e.g., bromodichloronitromethane, bromodichloroacetaldehyde, dichloroiodomethane, and chloroiodoacetic acid) had similar concentrations in the SDS and preformed samples (Tables S5−S8), indicating that their formation was precursor-limited; i.e., additional chlorine had little effect on their formation. In contrast, concentrations of all of the THM4, HAA9 species, and some unregulated DBPs (e.g., trichloroacetaldehyde, dichloroacetonitrile, bromochloroacetonitrile, dichloroacetamide, dibromoacetamide, trichloroacetamide) increased after SDS chlorination (Tables S5−S8), indicating chlorine-controlled DBP formation reactions; i.e., additional chlorine yielded additional DBPs. At Plants 1 and 2, preformed TOCl represented about 50% found in the SDS sample for the GAC influent. However, for TOBr, preformed and SDS concentrations were similar for the GAC influent, indicating bromide was the limiting reagent in Br-DBP formation.

For GAC effluent at Plants 1 and 2, the contribution of preformed DBPs to the SDS-DBP concentrations was 6−16% for the DBP sum and about 30−50% for TOCl (Tables S5−S8). These percentages were similar to those for SDS-treated GAC influents. Thus, on average, GAC was equally removing preformed DBPs and DBP precursors within these measures. For TOBr, GAC removed more preformed Br-DBPs, as the preformed TOBr to SDS-TOBr ratio decreased after GAC treatment.

DOI: 10.1021/acs.est.9b00023
Environ. Sci. Technol. 2019, 53, 5987−5999

In Plant 1, GAC treatment removed preformed IAAs (iodo-, chloroiodo-, bromoiodo-, and diiodoacetic acid) to below detection (<25 ng/L), yet some of these compounds formed in the SDS test following GAC, indicating adsorbability and/or biodegradability of these compounds might be higher than the corresponding precursor material. Some studies have shown GAC removal of iodide, and unlike bromide, iodide sorption is not affected by competing anions.[71−73] As iodide reacts with chlorine in GAC influent, it converts to HOI, which reacts with NOM to form organic iodine, which is more readily adsorbed by activated carbon than iodide. Iodide is also rapidly oxidized to iodate, which is less adsorbable but is a nontoxic inorganic sink for iodide.[74,75] It has been proposed that iodide can be converted to iodine by dissolved oxygen, which can then be easily removed by GAC, suggesting removal of iodide (and reduction in iodo-DBP formation) is dependent on dissolved oxygen concentration and disinfectant concentration.[71,73,76] Adsorption of IAAs to GAC has not been previously reported.

Calculated Water Toxicity. *Overall Results.* Because the use of GAC increased formation of some of the more toxic Br- and N-DBPs, it was not evident whether the effective control of overall DBP formation translated to safer drinking water. Therefore, cytotoxicity and genotoxicity associated with the 70 measured DBPs were calculated for GAC-treated samples across GAC service lives (Figures 2, S14, and S15).[14,50] Breakthrough of SDS cytotoxicity and genotoxicity is also shown in Figure S16. Calculated cytotoxicity and genotoxicity were substantially lower following GAC treatment at younger service lives, despite higher formation of some toxic Br- and N-DBPs. With increasing GAC run time, an increase in SDS-DBPs corresponded to increased calculated cytotoxicity and genotoxicity (Figure 2), but calculated toxicity values for all three plants remained below GAC influent values after preoxidation (without GAC treatment). Plant 1 had less significant reduction for calculated toxicity than its corresponding reduction in overall DBP formation following SDS. While overall DBP formation was reduced by 50−83%, cytotoxicity decreased only 7−17% and genotoxicity, by 29−34% following GAC (Figure 2). *This indicates that reductions in DBP concentrations do not necessarily reflect reductions in toxicity.* Plant 2 had the highest overall DBP formation, along with the highest calculated cytotoxicity and genotoxicity (Tables S13−S15); implementation of GAC treatment yielded 69%, 65%, and 34% reduction in calculated cytotoxicity and 50%, 76%, and 32% reduction in calculated genotoxicity for youngest, middle-aged, and oldest GAC, respectively, compared to not using GAC at all (Figure 2). Plant 3, which had the least impacted source water, formed lower calculated toxicity with 39−83% reduction in calculated cytotoxicity and 47−57% reduction in calculated genotoxicity following GAC (Figure 2).

Preformed DBPs. A reduction in calculated cytotoxicity and genotoxicity for preformed DBPs was substantial and consistent for Plant 1 (74−100% and 83−100% for cytotoxicity and genotoxicity, respectively; Table S13) but more variable for Plant 2 (43−100% and 74−100%, respectively, Table S14), which was driven by inconsistent breakthrough of bromoiodoacetamide. This compound is significantly more cytotoxic than most regulated DBPs (except bromoacetic acid).[50] At both plants, the preformed calculated toxicity in the GAC effluent was highest in the youngest GAC but was lower in older GAC, indicative of biological acclimation.[29]

At Plant 1, calculated cytotoxicity for preformed DBPs in the GAC influent was 70% of the value after SDS but dropped to <1−22% following GAC; calculated genotoxicity of the preformed DBPs in the GAC influent was 104% of the value after SDS and dropped to <1−22% following GAC (Tables S13 and S14). While preformed calculated toxicity was reduced by 74−100% in Plant 1, calculated cytotoxicity was only reduced by 7−17% following SDS procedures. Plant 2 preformed calculated cytotoxicity ranged from <1% to 61% of the value following SDS, and 0−34% of the calculated genotoxicity was preformed. Calculated toxicity is a function of both DBP concentration and toxicity index values and, therefore, does not always correlate with decreased DBP concentrations. This reduced efficiency of GAC following SDS procedures may indicate that individual DBPs may be more efficiently removed by GAC adsorption than corresponding precursors in some cases.

Drivers of Toxicity. At all three drinking water plants studied, THMs and HAAs constituted a majority of the quantified DBPs (Figure 2 and S6). For example, at Plant 1, THMs were 18−25% and HAAs were up to 9% of the TOX (Figure 5); however, THMs only contributed 2% to calculated cytotoxicity, and HAAs only contributed up to 3%. Cytotoxicity and genotoxicity drivers without GAC treatment were HNMs, IAAs, HALs, and HANs (Figure 5). Following GAC treatment, drivers of toxicity shifted to HNMs (70−76%), HANs (14−16%), and HAMs (9%), with little contribution of IAAs or HALs. The increase of tribromonitromethane after GAC treatment contributed up to 41% of the cytotoxicity and 37% of the genotoxicity (Figures 2 and 5). Formation of tribromonitromethane, like bromoiodoacetamide, may be due to desorption or to surface catalyzed reactions. Reduction of cytotoxicity and genotoxicity increases to 41−51% and 53−59%, respectively, if tribromonitromethane is not considered, *highlighting that the increase in concentration of toxic unregulated DBPs can have a dramatic impact on toxicity.* Dibromochloronitromethane and bromodichloronitromethane also contributed significantly to the calculated cytotoxicity and genotoxicity (16−20% and 14−16%, respectively).

At Plant 2, THMs were 34−75% and HAAs were 14−25% of the TOX, respectively (Figure S14). However, THMs contributed only ∼1% of the calculated cytotoxicity, while HAAs contributed 12−27%. Two groups contributing the most to cytotoxicity in the GAC influent of Plant 2 were HAMs and HANs, with 46% and 31%, respectively (Figure S14). Following GAC treatment, HAMs contributed to 21−32% and HANs to 43−50% of cytotoxicity. Major contributors to cytotoxicity were bromochloroacetamide (5−26%), dibromoacetamide (7−16%), bromochloroacetonitrile (14−20%), dibromoacetonitrile (11−31%), and bromoacetic acid (5−24%). Thus, while HAMs and HANs only contributed 4−8% and 1−3%, respectively, to TOX, they were the major drivers of cytotoxicity in the overall DBP mixture. *These results highlight that regulated DBP concentrations alone may not always provide an adequate basis for risk assessment.* THMs are not genotoxic in the Chinese hamster ovary (CHO) assay and, therefore, had no contribution to calculated genotoxicity. The drivers for genotoxicity at Plant 2 were HAAs (56% to 78%) and HANs (11% to 30%). Genotoxicity was largely driven by bromoacetic acid (40−81%) and dibromoacetonitrile (11−30%). For Plant 3 (2nd sampling) with and without GAC, HANs and HALs were drivers for cytotoxicity, while HNMs,

DOI: 10.1021/acs.est.9b00023
Environ. Sci. Technol. 2019, 53, 5987−5999

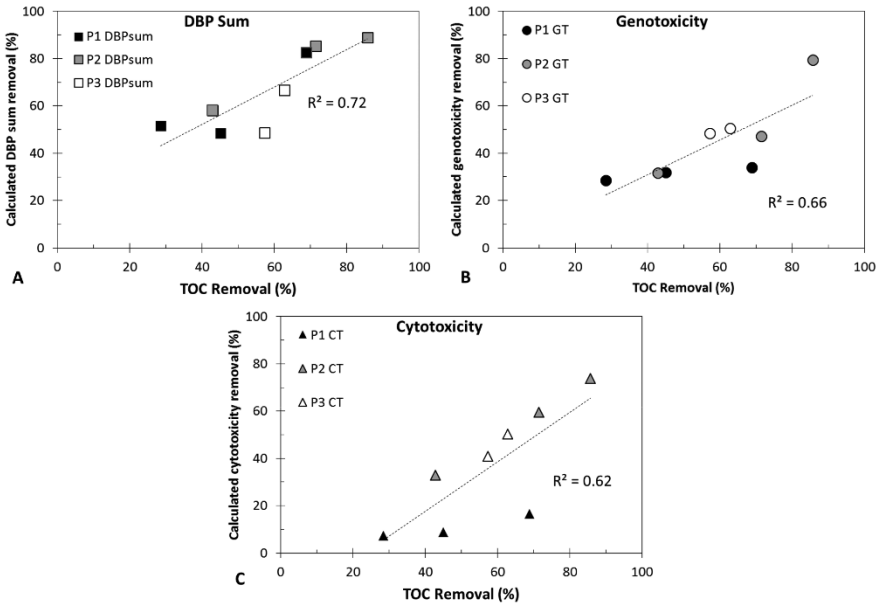

Figure 6. Relationship between TOC removal and removal of the SDS-DBP sum (A), genotoxicity (GT) (B), and cytotoxicity (CT) (C).

HANs, and HALs were the drivers for genotoxicity (Figure S15). This study represents the most extensive evaluation of calculated toxicity over the life of GAC.

Breakthrough Relationships to TOC. For preformed concentrations in Plants 1 and 2, TOC breakthrough was a useful conservative indicator for TOCl, TOBr, and the total DBP sum but not for TOI, which was present in the influent at 2 orders of magnitude lower than TOCl and 1 order of magnitude lower than TOBr (Figures S4 and S5). This pattern was also seen at Plant 1, and correlations between TOC removal and speciated TOX removal for the combined data sets from both plants are shown in Figure S17. At both plants, TOC was also a useful conservative indicator for calculated toxicity breakthrough, except at 3000 BV at Plant 2 for cytotoxicity (Figure S5). The relationships between TOC removal, removal of the SDS total DBP sum, and cytotoxicity and genotoxicity for all three plants are shown in Figure 6. The correlation coefficients (R^2 values) for TOC vs the SDS DBP sum, genotoxicity, and cytotoxicity are 0.72, 0.66, and 0.62, respectively. It should be noted that, if cytotoxicity for Plant 1 is excluded, the R^2 is 0.98 indicating much stronger correlations to TOC removal at Plants 2 and 3. The relationships between TOC and SDS TOCl, TOBr, TOI, and the DBP sum are shown in Figures S7, S8, and S9. As with preformed DBP results (Figure S17), TOC is an acceptable surrogate indicator for TOCl, TOBr, and DBP sum (but not for TOI), though TOC is not always the best indicator for the formation of specific compounds, e.g., N-DBPs,[77] which have strong impacts on calculated toxicity. Given the differences in DBP speciation between plants, the effectiveness of GAC for DBP and toxicity control was location specific and was likely a function of precursor characteristics, halide concentration, and GAC type.

Implications for Drinking Water Treatment and Risk Reduction. While concentrations of some Br- and N-DBPs increased following GAC treatment, the overall performance of GAC in decreasing DBP concentrations, calculated cytotoxicity, and calculated genotoxicity in finished waters is promising. However, it is clear that calculated toxicity reductions are not as dramatic as reduction in DBP levels. Moreover, decreased DBP concentrations do not necessarily reflect decreased toxicity, and small increases in some unregulated DBPs (such as tribromonitromethane) can have a dramatic impact on calculated toxicity. Thus, concentrations of regulated DBPs alone may not be adequate when conducting risk assessments.

The TIC-Tox method is a useful comparative tool, but it is based on *in vitro* models and excludes metabolic transformations. Future studies should also include real measurements of cytotoxicity and genotoxicity for GAC-treated waters to account for the total mixture toxicity, including unknown DBPs not measured in this study. In many cases, more than 50% of the halogenated material in chlorinated drinking water is not yet identified or quantified.[78] In this study, there was up to 79%, 45%, and 48% unknown TOX in Plants 1, 2, and 3, respectively (Figures 5, S14, and S15), indicating a need for further exploration of halogenated material in drinking waters and in particular I-DBPs. Low levels of bromide and iodide limit the formation of Br- and I-DBPs at the plants in this study, so future studies should address the impact that bromide and iodide may have on GAC efficiency to reduce toxicity. Finally, results indicate that prechlorination before GAC

DOI: 10.1021/acs.est.9b00023
Environ. Sci. Technol. 2019, 53, 5987−5999

treatment may be an effective strategy for further reducing DBP formation, but more research including measured toxicity is required.

■ ASSOCIATED CONTENT

Supporting Information

The Supporting Information is available free of charge on the ACS Publications website at DOI: 10.1021/acs.est.9b00023.

Additional details of materials and methods, bulk water parameters, and raw data with accompanying graphs (PDF)

■ AUTHOR INFORMATION

Corresponding Author

*Tel: 803-777-6932; fax: 803-777-9521; e-mail: richardson.susan@sc.edu.

ORCID

Amy A. Cuthbertson: 0000-0002-7634-3734
Hannah K. Liberatore: 0000-0001-7423-3251
Riley E. Mulhern: 0000-0001-6293-3672
Susan D. Richardson: 0000-0001-6207-4513

Notes

The authors declare no competing financial interest.

■ ACKNOWLEDGMENTS

The authors would like to acknowledge all the students and staff that contributed to this project including Joshua Allen, Alena Bensussan, Alex Bryer, Sami Cooler, Alejandro Ortega, Ashley Perkins, Taylor Hipp, Tiffany Crawford, Vincent Esposito, Meghan Franco, Jackson Crouse, Allison Reinert, and Rebekah Parris. Thanks to Eric Dickenson at the Southern Nevada Water Authority for valuable feedback. The authors also thank Lijian He from the Mass Spectrometry Center at the University of South Carolina for his help on ICP-MS measurements and use of their instrumentation as well as Dorothy Noble at the University of Colorado-Boulder for some of the regulated DBP analyses. Funding was provided by the Water Research Foundation (WRF) under Project 4560.

■ REFERENCES

(1) CDC. A Century of U.S. Water Chlorination and Treatment: One of the ten greatest public health achievements of the 20th century. *Morb. Mortal. Wkly. Rep.* **1999**, *48*, 621−629.

(2) Waller, K.; Swan, S. H.; DeLorenze, G.; Hopkins, B. Trihalomethanes in drinking water and spontaneous abortion. *Epidemiol.* **1998**, *9* (2), 134−140.

(3) Nieuwenhuijsen, M.; Toledano, M.; Eaton, N.; Fawell, J.; Elliott, P. Chlorination disinfection byproducts in water and their association with adverse reproductive outcomes: a review. *Occup. Environ. Med.* **2000**, *57* (2), 73−85.

(4) Villanueva, C. M.; Cantor, K.; Cordier, S.; Jaakkola, J.; King, W. D.; Lynch, C.; Porru, S.; Kogevinas, M. Disinfection byproducts and bladder cancer: a pool analysis. *Epidemiol.* **2004**, *15*, 357−367.

(5) Savitz, D. A.; Singer, P. C.; Hartmann, K. E.; Herring, A. H.; Weinberg, H. S.; Makarushka, C.; Hoffman, C.; Chan, R.; Maclehose, R. *Drinking Water Disinfection By-products and Pregnancy Outcome*; AWWA Research Foundation: Denver, CO, 2005.

(6) Richardson, S. D.; Plewa, M. J.; Wagner, E. D.; Schoeny, R.; DeMarini, D. M. Occurrence, genotoxicity, and carcinogenicity of regulated and emerging disinfection by-products in drinking water: A review and roadmap for research. *Mutat. Res., Rev. Mutat. Res.* **2007**, *636* (1−3), 178−242.

(7) Villanueva, C. M.; Cantor, K. P.; Grimalt, J. O.; Malats, N.; Silverman, D.; Tardon, A.; Garcia-Closas, R.; Serra, C.; Carrato, A.; Castaño-Vinyals, G.; Marcos, R.; Rothman, N.; Real, F. X.; Dosemeci, M.; Kogevinas, M. Bladder cancer and exposure to water disinfection by-Products through ingestion, bathing, showering, and swimming in pools. *Am. J. Epidemiol.* **2006**, *165* (2), 148−156.

(8) Cantor, K. P.; Villanueva, C. M.; Silverman, D. T.; Figueroa, J. D.; Real, F. X.; Garcia-Closas, M.; Malats, N.; Chanock, S.; Yeager, M.; Tardon, A.; Garcia-Closas, R.; Serra, C.; Carrato, A.; Castaño-Vinyals, G.; Samanic, C.; Rothman, N.; Kogevinas, M. Polymorphisms in GSTT1, GSTZ1, and CYP2E1, Disinfection by-products, and risk of bladder cancer in Spain. *Environ. Health Perspect.* **2010**, *118* (11), 1545−1550.

(9) Rahman, M. B.; Driscoll, T.; Cowie, C.; Armstrong, B. K. Disinfection by-products in drinking water and colorectal cancer: a meta-analysis. *Int. J. Epidemiol.* **2010**, *39*, 733−45.

(10) Costet, N.; Villanueva, C. M.; Jaakkola, J. J. K.; Kogevinas, M.; Cantor, K. P.; King, W. D.; Lynch, C. F.; Nieuwenhuijsen, M. J.; Cordier, S. Water disinfection by-products and bladder cancer: is there a European specificity? A pooled and meta-analysis of European case−control studies. *Occup. Environ. Med.* **2011**, *68* (5), 379.

(11) U.S. EPA. National Primary Drinking Water Regulations: Stage 2 Disinfectants and Disinfection Byproducts Rule. *Fed. Regist.* **2006**, *71*, 387−493.

(12) Jeong, C. H.; Wagner, E. D.; Siebert, V. R.; Anduri, S.; Richardson, S. D.; Daiber, E. J.; McKague, A. B.; Kogevinas, M.; Villanueva, C. M.; Goslan, E. H.; Luo, W.; Isabelle, L. M.; Pankow, J. F.; Grazuleviciene, R.; Cordier, S.; Edwards, S. C.; Righi, E.; Nieuwenhuijsen, M. J.; Plewa, M. J. The occurrence and toxicity of disinfection byproducts in European drinking waters in relation with the HIWATE epidemiology study. *Environ. Sci. Technol.* **2012**, *46* (21), 12120−12128.

(13) Krasner, S. W.; Lee, T. C. F.; Westerhoff, P.; Fischer, N.; Hanigan, D.; Karanfil, T.; Beita-Sandí, W.; Taylor-Edmonds, L.; Andrews, R. C. Granular activated carbon treatment may result in higher predicted genotoxicity in the presence of bromide. *Environ. Sci. Technol.* **2016**, *50* (17), 9583−9591.

(14) Plewa, M. J.; Wagner, E. D.; Richardson, S. D. TIC-Tox: A preliminary discussion on identifying the forcing agents of DBP-mediated toxicity of disinfected water. *J. Environ. Sci.* **2017**, *58* (Supplement C), 208−216.

(15) Richardson, S. D. Disinfection by-products: formation and occurrence of drinking water. In *The Encyclopedia of Environmental Health*; Nriagu, J. O., Ed.; Elsevier: Burlington, 2011; Vol. 2, pp 110−136.

(16) Chuang, Y. H.; McCurry, D. L.; Tung, H. H.; Mitch, W. A. Formation pathways and trade-offs between haloacetamides and haloacetaldehydes during combined chlorination and chloramination of lignin phenols and natural waters. *Environ. Sci. Technol.* **2015**, *49* (24), 14432−14440.

(17) Bond, T.; Templeton, M. R.; Graham, N. Precursors of nitrogenous disinfection by-products in drinking water-A critical review and analysis. *J. Hazard. Mater.* **2012**, *235*, 1−16.

(18) Kimura, S. Y.; Komaki, Y.; Plewa, M. J.; Marinas, B. J. Chloroacetonitrile and N,2-dichloroacetamide formation from the reaction of chloroacetaldehyde and monochloramine in water. *Environ. Sci. Technol.* **2013**, *47* (21), 12382−12390.

(19) Kimura, S. Y.; Vu, T. N.; Komaki, Y.; Plewa, M. J.; Marinas, B. J. Acetonitrile and N-chloroacetamide formation from the reaction of acetaldehyde and monochloramine. *Environ. Sci. Technol.* **2015**, *49* (16), 9954−9963.

(20) Shah, A. D.; Mitch, W. A. Halonitroalkanes, halonitriles, haloamides, and N-nitrosamines: A critical review of nitrogenous disinfection byproduct formation pathways. *Environ. Sci. Technol.* **2012**, *46* (1), 119−131.

(21) Richardson, S. D.; Thruston, A. D.; Rav-Acha, C.; Groisman, L.; Popilevsky, I.; Juraev, O.; Glezer, V.; McKague, A. B.; Plewa, M. J.; Wagner, E. D. Tribromopyrrole, brominated acids, and other

DOI: 10.1021/acs.est.9b00023
Environ. Sci. Technol. 2019, 53, 5987−5999

disinfection byproducts produced by disinfection of drinking water rich in bromide. *Environ. Sci. Technol.* **2003**, *37* (17), 3782−3793.
(22) Muellner, M. G.; Wagner, E. D.; McCalla, K.; Richardson, S. D.; Woo, Y.-T.; Plewa, M. J. Haloacetonitriles vs. regulated haloacetic acids: Are nitrogen-containing DBPs more toxic? *Environ. Sci. Technol.* **2007**, *41* (2), 645−651.
(23) Plewa, M. J.; Wagner, E. D.; Muellner, K. S.; Hsu, K. M.; Richardson, S. D. Comparative mammalian cell toxicity of N-DBPs and C-DBPs. In *Occurrence, Formation, Health Effects and Control of Disinfection By-Products in Drinking Water*; Karanfil, T. S., Krasner, S. W., Westerhoff, P., Xie, Y., Eds.; American Chemical Society: Washington, DC, 2008; pp 36−50.
(24) Plewa, M. J.; Muellner, M. G.; Richardson, S. D.; Fasano, F.; Buettner, K. M.; Woo, Y. T.; McKague, A. B.; Wagner, E. D. Occurrence, synthesis, and mammalian cell cytotoxicity and genotoxicity of haloacetamides: An emerging class of nitrogenous drinking water disinfection byproducts. *Environ. Sci. Technol.* **2008**, *42* (3), 955−961.
(25) Plewa, M. J.; Wagner, E. D.; Richardson, S. D.; Thruston, A. D.; Woo, Y. T.; McKague, A. B. Chemical and biological characterization of newly discovered iodoacid drinking water disinfection byproducts. *Environ. Sci. Technol.* **2004**, *38* (18), 4713−4722.
(26) Richardson, S. D.; Fasano, F.; Ellington, J. J.; Crumley, F. G.; Buettner, K. M.; Evans, J. J.; Blount, B. C.; Silva, L. K.; Waite, T. J.; Luther, G. W.; McKague, A. B.; Miltner, R. J.; Wagner, E. D.; Plewa, M. J. Occurrence and mammalian cell toxicity of iodinated disinfection byproducts in drinking water. *Environ. Sci. Technol.* **2008**, *42* (22), 8330−8338.
(27) Plewa, M. J.; Wagner, E. D.; Muellner, M. G.; Hsu, K. M.; Richardson, S. D. Comparative mammalian cell toxicity of N-DBPs and C-DBPs. In *Disinfection by-Products in Drinking Water: Occurrence, Formation, Health Effects, and Control*; Karanfil, T., Krasner, S. W., Xie, Y., Eds.; American Chemical Society: Washington, DC, 2008; Vol. *995*, pp 36−50.
(28) Liberatore, H. K.; Plewa, M. J.; Wagner, E. D.; VanBriesen, J. M.; Burnett, D. B.; Cizmas, L. H.; Richardson, S. D. Identification and comparative mammalian cell cytotoxicity of new iodo-phenolic disinfection byproducts in chloraminated oil and gas wastewaters. *Environ. Sci. Technol. Lett.* **2017**, *4* (11), 475−480.
(29) Knappe, D. R. U. Chapter 9 - Surface chemistry effects in activated carbon adsorption of industrial pollutants. In *Interface Science and Technology*; Newcombe, G., Dixon, D., Eds.; Elsevier: New York, 2006; Vol. *10*, pp 155−177.
(30) Summers, R. S.; Knappe, D. R. U.; Snoeyink, V. L. Adsorption of organic compounds by activated carbon. In *Water Quality and Treatment*, 6 ed.; American Water Works Association McGraw-Hill: New York, 2010.
(31) Chili, C. A.; Westerhoff, P.; Ghosh, A. GAC removal of organic nitrogen and other DBP precursors. *J. - Am. Water Works Assoc.* **2012**, *104* (7), E406−E415.
(32) Fu, J.; Lee, W. N.; Coleman, C.; Nowack, K.; Carter, J.; Huang, C. H. Removal of disinfection byproduct (DBP) precursors in water by two-stage biofiltration treatment. *Water Res.* **2017**, *123*, 224−235.
(33) Liu, C.; Olivares, C. I.; Pinto, A. J.; Lauderdale, C. V.; Brown, J.; Selbes, M.; Karanfil, T. The control of disinfection byproducts and their precursors in biologically active filtration processes. *Water Res.* **2017**, *124*, 630−653.
(34) Jiang, J. Y.; Zhang, X. R.; Zhu, X. H.; Li, Y. Removal of intermediate aromatic halogenated DBPs by activated carbon adsorption: A new approach to controlling halogenated DBPs in chlorinated drinking water. *Environ. Sci. Technol.* **2017**, *51* (6), 3435−3444.
(35) Symons, J. M.; Krasner, S. W.; Simms, L. A.; Sclimenti, M. J. Measurement of THM and precursor concentrations revisited: The effect of bromide ion. *J. - Am. Water Works Assoc.* **1993**, *85* (1), 51−62.
(36) Summers, R. S.; Benz, M. A.; Shukairy, M. H.; Cummings, L. Effect of separation processes on the formation of brominated THMs. *J. - Am. Water Works Assoc.* **1993**, *85* (1), 88−95.
(37) Smith, E. M.; Plewa, M. J.; Lindell, C. L.; Richardson, S. D.; Mitch, W. A. Comparison of byproduct formation in waters treated with chlorine and iodine: Relevance to point-of-use treatment. *Environ. Sci. Technol.* **2010**, *44* (22), 8446−8452.
(38) Allard, S.; Tan, J.; Joll, C. A.; von Gunten, U. Mechanistic study on the formation of Cl-/Br-/I-trihalomethanes during chlorination/chloramination combined with a theoretical cytotoxicity evaluation. *Environ. Sci. Technol.* **2015**, *49* (18), 11105−11114.
(39) Kristiana, I.; Lethorn, A.; Joll, C.; Heitz, A. To add or not to add: The use of quenching agents for the analysis of disinfection by-products in water samples. *Water Res.* **2014**, *59* (Supplement C), 90−98.
(40) Gong, T.; Tao, Y.; Xian, Q. Selection and applicability of quenching agents for the analysis of polar iodinated disinfection byproducts. *Chemosphere* **2016**, *163* (Supplement C), 359−365.
(41) Allen, J. M.; Cuthbertson, A. A.; Liberatore, H. K.; Kimura, S. Y.; Mantha, A.; Edwards, M. A.; Richardson, S. D. Showering in Flint, MI: Is there a DBP problem? *J. Environ. Sci.* **2017**, *58* (Supplement C), 271−284.
(42) U.S. EPA *Method 551.1: Determination of Chlorination Disinfection Byproducts, Chlorinated Solvents, and Halogenated Pesticides/Herbicides in Drinking Water by Liquid-Liquid Extraction and Gas Chromatography with Electron-Capture Detection*; Revision 1.0 ed.; U.S. EPA: Cincinnati, OH, 1995.
(43) U.S. EPA *Method 552.3. Determination of Haloacetic Acids and Dalapon in Drinking Water by Liquid-Liquid Microextraction, Derivatization, and Gas Chromatography with Electron Capture Detection*; U.S. EPA: Cincinnati, OH, 2003.
(44) Richardson, S. D. *Diazomethane Generation Using Sigma-Aldrich Diazaldehyde Generator and Methylation of Carboxylic Acid Compounds: SOP − RSB-010.1*; U.S. EPA: Athens, GA, 2009.
(45) Jeong, C. H.; Postigo, C.; Richardson, S. D.; Simmons, J. E.; Kimura, S. Y.; Mariñas, B. J.; Barcelo, D.; Liang, P.; Wagner, E. D.; Plewa, M. J. Occurrence and comparative toxicity of haloacetaldehyde disinfection byproducts in drinking water. *Environ. Sci. Technol.* **2015**, *49* (23), 13749−13759.
(46) Echigo, S.; Zhang, X.; Minear, R. A.; Plewa, M. Differentiation of total organic brominated and chlorinated compounds in total organic halide measurement: A new approach with an ion chromatographic technique. In *Natural Organic Matter and Disinfection By-Products: Characterization and Control in Drinking Water*; Barrett, S. E., Krasner, S. W., Amy, G., Eds.; American Chemical Society: Washington, DC, 2000; pp 330−342.
(47) Daiber, E. J.; DeMarini, D. M.; Ravuri, S. A.; Liberatore, H. K.; Cuthbertson, A. A.; Thompson-Klemish, A.; Byer, J. D.; Schmid, J. E.; Afifi, M. Z.; Blatchley, E. R.; Richardson, S. D. Progressive Increase in disinfection byproducts and mutagenicity from source to tap to swimming pool and spa water: Impact of human inputs. *Environ. Sci. Technol.* **2016**, *50* (13), 6652−6662.
(48) Kimura, S. Y.; Zheng, W.; Hipp, T. N.; Allen, J. M.; Richardson, S. D. Total organic halogen (TOX) in human urine: A halogen-specific method for human exposure studies. *J. Environ. Sci.* **2017**, *58* (Supplement C), 285−295.
(49) Yang, Y.; Komaki, Y.; Kimura, S. Y.; Hu, H.-Y.; Wagner, E. D.; Mariñas, B. J.; Plewa, M. J. Toxic impact of bromide and iodide on drinking water disinfected with chlorine or chloramines. *Environ. Sci. Technol.* **2014**, *48* (20), 12362−12369.
(50) Wagner, E. D.; Plewa, M. J. CHO cell cytotoxicity and genotoxicity analyses of disinfection by-products: An updated review. *J. Environ. Sci.* **2017**, *58* (Supplement C), 64−76.
(51) Westerhoff, P.; Mash, H. Dissolved organic nitrogen in drinking water supplies: a review. *Aqua* **2002**, *51* (8), 415−448.
(52) Mitch, W. A.; Schreiber, I. M. Degradation of tertiary alkylamines during chlorination/chloramination: Implications for formation of aldehydes, nitriles, haloni troalkanes, and nitrosamines. *Environ. Sci. Technol.* **2008**, *42* (13), 4811−4817.
(53) Joo, S. H.; Mitch, W. A. Nitrile, aldehyde, and halonitroalkane formation during chlorination/chloramination of primary amines. *Environ. Sci. Technol.* **2007**, *41* (4), 1288−1296.

DOI: 10.1021/acs.est.9b00023
Environ. Sci. Technol. 2019, 53, 5987−5999

(54) Liew, D.; Linge, K. L.; Joll, C. A. Formation of nitrogenous disinfection by-products in 10 chlorinated and chloraminated drinking water supply systems. *Environ. Monit. Assess.* **2016**, *188* (9), 16.
(55) Zhou, S. Q.; Zhu, S. M.; Shao, Y. S.; Gao, N. Y. Characteristics of C-, N-DBPs formation from algal organic matter: Role of molecular weight fractions and impacts of pre-ozonation. *Water Res.* **2015**, *72*, 381−390.
(56) Fang, J. Y.; Yang, X.; Ma, J.; Shang, C.; Zhao, Q. A. Characterization of algal organic matter and formation of DBPs from chlor(am)ination. *Water Res.* **2010**, *44* (20), 5897−5906.
(57) Fang, J. Y.; Ma, J.; Yang, X.; Shang, C. Formation of carbonaceous and nitrogenous disinfection by-products from the chlorination of Microcystis aeruginosa. *Water Res.* **2010**, *44* (6), 1934−1940.
(58) Yang, X.; Guo, W. H.; Shen, Q. Q. Formation of disinfection byproducts from chlor(am)ination of algal organic matter. *J. Hazard. Mater.* **2011**, *197*, 378−388.
(59) Wert, E. C.; Rosario-Ortiz, F. L. Intracellular organic matter from cyanobacteria as a precursor for carbonaceous and nitrogenous disinfection byproducts. *Environ. Sci. Technol.* **2013**, *47* (12), 6332−6340.
(60) Kennedy, A. M.; Reinert, A. M.; Knappe, D. R. U.; Ferrer, I.; Summers, R. S. Full- and pilot-scale GAC adsorption of organic micropollutants. *Water Res.* **2015**, *68*, 238−248.
(61) Wu, H. W.; Xie, Y. F. F. Effects of EBCT and water temperature on HAA removal using BAC. *J. - Am. Water Works Assoc.* **2005**, *97* (11), 94−101.
(62) Gibert, O.; Lefevre, B.; Fernandez, M.; Bernat, X.; Paraira, M.; Pons, M. Fractionation and removal of dissolved organic carbon in a full-scale granular activated carbon filter used for drinking water production. *Water Res.* **2013**, *47* (8), 2821−2829.
(63) Mohd Zainudin, F.; Abu Hasan, H.; Sheikh Abdullah, S. R. An overview of the technology used to remove trihalomethane (THM), trihalomethane precursors, and trihalomethane formation potential (THMFP) from water and wastewater. *J. Ind. Eng. Chem.* **2018**, *57*, 1−14.
(64) Dietrich, A. M.; Gallagher, D. L.; DeRosa, P. M.; Millington, D. S.; Digiano, F. A. Enhancement of N-nitrosamine formation on granular-activated carbon from N-methylaniline and nitrite. *Environ. Sci. Technol.* **1986**, *20* (10), 1050−1055.
(65) Duirk, S. E.; Lindell, C.; Cornelison, C. C.; Kormos, J.; Ternes, T. A.; Attene-Ramos, M.; Osiol, J.; Wagner, E. D.; Plewa, M. J.; Richardson, S. D. Formation of toxic iodinated disinfection by-products from compounds used in medical imaging. *Environ. Sci. Technol.* **2011**, *45*, 6845−6854.
(66) Tugulea, A.-M.; Aranda-Rodriguez, R.; Bérubé, D.; Giddings, M.; Lemieux, F.; Hnatiw, J.; Dabeka, L.; Breton, F. The influence of precursors and treatment process on the formation of iodo-THMs in Canadian drinking water. *Water Res.* **2018**, *130*, 215−223.
(67) Richardson, S. D.; Ternes, T. A. Water analysis: Emerging contaminants and current issues. *Anal. Chem.* **2018**, *90*, 398−428.
(68) Means, E. G., III; Krasner, S. W. D-DBP regulation: issues and ramifications. *J. - Am. Water Works Assoc.* **1993**, *85*, 68−73.
(69) Chuang, Y. H.; Shabani, F.; Munoz, J.; Aflaki, R.; Hammond, S. D.; Mitch, W. A. Formation of N-nitrosamines during the analysis of municipal secondary biological nutrient removal process effluents by US EPA method 521. *Chemosphere* **2019**, *221*, 597−605.
(70) Zeng, T.; Mitch, W. A. Impact of nitrification on N-nitrosamine and halogenated disinfection byproduct formation within drinking water storage facilities. *Environ. Sci. Technol.* **2016**, *50*, 2964−2973.
(71) Maes, N.; de Cannieére, P.; Sillen, X.; van Ravestyn, L.; Put, M. *Migration of Iodide in Backfill Materials Containing an Anion Getter*; SCK CEN: 2004; p 45.
(72) Kaufhold, S.; Pohlmann-Lortz, M.; Dohrmann, R.; Nüesch, R. About the possible upgrade of bentonite with respect to iodide retention capacity. *Appl. Clay Sci.* **2007**, *35* (1), 39−46.
(73) Watson, K.; Farré, M. J.; Knight, N. Strategies for the removal of halides from drinking water sources, and their applicability in disinfection by-product minimisation: A critical review. *J. Environ. Manage.* **2012**, *110* (Supplement C), 276−298.
(74) Bichsel, Y.; von Gunten, U. Oxidation of iodide and hypoiodous acid in the disinfection of natural waters. *Environ. Sci. Technol.* **1999**, *33* (22), 4040−4045.
(75) Bichsel, Y.; von Gunten, U. Hypoiodous acid: Kinetics of the buffer-catalyzed disproportionation. *Water Res.* **2000**, *34* (12), 3197−3203.
(76) Ikari, M.; Matsui, Y.; Suzuki, Y.; Matsushita, T.; Shirasaki, N. Removal of iodide from water by chlorination and subsequent adsorption on powdered activated carbon. *Water Res.* **2015**, *68* (SupplementC), 227−237.
(77) Mulhern, R. E.; Summers, R. S.; Dickenson, E. R. V. Evaluating and modeling the activated carbon adsorption of wastewater-derived N-nitrosodimethylamine precursors. *Environ. Sci.:Water Res. Technol.* **2017**, *3* (5), 844−856.
(78) Krasner, S. W.; Weinberg, H. S.; Richardson, S. D.; Pastor, S. J.; Chinn, R.; Sclimenti, M. J.; Onstad, G. D.; Thruston, A. D., Jr. Occurrence of a new generation of disinfection byproducts. *Environ. Sci. Technol.* **2006**, *40* (23), 7175−7185.

DOI: 10.1021/acs.est.9b00023
Environ. Sci. Technol. 2019, 53, 5987−5999

ACS OMEGA

Article

Cite This: ACS Omega 2019, 4, 8290−8298

http://pubs.acs.org/journal/acsodf

Probing the Formation of Reactive Oxygen Species by a Porous Self-Assembled Benzophenone Bis-Urea Host

Baillie A. DeHaven,[†] Hannah K. Liberatore,[†] Alexander Greer,[‡,§] Susan D. Richardson,[†] and Linda S. Shimizu*[,†]

[†]Department of Chemistry and Biochemistry, University of South Carolina, Columbia, South Carolina 29208, United States

[‡]Department of Chemistry, Brooklyn College, Brooklyn, New York 11210, United States

[§]Ph.D. Program in Chemistry, Graduate Center of City University of New York, New York, New York 10016, United States

Supporting Information

ABSTRACT: Herein, we examine the photochemical formation of reactive oxygen species (ROS) by a porous benzophenone-containing bis-urea host (**1**) to investigate the mechanism of photooxidations that occur within the confines of its nanochannels. UV irradiation of the self-assembled host in the presence of molecular oxygen generates both singlet oxygen and superoxide when suspended in solution. The efficiency of ROS generation by the host is lower than that of benzophenone (BP), which could be beneficial for reactions carried out catalytically, as ROS species react quickly and often unselectively. Superoxide formation was detected through reaction with 5,5-dimethyl-1-pyrroline *N*-oxide in the presence of methanol. However, it is not detected in $CHCl_3$, as it reacts rapidly with the solvent to generate methaneperoxy and chloride anions, similar to BP. The lifetime of airborne singlet oxygen ($\tau_{\Delta airborne}$) was examined at the air−solid outer surface of the host and host·quencher complexes and suggests that quenching is a surface phenomenon. The efficiency of the host and BP as catalysts was compared for the photooxidation of 1-methyl-1-cyclohexene in solution. Both the host and BP mediate the photooxidation in $CHCl_3$, benzene, and benzene-d_6, producing primarily epoxide-derived products with low selectivity likely by both type I and type II photooxidation processes. Interestingly, in $CHCl_3$, two chlorohydrins were also formed, reflecting the formation of chloride in this solvent. In contrast, UV irradiation of the host·guest crystals in an oxygen atmosphere produced no epoxide and appeared to favor mainly the type II processes. Photolysis afforded high conversion to only three products: an enone, a tertiary allylic alcohol, and a diol, which demonstrates the accessibility of the encapsulated reactants to oxygen and the influence of confinement on the reaction pathway.

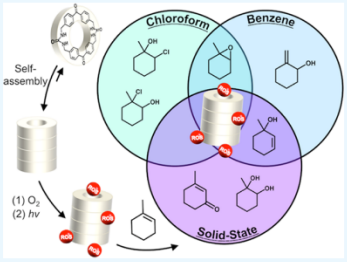

INTRODUCTION

Here, we investigate the selectivity and efficiency of reactive oxygen species (ROS) photogeneration by a self-assembled benzophenone *bis*-urea macrocycle (host **1**) and probe its utility for mediating the photooxidation of 1-methyl-1-cyclohexene (**2**) suspended in solution compared to the solid state. Host **1** presents two benzophenone (BP) photosensitizer units covalently attached to two urea groups through methylene bridges resulting in a *bis*-urea macrocycle. Self-assembly through bifurcated urea hydrogen-bonding interactions affords hexagonally packed columnar nanotubes that are activated by heating to generate accessible channels that can be readily loaded with guests and applied as a nanoreactor for selective photooxidations, Figure 1.[1,2]

Our previous report showed that photolysis of host **1** crystals in oxygenated $CHCl_3$ showed NIR photoluminescence of $^1O_2$ at 1270 nm.[1] Furthermore, UV irradiation (1 h) of the crystals generates low quantities (~1 in 30 000 molecules) of persistent triplet radical pairs consisting of a ketyl radical and benzylic radicals.[3] In the current work, we hypothesize that host **1** will photogenerate ROS in a controlled manner based on media (suspended in solution versus in the solid state). Our work is fundamental, in that controlling the type of ROS formed is challenging.

ROS can be employed in a diverse range of applications ranging from wastewater treatment to photodynamic therapy for cancer treatment[4−7] but are often produced as mixtures. This is because O_2 can be activated through type I and type II photosensitized oxidation processes.[8,9] Type I reactions produce species such as $O_2^{\bullet-}$, $HO_2\cdot$, ROO·, RO·, and ·OH.[9−11] Type II reactions mainly produce singlet oxygen ($^1O_2$) through a Dexter energy transfer of the triplet sensitizer with $^3O_2$.[8,12−14] Achieving high selectivity in photooxidations carried out by ROS is challenging due to their high reactivity. Thus, strategies to achieve control over selectivity are useful

Received: March 26, 2019
Accepted: April 25, 2019
Published: May 8, 2019

DOI: 10.1021/acsomega.9b00831
ACS Omega 2019, 4, 8290−8298

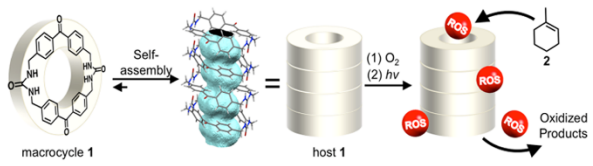

Figure 1. Macrocycle **1** is composed of two BP sensitizer units covalently bound through methylene urea groups. Self-assembly through bifurcated urea hydrogen-bonding interactions results in the formation of porous host **1** nanotubes with one-dimensional (1D) elliptical channels (highlighted in light blue). UV irradiation of the host crystals results in the generation of ROS through type I and type II pathways.

Scheme 1. Proposed Mechanism for the Photooxidation Pathways of Host 1

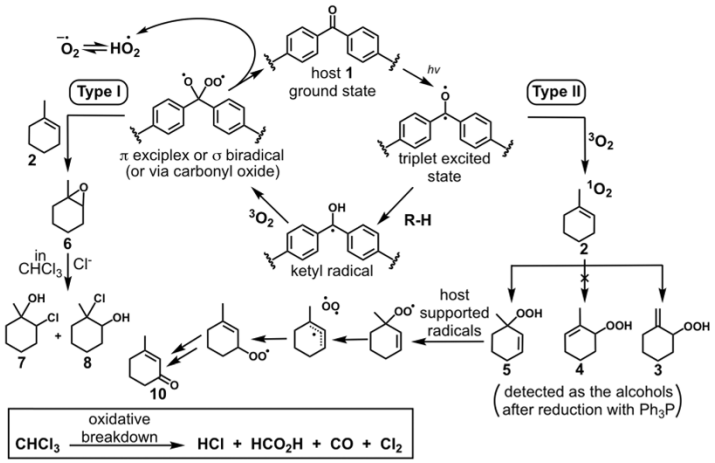

and include templating,[15] air−water interfacial effects,[16] and nanocavity confinement.[1,17,18]

Herein, we probe the channel confinement effect with host **1** in an effort to gain some control over the ROS mechanism. In this work, we found that photolysis of host **1** leads to (1) the detection of both $O_2^{\bullet-}$ and $^1O_2$, which was found to be dependent on its environment; (2) an $^1O_2$ quantum yield ($\Phi[^1O_2]$) of 1−12%; (3) outer wall quenching of $^1O_2$ by host **1**, reducing the lifetime of $^1O_2$ at the air−solid interface; and (4) some selectivity in photooxidations of 1-methyl-1-cyclohexene **2** in solution (type I and type II reactions) versus within the solid phase (favoring type II reactions). Selectivity comparisons of host **1** are made with homogeneous photooxidations with benzophenone[19] and selectivity achieved with octa acid hosts[20] and zeolites.[21]

Our data are consistent with the mechanism shown in Scheme 1, in which host **1** photogenerates both $^1O_2$ and $O_2^{\bullet-}$.[10,22] Selectivity for hydroperoxide **5** over **3** and **4** is seen in the solid state, where **5** undergoes a Schenk rearrangement to enone **10**. Superoxide generation by BP involves the formation of a ketyl radical, which will then undergo an electron-transfer process with $^3O_2$ to form $O_2^{\bullet-}$.[10,22,23] A π host/O_2 exciplex or σ $R_2C(O^{\bullet})O_2^{\bullet}$ biradical at a BP site is proposed as the epoxidizing agent due to the unusual formation of chlorohydrins in $CHCl_3$.

RESULTS AND DISCUSSION

ROS Generated by the Host 1 Crystals Suspended in Solution. The type of ROS generated by host **1** suspended in solution was investigated using electron paramagnetic resonance (EPR) and UV−vis spectroscopies. Literature examples show that BP photoactivates oxygen to $O_2^{\bullet-}$ in protic solvents, such as MeOH, ethanol, and 2-propanol.[10,22] Therefore, EPR spin-trapping experiments were used to probe if host **1**, like parent BP, generates $O_2^{\bullet-}$. 5,5-Dimethyl-1-pyrroline *N*-oxide (DMPO) was selected as the spin trap, which is known to form adducts (doublet of triplets) with $O_2^{\bullet-}$, hydroxide, or peroxyl radicals, where DMPO−OOH degrades to DMPO−OH adduct.[24−26] Interestingly, the detection of $O_2^{\bullet-}$ by EPR was found to be solvent-dependent using DMPO, where the DMPO−OOH adduct was detected in a solution of benzene containing catalytic amounts MeOH but was not detected in $CHCl_3$ (Figure 2).

Irradiation of a host **1** suspension of DMPO in benzene with a catalytic amount of MeOH resulted in the formation of a DMPO adduct evident (Figure 2A) by hyperfine splitting constants of a^N = 14.2 G and a^H = 9.2 G, which is in the range of typical DMPO−OOH adducts (Figure S8).[27−29] Furthermore, the irradiation of BP for 2 min in the presence of DMPO and MeOH also resulted in the formation of a four-line spectrum that overlays well with the spectra obtained by host **1**, with a^N = 13.8 G and a^H = 9.3 G (Figure S9). In the

DOI: 10.1021/acsomega.9b00831
ACS Omega 2019, 4, 8290−8298

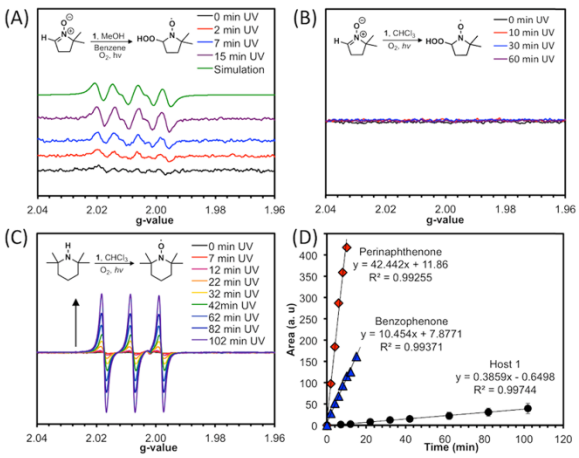

Figure 2. EPR studies of host **1** suspended in oxygen-saturated solutions of $O_2^{\bullet-}$ and $^1O_2$ quenchers. (A) DMPO was used to trap $O_2^{\bullet-}$ in benzene in the presence of **1** and MeOH. (B) DMPO $O_2^{\bullet-}$-trapping experiment in $CHCl_3$ in the presence of **1**. (C) Irradiation of **1** in a solution of 2,2,6,6-tetramethylpiperidine (TMP) in $CHCl_3$ results in the chemical quenching of $^1O_2$ to form 2,2,6,6-tetramethyl piperidine-1-yl oxidanyl (TEMPO) over time. (D) Comparison of the TMP chemical-quenching studies with three photosensitizers: perinaphthenone, BP, and host **1**. The error bars for the host **1** plot represent the standard deviation between triplicate trials.

presence of MeOH, the host can generate $O_2^{\bullet-}$, albeit ~15× slower than BP. The formation of superoxide is further supported by the direct detection of its λ_{max} at 255 nm, using UV−visible spectroscopy in acetonitrile (Figure S25).[10]

A similar experiment was carried out using chloroform as the solvent; however, no DMPO adduct was detected, Figure 4B. The lack of DMPO adduct suggests that the $[O_2^{\bullet-}]$ is very low, leaving little if any $O_2^{\bullet-}$ to form an adduct with DMPO. Relatedly, Roberts and Sawyer reported that $O_2^{\bullet-}$ reacts with $CHCl_3$ to generate methaneperoxy ($HC(=O)OO^-$) and chloride anions.[30] In addition, the oxidative breakdown of $CHCl_3$ is also known to produce HCl, HCO_2H, CO, and Cl_2. Therefore, it is likely that $O_2^{\bullet-}$ is indeed generated by **1** in $CHCl_3$ but quickly reacts with the solvent before any DMPO adduct can be formed. This result suggests that the use of $CHCl_3$ for $O_2^{\bullet-}$ detection by DMPO should be avoided.

Next, the formation of $^1O_2$ was probed using 2,2,6,6-tetramethylpiperidine (TMP), which is oxidized by $^1O_2$ to form a stable nitroxide radical 2,2,6,6-tetramethyl piperidine-1-yl oxidanyl (TEMPO), which gives rise to three-line EPR spectra.[24,26] Irradiation of an oxygen-saturated $CHCl_3$ solution with suspended host **1** led to the formation of a three-line TEMPO signal, indicating the formation of $^1O_2$ (Figure 2C). The areas obtained by the EPR signals for DMPO and TEMPO in $CHCl_3$ were found to be quite similar (5.8 vs 5.1) with the $O_2^{\bullet-}$ adduct generated ~1.1× faster than $^1O_2$. Thus, both $O_2^{\bullet-}$ and $^1O_2$ are photogenerated by host **1** in type I and type II processes.

Quantum Yields of $^1O_2$ Generation in Solution. The $^1O_2$ quantum yield of **1** while suspended in $CHCl_3$ was approximated using EPR and UV−visible spectroscopy and was found to be low, ranging from 1 to 12% depending on the method. Figure 2C shows the gradual formation of TEMPO from TMP. The $\Phi[^1O_2]^{host\ 1}$ was estimated to be ~1% in $CHCl_3$ when compared to the reference, perinapthenone (Figure 2D).[31] In some cases, the use of TMP in determining the quantum yield of $^1O_2$ production can be misleading when the excited photosensitizer is able to react with TMP, resulting in the $TMP^{\bullet+}$.[26] The radical cation can then undergo a reaction with molecular oxygen to form an EPR-detectable TEMPO signal that is not attributed to $^1O_2$ production.[26] While this process has been observed by the parent BP, it is not anticipated to occur (or be minimal at best) with host **1** because TMP is too large to fit into the host channels (Table S1).

In addition to EPR, the $\Phi[^1O_2]$ was also measured by UV−vis spectroscopy using 1,4-dimethylnaphthalene (DMN), an $^1O_2$ trap that absorbs at higher-energy wavelengths (~290 nm) than the 360 nm required for **1** to generate $^1O_2$. Figure 3 shows the decrease of the DMN absorbance signal with the time of irradiation, indicative of the DMN reaction with $^1O_2$ forming the 1,4-naphthalene endoperoxide product, which does not absorb in this region. From these data, we calculated the $\Phi[^1O_2]^{host\ 1}$ to be 12% in $CHCl_3$, when compared to the

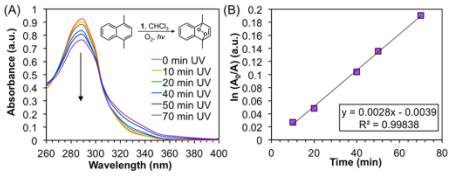

Figure 3. Indirect quantification of the quantum yield of $^1O_2$ generation by host **1** as monitored by the absorption loss of DMN. (A) Oxygen-saturated solution of DMN was irradiated in the presence of host **1** and the absorbance spectra recorded over time to monitor the loss of DMN. (B) Area of UV absorbance plotted versus time of UV irradiation for host **1**.

DOI: 10.1021/acsomega.9b00831
ACS Omega 2019, 4, 8290 8298

reference methylene blue.[32,33] We note that 1,4-dimethylnaphthalene-1,4-endoperoxide has a half-life ($t_{1/2}$) of 5 h at 25 °C and can serve as a chemical source of $^1O_2$;[34−36] however, this $^1O_2$ release was relatively low on the time scale of our quantum yield measurements. Furthermore, it is not surprising that the $\Phi[^1O_2]$ varies between the two techniques, as they show different sensitivity.[37]

Given these results, we conclude that the host generates low quantities of $^1O_2$ with $\Phi[^1O_2]^{host\ 1}$ ranging from 1 to 12%. The low $^1O_2$ quantum yield could be advantageous for suspended host catalytic studies, as it may encourage oxidations to occur within the confines of the host channels as opposed to free in solution.

Lifetime of $^1O_2$ at the Air−Solid Interface. Because selectivity was reported for the photooxidation of 2-methyl-2-butene in crystalline complexes with host **1**,[1] we are interested in the lifetime of $^1O_2$ at the air−solid interface of the host crystals. The lifetime reduction of $^1O_2$ by the **1**·DMSO complex and by solid Ph_3P was measured to give a sense of the outer-wall-quenching capacity. Solid Ph_3P was used for comparison, as it is a well-known chemical quencher of $^1O_2$ in the solution phase.[13,38] Other **1**·quencher complexes were prepared and include *N*,*N*-dimethylaniline, pyridine, and *N*,*N*,*N*′,*N*′-tetramethyl-ethane-1,2-diamine (Table S1).

Figure 4 shows the lifetime of airborne $^1O_2$ ($\tau_{\Delta airborne}$) generated by a three-phase apparatus to be ∼150 μs and thus

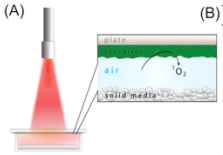

(B)

Entry	Sample	$\tau_{\Delta airborne}$(ms)
1	Pc plate	~0.15
2	**1**•DMSO + Pc plate	0.13±0.02
3	**1**•pyridine +Pc plate	0.12±0.06
4	Solid Ph_3P +Pc plate	0.10±0.03

Figure 4. Measurement of the airborne $^1O_2$ lifetime at the air−solid interface. (A) Simplified experimental setup, consisting of a sensitizer plate used to generate airborne $^1O_2$ whose lifetime was measured by a photomultiplier tube through a 1270 nm band-pass filter. (B) Table of the experimental $^1O_2$ lifetimes obtained in this study.

longer compared to $^1O_2$ solvated in benzene and toluene by ∼5-fold (31 and 29 μs, respectively), and MeOH and ethanol by ∼15-fold (10 and 13 μs, respectively).[39] The lifetime of $^1O_2$ in DMSO is 30 μs but is reduced in pyridine (5.7 μs).[39] The total quenching rate constant (k_T) for Ph_3P is 8.5 × 10^6 M^{-1} s^{-1}, and for other phosphines, it ranges from 0.1 to 2.0 × 10^7 M^{-1} s^{-1}.[38,40,41] The table in Figure 4 shows that the $\tau_{\Delta airborne}$ is reduced going from a sample absent of a solid-trapping agent (∼0.15 ms) to a sample containing solid host **1** (with DMSO or pyridine guests; 0.13 and 0.12 ms, respectively) and solid Ph_3P (0.10 ms). These data are in line with the quenching of $^1O_2$ in the solution phase. We attribute the decrease to be sensitive to factors such as the high oxophilicity of Ph_3P in solid-surface physical and chemical quenching. That is, once the $^1O_2$ was carried from the sensitizer plate to the air/solid interface of the solid host or solid Ph_3P, it was quenched. In the previous work, long and short $^1O_2$ lifetimes were found depending on whether it resided within a gas bubble or in the bulk aqueous solution.[42] In a gas bubble, an $^1O_2$ lifetime of 0.98 ms has been previously observed.[42] Seeing that the lifetime of $^1O_2$ in air is decreased in the presence of the host in comparison to the Pc plate or in a gas bubble, we wanted to next investigate ROS formation by the interior of the host.

Comparison of Photooxidations of 1-Methyl-1-cyclohexene (2) Sensitized by Host 1 and BP. Oxidation reactions were investigated in solution ($CHCl_3$, benzene, and benzene-d_6) and in the solid state to uncover differences in product distributions. Our goal is to correlate the products formed to specific photooxidation mechanisms (type I vs type II) and to uncover confinement effects. Substrate **2** and sensitizer (**1** or BP) were UV-irradiated in an oxygen-saturated environment (solution or solid state). The reactions were quenched with triphenylphosphine to reduce any hydroperoxides and analyzed by gas chromatography mass spectrometry (GC−MS) (Table 1).

Efficiency of Photooxidations in Heterogeneous Solutions. The photosensitizers investigated vary in solubility. Host **1** was used as a suspension, while BP was soluble. Photolysis of **2** mediated by sensitizer **1** in oxygen-saturated $CHCl_3$ (Table 1, entry 1) led to three major oxidation products, epoxide **6** (21%) and two chlorohydrins **7** (24%) and **8** (16%). Overall, 92% conversion was observed with other minor products consisting mainly of enones and ketones (Figure S20). The formation of the chlorohydrins reflects the degradation of the solvent by $O_2^{\bullet-}$, as indicated by the DMPO spin-trapping experiment in $CHCl_3$. Thus, we compared photolysis of **2** with BP sensitizer under similar conditions (Table 1, entry 2), which resulted in 100% conversion of **2**. Chlorohydrin **7** (37%) was the major product with multiple

Table 1. Product Distributions in Photosensitized Oxidation of Alkenes[a]

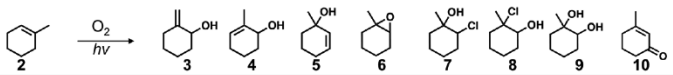

Entry	Conditions	Time (h)	% Conversion	% Selectivity							
1	Host **1** ($CHCl_3$)[b]	18	92%	--	--	--	21%	24%	16%	--	--
2	BP ($CHCl_3$)	18	~100%	--	--	--	--	37%	--	--	--
3	Host **1** (benzene)[b]	12	40%	15%	--	29%	28%	--	--	--	--
4	BP (benzene)	12	41%	6%	--	44%	21%	--	--	--	--
5	Host **1** (benzene-d_6)[b]	12	37%	11%	--	18%	25%	--	--	--	--
6	BP (benzene-d_6)	12	73%	29%	--	32%	9%	--	--	--	--
7	Host **1** (solid-state)	5	97%	--	--	32%	--	--	--	13%	42%

[a]Product distribution of the most prominent products formed by photooxidation. [b]Indicates that the photosensitizer was suspended in the solvent.

DOI: 10.1021/acsomega.9b00831
ACS Omega 2019, 4, 8290−8298

chlorinated alkenes, again confirming the degradation of $CHCl_3$ under these conditions.

With both sensitizers, epoxide-derived products are observed as well as chloride addition from the oxidative breakdown of solvent (Scheme 1, inset). Our hypothesis is that the epoxidizing agent is either a π BP/O_2 exciplex or σ $R_2C(O^{\bullet})O_2^{\bullet}$ biradical. Benzophenone has been reported to be an n−π^* triplet sensitizer, where cycloaddition to an alkene forms a dioxetane in addition to an allylic hydroperoxide formation from singlet oxygen.[19,43] BP is also a noted type I photosensitizer.[44−46] To avoid chloride production, we next examined these reactions in benzene.

Photolysis of **2** mediated by sensitizer **1** for 12 h in oxygen-saturated benzene or benzene-d_6 (Table 1, entries 3 and 5) gave similar conversions (40 vs 37%) despite a large variation of the $^1O_2$ lifetime from 30 to 731 μs.[47] Similarly, poor selectivity was seen in both cases with the major products being alcohols **3**, **5**, and epoxide **6**. In comparison, the photooxidation of **2** sensitized by BP under similar conditions was also unselective and gave the same major products **3**, **5**, and **6** (Table 1, entries 4 and 6). Interestingly, in the case of BP, the 25-fold difference in $^1O_2$ lifetime did play a role in conversion. Nearly, double the conversion of **2** was observed in benzene-d_6 (71%) compared to that in benzene (41%). Alcohols **3** and **5** are common oxidation products observed in type II $^1O_2$-mediated oxidations of cycloalkene **2**.[17,48−50] Furthermore, epoxide **6** could arise from either a type I or a type II process. We also observed the formation of significant amounts of biphenyl, which is expected to proceed via H-abstraction and coupling. Lack of mechanistic control likely lowers the selectivity in solution. The biradical is directed to the exterior of the assembled host and is not expected to be influential in reactions that proceed within its interior, for example, within the solid host·guest crystals.

Activated host **1** crystals were readily loaded with alkene **2** to afford a host/guest complex with a 2:1 stoichiometry. Remarkably, the photolysis of host **1**·**2** crystals in the solid state led to only three products in high conversion with shorter irradiation time (Table 1, entry 7). After just 5 h at 0 °C, two unexpected products were obtained, enone **10** (42%) and diol **9** (13%). Products **9** and **10** are not observed in solution, demonstrating the influence encapsulation of **2** on the photooxidation pathway. Indeed, the low temperature ensures that **2** remains in the channel during the photoreaction (Figure S19). Products are not released until the host is sonicated in a tetrahydrofuran (THF) solution of triphenylphosphine. A depiction of a potential host **1**·**2** complex is shown in Figure 5A. The high conversion demonstrates that oxygen readily enters the channels under these conditions. The only typical product observed was alcohol **5**, which was produced in 32% selectivity. Enone **10** is likely derived from $^1O_2$ through a Schenck allylic peroxyl radical rearrangement of **5**.[51,52] This rearrangement may be facilitated by confinement as well as by long-lived resonance-stabilized surface/host radicals, which form in low quantity (up to ∼1 in 10 000 molecules) upon irradiation of host **1** crystals, shown schematically in Figure 5B.[3]

Formation of diol **9** is particularly interesting and may suggest the formation of dioxetane-type intermediates within the narrow channels, Figure 5C. We are currently utilizing computations to investigate the stability of such intermediates within our frameworks. This diol can also be formed upon oxidation of **2** by enzyme P450.[53,54] In contrast to the solution,

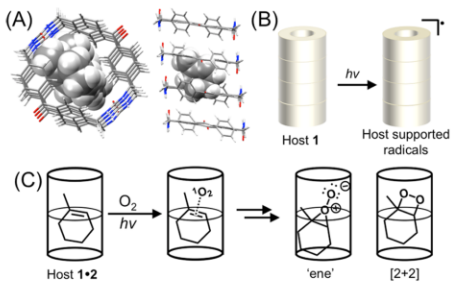

Figure 5. Depictions of host **1** complexes. (A) Top-down view (left) and side view (right) of the plausible host **1**·**2** complex. (B) Irradiation of the host **1** nanotubes results in the formation of host-supported radicals in low quantities.[3] (C) Vapor diffusion of **2** resulted in the formation of the host **1**·**2** complex, irradiation in an oxygen atmosphere results in the type II photooxidations via the "ene" or [2 + 2] cycloaddition pathways.

no epoxide was observed within the solid complexes. One plausible explanation is that the required biradical would not be accessible as it is formed on the exterior of host **1**. Thus, it is not surprising that no epoxide was observed.

In comparison to other molecular containers, the reaction of **2** encapsulated in Gibb's octa acid capsule (2:2) with the sensitizer, rose Bengal, in the surrounding D_2O solution favors the tertiary alcohol **5** with 90% selectivity at 60% conversion.[17] Individual octa acid cavitands have a deep cavity (13.73 Å) with a diameter of 11.36 Å to readily uptake guest molecules.[49] Hydrogen-bonding interactions allow two octa acid cavitands to form a closed capsule, which gives a discrete quaternary complex.[49] Interestingly, the hydroperoxide formed was stable in the capsule and showed no rearrangement to **10**. In comparison, host **1** displays a roughly elliptical one-dimensional channel of ∼150 μM in length with only two entrances and a diameter of 5 × 7.1 Å^2 (Figure 1, the channel highlighted in blue). Absorbed guests are trapped within the confined environment under these conditions and the ROS must diffuse within the long channels. Thus, host **1** is more similar to zeolites, such as ZSM-5 zeolite, which has both straight and elliptical pores with dimensions of approximately 5.2 × 5.8 Å^2. Photolysis of **2** in ZSM-5 forms alcohols **3**, **4**, and **5** upon photooxidation and subsequent reduction.[50] The selectivity of alkene photooxidation can be improved in cation-exchanged zeolites.[55−57] For example, Na-ZSM-5 Y-type zeolite produced secondary allylic alcohol **3** with 88% selectivity.[50] From the reactant's perspective, photooxidation in the "infinite" 1D channels of host **1** is a significantly different environment than in distinct molecular capsules.

In summary, the photooxidation studies of cyclohexene **2** in solution and in the solid state are consistent with the proposed mechanism in Scheme 1. Our findings shed light on the complex mechanistic pathways of photooxidations and highlight degradation reactions that are detrimental to selectivity. (i) $O_2^{\bullet-}$ and BP/O_2 exciplexes are important in solution, leading to the oxidative degradation of $CHCl_3$ and subsequent formation of chlorinated products. These biradical intermediates are likely also responsible for the formation of significant amounts of biphenyl observed in reactions carried out in

DOI: 10.1021/acsomega.9b00831
ACS Omega 2019, 4, 8290−8298

benzene. Epoxide formation that was observed in the solution could arise from either a type I or a type II process.

(ii) $^1O_2$ is important in the solid-state reaction. Cyclohexene **2** is a good match for the size and shape of the host **1** channel and forms 2:1 host/guest complexes. The encapsulated cyclohexene is accessible to oxygen gas and upon irradiation likely undergoes ene reactions with $^1O_2$.[17,49,50,58] Encapsulation dramatically influences the products observed. In particular, high selectivity was observed for **5**, which undergoes efficient allylic peroxyl radical rearrangement to enone **10** within the narrow channels. This pathway appears to represent the majority of the products (**5** + **10** ~74%). The unexpected diol **9**, observed within our crystalline host, may be due to steric constraints that aid the [2 + 2] process to give a proposed dioxetane intermediate (Figure 5C), which subsequently affords the observed diol either upon rearrangement in the channel or upon extraction into a solution of triphenylphosphine. The high conversion suggests that ROS readily diffuses along the ~150 μM channels.

(iii) The lifetime of airborne $^1O_2$ was also examined at the air−solid outer surface of the host. Airborne $^1O_2$ was generated by a Pc plate that was physically isolated from the host in the solid state. Minimal reduction in the lifetime of airborne $^1O_2$ was observed when it came in contact with the surface of host **1**. The data suggest that $^1O_2$ quenching is a surface phenomenon. Thus, we propose that $^1O_2$ via the type II process is involved in the air/solid reaction with cyclohexene **2** and is primarily within the confined channels of host **1**.

CONCLUSIONS

The assembled host **1** displays markedly different behaviors of ROS generated upon photolysis in solution and in the solid state. UV irradiation of photosensitizers host **1** and BP leads to the production of both $^1O_2$ and $O_2^{\bullet-}$ in solution. These represent key reactive species formed in the type I and type II mechanisms. These species undergo unselective reactions with 1-methyl-1-cyclohexene to afford epoxide-derived products as well as degradation of the solvent, which generated chloride in $CHCl_3$ and biphenyl in benzene. It would be advantageous to be able to select a single ROS to direct more selective photooxidations.

In contrast, within the nanochannels of the host in the solid state, mainly type II ($^1O_2$) processes were observed. UV irradiation of the crystalline host·guest complex in an oxygen atmosphere produced no epoxide and afforded the tertiary alcohol **5** with enone **10** as a downstream product of **5**. An unexpected diol, **9**, is proposed to form via formally a [2 + 2]-mediated dioxetane in confinement. Overall, while both $^1O_2$ and $O_2^{\bullet-}$ have access to the channels of **1**, it appears that $^1O_2$ is the main reactive species with the bound cyclohexene **2**. Comparison of reactions carried out in the air/solid and solution/solid interfaces suggests that selectivity arises primarily in the interior of the host. This is likely a result of confinement and/or directed mobility of ROS within the elliptical subnanometer channels. We are currently investigating the use of molecular dynamics to probe complexes of host **1** with $O_2^{\bullet-}$ and $^1O_2$ to see if these ROS species diffuse freely or adhere to the walls. In particular, how does the encapsulation of ROS species within nanochannels affect the mobility, lifetime, and stability of the proposed intermediates? A greater understanding of conditions that favor control over the selectivity of ROS generation and their mobility within confined environments would help in the development of more selective, next-generation photooxidation catalysts.

EXPERIMENTAL SECTION

Materials and Reagents. BP, benzophenone; $CHCl_3$, chloroform; MeOH, methanol; DMPO, 5,5-dimethyl-1-pyrroline *N*-oxide; Ph_3P, triphenylphosphine; DMSO, dimethylsulfoxide; TMP, 2,2,6,6-tetramethylpiperidine; TEMPO, 2,2,6,6-tetramethyl piperidin-1-yl oxidanyl; AlPcS, Al(III) phthalocyanine tetrasulfonate; Pc, phthalocyanine.

Host Synthesis and Guest Encapsulation. Host **1** was synthesized as previously reported.[1−3] Crystallization by slow cooling in DMSO (10 mg/mL) affords white needle-like crystals with regular channels (7.1 × 5.0 Å^2) that are filled with DMSO.[1−3] The host crystals were activated by heating to 180 °C using thermogravimetric analysis (TGA) at a ramp rate of 4 °C/min.[1−3] Once activated, the evacuated host can be readily loaded with guest molecules by soaking the crystals in guest solutions or through vapor diffusion.[1,2]

Photolysis. Irradiations were carried out in a Rayonet reactor at 350 nm in Norell quartz EPR tubes or sodium borosilicate vials.

EPR Spectroscopy. EPR was used to probe the types of ROS generated by host **1** upon UV irradiation while suspended in solution. In each experiment, the sensitizer (**1** or a standard) was added to oxygen-saturated stock solutions containing known ROS quenchers such as TMP, DMPO, or DMN. The solutions were UV-irradiated at 360 nm in a Rayonet reactor, and the reaction was monitored over time by EPR or UV−visible spectroscopy. More detail for each experiment can be found in the Supporting Information.

Quantum Yield Measurement by EPR. The $^1O_2$ quantum yield ($\Phi[^1O_2]$) was determined by plotting the area of TEMPO EPR signal versus time and obtaining the slope of each plot using the equation $\Phi[^1O_2]^{sample} = \Phi[^1O_2]^{ref}(m^{sample}/m^{ref})$, where perinaphthenone was used as the reference ($\Phi[^1O_2]^{ref} = 0.97$ in $CHCl_3$), m^{sample} is the slope of the host plot, and m^{ref} is the slope of the perinaphthenone plot (Figure 2D).[26,51] By this method, we estimate the $\Phi[^1O_2]^{host\ 1}$ to be ~1% in $CHCl_3$.

Quantum Yield Measurement by UV−Visible Spectroscopy. The $^1O_2$ quantum yield ($\Phi[^1O_2]$) was determined by plotting the difference between each absorbance signal versus time and obtaining the slope of each plot using the equation $\Phi[^1O_2]^{sample} = \Phi[^1O_2]^{ref}(m^{sample}/m^{ref})$, where methylene blue was used as the reference ($\Phi[^1O_2]^{ref} = 0.52$ in $CHCl_3$), m^{sample} is the slope of the host plot, and m^{ref} is the slope of the methylene blue plot.

Lifetime of $^1O_2$ at the Air−Solid Interface. An apparatus was constructed to deliver airborne $^1O_2$ to a solid-quenching agent. The reactor consisted of a sensitizing glass plate made by depositing Al(III) phthalocyanine tetrasulfonate (AlPcS) (~5 × 10^{-5} mol) onto the bottom side of a porous silica square (0.50 g, shape: 1.0 mm × 2.25 cm^2). A 0.8 mM solution of AlPcS in MeOH was deposited on the bottom face of the plate via slow evaporation. The glass plate was placed sensitizer-face down on top of a custom-made plate containing a well (sized: 1 mm × 1 cm × 1 cm). The solid trapping agent (10 mg) was placed in the well. The sensitizer plate was not in contact with the solid trapping agent and sat above it by 0.1 mm. A digital ruler with a precision of 0.01 mm was used to measure the distance between the sensitizer plate and the solid trapping agent in the well. The sensitizer plate was placed 3.0

DOI: 10.1021/acsomega.9b00831
ACS Omega 2019, 4, 8290−8298

cm below a terminus of a multimode FT-400-EMT optical fiber with an SMA 905 connector (Thorlabs, Inc.). The optical fiber was connected to a 630 nm light source from a Nd:YAG Q-switched laser pumping an optical parametric oscillator producing 5 ns ~0.2 mJ/pulses. The output of the 630 nm light from the laser yielded incident photons in a Gaussian distribution upon the sensitizer plate. The $^1O_2$ luminescence was detected by a photomultiplier tube (H10330A-45, Hamamatsu Corp.) through a 1270 nm band-pass filter (FWHM = 15 nm). The $^1O_2$ luminescence signals were registered on a 600 MHz oscilloscope, and the kinetic data for the $^1O_2$ lifetime ($\tau_{\Delta airborne}$) were determined by a least-square curve-fitting procedure. The $^1O_2$ decay was observed in the 1270 nm phosphorescence upon irradiation of the sensitizer particles with 630 nm light. A slow component for the $^1O_2$ signal was observed (tenths of microseconds), which is attributed to airborne $^1O_2$ in the air gap between the sensitizer plate of origin and the solid trapping agents. A reduction of the $^1O_2$ lifetime ($\tau_{\Delta airborne}$) arises when the $^1O_2$ encounters the air/solid interface of the trapping agent.

Host 1 in Photooxidations. Photooxidations by host **1** in $CHCl_3$ and benzene resulted in multiple products, and characterization was attempted only on key products. Relative conversion and selectivity were obtained by gas chromatography mass spectrometry (GC−MS), and the products were confirmed using standards and/or the NIST database and literature when applicable (Supporting Information Figures S20−S23).

Host 1 in Photooxidations in Solution. Cycloalkene **2** (21 mM) was stirred in oxygenated $CHCl_3$ or benzene with host **1** (2 mg, 20 mol %). The photooxidations in $CHCl_3$ were UV-irradiated for 18 h and diluted with CH_2Cl_2 solutions of triphenylphosphine (21 mM) for rapid analysis by GC−MS. The photooxidations in benzene were UV-irradiated over time, and aliquots (50 μL) of the reaction mixture were removed over time (4, 8, and 12 h), diluted into solutions of triphenylphosphine in benzene.

Host 1 Loading with Cycloalkene 2. The activated host was equilibrated with **2** for at least 24 h. TGA of the host **1**·**2** complex displayed one-step desorption from 25 to 80 °C with a weight loss of 8.2% (Figure S19 and Table S1). The host·guest stoichiometry was calculated from the weight loss and corresponded to a 2:1 host/guest ratio. Because the TGA indicates that alkene **2** slowly desorbs from the host at ambient temperature, all solid-state reactions were performed at lower temperatures (0 °C).

Solid-State Host 1 in Photooxidations. Host **1** (~16 mg) was UV-irradiated in a borosilicate vial saturated with oxygen for 5 h at 0 °C. After irradiation, the complex was immediately sonicated in a solution of triphenylphosphine (21 mM in THF) and analyzed by GC−MS.

■ ASSOCIATED CONTENT

Supporting Information

The Supporting Information is available free of charge on the ACS Publications website at DOI: 10.1021/acsomega.9b00831.

^{1}H NMR of 4,4′-bis(bromomethyl)benzophenone (Figure S1); ^{1}H NMR of protected benzophenone *bis*-urea macrocycle **1** (Figures S2); ^{1}H NMR of benzophenone *bis*-urea macrocycle **1** (Figures S3); space-filling model of **1** (Figure S4); self-assembly of macrocycle **1** (Figure S5); decolorization of DMPO in MeOH (Figure S6); EPR spectra (Figures S7−S14); EPR spectral simulation (Figures S8 and S9); comparison of area obtained in the formation of TEMPO (Figure S15); singlet oxygen quantum yield (Figure S16); absorption data (Figure S17); comparison of absorptions (Figure S18); TGA plots (Figure S19); GC−MS data (Figure S20); GC trace (Figures S21−S23); airborne singlet oxygen decay curve (Figure S24); direct detection of superoxide (Figure S25); and EPR spin-trapping study (Figure S26) (PDF)

■ AUTHOR INFORMATION

Corresponding Author

*E-mail: shimizls@mailbox.sc.edu.

ORCID

Hannah K. Liberatore: 0000-0001-7423-3251
Alexander Greer: 0000-0003-4444-9099
Susan D. Richardson: 0000-0001-6207-4513
Linda S. Shimizu: 0000-0001-5599-4960

Author Contributions

The manuscript was written through contributions of all authors.

Notes

The authors declare no competing financial interest.

■ ACKNOWLEDGMENTS

B.A.D. and L.S.S. acknowledge support from the National Science Foundation (CHE-1608874 and OIA-1655740) and a SPARC Graduate Research Grant from the Office of the Vice President for Research at the University of South Carolina. A.G. acknowledges support from the National Science Foundation (CHE-1464975).

■ REFERENCES

(1) Geer, M. F.; Walla, M. D.; Solntsev, K. M.; Strassert, C.; Shimizu, L. S. Self-assembled benzophenone bis-urea macrocycles facilitate selective oxidations by singlet oxygen. *J. Org. Chem.* **2013**, *78*, 5568−5578.

(2) Dewal, M. B.; Xu, Y.; Yang, J.; Mohammed, F.; Smith, M. D.; Shimizu, L. S. Manipulating the cavity of a porous material changes the photoreactivity of included guests. *Chem. Commun.* **2008**, 3909−3911.

(3) DeHaven, B. A.; Tokarski, J. T.; Korous, A. A.; Mentink-Vigier, F.; Makris, T. M.; Brugh, A. M.; Forbes, M. D. E.; van Tol, J.; Bowers, C. R.; Shimizu, L. S. Persistent radicals of self-assembled benzophenone bis-urea macrocycles: Characterization and application as a polarizing agent for solid-state DNP MAS Spectroscopy. *Chem. - Eur. J.* **2017**, *23*, 8315−8319.

(4) DeRosa, M.; Crutchley, R. Photosensitized singlet oxygen and its applications. *Coord. Chem. Rev.* **2002**, 233−234, 351−371.

(5) Kim, H.; Kim, W.; Mackeyev, Y.; Lee, G.-S.; Kim, H.-J.; Tachikawa, T.; Hong, S.; Lee, S.; Kim, J.; Wilson, L. J.; Majima, T.; Alvarez, P. J. J.; Choi, W.; Lee, J. Selective oxidative degradation of organic pollutants by singlet oxygen-mediated photosensitization: Tin porphyrin versus C_{60} aminofullerene systems. *Environ. Sci. Technol.* **2012**, *46*, 9606−9613.

(6) Ogilby, P. R. Singlet oxygen: there is indeed something new under the sun. *Chem. Soc. Rev.* **2010**, *39*, 3181−3209.

(7) Dąbrowski, J. M. Reactive oxygen species in photodynamic therapy: Mechanisms of their generation and potentiation. *Adv. Inorg. Chem.* **2017**, *70*, 343−394.

(8) Ghogare, A. A.; Greer, A. Using singlet oxygen to synthesize natural products and drugs. *Chem. Rev.* **2016**, *116*, 9994−10034.

DOI: 10.1021/acsomega.9b00831
ACS Omega 2019, 4, 8290−8298

(9) Baptista, M. S.; Cadet, J.; Di Mascio, P.; Ghogare, A. A.; Greer, A.; Hamblin, M. R.; Lorente, C.; Nunez, S. C.; Ribeiro, M. S.; Thomas, A. H.; Vignoni, M.; Yoshimura, T. M. Type I and Type II photosensitized oxidation reactions: Guidelines and mechanistic pathways. *Photochem. Photobiol.* **2017**, *93*, 912−919.
(10) Hayyan, M.; Hashim, M. A.; AlNashef, I. M. Superoxide ion: Generation and chemical implications. *Chem. Rev.* **2016**, *116*, 3029−3085.
(11) Lee-Ruff, E. The organic chemistry of superoxide. *Chem. Soc. Rev.* **1977**, *6*, 195−214.
(12) Skourtis, S. S.; Liu, C.; Antoniou, P.; Virshup, A. M.; Beratan, D. N. Dexter energy transfer pathways. *Proc. Natl. Acad. Sci. U.S.A.* **2016**, *113*, 8115−8120.
(13) Greer, A. Christopher Foote's discover of the role of singlet oxygen [$^1O_2(^1\Delta_g)$] in photosensitized oxidation reactions. *Acc. Chem. Res.* **2006**, *39*, 797−804.
(14) Foote, C. S.; Wexler, S. Olefin oxidations with excited singlet molecular oxygen. *J. Am. Chem. Soc.* **1964**, *86*, 3879−3880.
(15) Wiegand, C.; Herdtweck, E.; Bach, T. Enantioselectivity in visible light-induced, singlet oxygen [2+4] cylcoaddition reactions (type II photooxygenations) of 2-pyridones. *Chem. Commun.* **2012**, *48*, 10195−10197.
(16) Malek, B.; Fang, W.; Abramova, L.; Walalawela, N.; Ghogare, A. A.; Greer, A. "Ene" reactions of singlet oxygen at the air-water interface. *J. Org. Chem.* **2016**, *81*, 6395−6401.
(17) Natarajan, A.; Kaanumalle, L. S.; Jockusch, S.; Gibb, C. L. D.; Gibb, B. C.; Turro, N. J.; Ramamurthy, V. Controlling photoreactions with restricted spaces and weak intermolecular forces: Exquisite selectivity during oxidation of olefins by singlet oxygen. *J. Am. Chem. Soc.* **2007**, *129*, 4132−4133.
(18) Chen, Y.-Z.; Wang, Z. U.; Wang, H.; Lu, J.; Yu, S.-H.; Jiang, H.-L. Singlet oxygen-engaged selective photo-oxidation over Pt nanocrystals/porphyrinic MOF: The role of photothermal effect and Pt electronic state. *J. Am. Chem. Soc.* **2017**, *139*, 2035−2044.
(19) Shimizu, N.; Bartlett, P. D. Photooxidation of olefins sensitized by α-diketones and by benzophenone. A practical epoxidation method with biacetyl. *J. Am. Chem. Soc.* **1976**, *98*, 4193−4200.
(20) Gupta, S.; Ramamurthy, V. Characterization and singlet oxygen oxidation of 1-alkyl cyclohexenes encapsulated within a water-soluble organic capsule. *ChemPhotoChem* **2018**, *2*, 655−666.
(21) Pace, A.; Clennan, E. L. A new experimental protocol of intrazeolite photooxidations. The first product-based estimate of an upper limit for the intrazeolite singlet oxygen lifetime. *J. Am. Chem. Soc.* **2002**, *124*, 11236−11237.
(22) McDowell, M. S.; Bakac, A.; Espenson, J. H. A convenient route to superoxide ion in aqueous solution. *Inorg. Chem.* **1983**, *22*, 847−848.
(23) Sun, G.; Hong, K. H. Photo-induced antimicrobial and decontaminating agents: Recent progresses in polymer and textile applications. *Text. Res. J.* **2013**, *83*, 532−542.
(24) Nosaka, Y.; Nosaka, A. Y. Generation and detection of reactive oxygen species in photocatalysis. *Chem. Rev.* **2017**, *117*, 11302−11336.
(25) He, W.; Liu, Y.; Wamer, W. G.; Yin, J.-J. Electron spin resonance spectroscopy for the study of nanomaterial-mediated generation of reactive oxygen species. *J. Food Drug Anal.* **2014**, *22*, 49−63.
(26) Nardi, G.; Manet, I.; Monti, S.; Miranda, M. A.; Lhiaubet-Vallet, V. Scope and limitations of the TEMPO/EPR method for singlet oxygen detection: the misleading role of electron transfer. *Free Radical Biol. Med.* **2014**, *77*, 64−70.
(27) Buettner, G. R. Spin trapping: ESR parameters of spin adducts. *Free Radical Biol. Med.* **1987**, *3*, 259−303.
(28) Zang, L.-Y.; Misra, H. P. EPR kinetic studies of superoxide radicals generated during the autooxidation of 1-methyl-4-phenyl-2,3-dihydropyridinium, a bioactivated intermediate of parkinsonian-inducing neurotoxin 1-methyl-4-phenyl-1,2,3,6-tetrahydropyridine. *J. Biol. Chem.* **1992**, *267*, 23601−23608.
(29) Harbour, J. R.; Hair, M. L. Detection of superoxide ions in nonaqueous media. Generation by photolysis of pigment dispersions. *J. Phys. Chem.* **1978**, *82*, 1397−1399.
(30) Roberts, J. L.; Sawyer, D. T. Facile degradation by superoxide ion of carbon tetrachloride, chloroform, methylene chloride, and p,p'-DDT in aprotic media. *J. Am. Chem. Soc.* **1981**, *103*, 712−714.
(31) Schmidt, R.; Tanielian, C.; Dunsbach, R.; Wolff, C. Phenalone, a universal reference compound for the determination of quantum yields of singlet oxygen $O_2(^1\Delta_g)$ sensitization. *J. Photochem. Photobiol., A* **1994**, *79*, 11−17.
(32) Ogunsipe, A.; Maree, D.; Nyokong, T. Solvent effects on the photochemical and fluorescence properties of zing phthalocyanine derivatives. *J. Mol. Struct.* **2003**, *650*, 131−140.
(33) Borah, P.; Sreejith, S.; Anees, P.; Menon, N. V.; Kang, Y.; Ajayaghosh, A.; Zhao, Y. Near-IR squaraine dye-loaded gated periodic mesoporous organosilica for photo-oxidation of phenol in a continuous-flow device. *Sci. Adv.* **2015**, *1*, No. e1500390.
(34) Wasserman, H. H.; Larsen, D. L. Formation of 1,4-endoperoxides from the dye-sensitized photo-oxygenation of alkylnaphthalenes. *J. Chem. Soc., Chem. Commun.* **1972**, *5*, 253−254.
(35) Wasserman, H. H.; Wiberg, K. B.; Larsen, D. L.; Parr, J. Photooxidation of methylnaphthalenes. *J. Org. Chem.* **2005**, *70*, 105−109.
(36) Turro, N. J.; Chow, M.-F. Mechanism of thermolysis of endoperoxides of aromatic compounds. Activation parameters, magnetic field, and magnetic isotope effects. *J. Am. Chem. Soc.* **1981**, *103*, 7218−7224.
(37) Wu, H.; Song, Q.; Ran, G.; Lu, X.; Xu, B. Recent developments in the detection of singlet oxygen with molecular spectroscopic methods. *TrAC, Trends Anal. Chem.* **2011**, *30*, 133−141.
(38) Ho, D. G.; Gao, R.; Celaje, J.; Chung, H.-Y.; Selke, M. Phosphadioxirane: A peroxide from an ortho-substituted arylphosphine and singlet dioxygen. *Science* **2003**, *302*, 259−262.
(39) Wilkinson, F.; Helman, W. P.; Ross, A. B. Rate constants for the decay and reactions of the lowest electronically excited singlet state of molecular oxygen in solution. An expanded and revised compilation. *J. Phys. Chem. Ref. Data* **1995**, *24*, 663−1021.
(40) Zhang, D.; Gao, R.; Afzal, S.; Vargas, M.; Sharma, S.; McCurdy, A.; Yousufuddin, M.; Stewart, T.; Bau, R.; Selke, M. Intramolecular arene epoxidation by phosphadioxiranes. *Org. Lett.* **2006**, *8*, 5125−5128.
(41) Gao, R.; Ho, D. G.; Dong, T.; Khuu, D.; Franco, N.; Sezer, O.; Selke, M. Reaction of arylphosphines with singlet oxygen: Intra- vs. intermolecular oxidation. *Org. Lett.* **2001**, *3*, 3719−3722.
(42) Bartusik, D.; Aebisher, D.; Lyons, A. M.; Greer, A. Bacterial inactivation by a singlet oxygen bubbler: Identifying factors controlling the toxicity of $^1O_2$. *Environ. Sci. Technol.* **2012**, *46*, 12098−12104.
(43) Darmanyan, A. P.; Foote, C. S. Solvent effects on singlet oxygen yield from n,π* and π,π* triplet carbonyl compounds. *J. Phys. Chem.* **1993**, *97*, 5032−5035.
(44) Lacombe, S.; Cardy, H.; Simon, M.; Khoukh, A.; Soumillion, J. Ph; Ayadim, M. Oxidation of sulfides and disulfides under electron transfer or singlet oxygen photosensitization using soluble or grafted sensitizers. *Photochem. Photobiol. Sci.* **2002**, *1*, 347−354.
(45) Adam, W.; Saha-Moeller, C.; Schoenberger, A.; Berger, M.; Cadet, J. Formation of 7,8-dihydro-8-oxoguanine in the 1,2-dioxetane-induced oxidation of calf thymus DNA: Evidence for photosensitized DNA damage by thermally generated triplet ketones in the dark. *Photochem. Photobiol.* **1995**, *62*, 231−238.
(46) Davidson, R. S.; Bartholomew, R. F. The photosensitized oxidation of amines. Part I. The use of benzophenone as a sensitiser. *J. Chem. Soc. C* **1971**, *12*, 2342−2346.
(47) Bregnhøj, M.; Westberg, M.; Jensen, F.; Ogilby, P. R. Solvent-dependent singlet oxygen lifetimes: Temperature effects implicate tunneling and charge-transfer interactions. *Phys. Chem. Chem. Phys.* **2016**, *18*, 22946−22961.
(48) Chavan, S. A.; Maes, W.; Gevers, L. E. M.; Wahlen, J.; Vankelecom, I. F. J.; Jacobs, P. A.; Dehaen, W.; De Vos, D. E.

DOI: 10.1021/acsomega.9b00831
ACS Omega 2019, 4, 8290−8298

Porphyrin-functionalized dendrimers: Synthesis and applications as recyclable photocatalysts in a nanofiltration membrane reactor. *Chem. - Eur. J.* **2005**, *11*, 6754−6762.
(49) Ramamurthy, V. Photochemistry within a water-soluble organic capsule. *Acc. Chem. Res.* **2015**, *48*, 2904−2917.
(50) Chen, Y.-Z.; Wu, L.-Z.; Zhang, L.-P.; Tung, C.-H. Confined space-controlled hydroperoxidation of trisubstituted alkenes adsorbed on pentasil zeolites. *J. Org. Chem.* **2005**, *70*, 4676−4681.
(51) Davies, A. G. The Schenck rearrangement of allylic hydroperoxides. *J. Chem. Res.* **2009**, 533−544.
(52) Dussault, P. H.; Eary, C. T.; Woller, K. R. Total synthesis of the alkoxydioxines (+)- and (-)-chondrillin and (+)- and (-)-plakorin via singlet oxygenation/radical rearrangement. *J. Org. Chem.* **1999**, *64*, 1789−1797.
(53) Bellucci, G.; Chiappe, C.; Marioni, F.; et al. The cytochrome P-450 catalyzed oxidation of 1-methylcyclohexene. Competition between hydroxylation and epoxidation and absolute stereochemistry of the epoxidation. *Bioorg. Med. Chem. Lett.* **1991**, *1*, 121−124.
(54) Peter, S.; Kinne, M.; Ullrich, R.; Kayser, G.; Hofrichter, M. Epoxidation of linear, branched and cyclic alkenes catalyzed by unspecific peroxygenase. *Enzyme Microb. Technol.* **2013**, *52*, 370−376.
(55) Clennan, E. L.; Sram, J. P. Photooxidations in zeolites. Part 2: A new mechanistic model for reaction selectivity in singlet oxygen ene reactions in zeolitic media. *Tetrahedron Lett.* **1999**, *40*, 5275−5278.
(56) Stratakis, M.; Raptis, C.; Sofikiti, N.; Tsangarakis, C.; Kosmas, G.; Zaravinos, L-P.; Kalaitzakis, D.; Stavroulakis, D.; Baskakis, C.; Stathoulopoulou, A. Intrazeolite photooxygenation of chiral alkenes. Control of facial selectivity by confinement and cation-π interactions. *Tetrahedron* **2006**, *62*, 10623−10632.
(57) Robbins, R. J.; Ramamurthy, V. Generation and reactivity of singlet oxygen within zeolites: Remarkable control of hydroperoxidation of alkenes. *Chem. Commun.* **1997**, *11*, 1071−1072.
(58) Singleton, D. A.; Hang, C.; Szymanski, M. J.; Meyer, M. P.; Leach, A. G.; Kuwata, K. T.; Chen, J. S.; Greer, A.; Foote, C. S.; Houk, K. N. Mechanism of ene reactions of singlet oxygen. A two-step no-intermediate mechanism. *J. Am. Chem. Soc.* **2003**, *125*, 1328−1319.

DOI: 10.1021/acsomega.9b00831
ACS Omega 2019, 4, 8290−8298

Available online at www.sciencedirect.com

ScienceDirect

Current Opinion in Environmental Science & Health

Current methods for analyzing drinking water disinfection byproducts

Mengting Yang[1], Hannah K. Liberatore[2] and Xiangru Zhang[3]

Abstract

Disinfection byproducts (DBPs) are produced during the process of disinfecting drinking water. Toxicological and epidemiological studies have indicated that DBPs may pose adverse effects on human health, which is why their ubiquitous existence in drinking water supplies has aroused increasing concerns. With hundreds of known DBPs and many still unaccounted for, a variety of analytical methods are essential for investigating their formation and occurrence in drinking water. This review discusses current analytical methods and challenges associated with the identification and measurement of DBPs mainly published in the last two years.

Addresses

[1] Shenzhen Key Laboratory of Environmental Chemistry and Ecological Remediation, College of Chemistry and Environmental Engineering, Shenzhen University, Shenzhen 518060, China

[2] Department of Chemistry and Biochemistry, University of South Carolina, Columbia, SC 29208, United States

[3] Department of Civil and Environmental Engineering, The Hong Kong University of Science and Technology, Hong Kong, China

Corresponding author: Zhang, Xiangru. (xiangru@ust.hk)

Current Opinion in Environmental Science & Health 2019, **7**:98–107

This review comes from a themed issue on **Drinking water contaminants**

Edited by **Susan Richardson** and **Cristina Postigo**

For a complete overview see the Issue and the Editorial

https://doi.org/10.1016/j.coesh.2018.12.006

Introduction

Since 1974, when chloroform was detected and identified as the first disinfection byproduct (DBP) in chlorinated drinking water, many researchers have recognized the formation of DBPs during drinking water disinfection as a new issue of great concern for drinking water safety [1,2]. According to toxicological and epidemiological studies, the long-term consumption of drinking water containing low or trace levels (ng/L–μg/L) of DBPs may have chronic adverse effects on human health, potentially leading to bladder cancer, colorectal cancer, birth defects, and many other health issues [3–5]. Emerging DBPs may warrant greater concern than regulated DBPs (e.g. trihalomethanes [THMs] and haloacetic acids [HAAs]) because previous studies have demonstrated that many are much more toxic than the regulated DBPs [2,3,6,7]. Meanwhile, new DBPs continue to be detected and reported [8]. In this context, the detection, identification, and quantification of DBPs are of great significance as accurate and comprehensive knowledge of the composition of DBPs generated in drinking water under different conditions is essential in controlling their formation and reducing the resulting toxicity. This review discusses analytical methods for drinking water DBPs and current challenges, mainly based on peer-reviewed journal articles published between 2016 and 2018, with particular emphasis on current trends in the analysis of emerging DBPs. Studies and analytical methods discussed are summarized in Table 1.

Gas chromatography and related analytical methods

Gas chromatography (GC) has been frequently used in the identification and quantification of volatile and semivolatile DBPs. For analytes that are polar, thermally labile, or extremely hydrophilic, chemical derivatization is required. Electron capture detection (ECD) and mass spectrometry (MS) are the predominant detectors used for GC analysis of DBPs [9–21]. Its high sensitivity and low cost make ECD a go-to for the quantification of target DBPs. ECD is used in standard methods, U.S. EPA Methods 551.1 and 552.3, for commonly measured DBPs (THMs, HAAs, and haloacetonitriles, chloropropanones, chloropicrin, and chloral hydrate) [9,10]. It has also been used to measure emerging DBPs, including haloacetamides, in drinking water [11]. Although ECD has high sensitivity for halogenated compounds, it lacks selectivity, such that unknown DBPs or other compounds may interfere with the target analytes.

Owing to additional selectivity, which allows for both target and nontarget analyses, MS is preferred for coupling to GC. For quantification, selected ion monitoring using quadrupole-MS and multiple reaction monitoring (MRM) using triple quadrupole-MS are commonly used to enhance sensitivity and selectivity of target analytes. For example, Allen et al. [13] used a combination of selected ion monitoring and MRM to quantify 61 DBPs by GC-MS (/MS) in Flint, MI, in response to complaints of skin rashes in residents after

Table 1

Summary of pretreatment and determination methods of DBPs.

Analytes	Identification/ Quantification	Sample pretreatment	Analytical column	Detector/detection method
GC-related methods				
HAAs, THMs, HANs, HKs, TCAL, and TCNM [9,10]	Quantification	LLE with MTBE	DB-1; DB-1701	Electron capture detector
HAMs and HAAs [11]	Quantification	LLE with MTBE	Rtx-5MS (Restek)	Electron capture detector; Shimadzu QP2010plus quadrupole MS
N-Nitrosamines, THMs, Iodo-THMS, HAAs, IAA, HANs, HALs, HAMs, HKs, and TCNM [12]	Quantification	LLE with MTBE	DB-1701 (Agilent)	Agilent 240 Ion Trap MS
HALs, HANs, HKs, HNMs, I-THMs, HAMs, and IAAs [13]	Quantification	LLE with MTBE; derivatization with PFBHA and LLE with hexane for mono- and di-HALs	Rtx-200; Rxi-5MS (Restek)	Agilent 5977 A quadrupole MS; Thermo TSQ Quantum GC triple quadrupole MS
Iodo-THMs, HANs, and HNM [14]	Quantification	DLLME (optimized extraction/ dispersion solvent: dichloromethane/methanol)	Ultra-2 (J &W Scientific)	Agilent 5975 quadrupole MS
N-DBPs derived from amino acid phenylalanine [15]	Identification and quantification	SPME with PDMS-DVB fibers (Supelco)	Rtx-5MS (Restek)	Thermo DSQ II quadrupole MS
C-DBPs and N-DBPs derived from microcystin-LR [16]	Identification	LLE with MTBE	TG-5MS (Thermo Scientific)	Thermo TSQ Quantum XLS triple quadruple MS
New nitrogenous aromatic DBPs: chlorophenyl acetonitriles [17]	Identification	LLE with MTBE	Rtx-5MS (Restek)	Shimadzu QP2020 quadrupole MS
I-THMs, HANs, HAMs, HNMs, HALs, HKs, and nontarget contaminants/DBPs (e.g. *trans*-2,3,4-trichloro-2-butenenitrile) [18]	Identification and quantification	LLE with MTBE	Rtx-200 (Restek)	LECO Pegasus BT TOF MS; Agilent 5977 A quadrupole MS
HANs, HAMs, and nitrogenous heterocyclic DBPs formed during chloramination of phenolic compounds [19]	Identification	LLE with MTBE	DB-5MS Ultra Inert (Agilent)	Agilent 7200 Accurate-Mass QTOF
Iodophenolic DBPs in chloraminated oil and gas wastewater [20]	Identification	LLE with dichloromethane	Rxi-5MS (Restek)	LECO Pegasus GC-HRT TOF MS
Bromo-DBPs in pools and spas treated with bromine disinfection [21]	Identification	Resin extraction with Amberlite XAD-2 and Supelite DAX-8 resins	Rtx-5 (Restek)	LECO Pegasus GC-HRT TOF MS
LC-related methods				
N-Nitrosodimethylamine formation from dichloramine and *N,N*-dimethyl-α-arylamines [23]	Quantification	Aqueous	Poroshell 120C18 (Agilent)	Photodiode array detector at 228 nm
HAMs derived from antibiotic chloramphenicol and its analogs [24]	Quantification	SPE with Oasis HLB cartridges	Hypersil GOLD C18 packed	Thermo TSQ Quantum Access MAX triple quadrupole MS
DBPs derived from peptides (S-(1,2-dichlorovinyl)glutathione, etc) [25]	Identification	SPE with Oasis HLB/Bond Elut ENV/ Bond Elut C18 cartridges	Advance Bio Peptide Mapping C18 (Agilent) and TSKgel Amide-80 (Tosoh Bioscience)	AB Sciex TripleTOF 5600

(*continued on next page*)

Table 1. (*continued*)

Analytes	Identification/ Quantification	Sample pretreatment	Analytical column	Detector/detection method
Iodinated HAAs and aromatic iodinated DBPs [26]	Quantification	SPE with Oasis MAX/HLB/MCX cartridges	XSelect HSS T3 (Waters)	AB Sciex API4000 triple quadrupole MS
Nitrosamines [27]	Quantification	SPE with polypropylene cartridges	Synergi Fusion-RP 80 A C18	Agilent 6430 triple quadrupole MS
Polar, iodinated DBPs [28]	Quantification	LLE with MTBE	XSelect HSS T3 (Waters)	AB Sciex API4000 triple quadrupole MS
2,6-Dichloro-1,4-benzoquinone [29]	Quantification	SPE with Oasis HLB cartridges	BEH C18	AB Sciex 3200 QTrap MS
DBPs derived from antimicrobial preservatives [30]	Quantification	n.a.[a]	Extend C18 (Agilent)	Agilent G6490A triple quadrupole MS
Iodinated X-ray contrast media [31]	Quantification	SPE with LiChrolut EN and ENVI-Carb cartridges	BEH Shield RP18	Waters Acquity triple quadrupole MS
Polar, chlorinated, brominated, and iodinated DBPs (trihalomethanols, etc) in ClO_2-treated drinking water [34]	Identification	LLE with MTBE	Waters HSS T3	Waters Acquity triple quadrupole MS
New polar I-DBPs: I-HAAs, carbonaceous phenolic I-DBPs and nitrogenous phenolic I-DBPs [35]	Identification	LLE with MTBE	Waters HSS T3	Waters Xevo triple quadrupole MS
New polar I-DBPs (3-iodo-4-hydroxybenzaldehyde, etc) formed during cooking [36]	Identification	LLE with MTBE	Waters HSS T3 and Shimadzu Shim-pack XR-ODS II	Waters Acquity triple quadrupole MS; Shimadzu IT-TOF-MS
N-chlorinated dipeptides (*N*-Cl-tyrosylglycine, etc) [38]	Identification and quantification	SPE with Oasis HLB cartridges	Phenomenex Luna C18 (2)	TripleTOF 5600[b] and QTRAP 5500 MS[c] (AB Sciex)
Iodinated tyrosyl dipeptides (3,5-diiodo-*N*-chlorinated tyrosylalanine, etc) [39]	Identification and quantification	SPE with Oasis HLB cartridges	Phenomenex Luna C18 (2)	X500R QTOF[b] and QTRAP 5500 MS[c] (AB Sciex)
N-chloro-HAMs (as degradation products of HAMs in chlorinated drinking waters) [40]	Identification	SPE with Oasis MAX cartridges	Acquity UPLC HSS T3 (Waters)	Waters Xevo G2-XS QTof
Halogenated DBPs derived from bisphenols F and S (tetrachloro-bisphenol F, trichloro-bisphenol S, etc) [41,42]	Identification	n.a.	Acquity BEH C18 (Waters)	Waters SYNAPT G1 Q-TOF
DBPs derived from theophylline with Fe (VI) oxidation-chlorination treatment [43]	Identification	n.a.	Symmetry C18	QTOF X500R (AB Sciex)
Ultrahigh-resolution MS				
206 iodinated DBPs during chloramination and 15 iodinated DBPs during chlorination [45]	Identification	SPE with Sep-pak C18 cartridges	n.a.	Bruker apex ultra 9.4 T FT-ICR MS
193 one bromine–containing DBPs and 5 two bromine–containing DBPs during chloramination [46]	Identification	SPE with Sep-pak C18 cartridges	n.a.	Bruker apex ultra 9.4 T FT-ICR MS
Transformation products of X-ray contrast media iopamidol during ozonation and chlorination [47]	Identification	n.a.	Acquity UPLC HSS T3	Thermo Q Exactive hybrid quadrupole-orbitrap MS

DBPs derived from anticancer drugs vinca alkaloids [48]	Identification	n.a.	Purospher STAR RP-18 Hibar HR (Merck)	Thermo Q Exactive hybrid quadrupole-orbitrap MS
DBPs derived from sulfonamide antibiotics [49]	Identification	n.a.	Waters Atlantis T3	Thermo quadrupole-Orbitrap MS
DBPs derived from 17β-estradiol [50]	Identification	n.a.	Zorbax SB-C18	Thermo Q Exactive hybrid quadrupole-orbitrap MS
Iodo-DBPs from chlor(am)ination [51]	Identification	Resin extraction with XAD-2 and DAX-8 resins	TR-5MS (Thermo Scientific)	Thermo Q Exactive GC Orbitrap MS
TOX				
Halogen-specific TOX [52]	Quantification	Adsorption–pyrolysis–absorption with Mitsubishi modules (TX-3AA and AQF-100)	IonPac AS19 (Dionex)	On-line detection of halides by IC (ICS-3000, Dionex)
TOCl, TOBr, and TOI during chlor(am)ination [53]	Quantification	Adsorption–pyrolysis–absorption with Mitsubishi modules (TXA03C and AQF-100)	n.a.	Off-line detection of Cl^-/Br^- and I^- with IC (ICS-90, Dionex); UPLC-triple quadrupole MS (Waters)
Adsorbable organic bromine (AOBr) [54]	Quantification	Adsorption–pyrolysis–absorption with Mitsubishi modules (TX-3AA and AQF-100)	AG9H/AS9H	On-line detection of halides by IC (ICS-2000, Dionex)
TOCl, TOBr, and TOI formed during chlorination of algal organic matter [55]	Quantification	Adsorption–pyrolysis–absorption with Analytic Jena Multi X 2500 TOX Analyzer (Analytik Jena)	n.a.	Off-line detection of halides with IC (ICS-2100, Dionex)
TOCl, TOBr, and TOI in water under natural sunlight irradiation[d] [56]	Quantification	Adsorption–pyrolysis with Mitsubishi TOX-100 Analyzer	n.a.	On-line microcoulometric titration of halides with Mitsubishi TOX-100 Analyzer
TOCl, TOBr, and TOI in human urine [57]	Quantification	Adsorption–pyrolysis–absorption with Mitsubishi modules (TXA-04 and AQF-2100H)	IonPac AS9-HC (Dionex)	Off-line detection of Cl^- and Br^- with 1600 IC System (Dionex); ICP-MS (Finnigan ELEMENT XR) for I^- detection
Other methods				
Bromate [70]	Quantification	n.a.	IonPac AS19 (Dionex)	Detection by IC (ICS-2000, Dionex)
HAAs, iodo-HAAs, iodate, bromate, I^-, Br^- [71]	Quantification	Aqueous	IonPac AS21 (Dionex)	IC-MS/MS (AB Sciex 4000Q Trap)
HAAs, iodo-HAAs, bromate, and dalapon [72]	Quantification	Aqueous	Metrosep A Supp 7 (Metrohm USA, Inc.)	IC-MS/MS (Metrohm 850 Professional IC and Agilent 6490 triple quadrupole MS)
Properties of algal organic matter; cyanobacteria-related C- and N-DBPs (THMs, HANs, HKs, and TCNM) [74]	Identification and quantification	Aqueous	None	3D excitation–emission matrices measured with a Hitachi Fluorescence Spectrophotometer-4600; DBPs measured by Agilent GC-ECD
Halobenzoquinones [75]	Quantification	Aqueous sample added to sensing solution of quantum dots capped by amino acids	None	Photoluminescence spectra recorded on a Thermo Fisher Lumina fluorescence spectrophotometer

HANs: haloacetonitriles; HKs: haloketones; HNM: halonitromethane; HALs: haloacetaldehydes; HAMs: haloacetamides; TCAL: trichloroacetaldehyde (chloral hydrate); TCNM: trichloronitromethane (chloropicrin); IAA: iodoacetic acid; LLE: liquid-liquid extraction; MTBE: methyl tert-butyl ether; DLLME: dispersive liquid-liquid microextraction; SPME: solid-phase microextraction; SPE: solid-phase extraction; PDMS-DVB: polydimethylsiloxane-divinylbenzene; AOX: adsorbable organic halogen; THM: trihalomethane; DBP: disinfection by-product; HAA: haloacetic acid; TOX: Total organic halogen; MS: mass spectrometry; GC: gas chromatography.

[a] n.a., not available.

[b] Used for characterization.

[c] Used for quantification.

[d] Because pure chlorine, bromine, and iodine solutions were used for preparing disinfected artificial water samples, the TOX results were expressed as halogen-specific TOX concentrations in the study [56].

the 2014-2015 lead crisis. In 2018, On et al. [14] developed a dispersive liquid-liquid microextraction method for quantifying 11 priority emerging DBPs by GC-MS.

The most popular ionization technique for GC-MS analyses is electron ionization (EI), which uses a standardized ionization energy (70 eV) and results in distinctive fragmentation patterns that allow for convenient comparison to library databases (e.g. NIST), as well as characteristic fragments and patterns for manual interpretation and identification of new DBPs. Zhang et al. [17] used this method in the identification of a new group of nitrogenous DBPs, chlorophenyl acetonitriles, and confirmed their identities based on retention time and fragment ions of analytes compared to standards. Recently, Kimura et al. [18] developed a method for simultaneous quantification of 39 target DBPs and comprehensive identification of nontarget DBPs/contaminants using medium-resolution (two decimal place accuracy) GC–time-of-flight (TOF) MS. This method also allowed the identification of nontarget DBPs, including *trans*-2,3,4-trichloro-2-butenenitrile.

GC equipped with high-resolution mass spectrometry (HRMS) is an ideal tool for the identification of unknown volatile/semivolatile DBPs as accurate mass capabilities allow for enhanced structural elucidation of unknowns. Nihemaiti et al. [19] recently investigated the formation of nitrogenous DBPs during chloramination of aromatic model compounds (e.g. resorcinol). By using GC coupled to high-resolution quadrupole–time-of-flight–mass spectrometry (GC-QTOF-MS), they tentatively identified several intermediates/products and reported nitrogenous heterocyclic DBPs (e.g. 3-chloro-2,5-pyrroledione) generated during chloramination. In 2017, Liberatore et al. [20] identified two new classes of iodophenolic DBPs resulting from chloramination of oil and gas wastewater (including hydraulic fracturing) using GC–high resolution-TOF–MS.

In some cases, EI fragments molecules so intensely that no molecular ion is present in the mass spectrum, which makes it difficult to fully identify these unknowns. Chemical ionization (CI) is a softer ionization technique than EI, often affording the (pseudo)molecular ion with minimal fragmentation. Using EI and CI in combination can be beneficial for the identification of some unknowns. For example, Daiber et al. [21] used complementary EI and CI analyses by GC–HR-TOF–MS to identify a series of new sulfur-containing bromo-DBPs in swimming pools and spas treated by bromine disinfection.

Liquid chromatography and liquid chromatography–mass spectrometry methods

In contrast to GC-related methods, liquid chromatography (LC) methods are ideally suited for the analysis of polar, high-molecular-weight, and thermally labile DBPs [22]. LC-based analyses are most commonly detected using MS (or MS/MS) detectors, but spectrophotometric measurements can also be used for monitoring the formation of some DBPs. For example, Huang et al. [23] used high-performance LC (HPLC)-UV to monitor highly carcinogenic *N*-nitrosodimethylamine and discovered the role of dichloramine in its formation from dimethylarylamine precursors, including ranitidine. Reversed-phase columns and electrospray ionization (ESI) are the most commonly used chromatography and ionization techniques, respectively. Although studies applying atmospheric pressure chemical ionization are rare, this mode is well suited for analysis of less polar DBPs, such as haloacetamides [24]. It is also advantageous to use complementary column phases for more comprehensive identification of unknowns, as demonstrated by Tang et al. [25] in their 2016 study of peptide-related DBPs.

For analytes with known chemical identity and for which standards are available, MRM via LC–triple quadrupole tandem–MS is widely used for DBP monitoring and quantification. Using MRM, Hu et al. [26] developed a new solid-phase extraction–HPLC–MS/MS method to simultaneously measure iodinated HAAs and iodinated aromatic DBPs. In addition to the analysis of different groups of emerging DBPs, including nitrosamines, polar iodinated DBPs, halobenzoquinones (HBQs), and DBPs derived from antimicrobial preservatives [27–30], MRM has been used in the analysis of iodine-containing X-ray contrast media [31], which are of concern as important precursors of iodinated DBPs [31–33].

Furthermore, LC–MS/MS methods can be used as nontarget screening strategies to effectively detect and identify new DBPs. Han et al. [34] recently characterized the formation of halogenated DBPs and identified a new class, trihalomethanols, in drinking water disinfected with chlorine dioxide using an ultra-performance LC (UPLC)–MS/MS precursor ion scan (PIS) technique, which selectively detects compounds that generate bromide and chloride fragment ions via collision-induced dissociation. Compounds of interest from PIS analyses can be further analyzed in product ion scan mode to obtain structural information. In a similar manner, many new iodinated DBPs have also been identified in drinking water [35–37].

The use of HRMS further aids in the identification of unknown DBPs. The most common type of HRMS is QTOF-MS, which has been applied in the analysis of a wide range of emerging DBPs. For example, a high-throughput approach using HPLC–QTOF–MS was developed by Tang et al. [25] for the identification of peptide-derived DBPs and their precursors. Based on the strategy of nontarget detection with precursor ion exclusion and database searching, hundreds of peptides

[25], as well as *N*-chlorinated dipeptides and iodinated tyrosyl dipeptides [38,39], were identified and formation pathways were determined. Other interesting studies reported QTOF applications in the identification of *N*-chloro-haloacetamides as degradation products of haloacetamides in chlorinated water, halogenated DBPs produced from the chlorination of environmental contaminants bisphenol F and bisphenol S, and DBPs derived from the contaminant theophylline after Fe (VI) oxidation–chlorination treatment [40–43].

Ultrahigh resolution mass spectrometry

HRMS and ultrahigh-resolution MS are capable of accurately determining the mass of analytes and thus are becoming promising techniques for exploring the chemical structures of unknown DBPs, especially in a complex matrix. One disadvantage of TOF and QTOF analyses is that with higher resolution, some sensitivity is sacrificed, which limits capabilities in identifying new trace-level compounds. However, ultrahigh resolution Fourier-transform (FT) ion cyclotron resonance (ICR) and Orbitrap mass spectrometers are capable of performing sensitive accurate mass analyses.

FT-ICR MS is the most powerful HR mass spectrometer as it can achieve higher resolution and mass accuracy (parts-per-billion) than any other mass spectrometer [44]. However, its high cost currently limits its widespread use. With a state-of-the-art FT-ICR MS instrument, Wang et al. [45] characterized the formation of iodinated DBPs during chlor(am)ination of water containing iodide and humic substances, detecting over 10 times more iodo-DBPs from chloramination than from chlorination. Using accurate molecular formulas, a parameter called the 'modified aromaticity index' was calculated, and results indicated that most detected iodinated DBPs may have (polycyclic) aromatic structures. In subsequent research [46], brominated DBPs from chloramine disinfection of bromide- and fulvic acid-containing water were similarly characterized via FT-ICR. In addition to expense, another disadvantage to FT-ICR MS is its slower acquisition rate, which limits its pairing with chromatography systems.

Recently, LC-Orbitrap instruments have been used to analyze DBPs of the X-ray contrast media iopamidol [47], anticancer drugs [48], sulfonamide antibiotics [49], and hormones [50] formed during chlorination. In 2016, Postigo et al. [51] characterized iodinated DBP formation in chlorinated and chloraminated water, including two never-before-reported iodo-DBPs, using the newly developed GC-Orbitrap mass spectrometer. For most high-resolution needs, Orbitrap MS can be a feasible alternative to ICR as the two share similarities in many aspects, and Orbitrap MS is less expensive and more easily coupled with chromatography.

Total organic halogen analysis

Total organic halogen (TOX) analysis is often used as a surrogate measurement to quantify both known and unknown DBPs in drinking water. In general, TOX analysis involves four major steps: (1) concentration of halogenated DBPs in water samples by adsorption onto activated carbon columns; (2) removal of inorganic halides with a nitrate solution; (3) pyrolysis of carbon columns at approximately 1000 °C to convert organic halogens to hydrogen halides; and (4) on-line microcoulometric titration of halides [52].

Using an off-line ion chromatograph equipped with a conductivity detector instead of an on-line titration system, halogen-specific TOX (total organic chlorine [TOCl], bromine [TOBr], and iodine [TOI]) can be measured. As iodinated and brominated DBPs show higher toxic potency than their chlorinated analogs, halogen-specific TOX analysis is becoming increasingly popular. Based on TOX analysis and careful selection of halogen-related reactions, Zhu and Zhang [53] developed two kinetic models that accurately predicted the formation of halogenated DBPs during chlorination and chloramination. With an emphasis on brominated DBPs generated during chlorination, TOBr was used to elucidate mechanisms of bromo-DBP formation (involving bromine electrophilic substitution, electron transfer, and recycling) [54]. Two other studies focused on algae-derived [55] and wastewater-derived [56] DBPs as they may be present in drinking water due to seasonal algal blooms and water reuse, respectively. Through TOX analysis, Liu et al. [55] reported the effects of bromide and iodide on formation and speciation of TOX during chlorination of algal organic matter extracted from three freshwater/marine algae, and Abusallout and Hua [56] revealed photolytic degradation kinetics of TOCl, TOBr, and TOI in drinking water/wastewater under natural solar irradiation. In addition to drinking water analyses, Kimura et al. [57] developed a method for TOX quantification in urine as an indicator for human exposure to DBPs. This method utilizes inductively coupled plasma (ICP)–MS for more sensitive detection of TOBr and TOI.

Recent studies have indicated that for the same source water, the toxic potency of the disinfected water is positively correlated with the TOX level of the disinfected water [3,34,58–69], thus, the toxicity trend of a water sample that is disinfected under different scenarios can be well explained by the TOX trend of the disinfected water sample. For example, to better assess the toxicity of disinfected drinking water via bioassays and to minimize the loss of DBPs during sample enrichment, Stalter et al. [59] compared different methods for sample enrichment. The recoveries from the sample enrichment of TOX were used to evaluate the DBP extraction efficiency, and bioassay results

demonstrated that samples with higher TOX recoveries generally showed higher levels of cytotoxicity.

Other analytical methods

Besides analyzing inorganic DBPs (such as bromate) and related halocontaminants (e.g. bromide and iodide), ion chromatography enables the effective separation of organic compounds with relatively high polarity; thus, ion chromatography coupled with tandem MS can provide an alternative approach to detecting HAAs [70–72].

Moreover, spectroscopic methods have the potential to monitor DBPs generated during ozonation. A recent review reported that the generation of bromate was strongly correlated with variations in the absorbance and fluorescence of ozonated water [73]. Also, using fluorescence excitation–emission matrices with parallel factor analysis, Ma et al. [74] observed that a tryptophan-like substance was strongly correlated with the formation of carbonaceous/nitrogenous DBPs in cyanobacteria-laden drinking water. Jiao et al. [75] developed a selective and cost-effective fluorescence-based method for the direct detection of emerging HBQs in drinking water. Mn-doped ZnS quantum dots were capped with amino acids to serve as probes, and the charge-transfer interaction between HBQs and amino acids enabled the aggregation of quantum dots, leading to decreasing fluorescence.

'Total ion current-toxic potencies' calculated toxicity

In addition to identifying and monitoring DBP formation, a method for assessing individual DBPs as forcing agents of toxicity in drinking water has become increasingly common [76]. By using DBP relative concentrations (total ion current [TIC]) obtained via any of the aforementioned types of analyses combined with corresponding literature values of toxic potencies (Tox), one can estimate the toxicity contribution of specific DBPs in finished water. This method allows for prioritization of DBPs based on their toxicological contribution, rather than on concentration alone, as some of the highest-forming DBPs (e.g. THMs) have little contribution to overall toxicity. For example, in 2018, this method was applied in determining that haloacetonitriles were the major drivers of toxicity from chlorination of algal organic matter [55].

Conclusions and recommendations

Analytical methods for the detection, identification, and quantification of DBPs are of great significance to DBP-related studies, and reliable data are essential for the evaluation of drinking water toxicity and the development of DBP control strategies. Frequently used techniques for DBP detection and determination mainly include TOX, GC–ECD, GC-MS, UPLC–MS/MS, and HRMS. TOX measurements are used to represent total halogenated DBP concentrations in a sample. However, the adsorption efficiencies of certain polar DBPs on activated carbon (e.g. HAAs) may be low and could result in bias during TOX analysis. Alternative adsorption materials (e.g. modified activated carbon) should be investigated to enhance the adsorption efficiency. In addition, GC-related methods are suitable for the detection of volatile and semivolatile DBPs, whereas LC–MS is an ideal tool for analyzing polar DBPs or thermally unstable DBPs. Although EI and ESI are the most common ionization modes for pairing MS with GC and LC, respectively, both have their limitations in analysis for some DBP classes. Accordingly, other ionization modes, including CI, atmospheric pressure photoionization, and atmospheric pressure chemical ionization, should be incorporated for the detection of previously overlooked DBPs. Given that fluorescence measurements are fast, convenient, and nondestructive, fluorescence-based methods could be adopted to establish monitoring strategies for halogenated DBPs in water in the future. In addition, toxicity testing of waters is sometimes budget-limited in projects, but the method of 'TIC-Tox' provides a way to analytically compare treated waters without measuring mixture toxicities. It can serve as a surrogate for toxicity measurements in estimating the 'known' toxicity (i.e. the toxicity contributed by the things we measure). Most importantly, there is no universal method for DBP analysis, and continued implementation of a variety of methods by the DBP research community is necessary for comprehensive understanding of DBP impacts and control.

Conflict of interest statement

Nothing declared.

Acknowledgements

The authors acknowledge the support from the National Natural Science Foundation of China (Grant 51508335), the Natural Science Foundation of Guangdong Province (Grant 2016A030310061), and the Shenzhen Science and Technology Project (Grant JCYJ20170818091859147 and Grant ZDSYS201606061530079).

References

Papers of particular interest, published within the period of review, have been highlighted as:

* of special interest

1. Rosario-Ortiz F, Rose J, Speight V, Von Gunten U, Schnoor J: **How do you like your tap water?** *Science* 2016, **351**:912–914.

2. Richardson SD, Temes TA: **Water analysis: emerging contaminants and current issues**. *Anal Chem* 2017, **90**:398–428.

3. * Li XF, Mitch WA: **Drinking water disinfection byproducts (DBPs) and human health effects: multidisciplinary challenges and opportunities**. *Environ Sci Technol* 2018, **52**: 1681–1689.
In this review, the authors discuss new efforts made by the DBP research community to assess DBP impacts on water toxicity and health effects.

4. Gängler S, Charisiadis P, Seth R, Chatterjee S, Makris KC: **Time of the day dictates the variability of biomarkers of exposure to disinfection byproducts**. *Environ Int* 2018, **112**:33–40.

5. Freeman LEB, Cantor KP, Baris D, Nuckols JR, Johnson A, Colt JS, Schwenn M, Ward MH, Lubin JH, Waddell R: **Bladder cancer and water disinfection by-product exposures through**

multiple routes: a population-based case–control study (New England, USA). *Environ Health Perspect* 2017, **125**. 067010-1–067010-9.

6. Yang M, Zhang X: **Comparative developmental toxicity of new aromatic halogenated DBPs in a chlorinated saline sewage effluent to the marine polychaete *Platynereis dumerilii***. *Environ Sci Technol* 2013, **47**:10868–10876.

7. Li J, Moe B, Vemula S, Wang W, Li XF: **Emerging disinfection byproducts, halobenzoquinones: effects of isomeric structure and halogen substitution on cytotoxicity, formation of reactive oxygen species, and genotoxicity**. *Environ Sci Technol* 2016, **50**:6744–6752.

8. Yang M, Zhang X: **Current trends in the analysis and identification of emerging disinfection byproducts**. *Trends Environ Anal Chem* 2016, **10**:24–34.

9. Hodgeson JW, Cohen AL, Munch DJ, Hautman DP: *Method 551.1 – Determination of chlorination disinfection byproducts, chlorinated solvents, and halogenated pesticides/herbicides in drinking water by liquid-liquid extraction and gas chromatography with electron-capture detection*. Cincinnati, OH: EPA National Exposure Research Laboratory, Office of Research and Development; 1995.

10. Domino MM, Pepich BV, Munch DJ, Fair PS, Xie Y, Munch JW, Pawlecki-Vonderheide AM, Hodgeson JW, Becker D, Collins J, Barth RE: *Method 552.3 – Determination of haloacetic acids and dalapon in drinking water by liquid-liquid microextraction, derivatization, and gas chromatography with electron capture detection*. Cincinnati, OH: EPA Office of Ground Water and Drinking Water; 2003.

11. Ding S, Chu W, Krasner SW, Yu Y, Fang C, Xu B, Gao N: **The stability of chlorinated, brominated, and iodinated haloacetamides in drinking water**. *Water Res* 2018, **142**:490–500.

12. Zeng T, Plewa MJ, Mitch WA: **N-Nitrosamines and halogenated disinfection byproducts in US Full Advanced Treatment trains for potable reuse**. *Water Res* 2016, **101**:176–186.

13. Allen JM, Cuthbertson AA, Liberatore HK, Kimura SY, Mantha A, Edwards MA, Richardson SD: **Showering in Flint, MI: is there a DBP problem?** *J Environ Sci* 2017, **58**:271–284.

14. On J, Pyo H, Myung SW: **Effective and sensitive determination of eleven disinfection byproducts in drinking water by DLLME and GC–MS**. *Sci Total Environ* 2018, **639**:208–216.

15. Ma X, Deng J, Feng J, Shanaiah N, Smiley E, Dietrich AM: **Identification and characterization of phenylacetonitrile as a nitrogenous disinfection byproduct derived from chlorination of phenylalanine in drinking water**. *Water Res* 2016, **102**:202–210.

16. Zhang Y, Shao Y, Gao N, Chu W, Sun Z: **Removal of microcystin-LR by free chlorine: identify of transformation products and disinfection by-products formation**. *Chem Eng J* 2016, **287**:189–195.

17. Zhang D, Chu W, Yu Y, Krasner SW, Pan Y, Shi J, Yin D, Gao N: **Occurrence and stability of chlorophenyl acetonitriles, a new class of nitrogenous aromatic DBPs, in chlorinated and chloraminated drinking waters**. *Environ Sci Technol Lett* 2018, **5**:394–399.

18. * Kimura SY, Cuthbertson AA, Byer JD, Richardson SD: **The DBP exposome: development of a new method to simultaneously quantify priority disinfection by-products and comprehensively identify unknowns**. *Water Res* 2019, **148**:324–333.
Using GC time-of-flight mass spectrometry, a method for simultaneous quantification of target DBPs and non-target analysis was developed. This method led to the identification of non-target DBPs, including *trans*-2,3,4-trichloro-2-butenenitrile.

19*. Nihemaiti M, Le Roux J, Hoppe-Jones C, Reckhow DA, Croué JP: **Formation of haloacetonitriles, haloacetamides, and nitrogenous heterocyclic byproducts by chloramination of phenolic compounds**. *Environ Sci Technol* 2017, **51**:655–663.
Authors investigated the formation of nitrogenous DBPs during chloramination of model compounds using GC-high resolution quadrupole time-of-flight mass spectrometry (GC-QTOF-MS). Several chloramination intermediates/products were tentatively identified, including heterocyclic N-DBPs like 3-chloro-2,5-pyrroledione.

20. Liberatore HK, Plewa MJ, Wagner ED, VanBriesen JM, Burnett DB, Cizmas LH, Richardson SD: **Identification and comparative mammalian cell cytotoxicity of new iodophenolic disinfection byproducts in chloraminated oil and gas wastewaters**. *Environ Sci Technol Lett* 2017, **4**:475–480.

21. Daiber EJ, DeMarini DM, Ravuri SA, Liberatore HK, Cuthbertson AA, Thompson-Klemish A, Byer JD, Afifi MZ, Blatchley ER, Richardson SD: **Progressive increase in disinfection byproducts and mutagenicity from source to tap to swimming pool and spa water: impact of human inputs**. *Environ Sci Technol* 2016, **50**:6652–6662.

22. Richardson SD, Postigo C: **Liquid chromatography–Mass spectrometry of emerging disinfection by-products**. *Compr Anal Chem* 2018, **79**:267–295.

23. Huang ME, Huang S, McCurry DL: **Re-examining the role of dichloramine in high-yield N-nitrosodimethylamine formation from N,N-dimethyl-α-arylamines**. *Environ Sci Technol Lett* 2018, **5**:154–159.

24. Chu W, Krasner SW, Gao N, Templeton MR, Yin D: **Contribution of the antibiotic chloramphenicol and its analogues as precursors of dichloroacetamide and other disinfection byproducts in drinking water**. *Environ Sci Technol* 2016, **50**:388–396.

25. * Tang Y, Xu Y, Li F, Jmaiff L, Hrudey SE, Li XF: **Nontargeted identification of peptides and disinfection byproducts in water**. *J Environ Sci* 2016, **42**:259–266.
Using HPLC-QTOF-MS and a precursor ion exclusion technique, authors developed a method for the identification of peptide-derived DBPs and precursors, leading to the identification of hundreds of compounds.

26. Hu S, Gong T, Ma J, Tao Y, Xian Q: **Simultaneous determination of iodinated haloacetic acids and aromatic iodinated disinfection byproducts in waters with a new SPE-HPLC-MS/MS method**. *Chemosphere* 2018, **198**:147–153.

27. Chen WH, Wang CY, Huang TH: **Formation and fates of nitrosamines and their formation potentials from a surface water source to drinking water treatment plants in Southern Taiwan**. *Chemosphere* 2016, **161**:546–554.

28. Gong T, Tao Y, Xian Q: **Selection and applicability of quenching agents for the analysis of polar iodinated disinfection byproducts**. *Chemosphere* 2016, **163**:359–365.

29. Kosaka K, Nakai T, Hishida Y, Asami M, Ohkubo K, Akiba M: **Formation of 2, 6-dichloro-1, 4-benzoquinone from aromatic compounds after chlorination**. *Water Res* 2017, **110**:48–55.

30. Yoom H, Shin J, Ra J, Son H, Ryu D, Kim C, Lee Y: **Transformation of methylparaben during water chlorination: effects of bromide and dissolved organic matter on reaction kinetics and transformation pathways**. *Sci Total Environ* 2018, **634**:677–686.

31. Xu Z, Li X, Hu X, Yin D: **Distribution and relevance of iodinated X-ray contrast media and iodinated trihalomethanes in an aquatic environment**. *Chemosphere* 2017, **184**:253–260.

32. Duirk SE, Lindell C, Cornelison CC, Kormos J, Ternes TA, Attene-Ramos M, Osiol J, Wagner ED, Plewa MJ, Richardson SD: **Formation of toxic iodinated disinfection by-products from compounds used in medical imaging**. *Environ Sci Technol* 2011, **45**:6845–6854.

33. Wendel FM, Lütke Eversloh C, Machek EJ, Duirk SE, Plewa MJ, Richardson SD, Ternes TA: **Transformation of iopamidol during chlorination**. *Environ Sci Technol* 2014, **48**:12689–12697.

34. * Han J, Zhang X, Liu J, Zhu X, Gong T: **Characterization of halogenated DBPs and identification of new DBPs trihalomethanols in chlorine dioxide treated drinking water with multiple extractions**. *J Environ Sci* 2017, **58**:83–92.
Using a precursor ion scan (PIS) technique, authors characterized the formation of halogenated DBPs and identified a new class, trihalomethanols, in chlorine dioxide-disinfected drinking water by UPLC-MS/MS.

35. Pan Y, Li W, An H, Cui H, Wang Y: **Formation and occurrence of new polar iodinated disinfection byproducts in drinking water**. *Chemosphere* 2016, **144**:2312–2320.

36. Pan Y, Zhang X, Li Y: **Identification, toxicity and control of iodinated disinfection byproducts in cooking with simulated chlor (am) inated tap water and iodized table salt**. *Water Res* 2016, **88**:60–68.

37. Gong T, Tao Y, Zhang X, Hu S, Yin J, Xian Q, Ma J, Xu B: **Transformation among aromatic iodinated disinfection byproducts in the presence of monochloramine: from monoiodophenol to triiodophenol and diiodonitrophenol**. *Environ Sci Technol* 2017, **51**:10562–10571.

38. Huang G, Jiang P, Li XF: **Mass spectrometry identification of N-chlorinated dipeptides in drinking water**. *Anal Chem* 2017, **89**:4204–4209.

39. Huang G, Jiang P, Jmaiff Blackstock LK, Tian D, Li XF: **formation and occurrence of iodinated tyrosyl dipeptides in disinfected drinking water**. *Environ Sci Technol* 2018, **52**:4218–4226.

40. Yu Y, Reckhow DA: **Formation and occurrence of N-chloro-2, 2-dichloroacetamide, a previously overlooked nitrogenous disinfection byproduct in chlorinated drinking waters**. *Environ Sci Technol* 2017, **51**:1488–1497.

41. Zheng S, Shi JC, Hu JY, Hu WX, Zhang J, Shao B: **Chlorination of bisphenol F and the estrogenic and peroxisome proliferator-activated receptor gamma effects of its disinfection byproducts**. *Water Res* 2016, **107**:1–10.

42. Zheng S, Shi J, Zhang J, Yang Y, Hu J, Shao B: **Identification of the disinfection byproducts of bisphenol S and the disrupting effect on peroxisome proliferator-activated receptor gamma (PPARγ) induced by chlorination**. *Water Res* 2018, **132**:167–176.

43. Sun S, Jiang J, Pang S, Ma J, Xue M, Li J, Liu Y, Yuan Y: **Oxidation of theophylline by Ferrate (VI) and formation of disinfection byproducts during subsequent chlorination**. *Separ Purif Technol* 2018, **201**:283–290.

44. Ghaste M, Mistrik R, Shulaev V: **Applications of Fourier transform ion cyclotron resonance (FT-ICR) and Orbitrap based high resolution mass spectrometry in metabolomics and lipidomics**. *Int J Mol Sci* 2016, **17**:816–837.

45. * Wang X, Wang J, Zhang Y, Shi Q, Zhang H, Zhang Y, Yang M: **Characterization of unknown iodinated disinfection byproducts during chlorination/chloramination using ultrahigh resolution mass spectrometry**. *Sci Total Environ* 2016, **554**:83–88.
Using Fourier transform ion cyclotron resonance MS, authors characterized iodo-DBP formation from iodide and humic substances during chlor(am)ination. Results showed that chloramination formed over 10 times more iodo-DBPs than chlorination, and the majority of them likely possessed aromatic structures.

46. Zhang H, Yang M: **Characterization of brominated disinfection byproducts formed during chloramination of fulvic acid in the presence of bromide**. *Sci Total Environ* 2018, **627**:118–124.

47. Matsushita T, Hashizuka M, Kuriyama T, Matsui Y, Shirasaki N: **Use of orbitrap-MS/MS and QSAR analyses to estimate mutagenic transformation products of iopamidol generated during ozonation and chlorination**. *Chemosphere* 2016, **148**:233–240.

48. Negreira N, Regueiro J, de Alda ML, Barceló D: **Reactivity of vinca alkaloids during water chlorination processes: identification of their disinfection by-products by high-resolution quadrupole-Orbitrap mass spectrometry**. *Sci Total Environ* 2016, **544**:635–644.

49. Wang M, Helbling DE: **A non-target approach to identify disinfection byproducts of structurally similar sulfonamide antibiotics**. *Water Res* 2016, **102**:241–251.

50. Shao Y, Pan Z, Rong C, Wang Y, Zhu H, Zhang Y, Yu K: **17β-estradiol as precursors of Cl/Br-DBPs in the disinfection process of different water samples**. *Environ Pollut* 2018, **241**:9–18.

51. * Postigo C, Cojocariu CI, Richardson SD, Silcock PJ, Barcelo D: **Characterization of iodinated disinfection by-products in chlorinated and chloraminated waters using Orbitrap based gas chromatography-mass spectrometry**. *Anal Bioanal Chem* 2016, **408**:3401–3411.
Using GC-Orbitrap MS, the authors characterized iodo-DBP formation during chlor(am)ination, which led to the identification of new iodinated DBPs.

52. Kristiana I, McDonald S, Tan J, Joll C, Heitz A: **Analysis of halogen-specific TOX revisited: method improvement and application**. *Talanta* 2015, **139**:104–110.

53. * Zhu X, Zhang X: **Modeling the formation of TOCl, TOBr and TOI during chlor (am) ination of drinking water**. *Water Res* 2016, **96**:166–176.
Based on TOX analysis, authors developed kinetic models to predict the formation of DBPs during chlorination and chloramination. Mechanisms of Br-DBP formation were elucidated.

54. Langsa M, Heitz A, Joll CA, Von Gunten U, Allard S: **Mechanistic aspects of the formation of adsorbable organic bromine during chlorination of bromide-containing synthetic waters**. *Environ Sci Technol* 2017, **51**:5146–5155.

55. Liu C, Ersan MS, Plewa MJ, Amy G, Karanfil T: **Formation of regulated and unregulated disinfection byproducts during chlorination of algal organic matter extracted from freshwater and marine algae**. *Water Res* 2018, **142**:313–324.

56. Abusallout I, Hua G: **Natural solar photolysis of total organic chlorine, bromine and iodine in water**. *Water Res* 2016, **92**:69–77.

57. Kimura SY, Zheng W, Hipp TN, Allen JM, Richardson SD: **Total organic halogen (TOX) in human urine: a halogen-specific method for human exposure studies**. *J Enivron Sci* 2017, **58**:285–295.

58. Jiang J, Zhang X, Zhu X, Li Y: **Removal of intermediate aromatic halogenated DBPs by activated carbon adsorption: a new approach to controlling halogenated DBPs in chlorinated drinking water**. *Environ Sci Technol* 2017, **51**:3435–3444.

59. Stalter D, Peters LI, O'Malley E, Tang JYM, Revalor M, Farré MJ, Watson K, von Gunten U, Escher BI: **Sample enrichment for bioanalytical assessment of disinfected drinking water: concentrating the polar, the volatiles, and the unknowns**. *Environ Sci Technol* 2016, **50**:6495–6505.

60. Savitz DA, Singer PC, Herring AH, Hartmann KE, Weinberg HS, Makarushka C: **Exposure to drinking water disinfection byproducts and pregnancy loss**. *Am J Epidemiol* 2006, **164**:1043–1051.

61. Itoh S, Gordon BA, Callan P, Bartram J: **Regulations and perspectives on disinfection by-products: importance of estimating overall toxicity**. *J Water Supply Res Technol* 2011, **60**:261–274.

62. Pan Y, Zhang X, Wagner ED, Osiol J, Plewa MJ: **Boiling of tap water: effect on polar brominated disinfection byproducts, halogen speciation, and cytotoxicity**. *Environ Sci Technol* 2014, **48**:149–156.

63. Yang M, Liu J, Zhang X, Richardson SD: **Comparative toxicity of chlorinated saline and freshwater wastewater effluents to marine organisms**. *Environ Sci Technol* 2015, **49**:14475–14483.

64. Liu J, Zhang X, Li Y: **Effect of boiling on halogenated DBPs and their developmental toxicity in real tap waters**. In *Recent advances in disinfection by-products*. Edited by Karanfil T, Mitch B, Westerhoff T, Xie Y, American Chemical Society; 2015:45–60.

65. Liu J, Zhang X, Li Y: **Photoconversion of chlorinated saline wastewater DBPs in receiving seawater is overall a detoxification process**. *Environ Sci Technol* 2017, **51**:58–67.

66. Li Y, Zhang X, Yang M, Liu J, Li W, Graham NJD, Li X, Yang B: **Three-step chlorination increases disinfection efficiency and reduces DBP formation and toxicity**. *Chemosphere* 2017, **168**:1302–1308.

67. Lv X, Zhang X, Du Y, Wu Q, Lu Y, Hu H: **Solar light irradiation significantly reduced cytotoxicity and disinfection byproducts in chlorinated reclaimed water**. *Water Res* 2017, **125**:162–169.

68. Han J, Zhang X: **Evaluating the comparative toxicity of DBP mixtures from different disinfection scenarios: a new approach by combining freeze-drying or rotoevaporation with a marine polychaete bioassay**. *Environ Sci Technol* 2018, **52**:10552–10561.

69. Sun H, Liu H, Han J, Zhang X, Cheng F, Liu Y: **Chemical cleaning-associated generation of dissolved organic matter and halogenated byproducts in ceramic MBR: ozone versus hypochlorite**. *Water Res* 2018, **140**:243–250.

70. Hu J, Qiang Z, Dong H, Qu J: **Enhanced formation of bromate and brominated disinfection byproducts during chlorination of bromide-containing waters under catalysis of copper corrosion products**. *Water Res* 2016, **98**:302–308.

71. Xue R, Donovan A, Shi H, Yang J, Hua B, Inniss E, Eichholz T: **Rapid simultaneous analysis of 17 haloacetic acids and related halogenated water contaminants by high-performance ion chromatography-tandem mass spectrometry**. *Anal Bioanal Chem* 2016, **408**:6613–6622.

72. Wu S, Anumol T, Gandhi J, Snyder SA: **Analysis of haloacetic acids, bromate, and dalapon in natural waters by ion chromatography–tandem mass spectrometry**. *J Chromatogr A* 2017, **1487**:100–107.

73. Korshin GV, Sgroi M, Ratnaweera H: **Spectroscopic surrogates for real time monitoring of water quality in wastewater treatment and water reuse**. *Curr Opin Environ Sci Health* 2018, **2**: 12–19.

74. Ma C, Xu H, Zhang L, Pei H, Jin Y: **Use of fluorescence excitation–emission matrices coupled with parallel factor analysis to monitor C-and N-DBPs formation in drinking water recovered from cyanobacteria-laden sludge dewatering**. *Sci Total Environ* 2018, **640**:609–618.

75. Jiao Z, Zhang P, Chen H, Li J, Zhong Z, Fan H, Cheng F: **Halobenzoquinone-mediated assembly of amino acid modified Mn-doped ZnS quantum dots for halobenzoquinones detection in drinking water**. *Anal Chim Acta* 2018, **1026**: 147–154.

76. * Plewa MJ, Wagner ED, Richardson SD: **TIC-Tox: a preliminary discussion on identifying the forcing agents of DBP-mediated toxicity of disinfected water**. *J Environ Sci* 2017, **58**: 208–216.

Authors combined chemical and biological data to determine the DBPs that drive drinking water toxicity. Results showed that the major forcing agents of cyto- and genotoxicity are nitrogenous DBPs, and regulated DBPs seem to have little contribution.

Environmental Science & Technology

Article

Cite This: Environ. Sci. Technol. 2018, 52, 13047−13056

pubs.acs.org/est

Chlorination of Source Water Containing Iodinated X-ray Contrast Media: Mutagenicity and Identification of New Iodinated Disinfection Byproducts

Cristina Postigo,[*,†,#] David M. DeMarini,[‡] Mikayla D. Armstrong,[§] Hannah K. Liberatore,[∥] Karsten Lamann,[∥,$] Susana Y. Kimura,[∥,@] Amy A. Cuthbertson,[∥] Sarah H. Warren,[‡] Susan D. Richardson,[∥] Tony McDonald,[‡] Yusupha M. Sey,[‡] Nana Osei B. Ackerson,[⊥] Stephen E. Duirk,[⊥] and Jane Ellen Simmons[‡]

[†]Institute of Environmental Assessment and Water Research (IDAEA-CSIC), Water and Soil Quality Research Group, Department of Environmental Chemistry, Barcelona, 08034, Spain

[#]Marie Curie Fellow, National Health and Environmental Effects Research Laboratory, U.S. Environmental Protection Agency, Research Triangle Park, North Carolina 27711, United States

[‡]National Health and Environmental Effects Research Laboratory, U.S. Environmental Protection Agency, Research Triangle Park, North Carolina 27711, United States

[§]Department of Environmental Sciences and Engineering, University of North Carolina, Chapel Hill, North Carolina 27599, United States

[∥]Department of Chemistry and Biochemistry, University of South Carolina, 631 Sumter Street, Columbia, South Carolina 29208, United States

[⊥]Department of Civil Engineering, University of Akron, Akron, Ohio 44235, United States

Supporting Information

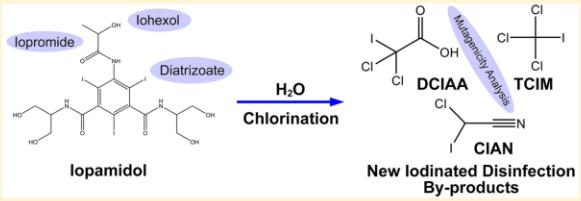

ABSTRACT: Iodinated contrast media (ICM) are nonmutagenic agents administered for X-ray imaging of soft tissues. ICM can reach μg/L levels in surface waters because they are administered in high doses, excreted largely unmetabolized, and poorly removed by wastewater treatment. Iodinated disinfection byproducts (I-DBPs) are highly genotoxic and have been reported in disinfected waters containing ICM. We assessed the mutagenicity in *Salmonella* of extracts of chlorinated source water containing one of four ICM (iopamidol, iopromide, iohexol, and diatrizoate). We quantified 21 regulated and nonregulated DBPs and 11 target I-DBPs and conducted a nontarget, comprehensive broad-screen identification of I-DBPs. We detected one new iodomethane (trichloroiodomethane), three new iodoacids (dichloroiodoacetic acid, chlorodiiodoacetic acid, bromochloroiodoacetic acid), and two new nitrogenous I-DBPs (iodoacetonitrile and chloroiodoacetonitrile). Their formation depended on the presence of iopamidol as the iodine source; identities were confirmed with authentic standards when available. This is the first identification in simulated drinking water of chloroiodoacetonitrile and iodoacetonitrile, the latter of which is highly cytotoxic and genotoxic in mammalian cells. Iopamidol (5 μM) altered the concentrations and relative distribution of several DBP classes, increasing total haloacetonitriles by >10-fold. Chlorination of ICM-containing source water increased I-DBP concentrations but not mutagenicity, indicating that such I-DBPs were either not mutagenic or at concentrations too low to affect mutagenicity.

INTRODUCTION

Disinfecting source water used for drinking water or wastewater prior to discharge into distribution systems or the environment is important for inactivating pathogenic microorganisms. Disinfection byproducts (DBPs) are formed by the reaction of oxidizing disinfectants, such as chlorine, chloramines, or chlorine dioxide with natural organic matter (NOM) and/or bromide/iodide in water. Although the use of alternative disinfectants has increased over time, chlorine remains the most frequently used

Received: August 17, 2018
Revised: October 15, 2018
Accepted: October 19, 2018
Published: October 19, 2018

DOI: 10.1021/acs.est.8b04625
Environ. Sci. Technol. 2018, 52, 13047−13056

disinfectant for both surface and ground waters in the United States.[1] Many of the resulting DBPs are mutagenic, genotoxic, cytotoxic, and/or carcinogenic.[2−5] Thus, water systems must operate their disinfection procedures to balance inactivating harmful pathogens with forming potentially harmful DBPs.

Epidemiologic studies have found a positive association between exposure to chlorinated water and increased risk for bladder cancer.[6−9] Increased risks of colon cancer[10] and adverse reproductive and developmental outcomes, including spontaneous abortion, heart defects, low birth weight at term, still birth, and preterm delivery,[11−21] have also been reported in some epidemiologic studies. Although the majority of DBPs that have been evaluated are genotoxic,[4] the iodine-containing DBPs (I-DBPs) are 10−1000 times more potent in Chinese hamster ovary (CHO) cells than their chlorinated and brominated counterparts,[3,5,22−25] raising special concerns regarding waters with high concentrations of I-DBPs. This DBP class was also recently reported to show significant developmental toxicity in marine polychaete[26,27] and in zebrafish embryos.[28]

I-DBPs are formed during disinfection of waters containing iodide, including freshwaters impacted by seawater intrusion or fossilized seawater,[3,5,29,30] wastewaters,[31] saline wastewater effluents,[32] or bromide-rich desalinated seawater[33] and also after iodine-based water disinfection treatments.[34] Furthermore, they may also form during household cooking processes when using chloraminated tap water and iodized salt.[27] A number of low- and high-molecular weight I-DBPs have been identified in recent years,[3,5,29,35−40] and their formation is influenced by a variety of factors, including the levels of iodide present in source waters,[41,42] molecular size of NOM,[43] presence of microbial organic matter,[44] and the presence of other iodine sources, such as iodinated X-ray contrast media (ICM).[45,46]

ICM are commonly administered for medical imaging of soft tissues; they are administered in high doses (up to 200 g/person/day), excreted mostly unchanged, and poorly removed in wastewater treatment plants. Therefore, they can be present at levels in the μg/L range in surface waters impacted by effluents from wastewater treatment plants.[47,48] For example, diatrizoate (DTZ) has been quantified at levels between 20 and 100 μg/L,[47] and ICM have also been detected in finished drinking waters.[46,49,50] Among the ICM, iopamidol (IPAM),[40,45,46,51−55] iohexol (IHX),[45,46,54] iopromide (IPR),[45,46,54] DTZ,[45,46,54] iomeprol,[46] and iodixanol,[54] have been investigated as potential precursors of I-DBPs during chlorination or chloramination of water. According to these studies, IPAM is the ICM that is most reactive with chlorine. Further, UV irradiation of ICM-containing waters also causes iodide to be released from ICM, increasing the possibility of I-DBP formation during subsequent disinfection treatments.[56,57]

Under chlorination, IPAM has yielded the highest concentrations of I-DBPs, such as iodine-containing trihalomethanes (I-THMs) and iodine-containing haloacetic acids (I-HAAs). In contrast to chlorination, chloramination has been shown to enhance I-DBP formation in waters containing other ICM;[54] however, the resulting concentrations are lower than those observed for chlorinated IPAM-containing waters.

Although ICM are not mutagenic or generally toxic *per se*,[58,59] IPAM has been shown to induce DNA damage in CHO cells as measured by the comet assay.[52] In addition, chlorinating or chloraminating source waters containing IPAM increased the level of DNA damage relative to that of source water without IPAM.[45,52,58,60] Chlorination of source water containing IHX also increased the level of DNA damage relative to that of chlorinated source water without IHX.[52]

To explore this issue further, we determined the DBP concentrations and mutagenicity after laboratory-scale chlorination of source water containing one of four ICM: IPAM, IPR, DTZ, or IHX. We quantitatively analyzed the disinfected waters for 11 I-DBPs and 21 target non-I-DBPs. In addition, we also performed for the first time a nontarget, comprehensive, broad-screen analysis in large-volume extracts of waters for detecting unknown I-DBPs that form in ICM-containing waters during chlorination. We determined the mutagenic potencies of the extracts in the *Salmonella* mutagenicity assay using strains TA98 and TA100 with or without metabolic activation (S9). We also used strain RSJ100, which expresses the *GSTT1* gene, to determine whether any portion of the activity was due to the presence of DBPs that are activated by GSTT1 enzyme, such as brominated trihalomethanes (Br-THMs).[4] This is important because approximately 80% of the U.S. population carries this gene,[61] and a case-controlled epidemiologic study by Canter et al.[6] demonstrated an increased risk for DBP-related bladder cancer for such people who have sufficient exposure to chlorinated water.

This approach has resulted in the most extensive study to date on the formation of DBPs and mutagenicity resulting from chlorination of ICM-containing waters, encompassing both quantitative analysis of 32 target DBPs and the identification of never-before-reported iodinated DBPs. In addition, this is the first mutagenicity study of chlorinated ICM-containing waters in the presence of NOM, which is an important factor in the formation of DBPs,[45] and the first study to combine complementary chemical and mutagenicity analyses in the comparison of multiple ICMs.

EXPERIMENTAL PROCEDURES

Chemicals and Reagents. Chemicals and reagents were of the highest purity commercially available. Physical-chemical properties, purity, sources of the ICM, and molecular structures are described in the Supporting Information (SI) in Table S1 and Figure S1. Chloroiodoacetonitrile was synthesized as described in the SI and shown in Figure S2. Relevant information on the other chemicals and reagents used is provided in the SI.

Disinfection Reactions. The source water used in these experiments was collected at a water treatment plant after coagulation, flocculation, sedimentation, and filtration, but prior to disinfection. Water was collected by gravity flow through Teflon tubing into 35-gallon linear-low-density polyethylene, open-head barrels (Super Shipper, Bergan Barrel & Drum Co., Kearny, NJ) equipped with Teflon liners (24″ × 24″, open end 31.25″, Welch Fluorocarbon Inc., Dover, NH) with a Teflon sheet between the water and the barrel lid. After collection, the water was stored at 4 °C in the dark until use. As reported in Table S2, the concentration of total organic carbon (TOC) was 2.1 mg/L, and both bromide and iodide were below their limits of detection.

Large-volume (up to 125 L) chlorination reactions were performed with source water brought to and held at room temperature (21−22 °C) (Table S3), headspace-free, in the dark. Reactions were performed for each ICM using an ICM concentration of 5 μM (3.88, 3.95, 4.10, and 3.39 mg/L for IPAM, IPR, IHX, and DTZ, respectively) and chlorine doses of 100 μM (7.09 mg/L) as Cl_2. This ICM:Cl_2 molar ratio was selected based on previous experiments performed with IPAM.[45] An advantage to higher chlorine concentrations than would typically be employed at water treatment plants, along

DOI: 10.1021/acs.est.8b04625
Environ. Sci. Technol. 2018, 52, 13047−13056

with higher levels of ICM than those typically observed in actual impacted source waters, was the increased likelihood of formation of iodinated DBPs at concentrations above their limits of quantification. Chlorine-demand tests were performed with the source water to confirm that the selected amount of disinfectant was not completely consumed upon reaction time.

Reactions were conducted over 72 h with continuous stirring. Because we discovered that the stirring had ceased and was not continuous during the preparation of the first IPAM-containing water (IPAM1), we prepared a second sample (IPAM2). Consequently, we generated chemistry and mutagenicity data on both IPAM-containing water samples, which provided some opportunity to compare the reproducibility of the preparation method. In all cases, water was buffered with 10 mM phosphate buffer, using H_2SO_4 and NaOH to achieve pH 7.5 prior to disinfection. The pH was monitored with a pH 2100-benchtop meter (Oakton instruments, Vernon Hills, IL). The custom disinfection system has been described in detail previously.[62]

The *N*,*N*-diethyl-*p*-phenylenediamine (DPD)-ferrous ammonium sulfate (FAS) titrimetric method[63] was used to measure both the chlorine concentration (as mg/L Cl_2) in the disinfectant solution prepared prior to each reaction and the free chlorine concentrations in the water after each experiment (mean residual free chlorine, 1.4 mg/L Cl_2).

XAD Resin Extractions. DBPs were extracted from measured volumes of treated waters (up to 120 L) using XAD resins/ethyl acetate as published previously[64] and described in SI.

QA/QC. Controls included source waters spiked with each of the four ICM (no disinfectant) and source water disinfected with chlorine (no ICM). In addition to these source water controls, an XAD resin blank (method blank) was also generated by passing Milli-Q water through the XAD resins and eluting with ethyl acetate. The extract from the method blank was then analyzed for contaminants resulting from impurities in the solvent or the resin. Blanks consisting of disinfected water (Milli-Q and source water) containing the individual ICM were also processed for chemical characterization of target iodo-DBPs. Efforts to ensure integrity of the source water samples and reduce the possibility of confounding are outlined in the SI (Characteristics of the Source Water).

Quantitative Analyses of 21 Target Non-I-DBPs. Although only 9 DBPs (4 THMs and 5 HAAs) are required for monitoring by the U.S. EPA for water systems that disinfect with chlorine, we quantified a total of 21 DBPs that are measured routinely for research purposes in disinfected water by EPA Methods 552.2[65] and 551.1.[66] Analytes included nine chloro-/bromoacetic acids (HAA9); the four regulated trihalomethanes (THM4); chloral hydrate (CH); two haloketones (dichloropropanone and trichloropropanone); four haloacetonitriles (dichloro-, bromochloro-, dibromo-, and trichloroacetonitrile); and trichloronitromethane.

Quantitative Analyses of 11 Target I-DBPs. The 11 target I-DBPs and their physical-chemical properties are listed in Table S4. The unregulated I-DBPs (iodotrihalomethanes (I-THMs), iodoacids, and iodoacetaldehyde) were quantified using published methods.[35,45] Specific details, such as the instruments used and their operating conditions, are included in the SI. Thus, a total of 32 target DBPs were measured quantitatively (21 non-I-DBPs and 11 I-DBPs). Formation of iodate, a nontoxic sink of iodide, was not monitored in the solutions. Previous studies have shown the absence of detectable levels of this inorganic iodine species in chlorinated ICM-containing source waters.[45,51]

Analysis of Nontarget I-DBPs. To detect relevant I-DBPs not included in the list of target compounds, diazomethane-derivatized and nonderivatized XAD resin extracts (blanks and samples) were analyzed by GC-electron ionization (EI) high-resolution mass spectrometry (HR-MS) using a LECO HRT time-of-flight mass spectrometer (St. Joseph, MI) in full-scan mode. Tentative molecular structures were proposed according to the evidence obtained from the National Institute of Standards and Technology (NIST) and Wiley mass spectral databases and by manual interpretation when not present in the library. For manual interpretation of mass spectra, the presence of isotopic patterns and elemental composition of the molecular and fragment ions provided by EI-HR-MS data were taken into consideration. Tentative identifications were confirmed by analysis of analytical standards (when available) and comparing the GC retention times and mass spectra.

Mutagenicity. XAD/ethyl acetate extracts were solvent-exchanged into dimethyl sulfoxide (DMSO). Appropriate dilutions with DMSO were done for evaluation of the mutagenicity of each extract with the *Salmonella* mutagenicity assay. For this we used the standard plate-incorporation method in strains TA100 and TA98 with and without metabolic activation (S9) provided by Aroclor-induced Sprague−Dawley rat liver (Moltox, Boone, NC).[67] These strains are commonly used to assess the mutagenicity of DBPs and drinking water.[4] In addition, we evaluated the extracts in *Salmonella* strains RSJ100 (*GSTT1+*) and TPT100 (*GSTT1-*) in the absence of S9 to assess if the mutagenicity of the extracts was enhanced by the presence of the GSTT1 enzyme, which activates brominated trihalomethanes (Br-THMs) to mutagens.[4] RSJ100 and TPT100 are otherwise isogenic to TA100 except that they do not contain the pKM101 plasmid.

We also evaluated the mutagenicity of chloro-, bromo-, and iodoacetic acid (Sigma, St. Louis, MO) in TA100, TA1535 (the parent strain of TA100 that does not have the pKM101 plasmid), as well as RSJ100 and TPT100 in the absence of S9 to assess the ability of the GSTT1 enzyme to activate these DBPs to mutagens. However, because these are semivolatiles, we performed the preincubation assay, where the cells and each HAA were incubated at 37 °C for 30 min. Then the top agar was added, and the mixture was vortexed and poured onto the bottom agar.

Extracts were tested at 1 plate per dose over a dose range of 0.01 to 1 L-equivalent (L-eq) per plate in TA100 and TA98 and at 0.05 to 0.5 L-eq per plate in RSJ100 and TPT100. The haloacetic acids were tested at 1 plate per dose over a dose range of 1−500 μg/plate. For the extracts, two experiments were performed in the absence of S9 in both TA98 and TA100; however, due to limited sample, experiments with S9 were conducted only once. Two to three experiments were performed with the extracts in RSJ100 and TPT100, and two experiments were performed with the haloacetic acids.

Plates were incubated for 3 days at 37 °C, and mutant colonies (revertants, rev) were counted on an automatic colony counter (Accura 1000, Manassas, VA). A dose-related response that approached or exceeded a 2-fold increase in rev/plate compared to the DMSO control was defined as a positive mutagenic response. Linear regressions were calculated over the linear portion of the dose−response curves as defined by the r^2-value to calculate the mutagenic potencies of the water samples expressed as the slopes of the regressions (rev/L-eq).[67] Regressions with *P*-values ≤0.05 were considered a mutagenic response. Unpaired, 2-tailed *t* tests were used to compare the mutagenic potencies, with $P \leq 0.05$ for significance.

DOI: 10.1021/acs.est.8b04625
Environ. Sci. Technol. 2018, 52, 13047−13056

RESULTS AND DISCUSSION

Quantification of 21 Target Noniodinated DBPs. The occurrence in the samples of the regulated THMs, regulated and other chloro/bromo HAAs (Tables S5 and S6), investigated haloacetonitriles (HANs), trichloronitromethane, haloketones, and chloral hydrate (Table S7) is summarized in Figure 1.

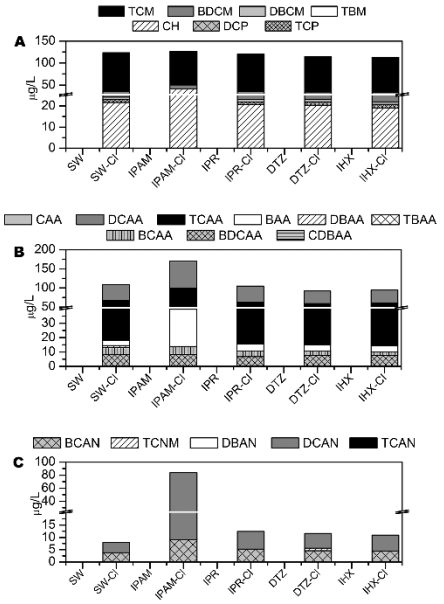

Figure 1. Concentration (μg/L) of (A) regulated trihalomethanes (THM4), chloral hydrate, selected chlorine-containing haloketones, (B) haloacetic acids (HAA9), and (C) trichloronitromethane and chloro-bromo-containing haloacetonitriles in blank and chlorinated waters. TCM: Chloroform or trichloromethane. BDCM: Bromodichloromethane. DBCM: dibromochloromethane. TBM: tribromomethane or bromoform. CH: chloral hydrate or trichloroacetaldehyde. DCP: dichloropropanone. TCP: trichloropropanone. CAA: chloroacetic acid. DCAA: dichloroacetic acid. TCAA: trichloroacetic acid. BCAA: bromochloroacetic acid. BDCAA: bromodichloroacetic acid. CDBAA: chlorodibromoacetic acid. BAA: bromoacetic acid. DBAA: dibromoacetic acid. TBAA: tribromoacetic acid. BCAN: bromochloroacetonitrile. DBCAN: dibromochloroacetonitrile. DCAN: dichloroacetonitrile. TCAN: trichloroacetonitrile. TCNM: trichloronitromethane. SW = source water and SW-Cl = chlorinated source water.

As expected, and without exception, none of these DBPs was present above the detection limit in nondisinfected waters, including the source water (SW) as well as the SW containing any of the ICM.

ICM had no effect on the total concentrations or speciation of the four regulated THMs resulting from chlorination, with chloroform being the most abundant THM, followed by bromodichloromethane and dibromochloromethane. Of the four ICM tested, only IPAM, as expected due to its high reactivity with chlorine, increased the concentrations of the 9 HAAs quantified (5 regulated and 4 unregulated), especially dichloroacetic acid (DCAA) and bromoacetic acid (BAA). DCAA and trichloroacetic acid (TCAA) were the most abundant HAAs in the chlorinated source water, followed by either bromodichloroacetic acid (BDCAA) or BAA. These results are consistent with those of a recent study,[51] which also found chloroform and TCAA to be the predominant THM and HAA species formed in chlorinated IPAM-containing source water.

When source water without IPAM was chlorinated, the HAAs and THMs contributed the most and equally to the total DBP concentrations, followed by chloral hydrate and HANs. However, this contribution pattern of DBP classes was altered considerably after chlorination of source water containing IPAM, resulting in the initial total HAN concentration of 7.8 μg/L increasing to 83.7 μg/L. Although ICM reactivity to form HANs has not been studied previously, IPAM is the ICM that is generally most reactive with chlorine.[45,51] This is borne out in the lower amounts of residual free chlorine remaining after the 72 h reaction for IPAM than for the other three ICM evaluated (Table S3). In addition to IPAM being an iodine source for iodo-DBP formation, it may also serve as a source of nitrogen (three secondary amides) in the formation of N-DBPs such as DCAN.

Quantification of 11 Target I-DBPs. The concentration of the 11 target I-DBPs (Figure 2A, Table S8) in the chlorinated

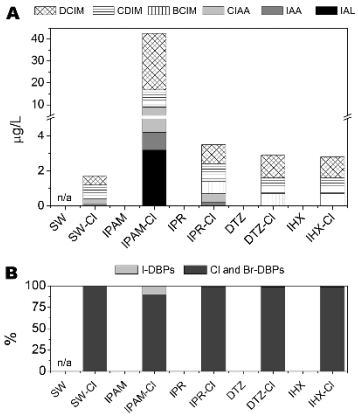

Figure 2. (A) Concentration (μg/L) of the target I-DBPs and (B) contribution of I-DBPs (%) to the total mass of the 32 target DBPs measured in the samples. DCIM: dichloroiodomethane. CDIM: chlorodiiodomethane. BCIM: bromochloroiodomethane. CIAA: chloroiodoacetic acid. IAA: iodoacetic acid. IAL: iodoacetaldehyde. n/a: not analyzed.

samples represented <10% of the total concentration of the total quantified 32 target DBPs (Figure 2B). Overall, the addition of each ICM increased slightly the concentrations of the different classes of I-DBPs in the disinfected waters. The highest increase in the concentration of I-DBPs was observed in chlorinated source water containing IPAM, as previously reported[45] (Figure 2A and Table S8). Only a few I-DBPs were formed in reaction blanks (chlorinated IPAM solutions in the absence of NOM), 0.1 μg/L of iodoacetic acid (IAA) and 3.9 μg/L of dichloroiodomethane, and at much lower concentrations than in the presence of NOM (Table S8), which is consistent with previous findings from Duirk et al.[45]

DOI: 10.1021/acs.est.8b04625
Environ. Sci. Technol. 2018, 52, 13047−13056

As for the classes of I-DBPs formed (Figure 2A, Table S8), I-THMs were always more abundant than I-HAAs and iodoacetaldehyde (IAL). Of all the targeted I-THMs, dichloriodomethane (>50-fold increase with IPAM compared to SW-Cl) followed by chlorodiiodomethane (>8-fold increase with IPAM) and bromochloroiodomethane were the most abundant in chlorinated source waters containing ICM.

In the case of I-HAAs, chloroiodoacetic acid and IAA were produced at low levels (<300 ng/L) in chlorinated source waters in the absence of ICM and at higher concentrations in chlorinated source waters containing IPR and IPAM. Chlorinated IPAM-containing waters produced higher levels of these I-HAAs (up to 5.9 μg/L in total) than did chlorinated IPR-containing waters (0.7 μg/L). IAL was detected only in chlorinated IPAM-containing waters (3.2 μg/L). The high I-DBP concentrations formed by chlorinated IPAM-containing waters could be attributed to the potentially high reactivity of chlorine toward IPAM. For example, chlorine is known to attack a specific amide side chain in the molecule that leads to the further release of iodine and other reactions.[40]

Identification and Quantification of Nontarget I-DBPs. Because ICM may serve as iodine sources in water, we performed a nontarget screening to potentially identify new I-DBPs in the extracts. To aid in the identification of iodine-containing peaks, we utilized extracted ion chromatograms of the m/z 126.904 fragment ion (iodine; I^+) from GC/HR-EI-MS full-scan data obtained for each extract, using a strategy described previously.[36,38] New I-DBPs, namely, iodoacetonitrile (Figure 3A), chloroiodoacetonitrile (Figure 3B), and trichloroiodomethane (Figure 3C), were tentatively identified using HR-MS data in the chlorinated IPAM-containing water (Figure S3), which was also the water sample with the highest concentrations of the 11 target I-DBPs. Iodoacetonitrile and trichloroiodomethane both had high similarity library matches with the NIST mass spectral database; however, chloroiodoacetonitrile did not have any sufficient matches. In all three cases, especially for chloroiodoacetonitrile, structures were elucidated via mass spectral interpretation of the EI fragmentation patterns, and molecular formulas for each molecular ion and fragment ion were determined from the accurate mass, as shown in Figure 3. The presence of chlorine(s) was determined from characteristic isotopic patterns.[68] Common fragment ions included the losses of chlorine ($\Delta m/z$ between successive fragments of 34.9688 and 36.9659) and iodine ($\Delta m/z$ of 126.9045), as well as the presence of iodine fragment ions (I^+; m/z 126.9039).

The identities of iodoacetonitrile and chloroiodoacetonitrile were confirmed through the analysis of pure standards that were available commercially for the former and synthesized for the latter (Figures 3 and S2). Although trichloroiodomethane had a high-similarity NIST mass spectral library match, its identity is still tentative because a pure standard could not be obtained.

Iodoacetonitrile is extremely cytotoxic and genotoxic in mammalian cells and has the highest genotoxicity among an entire class of seven haloacetonitriles.[2] Both iodoacetonitrile and chloroiodoacetonitrile are nitrogen-containing DBPs (N-DBPs), which are generally much more toxic than DBPs without nitrogen.[4,69] Iodinated DBPs are also consistently more toxic than brominated and chlorinated DBPs.[4] Thus, it is highly likely that chloroiodoacetonitrile (having both nitrogen and iodine in its structure) is highly cytotoxic and genotoxic in mammalian cells.

New iodoacids were also tentatively identified in the derivatized IPAM-Cl extract by selected reaction monitoring (SRM) of expected fragment ions and MS/MS transitions for these

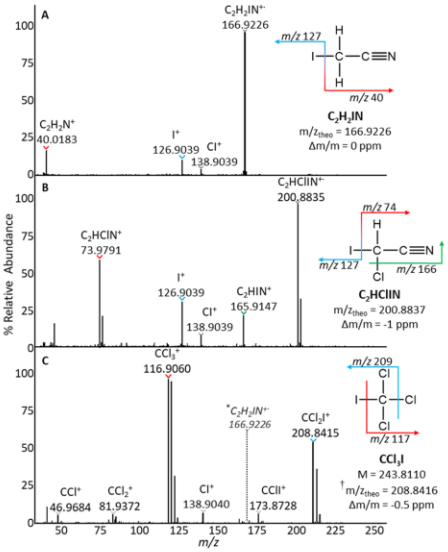

Figure 3. High-resolution EI mass spectra of (A) iodoacetonitrile (t_R = 9.12 min), (B) chloroiodoacetonitrile (t_R = 10.27 min), and (C) trichloroiodomethane (t_R = 9.15 min) in chlorinated IPAM-containing source water. †Electron ionization of trichloroiodomethane (TCIM; CCl_3I) does not produce a molecular ion; therefore, mass accuracy ($\Delta m/m$) is shown for its highest m/z fragment (CCl_2I^+). *Due to chromatographic coelution of TCIM with iodoacetonitrile (IAN), the high-abundance IAN molecular ion ($C_2H_2IN^{+\cdot}$) is observed in the mass spectrum of TCIM.

compounds. These were the following trihaloiodoacetic acids: dichloroiodoacetic acid (DCIAA), chlorodiiodoacetic acid (CDIAA), and bromochloroiodoacetic acid (BCIAA), identified in their methyl ester forms (Figure 4). The predicted SRM transitions utilized for their detection included losses of the methyl ester group ($-COOCH_3$; −59), methoxy group ($-OCH_3$; −31), iodine (−I; −127), and a rearrangement resulting in a loss of iodine and CO (−I, CO; −155). For example, the exhibited transitions from m/z 268 > 209 ($-COOCH_3$) and 268 > 237 ($-OCH_3$) at the same retention time of 13.72 min should be characteristic of DCIAA, whereas transitions from m/z 312 > 185 (−I) and 312 > 157 (−I, CO) at 18.38 min could be attributed to BCIAA.

Although their identities could not be confirmed, due to lack of available chemical standards, their GC retention times occurred in regions that would be expected for these compounds based on comparison to mono- and dihaloacetic acids. It is likely that these never-before-reported trihalo-I-HAAs were formed at low levels because they were not detected in the comprehensive full-scan MS analyses but were seen using the much more sensitive and selective SRM tandem mass spectrometry method. The detection of these six new I-DBPs in the IPAM-Cl water samples and not in the corresponding controls without IPAM confirmed IPAM as the source of iodine in their formation.

Mutagenicity of Chlorinated Waters. We analyzed the mutagenicity data in strains TA98 and TA100 (Table S9) by

DOI: 10.1021/acs.est.8b04625
Environ. Sci. Technol. 2018, 52, 13047−13056

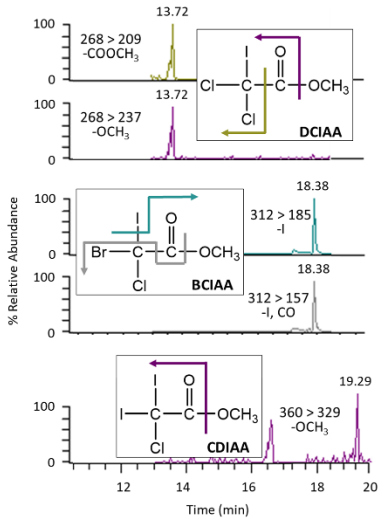

Figure 4. Selected reaction monitoring (SRM) of expected fragment ions and MS/MS transitions for new iodo-acids tentatively identified in the derivatized extract of chlorinated IPAM-containing source water. Possible identifications are dichloroiodoacetic acid (DCIAA), bromochloroiodoacetic acid (BCIAA), and chlorodiiodoacetic acid (CDIAA).

linear regression analysis (Figure S4) to calculate the slope values, which were the mutagenic potencies (rev/L-eq) of the samples in those strains (Table S10). The method blank (an ethyl acetate extract of the XAD that had been solvent-exchanged into DMSO) was not mutagenic relative to the DMSO control (Table S9), indicating that the mutagenicity observed throughout the study was not due to mutagens from the extraction procedure itself.

Statistical analyses of the mutagenic potency of the chlorinated source water (no ICM) (Figure 5A and 5B) confirmed a previous study on disinfected waters[67] in that the extract (a) was more mutagenic in the absence than the presence of S9, (b) was more mutagenic in TA100 than in TA98, and (c) had a mutagenic potency in TA100-S9 (1388.0 rev/L-eq) that was similar to that found in previous studies (~1200 rev/L-eq).[4,67,70,71]

Overall, both the mutagenicity and DBP data confirmed that the source water was typical of other source waters studied previously and that the laboratory-based disinfection procedure simulated those of commercial drinking water plants.[70] Although sample limitation prevented us from assessing the mutagenicity of the source water prior to disinfection, previous studies have shown most source waters (85−100%) are weakly or not mutagenic.[67,70,72] Supporting this is the absence of detectable DBPs in the nondisinfected source water with or without the addition of the ICM (Figure 1 and Tables S5 and S7).

Mutagenicity of Chlorinated Source Water Containing ICM. None of the ICM increased the mutagenicity of the source water after the waters were chlorinated, and this was the case in both TA98 and TA100 of *Salmonella* with or without S9 (Figure 5A and 5B). Other than IHX, none of these four ICM enhanced the genotoxicity (DNA damage measured by the comet assay in CHO cells) of chlorinated ICM-containing source water relative to chlorinated source alone.[52] On the contrary, in this study, the discovery of a highly cytotoxic and genotoxic compound (e.g., iodoacetonitrile)[2] in chlorinated IPAM-containing water could increase the cytotoxicity and genotoxicity of chlorinated source water.

In contrast, chlorinated water containing IPAM was less mutagenic than chlorinated source water alone in some strain/S9 combinations (Figure 5A and 5B). A similar phenomenon was found for IPR for DNA damage; chlorinated water containing IPR was less genotoxic than chlorinated water alone.[52] Although the basis for these findings is unclear, it is possible that the observed lower mutagenicity is due to lower formation of highly mutagenic DBPs in chlorinated IPAM-containing source waters. This finding could also be due to the competitive reaction of free chlorine with IPAM (versus NOM) to form high molecular weight DBPs, which have been found to be significantly less toxic than iodo-DBPs measured in this study.[40,60]

As an indication of the reproducibility of our laboratory-based chlorination procedure, the mutagenic potencies of the extracts from two independently conducted chlorination reactions of IPAM-containing waters (IPAM1 and IPAM2) were not significantly different from each other in either strain with or without S9 ($P > 0.217$); however, due to the lack of sample, no data were generated in TA98 + S9 with the IPAM1 extract (Table S10).

Although we did not find that any of the ICM increased the bacterial cell mutagenicity of the water extracts after chlorination, Duirk et al.[75] found a significant but modest (1.3-fold) increase in DNA damage induced by extracts of chlorinated IPAM-containing waters in mammalian cells *in vitro*. The

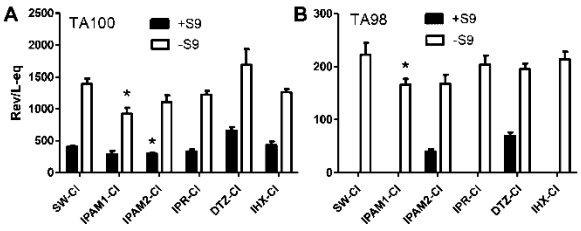

Figure 5. Mutagenic potencies (rev/L-eq) in TA100 (A) and TA98 (B) of extracts of chlorinated source water and chlorinated source water containing each of the four ICM. Asterisks indicate a significantly different mutagenic potency relative to that of the comparable chlorinated source water ($P < 0.05$).

DOI: 10.1021/acs.est.8b04625
Environ. Sci. Technol. 2018, 52, 13047−13056

Salmonella mutagenicity assay detects mutations (i.e., a change in DNA sequence), whereas the comet assay used by Duirk et al.[45] detects DNA damage (i.e., a DNA strand break or a molecule bound covalently to the DNA). Such DNA damage can be either repaired by the cell or processed by the cell into a mutation. Thus, it is possible that the small amount of DNA damage induced by chlorinating IPAM-containing water may be repaired and not result in mutation detectable in the *Salmonella* mutagenicity assay.

Correlations between Mutagenic Potencies and Concentrations of Target DBPs. Using the data in Table S10 to calculate Pearson *r* correlation coefficients, we found no significant ($P > 0.05$) positive correlations between the mutagenic potencies of any of the 11 water extracts and the total concentrations of the 21 target noniodinated DBPs, the 11 target I-DBPs, or all 32 target DBPs (data not shown). In contrast, we found strong correlations between the concentrations of the 21 target noniodinated DBPs and the mutagenicity of chlorinated or brominated finished, tap, swimming pool, or spa (hot tub) waters in a previous study.[70] Some of the pool and spa water samples of our previous study had concentrations of the 21 target DBPs and levels of mutagenicity that were nearly twice as high as those reported here. In addition, our present study had only one chlorinated water sample without ICM, so we could not perform a correlation analysis to confirm the correlation between DBP concentrations and mutagenicity that we found in our pool and spa study.

Chlorinated IPAM-containing waters generated the highest DBP concentrations, especially I-DBPs (Table S8); however, as stated earlier, IPAM did not increase the mutagenicity of chlorinated water (Figure 5A and 5B). This is likely because IAA is only weakly mutagenic in TA100 (2.8 rev/μg) (Table S12). Other I-DBPs have not been studied extensively for mutagenicity.

A previous study showed that methanol extracts of chlorinated IPAM-containing buffer or purified water (no NOM) were mutagenic in *Salmonella*.[58] The authors also identified several high-molecular weight structures that structure−activity relationship models predicted to be mutagenic.[55,58] Wendel et al.[40] found that <2% of the IPAM in chlorinated IPAM-containing water in the absence of NOM was converted to low-molecular-weight I-DBPs, and they identified a variety of high-molecular-weight I-DBPs. However, of the five high-molecular-weight DBPs evaluated for induction of DNA damage in mammalian cells *in vitro* (comet assay), none were genotoxic.[60]

Role of *GSTT1*. The mutagenicity of the extracts in strain RSJ100 (*GSTT1+*) and strain TPT100 (*GSTT1−*) is shown in Table S11. We subjected these data to linear regression analysis (Figure S5) to determine the slope values, which were the mutagenic potencies (Table S11 and Figure 6). The GSTT1 enzyme enhanced the mutagenic potencies of the extracts of the chlorinated SW+IPAM by 4.6-fold and of the chlorinated SW +IHX by 2-fold. Again, the two preparations of SW+IPAM replicated well. These results imply that some of the mutagenicity of these samples is due to the formation of Br-THMs and/or possibly the I-THMs. No I-THMs have been evaluated in the GSTT1-expressing strain of *Salmonella* to know if they are activated to mutagens by this enzyme.

We also examined the ability of the GSTT1 enzyme to activate the I-DBP iodoacetic acid (IAA) to a mutagen, as well as its homologues, bromoacetic acid (BAA), and chloroacetic acid (CAA). The results (Table S12) showed that the GSTT1 enzyme did not activate any of these three DBPs. For comparison, we showed that only IAA was mutagenic in the standard strain, TA100 (Table S12). Thus, it seems that the enhancements by the GSTT1 enzyme of the selected water extracts noted above were due to the presence of Br-THMs and/or possibly I-THMs.

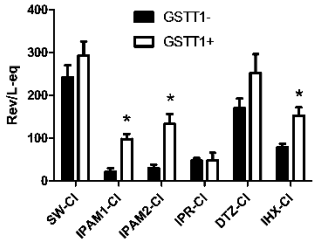

Figure 6. Mutagenic potencies of extracts in *Salmonella* strains either expressing (+) or not (−) the *GSTT1* gene. Higher mutagenic potencies in *GSTT1+* imply that some of the mutagenesis of that sample may be due to the presence of Br-THMs and/or I-THMs. $P < 0.05$.

Implications for Public Health. This study confirms IPAM as a relevant iodine source of I-DBPs in drinking water. However, the DBPs formed in the presence of IPAM or any of the other three ICM did not increase the mutagenicity of chlorinated water. Further characterization of I-DBPs formed after disinfection of ICM-containing waters is warranted given the generally potent genotoxicity of such DBPs relative to chlorinated or brominated DBPs.

DBP formation and mutagenicity of disinfected waters will depend on the type of NOM present in the source waters, which may produce different results than those reported here. Nonetheless, the potential associated risk could be diminished by reducing ICM release into drinking water sources. This requires advanced treatment of municipal and hospital wastewaters, which are the main sources of ICM into the environment. In addition, a feasibility study has demonstrated collection of ICM from hospitalized patients through decentralized urine collection,[73] and decreasing the amount of ICM entering hospital wastewater could potentially decrease requirements for advanced treatment.

■ ASSOCIATED CONTENT

Supporting Information

The Supporting Information is available free of charge on the ACS Publications website at DOI: 10.1021/acs.est.8b04625.

Physical-chemical properties, structures, and CAS numbers of ICMs; chemicals and reagents; synthesis of chloroiodoacetonitrile; characteristics of the source water; TOC, bromide, and iodide concentrations of water; reaction temperature and chlorine residual; CAS nos. and physical-chemical properties of target I-DPBs; purification of XAD resins; organic extractions by XAD/ethyl acetate; quantitative analysis of 11 target I-DBPs; analysis of nontarget I-DPBs; concentrations of regulated THMs and regulated and chloro/bromo HAAs; summed DBP concentrations; concentrations of 11 target I-DBPs; chromatograms from chlorinated IPAM-containing water; mutagenicity of chlorinated water extracts in TA100 and TA98; mutagenicity dose−response curves of water extracts in TA100 and TA98; mutagenic potencies of water samples and concentrations of target DBPs; mutagenicity of water extracts in RSJ100 and TPT100;

DOI: 10.1021/acs.est.8b04625
Environ. Sci. Technol. 2018, 52, 13047−13056

mutagenicity dose−response curves of water extracts in RSJ100 and TPT100; and mutagenicity of chloro-, bromo-, and iodoacetic acid (PDF)

AUTHOR INFORMATION

Corresponding Author

*Phone: +34-93-400-6100; e-mail: cprqam@cid.csic.es.

ORCID

David M. DeMarini: 0000-0001-8357-7988
Hannah K. Liberatore: 0000-0001-7423-3251
Amy A. Cuthbertson: 0000-0002-7634-3734

Present Addresses

[@]Department of Chemistry, University of Calgary, Alberta T2N 1N4, Canada.
[$]Institute of Inorganic and Analytical Chemistry, University of Muenster, Muenster, Germany.

Notes

The authors declare no competing financial interest.

ACKNOWLEDGMENTS

C.P. acknowledges support provided by the European Union Seventh R&D Framework Programme (FP7/2007-2013) under grant agreement 274379 (Marie Curie IOF). M.D.A. acknowledges funding from the U.S. EPA-UNC-CH Cooperative Training Agreement CR-83591401-0. This work was financially supported by the Office of Research and Development, U.S. Environmental Protection Agency, Research Triangle Park, NC. The EU is not liable for any use that may be made of the information contained therein. H.K.L. acknowledges financial support from the Department of Education through GAANN award P200A120075. This article was reviewed by the National Health and Environmental Effects Research Laboratory, U.S. EPA, and approved for publication. Approval does not signify that the contents reflect the views of the agency, nor does mention of trade names or commercial products constitute endorsement or recommendation for use.

REFERENCES

(1) EPA, U. In *U.S. EPA. 2016. Six-Year Review 3 Technical Support Document for Disinfectants/Disinfection Byproducts Rules. Office of Water. EPa-810-R-16-012*, 2016.

(2) Muellner, M. G.; Wagner, E. D.; McCalla, K.; Richardson, S. D.; Woo, Y. T.; Plewa, M. J. Haloacetonitriles vs. regulated haloacetic acids: are nitrogen-containing DBPs more toxic? *Environ. Sci. Technol.* **2007**, *41* (2), 645−651.

(3) Richardson, S. D.; Fasano, F.; Ellington, J. J.; Crumley, F. G.; Buettner, K. M.; Evans, J. J.; Blount, B. C.; Silva, L. K.; Waite, T. J.; Luther, G. W.; McKague, A. B.; Miltner, R. J.; Wagner, E. D.; Plewa, M. J. Occurrence and mammalian cell toxicity of iodinated disinfection byproducts in drinking water. *Environ. Sci. Technol.* **2008**, *42* (22), 8330−8338.

(4) Richardson, S. D.; Plewa, M. J.; Wagner, E. D.; Schoeny, R.; DeMarini, D. M. Occurrence, genotoxicity, and carcinogenicity of regulated and emerging disinfection by-products in drinking water: A review and roadmap for research. *Mutat. Res., Rev. Mutat. Res.* **2007**, *636* (1−3), 178−242.

(5) Plewa, M. J.; Muellner, M. G.; Richardson, S. D.; Fasano, F.; Buettner, K. M.; Woo, Y. T.; McKague, A. B.; Wagner, E. D. Occurrence, synthesis, and mammalian cell cytotoxicity and genotoxicity of haloacetamides: an emerging class of nitrogenous drinking water disinfection byproducts. *Environ. Sci. Technol.* **2008**, *42* (3), 955−961.

(6) Cantor, K. P.; Villanueva, C. M.; Silverman, D. T.; Figueroa, J. D.; Real, F. X.; Garcia-Closas, M.; Malats, N.; Chanock, S.; Yeager, M.; Tardon, A.; Garcia-Closas, R.; Serra, C.; Carrato, A.; Castano-Vinyals, G.; Samanic, C.; Rothman, N.; Kogevinas, M. Polymorphisms in GSTT1, GSTZ1, and CYP2E1, disinfection by-products, and risk of bladder cancer in Spain. *Environ. Health Perspect* **2010**, *118* (11), 1545−50.

(7) Costet, N.; Villanueva, C. M.; Jaakkola, J. J.; Kogevinas, M.; Cantor, K. P.; King, W. D.; Lynch, C. F.; Nieuwenhuijsen, M. J.; Cordier, S. Water disinfection by-products and bladder cancer: is there a European specificity? A pooled and meta-analysis of European case-control studies. *Occup. Environ. Med.* **2011**, *68* (5), 379−385.

(8) Villanueva, C. M.; Cantor, K. P.; Cordier, S.; Jaakkola, J. J.; King, W. D.; Lynch, C. F.; Porru, S.; Kogevinas, M. Disinfection byproducts and bladder cancer: a pooled analysis. *Epidemiology* **2004**, *15* (3), 357−367.

(9) Villanueva, C. M.; Cantor, K. P.; Grimalt, J. O.; Malats, N.; Silverman, D.; Tardon, A.; Garcia-Closas, R.; Serra, C.; Carrato, A.; Castano-Vinyals, G.; Marcos, R.; Rothman, N.; Real, F. X.; Dosemeci, M.; Kogevinas, M. Bladder cancer and exposure to water disinfection by-products through ingestion, bathing, showering, and swimming in pools. *Am. J. Epidemiol.* **2007**, *165* (2), 148−156.

(10) Rahman, M. B.; Driscoll, T.; Cowie, C.; Armstrong, B. K. Disinfection by-products in drinking water and colorectal cancer: a meta-analysis. *Int. J. Epidemiol.* **2010**, *39* (3), 733−745.

(11) Costet, N.; Garlantezec, R.; Monfort, C.; Rouget, F.; Gagniere, B.; Chevrier, C.; Cordier, S. Environmental and urinary markers of prenatal exposure to drinking water disinfection by-products, fetal growth, and duration of gestation in the PELAGIE birth cohort (Brittany, France, 2002−2006). *Am. J. Epidemiol.* **2012**, *175* (4), 263−275.

(12) Grellier, J.; Bennett, J.; Patelarou, E.; Smith, R. B.; Toledano, M. B.; Rushton, L.; Briggs, D. J.; Nieuwenhuijsen, M. J. Exposure to disinfection by-products, fetal growth, and prematurity: a systematic review and meta-analysis. *Epidemiology* **2010**, *21* (3), 300−313.

(13) Hinckley, A. F.; Bachand, A. M.; Reif, J. S. Late pregnancy exposures to disinfection by-products and growth-related birth outcomes. *Environ. Health Perspect.* **2005**, *113* (12), 1808−1813.

(14) Jeong, C. H.; Wagner, E. D.; Siebert, V. R.; Anduri, S.; Richardson, S. D.; Daiber, E. J.; McKague, A. B.; Kogevinas, M.; Villanueva, C. M.; Goslan, E. H.; Luo, W.; Isabelle, L. M.; Pankow, J. F.; Grazuleviciene, R.; Cordier, S.; Edwards, S. C.; Righi, E.; Nieuwenhuijsen, M. J.; Plewa, M. J. The occurrence and toxicity of disinfection byproducts in European drinking waters in relation with the HIWATE epidemiology study. *Environ. Sci. Technol.* **2012**, *46* (21), 12120−12128.

(15) Nieuwenhuijsen, M. J.; Grellier, J.; Smith, R.; Iszatt, N.; Bennett, J.; Best, N.; Toledano, M. The epidemiology and possible mechanisms of disinfection by-products in drinking water. *Philos. Trans. R. Soc., A* **2009**, *367* (1904), 4043−4076.

(16) Savitz, D. A.; Singer, P. C.; Hartmann, K. E.; Herring, A. H.; Weinberg, H. S.; Makarushka, C.; Hoffman, C.; Chan, R.; Maclehose, R. *Drinking Water Disinfection By-products and Pregnancy Outcome*; Awwa Research Foundation: Denver, CO, 2005.

(17) Villanueva, C. M.; Gracia-Lavedan, E.; Ibarluzea, J.; Santa Marina, L.; Ballester, F.; Llop, S.; Tardon, A.; Fernandez, M. F.; Freire, C.; Goni, F.; Basagana, X.; Kogevinas, M.; Grimalt, J. O.; Sunyer, J.; Project, I. Exposure to trihalomethanes through different water uses and birth weight, small for gestational age, and preterm delivery in Spain. *Environ. Health Perspect.* **2011**, *119* (12), 1824−1830.

(18) Waller, K.; Swan, S. H.; DeLorenze, G.; Hopkins, B. Trihalomethanes in drinking water and spontaneous abortion. *Epidemiology* **1998**, *9* (2), 134−140.

(19) Wright, J. M.; Evans, A.; Kaufman, J. A.; Rivera-Nunez, Z.; Narotsky, M. G. Disinfection by-product exposures and the risk of specific cardiac birth defects. *Environ. Health Perspect.* **2017**, *125* (2), 269−277.

(20) Wright, J. M.; Schwartz, J.; Dockery, D. W. Effect of trihalomethane exposure on fetal development. *Occup. Environ. Med.* **2003**, *60* (3), 173−180.

(21) Yang, C. Y.; Xiao, Z. P.; Ho, S. C.; Wu, T. N.; Tsai, S. S. Association between trihalomethane concentrations in drinking water

DOI: 10.1021/acs.est.8b04625
Environ. Sci. Technol. 2018, 52, 13047−13056

and adverse pregnancy outcome in Taiwan. *Environ. Res.* **2007**, *104* (3), 390−395.
(22) Pals, J.; Ang, J.; Wagner, E. D.; Plewa, M. J. Biological mechanism for the toxicity of haloacetic acid drinking water disinfection byproducts. *Environ. Sci. Technol.* **2011**, *45*, 5791−5797.
(23) Plewa, M. J.; Simmons, J. E.; Richardson, S. D.; Wagner, E. D. Mammalian cell cytotoxicity and genotoxicity of the haloacetic acids, a major class of drinking water disinfection by-products. *Environ. Mol. Mutagen.* **2010**, *51*, 871−878.
(24) Yang, Y.; Komaki, Y.; Kimura, S. Y.; Hu, H. Y.; Wagner, E. D.; Mariñas, B. J.; Plewa, M. J. Toxic impact of bromide and iodide on drinking water disinfected with chlorine or chloramines. *Environ. Sci. Technol.* **2014**, *48* (20), 12362−12369.
(25) Zhang, S.-H.; Miao, D.-Y.; Liu, A.-L.; Zhang, L.; Wei, W.; Xie, H.; Lu, W.-Q. Assessment of the cytotoxicity and genotoxicity of haloacetic acids using microplate-based cytotoxicity test and CHO/HGPRT gene mutation assay. *Mutat. Res., Genet. Toxicol. Environ. Mutagen.* **2010**, *703* (2), 174−179.
(26) Yang, M.; Zhang, X. Comparative developmental toxicity of new aromatic halogenated DBPs in a chlorinated saline sewage effluent to the marine polychaete Platynereis dumerilii. *Environ. Sci. Technol.* **2013**, *47* (19), 10868−10876.
(27) Pan, Y.; Zhang, X.; Li, Y. Identification, toxicity and control of iodinated disinfection byproducts in cooking with simulated chlor(am)inated tap water and iodized table salt. *Water Res.* **2016**, *88*, 60−68.
(28) Hanigan, D.; Truong, L.; Simonich, M.; Tanguay, R.; Westerhoff, P. Zebrafish embryo toxicity of 15 chlorinated, brominated, and iodianted disinfection by-products. *J. Environ. Sci.* **2017**, *58*, 302−310.
(29) Plewa, M. J.; Wagner, E. D.; Richardson, S. D.; Thruston, A. D.; Woo, Y. T.; McKague, A. B. Chemical and biological characterization of newly discovered iodoacid drinking water disinfection byproducts. *Environ. Sci. Technol.* **2004**, *38* (18), 4713−4722.
(30) Agus, E.; Voutchkov, N.; Sedlak, D. L. Disinfection by-products and their potential impact on the quality of water produced by desalination systems: A literature review. *Desalination* **2009**, *237* (1), 214−237.
(31) Krasner, S. W.; Westerhoff, P.; Chen, B.; Rittmann, B. E.; Amy, G. L. Occurrence of disinfection byproducts in United States wastewater treatment plant effluents. *Environ. Sci. Technol.* **2009**, *43*, 8320−8325.
(32) Gong, T.; Zhang, X. Detection, identification and formation of new iodinated disinfection byproducts in chlorinated saline wastewater effluents. *Water Res.* **2015**, *68*, 77−86.
(33) Kim, D.; Amy, G. L.; Karanfil, T. Disinfection by-product fomation during seawater desalination: a review. *Water Res.* **2015**, *81*, 343−355.
(34) Smith, E. M.; Plewa, M. J.; Lindell, C. L.; Richardson, S. D.; Mitch, W. A. Comparison of byproduct formation in waters treated with chlorine and iodine: Relevance to point-of-use treatment. *Environ. Sci. Technol.* **2010**, *44* (22), 8446−8452.
(35) Jeong, C. H.; Postigo, C.; Richardson, S. D.; Simmons, J. E.; Kimura, S. Y.; Mariñas, B. J.; Barcelo, D.; Liang, P.; Wagner, E. D.; Plewa, M. J. Occurrence and comparative toxicity of haloacetaldehyde disinfection byproducts in drinking water. *Environ. Sci. Technol.* **2015**, *49* (23), 13749−13759.
(36) Liberatore, H. K.; Plewa, M. J.; Wagner, E. D.; Vanbriesen, J. M.; Burnett, D. B.; Cizmas, L. H.; Richardson, S. D. Identification and comparative mammalian cell cytotoxicity of new iodo-phenolic disinfection byproducts in chloraminated oil and gas wastewaters. *Environ. Sci. Technol. Lett.* **2017**, *4* (11), 475−480.
(37) Pan, Y.; Li, W.; An, H.; Cui, H.; Wang, Y. Formation and occurrence of new polar iodinated disinfection byproducts in drinking water. *Chemosphere* **2016**, *144*, 2312−20.
(38) Postigo, C.; Cojocariu, C. I.; Richardson, S. D.; Silcock, P. J.; Barcelo, D. Characterization of iodinated disinfection by-products in chlorinated and chloraminated waters using Orbitrap based gas chromatography-mass spectrometry. *Anal. Bioanal. Chem.* **2016**, *408* (13), 3401−3411.
(39) Wang, X.; Wang, J.; Zhang, Y.; Shi, Q.; Zhang, H.; Zhang, Y.; Yang, M. Characterization of unknown iodinated disinfection by-products during chlorination/chloramination using ultrahigh resolution mass spectrometry. *Sci. Total Environ.* **2016**, *554−555*, 83−88.
(40) Wendel, F. M.; Lütke Eversloh, C.; Machek, E. J.; Duirk, S. E.; Plewa, M. J.; Richardson, S. D.; Ternes, T. A. Transformation of iopamidol during chlorination. *Environ. Sci. Technol.* **2014**, *48* (21), 12689−12697.
(41) Jones, D. B.; Saglam, A.; Song, H.; Karanfil, T. The impact of bromide/iodide concentration and ratio on iodinated trihalomethane formation and speciation. *Water Res.* **2012**, *46* (1), 11−20.
(42) Postigo, C.; Richardson, S. D.; Barcelo, D. Formation of iodo-trihalomethanes, iodo-haloacetic acids, and haloacetaldehydes during chlorination and chloramination of iodine containing waters in laboratory controlled reactions. *J. Environ. Sci. (Beijing, China)* **2017**, *58*, 127−134.
(43) Zhang, J.; Chen, D. D.; Li, L.; Li, W. W.; Mu, Y.; Yu, H. Q. Role of NOM molecular size on iodo-trihalomethane formation during chlorination and chloramination. *Water Res.* **2016**, *102*, 533−541.
(44) Wei, Y.; Liu, Y.; Ma, L.; Wang, H.; Fan, J.; Liu, X.; Dai, R. H. Speciation and formation of iodinated trihalomethane from microbially derived organic matter during the biological treatment of micro-polluted source water. *Chemosphere* **2013**, *92* (11), 1529−1535.
(45) Duirk, S. E.; Lindell, C.; Cornelison, C. C.; Kormos, J.; Ternes, T. A.; Attene-Ramos, M.; Osiol, J.; Wagner, E. D.; Plewa, M. J.; Richardson, S. D. Formation of toxic iodinated disinfection by-products from compounds used in medical imaging. *Environ. Sci. Technol.* **2011**, *45* (16), 6845−6854.
(46) Xu, Z. F.; Li, X.; Hu, X. L.; Yin, D. Q. Distribution and relevance of Iodinated X-Ray contrast media and Iodinated trihalomethanes in an aquatic environment. *Chemosphere* **2017**, *184*, 253−260.
(47) Ternes, T. A.; Hirsch, R. Occurrence and behavior of X-ray contrast media in sewage facilities and the aquatic environment. *Environ. Sci. Technol.* **2000**, *34*, 2741−2748.
(48) Zonja, B.; Delgado, A.; Pérez, S.; Barceló, D. LC-HRMS suspect screening for detection-based prioritization of iodinated contrast media photodegradates in surface waters. *Environ. Sci. Technol.* **2015**, *49* (6), 3464−3472.
(49) Kormos, J. L.; Schulz, M.; Ternes, T. A. Occurrence of iodinated X-ray contrast media and their biotransformation products in the urban water cycle. *Environ. Sci. Technol.* **2011**, *45*, 8723−8732.
(50) Mendoza, A.; Zonja, B.; Mastroianni, N.; Negreira, N.; López de Alda, M.; Pérez, S.; Barceló, D.; Gil, A.; Valcárcel, Y. Drugs of abuse, cytostatic drugs and iodinated contrast media in tap water from the Madrid region (central Spain): A case study to analyse their occurrence and human health risk characterization. *Environ. Int.* **2016**, *86*, 107−118.
(51) Ackerson, N. O. B.; Machek, E. J.; Killinger, A. H.; Crafton, E. A.; Kumkum, P.; Liberatore, H. K.; Plewa, M. J.; Richardson, S. D.; Ternes, T. A.; Duirk, S. E. Formation of DBPs and halogen-specific TOX in the presence of iopamidol and chlorinated oxidants. *Chemosphere* **2018**, *202*, 349−357.
(52) Jeong, C. H.; Machek, E. J.; Shakeri, M.; Duirk, S. E.; Ternes, T. A.; Richardson, S. D.; Wagner, E. D.; Plewa, M. J. The impact of iodinated X-ray contrast agents on formation and toxicity of disinfection by-products in drinking water. *J. Environ. Sci. (Beijing, China)* **2017**, *58*, 173−182.
(53) Wang, Z.; Xu, B.; Lin, Y. L.; Hu, C. Y.; Tian, F. X.; Zhang, T. Y.; Gao, N. Y. A comparison of iodinated trihalomethane formation from iodide and iopamidol in the presence of organic precursors during monochloramination. *Chem. Eng. J.* **2014**, *257*, 292−298.
(54) Ye, T.; Xu, B.; Wang, Z.; Zhang, T. Y.; Hu, C. Y.; Lin, L.; Xia, S. J.; Gao, N. Y. Comparison of iodinated trihalomethanes formation during aqueous chlor(am)ination of different iodinated X-ray contrast media compounds in the presence of natural organic matter. *Water Res.* **2014**, *66*, 390−398.
(55) Matsushita, T.; Hashizuka, M.; Kuriyama, T.; Matsui, Y.; Shirasaki, N. Use of orbitrap-MS/MS and QSAR analyses to estimate

DOI: 10.1021/acs.est.8b04625
Environ. Sci. Technol. 2018, 52, 13047−13056

mutagenic transformation products of iopamidol generated during ozonation and chlorination. *Chemosphere* **2016**, *148*, 233−240.
(56) Allard, S.; Criquet, J.; Prunier, A.; Falantin, C.; Le Person, A.; Yat-Man Tang, J.; Croué, J. P. Photodecomposition of iodinated contrast media and subsequent formation of toxic iodinated moieties during final disinfection with chlorinated oxidants. *Water Res.* **2016**, *103*, 453−461.
(57) Wang, Z.; Lin, Y. L.; Xu, B.; Xia, S. J.; Zhang, T. Y.; Gao, N. Y. Degradation of iohexol by UV/chlorine process and formation of iodinated trihalomethanes during post-chlorination. *Chem. Eng. J.* **2016**, *283*, 1090−1096.
(58) Matsushita, T.; Kobayashi, N.; Hashizuka, M.; Sakuma, H.; Kondo, T.; Matsui, Y.; Shirasaki, N. Changes in mutagenicity and acute toxicity of solutions of iodinated X-ray contrast media during chlorination. *Chemosphere* **2015**, *135*, 101−107.
(59) Nelson, J. A.; Livingston, G. K.; Moon, R. G. Mutagenic evaluation of radiographic contrast media. *Invest. Radiol.* **1982**, *17*, 183−185.
(60) Wendel, F. M.; Ternes, T. A.; Richardson, S. D.; Duirk, S. E.; Pals, J. A.; Wagner, E. D.; Plewa, M. J. Comparative toxicity of high-molecular weight iopamidol disinfection byproducts. *Environ. Sci. Technol. Lett.* **2016**, 3 (3), 81−84.
(61) Regli, S.; Chen, J.; Messner, M.; Elovitz, M. S.; Letkiweicz, F. J.; Pegram, R. A.; Pepping, T. J.; Richardson, S. D.; Wright, J. M. Estimating potential increased bladder cancer risk due to increased bromide concentrations in sources of disinfected drinking waters. *Environ. Sci. Technol.* **2015**, *49*, 13094−13102.
(62) Pressman, J. G.; Richardson, S. D.; Speth, T. F.; Miltner, R. J.; Narotsky, M. G.; Hunter, E. S., III; Rice, G. E.; Teuschler, L. K.; McDonald, A.; Parvez, S.; Krasner, S. W.; Weinberg, H. S.; McKague, A. B.; Parrett, C. J.; Bodin, N.; Chinn, R.; Lee, C.-F. T.; Simmons, J. E. Concentration, chlorination, and chemical analysis of drinking water for disinfection byproduct mixtures health effects research: U.S. EPA's Four Lab study. *Environ. Sci. Technol.* **2010**, *44* (19), 7184−7192.
(63) APHA. In *American Public Health Association (APHA), American Water Works Association (AWWA), Water Environment Federation (WEF) 4500-Cl F. DPD Ferrous Titrimetric Method. In: Standard Methods for the Examination of Water and Wastewater*, 16th ed.; American Public Health Association: Washington, DC; 1985; pp 306−309.
(64) Richardson, S. D.; Thruston, A. D.; Collette, T. W.; Patterson, K. S.; Lykins, B. W.; Majetich, G.; Zhang, Y. Multispectral identification of chlorine dioxide disinfection byproducts in drinking water. *Environ. Sci. Technol.* **1994**, *28* (4), 592−599.
(65) Munch, D. J.; Munch, J. W.; Pawlecki, A. M. EPA Method 552.2. *Determination of haloacetic acids and dalapon in drinking water by liquid-liquid extraction, derivatization and gas chromatography with electron capture detection. Revision 1*; National Exposure Research Laboratory Office of Research and Development, US Environmental Protection Agency: Cincinnati, OH, 1995.
(66) Munch, D. J.; Hautman, D. P. EPA Method 551.1. *Determination of chlorination disinfection by-products, chlorinated solvents, and halogenated pesticide/herbicides in drinking water by liquid-liquid extraction and gas chromatography with electron-capture detection. Revision 1*; National Exposure Research Laboratory Office of Research and Development, US Environmental Protection Agency: Cincinnati, OH. 1995.
(67) DeMarini, D. M.; Abu-Shakra, A.; Felton, C. F.; Patterson, K. S.; Shelton, M. L. Mutation spectra in Salmonella of chlorinated, chloraminated, or ozonated drinking water extracts. Comparison to MX. *Environ. Mol. Mutagen.* **1995**, *26*, 270−285.
(68) McLafferty, F. M.; Turacek, F. *Interpretation of Mass Spectra*, 4th ed.; University Science Books: Sausalito, CA, 1993.
(69) Plewa, M. J.; Wagner, E. D.; Muellner, M. G.; Hsu, K.-M.; Richardson, S. D. Comparative mammalian cell toxicity of N-DBPs and C-DBPs. In *Disinfection By-Products in Drinking Water: Occurrence, Formation, Health Effects, and Control*; Karanfil, T., Krasner, S. W., Westerhoff, P., Xie, Y., Eds.; American Chemical Society: Washington, D.C., 2008; pp 36−50.
(70) Daiber, E. J.; DeMarini, D. M.; Ravuri, S. A.; Liberatore, H. K.; Cuthbertson, A. A.; Thompson-Klemish, A.; Byer, J. D.; Schmid, J. E.; Afifi, M. Z.; Blatchley, E. R.; Richardson, S. D. Progressive increase in disinfection byproducts and mutagenicity from source to tap to swimming pool and spa water: Impact of human inputs. *Environ. Sci. Technol.* **2016**, *50* (13), 6652−6662.
(71) Takanashi, H.; Kishida, M.; Nakajima, T.; Ohki, A.; Akiba, M.; Aizawa, T. Surveying the mutagenicity of tap water to elicit the effects of purification processes on Japanese tap water. *Chemosphere* **2009**, *77*, 434−439.
(72) Umbuzeiro, G. A.; Roubicek, D. A.; Sanchez, P. S.; Sato, M. I. The Salmonella mutagenicity assay in a surface water quality monitoring program based on a 20-year survey. *Mutat. Res., Genet. Toxicol. Environ. Mutagen.* **2001**, *491*, 119−126.
(73) Heinzmann, B.; Schwarz, R.-J.; Schuster, P.; Pineau, C. Decentralized collection of iodinated x-ray contrast media in hospitals−results of the feasibility study and the practice test phase. *Water Sci. Technol.* **2008**, *57* (2), 209−215.

DOI: 10.1021/acs.est.8b04625
Environ. Sci. Technol. 2018, 52, 13047−13056

JOURNAL OF ENVIRONMENTAL SCIENCES 78 (2019) 204–214

Available online at www.sciencedirect.com

ScienceDirect

www.elsevier.com/locate/jes

JES JOURNAL OF ENVIRONMENTAL SCIENCES

www.jesc.ac.cn

Impact of chlorine exposure time on disinfection byproduct formation in the presence of iopamidol and natural organic matter during chloramination

Nana Osei B. Ackerson[1], *Alexis H. Killinger*[1], *Hannah K. Liberatore*[2], *Thomas A. Ternes*[3], *Michael J. Plewa*[4], *Susan D. Richardson*[2], *Stephen E. Duirk*[1,*]

1. *Department of Civil Engineering, University of Akron, Akron, OH 44325, USA*
2. *Department of Chemistry and Biochemistry, University of South Carolina, 631 Sumter St., Columbia, SC 29208, USA*
3. *Federal Institute of Hydrology (BfG), Am Mainzer Tor 1, D-56068 Koblenz, Germany*
4. *Department of Crop Sciences and Safe Global Water Institute and NSF Science and Technology Center of Advanced Materials for the Purification of Water with Systems, University of Illinois at Urbana-Champaign, 1101 West Peabody Drive, Urbana, IL 61801, USA*

ARTICLE INFO

Article history:
Received 19 July 2018
Revised 17 September 2018
Accepted 19 September 2018
Available online 29 September 2018

Keywords:
Prechlorinaton
Iopamidol
Monochloramine
Disinfection byproducts (DBPs)
Total organic chlorine (TOCl)
Total organic iodine (TOI)

ABSTRACT

Chloramines, in practice, are formed onsite by adding ammonia to chlorinated drinking water to achieve the required disinfection. While regulated disinfection byproducts (DBPs) are reduced during chloramine disinfection, other DBPs such as iodinated (iodo-) DBPs, that elicit greater toxicity are formed. The objective of this study was to investigate the impact of prechlorination time on the formation of both halogen-specific total organic halogen (TOX) and iodo/chlorinated (chloro-) DBPs during prechlorination/chloramination in source waters (SWs) containing iopamidol, an X-ray contrast medium. Barberton SW (BSW) and Cleveland SW (CSW) containing iopamidol were prechlorinated for 5–60 min and afterwards chloraminated for 72 hr with ammonium chloride. Chlorine contact time (CCT) did not significantly impact total organic iodine (TOI) concentrations after prechlorination or chloramination. Concentrations of total organic chlorine (TOCl) formed during prechlorination did not significantly change regardless of pH and prechlorination time, while TOCl appeared to decrease after 72 hr chloramination period. Dichloroiodomethane ($CHCl_2I$) formation during prechlorination did not exhibit any significant trends as a function of pH or CCT, but after chloramination, significant increases were observed at pHs 6.5 and 7.5 with respect to CCT. Iodo-HAAs were not formed during prechlorination but were detected after chloramination. Significant quantities of chloroform ($CHCl_3$) and trichloroacetic acid (TCAA) were formed during prechlorination but formation ceased upon ammonia addition. Therefore, prechlorination studies should measure TOX and DBP concentrations prior to ammonia addition to obtain data regarding the initial conditions.

* *Corresponding author.*
E-mail address: duirk@uakron.edu. (S.E. Duirk).

https://doi.org/10.1016/j.jes.2018.09.022
1001-0742/© 2018 The Research Center for Eco-Environmental Sciences, Chinese Academy of Sciences. Published by Elsevier B.V.

Introduction

Chloramines have been used primarily for disinfection when chlorination of waters containing high concentrations of natural organic matter (NOM) or other precursors lead to excessive formation of disinfection by-products (DBPs) (Bougeard et al., 2010). Trihalomethanes (THMs) and haloacetic acids (HAAs) are two classes of halogenated DBPs that are formed in high concentrations; which are just a fraction of total organic halogen (TOX) formed during chlorination. Epidemiological studies have linked DBPs in chlor(am) inated waters to cancer of the bladder, pancreas, rectum, kidney, as well as Hodgkin's and non-Hodgkin's lymphomas, spontaneous abortions, and birth defects in consumers exposed for prolonged periods (Morris et al., 1992; Koivusalo et al., 1994; Bull et al., 1995; Nieuwenhuijsen et al., 2000; Waller et al., 2001; Villanueva et al., 2004; Regli et al., 2015). Reducing the concentration of TOX and known DBPs in drinking water will minimize the public health risks associated with exposure to these halogenated compounds (Richardson et al., 2007; Plewa et al., 2010). Therefore, water utilities should balance the need to adequately disinfect drinking water while minimizing the formation of toxic/carcinogenic by-products.

Chloramines are formed by the addition of ammonia to chlorine. In drinking water treatment plants, treated waters are exposed to aqueous chlorine for different contact times before the addition of ammonia to form chloramines. Chloramines are known to be less reactive than aqueous chlorine and are comprised of three dominant species under drinking water treatment conditions: monochloramine (NH_2Cl), dichloramine ($NHCl_2$), and trichloramine (NCl_3) (Vikesland et al., 2001). Water utilities use chloramines at $pH \geq 8$ so that NH_2Cl is the predominant chloramine species for disinfection, which increases chloramine stability and prevents monochloramine autodecomposition (Jafvert and Valentine, 1992). Monochloramine reacts with NOM and other precursors in water or hydrolyzes to form aqueous chlorine to react with precursors to form unregulated DBPs such as iodinated DBPs (iodo-DBPs), nitrogenous DBPs (N-DBPs), and haloacetaldehydes (Bichsel and von Gunten, 2000a; Choi and Valentine, 2002; Plewa et al., 2004, 2008; Krasner et al., 2006; Hua and Reckhow, 2007b; Chen and Young, 2008; Richardson et al., 2008; Jones et al., 2011; Huang et al., 2012; Shah and Mitch, 2012; Chuang et al., 2015; Jeong et al., 2015; Postigo et al., 2017). Moreover, in vitro mammalian cell studies have revealed that these classes of DBPs elicit higher cytotoxicity and genotoxicity responses compared to the regulated DBPs (Plewa et al., 2004, 2008; Richardson et al., 2008; Duirk et al., 2011; Jeong et al., 2015). As water utilities reduce the levels of regulated DBPs by using monochloramine disinfection, an understanding of aqueous chlorine contact time prior to ammonia addition is pertinent to decreasing both regulated and unregulated DBPs.

Prechlorination has been found to significantly change DBP formation trends from organic contaminant precursors, including pharmaceuticals and pesticides, prior to ammonia addition. In the absence of NOM, N-nitrosodimethylamine (NDMA) formation increased with aqueous chlorine contact time (0–120 min) for sumatriptan and diltiazem but decreased with chlorine exposure time for ranitidine, nizatidine, and tetracycline (Shen and Andrews, 2013). The authors reported similar trends for ranitidine, but different trends for sumatriptan in the presence of NOM. Also, Chuang et al. (2015) reported that the formation of dichloroacetamide and trichloroacetamide after 24 hr chloramination of 2,4,6-trichlorophenol increased with aqueous chlorine contact time from 0.5 to 5 min. However, the highest concentration of dichloroacetonitrile from the same precursor formed during chloramination was observed at 0.5 min chlorine exposure time. Therefore, factors causing different DBP trends during prechlorination before ammonia addition to form chloramine include chlorine exposure time, type of aqueous precursor, and pH.

Chloramination has also been found to promote the formation of iodo-DBPs (Bichsel and von Gunten, 2000a; Plewa et al., 2004, 2008; Krasner et al., 2006; Richardson et al., 2008; Jones et al., 2011; Postigo et al., 2017). NH_2Cl oxidizes iodide to hypoiodous acid (HOI) and then rapidly incorporates into NOM, forming iodo-DBP (Bichsel and von Gunten, 2000b). Since the competing reaction to form iodate is extremely slow with monochloramine, an increase in chlorine contact time can result in the complete oxidation of HOI to iodate (Bichsel and von Gunten, 1999; Allard et al., 2015). Therefore, it has been observed in actual drinking waters that an increase in aqueous chlorine exposure to iodide-containing waters prior to chloramine formation decreases the quantities of iodo-DBPs produced (Richardson et al., 2008). Allard et al. (2015) found that iodoform (CHI_3) formation increased as prechlorination time increased to 5 min but decreased at 30 min aqueous chlorine exposure. This happened because as chlorine exposure time increased HOI was oxidized to iodate (IO_3^-) and thus limited triiodination to form CHI_3. However, dichloroiodomethane ($CHCl_2I$) and chlorodiiodomethane ($CHClI_2$) increased with prechlorination time since both involve the incorporation of both residual HOI and chlorine.

To-date, prechlorination studies investigating iodo-DBP formation have mostly used inorganic iodide. However, iodinated X-ray contrast media (ICM), particularly iopamidol, also contain 3 iodine atoms and have been shown to be a precursor in the formation of iodo-DBPs (Duirk et al., 2011; Tian et al., 2014; Wendel et al., 2014; Ye et al., 2014). In the United States (US) iopamidol was detected in source waters at 6 out of 10 drinking water treatment plants with concentrations up to 2700 ng/L (Duirk et al., 2011). The objective of this study was to investigate the impact of prechlorination contact time on the formation and speciation of halogen-specific TOX and DBPs prior to and post ammonia addition in source waters containing iopamidol. Therefore, the formation of both chlorinated (chloro-) and iodinated (iodo-) DBPs and TOX was measured at the end of the prechlorination time and after the 72-hr chloramination period.

1. Materials and methods

1.1. Standards and reagents

All DBP standards and reagents were purchased at the highest possible purities. All other (in)organic chemicals

used were certified American Chemical Society reagent grade and were used without further purification. Iopamidol (99.5%) was purchased from U.S. Pharmacopeia (Rockville, MD, USA). All other standards and reagents used can be found in Appendix A.

Purified water (18.2 MΩ/cm) was produced from a Barnstead ROPure Infinity/NANOPure system (Barnstead-Thermolyne Corp. Dubuque, IA, USA). Phosphate (for pH 6.5 and 7.5) and borate (for pH 8.5 and 9.0) buffers were used to maintain pH while pH adjustments were achieved with 0.5 mol/L H_2SO_4 and 1 mol/L NaOH. Experimental pH was monitored with Orion 5-star pH meter equipped with Ross ultra-combination electrode (Thermo Fisher Scientific, Pittsburgh, PA). Aqueous chlorine prepared from commercial 5.75%-6% sodium hypochlorite (NaOCl) containing equimolar quantities of OCl^- and Cl^- was purchased from Thermo Fisher Scientific (Pittsburgh, PA). Prior to each experiment, the concentration of aqueous chlorine was verified using ferrous ammonium sulfate (FAS)/N,N′-diphenyl-p-phenylenediamine (DPD) titration (APHA et al., 2005). All glassware and polytetrafluoroethylene containers were conditioned by soaking them in a chlorine bath for 24 hr, rinsed with copious amounts of purified water, and dried before use.

1.2. Experimental procedure

Source waters (SWs) from the intake structures of Barberton and Cleveland Water Treatment Plants (WTPs) in Northeast Ohio, USA, were used in this study. Detailed chemical and fluorescence spectral characteristics of Barberton source water (BSW) and Cleveland source water (CSW) have previously been characterized (Ackerson et al., 2018). Also, iopamidol concentration in the SWs were below detection limit (Wendel et al., 2014). A summary of the SW characteristics, including fluorescence data, can be found Appendix A Tables S1 and S2. SWs were filtered with 0.45 μm Whatman nylon membrane filter (West Chester, PA) and stored at 4 °C until use.

Reaction mixtures containing filtered BSW or CSW, 4 mmol/L buffer, and 5 μmol/L iopamidol in a 1000 mL Erlenmeyer flask were spiked with 100 μmol/L of aqueous chlorine at pH 6.5–9.0 under rapid mixing. Aliquots of chlorinated samples were transferred to 120 mL and 40 mL batch reactors to be extracted entirely at each discrete sample interval. After 5, 30, and 60 min of aqueous chlorine exposure, 143 μmol/L of aqueous ammonium chloride (NH_4Cl) was added to the sample to form monochloramine with a minimum Cl/N molar ratio of 0.7. At pH 7.5 and above NH_2Cl is the predominant combined chlorine while $NHCl_2$ is the major combined chlorine at pH 4.0 to 6.0 due to acid-catalyzed disproportionation of NH_2Cl (Jafvert and Valentine, 1992). A study by Yang et al. (2007) found that the proportion of $NHCl_2$ in combined chlorine oxidant increased from 3.6% at pH 7.0 to 63% at pH 6.0. Therefore, in this study, NH_2Cl will be the most abundant (approximately >98%) chloramine species at pH 7.5 and above. At pH 6.5, it is possible the proportion of NH_2Cl is more than 60%.

Aliquots of samples were taken before ammonia addition at the end of chlorine exposure time and quenched with aqueous sulfite solution and were immediately extracted and analyzed for halogen-specific TOX and DBPs. Samples spiked with NH_4Cl were kept in the dark at 25 ± 1 °C for 72 hr. Afterwards, residual oxidant was quenched with 120 μmol/L sulfite solution and extracted immediately for both TOX and DBP analyses. Extraction for DBPs was achieved using liquid–liquid extraction in methyl tert-butyl ether (MtBE) and 1,2-dibromopropane as the internal standard. An aliquot of the organic extract was used for THM analysis, while the remaining was used for HAA derivatization. TOX samples were acidified (pH 2) with HNO_3. I^- and IO_3^- were analyzed after oxidant quenching. Details of extraction procedures for TOX and DBPs, TOX combustion, and HAA derivatization were described by Ackerson et al. (2018).

1.3. Analytical methods

The acidified TOX samples were adsorbed on activated carbon using TOX-100 adsorption module (Cosa Instruments/Mitsubishi, NY, USA), combusted in TOX-100 analyzer (Cosa Instruments/Mitsubishi, Horseblock Road, NY, USA), and collected in a phosphate solution (100 μmol/L). Halogen-specific TOX, I^-, and IO_3^- analysis was performed on a Dionex ICS-3000 ion chromatography (Dionex Corporation, Sunnyvale, CA) with a conductivity detector and an ASRS®300 4 mm anion self-regenerating suppressor. Using KOH as the mobile phase (flow rate of 1 mL/min), total organic chlorine (TOCl) and total organic iodine (TOI) were respectively detected as Cl^- and I^- on an AS20 analytical column (4 × 250 mm) with guard column (Dionex Corporation, Sunnyvale, CA). THMs, haloacetonitriles (HANs), and non-iodinated HAAs analyses were accomplished with 7890A GC system equipped with ^{63}Ni microelectron capture detector (μECD) from Agilent Technologies (Santa Clara, CA). Splitless injection was used with a Rxi-5Sil MS GC column (Restek Corporation, Bellefonte, PA) of dimensions 30 m × 0.5 μm and 0.25 mm i.d., for analyte separation. Ultrahigh purity nitrogen and helium gases were used as the make-up gas and carrier gas, respectively. The μECD temperature was 250 °C. Iodo-HAAs were analyzed using a GC-triple quadrupole mass spectrometer (GC–MS–MS). A flow rate of 1.2 mL/min was used in a Rxi-5 ms column (30 m × 0.25 mm i.d × 0.25 μm). Injections of 2.0 μL by splitless mode were carried out at an inlet temperature of 250 °C. The temperature of the transfer line was held at 280 °C. The temperature, emission current, and electron energy of the electron ionization source were 200 °C, 50 μA, and 70 eV, respectively. Oven temperature programming for THMs, HANs, and HAAs, as well as MS–MS transitions, are indicated elsewhere (Ackerson et al., 2018). THM species analyzed were chloroform ($CHCl_3$), dichloroiodomethane ($CHCl_2I$), chlorodiiodomethane ($CHClI_2$), and iodoform (CHI_3). Dichloroacetic acid (DCAA), trichloroacetic acid (TCAA), iodoacetic acid (IAA), chloroiodoacetic acid (CIAA), and diiodoacetic acid (DIAA) were the HAA compounds analyzed, while dichloroacetonitrile (DCAN) and chloroacetonitrile (CAN) comprised the HAN compounds analyzed.

The data were analyzed with Microsoft Excel and Minitab 17. Test of statistical significance was achieved with Minitab 17 using one-way analysis of variance (ANOVA) at 95% confidence interval.

2. Results and discussion

2.1. Prechlorination time and TOX formation

Iopamidol degradation in the presence of NOM and aqueous chlorine or chloramine resulted in minimal TOI degradation. The initial TOI concentration was 15 μmol/L which is due to the three iodine atoms from 5 μmol/L iopamidol. In both BSW and CSW, TOI did not show any appreciable differences in concentrations at the end of each aqueous chlorine contact time and chloramination of 72 hr as a function of pH (Fig. 1), which agrees with previous results (Ackerson et al., 2018). Chlorination of iopamidol-containing SWs results in OCl^- cleaving one of the iopamidol amide side chains, resulting in the formation of a secondary amine, which undergoes chlorine-iodine exchange to form HOI and other DBPs (Wendel et al., 2014). HOI rapidly reacts with NOM, resulting in the formation of TOI. Since iopamidol transformation during chlorination is slow, greater than 80% of iopamidol remained in chlorinated aqueous solution after 1 hr of prechlorination based on previous work (Wendel et al., 2014). Therefore, the bulk of TOI was contributed by unreacted iopamidol at the end of prechlorination. In addition, iodine-containing iopamidol transformation products (TPs), formed from the reaction of the remaining iopamidol with aqueous chlorine, contributed to the observed TOI concentrations (Ackerson et al., 2018). The addition of ammonia results in the rapid formation ($k = 4.2 \times 10^6$ L/mol/sec) of NH_2Cl (Morris and Isaac, 1981), which slowly reacts with the unreacted iopamidol and iopamidol TPs to form other TPs and low amount of HOI. Because more than 90% of iopamidol remains during chloramination (Wendel et al., 2016; Ackerson et al., 2018), the unreacted iopamidol, iodine-bearing TPs, and the HOI which incorporated in NOM structures produced the TOI observed after chloramination. Therefore, TOI concentrations after both prechlorination and chloramination were equal. Also, since NH_2Cl is very slow to oxidize HOI to iodate, there was sufficient time for HOI to react with NOM (Bichsel and von Gunten, 1999). However, the formation of HOI in the presence of monochloramine is significantly reduced due to the minimal concentrations of aqueous chlorine produced from the hydrolysis of monochloramine (Jafvert and Valentine, 1992), to react with iopamidol or iodine-containing DBPs.

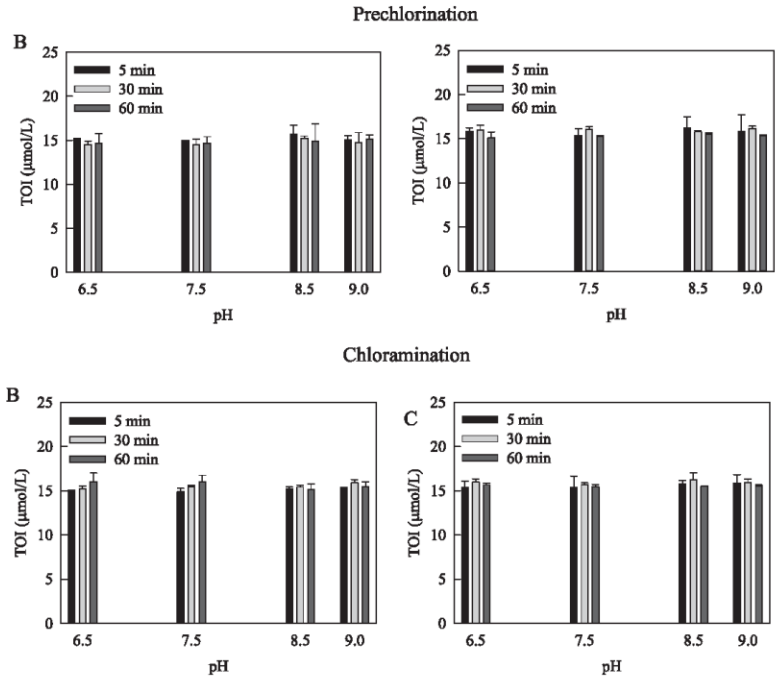

Fig. 1 – Formation of TOI in Barberton (B) and Cleveland (C) source waters during prechlorination and chloramination as a function of pH and prechlorination time. [Iopamidol] = 5 μmol/L, [HOCl] = 100 μmol/L, [NH4Cl] = 143 μmol/L, [Buffer]T = 4 mmol/L, Temp = 25 °C, DOC = 2.51 mg/LC, DOCBarberton = 4.47 mg/L-C, DOCCleveland = 2.51 mg/L-C. Error bars represent 95% confidence interval for two replicates. Legend represents prechlorination time.

Previous study showed that less than 10% of TOI degraded after 6 hr of chlorine contact time in the presence of iopamidol in the same SWs (Ackerson et al., 2018). This suggests that TOI loss from iopamidol transformation in the presence of aqueous chlorine and NOM would be negligible at the prechlorination times used in the study. HOI, I^-, and IO_3^- were not detected in any of the samples after either prechlorination or chloramination; possibly due to incomplete transformation of iopamidol.

TOCl, on the contrary, exhibited different formation trends with respect to the SWs and aqueous chlorine exposure times. Generally, in BSW, TOCl concentrations increased as prechlorination time increased from 5 to 60 min regardless of pH (Fig. 2). However, the statistical significance of TOCl formation as a function of prechlorination time diminishes at pH 8.5 (p =0.291) and 9 (p =0.225). As pH increased, TOCl formation appears to increase especially at prechlorination time of 5 min. This would appear to indicate TOCl formation is very rapid at pH greater than 7.5 for the first 5 min. At pH 6.5, TOCl formation in BSW increased by 47% and 31% as prechlorination time increased from 5 to 30 min and 30 to 60 min, respectively. However, TOCl formation at pH 7.5 increased from prechlorination time of 5–30 min and 30–60 min by 13% and 43%, respectively. In the CSW, regardless of pH or prechlorination time, TOCl formation was approximately 5 μmol/L; although, the 30 min prechlorination time appeared to form slightly more TOCl compared to the 5 and 60 min prechlorination times (Fig. 2). However, there is no statistical significance as a function of prechlorination time (p =0.245–0.814) and pH (p =0.537–0.974). It is very noticeable that significantly more TOCl formed in the BSW compared to CSW, which would be attributed to the relatively higher humic/fulvic concentrations in the BSW (Ackerson et al., 2018; Parsons et al., 2004; Hua and Reckhow, 2007a). However, TOCl concentration decreased at the end of chloramination relative to TOCl concentration formed at the end of prechlorination. The reduction in TOCl formation was generally statistically significant in BSW (p <0.05) as a function of prechlorination time and pH, but no statistical significance was observed in CSW. Relative to the amount of TOCl formed during prechlorination, the concentration of TOCl formed in BSW during chloramination decreased by 34%-67%, 37%-68%, and 32%-52% for samples exposed to aqueous chlorine for 5, 30, and 60 min, respectively. In CSW, TOCl formation after

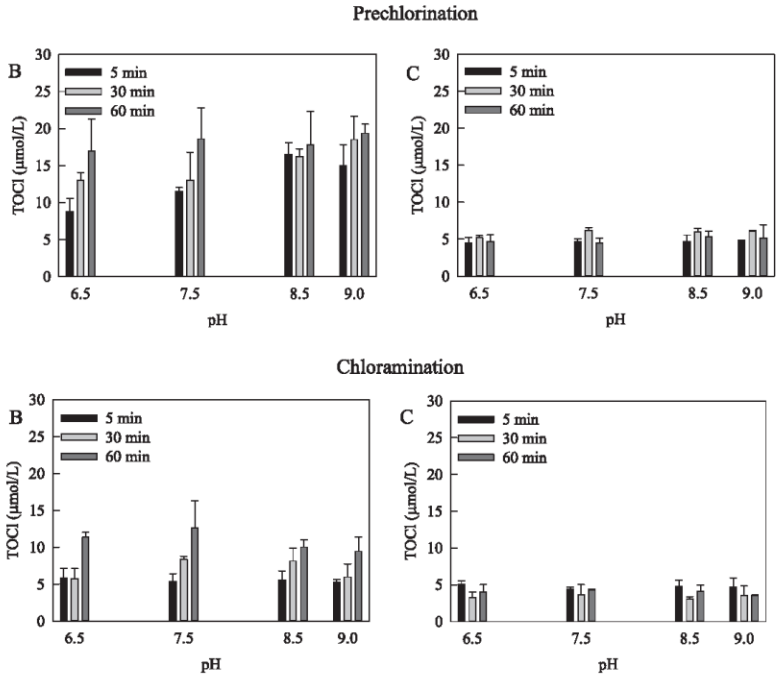

Fig. 2 – Formation of TOCl in Barberton (B) and Cleveland (C) source waters during prechlorination and chloramination as a function of pH and prechlorination time. [Iopamidol] = 5 μmol/L, [HOCl] = 100 μmol/L, [NH4Cl] = 143 μmol/L, [Buffer]T = 4 mmol/L, Temp = 25 °C, DOCBarberton = 4.47 mg/L-C, DOCCleveland = 2.51 mg/L-C. Error bars represent 95% confidence interval for two replicates. Legend represents prechlorination time.

chloramination was approximately 4 μmol/L regardless of chlorine contact time and pH.

Generally, concentration of TOCl formed in CSW during prechlorination decreased at chloramination except at 5 min prechlorination when a marginal increase of less than 15% was observed at pH 6.5 and 8.5. However, it was more significant in BSW due to the higher concentration of reactive hydrophobic acids (Hua and Reckhow, 2007a). The authors observed that water containing higher amount of hydrophobic acids (fulvic and humic regions) (Appendix A Table S2) produced more DBPs. Also, formation of TOCl during chloramination only in BSW increased with increasing aqueous chlorine contact times at all pH. The increase (55%) was statistically significant (p =0.038) at pH 7.5 as chlorine contact time increased from 5 to 30 min. Also, the increase during chloramination for chlorine contact time from 30 to 60 min was statistically significant (p =0.015) at pH 6.5 in BSW. No pH trends were observed for either SW in the degradation of TOCl.

TOCl degradation after ammonia addition relative to prechlorination could be attributed to the formation of organic chloramines during prechlorination and subsequent degradation upon ammonia addition. Both BSW and CSW contain relatively high concentrations of aromatic protein-like (region II) and soluble microbial substances (region IV) (Ackerson et al., 2018). Chen et al. (2003) linked these regions to tryptophan-like, tyrosine-like, and protein-like components; which may form organic chloramines when these nitrogen-containing compounds react with aqueous chlorine (Lee and Westerhoff, 2009). The authors observed that maximum formation of organic chloramines was produced at 10 min during chlorination of NOM isolates. However, other studies have shown that formation of organic chloramines depends on the type of nitrogenous precursor in the water (How et al., 2017). Once formed, organic chloramines decrease with increasing chlorine exposure time (Lee and Westerhoff, 2009). In addition, the presence of α-hydrogen enhances organic chloramines degradation via dehydrohalogenation (Hui and Debiemme-Chouvy, 2013). Half-life for organic chloramines degradation ranges from 0.1 to 240 hr (How et al., 2016) depending on the precursor. The organic chloramines also contribute to TOCl concentration. Nonetheless, when inorganic chloramines are formed after ammonia addition, degradation of residual organic chloramines were very slow with half-life of 5 days (Lee and Westerhoff, 2009). Yang et al. (2008) suggested that the organic chloramines can potentially decrease or suppress the generation of TOCl and chlorinated DBPs like $CHCl_3$, DCAA, and DCAN. Thus, in the presence of monochloramine, while the residual organic chloramines were slowly degrading, TOCl concentration decreased.

2.2. Formation of DBPs as a function of chlorine contact time

$CHCl_2I$, $CHCl_3$, and TCAA were specifically monitored for pH and contact time-dependence, as iopamidol is a direct precursor in their formation. Both CHI_3 and $CHCl I_2$ were below detection limit. In addition, iodo-HAAs were monitored in the disinfected SWs. $CHCl_2I$ was the only iodo-THM formed at sufficient concentrations (Fig. 3). Regardless of SW or prechlorination time, $CHCl_2I$ did not exhibit any real formation trend as function of pH or prechlorination time with concentrations ranging from 6 to 28 nmol/L. This could be due to the rate limiting step of iopamidol transformation into iodine-containing TPs that participate in chlorine-iodine exchange resulting in the formation of HOI. HOI will then incorporate into the NOM structure yielding iodo-DBPs as the NOM is further oxidized.

Chloramination did not suppress or result in the degradation of $CHCl_2I$, but concentrations increased over the 72-h chloramination period. Regardless of SW, aqueous chlorine contact time, or pH, the amount of $CHCl_2I$ formed after monochloramine exposure was greater than the amount of $CHCl_2I$ formed during prechlorination and decreased as pH increased. In BSW, $CHCl_2I$ increased during chloramination by 1.2–12, 1.4–8, and 1.4–7 times in samples exposed to aqueous chlorine for 5, 30, and 60 min, respectively. In addition, 1.3–10, 1.9–9, and 1.2–5 times increases in $CHCl_2I$ concentrations were observed in CSW samples chlorinated for 5, 30, and 60 min, respectively. Relative to prechlorination, there was significant increase in $CHCl_2I$ formation in BSW and CSW during chloramination at pH 6.5 and 7.5. However, ammonia addition did not significantly affect $CHCl_2I$ formation at pH 8.5 and 9.0. Generally, the highest concentration of $CHCl_2I$ formed during chloramination occurred at 60 min prechlorination time in BSW (except at pH 6.5) and 30 min prechlorination time in CSW. The increased formation of the $CHCl_2I$ during chloramination can be attributed to NH_2Cl being slow at oxidizing HOI to IO_3^-. Thus, HOI, NH_2Cl, and HOCl/OCl^- (from NH_2Cl hydrolysis) were the active oxidants which reacted with NOM to form $CHCl_2I$. Formation of $CHCl_2I$ during chloramination decreased with increasing pH at all aqueous chlorine contact times. While not significant as pH increased, a significant decrease in $CHCl_2I$ concentrations was observed when comparing pH 6.5 and 8.5 for both SWs. The predominance of $CHCl_2I$ in the SWs agrees with the chloramination of fulvic and humic acid isolates dosed with iopamidol (Wang et al., 2014).

When comparing iodo-DBP formation in waters where inorganic iodide was the precursor, higher concentrations of iodo-DBPs were formed with preformed monochloramine. Dosing Pony Lake fulvic acid with inorganic iodide, Allard et al. (2015) detected $CHCl_2I$, $CHClI_2$, and CHI_3 at the end of 24-hr chloramination after initial chlorine contact times of 2–30 min. Also, when humic and fulvic acid isolates were spiked with iodide and iopamidol in separate experiments using monochloramine, $CHCl_2I$, $CHClI_2$, and CHI_3 were formed in the iodide-containing sample whereas only $CHCl_2I$ was observed in significant quantities in the iopamidol-containing samples (Wang et al., 2014). Comparing this study to other studies (Duirk et al., 2011; Jones et al., 2011; Wang et al., 2014; Allard et al., 2015), iodide-containing waters produce more iodo-THMs than waters containing iopamidol during prechlorination before ammonia addition because iodide ions are more easily transformed to HOI by HOCl than iodine atoms from iopamidol. Thus, the iodo-THMs formed during prechlorination/chloramination may depend on the type of iodine species (I^-, HOI, organic iodine) present and the NOM characteristics.

IAA, DIAA, and CIAA were also detected in both SWs only during chloramination (Appendix A Fig. S1). During

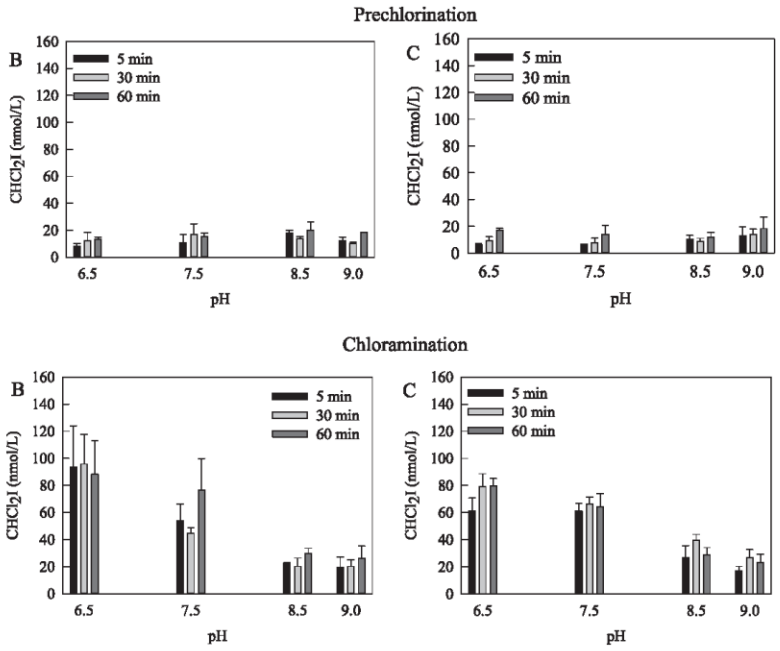

Fig. 3 – Formation of CHCl2I in Barberton (B) and Cleveland (C) source waters during prechlorination and chloramination as a function of pH and prechlorination time. [Iopamidol] = 5 μmol/L, [HOCl] = 100 μmol/L, [NH4Cl] = 143 μmol/L, [Buffer]T = 4 mmol/L, Temp = 25 °C, DOCBarberton = 4.47 mg/L-C, DOCCleveland = 2.51 mg/L-C. Error bars represent 95% confidence interval for triplicate samples. Legend represents prechlorination time.

prechlorination, all iodo-acids were either below the limit of detection or limit of quantification. The concentrations of the iodo-acids were higher in CSW than BSW, with highest concentrations formed at pH 6.5 and 7.5 during the 5-min chlorine contact time. Other studies have also reported greater iodo-acid formation in chloraminated waters with short (or no) free chlorine contact times (Richardson et al., 2008). At higher pH, the concentration of iodo-acids in CSW was below 3 nmol/L. Finally, the concentrations of each iodo-acid formed in BSW was less than 5 nmol/L.

Chloroform ($CHCl_3$) formation was determined after 5–60 min aqueous chlorine contact times and compared to 72-hr chloramination concentrations (Fig. 4). While chloroform formation was rapid, it did not exhibit any statistically significant formation with respect to prechlorination time and pH ($p > .05$) except at pH 9.0 in BSW. Generally, $CHCl_3$ formation during prechlorination increased with chlorine contact time at each pH. Marginal increases were observed when chlorine contact time increased from 5 to 30 min at all pH, but substantial increase was recorded at chlorine contact time from 30 to 60 min at pH 9.0. From chlorine contact time of 5 to 30 min in BSW, the minimum increase in $CHCl_3$ formation was 7.1% at pH 7.5 while the maximum increase was 22.4% at pH 6.5 during prechlorination. Also, the minimum increase in $CHCl_3$ concentration from 30 to 60 min prechlorination time occurred at pH 8.5 (1.3%) whereas the maximum increase occurred at pH 9.0 (50%) during prechlorination. In CSW, the minimum and maximum increase in $CHCl_3$ formation from chlorine contact time of 5 to 60 min occurred at pH 9.0 (6.6%) and 6.5 (51%), respectively.

The addition of ammonia effectively stopped $CHCl_3$ formation with only minor increases observed in BSW. In addition, significantly more $CHCl_3$ formed in BSW than CSW because of the relatively higher $SUVA_{254}$ and, humic and fulvic concentrations in BSW. Comparatively, higher concentrations of $CHCl_3$ (8–35 times) were formed in this study than previous study that used preformed monochloramine in the same SWs containing the same quantity of iopamidol (Ackerson et al., 2018). Also, higher quantities of $CHCl_3$ were formed in chlorinated BSW (2–6 times) and CSW (1.5–4 times) containing 5 μmol/L iopamidol (Ackerson et al., 2018) than the concentration of $CHCl_3$ formed during 72 hr of chloramination in this study.

TCAA formation was rapid and observed to be more substantial in the BSW than CSW at the longest prechlorination time (Fig. 5). Formation of TCAA in BSW at each chlorine contact time decreased with increasing pH

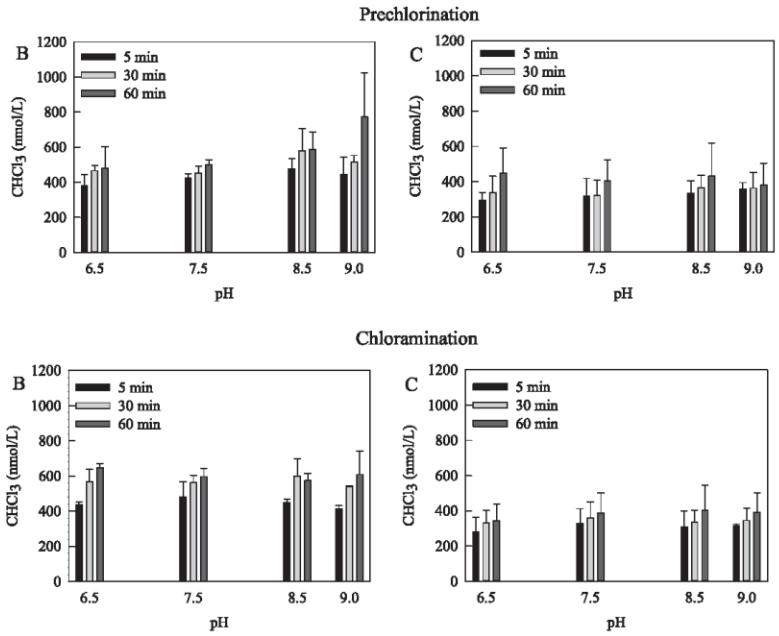

Fig. 4 – Formation of CHCl3 in Barberton (B) and Cleveland (C) source waters during prechlorination and chloramination as a function of pH and prechlorination time. [Iopamidol] = 5 μmol/L, [Cl2]T = 100 μmol/L, [NH4Cl] = 143 μmol/L, [Buffer]T = 4 mmol/L, Temp = 25 °C, DOCBarberton = 4.47 mg/L-C, DOCCleveland = 2.51 mg/L-C. Error bars represent 95% confidence interval for triplicate samples. Legend represents prechlorination time.

except at 30 min when approximately equal concentration was formed at pH 8.5 and 9.0. However, no discernible pH trends were found at each chlorine contact time in CSW. The concentration of TCAA formed in CSW during prechlorination increased with chlorine contact time at each pH except at pH 6.5 where substantial concentration was observed at 30 min. The addition of ammonia ceased TCAA formation in BSW. Generally, TCAA formation increased in CSW after chloramination, though the increases were found not to be statistically significant except at chlorine contact time of 60 min at pH 6.5 (p =0.040). TCAA formation during both prechlorination and chloramination increased with chlorine contact time. TCAA formation during chloramination decreased with increasing pH for BSW (15%-65%) and CSW (1%-30%) at each chlorine contact time and, appeared to be more significant at the 30–60 min prechlorination time from pH 6.5 to 9.0. The formation of TCAA in BSW and CSW showed different pattern because of the differences in the concentrations of $SUVA_{254}$ and NOM characteristics. The study by Hua and Reckhow (2007a) observed different trihaloacetic acid formation in three different SWs. The concentrations of TCAA formed in this study were about 8–33 times more than the amount detected in BSW and CSW containing iopamidol and preformed monochloramine (Ackerson et al., 2018).

2.3. DBP proportions in TOX

The percentage of each class of DBP was determined by multiplying the concentration of the DBP by the number of atoms of the specific halogen, and the product normalized to the halogen-specific TOX. A similar procedure was used previously (Ackerson et al., 2018). TOI included concentrations of chloro-iodo-THMs, iodo-HAAs (both IAA and DIAA), chloro-iodo-HAAs, and unknown TOI (UTOI). In both SWs, regardless of the prechlorination time, the percentage of known DBPs relative to TOI at the end of chlorination and chloramination was <1%. Generally, the percentages of chloro-iodo-THMs, iodo-HAAs, and chloro-iodo-HAA were higher in chloramination than chlorination, since over time HOI was able to react with NOM due to increased HOI stability in the presence of monochloramine than aqueous chlorine. Further, the fraction of chloro-iodo-THMs did not show any discernible trend with prechlorination time during prechlorination and chloramination in BSW and CSW (Appendix A Table S3). Similarly, the fractions of iodo-HAAs and chloro-iodo-HAA did not exhibit any observed trends with respect to pH or chlorine contact time during chloramination (Appendix A Table S4). The high proportions of UTOI (>99%) is predominantly attributed to iopamidol TPs produced in the aqueous system.

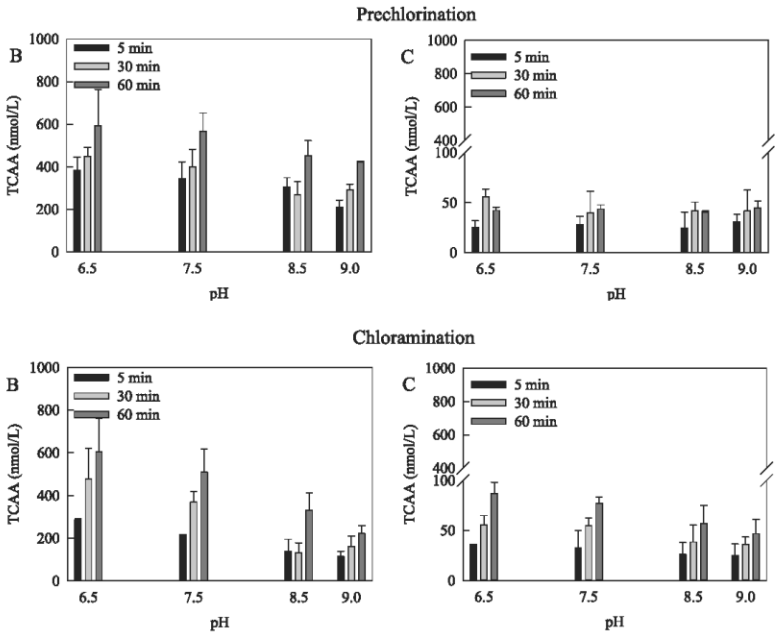

Fig. 5 – Formation of TCAA in Barberton (B) and Cleveland (C) source waters during prechlorination and chloramination as a function of pH and prechlorination time. [Iopamidol] = 5 μmol/L, [Cl2]T = 100 μmol/L, [NH4Cl] = 143 μmol/L, [Buffer]T = 4 mmol/L, Temp = 25 °C, DOCBarberton = 4.47 mg/L-C, DOCCleveland = 2.51 mg/L-C. Error bars represent 95% confidence interval for triplicate samples. Legend represents prechlorination time.

Generally, all the choro-DBPs formed were found to contribute significantly to the fractions of identifiable TOCl especially at the end of chloramination, except chloro-iodo-HAAs, which were present at low concentrations. The fractions of TOCl detected in the SWs during prechlorination and chloramination did not exhibit consistent trends regardless of pH or chlorine contact time. During prechlorination, the highest fraction of known DBPs in BSW (6%–13%) and CSW (13%–21%) was chloro-THM (Appendix A Table S5). Also, the fraction of chloro-HAA during prechlorination was between 3%-13% in BSW and 1%-5% in CSW. Therefore, on the average, the fully chlorinated DBPs contributed to 20% of TOCl concentration. This means greater than 70% of TOCl are other iopamidol DBPs and unknown DBPs formed from chlorination of NOM. During chloramination, the fractions of chloro-THM, chloro-HAA, and chloro-iodo-THMs increased while the fractions of unknown TOCl (UTOCl) generally decreased in both SWs (Appendix A Table S6) since $CHCl_3$ and TCAA ceased after ammonia addition, leading to a decrease in UTOCl. Thus, it could be inferred that the decrease in TOCl formation was due to the possible degradation of unknown chloro-DBPs. The fractions of chloro-THM increased to 14%-38% in BSW and 14%-35% in CSW while the fraction of chloro-HAA increased to 4%-28% in BSW and 2%-9% in CSW. The fractions of UTOCl during chloramination was in the range of 52%-75% in BSW and 54%-81% in CSW. UTOCl formed the predominant fraction of TOCl in the SWs during both prechlorination and chloramination. Nevertheless, the fractions of UTOCl formed in the SWs were less than UTOI. Similarly, higher concentrations of UTOI were generally formed in the SWs than UTOCl.

3. Conclusion

Regardless of chlorine contact time, TOI concentrations were not affected by either prechlorination and chloramination. On the contrary, higher concentrations of TOCl were formed during prechlorination than during chloramination. In BSW, TOCl formation generally increased with chlorine contact time during prechlorination but the increase was not statistically significant (p >0.05). The concentrations of TOCl generally decreased after chloramination. The formation of iodo-THMs increased during chloramination compared to prechlorination for both SWs. However, iodo-HAAs were not formed during prechlorination but were detected after the 72-hr chloramination period. The concentrations for both iodo-THMs and iodo-HAAs decreased as pH increased from 6.5–9.0.

$CHCl_3$ and TCAA concentrations in the SWs increased with chlorine contact time; however, formation of both chloro-DBP classes stopped after ammonia addition in the chlorinated SWs. Finally, water utilities practicing prechlorination may want to consider prechlorination for shorter time to achieve minimal DBP formation.

Acknowledgements

This study was supported by the National Science Foundation (NSF, project numbers NSF1124865 and NSF1124844) and the German Research Foundation (Deutsche Forschungsgemeinschaft, DFG, project number TE 533/4-1).

Appendix A. Supplementary data

Supplementary data to this article can be found online at https://doi.org/10.1016/j.jes.2018.09.022.

REFERENCES

Ackerson, N.O.B., Machek, E.J., Killinger, A.H., Crafton, E.A., Kumkum, P., Liberatore, H.K., et al., 2018. Formation of DBPs and halogen-specific TOX in the presence of iopamidol and chlorinated oxidants. Chemosphere https://doi.org/10.1016/j.chemosphere.2018.03.102.

Allard, S., Tan, J., Joll, C.A., von Gunten, U., 2015. Mechanistic study on the formation of Cl-/Br-/I-trihalomethanes during chlorination/chloramination combined with a theoretical cytotoxicity evaluation. Environ. Sci. Technol. 49, 11105–11114.

APHA, AWWA, WEF, 2005. Standard Methods for the Examination of Water and Wastewater. 20 ed. American Public Health Association, Washington, DC.

Bichsel, Y., von Gunten, U., 1999. Oxidation of iodide and hypoiodous acid in the disinfection of natural waters. Environ. Sci. Technol. 33, 4040–4045.

Bichsel, Y., von Gunten, U., 2000a. Formation of iodo-trihalomethanes during disinfection and oxidation of iodide containing waters. Environ. Sci. Technol. 34, 2784–2791.

Bichsel, Y., von Gunten, U., 2000b. Hypoiodous acid: Kinetics of the buffer-catalyzed disproportionation. Water Res. 34, 3197–3203.

Bougeard, C.M., Goslan, E.H., Jefferson, B., Parsons, S.A., 2010. Comparison of the disinfection by-product formation potential of treated waters exposed to chlorine and monochloramine. Water Res. 44 (3), 729–740. https://doi.org/10.1016/j.watres.2009.10.008.

Bull, R.J., Birnbaum, L.S., Cantor, K.P., Rose, J.B., Butterworth, B.E., Pegram, R., et al., 1995. Water chlorination: Essential process or cancer hazard? Fundam. Appl. Toxicol. 28, 155–166.

Chen, W.H., Young, T.M., 2008. NDMA formation during chlorination and chloramination of aqueous diuron solutions. Environ. Sci. Technol. 42, 1072–1077.

Chen, W., Westerhoff, P., Leenheer, J.A., Booksh, K., 2003. Fluorescence excitation-emission matrix regional integration to quantify spectra for dissolved organic matter. Environ. Sci. Technol. 37, 5701–5710.

Choi, J., Valentine, R.L., 2002. Formation of N-nitrosodimethylamine (NDMA) from reaction of monochloramine: A new disinfection by-product. Water Res. 36, 817–824.

Chuang, Y.-H., McCurry, D.L., Tung, H.-H., Mitch, W.A., 2015. Formation pathways and trade-offs between haloacetamides and haloacetaldehydes during combined chlorination and chloramination of lignin phenols and natural waters. Environ. Sci. Technol. 49, 14432–14440.

Duirk, S.E., Lindell, C., Cornelison, C.C., Kormos, J., Temes, T.A., Attene-Ramos, M., et al., 2011. Formation of toxic iodinated disinfection by-products from compounds used in medical imaging. Environ. Sci. Technol. 45, 6845–6854.

How, Z.T., Linge, K.L., Busetti, F., Joll, C.A., 2016. Organic chloramines in drinking water: An assessment of formation, stability, reactivity and risk. Water Res. 93, 65–73.

How, Z.T., Kristiana, I., Busetti, F., Linge, K.L., Joll, C.A., 2017. Organic chloramines in chlorine-based disinfected watersystems: A critical review. Journal of Environmental Sciences 58, 2–18.

Hua, G., Reckhow, D.A., 2007a. Characterization of disinfection byproduct precursors based on hydrophobicity and molecular size. Environ. Sci. Technol. 41, 3309–3315.

Hua, G., Reckhow, D.A., 2007b. Comparison of disinfection byproduct formation from chlorine and alternative disinfectants. Water Research 41, 1667–1678.

Huang, H., Wu, Q.-Y., Hu, H.-Y., Mitch, W.A., 2012. Dichloroacetonitrile and dichloroacetamide can form independently during chlorination and chloramination of drinking waters, model organic matters, and wastewater effluents. Environ. Sci. Technol. 46, 10624–10631.

Hui, F., Debiemme-Chouvy, C., 2013. Antimicrobial N-halamine polymers and coatings: A review of their synthesis, characterization, and applications. Biomacromolecules 14 (3), 585–601.

Jafvert, C.T., Valentine, R.L., 1992. Reaction scheme for the chlorination of ammoniacal water. Environ. Sci. Technol. 26, 577–586.

Jeong, C.H., Postigo, C., Richardson, S.D., Simmons, J.E., Kimura, S.Y., Marinas, B.J., et al., 2015. Occurrence and comparative toxicity of haloacetaldehyde disinfection byproducts in drinking water. Environ. Sci. Technol. 49, 13749–13759.

Jones, D.B., Saglam, A., Triger, A., Song, H., Karanfil, T., 2011. I-THM formation and speciation: preformed monochloramine versus prechlorination followed by ammonia addition. Environ. Sci. Technol. 45, 10429–10437.

Koivusalo, M., Jaakkola, J.J.K., Vartiainen, T., Hakulinen, T., Karjalainen, S., Pukkala, E., et al., 1994. Drinking-water mutagenicity and gastrointestinal and urinary-tract cancers - An ecological study in Finland. Am. J. Public Health 84, 1223–1228.

Krasner, S.W., Weinberg, H.S., Richardson, S.D., Pastor, S.J., Chinn, R., Sclimenti, M.J., et al., 2006. Occurrence of a new generation of disinfection byproducts. Environ. Sci. Technol. 40, 7175–7185.

Lee, W., Westerhoff, P., 2009. Formation of organic chloramines during water disinfection – Chlorination versus chloramination. Water Res. 43, 2233–2239.

Morris, J.C., Isaac, R.A., 1981. A critical review of kinetic and thermodynamic constants for the aqueous chlorine-ammonia system. In: Jolley, R.L., Brungs, W.A., Cotruvo, J.A., et al. (Eds.), Water Chlorination: Environmental Impact and Health Effects. Ann Arbor Science, Ann Arbor, MI, pp. 49–62.

Morris, R.D., Audet, A.M., Angelillo, I.F., Chalmers, T.C., Mosteller, F., 1992. Chlorination, chlorination by-products, and cancer - A metaanalysis. Am. J. Public Health 82, 955–963.

Nieuwenhuijsen, M.J., Toledano, M.B., Eaton, N.E., Fawell, J., Elliott, P., 2000. Chlorination disinfection byproducts in water and their association with adverse reproductive outcomes: a review. Occup. Environ. Med. 57, 73–85.

Parsons, S.A., Jefferson, B., Goslan, E.H., Jarvis, P.R., Fearing, D.A., 2004. Natural organic matter – The relationship between

character and treatability. Water Sci. Technol.: Water Supply 4, 43–48.
Plewa, M.J., Wagner, E.D., Richardson, S.D., Thruston, A.D., Woo, Y. T., McKague, A.B., 2004. Chemical and biological characterization of newly discovered iodoacid drinking water disinfection byproducts. Environ. Sci. Technol. 38, 4713–4722.
Plewa, M.J., Muellner, M.G., Richardson, S.D., Fasanot, F., Buettner, K.M., Woo, Y.-T., et al., 2008. Occurrence, synthesis, and mammalian cell cytotoxicity and genotoxicity of haloacetamides: An emerging class of nitrogenous drinking water disinfection byproducts. Environ. Sci. Technol. 42, 955–961.
Plewa, M.J., Simmons, J.E., Richardson, S.D., Wagner, E.D., 2010. Mammalian cell cytotoxicity and genotoxicity of the haloacetic acids, a major class of drinking water disinfection by-products. Environ. Mol. Mutagen. 51, 871–878.
Postigo, C., Richardson, S.D., Barcelo, D., 2017. Formation of iodo-trihalomethanes, iodo-haloacetic acids, and haloacetaldehydes during chlorination and chloramination of iodine containing waters in laboratory controlled reactions. J. Environ. Sci. 58, 127–134.
Regli, S., Chen, J., Messner, M., Elovitz, M.S., Letkiewicz, F.J., Pegram, R.A., et al., 2015. Estimating potential increased bladder cancer risk due to increased bromide concentrations in sources of disinfected drinking waters. Environ. Sci. Technol. 49, 13094–13102.
Richardson, S.D., Plewa, M.J., Wagner, E.D., Schoeny, R., DeMarini, D.M., 2007. Occurrence, genotoxicity, and carcinogenicity of regulated and emerging disinfection by-products in drinking water: A review and roadmap for research. Mutat. Res.-Rev. Mutat. Res. 636, 178–242.
Richardson, S.D., Fasano, F., Ellington, J.J., Crumley, F.G., Buettner, K.M., Evans, J.J., et al., 2008. Occurrence and mammalian cell toxicity of iodinated disinfection byproducts in drinking water. Environ. Sci. Technol. 42, 8330–8338.
Shah, A.D., Mitch, W.A., 2012. Halonitroalkanes, halonitriles, haloamides, and n-nitrosamines: A critical review of nitrogenous disinfection byproduct formation pathways. Environ. Sci. Technol. 46, 119–131.
Shen, R.Q., Andrews, S.A., 2013. NDMA formation from amine-based pharmaceuticals – Impact from prechlorination and water matrix. Water Res. 47, 2446–2457.
Tian, F.-X., Xu, B., Lin, Y.-L., Hu, C.-Y., Zhang, T.-Y., Gao, N.-Y., 2014. Photodegradation kinetics of iopamidol by UV irradiation and enhanced formation of iodinated disinfection by-products in sequential oxidation processes. Water Res. 58, 198–208.
Vikesland, P.J., Ozekin, K., Valentine, R.L., 2001. Monochloramine decay in model and distribution system waters. Water Res. 35 (7), 1766–1776.
Villanueva, C.M., Cantor, K.P., Cordier, S., Jaakkola, J.J.K., King, W. D., Lynch, C.F., et al., 2004. Disinfection byproducts and bladder cancer - A pooled analysis. Epidemiology 15, 357–367.
Waller, K., Swan, S.H., Windham, S.C., Fenster, L., 2001. Influence of exposure assessment methods on risk estimates in an epidemiologic study of total trihalomethane exposure and spontaneous abortion. J. Exp. Anal. Environ. Epidemiol. 11, 522–531.
Wang, Z., Xu, B., Lin, Y.-L., Hu, C.-Y., Tian, F.-X., Zhang, T.-Y., et al., 2014. A comparison of iodinated trihalomethane formation from iodide and iopamidol in the presence of organic precursors during monochloramination. Chem. Eng. J. 257, 292–298.
Wendel, F.M., Eversloh, C.L., Machek, E.J., Duirk, S.E., Plewa, M.J., Richardson, S.D., et al., 2014. Transformation of Iopamidol during chlorination. Environ. Sci. Technol. 48, 12689–12697.
Wendel, F.M., Temes, T.A., Richardson, S.D., Duirk, S.E., Pals, J.A., Wagner, E.D., Plewa, M.J., 2016. Comparative Toxicity of High-Molecular Weight Iopamidol Disinfection Byproducts. Environmental Science & Technology Letters 3, 81–84.
Yang, X., Shang, C., Westerhoff, P., 2007. Factors affecting formation of haloacetonitriles, haloketones, chloropicrin and cyanogen halides during chloramination. Water Res. 41 (6), 1193–1200.
Yang, X., Shang, C., Lee, W., Westerhoff, P., Fan, C.H., 2008. Correlations between organic matter properties and DBP formation during chloramination. Water Res. 42, 2329–2339.
Ye, T., Xu, B., Wang, Z., Zhang, T.-Y., Hu, C.-Y., Lin, L., et al., 2014. Comparison of iodinated trihalomethanes formation during aqueous chlor(am)ination of different iodinated X-ray contrast media compounds in the presence of natural organic matter. Water Res. 66, 390–398.

Chemosphere 202 (2018) 349–357

Contents lists available at ScienceDirect

Chemosphere

journal homepage: www.elsevier.com/locate/chemosphere

Formation of DBPs and halogen-specific TOX in the presence of iopamidol and chlorinated oxidants

Nana Osei B. Ackerson [a], Edward J. Machek [a], Alexis H. Killinger [a], Elizabeth A. Crafton [a], Pushpita Kumkum [a], Hannah K. Liberatore [b], Michael J. Plewa [c], Susan D. Richardson [b], Thomas A. Ternes [d], Stephen E. Duirk [a, *]

[a] Department of Civil Engineering, University of Akron, Akron, OH 44325, United States
[b] Department of Chemistry and Biochemistry, University of South Carolina, 631 Sumter St., Columbia, SC 29208, United States
[c] Department of Crop Sciences and Safe Global Water Institute and NSF Science and Technology Center of Advanced Materials for the Purification of Water with Systems, University of Illinois at Urbana-Champaign, 1101 West Peabody Drive, Urbana, IL 61801, United States
[d] Federal Institute of Hydrology (BfG), Am Mainzer Tor 1, D-56068 Koblenz, Germany

HIGHLIGHTS

- Iopamidol is a direct and indirect precursor in the formation of chloro/iodo-DBPs.
- Dichloroiodomethane formation increased as iopamidol concentration increased.
- Chloroform yields were increased with iopamidol present during chlorination.
- Trichloroacetic acid yields were unchanged or suppressed with iopamidol present.
- Iopamidol substantially increased total organic chloride yield during chlorination.

ARTICLE INFO

Article history:
Received 26 October 2017
Received in revised form
7 March 2018
Accepted 15 March 2018
Available online 16 March 2018

Handling Editor: W. Mitch

Keywords:
Iopamidol
Aqueous chlorine
Monochloramine
Total organic halogen
Disinfection byproducts
Natural organic matter

ABSTRACT

Iopamidol is a known direct precursor to iodinated and chlorinated DBP formation; however, the influence of iopamidol on both iodo/chloro-DBP formation has yet to be fully investigated. This study investigated the effect of iopamidol on the formation and speciation of halogen-specific total organic halogen (TOX), as well as iodo/chloro-DBPs, in the presence of 3 source waters (SWs) from Northeast Ohio and chlorinated oxidants. Chlorination and chloramination of SWs were carried out at pH 6.5–9.0 and, different iopamidol and dissolved organic carbon (DOC) concentrations. Total organic iodine (TOI) loss was approximately equal (22–35%) regardless of SW. Total organic chlorine (TOCl) increased in all SWs and was substantially higher in the higher $SUVA_{254}$ SWs. Iopamidol was a direct precursor to chloroform ($CHCl_3$), trichloroacetic acid (TCAA), and dichloroiodomethane ($CHCl_2I$) formation. While $CHCl_3$ and TCAA exhibited different formation trends with varying iopamidol concentrations, $CHCl_2I$ increased with increasing iopamidol and DOC concentrations. Low concentrations of iodo-acids were detected without discernible trends. Total trihalomethanes (THMs), total haloacetic acids (HAAs), TOCl, and unknown TOCl (UTOCl) were correlated with fluorescence regional volumes and $SUVA_{254}$. The yields of all these species showed a strong positive correlation with fulvic, humic, and combined humic and fulvic regions, as well as $SUVA_{254}$. Iopamidol was then compared to the 3 SWs with respect to DBP yield. Although the $SUVA_{254}$ of iopamidol was relatively high, it did not produce high yields of THMs and HAAs compared to the 3 SWs. However, chlorination of iopamidol did result in high yields of TOCl and UTOCl.

1. Introduction

Disposal of treated or partially treated wastewater treatment plant (WWTP) effluent into drinking water sources has resulted in the accumulation of micropollutants like pharmaceuticals in the

* Corresponding author.
E-mail address: duirk@uakron.edu (S.E. Duirk).

https://doi.org/10.1016/j.chemosphere.2018.03.102
0045-6535/

aquatic environment. The proliferation of pharmaceuticals in the aquatic environment is due to unprecedented increase in their sales and uses, especially, in the United States. An approximately 62% increase in pharmaceuticals sales was observed in the U.S. from 2000 to 2004 (Khetan and Collins, 2007). In addition, other factors like low or no removal of pharmaceuticals during conventional wastewater treatment, seepage from unlined landfills, as well as leaking sewer lines and septic systems, contribute significantly to the concentrations of pharmaceutical in drinking water sources (Glassmeyer et al., 2005; Wu et al., 2009; Kovalova et al., 2012). Furthermore, Sharma (2008) indicated that unused pharmaceuticals, as well as waste from medical/pharmaceutical facilities, contribute to the increasing concentration of pharmaceuticals in the environment.

Iodinated X-ray contrast media (ICM) are a class of pharmaceuticals with a triiodinated benzene ring and different amide side chains. They are used in the imaging of soft tissues and are administered at a 200-g dose and are metabolically stable. Worldwide, about 12.5% of more than 600 million X-ray examinations conducted annually use ICM (Christiansen, 2005). Due to their relatively high solubility, some ICM are almost totally excreted through urine and feces within 24 h of being administered (Christiansen, 2005; Perez and Barcelo, 2007). Due to their chemical properties, ICM are recalcitrant to conventional wastewater treatment and are one of the most frequently detected pharmaceuticals in wastewater effluents, lakes, rivers, creeks, and other water sources (Ternes and Hirsch, 2000; Seitz et al., 2006; Ternes et al., 2007). Diatrizoate, iohexol, iomeprol, iopamidol, and iopromide were the 5 most detected ICM in drinking water sources at 10 drinking water treatment plants in U.S., with iopamidol being the predominant ICM (Duirk et al., 2011). ICM have been detected in wastewater and drinking water sources in concentrations up to 2600 μg/L and 2700 ng/L respectively (Duirk et al., 2011; Kovalova et al., 2012). When wastewater from medical facilities was treated with powdered activated carbon, the concentration of iopamidol in the effluent was 900 μg/L (McArdell et al., 2010).

To eliminate/minimize ICM and other micropollutants in source waters, different treatment methods have been investigated, which have resulted in complete removal or degradation to form transformation products (TPs) or disinfection by-products (DBPs) (Wendel et al., 2014). Nineteen DBPs (i.e. TPs) were formed when deionized water spiked with iopamidol was dosed with aqueous chlorine. Four of the 19 DBPs were found to exhibit some cytotoxicity but no genotoxicity (Wendel et al., 2014, 2016). Similarly, Matsushita et al. (2015) suggested 3 additional DBPs from chlorination of iopamidol that contributed to the observed mutagenicity. In addition, deiodinated and hydroxylated TPs of iopamidol were detected during ultraviolet (UV) irradiation of water containing iopamidol (Tian et al., 2014). The treatment of iopamidol with Fe(III) oxalate/H_2O_2 under UV irradiation, produced other high molecular weight TPs, as well (Zhao et al., 2014). Also, photodecomposition of iopromide and the subsequent addition of HOCl or NH_2Cl in the presence of NOM formed iodinated DBPs (iodo-DBPs) (Allard et al., 2016). Further, several biotransformation products of iopromide, iohexol, and iopamidol were formed in aerobic soil-water systems (Schulz et al., 2008; Kormos et al., 2010). The DBPs identified under simulated drinking water treatment to date are both low- and high-molecular weight (Duirk et al., 2011; Wendel et al., 2014).

DBPs are formed when disinfectants like chlorine, chloramines, among others react with natural organic matter (NOM), halide ions, ammonia, personal care products, and pharmaceuticals like ICM. Speciation and distribution of regulated and unregulated DBPs are dependent on the pH, oxidant type, and the constituents in the water matrix (Richardson et al., 2007; Krasner, 2009). An occurrence study in the United States and Canada revealed the formation of iodo-DBPs in chloraminated drinking waters that did not contain inorganic iodide (Richardson et al., 2008). Further work has shown that iodinated trihalomethanes (iodo-THMs) and acids (iodo-acids), which are more cytotoxic and genotoxic than their brominated/chlorinated analogues, were formed from ICM when chlorinated in the presence of NOM (Duirk et al., 2011). Recent studies have revealed that iopamidol is the only ICM among the 5 frequently detected ICM that exhibits significant reactivity with aqueous chlorine (Duirk et al., 2011; Wendel et al., 2014; Matsushita et al., 2015). Also, because iopamidol reacts with aqueous chlorine to form significant quantities of iodo-DBPs, iopamidol was the focus of this study.

Since iopamidol is a direct precursor in the formation of dichloroiodomethane ($CHCl_2I$), trichloroacetic acid (TCAA), chloroform ($CHCl_3$), and total organic chlorine (TOCl); the main objective was to investigate the influence of iopamidol on both chlorinated and iodinated DBP formation in the presence of NOM from three different source waters and chlorinated oxidants. Initially, pH was varied to investigate the effect of iopamidol/NOM precursors on DBP formation in the presence of both aqueous chlorine and monochloramine. Then, the concentrations of iopamidol and NOM were varied and DBP formation was monitored as a function of pH and chlorinated oxidant. Finally, DBP yields were then correlated to NOM properties, such as $SUVA_{254}$ and the fluorescence regional volumes of the excitation-emission (EEM) spectra.

2. Materials and methods

2.1. Standards and reagents

Iopamidol was purchased from U.S. Pharmacopeia (Rockville, MD, USA). All DBPs were purchased at the highest possible purities. All other (in)organic chemicals used were certified American Chemical Society (ACS) reagent grade and were used without further purification. Information regarding all standards and reagents used are available in Supporting Information (SI).

Purified water (18.2 MΩ cm $^{-1}$), prepared from a Barnstead ROPure Infinity/NANOPure system (Barnstead-Thermolyne Corp. Dubuque, IA, USA) was used for preparations of aqueous stock solutions, as well as phosphate and borate buffer solutions. Experimental pH was monitored with an Orion 5-star pH meter equipped with Ross ultra-combination electrode (Thermo Fisher Scientific, Pittsburgh, PA); pH adjustments for the experiments were achieved with 1 N H_2SO_4 and 1 N NaOH. Phosphate buffer was used to maintain pH 6.5 and 7.5, while borate was used to maintain pH 8.5 and 9.0. Commercial 10–15% sodium hypochlorite (NaOCl) which contained equimolar amounts of OCl^- and Cl^- was purchased from Sigma Aldrich (St. Louis, MO). This was used to prepare aqueous chlorine solutions monthly. For each experiment, the concentration of aqueous chlorine was verified using ferrous ammonium sulfate (FAS)/N,N′-diphenyl-*p*-phenylenediamine (DPD) titration (APHA et al., 2005). Also, all glassware and polytetrafluoroethylene (PTFE) bottles were soaked in a chlorine bath for 24 h, rinsed with a large amount of purified water and dried before use.

2.2. Source waters

Three source waters from the intake of drinking water treatment plants (WTPs) in Northeast Ohio were used in the experiments. They included Akron source water (ASW) from the Akron WTP (Akron, OH), Barberton source water (BSW) from the Barberton WTP (Barberton, OH), and Cleveland source water (CSW) from the Garret Morgan WTP (Cleveland, OH). The characteristics of

the source waters and the procedures for the source water characterization can be found in SI.

2.3. Monochloramine solution preparation

The preparation of pre-formed monochloramine solution was achieved by mixing 5.64 mM ammonium chloride with 3.7 mM hypochlorous acid to achieve a Cl/N molar ratio of 0.7 in a 4.0 mM borate buffer solution. The solution, under rapidly mixed conditions on a magnetic stir plate using a PTFE stir bar at pH 8.5, was allowed to react and reach equilibrium for 50 min in the dark. The concentration of the pre-formed monochloramine was determined with an ultraviolet (UV) visible spectrophotometer and FAS/DPD titration (APHA et al., 2005). Monochloramine was freshly prepared for each experiment.

2.4. Experimental procedures

Each source water or purified water was dosed with iopamidol (1.0–5.0 μM), buffer solution (1.0 or 4.0 mM), and chlorinated oxidant (100 μM). The 1.0 and 4.0 mM buffer solutions were used for TOX and DBP experiments respectively. The chlorinated oxidant was either aqueous chlorine or monochloramine. Each experiment was carried out between pH 6.5–9.0 and in the presence of 4 mM buffer. Samples were stored in the incubator (25 ± 1 °C) for 0–72 h. More details of the experimental procedures used can be found in the SI.

2.5. Analytical methods

Residual oxidant in TOX and DBP samples were quenched with 120 μM aqueous sulfite solution after each reaction time (i.e. before extraction and analysis). Also, residual oxidant in iodate samples were quenched with 120 μM resorcinol solution following the same protocol. TOX samples were concentrated on activated carbon, combusted, absorbed in phosphate solution, and analyzed on the ion chromatography system (ICS-3000). Iodide and iodate were directly analyzed on the ICS-3000. Samples for DBP analyses were extracted with methyl *tert*-butyl ether (MtBE). Each organic extract was split into two; one for THM and haloacetonitrile (HAN) analyses and the other was derivatized with diazomethane for haloacetic acid (HAA) analyses. THMs, HANs, and non-iodinated HAAs were analyzed on a gas chromatograph (GC) equipped with a micro electron capture detector (ECD). Iodinated HAAs (iodo-HAAs) were analyzed using a GC-triple quadrupole mass spectrometer (GC-MS-MS). Detailed analytical procedures are described in SI.

3. Results and discussion

3.1. Formation of TOX and DBPs in the absence of NOM

The reaction of iopamidol with aqueous chlorine in buffered pure water resulted in the formation of both organic and inorganic products. Total organic iodine (TOI), iodate, and TOCl were detected at the end of 72 h (Fig. S2). This has been previously observed at iopamidol and aqueous chlorine concentrations of 1.29 mM and 25.8 mM respectively (Wendel et al., 2014). TOI concentration at the start of the reaction was high (15 μM). This effect is due to the presence of iopamidol (5.0 μM), which has 3 iodine atoms attached to the benzene ring. Iopamidol and iopamidol TPs contributed to TOI concentrations detected in the samples. The highest and lowest TOI remaining occurred at pH 9.5 and 7.5, respectively. The formation trend is due to the participation of both HOCl and OCl in the reaction with iopamidol and iopamidol TPs. It has been observed that during chlorination of iopamidol, OCl cleaves one of the amide side chains exposing the iopamidol TP to further electrophilic attack (Duirk et al., 2011; Wendel et al., 2014). Chlorine and iodine exchange occurs at the triiodinated benzene moiety (Wendel et al., 2014; Tian et al., 2017), producing hypoiodous acid (HOI), as well as additional iopamidol TPs (i.e., TOI). Oxidation of HOI by aqueous chlorine results in the formation of iodate, with the highest yield produced at pH 7.5. This would suggest that both HOCl and OCl are needed to participate in halogen exchange with the iodine on the benzene ring and oxidize HOI to iodate (Bichsel and von Gunten, 1999; Wendel et al., 2014). The two major iodine species (TOI and iodate) balanced out the iodine mass balance (Fig. S3). The incorporation of aqueous chlorine into iopamidol TPs formed TOCl; the highest formation occurred at pH 7.5. Also, the degradation of iopamidol (in the absence of NOM) produced $CHCl_3$, $CHCl_2I$, and TCAA at the end of 72 h (Fig. S4). $CHCll_2$ was detected but below limit of quantitation. This suggests that under the experimental conditions, iopamidol is a direct precursor to $CHCl_3$ and TCAA formation (i.e., regulated DBPs) as well as $CHCl_2I$ at very low concentrations.

3.2. Formation and speciation of TOX in the presence of NOM

In the presence of aqueous chlorine, iopamidol, and NOM, TOI slowly degraded with time in all source waters. No significant pH dependence was observed (Fig. S5), and TOI loss was about 22–35% in all source waters regardless of pH or source water at the end of 72 h. In the presence of NOM, TOI was simultaneously degrading and forming due to the degradation of iopamidol and high molecular weight DBPs of iopamidol forming HOI. For iopamidol, HOI formation is delayed; that is, the formation of HOI does not take place until the amide side chain is initially cleaved by OCl ($k = 0.94\ M^{-1}s^{-1}$) (Wendel et al., 2014). However, inorganic iodide is rapidly oxidized directly by aqueous chlorine to HOI ($k = 4.3 \times 10^8\ M^{-1}s^{-1}$) (Nagy et al., 1988). HOI reacted with NOM to form both identified and unidentified iodinated products (Duirk et al., 2011; Wendel et al., 2014). Both known and unknown iodo-DBPs, as well as other iopamidol TPs, contributed to the TOI concentration in the source waters. Also, no inorganic iodine species (i.e., iodide, iodate or HOI) were detected. The use of aqueous sulfite solution to quench residual aqueous chlorine would reduce residual HOI to I . Since I was not detected, HOI could not be present in the reaction mixture. Finally, about 3.5 μM of iodine species (initial concentration of ipamidol was 5 μM) could not be accounted for to achieve a complete iodine mass balance. In the absence of NOM, only the iopamidol transformation products were detected. In the presence of NOM, highly soluble iodide containing transformation products could be formed that may have not been adsorbed on the powdered activated carbon used to extract TOX from the aqueous samples.

TOCl formation was also monitored as a function of pH over time. In Fig. S5, the TOCl formed was due to the incorporation of chlorine into NOM and iopamidol TPs. Wendel et al. (2014) observed that in the degradation of iopamidol in deionized water in the presence of aqueous chlorine, deiodination, and chlorine incorporation occurred simultaneously. Approximately equal concentrations of TOCl were formed in reactions with both ASW and BSW, while lower concentrations were detected with CSW. The higher TOCl formation in both ASW and BSW may be due to the relative high percentage of humic and fulvic acid composition in the NOM (Table S1 and Fig. S1).

When monochloramine (100 μM) was the active chlorinated oxidant, TOI loss in all 3 source waters dosed with iopamidol (5.0 μM) was minimal (Fig. S6). In the absence of NOM and similar concentrations of monochloramine and iopamidol, less than 10% loss of TOI was observed (Fig. S7). However, the loss was not

statistically significant. The result is different from earlier studies which did not observe iopamidol degradation in chloraminated purified water because the concentrations of iopamidol (1 μM) and monochloramine (42 μM) were low (Wendel et al., 2014). Tian et al. (2017) detected iopamidol TPs when they dosed purified water with 25 μM iopamidol and 250 μM monochloramine. It has been proposed that aqueous chlorine, a hydrolysis product of NH_2Cl, is the active oxidant participating in the reaction iopamidol (Duirk et al., 2011). Chlorine to nitrogen molar ratio (Cl/N) affects monochloramine hydrolysis, i.e. decrease in monochloramine stability results in a more rapid formation of aqueous chlorine. Duirk et al. (2011) showed that as you increase monochloramine stability through the addition of excess ammonia to a Cl/N ratio of 0.5 or less, iodo-DBP formation was significantly reduced by 60% and continued to decease until no iodo-DBP formation was observed at a Cl/N ratio of 0.025. The preformed monochloramine used in this study had a Cl/N ratio of 0.7, which favors monochloramine hydrolysis. In addition, the concentration of TOCl formed in the chloraminated source waters (Fig. S6) was about four times lower than what was observed in the chlorinated source waters since monochloramine is less reactive than chlorine. The low concentrations of TOCl would be attributed to HOCl reacting with NOM (Duirk and Valentine, 2006).

3.3. DBP formation and speciation

The impact of iopamidol on DBP formation was studied in ASW, BSW, and CSW. Of the DBPs monitored, 10 THMs, 13 HAAs, and 7 HANs (see SI), chlorination of iopamidol-spiked waters was found to abundantly form $CHCl_3$, TCAA, and $CHCl_2I$. Iodo-HAAs; iodoacetic acid (IAA), chloroiodoacetic acid (CIAA), and diiodoacetic acid (DIAA) were formed in chlorinated ASW and BSW but were not consistent in every replicate sample. Iodo-HAAs concentrations increased in ASW from pH 6.5 to 7.5, with similar concentrations at pH 7.5 and 8.5, and a slight decrease in formation at pH 9.0 (Fig. S8). However, in BSW, no discernible pH trend was observed (Fig. S8).

Further studies were conducted to assess the effect of iopamidol as a function of pH, SW, and chlorinated oxidant on the formation of $CHCl_3$, TCAA, and $CHCl_2I$. DBP formation in BSW and CSW was investigated at iopamidol concentrations ranging from 1.0 to 5.0 μM and aqueous chlorine concentration of 100 μM. Fig. 1 shows that $CHCl_2I$ concentrations generally increased with increasing iopamidol concentrations as pH increased from pH 6.5–9.0 in both source waters. However, $CHCl_2I$ was below the detection limit in the CSW when iopamidol concentration was 1.0 μM except at pH 9. Significantly higher concentrations of $CHCl_2I$ were formed (i.e., 7–10 times greater) in the BSW than CSW regardless of iopamidol concentration. This was due to higher concentration of DOC in BSW (4.47 mg/L C), as well as BSW having greater humic and fulvic components (i.e., DBP precursors) than CSW (Table S2). Since iopamidol was observed to form $CHCl_2I$ in pure water, increasing iopamidol levels would have possibly increased HOI formation that incorporated into NOM structure. It was observed that little to no quantities of $CHCll_2$ were formed in the source waters. Furthermore, $CHCl_3$ concentrations were similar at iopamidol concentrations of 1 and 5 μM but were greater at 2.5 μM in BSW (Fig. S9). However, $CHCl_3$ concentration in CSW was not statistically different with increasing iopamidol concentrations at each pH. This could be due to the competitive kinetics in DBP formation between BSW and iopamidol. Iopamidol in a known direct precursor in the formation of known regulated DBPs (Fig. S4). With only 2.5 μM iopamidol present, this could have resulted in an optimal chloroform formation condition where the NOM contributed early and iopamidol later in the experiment. However, kinetic data was not obtained to fully substantiate this hypothesis. Fig. S9 illustrates that there was no statistically significant change in the quantities of TCAA produced in BSW as iopamidol concentrations increased. Nonetheless, an enhanced formation of TCAA was seen at iopamidol concentration of 2.5 μM, while TCAA formation at 1 and 5 μM iopamidol concentrations in CSW were similar with respect to each pH. In the absence of NOM, TCAA formation is highest at pH 7.5 (Fig. S4). This could indicate that more TCAA was formed from the reaction of aqueous chlorine and iopamidol in CSW at pH 7.5. Although some studies have been carried out in the absence of NOM (Wendel et al., 2014; Tian et al., 2017), the mechanism for iopamidol degradation in the presence of aqueous chlorine and NOM is not fully understood and experiments have suggested significantly simpler transformation pathways. Currently, experiments in the presence of NOM are being conducted to elucidate iopamidol transformation products and pathways. As pH increased, TCAA concentrations decreased slightly because TCAA formation is generally an acid-catalyzed process and formation at high pH is suppressed (Hua and Reckhow, 2012).

The effect of DOC concentration on DBP speciation was investigated at iopamidol and aqueous chlorine levels of 5.0 and 100 μM, respectively. The concentration of $CHCl_2I$ generally increased with increasing DOC levels in BSW (Fig. 2). As DOC levels increased, there were more DBP precursors in the NOM structure to react with both chlorine and iodine to form $CHCl_2I$. Thus, dilution of the source water limited the available NOM reaction sites, resulting in the reduced formation of known low molecular weight DBPs. In the CSW, $CHCl_2I$ concentrations were the highest at the lowest DOC concentrations (Fig. 2). This could be due to the less DOC present to react with the aqueous chlorine, allowing for more complete transformation of iopamidol, and yielding more HOI to incorporate in the DBP precursors in the CSW. Increasing DOC levels in BSW corresponded with increasing $CHCl_3$ and TCAA concentrations except at pH 7.5 for TCAA (Fig. S10). In CSW, the quantities of $CHCl_3$ exhibited a marginal increase as DOC concentrations increased except at pH 9.0. Increased TCAA formation in CSW at half DOC concentration (1.26 mg/L-C) was observed; however, lower concentrations were formed at full DOC (2.51 mg/L-C). Since CSW NOM is not very reactive, diluting the DOC would limit reactive NOM sites and enhance the reaction between aqueous chlorine and iopamidol to form TCAA and chloroform. Both iopamidol and NOM in CSW produced $CHCl_3$ and TCAA upon chlorination; therefore, the concentration of each precursor would impact the amount of TCAA formed in CSW.

DBP formation kinetics were measured at 2.5 μM iopamidol and 100 μM aqueous chlorine in each of the three source waters. The Cl/DOC ratios for ASW, BSW, and CSW are 1.27, 1.59, and 2.83 mg Cl/mg C respectively and were within the range of drinking water practice (Reckhow and Singer, 2011). $CHCl_3$ was the most predominant chloro-DBP formed in all source waters (Fig. S11). Formation of $CHCl_3$ was due to the reactions of aqueous chlorine with iopamidol and NOM. The highest $CHCl_3$ levels were formed in BSW (Tables S1 and S2). The chemistry of the DOC (Fig. S1) in the source waters appears to have influenced the kinetics of $CHCl_3$ formation. About 57–67% and 46–55% of $CHCl_3$ concentrations produced at 72 h at each pH was formed at 12 h in both BSW and ASW, respectively (i.e. the quantities of $CHCl_3$ formed at 12 h were normalized to the quantities at 72 h at each pH). However, only 23–44% of $CHCl_3$ quantities formed in CSW at 72 h at each pH was formed at 12 h. In addition, $CHCl_3$ formation in the source waters increased with pH. This is consistent with other studies and can be ascribed to base-catalyzed hydrolysis of other DBPs like TCAA, to form $CHCl_3$ (Hua et al., 2006).

TCAA was detected in all three source waters (Fig. S11). Like $CHCl_3$, TCAA formation was associated with degradation of iopamidol and oxidation of NOM by aqueous chlorine. TCAA formation

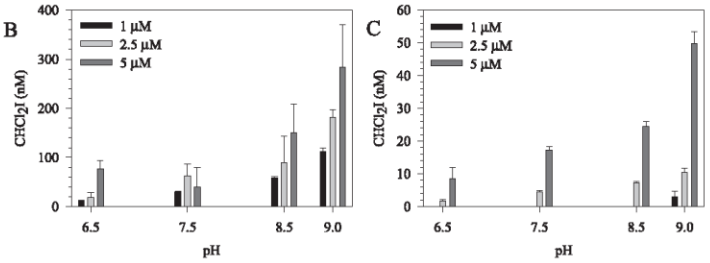

Fig. 1. $CHCl_2I$ formation in Barberton (B) and Cleveland (C) source waters at 72 h as a function of iopamidol concentration and pH. $[Cl_2]_T = 100\ \mu M$, [Iopamidol] = 1.0–5.0 μM, $[Buffer]_T = 4.0$ mM, temperature = 25 °C, $DOC_{Barberton} = 4.47$ mg/L C, $DOC_{Cleveland} = 2.51$ mg/L C. Error bars represent 95% confidence intervals of triplicate samples.

was highest in ASW, then BSW and CSW, in that order. Approximately 53–73% of TCAA concentration formed in ASW and BSW at 72 h at each pH was observed at 12 h, while 38–75% was produced in CSW at 12 h. Generally, TCAA formation was high at lower pH except in the CSW, where TCAA formation was more rapid at pH 7.5. This could be a result of the low DOC concentration (2.51 mg/L-C) in CSW and its less reactivity towards aqueous chlorine. Therefore, it was consistent with iopamidol forming significant concentration of TCAA (approximately 265 nM) in purified water at pH 7.5.

$CHCl_2I$ was consistently detected in all the three chlorinated source waters (Fig. S12). Although approximately the same concentration of $CHCl_2I$ was formed at pH 9.0 in ASW and BSW, higher levels were formed in ASW than BSW at lower pH. Nevertheless, lower levels were detected in CSW. The trend may be attributed to the high volume of reactive fulvic and humic fractions in ASW and BSW NOM. Notwithstanding, the higher concentration of DOC in ASW likely resulted in the higher amounts of $CHCl_2I$ in ASW. Generally, $CHCl_2I$ formation exhibited an initial lag, regardless of NOM type because iopamidol needs to be initially transformed into TPs that yield HOI. Further, $CHCII_2$ was also formed, but less than 3.0 nM was detected in BSW at all levels of pH.

Additionally, all three source waters were spiked with 2.5 μM iopamidol and treated with 100 μM monochloramine. Generally, in chloramination, $CHCl_3$ formation is highest at pH 6.5, with relatively small quantities of HAAs produced (Duirk and Valentine, 2006; Bougeard et al., 2010). It was observed that $CHCl_3$ was the dominant DBP formed in all chloraminated source waters at 72 h (Fig. 3), but in comparison to chlorination, approximately a 40 times lower yield was observed. Low quantities of TCAA were produced and $CHCl_2I$ was the predominant iodo-DBP formed in all chloraminated source waters (Fig. 3). Higher concentrations of $CHCl_2I$ were formed in ASW than BSW. Hua and Reckhow (2007a) noted that more iodo-THMs were formed in chloraminated waters containing hydrophilic and low molecular weight precursors than in waters containing hydrophobic and high molecular weight precursors at pH 7.0.

Monochloramine is less reactive than aqueous chlorine and inherently unstable in the presence or absence of NOM. This process, known as monochloramine autodecomposition, is due to the acid catalyzed reaction of NH_2Cl reacting with itself and the accelerated monochloramine hydrolysis (Jafvert and Valentine, 1992). This process is accelerated near neutral pH and rapidly decreases as pH increases to 8.5 and above. In the presence of NOM, Duirk et al. (2005) reported monochloramine may react directly with NOM or by HOCl due to monochloramine hydrolysis resulting in DBP formation. Therefore, faster autodecomposition of NH_2Cl at lower pH results in greater iodo/chloro-DBP concentrations due to the greater formation of HOCl and less as the pH increases (Fig. 3). Formation of iodo-THMs in chloraminated source waters may be explained by HOI formation, from iopamidol degradation, and stability in the presence of monochloramine (Bichsel and von Gunten, 1999).

3.4. TOX distribution

TOX is made up of both the known halogenated DBPs and unknown DBPs. The unknown TOX (UTOX) is comprised of the unknown iopamidol TPs and other unknown halogenated by-

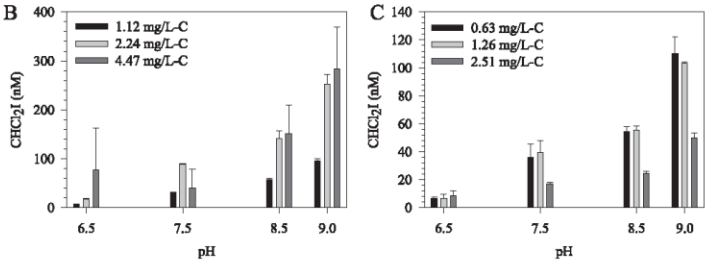

Fig. 2. $CHCl_2I$ formation in Barberton (B) and Cleveland (C) source waters at 72 h as a function of DOC concentration and pH. $[Cl_2]_T = 100\ \mu M$, [Iopamidol] = 5.0 μM, $[Buffer]_T = 4.0$ mM, temperature = 25 °C, $DOC_{Barberton} = 1.12–4.47$ mg/L C, $DOC_{Cleveland} = 0.63–2.51$ mg/L C. Error bars represent 95% confidence intervals of triplicate samples. Source waters were diluted with pure water to achieve the desired DOC concentrations.

products from HOCl/HOI incorporation into the NOM structure. For each halogen-specific TOX, DBPs formed in source water dosed with 5.0 and 100 μM iopamidol and chlorinated oxidants respectively, at 72 h, were normalized to their respective iodinated or chlorinated TOX concentration. TOX distribution was carried out in all three source waters under both chlorinated and chloraminated conditions.

Fig. S13 illustrates the distribution of TOI in chlorinated ASW, BSW, and CSW at 72 h. The TOI fractions included iodo-DBPs (comprises iodo-THMs and iodo-HAAs) and unknown TOI (UTOI). The proportions of iodo-DBPs were higher in BSW (2.6–3.9%) than ASW (2.5–3.2%) at pH 7.5 and 8.5. In CSW, <1% of TOI was iodo-DBPs. As pH increased, all source waters showed an increase in the percentage of TOI associated with iodo-DBPs. This is possibly because of base-catalyzed hydrolysis that increases iodo-THM (the predominant iodo-DBP) formation at higher pH. It was observed that more than 96% of TOI was UTOI. The possible high proportion of UTOI in the source waters would be due to iopamidol TPs, residual iopamidol, and/or unknown iodo-DBPs formed from the incorporation of iodide into the NOM (Hua and Reckhow, 2007a; Wendel et al., 2014; Matsushita et al., 2015). This is currently under investigation since the only known iopamidol transformation product detected was $C_{14}H_{19}I_3O_3N_6$ (DBP 705), which is a result of OCl-nucleophilic attack at the amide functional group in the A-side chain of the iopamidol molecule (Wendel et al., 2014). Work to resolve the iodide mass balance in the presence of NOM is in progress.

Fig. S14 depicts the fractions of chloro-DBPs per TOCl at 72 h in the chlorinated source waters with respect to pH. Unknown TOCl (UTOCl) represented the largest percentage of TOCl in all source waters. Mostly, the highest proportions of known chloro-THMs (i.e., $CHCl_3$ and $CHCl_2I$) were identified in BSW except at pH 6.5. This could be due to the more reactive moieties in the NOM structure in BSW. About 24–35%, 27–30%, and 12–22% of TOCl was detected as chloro-THM in BSW, ASW, and CSW, respectively. In general, the proportion of TOCl associated with HAAs (i.e., TCAA, ClAA, and dichloroacetic acid (DCAA)) in the three source waters accounted for <10% except at pH 6.5 in BSW. Other studies have also observed that more THMs were formed in chlorinated raw water samples than HAAs (Hua and Reckhow, 2012).

ASW, BSW, and CSW dosed with 5.0 μM iopamidol and 100 μM pre-formed monochloramine showed different fractions of TOX. In general, less than 1% of TOI produced in all source waters at all pH levels could be attributed to iodo-DBPs (Fig. S15). Monochloramine is known to form higher levels of iodo-DBPs in the presence of iodide as compared to aqueous chlorine (Bichsel and von Gunten, 2000; Hua and Reckhow, 2007b). However, because iopamidol goes through a slow transformation, lower quantities of iodo-DBPs but higher amount of TOI (Fig. S6) were observed due to iodide containing iopamidol TPs. In Fig. S16, UTOCl proportions in TOCl for the chloraminated source waters were >95%. Chloro-THMs, the highest identified known class of DBPs, accounted for 0.3–4.3% of TOCl in the source waters. HAAs were mainly <1% in both ASW and BSW but were rarely detected in CSW, as previously observed (Hua and Reckhow, 2007b). Due to monochloramine being a weaker oxidant, the slow degradation of iopamidol and TPs resulted in lower iodo-DBP formation.

3.5. DBP correlation with EEM regional volumes and SUVA

The amount of each class of DBPs formed in the three source waters containing iopamidol and aqueous chlorine concentrations

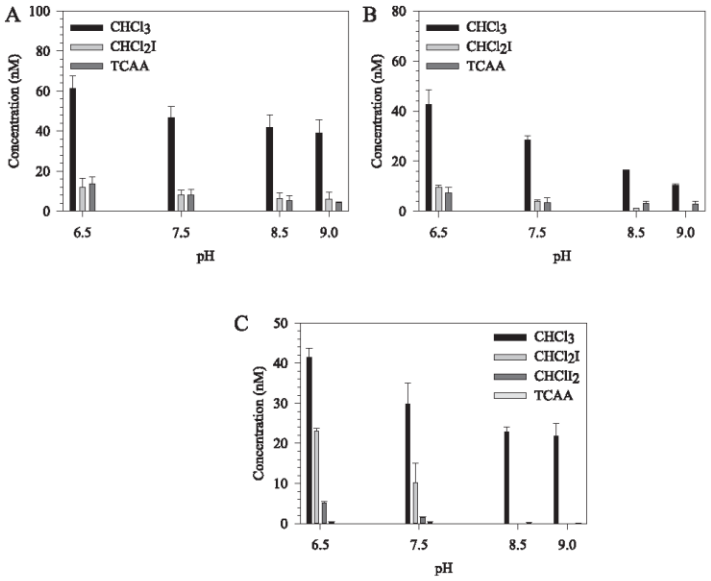

Fig. 3. Formation of DBPs in chloraminated source waters from Northeast Ohio as a function of pH. $[NH_2Cl]_T = 100\ \mu M$, [Iopamidol] = 2.5 μM, Reaction time = 72 h, $[Buffer]_T = 4.0$ mM, temperature = 25 °C, $DOC_{Akron} = 5.57$ mg/L C, $DOC_{Barberton} = 4.47$ mg/L C, $DOC_{Cleveland} = 2.51$ mg/L C. Error bars represent 95% confidence intervals of triplicate samples. (A) – Akron, (B) – Barberton, (C) – Cleveland source waters.

of 5.0 and 100 μM, respectively, at pH 7.5 were normalized to the DOC of the source waters to represent the respective DBP yields. The yields of total THMs (TTHMs), total HAAs (HAAs), TOCl, and UTOCl were correlated with their initial NOM fluorescence regional volumes (FRV) (Table S2 and Fig. S1), as well as $SUVA_{254}$ of only the SW or only iopamidol. The $SUVA_{254}$ of each precursor (i.e. NOM in SW and iopamidol) was used separately to reflect the influence of each precursor on DBP formation. Also, the sum of fulvic and humic regional volumes, designated as combined fulvic and humic, were included because the two fractions predominantly form the hydrophobic reactive portion of NOM precursor (Leenheer and Croue, 2003). In these analyses, TTHMs included $CHCl_3$, $CHCl_2I$, and $CHClI_2$, while HAAs were predominately comprised of TCAA and DCAA, and did not include IAA. Using a linear regression analysis, the yield of each class of DBP formed in the source waters was then correlated with each FRV. TTHM yields ($Yield_{TTHM}$) showed a strong positive correlation ($R^2 = 0.86–0.92$) with fulvic, humic, and combined fulvic and humic fraction (Fig. 4). Similarly, a strong positive correlation ($R^2 = 0.94–0.98$) was found between HAA yields ($Yield_{HAA}$) and fulvic, humic, and combined humic and fulvic fractions (Fig. 4). Further, TOCl ($R^2 = 0.97–0.99$) and UTOCl ($R^2 = 0.99$) exhibited strong correlations with fulvic, humic and combined fuvic and humic fractions (Fig. 4). The higher correlations between TOCl/UTOCl and FRV show that under the experimental conditions, fulvic and humic precursors predominantly contributed to TOCl and UTOCl formation. Nevertheless, iodo-THMs did not correlate, due to the delayed release and formation of HOI from the transformation of iopamidol.

Fulvic and humic acids contain aromatic carbon, phenolic structures, and conjugated double bonds that are highly reactive with chlorinated oxidants (Leenheer, 2004). During chlorination, the fulvic and humic fractions have been found to be the primary DBP precursors forming THMs and HAAs (Liang and Singer, 2003). Therefore, the fulvic and humic fractions in the source waters could be the principal precursors to form the known DBPs, as well as TOCl and UTOCl formation. Also, because iopamidol is a precursor to $CHCl_3$, TCAA, TOCl, and UTOCl formation, iopamidol may have augmented the formation of the species. Thus, two precursors – iopamidol and NOM fractions, could have enhanced the correlations observed in Fig. 4. The higher molecular weight of humic acids (Thurman, 1985) could have contributed to humic fractions exhibiting higher correlation (R^2 values) with TTHMs/HAAs/TOCl/UTOCl than fulvic fractions.

To further assess the impact of iopamidol on DBP formation, DBP yields were correlated to $SUVA_{254}$ of the three source waters with and without iopamidol present, as well as to the $SUVA_{254}$ of iopamidol. Under the experimental conditions, it was observed that the yields of TTHMs were higher in source waters containing iopamidol than source waters without iopamidol (Fig. 5). From the slopes of the two regression lines (slope = 0.0008), they are parallel, but the

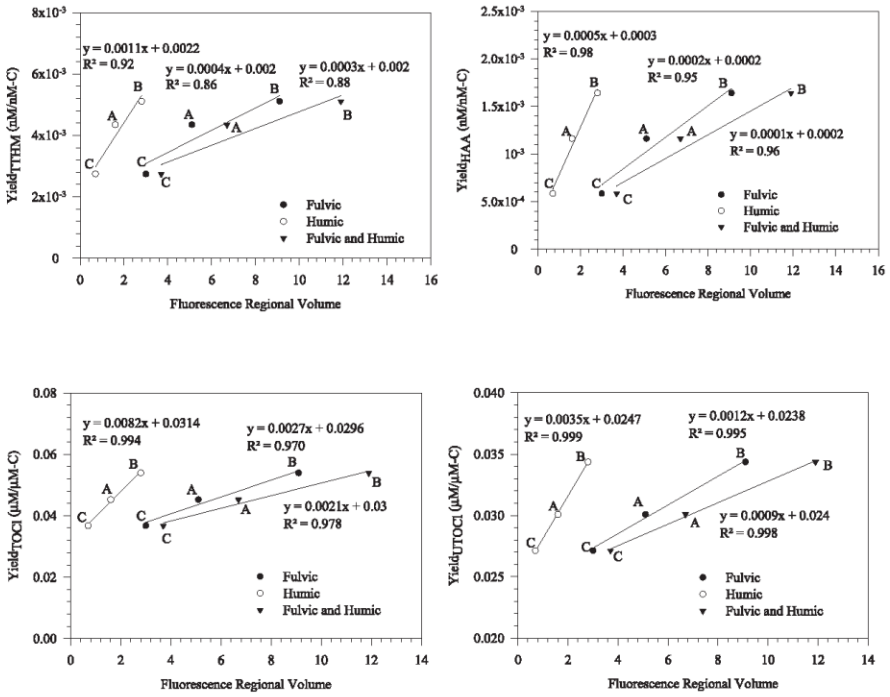

Fig. 4. Correlation between yields of TTHMs ($Yield_{TTHM}$), HAAs ($Yield_{HAA}$), TOCl ($Yield_{TOCl}$), and UTOCl ($Yield_{UTOCl}$) and fluorescence regional volume of three chlorinated source waters from Northeast Ohio: Akron (A), Barberton (B), and Cleveland (C). [Iopamidol] = 5.0 μM, $[Cl_2]_T = 100$ μM, pH = 7.5, $DOC_{Akron} = 5.57$ mg/L-C, $DOC_{Barberton} = 4.47$ mg/L-C, $DOC_{Cleveland} = 2.51$ mg/L-C.

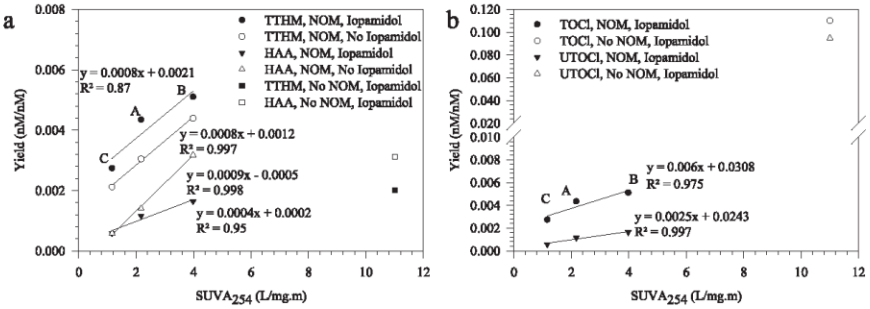

Fig. 5. Correlation between yields of TTHMs ($Yield_{TTHM}$), HAAs ($Yield_{HAA}$), TOCl ($Yield_{TOCl}$), and UTOCl ($Yield_{UTOCl}$) and $SUVA_{254}$ of three chlorinated source waters from Northeast Ohio: Akron (A), Barberton (B), and Cleveland (C). [Iopamidol] = 5 μM, $[Cl_2]_T$ = 100 μM, pH = 7.5, DOC_{Akron} = 5.57 mg/L-C $DOC_{Barberton}$ = 4.47 mg/L-C, $DOC_{Cleveland}$ = 2.51 mg/L-C.

regression line for source waters with iopamidol showed greater yield on the intercept. On the contrary, iopamidol seemed to suppress the impact of NOM in the formation of HAAs, as lower yields of HAAs were found in chlorinated source waters containing iopamidol (Fig. 5a). Although the $SUVA_{254}$ of iopamidol was high (11 L/mg.m), the impact it had on DBP formation in chlorinated water without NOM, was somewhat minimal as seen in Fig. 5 (i.e., the two isolated points). The yields of TOCl and UTOCl were higher in chlorinated water without NOM than in the presence of NOM (Fig. 5b). It was observed that the yields of UTOCl (Fig. 5b) produced in the absence of NOM are greater than the yields of TTHMs and HAAs (Fig. 5b) in the sample. This could imply a higher formation of unidentified DBPs from iopamidol. Although iopamidol has a high $SUVA_{254}$, the yields of chlorinated DBPs and TOCl in the 3 SWs were not linearly proportional to the yields of chlorinated DBPs and TOCl in water samples without NOM. While iopamidol is an organic precursor in the formation the $CHCl_3$ and TCAA, it does not exhibit DBP formation characteristics like NOM.

4. Conclusion

Chlorination of iopamidol in the absence of NOM resulted in the loss of TOI and the simultaneous formation of iodate and TOCl. In presence of NOM, TOI and TOCl formation were enhanced in chlorinated source waters containing iopamidol. In the presence of monochloramine, TOI loss was marginal but lower concentrations of TOCl was formed in the source waters compared to aqueous chlorine.

Increasing iopamidol concentrations from 1 to 5 μM in BSW and CSW dosed with 100 μM aqueous chlorine formed increasing concentrations of $CHCl_2I$ regardless of pH; indicating that iopamidol is also an indirect precursor to iodo-DBP formation. Approximately the same quantities of $CHCl_3$ and TCAA were formed at low and high iopamidol concentrations, but slightly elevated DBP concentrations were seen at the 2.5 μM iopamidol concentration in BSW and CSW. Further, $CHCl_2I$, $CHCl_3$, and TCAA increased with increasing DOC concentrations of BSW dosed with iopamidol (5 μM) and aqueous chlorine (100 μM). Conversely, $CHCl_2I$ decreased with increasing DOC concentrations in CSW. $CHCl_3$ formed in CSW increased marginally with DOC concentration. Higher concentrations of DBPs were formed in BSW than CSW. Kinetically, a lag in the formation of $CHCl_2I$ was observed in all 3 source waters that is consistent with the lag in iopamidol degradation, yielding HOI.

Yields of TTHMs, HAAs, TOCl, and UTOCl in all source waters at pH 7.5 exhibited a strong correlation with humic fractions, fulvic fractions, combined fulvic and humic fractions, and $SUVA_{254}$. Iopamidol was a precursor to chlorinated and iodinated DBPs but did not behave like NOM; since its $SUVA_{254}$ was higher than all the NOM of the source waters but formed lower concentrations of DBPs.

In drinking water treatment, some amount of the NOM in the water is removed. Thus, during disinfection, the iopamidol in the source water (usually up to 2.8 μg/L in water sources (Duirk et al., 2011; Ternes and Hirsch, 2000)) will react with the oxidant to form low concentrations of DBPs. Since iopamidol is usually found in wastewater from medical facilities, the use of iopamidol in medical imaging should be restricted.

Acknowledgements

This study was financially supported by the German Research Foundation (Deutsche Forschungsgemeinschaft, DFG, project number TE 533/4-1) and the National Science Foundation (NSF, project numbers NSF1124865 and NSF1124844).

Appendix A. Supplementary data

Supplementary data related to this article can be found at https://doi.org/10.1016/j.chemosphere.2018.03.102.

References

APHA, AWWA, WEF, 2005. Standard Methods for the Examination of Water and Wastewater, 20 ed. American Public Health Association, Washington DC.
Allard, S., Crique, J., Prunier, A., Falantin, C., Le Person, A., Tang, J.Y., Croue, J.-P., 2016. Photodecomposition of iodinated contrast media and subsequent formation of toxic iodinated moieties during final disinfection with chlorinated oxidants. Water Res. 103, 453–461.
Bichsel, Y., von Gunten, U., 1999. Oxidation of iodide and hypoiodous acid in the disinfection of natural waters. Environ. Sci. Technol. 33, 4040–4045.
Bichsel, Y., von Gunten, U., 2000. Formation of iodo-trihalomethanes during disinfection and oxidation of iodide containing waters. Environ. Sci. Technol. 34, 2784–2791.
Bougeard, C.M.M., Goslan, E.H., Jefferson, B., Parsons, S.A., 2010. Comparison of the disinfection by-product formation potential of treated waters exposed to chlorine and monochloramine. Water Res. 44, 729–740.
Christiansen, C., 2005. X-ray contrast media - an overview. Toxicology 209, 185–187.
Duirk, S.E., Gombert, B., Croue, J.P., Valentine, R.L., 2005. Modeling monochloramine loss in the presence of natural organic matter. Water Res. 39, 3418–3431.
Duirk, S.E., Lindell, C., Cornelison, C.C., Kormos, J., Ternes, T.A., Attene-Ramos, M., Osiol, J., Wagner, E.D., Plewa, M.J., Richardson, S.D., 2011. formation of toxic iodinated disinfection by-products from compounds used in medical imaging. Environ. Sci. Technol. 45, 6845–6854.
Duirk, S.E., Valentine, R.L., 2006. Modeling dichloroacetic acid formation from the

reaction of monochloramine with natural organic matter. Water Res. 40, 2667–2674.
Glassmeyer, S.T., Furlong, E.T., Kolpin, D.W., Cahill, J.D., Zaugg, S.D., Werner, S.L., Meyer, M.T., Kryak, D.D., 2005. Transport of chemical and microbial compounds from known wastewater discharges: potential for use as indicators of human fecal contamination. Environ. Sci. Technol. 39, 5157–5169.
Hua, G., Reckhow, D.A., 2007a. Characterization of disinfection byproduct precursors based on hydrophobicity and molecular size. Environ. Sci. Technol. 41, 3309–3315.
Hua, G., Reckhow, D.A., 2007b. Comparison of disinfection byproduct formation from chlorine and alternative disinfectants. Water Res. 41, 1667–1678.
Hua, G., Reckhow, D.A., 2012. Evaluation of bromine substitution factors of DBPs during chlorination and chloramination. Water Res. 46, 4208–4216.
Hua, G.H., Reckhow, D.A., Kim, J., 2006. Effect of bromide and iodide ions on the formation and speciation of disinfection byproducts during chlorination. Environ. Sci. Technol. 40, 3050–3056.
Jafvert, C.T., Valentine, R.L., 1992. Reaction scheme for the chlorination of ammoniacal water. Environ. Sci. Technol. 26, 577–586.
Khetan, S.K., Collins, T.J., 2007. Human pharmaceuticals in the aquatic environment: a challenge to Green chemistry. Chem. Rev. 107, 2319–2364.
Kormos, J.L., Schulz, M., Kohler, H.-P.E., Ternes, T.A., 2010. Biotransformation of selected iodinated x-ray contrast media and characterization of microbial transformation pathways. Environ. Sci. Technol. 44, 4998–5007.
Kovalova, L., Siegrist, H., Singer, H., Wittmer, A., McArdell, C.S., 2012. Hospital wastewater treatment by membrane bioreactor: performance and efficiency for organic micropollutant elimination. Environ. Sci. Technol. 46, 1536–1545.
Krasner, S.W., 2009. The formation and control of emerging disinfection by-products of health concern. Phil. Trans. Math. Phys. Eng. Sci. 367, 4077–4095.
Leenheer, J.A., 2004. Comprehensive assessment of precursors, diagenesis, and reactivity to water treatment of dissolved and colloidal organic matter. In: Newcombe, G., Ho, L (Eds.), Natural Organic Material Research: Innovations and Applications for Drinking Water, pp. 1–9.
Leenheer, J.A., Croue, J.P., 2003. Characterizing aquatic dissolved organic matter. Environ. Sci. Technol. 37, 18A–26A.
Liang, L., Singer, P.C., 2003. Factors influencing the formation and relative distribution of haloacetic acids and trihalomethanes in drinking water. Environ. Sci. Technol. 37, 2920–2928.
McArdell, C.S., Kovalova, L., Eugster, J., Hagenbuch, M., Wittmer, A., Siergrist, H., 2010. Elimination of pharmaceuticals from hospital wastewater in a pilot membrane bioreactor with PAC or ozone post-treatment. In: Conference Proceeding: SETAC Europe, 20th Annual Meeting, 23 – 27 May 2010. Seville, Spain).
Matsushita, T., Kobayashi, N., Hashizuka, M., Sakuma, H., Kondo, T., Matsui, Y., Shirasaki, N., 2015. Changes in mutagenicity and acute toxicity of solutions of iodinated X-ray contrast media during chlorination. Chemosphere 135, 101–107.
Nagy, J.C., Kumar, K., Margerum, D.W., 1988. Non-metal redox kinetics - oxidation of iodide by hypochlorous acid and by nitrogen trichloride measured by the pulsedaccelerated-flow method. Inorganic Chemistry 27, 2773–2780.
Perez, S., Barcelo, D., 2007. Fate and occurrence of X-ray contrast media in the environment. Anal. Bioanal. Chem. 387, 1235–1246.
Reckhow, D.A., Singer, P.C., 2011. Formation and control of disinfection by products. In: Edzwald, J.K (Ed.), Water Quality and Treatment: a Handbook of Drinking Water. McGraw Hill., NY, pp. 17 11–17 56.
Richardson, S.D., Fasano, F., Ellington, J.J., Crumley, F.G., Buettner, K.M., Evans, J.J., Blount, B.C., Silva, L.K., Waite, T.J., Luther, G.W., McKague, A.B., Miltner, R.J., Wagner, E.D., Plewa, M.J., 2008. Occurrence and mammalian cell toxicity of iodinated disinfection byproducts in drinking water. Environ. Sci. Technol. 42, 8330–8338.
Richardson, S.D., Plewa, M.J., Wagner, E.D., Schoeny, R., DeMarini, D.M., 2007. Occurrence, genotoxicity, and carcinogenicity of regulated and emerging disinfection by-products in drinking water: a review and roadmap for research. Mutat. Res. Rev. Mutat. Res. 636, 178–242.
Schulz, M., Loeffler, D., Wagner, M., Ternes, T.A., 2008. Transformation of the X-ray contrast medium Iopromide in soil and biological wastewater treatment. Environ. Sci. Technol. 42, 7207–7217.
Seitz, W., Weber, W.H., Jiang, J.-Q., Lloyd, B.J., Maier, M., Maier, D., Schulz, W., 2006. Monitoring of iodinated X-ray contrast media in surface water. Chemosphere 64, 1318–1324.
Sharma, V.K., 2008. Oxidative transformations of environmental pharmaceuticals by Cl(2), ClO(2), O(3), and Fe(VI): kinetics assessment. Chemosphere 73, 1379–1386.
Ternes, T.A., Bonerz, M., Herrmann, N., Teiser, B., Andersen, H.R., 2007. Irrigation of treated wastewater in Braunschweig, Germany: an option to remove pharmaceuticals and musk fragrances. Chemosphere 66, 894–904.
Ternes, T.A., Hirsch, R., 2000. Occurrence and behavior of X-ray contrast media in sewage facilities and the aquatic environment. Environ. Sci. Technol. 34, 2741–2748.
Thurman, E.M., 1985. Developments in Biogeochemistry: Organic Geochemistry of Natural Waters.
Tian, F.-X., Xu, B., Lin, Y.-L., Hu, C.-Y., Zhang, T.-Y., Gao, N.-Y., 2014. Photodegradation kinetics of iopamidol by UV irradiation and enhanced formation of iodinated disinfection by-products in sequential oxidation processes. Water Res. 58, 198–208.
Tian, F.-X., Xu, B., Lin, Y.-L., Hu, C.-Y., Zhang, T.-Y., Xia, S.-J., Chu, W.-H., Gao, N.-Y., 2017. Chlor(am)ination of iopamidol: kinetics, pathways and disinfection by-products formation. Chemosphere 184, 489–497.
Wendel, F.M., Eversloh, C.L., Machek, E.J., Duirk, S.E., Plewa, M.J., Richardson, S.D., Ternes, T.A., 2014. Transformation of Iopamidol during chlorination. Environ. Sci. Technol. 48, 12689–12697.
Wendel, F.M., Ternes, T.A., Richardson, S.D., Duirk, S.E., Pals, J.A., Wagner, E.D., Plewa, M.J., 2016. Comparative toxicity of high-molecular weight iopamidol disinfection byproducts. Environ. Sci. Technol. Lett. 3, 81–84.
Wu, C., Witter, J.D., Spongberg, A.L., Czajkowski, K.P., 2009. Occurrence of selected pharmaceuticals in an agricultural landscape, western Lake Erie basin. Water Res. 43, 3407–3416.
Zhao, C., Arroyo-Mora, L.E., DeCaprio, A.P., Sharma, V.K., Dionysiou, D.D., O'Shea, K.E., 2014. Reductive and oxidative degradation of iopamidol, iodinated X-ray contrast media, by Fe(III)-oxalate under UV and visible light treatment. Water Res. 67, 144–153.

JOURNAL OF ENVIRONMENTAL SCIENCES 58 (2017) 271–284

Available online at www.sciencedirect.com

ScienceDirect

www.elsevier.com/locate/jes

JES JOURNAL OF ENVIRONMENTAL SCIENCES

www.jesc.ac.cn

Showering in Flint, MI: Is there a DBP problem?

Joshua M. Allen[1,3], *Amy A. Cuthbertson*[1,3], *Hannah K. Liberatore*[1], *Susana Y. Kimura*[1,4], *Anurag Mantha*[2], *Marc A. Edwards*[2], *Susan D. Richardson*[1,*]

1. *Department of Chemistry and Biochemistry, University of South Carolina, Columbia, SC 29208, USA*
2. *Civil and Environmental Engineering, Virginia Tech, Blacksburg, VA 24061, USA*

ARTICLE INFO

Article history:
Received 23 May 2017
Accepted 11 June 2017
Available online 22 June 2017

Keywords:
Disinfection by-products
Disinfection byproducts
DBPs
Flint
Hot water
Showering
Bathing
Drinking water

ABSTRACT

Lead contamination in the City of Flint, MI has been well documented over the past two years, with lead levels above the EPA Action Level until summer 2016. This resulted from an ill-fated decision to switch from Detroit water (Lake Huron) with corrosion control, to Flint River water without corrosion control. Although lead levels are now closer to normal, reports of skin rashes have sparked questions surrounding tap water in some Flint homes. This study investigated the presence of contaminants, including disinfection by-products (DBPs), in the hot tap water used for showering in the homes of residents in Flint. Extensive quantitative analysis of 61 regulated and priority unregulated DBPs was conducted in Flint hot and cold tap water, along with the analysis of 50 volatile organic compounds and a nontarget comprehensive, broadscreen analysis, to identify a possible source for the reported skin rashes. For comparison, chlorinated hot and cold waters from three other cities were also sampled, including Detroit, which also uses Lake Huron as its source water. Results showed that hot water samples generally contained elevated levels of regulated and priority unregulated DBPs compared to cold water samples, but trihalomethanes were still within regulatory limits. Overall, hot shower water from Flint was similar to waters sampled from the three other cities and did not have unusually high levels of DBPs or other organic chemicals that could be responsible for the skin rashes observed by residents. It is possible that an inorganic chemical or microbial contaminant may be responsible.

Introduction

The Flint Water Crisis began in April 2014 when the City of Flint made an unfortunate decision, driven by costs, to switch source waters from Lake Huron in Detroit to the Flint River, while eliminating corrosion control (Pieper et al., 2017; Del Toral, 2015; Croft et al., 2015). This switch immediately led to violations for bacteria (including legionella), then total trihalomethanes (TTHMs), unprecedented corrosion of iron mains, main breaks, and elevated lead in drinking water (Del Toral, 2015; Croft et al., 2015; Edwards, 2015; Smith, 2015; Washington Post, 2016). While Lake Huron source water is regarded as a relatively pristine source of drinking water, the Flint River is highly corrosive, containing approximately eight times the normal level of chloride (Pieper et al., 2017). Corrosion inhibitors, such as orthophosphate, are commonly added to distribution systems to prevent the leaching of lead from pipes, but this practice was discontinued following the

* *Corresponding author*. E-mail: richardson.susan@sc.edu (Susan D. Richardson).
[3] Co-principal authors.
[4] Currently at the Department of Chemistry, University of Calgary, Calgary, AB T2N 1N4, Canada.

http://dx.doi.org/10.1016/j.jes.2017.06.009
1001-0742/

switch to the Flint River. Recent research has shown elevated blood lead levels in Flint children that was associated with the switch in water sources (Hanna-Attisha et al., 2016). In response to these findings, the water source was shifted back to Detroit (Lake Huron) in October 2015, and extra orthophosphate corrosion inhibitor was added in December 2015.

More recently, there have been questions raised about possible links between skin rashes and the quality of hot water in some Flint homes (Flint Water Study, 2016a, 2016b). Many residents have complained about skin rashes when showering or bathing in hot water, and it had been suggested to them that high levels of disinfection by-products (DBPs), particularly dichlorobenzene, may be the cause. DBPs are formed by the reaction of disinfectants with organic matter, bromide, and iodide, and 11 of the approximately 700 known DBPs are currently regulated in the U.S. (U.S. EPA, 2006). While regulated THM levels did spike to high levels during the switch to the Flint River source, residents still complained about skin rashes even after the switch back to Lake Huron, and they were reluctant to shower or bathe in their tap water. While DBPs, such as dichlorobenzene, dichloroacetonitrile, bromoform, and bromodichloromethane, are classified as skin irritants in their pure forms, no studies have been conducted to determine irritant characteristics of them at levels that would be present in shower water.

To determine whether there might be unusually high levels of DBPs or other organic chemicals present in the Flint tap water that could be causing these effects, we sampled both hot and cold water from showers in homes where skin rashes had been reported, quantifying a broad suite of 61 regulated and priority unregulated DBPs, including chlorinated, brominated, and iodinated haloacids, halomethanes, haloacetonitriles, haloacetamides, halonitromethanes, haloaldehydes, haloketones, and a suite of 50 volatile organic compounds (VOCs). In addition, mass spectrometry (MS) was used to comprehensively identify DBPs and other chemicals using a nontarget, broadscreen approach. Because DBPs are always formed when waters are chemically disinfected, we compared the results from Flint to hot and cold tap water from other representative cities to determine whether there was anything unusual in Flint. These cities included Detroit, which chlorinates the same source water (Lake Huron) and two cities in Georgia that chlorinate a surface water and a groundwater, respectively.

1. Material and methods

1.1. Water sampling

Hot and cold tap water samples were collected from showers from homes in four cities: Flint, MI, Detroit, MI, Grovetown, GA, and Lyons, GA in July 2016. Each residence used a tank hot water heater to generate hot water. The sampling design allowed comparisons of the Flint chlorinated tap water with two other cities that also chlorinate a surface water source (Detroit and Grovetown), as well as a city that chlorinates a groundwater source (Lyons). As mentioned earlier, Flint and Detroit use the same source water (Lake Huron); Grovetown uses the Savannah River and Clark Hill Reservoir.

Water samples for quantitative priority DBP analysis were collected headspace-free in amber glass bottles (1 L total volume) with quenching and preservation as described below in Chemical analyses section. Prior to extraction and analysis, samples were stored at 4°C with holding times between <24 hr to 72 hr. Samples for the analysis of 50 volatile organic compounds (VOCs, including four regulated THMs) were collected headspace-free in 40 mL vials. Water samples (10 L each) for comprehensive, broadscreen analysis were collected headspace-free in 2 L Teflon bottles. Samples were shipped overnight or same-day on ice packs to the University of South Carolina for analysis.

1.2. Chemicals and reagents

General reagents were ACS reagent grade and were purchased from Sigma-Aldrich (St. Louis, MO) and Fisher Scientific (Waltham, MA). DBP standards were purchased or custom synthesized from Sigma-Aldrich, CanSyn Chem. Corp. (Toronto, ON), Aldlab Chemicals (Woburn, MA), and TCI America (Waltham, MA) at the highest level of purity (Table 1). Fluorobenzaldehyde and 1,2-dibromopropane, used as the surrogate standard and the internal standard, respectively, O-(2,3,4,5,6-pentafluorobenzyl)hydroxylamine (PFBHA), used as the derivatizing agent for monohaloaldehydes, and Diazald, used as the methylating agent for halo-acids, were purchased from Sigma-Aldrich. All solvents (acetonitrile, hexanes, methyl *tert*-butyl ether (MTBE), methanol, and ethyl acetate) were of highest purity and were purchased from Sigma-Aldrich (St. Louis, MO) or VWR International (Radnor, PA).

1.3. Chemical analyses

Analytical methods were created for three different groups of priority unregulated DBPs, and all samples were measured in duplicate. Method 1 included the trihaloacetaldehydes (trichloroacetaldehyde, bromodichloroacetaldehyde, dibromochloroacetaldehyde and tribromoacetaldehyde), haloacetonitriles (HANs), haloketones (HKs), halonitromethanes (HNMs), and iodinated trihalomethanes (I-THMs) (Table 1). Stock solutions of DBP standards were made by dissolving DBP standards in anhydrous acetonitrile or methanol; calibration curves were made with the following concentrations: 0.1, 0.25, 0.50, 1.0, 2.5, 5.0, and 10 μg/L. Method 2 included haloacetamides (HAMs), trihalonitromethanes (THNMs), tribromoacetonitrile (TBAN), and iodinated acetic acids (IAAs), whose stock solutions were prepared in methanol; two separate calibration curves were prepared, one for HAMs, and another for THNMs and TBAN at 0.1, 0.25, 0.50, 1.0, 2.5, 5.0, 10, and 20 μg/L. Individual IAAs were prepared in methyl *tert*-butyl ether (MTBE), and a mix of all four IAAs was prepared in methanol with concentrations of 1 mg/L, which was used to spike pure water to prepare calibration curves at 0.005–0.1 μg/L for iodoacetic acid (IAA) and 0.1–5 μg/L for chloroiodoacetic acid (ClAA), bromoiodoacetic acid (BIAA), and diiodoacetic acid (DIAA). Method 3 included mono- and dihaloacetaldehydes, which were dissolved in anhydrous acetonitrile. Chloroacetaldehyde solution (50%) was standardized using a National Institute for Occupational Safety and Health (NIOSH) titration method (NIOSH, 1994). These

Table 1 – Retention time (R.T.), vendor information, quantifier and qualifier ions for priority DBPs quantified in this study. DBPs are classified by their corresponding analytical method and DBP class.

DBP class	DBP name	Abbreviation	R.T. (min)	Quantifier ion (m/z)	Qualifier ion (m/z)
Method 1					
HAL	Trichloroacetaldehyde[a]	TCAL	3.82	82	110.9
HAL	Bromodichloroacetaldehyde[b]	BDCAL	5.17	83	111/163.8
HAL	Dibromochloroacetaldehyde[b]	DBCAL	7.17	128.9	127.9
HAL	Tribromoacetaldehyde[a]	TBAL	9.10	172.8	171.8
HAN	Trichloroacetonitrile[a]	TCAN	3.42	108	110
HAN	Dichloroacetonitrile[a]	DCAN	4.22	74	82
HAN	Chloroacetonitrile[a]	CAN	4.36	75	48
HAN	Bromochloroacetonitrile[a]	BCAN	6.00	74	155
HAN	Bromoacetonitrile[a]	BAN	6.16	118.9	120.9
HAN	Dibromoacetonitrile[a]	DBAN	8.17	117.9	199
HAN	Iodoacetonitrile[a]	IAN	8.85	167	126.9
HK	1,1-Dichloropropanone[a]	11DCP	4.63	43	83
HK	Chloropropanone[a]	CP	4.73	92	43
HK	1,1,1-Trichloropropanone[a]	111TCP	6.88	43	125
HK	1,1-Dibromopropanone[b]	11DBP	8.17	43	215.9
HK	1-Bromo-1,1-dichloropropanone[b]	1B11DCP	8.80	43	125
HK	1,3-Dichloropropanone[b]	13DCP	8.95	77	49
HK	1,1,3-Trichloropropnanone[a]	113TCP	10.02	77	83
HK	1,1,3,3-Tetrachloropropanone[b]	1133TeCP	10.92	83	85
HK	1,1,3,3-Tetrabromopropanone[c]	1133TeBP	16.13	200.8	119.9
HNM	Trichloronitromethane[a]	TCNM	4.67	116.9	119
HNM	Dichloronitromethane[b]	DCNM	4.77	83	85
HNM	Bromochloronitromethane[b]	BCNM	6.64	129	127
HNM	Dibromonitromethane[b]	DBNM	8.51	172.8	171
I-THM	Dichloroiodomethane[b]	DCIM	4.34	83	126.9
I-THM	Bromochloroiodomethane[b]	BCIM	5.95	128.9	126.9
I-THM	Dibromoiodomethane[b]	DBIM	7.83	172.8	299.7
I-THM	Chlorodiiodomethane[b]	CDIM	8.33	174.9	126.9
I-THM	Bromodiiodomethane[b]	BDIM	10.09	218.8	220.8
I-THM	Iodoform[a]	TIM	12.06	393.7	266.8
Method 2					
HAM	Chloroacetamide[a]	CAM	10.08	93	44
HAM	Bromoacetamide[a]	BAM	11.73	137	44
HAM	Dichloroacetamide[d]	DCAM	12.03	44	127
HAM	Bromochloroacetamide[b]	BCAM	13.38	44	173
HAM	Trichloroacetamide[a]	TCAM	13.92	44	82
HAM	Iodoacetamide[a]	IAM	14.07	185	58
HAM	Dibromoacetamide[b]	DBAM	14.08	44	217
HAM	Chloroiodoacetamide[b]	CIAM	15.15	92	219
HAM	Bromodichloroacetamide[b]	BDCAM	15.21	44	128
HAM	Bromoiodoacetamide[b]	BIAM	16.28	136	138
HAM	Dibromochloroacetamide[b]	DBCAM	16.44	44	128
HAM	Tribromoacetamide[b]	TBAM	17.59	44	173
HAM	Diiodoacetamide[b]	DIAM	17.91	184	311
HAN	Tribromoacetonitrile[b]	TBAN	9.11	197.8	195.8
HNM	Bromodichloronitromethane[b]	BDCNM	6.71	163	161
HNM	Dibromochloronitromethane[b]	DBCNM	8.87	206.8	209
HNM	Tribromonitromethane[b]	TBNM	10.81	251	253
IAA	Iodoacetic acid[a]	IAA	7.53	200 > 73	169 > 141
IAA	Chloroiodoacetic acid[b]	CIAA	9.68	234 > 79	234 > 107
IAA	Bromoiodoacetic acid[b]	BIAA	11.08	278 > 123	278 > 151
IAA	Diiodoacetic acid[b]	DIAA	12.91	326 > 171	326 > 199
Method 3					
HAL	Chloroacetaldehyde[a]	CAL	14.62	238	181/182
HAL	Bromoacetaldehyde[c]	BAL	15.87	287	238
HAL	Iodoacetaldehyde[c]	IAL	17.48	293	335
HAL	Dichloroacetaldehyde[d]	DCAL	15.49	272	181/182
HAL	Bromochloroacetaldehyde[b]	BCAL	16.80	272	238
HAL	Dibromoacetaldehyde[b]	DBAL	18.21	137	135

compounds were combined in acetonitrile and spiked into pure water to prepare a calibration curve at 0.1, 0.25, 0.5, 1.0, 2.5, 5.0, 10, and 20 μg/L levels.

For this list of compounds, there are three extraction procedures and two derivatization procedures.

1.3.1. Method 1

Method 1 involved a single liquid–liquid extraction (LLE) for volatile DBPs. Samples were quenched with ascorbic acid in slight excess (chlorine to ascorbic acid molar ratio of 1:1.3) and adjusted to pH 3.5–4 with 1 M sulfuric acid. Aliquots of 100 mL were spiked with 30 g of sodium sulfate and 2 mL of MTBE in 125 mL amber bottles. Samples were shaken for 30 min on a mechanical shaker, followed by a 10 min hold to allow the organic phase to separate, which was immediately removed into a conical test tube. Sodium sulfate was added to the extract to remove any excess water, and 250 μL was transferred with a syringe into a gas chromatography (GC) vial. Final extracts were spiked with internal standard 1,2-dibromopropane.

Analyte detection was performed by an Agilent 7890 GC coupled to an Agilent 5977A mass spectrometer with electron ionization (Agilent Technologies, Santa Clara, CA), which was carried out in selected ion monitoring (SIM) mode. The samples (1.0 μL) were injected using a multi-mode inlet (MMI) in pulsed splitless mode with the following program: initial temperature of 35°C held for 0.1 min, ramped at a rate of 360°C/min to 220°C, held for 5 min, and then ramped at 720°C/min to 280°C for the remainder of the run. Samples were injected onto a Restek Rtx-200 column (30 m × 0.25 mm ID × 0.25 μm film thickness; Restek Corporation, Bellefonte, PA). The GC program was as follows: an initial temperature of 35°C held for 5 min, then ramped at 9°C/min to 200°C, then ramped at 20°C/min to 280°C, and held for 20 min. The transfer line temperature was maintained at 250°C, the source temperature at 200°C with an electron energy of 70 eV, and the quadrupole at 150°C. The retention times and the ions (*m/z* values) selected to monitor each compound can be found in Table 1. Quantification ions had a dwell time of 100 ms, and qualifier ions had a dwell time ranging from 50 to 75 ms. Quantification ions were selected based on relative abundance, generally selecting the most abundant ions.

1.3.2. Method 2

Method 2 involved a multiple-LLE for semi-volatile DBPs. Samples were quenched with ammonium chloride based on a chlorine to ammonium chloride molar ratio of 1:1.3 and adjusted to pH <1.0 with concentrated sulfuric acid. Aliquots of 100 mL were spiked with 30 g of sodium sulfate and 5 mL of MTBE in 125 mL amber bottles. Samples were shaken for 15 min on a mechanical shaker, followed by a 10 min wait to allow the organic phase to separate out, which was immediately removed into a separate container. Samples were extracted again for a total of three LLEs and a total of 15 mL of MTBE. The collected extract was passed through a sodium sulfate column to remove water, and concentrated under nitrogen to a final volume of 200 μL. Final extracts were transferred to two GC vials containing 100 μL each. One 100 μL extract was spiked with internal standard 1,2-dibromopropane for analysis of THNMs, HAMs, and TBAN by GC–MS. These compounds were analyzed using the same GC-EI-MS method in Method 1. The retention times and ions (*m/z* values) used for SIM analysis can be found in Table 1.

The second 100 μL extract underwent diazomethane derivatization for analysis of IAAs. A 100 μL portion of the extract was spiked with 1,2-dibromopropane internal standard and derivatized using freshly-generated diazomethane according to a U.S. Environmental Protection Agency Standard Operating Procedure (Richardson, 2009). An Aldrich® diazomethane-generator apparatus was used. Approximately 0.367 g of Diazald® and 1.0 mL of CARBITOL™ were added to the inner piece of the apparatus and 3.0 mL of MTBE was added to the outer portion. The apparatus was assembled, placed in ice, and 1.5 mL of 37% potassium hydroxide (KOH) was injected dropwise through the septum into the inner tube. After reacting for 1 hr, 50 μL of the diazomethane (dissolved in MTBE in the outer tube) was added to each 100 μL sample. After 30 min of reaction, excess diazomethane in the samples was quenched with approximately 10 mg of silica gel. Derivatized extracts were transferred to new vials to remove solid silica from the samples. Derivatized samples were analyzed by GC-tandem mass spectrometry (MS–MS) for four IAAs, including IAA, CIAA, BIAA, and DIAA, using a Quantum GC™ triple quadrupole mass spectrometer coupled to a TRACE GC Ultra gas chromatograph (Thermo Scientific, Waltham, MA). Sample volumes of 2.0 μL were injected at an inlet temperature of 250°C with a splitless time of 0.80 min and split flow of 50 mL/min. GC separations were performed using an Rxi-5ms (30 m × 0.25 mm ID × 0.25 μm film thickness; Restek Corporation, Bellefonte, PA), with the following oven temperature program: 35°C for 2 min, followed by a 9°C/min ramp to 280°C, and held for 20 min. The transfer line temperature was controlled at 280°C. An EI source was used at a temperature of 200°C, emission current of 50 μA, and electron energy of 70 eV. Multiple reaction monitoring (MRM) was used to quantify IAA, CIAA, BIAA, and DIAA. Two MS–MS transitions, one quantitative and one qualitative, were used for each of the IAAs, along with 1,2-dibromopropane internal standard as shown in Table 1.

1.3.3. Method 3

Method 3 was used for mono- and di-halogenated acetaldehydes, according to a published method by Jeong et al. (2015) with minor alterations. Samples were quenched with ascorbic acid in slight excess (chlorine to ascorbic acid molar ratio of 1:1.3) and adjusted to pH 3.5–4 with 1 M sulfuric acid. A 100 mL sample was spiked with a surrogate standard, ammonium sulfate, potassium hydrogen phthalate/sodium hydroxide buffer, and PFBHA and reacted for two hours in a temperature controlled water bath at 35°C. Samples were cooled down to room temperature, and concentrated sulfuric acid and 1,2-dibromopropanone internal standard were added. Then,

Notes to Table 1:
DBP: disinfection by-product; HAL: haloacetaldehyde; HAN: haloacetonitriles; HK: haloketones; HNM: halonitromethanes; I-THM: iodinated trihalomethanes; HAM: haloacetamides; IAA: iodinated acetic acid.
[a] Sigma Aldrich. [b] CanSyn Chem. Corp. [c] Aldlab Chemicals. [d] TCI America.

Table 2 – DBPs quantified and identified in finished water from showers in Detroit, Flint, Grovetown, and Lyons (μg/L).

DBP	LOQ[a] (μg/L)	Detroit 1		Detroit 2	Flint 1		Flint 2	Grovetown		Lyons	
		Cold	Hot	Hot	Cold	Hot	Hot	Cold	Hot	Cold	Hot
Halomethanes											
Chloromethane	1.0	<1.0	<1.0	<1.0	<1.0	<1.0	<1.0	<1.0	<1.0	<1.0	<1.0
Bromomethane	2.0	<2.0	<2.0	<2.0	<2.0	<2.0	<2.0	<2.0	<2.0	<2.0	<2.0
Chloroform	1.0	20.0 ± 0.7	30.0 ± 0.0	41.0 ± 4.2	25.0 ± 3.5	58.0 ± 3.5	50.0 ± 1.4	45.0 ± 0.0	54.0 ± 1.4	<1.0	1.6 ± 0.1
Bromodichloromethane	1.0	8.9 ± 0.1	11.0 ± 0.0	12.0 ± 1.4	10.0 ± 1.0	16.0 ± 0.7	15.0 ± 0.0	7.7 ± 0.0	8.4 ± 0.1	<1.0	1.8 ± 0.0
Dibromochloromethane	1.0	2.8 ± 0.0	3.4 ± 0.1	3.5 ± 0.3	3.4 ± 0.2	4.8 ± 0.1	4.5 ± 0.1	<1.0	<0.1	<1.0	1.5 ± 0.0
Bromoform	1.0	<1.0 (X)	<1.0 (X)	<1.0 (X)	<1.0 (X)	<1.0 (X)	<1.0 (X)	<1.0 (X)	<1.0 (X)	<1.0 (X)	<1.0 (X)
THM4		31.7 ± 0.7	44.4 ± 0.1	56.5 ± 4.4	38.4 ± 3.6	78.8 ± 3.6	69.5 ± 1.4	52.7 ± 0.0	62.4 ± 1.4	-	4.9 ± 0.1
Dichloroiodomethane	0.1	<0.1	<0.1	<0.1	NM	<0.1	<0.1	0.9 ± 0.17	0.7 ± 0.12	<0.1	<0.1
Bromochloroiodomethane	0.1	<0.1	<0.1	<0.1	NM	<0.1	<0.1	<0.1	<0.1	<0.1	<0.1
Dibromoiodomethane	0.1	<0.1	<0.1	<0.1	NM	<0.1	<0.1	<0.1	<0.1	<0.1	<0.1
Chlorodiiodomethane	0.1	<0.1	<0.1	<0.1	NM	<0.1	<0.1	<0.1	<0.1	<0.1	<0.1
Bromodiiodomethane	0.1	<0.1	<0.1	<0.1	NM	<0.1	<0.1	<0.1	<0.1	<0.1	<0.1
Iodoform	0.1	<0.1	<0.1	<0.1	NM	<0.1	<0.1	<0.1	<0.1	<0.1	<0.1
Carbon tetrachloride	1.0	<1.0	<1.0	<1.0	<1.0	<1.0	<1.0	<0.1	<1.0	<1.0	<1.0
Haloacids											
Monochloroacetic acid		X	X	X	X	X	X	X	X	X	X
Monobromoacetic acid		X	X	X	X	X	X	X	X	X	X
Dichloroacetic acid		X	X	X	X	X	X	X	X	X	X
Bromochloroacetic acid		X	X	X	X	X	X	X	X	X	X
Dibromoacetic acid		X	X	X	X	X	X	X	X	X	X
Trichloroacetic acid		X	X	X	X	X	X	X	X	X	X
Bromodichloroacetic acid		X	X	X	X	X	X	X	X	X	X
Dibromochloroacetic acid		X			X			X	X		
Monoiodoacetic acid	0.005	<0.005	<0.005	<0.005	<0.005	<0.005	<0.005	0.079 ± 0.020	0.075 ± 0.014	<0.005	<0.005
Bromoiodoacetic acid	0.1	<0.1	<0.1	<0.1	<0.1	<0.1	<0.1	<0.1	<0.1	<0.1	<0.1
Chloroiodoacetic acid	0.1	<0.1	<0.1	<0.1	<0.1	<0.1	<0.1	0.6 ± 0.13	0.7 ± 0.06	<0.1	<0.1
Diiodoacetic acid	0.1	<0.1	<0.1	<0.1	<0.1	<0.1	<0.1	<0.1	<0.1	<0.1	<0.1
2,2-Dichloropropenoic acid		X	X	X	X	X	X	X	X	X	X
Haloacetonitriles											
Chloroacetonitrile	0.1	<0.1	<0.1	<0.1	NM	<0.1	<0.1	<0.1	<0.1	<0.1	<0.1
Bromoacetonitrile	0.1	<0.1	<0.1	<0.1	NM	<0.1	<0.1	<0.1	<0.1	<0.1	<0.1
Dichloroacetonitrile	0.1	1.5 ± 0.25	2.1 ± 0.00	1.9 ± 0.04	NM (X)	0.4 ± 0.04	<0.1	3.3 ± 0.08	3.6 ± 0.05	<0.1 (X)	<0.1 (X)
Bromochloroacetonitrile	0.1	0.3 ± 0.11	0.2 ± 0.02	0.2 ± 0.02	NM (X)	<0.1	<0.1 (X)	0.4 ± 0.12	0.3 ± 0.02	<0.1	<0.1
Dibromoacetonitrile	0.1	<0.1 (X)	<0.1 (X)	<0.1 (X)	NM (X)	<0.1 (X)	<0.1 (X)	<0.1 (X)	<0.1 (X)	<0.1 (X)	<0.1 (X)
Trichloroacetonitrile	0.1	<0.1	<0.1	<0.1	NM	<0.1	<0.1	<0.1	<0.1	<0.1	<0.1
Bromodichloroacetonitrile	0.1	<0.1	<0.1	<0.1	NM	<0.1	<0.1	<0.1	<0.1	<0.1	<0.1
Dibromochloroacetonitrile	0.1	<0.1	<0.1	<0.1	NM	<0.1	<0.1	<0.1	<0.1	<0.1	<0.1
Tribromoacetonitrile	0.25	<0.25	<0.25	<0.25	NM	<0.25	<0.25	<0.25	<0.25	<0.25	<0.25
Iodoacetonitrile	0.1	<0.1	<0.1	<0.1	NM	<0.1	<0.1	<0.1	<0.1	<0.1	<0.1

(continued on next page)

Table 2 (*continued*)

DBP	LOQ[a] (μg/L)	Detroit 1		Detroit 2	Flint 1		Flint 2	Grovetown		Lyons	
		Cold	Hot	Hot	Cold	Hot	Hot	Cold	Hot	Cold	Hot
Haloaldehydes											
Monochloroacetaldehyde	0.1	<0.1	<0.1	<0.1	NM	<0.1	<0.1	<0.1	0.3 ± 0.12	<0.1	<0.1
Monobromoacetaldehyde	0.1	<0.1	<0.1	<0.1	<0.1	<0.1	<0.1	<0.1	<0.1	<0.1	<0.1
Dichloroacetaldehyde	0.1	0.4 ± 0.01	0.3 ± 0.25[b]	0.3 ± 0.25[b]	NM	0.5 ± 0.05	0.4 ± 0.40[b]	0.5 ± 0.07	0.5 ± 0.03	<0.1	<0.1
Bromochloroacetaldehyde	0.1	<0.1	<0.1 (X)	<0.1	NM	<0.1	<0.1	<0.1	<0.1	<0.1	<0.1
Dibromoacetaldehyde	0.1	<0.1	<0.1	<0.1	NM	<0.1	<0.1	<0.1	<0.1	<0.1	<0.1
Bromodichloroacetaldehyde	0.1	<0.1	<0.1	<0.1	NM	<0.1	<0.1	0.5 ± 0.34	<0.1 (X)	<0.1	<0.1
Trichloroacetaldehyde	0.1	7.8 ± 1.17	18.8 ± 0.98	20.3 ± 0.01	NM (X)	7.1 ± 0.14	1.9 ± 0.07	18.3 ± 0.32	23.0 ± 1.60	<0.1	<0.1
Tribromoacetaldehyde	0.1	<0.1	<0.1	<0.1	NM	<0.1	<0.1	<0.1	<0.1	<0.1	<0.1
Dibromochloroacetaldehyde	0.1	<0.1	<0.1	<0.1	NM	<0.1	<0.1	<0.1	<0.1	<0.1	<0.1
Iodoacetaldehyde	0.1	<0.1	<0.1	<0.1	NM	<0.1	<0.1	<0.1	<0.1	<0.1	<0.1
Haloketones											
Chloropropanone	0.1	<0.1	<0.1	<0.1	NM	1.4 ± 0.14	1.5 ± 0.17	1.9 ± 0.51	1.9 ± 0.73	<0.1	<0.1
1,1-Dichloropropanone	0.1	<0.1	0.1 ± 0.02	<0.1	NM	0.5 ± 0.05	0.3 ± 0.06	<0.1	<0.1	<0.1	<0.1
1,3-Dichloropropanone	0.1	<0.1	<0.1	<0.1	NM	<0.1	<0.1	<0.1	<0.1	<0.1	<0.1
1,1-Dibromopropanone	0.1	<0.1	<0.1	<0.1	NM	<0.1	<0.1	<0.1	<0.1	<0.1	<0.1
1,1,1-Trichloropropanone	0.1	2.0 ± 0.40	0.3 ± 0.01	0.4 ± 0.00	NM (X)	0.1 ± 0.03	<0.1	5.8 ± 0.67	2.2 ± 0.12	<0.1	<0.1
1,1,3-Trichloropropanone	0.1	<0.1	<0.1	<0.1	NM (X)	<0.1	<0.1	<0.1	<0.1 (X)	<0.1 (X)	<0.1 (X)
1-Bromo-1,1-dichloropropanone	0.1	<0.1	<0.1	<0.1	NM	<0.1	<0.1	0.1 ± 0.03	0.1 ± 0.07	0.1 ± 0.07	0.1 ± 0.08
1,1,3,3-Tetrachloropropanone	0.1	<0.1	<0.1	<0.1 (X)	NM (X)	<0.1	<0.1 (X)	<0.1	<0.1	<0.1 (X)	<0.1 (X)
1,1,3,3-Tetrabromopropanone	0.1	<0.1	<0.1	<0.1	NM	<0.1	<0.1	<0.1	<0.1	<0.1	<0.1
Halonitromethanes											
Dichloronitromethane	0.1	<0.1	<0.1	<0.1	NM	<0.1	<0.1	<0.1	<0.1	<0.1	<0.1
Bromochloronitromethane	0.1	<0.1	<0.1	<0.1	NM	<0.1	<0.1	<0.1	<0.1	<0.1	<0.1
Dibromonitromethane	0.1	<0.1	<0.1	<0.1	NM	<0.1	<0.1	<0.1	<0.1	<0.1	<0.1
Trichloronitromethane	0.1	<0.1	<0.1	<0.1	NM	0.2 ± 0.00	0.1 ± 0.00	0.5 ± 0.08	0.4 ± 0.00	<0.1	<0.1
Bromodichloronitromethane	0.1	0.9 ± 0.00	1.0 ± 0.01	1.0 ± 0.00	NM	0.9 ± 0.00	<0.1	<0.1	<0.1	<0.1	<0.1
Dibromochloronitromethane	0.1	<0.1	<0.1	<0.1	NM	<0.1	<0.1	<0.1	<0.1	<0.1	<0.1
Tribromonitromethane	0.1	<0.1	<0.1	<0.1	NM	<0.1	<0.1	<0.1	<0.1	<0.1	<0.1
Other halogenated DBPs											
2,4,6-Trichlorophenol		–	–	–	–	–	–	X	X	X	X
Dichlorophenol		–	–	–	–	–	–	X	X	X	X
2-Chlorophenol		X	–	X	X	–	–	X	X	X	X
4-Chlorophenol		X	–	–	X	–	–	X	X	X	X
Haloamides											
Monochloroacetamide	0.1	<0.1	<0.1	<0.1	NM	<0.1	<0.1	<0.1	<0.1	<0.1	<0.1
Monobromoacetamide	0.1	<0.1	<0.1	<0.1	NM	<0.1	<0.1	<0.1	<0.1	<0.1	<0.1
Dichloroacetamide	0.1	1.7 ± 0.07	2.1 ± 0.36	3.3 ± 0.90	NM	6.4 ± 2.21	4.0 ± 0.28	0.6 ± 0.17	1.7 ± 1.11	<0.1	<0.1
Dibromoacetamide	0.1	0.4 ± 0.03	0.4 ± 0.03	0.4 ± 0.04	NM	0.5 ± 0.15	0.4 ± 0.03	<0.1	<0.1	<0.1	0.2 ± 0.15[b]
Trichloroacetamide	0.1	0.3 ± 0.01	0.2 ± 0.04	0.3 ± 0.08	NM (X)	0.4 ± 0.15	0.4 ± 0.03	0.1 ± 0.02	0.2 ± 0.15	<0.1	<0.1
Bromochloroacetamide	0.1	0.8 ± 0.03	0.8 ± 0.16	1.1 ± 0.19	NM (X)	2.0 ± 0.68	1.1 ± 0.11	0.2 ± 0.03	0.4 ± 0.23	<0.1	<0.1

Bromodichloroacetamide	0.1	<0.1	<0.1	<0.1	NM	<0.1	<0.1	<0.1	<0.1	<0.1	<0.1
Dibromochloroacetamide	0.1	<0.1	<0.1	<0.1	NM	<0.1	<0.1	<0.1	<0.1	<0.1	<0.1
Tribromoacetamide	0.1	<0.1	<0.1	<0.1	NM	<0.1	<0.1	<0.1	<0.1	<0.1	<0.1
Bromoiodoacetamide	0.1	<0.1	<0.1	<0.1	NM	<0.1	<0.1	<0.1	<0.1	<0.1	<0.1
Haloamides											
Iodoacetamide	0.1	<0.1	<0.1	<0.1	NM	<0.1	<0.1	<0.1	<0.1	<0.1	<0.1
Chloroiodoacetamide	0.1	<0.1	<0.1	<0.1	NM	<0.1	<0.1	<0.1	<0.1	<0.1	<0.1
Diiodoacetamide	0.1	<0.1	<0.1	<0.1	NM	<0.1	<0.1	<0.1	<0.1	<0.1	<0.1
Non-halogenated compounds											
2-Methylpropanoic acid		X	X	X	X	X	X	X	X	X	X
2-Methylbutanoic acid		X	–	–	X	–	X	–	–	X	X
Butanoic acid		X	X	–	X	X	–	–	–	–	–
Dodecanoic acid		X	X	X	X	X	X	X	X	X	X
Tetradecanoic acid		X	X	X	X	X	X	X	X	X	X
Hexadecanoic acid		X	X	X	X	X	X	X	X	X	X
Octadecanoic acid		X	X	X	X	X	X	X	X	X	X
Pentadecanoic acid		X	X	X	X	X	X	–	–	X	X
Other volatile organic compounds											
Acetone	20	<20	<20	<20	<20	<20	<20	<20	<20	<20	<20
Benzene	1.0	<1.0	<1.0	<1.0	<1.0	<1.0	<1.0	<1.0	<1.0	<1.0	<1.0
2-Butanone	10	<10	<10	<10	<10	<10	<10	<10	<10	<10	<10
Carbon disulfide	1.0	<1.0	<1.0	<1.0	<1.0	<1.0	<1.0	<1.0	<1.0	<1.0	<1.0
Chlorobenzene	1.0	<1.0	<1.0	<1.0	<1.0	<1.0	<1.0	<1.0	<1.0	<1.0	<1.0
Chloroethane	1.0	<1.0	<1.0	<1.0	<1.0	<1.0	<1.0	<1.0	<1.0	<1.0	<1.0
Cyclohexane	1.0	<1.0	<1.0	<1.0	<1.0	<1.0	<1.0	<1.0	<1.0	<1.0	<1.0
1,2-Dibromo-3-chloropropane	1.0	<1.0	<1.0	<1.0	<1.0	<1.0	<1.0	<1.0	<1.0	<1.0	<1.0
1,2-Dibromoethane	1.0	<1.0	<1.0	<1.0	<1.0	<1.0	<1.0	<1.0	<1.0	<1.0	<1.0
1,4-Dichlorobenzene	1.0	<1.0	<1.0	<1.0	<1.0	<1.0	<1.0	<1.0	<1.0	<1.0	<1.0
1,3-Dichlorobenzene	1.0	<1.0	<1.0	<1.0	<1.0	<1.0	<1.0	<1.0	<1.0	<1.0	<1.0
1,2-Dichlorobenzene	1.0	<1.0	<1.0	<1.0	<1.0	<1.0	<1.0	<1.0	<1.0	<1.0	<1.0
Dichlorodifluoromethane	2.0	<2.0	<2.0	<2.0	<2.0	<2.0	<2.0	<2.0	<2.0	<2.0	<2.0
1,2-Dichloroethane	1.0	<1.0	<1.0	<1.0	<1.0	<1.0	<1.0	<1.0	<1.0	<1.0	<1.0
1,1-Dichloroethane	1.0	<1.0	<1.0	<1.0	<1.0	<1.0	<1.0	<1.0	<1.0	<1.0	<1.0
trans-1,2-Dichloroethene	1.0	<1.0	<1.0	<1.0	<1.0	<1.0	<1.0	<1.0	<1.0	<1.0	<1.0
cis-1,2-Dichloroethene	1.0	<1.0	<1.0	<1.0	<1.0	<1.0	<1.0	<1.0	<1.0	<1.0	<1.0
Ethylbenzene	1.0	<1.0	<1.0	<1.0	<1.0	<1.0	<1.0	<1.0	<1.0	<1.0	<1.0
2-Hexanone	10	<10	<10	<10	<10	<10	<10	<10	<10	<10	<10
Isopropylbenzene	1.0	<1.0	<1.0	<1.0	<1.0	<1.0	<1.0	<1.0	<1.0	<1.0	<1.0
Methyl acetate	1.0	<1.0	<1.0	<1.0	<1.0	<1.0	<1.0	<1.0	<1.0	<1.0	<1.0
4-Methyl-2-pentanone	10	<10	<10	<10	<10	<10	<10	<10	<10	<10	<10
Methylcyclohexane	5.0	<5.0	<5.0	<5.0	<5.0	<5.0	<5.0	<5.0	<5.0	<5.0	<5.0
Methylene chloride	1.0	<1.0	<1.0	<1.0	<1.0	<1.0	<1.0	<1.0	<1.0	<1.0	<1.0
Styrene	1.0	<1.0	<1.0	<1.0	<1.0	<1.0	<1.0	<1.0	<1.0	<1.0	<1.0
1,1,2,2-Trichloroethane	1.0	<1.0	<1.0	<1.0	<1.0	<1.0	<1.0	<1.0	<1.0	<1.0	<1.0
Tetrachloroethene	1.0	<1.0	<1.0	<1.0	<1.0	<1.0	<1.0	<1.0	<1.0	<1.0	<1.0
Toluene	1.0	<1.0	<1.0	<1.0	<1.0	<1.0	<1.0	<1.0	<1.0	<1.0	<1.0

(continued on next page)

Table 2 (*continued*)

DBP	LOQ[a] (μg/L)	Detroit 1		Detroit 2	Flint 1		Flint 2	Grovetown		Lyons	
		Cold	Hot	Hot	Cold	Hot	Hot	Cold	Hot	Cold	Hot
1,1,2,2-Trichloro-1,2,2-trifluoroethane	1.0	<1.0	<1.0	<1.0	<1.0	<1.0	<1.0	<1.0	<1.0	<1.0	<1.0
1,2,4-Trichlorobenzene	1.0	<1.0	<1.0	<1.0	<1.0	<1.0	<1.0	<1.0	<1.0	<1.0	<1.0
1,1,2-Trichloroethane	1.0	<1.0	<1.0	<1.0	<1.0	<1.0	<1.0	<1.0	<1.0	<1.0	<1.0
1,1,1-Trichloroethane	1.0	<1.0	<1.0	<1.0	<1.0	<1.0	<1.0	<1.0	<1.0	<1.0	<1.0
Trichloroethene	1.0	<1.0	<1.0	<1.0	<1.0	<1.0	<1.0	<1.0	<1.0	<1.0	<1.0
Trichlorofluoromethane	1.0	<1.0	<1.0	<1.0	<1.0	<1.0	<1.0	<1.0	<1.0	<1.0	<1.0
Vinyl chloride	1.0	<1.0	<1.0	<1.0	<1.0	<1.0	<1.0	<1.0	<1.0	<1.0	<1.0
Xylenes (total)	1.0	<1.0	<1.0	<1.0	<1.0	<1.0	<1.0	<1.0	<1.0	<1.0	<1.0

Key to table: Underlined compounds were quantified. DBPs identified in qualitative, broadscreen analyses are noted with an X; lack of detection by broadscreen methods is noted with a –. Halo-acids and non-halogenated acids were identified in their methyl ester forms. NM = not measured (due to broken bottle in shipment). "Flint 1, 2" and "Detroit 1, 2" refer to samples taken from two separate residences in each city. Samples were analyzed in duplicate with reported standard deviation unless otherwise noted.

[a] LOQ: Limit of quantification; [b] Compound was not detected in replicate sample; reported value is averaged with zero.

10 mL of hexane was added to samples, shaken for 3 min with a mechanical shaker, transferred to separatory funnels, and held for 5 min for phases to separate. The organic extract was collected in 40 mL vials and the LLE was repeated two more times for a total of 30 mL of organic extract. The final extract was dried over a sodium sulfate column and concentrated with nitrogen to 0.5 mL for GC–MS analysis.

Analyte detection was performed by GC-EI-MS analysis, which was carried out in SIM mode. The injection port was run in splitless mode at 250°C at 15.5 psi. GC separations were performed using a Rxi-5ms (30 m × 0.25 mm ID × 0.25 μm film thickness; Restek Corporation, Bellefonte, PA), with the following oven temperature program: 35°C for 2 min, followed by a 9°C/min ramp to 160°C, a 5°C/min ramp to 180°C, and a final ramp of 22°C/min to 280°C, which was held for 20 min. The transfer line temperature was controlled at 280°C, the source temperature at 200°C with an electron energy at 70 eV, and the quadrupole at 150°C. The retention times and the ions (*m/z* values) selected to monitor each compound can be found in Table 1. Quantification ions had a dwell time of 100 ms, and qualifier ions had a dwell time ranging from 50 to 75 ms. Quantification ions were selected based on relative abundance.

1.3.4. VOCs

Fifty VOCs, including the four regulated THMs, were measured using EPA Method 8260B and prepped following EPA Method 5030B (U.S. EPA, 1996a, 1996b). Briefly, 5 mL of each water sample was purged at ambient temperature for 11 min with helium flowing at a rate of 40 mL/min. The purged gas was desorbed for 4 min on the trap operating at a temperature of 180°C and carried by helium for GC–MS analysis. Bromofluorobenzene, 1,2-dichloroethane-d4, and toluene-d8 were used as surrogate standards.

1.3.5. Comprehensive, broadscreen analyses

Water samples (10 L each of hot and cold water) for comprehensive, broadscreen analysis were extracted immediately upon arrival using XAD resins (DAX-8 over XAD-2, 55 mL of each), according to a previously published procedure (Richardson et al., 2008b). Prior to use, new resins were extensively cleaned using Soxhlet extraction (Richardson et al., 1994). Briefly, water samples were acidified to pH 1 with sulfuric acid and were poured over the XAD resins in a glass column containing glass wool at the top and bottom. Once the water had eluted completely, organic compounds were eluted with 400 mL of ethyl acetate, a separatory funnel was used to remove the water layer, and 30 g of sodium sulfate was used to further dry the extract. A Turbovap (Turbovap®II, Biotage), followed by a gentle flow of nitrogen was used to concentrate the extract to 1.0 mL, which was divided into two aliquots: one for direct analysis by GC–MS, and the other for derivatization of halo-acids with diazomethane (as described above) for analysis of haloacid methyl esters. Comprehensive GC–MS analyses were performed on the Agilent mass spectrometer described above. Injections of 1.0 μL of the extracts were introduced *via* a split/splitless injector (in splitless mode) onto a Restek Rxi-5ms GC column (30 m × 0.25 mm ID × 0.25 μm film thickness; Restek Corporation, Bellefonte, PA), with the following oven temperature program: 35°C for 4 min, followed by a 9°C/min ramp to 280°C, which was held for 30 min. The transfer line temperature was controlled at 280°C, the source temperature at 200°C with an electron energy at 70 eV.

Mass spectra of unknown compounds in the drinking water extracts were subjected to library database searching (National Institute of Standards and Technology and user-created databases. Mass spectra were also manually interpreted to provide tentative structural identifications.

2. Results and discussion

2.1. Overall findings

Quantitative and comprehensive broadscreen results are shown in Table 2. Of the 50 VOCs, quantified, only chloroform, bromodichloromethane, and chlorodibromomethane were detected in the quantitative screening; bromoform was also observed in the comprehensive, broadscreen analysis, owing to the greater concentration of water (10,000-fold concentration factor), which allows lower detection limits for analytes, even in full-scan mode (providing a complete library-searchable mass spectrum). It is notable that none of the three possible dichlorobenzene isomers (1,2-dichlorobenzene, 1,3-dichlorobenzene, or 1,4-dichlorobenzene) were detected in the VOC analysis or in the comprehensive, broadscreen analysis, which had been initially suspected as the potential cause of the skin rashes by the residents. It is noteworthy that THM levels were significantly increased in the hot water from all four cities, with increases of 103%, 42%, 22%, and 100% for Flint, Detroit, Grovetown, and Lyons, respectively (Fig. 1). Levels were highest in the Flint hot shower water, with an average of 74 μg/L for the two residences as compared to 38 μg/L for the cold shower water. Chloroform was the dominant THM detected, up to 58 μg/L. Lyons hot water had the lowest levels of THMs, with only 4.9 μg/L measured in the hot water, and none detected in the cold water. These lower levels were expected, as Lyons treats groundwater, which typically contain much lower concentrations of natural organic matter (NOM) precursors than surface waters.

Increased formation of THMs in the hot water was not unexpected because higher temperatures will increase the reaction rate between chlorine and NOM, and this has been observed in previous studies (Zhang et al., 2013; Dion-Fortier et al., 2009). Interestingly, Flint did have significantly higher levels of total THMs compared to other cities, but these were still below the regulatory limit of 80 μg/L, even in the hot water. It should be noted that the U.S. Environmental Protection Agency does not regulate hot water or shower water. Drinking water plants sample ambient temperature water at the plant and in locations throughout the distribution system to be analyzed for regulated contaminants (U.S. EPA, 2006).

Priority unregulated DBPs were also found from every class investigated, including haloacetaldehydes (HALs), HANs, HAMs, HNMs, and HKs (Table 2). When present, they were generally found at low and sub-μg/L levels, with trichloroacetaldehyde, dichloroacetamide, 1,1,1-trichloropropanone, and dichloroacetonitrile among the highest levels of priority unregulated DBPs, up to 23, 6.4, 5.8, and 3.6 μg/L in tap water from Grovetown, Flint, Grovetown, and Grovetown, respectively. While these levels are generally lower than most individual

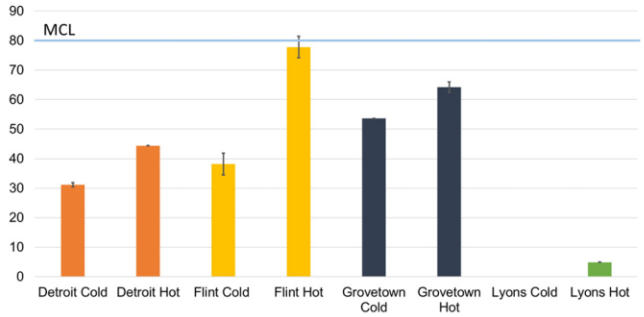

Fig. 1 – Total regulated THMs (chloroform, bromodichloromethane, chlorodibromomethane, and bromoform) in Flint, Detroit, Grovetown, and Lyons hot and cold water. MCL = Maximum contaminant level (80 μg/L regulatory limit in U.S.). Error bars represent propagated standard deviations of replicate samples.

THM levels, most of these priority unregulated DBPs are much more cytotoxic and genotoxic than the regulated THMs (Richardson et al., 2007, 2008a; Plewa et al., 2004a, 2004b, 2008a, 2008b; Muellner et al., 2007; Wagner and Plewa, 2017).

2.2. *Hot vs. cold*

As with the THMs, levels of priority unregulated DBPs were generally significantly higher in hot water compared to cold water. For example, trichloroacetaldehyde increased from 7.8 to 18.8 μg/L and dichloroacetonitrile increased from 1.5 to 2.1 μg/L in cold *vs.* hot water, respectively from Detroit. A notable exception is 1,1,1-trichloropropanone (111TCP), which was higher in Detroit cold *vs.* hot (2.0 *vs.* 0.3 μg/L) and Grovetown cold *vs.* hot (5.8 *vs.* 2.2 μg/L). This is likely due to degradation of 111TCP in the hot water tank in these residences. It should be noted that while increased temperatures can increase formation of some DBPs when residual chlorine and NOM are present, not all DBPs will be expected to be stable over time. In fact, a previous Nationwide Occurrence Study demonstrated that 111TCP and other haloketones readily degraded in the presence of chlorine in the distribution system (Weinberg et al., 2002; Krasner et al., 2006), and this was also observed in other studies (Stevens et al., 1989; Liu and Reckhow, 2013).

Haloacids, including regulated haloacetic acids, were also identified in all the water samples, and while they were not quantified in this study, their relative levels in the broadscreen analyses were semi-quantified based on relative responses to the 1,2-dibromopropane internal standard (Table 3). In most cases, trihaloacetic acids decreased from cold to hot, while dihalo- and monohaloacetic acids increased. Trichloroacetic acid (TCAA) decreased in all cases, likely as a result of thermal decomposition (Liu and Reckhow, 2013). Dichloroacetic acid (DCAA) increased in all locations except Grovetown, where increases in CIAA and chloroacetic acid (CAA) were observed (Tables 2 and 3). Enhanced formation of DCAA in hot water *vs.* cold is not unexpected, as its formation has been shown to increase with temperature (Liu and Reckhow, 2013). Notably, the highly genotoxic iodoacetic acid (IAA) was not detected in Flint or Detroit water, but was detected in Grovetown shower water, along with CIAA (Table 2).

Previously published studies have assessed the formation of common DBPs (the four regulated THMs [THM4], the

Table 3 – Semi-quantitative haloacetic acid data for Detroit, Flint, Grovetown, and Lyons shower waters. [a]

Sample		Mono-HAAs		Di-HAAs			Tri-HAAs [b]		
		CAA	BAA	DCAA	BCAA	DBAA	TCAA	BDCAA	DBCAA
Detroit	Cold	0.062	0.028	2.193	1.015	0.301	0.604	0.022	0.001
	Hot	0.110	0.053	2.926	1.261	0.301	0.209	0.005	–
Flint	Cold	0.053	0.018	2.765	1.443	0.346	0.527	0.008	0.001
	Hot	0.141	0.056	2.912	1.358	0.335	0.102	0.004	–
Grovetown	Cold	0.062	0.006	2.408	0.719	0.087	1.480	0.001	0.001
	Hot	0.081	0.006	2.199	0.844	0.093	0.856	0.001	0.001
Lyons	Cold	0.044	0.112	0.870	0.193	0.158	0.071	0.003	–
	Hot	0.015	0.004	0.878	0.328	0.377	0.053	0.002	–

Table Key: CAA = chloroacetic acid, BAA = bromoacetic acid, DCAA = dichloroacetic acid, BCAA = bromochloroacetic acid, DBAA = dibromoacetic acid, TCAA = trichloroacetic acid, BDCAA = bromodichloroacetic acid, DBCAA = dibromochloroacetic acid, TBAA = tribromoacetic acid.

[a] Semi-quantitative data is reported as the relative responses (ratio of peak areas) of each HAA to that of 1,2-dibromopropane internal standard.

[b] TBAA was not detected in any of the samples; lack of detection is indicated by a –.

nine bromo-chloro-haloacetic acids [HAA9], dichloroacetonitrile, trichloronitromethane, 1,1-dichloropropanone, and 1,1,1-trichloropropanone) in hot *vs.* cold tap water (Dion-Fortier et al., 2009; Liu and Reckhow, 2013). However, to the best of our knowledge, this study is the first to incorporate a more extensive analysis of over 50 priority unregulated DBPs in hot *vs.* cold water and indicates that many of these more toxic DBPs can be present at higher levels in hot water *vs.* cold water. This could present higher levels of exposure in showering and bathing and may be an important factor to consider in future epidemiologic studies.

2.3. Chlorinated, brominated, iodinated, and nitrogenous DBPs

Fig. 2 shows a comparison of the priority unregulated DBPs in hot water from the four cities, grouped according to chlorinated, brominated, iodinated, and nitrogen-containing species. These groupings are important to consider because brominated and iodinated DBPs are generally much more toxic than chlorinated DBPs (Plewa et al., 2004a; Richardson et al., 2007, 2008a; Jeong et al., 2015), and nitrogen-containing DBPs (N-DBPs) are generally more toxic than DBPs without nitrogen (Muellner et al., 2007; Plewa et al., 2004b, 2008a, 2008b). Chlorinated, brominated, and N-DBPs were present in all cities sampled, while iodinated DBPs were only found in water from Grovetown, likely due to natural iodide present in the source waters.

Fig. 3 shows the total concentrations (nM) of classes of priority unregulated DBPs measured in hot waters from the four sites. Different class-speciation was observed between Flint and Detroit, despite their use of the same source water. This difference may be a result of differences in the two cities' overall treatment processes (filtration, coagulation, chlorine dose, time spent in the distribution system, etc.). While Flint hot water exhibited higher THM4 levels than the other three sites (Fig. 1), it had lower total unregulated DBPs (149 nM) than both Detroit (183 nM) and Grovetown (252 nM). Not surprisingly, the total concentration observed for Lyons (1.9 nM) was much lower than that of the three surface water systems. The speciation of N-DBPs based on nM class totals indicates significantly higher total HAMs in Flint hot water *vs.* other cities, while Detroit had higher levels of total HANs than Flint but slightly less than Grovetown.

Two haloacetamides, dichloroacetamide (DCAM) and bromochloroacetamide (BCAM), were the main drivers of the higher N-DBP levels in Flint hot water, with 6.4 and 4.0 μg/L of DCAM and 2.0 and 1.1 μg/L of BCAM observed in two homes from Flint.

2.4. Nontarget identification of unknown DBPs

The nontarget (comprehensive, broadscreen) approach was helpful for uncovering other DBPs and organic compounds present in these waters, in addition to finding a few DBPs that were not detected in target analyses (Table 2). These included bromoform, 1,1,3-trichloropropanone, and 1,1,3,3-tetrachloropropanone, which were target DBPs in the quantitative analyses. As alluded to earlier, the greater concentration factor (10,000-fold) afforded with XAD extraction of larger quantities of water (10 L *vs.* 40 or 100 mL) allows even lower detection than these sensitive quantitative methods. In fact, nearly all of the priority unregulated DBPs quantified were also detected in the broadscreen analyses. Other DBPs and organic chemicals identified include 2-chlorophenol, 4-chlorophenol, dichlorophenol, 2,4,6-trichlorophenol, 2-methylpropanoic acid, 2-methylbutanoic acid, butanoic acid, dodecanoic acid, tetradecanoic acid, hexadecanoic acid, octadecanoic acid, and pentadecanoic acid. Chlorophenols are commonly used as agricultural pesticides, which can leach into source waters. This could account for their presence in all waters studied, especially Lyons, due to the large agricultural focus in the area. (U.S. DHHS, 1999). But, they can also be found as DBPs. While there would not be much concern for toxicity of the non-halogenated carboxylic acids, there is some toxicity associated with the chlorophenols (U.S. DHHS, 1999).

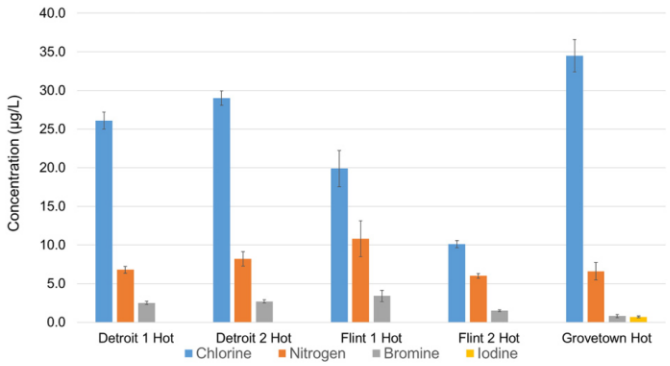

Fig. 2 – Classes of priority, unregulated DBPs in Flint, Detroit, and Grovetown hot water. Error bars represent propagated standard deviations for replicate samples.

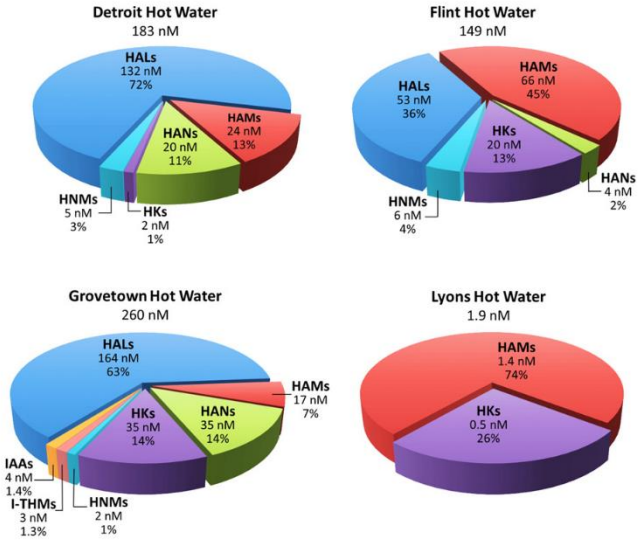

Fig. 3 – Total class concentrations (nM) and percentages of priority unregulated DBPs quantified in Detroit and Flint hot water.

2.5. *Flint vs. other water*

Overall, nothing unusual was detected in the hot or cold water from Flint, MI as compared to the other waters sampled. This is clear from both the extensive quantitative data collected, as well as from the comprehensive broadscreen analyses (Figs. 1–4, Tables 2 and 3). Fig. 4 illustrates this in a comparison of GC–MS chromatograms from Flint and Detroit hot water. Chromatograms are displayed in the regions where most DBPs elute, and are nearly identical. This is not completely unexpected because Flint has switched back to the same water source as Detroit (Lake Huron) and they are both treated

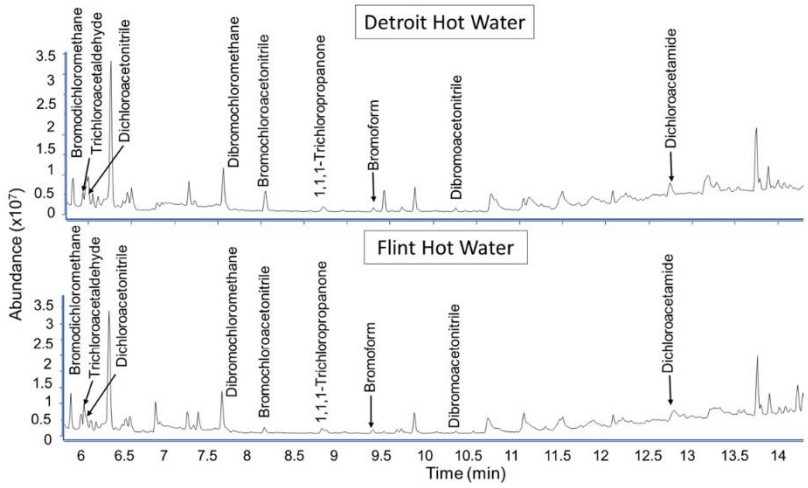

Fig. 4 – GC–MS chromatograms from comprehensive, broadscreen analysis of Flint and Detroit hot water.

with chlorine. However, it was important to thoroughly investigate the Flint hot water in case something unexpected was formed in the distribution system or in the hot water tank heaters, due to compromised distribution systems and plumbing (i.e., excessive corrosion).

3. Conclusions

In conclusion, hot shower water from Flint, MI was similar to waters sampled from three other cities and did not have unusually high levels of DBPs that could be responsible for the skin rashes observed by residents. Further, dichlorobenzene, which had been suspected as a potential cause of the skin rashes was not detected. Extensive analysis of priority unregulated DBPs and VOCs, as well as nontarget broadscreen analysis, were key in providing a more complete picture of DBP exposure for residents of Flint, and to our knowledge, this study reports the most extensive comparison of hot water to cold water in the literature for DBP concentrations. While hot water generally had higher levels of DBPs formed, likely due to increased reaction rates, average levels were still below regulatory limits. At the same time, results suggest that future epidemiologic studies may want to consider also measuring DBPs in hot water to more completely account for higher levels in showering or bathing exposures. Finally, while we did not find a "smoking gun" as the cause of the skin rashes, we only measured DBPs and other *organic* chemicals. It is possible that an inorganic chemical or microbial contaminant may be responsible.

Acknowledgments

The authors would like to acknowledge funding from the U.S. Environmental Protection Agency, Meghan Franco for assistance with XAD resin extractions, Shealy Environmental, Inc. for VOC analyses, as well as the citizens of Flint, Detroit, Grovetown, and Lyons who graciously allowed us to collect samples from their homes.

REFERENCES

Croft, H.D., Walling, D., Ambrose, G., 2015. City of Flint: Water System Questions & Answers. Department of Public Works, Flint, MI:p. 2015 (https://www.cityofflint.com/wp-content/uploads/2015_01_15-Water-System-Q-A.pdf).

Del Toral, M.A., 2015. High Lead Levels in Flint, Michigan – Interim Report. WG-15J. U.S. Environmental Protection Agency Region, Chicago, IL:p. 5. http://flintwaterstudy.org/wp-content/uploads/2015/11/Miguels-Memo.pdf.

Dion-Fortier, A., Rodriguez, M.J., Serodes, J., Proulx, F., 2009. Impact of water stagnation in residential cold and hot water plumbing on concentrations of trihalomethanes and haloacetic acids. Water Res. 43, 3057–3066.

Edwards, M., 2015. Our Sampling of 252 Homes Demonstrates a High Lead in Water Risk: Flint should be Failing to Meet the EPA Lead and Copper Rule. FlintWaterStudy, Blacksburg, VA (September 8, 2015. http://flintwaterstudy.org/2015/09/our-sampling-of-252-homesdemonstrates-a-high-lead-in-water-risk-flint-should-be-failing-to-meetthe-epa-lead-and-copper-rule/).

Flint Water Study website article, 2016a. Should You Bathe/Shower in Flint Water (or Any Water)? May 17.

Flint Water Study website article, 2016b. Some Perspectives on Rashes and Health Problems from Bathing or Showering; whether You are in Flint MI or Elsewhere in the USA. April 25.

Hanna-Attisha, M., LaChance, J., Sadler, R.C., Champney Schnepp, A., 2016. Elevated blood lead levels in children associated with the Flint Drinking Water Crisis: a spatial analysis of risk and public health response. Am. J. Public Health 106, 283–290.

Jeong, C.H., Postigo, C., Richardson, S.D., Simmons, J.E., Kimura, S.Y., Marinas, B.J., Barcelo, D., Liang, P., Wagner, E.D., Plewa, M.J., 2015. Occurrence and comparative toxicity of haloacetaldehyde disinfection byproducts in drinking water. Environ. Sci. Technol. 49, 13749–13759.

Krasner, S.W., Weinberg, H.S., Richardson, S.D., Pastor, S.J., Chinn, R., Sclimenti, M.J., Onstad, G.D., Thruston Jr., A.D., 2006. Occurrence of a new generation of disinfection byproducts. Environ. Sci. Technol. 40, 7175–7185.

Liu, B., Reckhow, D.A., 2013. DBP formation in hot and cold water across a simulated distribution system: effect of incubation time, heating time, pH, chlorine dose, and incubation temperature. Environ. Sci. Technol. 47, 11584–11591.

Muellner, M.G., Wagner, E.D., McCalla, K., Richardson, S.D., Woo, Y.-T., Plewa, M.J., 2007. Haloacetonitriles vs regulated haloacetic acids are nitrogen-containing DBPs more toxic. Environ. Sci. Technol. 41, 645–651.

NIOSH, 1994. Manual of Analytical Methods. 4th ed. Publication No. 94-113, U.S. Department of Health and Human Services (NIOSH), Cincinnati, OH.

Pieper, K.J., Tang, M., Edwards, M.A., 2017. Flint water crisis caused by interrupted corrosion control: investigating "ground zero". Environ. Sci. Technol. 51, 2007–2014.

Plewa, M.J., Wagner, E.D., Richardson, S.D., Thruston, A.D., Woo, Y.-T., McKague, A.B., 2004a. Chemical and biological characterization of newly discovered iodoacid drinking water disinfection byproducts. Environ. Sci. Technol. 38, 4713–4722.

Plewa, M.J., Wagner, E.D., Jazwierska, P., Richardson, S.D., Chen, P.H., McKague, A.B., 2004b. Halonitromethane drinking water disinfection byproducts: chemical characterization and mammalian cell cytotoxicity and Genotoxicity. Environ. Sci. Technol. 38, 62–68.

Plewa, M.J., Wagner, E.D., Muellner, M.G., Hsu, K.-M., Richardson, S.D., 2008a. Comparative Mammalian Cell Toxicity of N-DBPs and C-DBPs, in: Disinfection By-products in Drinking Water: Occurrence, Formation, Health Effects, and Control. American Chemical Society, Washington, D.C.

Plewa, M.J., Muellner, M.G., Richardson, S.D., Fasano, F., Buettner, K.M., Woo, Y.T., McKague, A.B., Wagner, E.D., 2008b. Occurrence, synthesis, and mammalian cell cytotoxicity and genotoxicity of haloacetamides: an emerging class of nitrogenous drinking water disinfection byproducts. Environ. Sci. Technol. 42, 955–961.

Richardson, S.D., Thruston Jr., A.D., Collette, T.W., Patterson, K.S., Lykins Jr., B.W., 1994. Multispectral identification of chlorine dioxide disinfection byproducts in drinking water. Environ. Sci. Technol. 28, 592–599.

Richardson, S.D., Plewa, M.J., Wagner, E.D., Schoeny, R., DeMarini, D.M., 2007. Occurrence, genotoxicity, and carcinogenicity of emerging disinfection by-products in drinking water: a review and roadmap for research. Mutat. Res. 636, 178–242.

Richardson, S.D., Fasano, F., Ellington, J.J., Crumley, F.G., Buettner, K.M., Evans, J.J., Blount, B.C., Silva, L.K., Waite, T.J., Luther, G.W., McKague, A.B., Miltner, R.J., Wagner, E.D., Plewa, M.J., 2008a. Occurrence and mammalian cell toxicity of iodinated disinfection byproducts in drinking water. Environ. Sci. Technol. 42, 8330–8338.

Richardson, S.D., Thruston Jr., A.D., Krasner, S.W., Weinberg, H.S., Miltner, R.J., Narotsky, M.G., Simmons, J.E., 2008b. Integrated disinfection byproducts mixtures research: comprehensive characterization of water concentrates prepared from chlorinated and ozonated/postchlorinated drinking water. J. Toxicol. Environ. Health A 71, 1165–1186.

Richardson, S.D., 2009. Diazomethane Generation Using Sigma-Aldrich Diazald Generator and Methylation of Carboxylic Acid Compounds: SOP – RSB-010.1 – Revision No. 0. U.S. Environmental Protection Agency, Athens, GA.

Smith, L., 2015. This mom helped uncover what was really going on with Flint's water. Michigan Radio. December 14, 2015. http://michiganradio.org/post/mom-helped-uncover-what-was-really-goingflint-s-water#stream/02.

Stevens, A.A., Moore, L.A., Miltner, R.J., 1989. Formation and control of non-trihalomethane disinfection by-products. J. Am. Water Works Assoc. 81, 54.

U.S. Department of Health and Human Services, 1999. Agency for Toxic Substances and Disease Registry. Toxicological Profile for Chlorophenols.

U.S. Environmental Protection Agency, 1996a. Method 5030B: Purge-and-Trap for Aqueous Samples – Revision 2.

U.S. Environmental Protection Agency, 1996b. Method 8260B: Volatile Organic Compounds by Gas Chromatography/Mass Spectrometry (GC/MS) – Revision 2.

U.S. Environmental Protection Agency, 2006. National primary drinking water regulations: stage 2 disinfectants and disinfection byproducts rule. Fed. Regist. 71, 387–493.

Wagner, E.D., Plewa, M.J., 2017. CHO cell cytotoxicity and genotoxicity analyses of disinfection by-products: an updated review. J. Environ. Sci. 58, 64–76.

Washington Post, 2016. Flint Residents Too Scared of the Water to Wash. That's Making them Sick. October 4. p. 2016.

Weinberg, H.S., Krasner, S.W., Richardson, S.D., Thruston Jr., A.D., 2002. The occurrence of disinfection by-products (DBPs) of health concern in drinking water: results of a nationwide DBP occurrence study. EPA/600/R02/068. U.S. Environmental Protection Agency, National Exposure Research Laboratory, Athens, GA (www.epa.gov/athens/publications/EPA_600_R02_068.pdf).

Zhang, X., Yang, H., Wang, X., Fu, J., Xie, Y., 2013. Formation of disinfection byproducts: effect of temperature and kinetic modeling. Chemosphere 90, 634–639.

Environmental Science & Technology

Article

pubs.acs.org/est

Progressive Increase in Disinfection Byproducts and Mutagenicity from Source to Tap to Swimming Pool and Spa Water: Impact of Human Inputs

Eric J. Daiber,[†,▽] David M. DeMarini,[‡] Sridevi A. Ravuri,[†,○] Hannah K. Liberatore,[§] Amy A. Cuthbertson,[§] Alexis Thompson-Klemish,[§] Jonathan D. Byer,[∥] Judith E. Schmid,[‡] Mehrnaz Z. Afifi,[⊥] Ernest R. Blatchley, III,[⊥,#] and Susan D. Richardson*[,§]

[†]Student Services Authority, U.S. Environmental Protection Agency, National Exposure Research Laboratory, Athens, Georgia 30605, United States

[‡]National Health and Environmental Effects Research Laboratory, U.S. Environmental Protection Agency, Research Triangle Park, North Carolina 27711, United States

[§]Department of Chemistry and Biochemistry, University of South Carolina, 631 Sumter St., Columbia, South Carolina 29208, United States

[∥]LECO Corp., 3000 Lakeview Ave., St. Joseph, Michigan 49085, United States

[⊥]Lyles School of Civil Engineering, Purdue University, 550 Stadium Mall Drive, West Lafayette, Indiana 47907, United States

[#]Division of Environmental & Ecological Engineering, Purdue University, 500 Central Drive, West Lafayette, Indiana 47907, United States

Supporting Information

ABSTRACT: Pools and spas are enjoyed throughout the world for exercise and relaxation. However, there are no previous studies on mutagenicity of disinfected spa (hot tub) waters or comprehensive identification of disinfection byproducts (DBPs) formed in spas. Using 28 water samples from seven sites, we report the first integrated mutagenicity and comprehensive analytical chemistry of spas treated with chlorine, bromine, or ozone, along with pools treated with these same disinfectants. Gas chromatography (GC) with high-resolution mass spectrometry, membrane-introduction mass spectrometry, and GC-electron capture detection were used to comprehensively identify and quantify DBPs and other contaminants. Mutagenicity was assessed by the *Salmonella* mutagenicity assay. More than 100 DBPs were identified, including a new class of DBPs, bromoimidazoles. Organic extracts of brominated pool/spa waters were 1.8× more mutagenic than chlorinated ones; spa waters were 1.7× more mutagenic than pools. Pool and spa samples were 2.4 and 4.1× more mutagenic, respectively, than corresponding tap waters. The concentration of the sum of 21 DBPs measured quantitatively increased from finished to tap to pool to spa; and mutagenic potency increased from finished/tap to pools to spas. Mutagenic potencies of samples from a chlorinated site correlated best with brominated haloacetic acid concentrations (Br-HAAs) (r = 0.98) and nitrogen-containing DBPs (N-DBPs) (r = 0.97) and the least with Br-trihalomethanes (r = 0.29) and Br−N-DBPs (r = 0.04). The mutagenic potencies of samples from a brominated site correlated best (r = 0.82) with the concentrations of the nine HAAs, Br-HAAs, and Br-DBPs. Human use increased significantly the DBP concentrations and mutagenic potencies for most pools and spas. These data provide evidence that human precursors can increase mutagenic potencies of pools and spas and that this increase is associated with increased DBP concentrations.

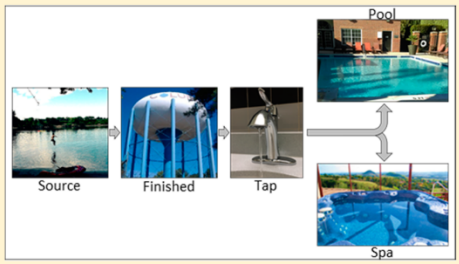

INTRODUCTION

Although swimming is regarded as a safe and healthy form of exercise, disinfection byproducts (DBPs) are formed in pools when chlorine or other disinfectants are used. DBPs are formed by the reaction of disinfectants with organic matter,[1−19] including natural organic matter from source water and human inputs, such as sweat, urine, pharmaceuticals, and

Special Issue: Jerry Schnoor's Lasting Influence on Global and Regional Environmental Research

Received: February 16, 2016
Revised: April 27, 2016
Accepted: April 28, 2016
Published: April 28, 2016

DOI: 10.1021/acs.est.6b00808
Environ. Sci. Technol. 2016, 50, 6652−6662

Table 1. Samples Collected[a]

samples	collection date	disinfectant	location
1-Raw	9/15/11	none	drinking water treatment plant (site 1)
1-Cl Finished	9/15/11	hypochlorite	drinking water treatment plant (site 1)
1-Cl Tap	9/16/11	hypochlorite	large university aquatic center (site 1)
1-Cl Average Use Public Pool (Indoor)	9/16/11	hypochlorite	large university aquatic center (site 1)
1-Cl Clean Public Pool (Indoor)	1/3/12	hypochlorite	large university aquatic center (site 1)
1-Cl Heavily Used Public Pool (Indoor)	11/2/11	hypochlorite	large university aquatic center (site 1)
1-Cl Clean Public Spa (Indoor)	9/16/11	hypochlorite	large university aquatic center (site 1)
1-Cl Heavily Used Public Spa (Indoor)	11/2/11	hypochlorite	large university aquatic center (site 1)
2-Raw	11/15/11	none	drinking water treatment plant (site 2)
2-Cl Finished	11/15/11	hypochlorite	drinking water treatment plant (site 2)
2-Cl Tap	11/16/11	hypochlorite	large university aquatic center (site 2)
2-Br Average Use Public Pool (Indoor)	11/16/11	bromine	large university aquatic center (site 2)
2-Br Average Use Public Spa (Indoor)	11/16/11	bromine	large university aquatic center (site 2)
2-Br Clean Public Pool (Indoor)	1/5/12	bromine	large university aquatic center (site 2)
2-Br Clean Public Spa (Indoor)	1/6/12	bromine	large university aquatic center (site 2)
2-Br Heavily Used Public Spa (Indoor)	1/5/12	bromine	large university aquatic center (site 2)
3-Cl Public Pool (Indoor)	10/21/11	hypochlorite	large university aquatic center (site 3)
3-Cl Public Spa (Indoor)	10/21/11	hypochlorite	large university aquatic center (site 3)
4-Raw	11/8/11	none	drinking water treatment plant (site 4)
4-Cl Finished	11/8/11	hypochlorite	drinking water treatment plant (site 4)
4-Cl Tap	11/9/11	hypochlorite	private residence (site 4)
4-Cl Private Spa (Outdoor)	11/9/11	dichloroisocyanuric acid	private residence (site 4)
5-Cl Tap	2/7/12	hypochlorite	private residence (site 5)
5-Br Private Spa (Outdoor)	2/7/12	bromine	private residence (site 5)
6-O_3–Cl Tap	12/21/11	ozone, hypochlorite	neighborhood pool (site 6)
6-O_3–Cl Public Pool (Outdoor)	12/21/11	ozone, hypochlorite	neighborhood pool (site 6)
7-Tap-Undisinfected Groundwater	12/19/11	none	private residence (site 7)
7-O_3 Private Spa (Outdoor)	12/19/11	ozone	private residence (site 7)

[a]"Clean" situations for spas correspond to 24 h after draining, cleaning, and disinfection; "heavily used" is after 3 weeks, just prior to draining and cleaning. "Clean" situation for Pool 1 and 2 denotes sampling after winter holidays when pool was not used; "heavily used" was 24 h after a major swim meet. All other pool and spa situations represent average use. "Bromine" at Site 2 was 1-bromo-3-chloro-5,5-dimethyl hydantoin (BCDMH); "bromine" at Site 5 was created by mixing NaBr and trichloroisocyanuric acid.

personal-care products. Although disinfection is important to inactivate harmful pathogens, adverse health effects associated with exposure to DBPs, such as asthma and bladder cancer, have been noted in human epidemiologic studies.

Increased incidences of asthma and other respiratory effects were found in several epidemiologic studies of Olympic swimmers and pool workers, with less clear evidence for recreational adult swimmers and children.[20−25] There are also recent reports of increased ocular, respiratory, and cutaneous symptoms for swimmers and pool workers,[26−28] as well as sore throat and phlegm reported more frequently for lifeguards and swimming instructors.[29] Short-term changes in respiratory biomarkers were also reported for swimmers in a chlorinated pool.[30] In addition, an association was found between testicular hormones at adolescence and attendance at chlorinated swimming pools during childhood, with swimmers strongly associated with lower levels of serum inhibin B and total testosterone.[31] Increased bladder cancer[32−34] and genotoxic effects[35] were also reported in swimmers. A new study in rats showed effects on their health, training, and metabolic profiles when tested in a 12-week swimming training program in simulated chlorinated pools.[36]

Trichloramine, formed by the reaction of chlorine with constituents of human urine and sweat,[2,37,38] is suspected to be associated with asthma and other respiratory effects, but causality is not yet proven. Trichloramine has a high Henry's law constant, so it is present at high concentrations in pool air.[39,40] Indoor swimming pool air shows similar inflammatory effects. However, it is likely that other air contaminants (i.e., DBPs) also contribute.[41]

Trihalomethanes (THMs) were the first class of DBPs studied in pools,[5,9] and now there are quantitative data for many other classes.[4,42−49] Although DBPs are regulated in drinking water, only Germany has a regulation for pools, with a maximum level of 20 μg/L for total THMs.[50] France recently set a recommended limit of 100 μg/L for total THMs.[51]

The first comprehensive, broadscreen studies of DBPs in pools were published in 2007 (outdoor pools)[1] and 2010 (indoor pools).[52] These studies went beyond target analysis of a few DBPs like THMs and HAAs to comprehensively identify all DBPs detected by GC−MS. Membrane-introduction mass spectrometry (MIMS) and liquid chromatography (LC)-MS also have been used to identify volatile amines[2,4,53] and halophenols.[54] In 2016, a study of DBPs and mutagenicity in freshwater and seawater pools disinfected with chlorine was published in which THMs, haloacetic acids (HAAs), haloacetonitriles, haloketones, chloral and bromal hydrate, and halonitromethanes were quantified.[49]

For DBPs quantified in pools, HAA concentrations are among the highest, up to 6800 μg/L for dichloroacetic acid.[55] HAAs are not volatile and will accumulate in pool waters. Although studies on DBPs in pools have increased over the last 5 years, there are only a few studies of spas, including measurements of THMs and nitrosamines.[53,56] Recent reviews

DOI: 10.1021/acs.est.6b00808
Environ. Sci. Technol. 2016, 50, 6652−6662

summarize the occurrence, implications, and control of DBPs in swimming pools.[12,57]

There is also a paucity of toxicity data for spas. Recent mammalian cell genotoxicity data for a chlorinated spa revealed significantly higher genotoxicity than the incoming tap water, but less than an unheated chlorinated pool at the same facility.[57] To the best of our knowledge, there are no reports on mutagenicity of spa water, and only three on pool water.[49,52,58] All found that pool waters were mutagenic, but did not evaluate source or tap water for comparison. Three studies evaluated the ability of pool and spa waters to induce DNA damage; all found these waters to be genotoxic;[59−63] one study evaluated only cytotoxicity.[64] Collectively, the genotoxicity studies demonstrated that disinfection of recreational waters by brominating agents resulted in more genotoxic waters than by chlorinating agents.

Here we report the first integrated mutagenicity and comprehensive chemistry analysis of spa water, as well as the first comprehensive study of the progression of DBP formation and accompanying mutagenicity from source water to finished water at the drinking water treatment plant, to tap water at the pool/spa facility, to the spa and swimming pool. We sampled public and private pools and spas from seven locations in the U.S. where chlorine, bromine, ozone, or ozone-chlorine was used for disinfection. Two sites were also sampled during heavily used situations following large swimming competitions (pools) or after 3 weeks of continuous use (spas). These heavily used situations were compared to clean situations, sampling 24 h following draining-cleaning-refilling-disinfection of the spas and after normal or limited use of the pools (no swimming competitions). In this way, the effect of increased human inputs or bather load (precursors) could be assessed.

EXPERIMENTAL METHODS

Sampling. Water samples (52 L) were collected from indoor (Sites 1−3) and outdoor (Sites 4−7) spas and swimming pools from 7 locations in the U.S. where chlorine, bromine, ozone, or ozone-chlorine was used for disinfection (Table 1). At 6 sites, we also collected the corresponding tap waters used to fill these spas and pools; at 2 sites we collected water from the corresponding drinking water treatment plants and the untreated source water. Collectively, these samples encompassed the complete source → finished → tap → spa/pool pathway. Public pool and spa samples were collected from three large university aquatic centers in the U.S., which used the same disinfectant for both their pool and spa, and each had the same tap water feeding both. Sites 1 and 3 used chlorine (hypochlorite); Site 2 used bromine (1-bromo-3-chloro-5,5-dimethylhydantoin [BCDMH]). Pool and spa samples were also collected from private homeowners who disinfected using either chlorine (dichloroisocyanuric acid; Site 4), bromine (NaBr and trichloroisocyanuric acid; Site 5), or ozone (Site 7). One public pool (Site 6) used ozone-chlorine.

Public pools and spas at two large university aquatic centers (Sites 1 and 2) were also sampled during heavily used situations following large swimming competitions (pools) or after 3 weeks of continuous use (spas). These heavily used situations were compared to "clean" situations (24 h following draining-cleaning-refilling-disinfection of the spa or after normal use of pools and no swimming competitions or after winter holidays). Water samples were collected headspace-free in 2 L Teflon bottles.

XAD Resin Extraction. For comprehensive DBP identification and mutagenicity analyses, samples (52 L) were acidified to pH between 1 and 2 and extracted using XAD resins and ethyl acetate.[63] Final extracts were concentrated using a Turbovap and a gentle stream of nitrogen and were divided three ways (each 1.0 mL, equivalent to 17.33 L water) for comprehensive GC−MS, mutagenicity, and genotoxicity analysis. Site 1, 2, 4, and 5 samples were extracted within 2 h after sampling. Samples from Sites 3, 6, and 7 were extracted 24 h after overnight shipment on ice.

Comprehensive GC−MS Analysis. Half of the 1.0 mL XAD resin extract was derivatized with diazomethane for identification of halo-acids (through their corresponding methyl esters);[63] the other half was analyzed directly. Ozonated pool and spa samples (750 mL) were derivatized using pentafluorobenzylhydroxylamine for detection of aldehydes and ketones.[64] DBP standards, solvents, and reagents were purchased at highest purity from CanSyn Chem. Corp. (Toronto, ON, Canada), Oakwood Chemical (Columbia, SC), Sigma-Aldrich (Milwaukee, WI), VWR (Radnor, PA), and Fisher Scientific (Waltham, MA).

Comprehensive GC−MS analyses were performed using electron ionization (EI) on a Waters Autospec high-resolution magnetic-sector mass spectrometer (Milford, MA) equipped with an Agilent model 6890 GC and operated at an accelerating voltage of 8 kV and source temperature of 200 °C, in both low-resolution (1000) and high-resolution (10 000) modes. Injections of 1 μL of the extracts were introduced via a split/splitless injector (in splitless mode) onto a GC column (Rtx-5, 30 m × 0.25 mm i.d., 0.25 μm film thickness, Restek, Bellefonte, PA). The GC temperature program consisted of an initial temperature of 35 °C (4 min), increased at 9 °C/min to 285 °C, and held for 30 min. Transfer lines were held at 280 °C and the injection port at 250 °C.

Samples were also analyzed on a LECO GC−HRT high-resolution time-of-flight mass spectrometer (St. Joseph, MI) operated in EI and chemical ionization (CI) modes at high resolution (25 000) and ultrahigh resolution (50 000) (full-width-at-half-maximum, fwhm), with a mass range m/z 30−650, 5 spectra/s, and source at 200 °C. Extracts were introduced using an Agilent 7693 autosampler with a 7890B GC equipped with a multimode inlet operated in cold splitless mode. The GC column and oven program were the same as described above.

Mass spectra of unknown compounds were subjected to library database searching (using the National Institute of Standards and Technology [NIST] and Wiley databases). However, many DBPs were not present in either database; in those cases, and also where a library match was insufficient to offer a tentative identification, high-resolution MS was used to provide empirical formulas for molecular ions and fragments. Mass spectra were also interpreted extensively to provide tentative structural identifications. When possible, pure standards were obtained to confirm identifications through a match of retention times and mass spectra.

Quantitative Analyses. Twenty-one target DBPs were quantified by EPA methods; six were quantified by MIMS. These included four THMs (THM4; chloroform, bromodichloromethane, dibromochloromethane, and bromoform), nine HAAs (HAA9; chloro-, bromo-, dichloro-, bromochloro-, dibromo-, bromodichloro-, dibromochloro-, and tribromoacetic acid), four haloacetonitriles (dichloroacetonitrile, trichloroacetonitrile, bromochloroacetonitrile, and dibromoacetonitrile),

DOI: 10.1021/acs.est.6b00808
Environ. Sci. Technol. 2016, 50, 6652−6662

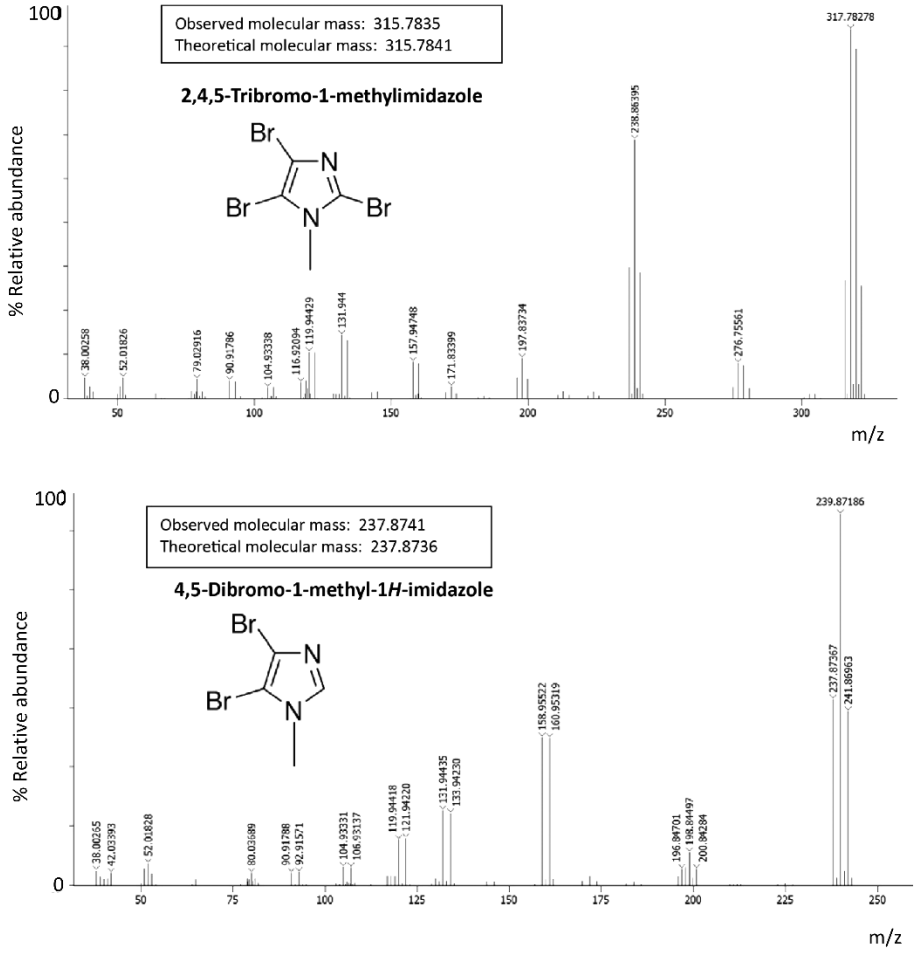

Figure 1. Mass spectra for confirmed brominated methylimidazoles.

two haloketones (1,1-dichloro- and 1,1,1-trichloropropanone), two cyanogen halides (cyanogen chloride and cyanogen bromide), one haloaldehyde (trichloroacetaldehyde [chloral hydrate]), one halonitromethane (trichloronitromethane [chloropicrin]), and four chloramines (dichloromethylamine, monochloramine, dichloramine, and trichloramine). HAAs were measured by EPA Method 552.2, quenching samples with ammonium chloride. Chloramines and cyanogen halides were measured using MIMS.[2,4,40,53] Other DBPs were measured by EPA Method 551.1, quenching with ammonium chloride and sodium sulfite. Sites 1, 2, and 4 water samples for MIMS analysis were shipped overnight on ice to Purdue University; because the disinfectant was not quenched for these samples, some changes in DBP concentrations may have occurred. Therefore, MIMS concentrations should be viewed as approximate. Total organic carbon (TOC) of source waters was measured using a Shimadzu 5000 TOC Analyzer (Table S1, Supporting Information (SI)).

Total Organic Halogen. Total organic chlorine (TOCl), bromine (TOBr), and iodine (TOI) measurements were made using a published procedure.[65] Briefly, a Mitsubishi AQF-100 precombustion station (Cosa Instruments, Norwood, NJ) was interfaced to an ion chromatography system (Dionex, Sunnyvale, CA) to separate and detect the halide ions. Further details available in SI.

Mutagenicity. Ethyl acetate extracts were solvent-exchanged into dimethyl sulfoxide (DMSO) at 10 000× and evaluated in the *Salmonella* plate-incorporation mutagenicity assay in strain TA100 in the absence of metabolic activation as described previously.[52] Briefly, various amounts of the extract

DOI: 10.1021/acs.est.6b00808
Environ. Sci. Technol. 2016, 50, 6652−6662

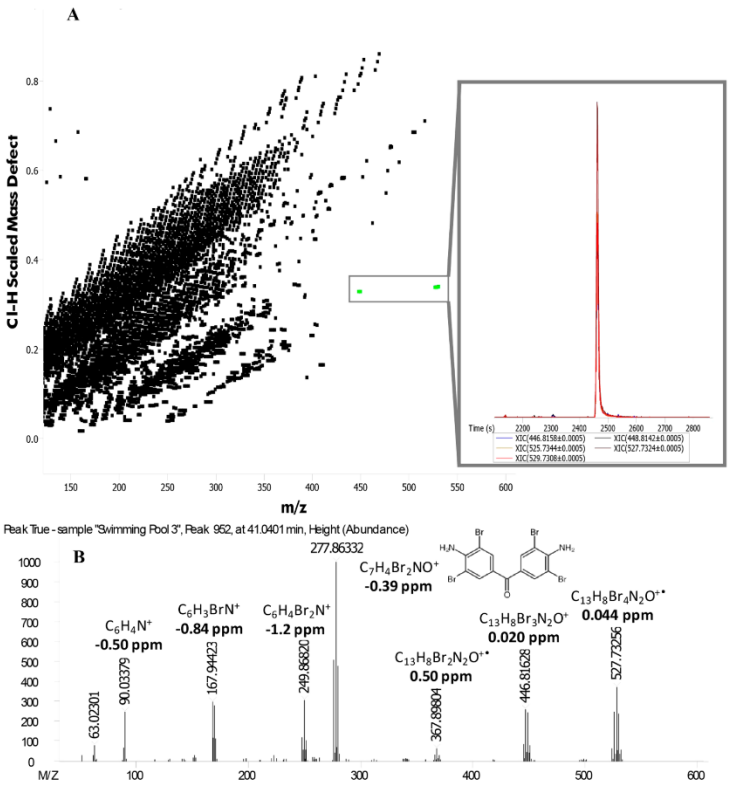

Figure 2. (A) Cl−H mass-defect plot for Site 2 Average Use Public Pool (brominated) water extract. The m/z ions shown in green belong to one unique chromatographic peak represented with (B) its deconvoluted mass spectrum. The compound was tentatively identified as 4,4′-diamino-3,5,3′,5′-tetrabromo-benzophenone, a new DBP.

and 100 μL of overnight cell culture were added to 2.5 mL of molten top-agar and poured onto bottom-agar plates containing VBME medium with a trace amount of histidine; plates were incubated for 3 days at 37 °C; colonies were counted using an automatic colony counter. Samples were viewed as mutagenic if they produced a dose-related increase in revertants (rev)/plate that reached or exceeded 2-fold relative to the DMSO controls. Details of positive controls are provided in footnotes of the mutagenicity data tables in SI.

To assess whether any environmental mutagens requiring metabolic activation were present in the source waters, all three source waters were also tested with metabolic activation using Aroclor-induced Sprague−Dawley male rat liver S9 at 1 mg of protein/plate (Moltox, Boone, NC). S9 is the supernatant from a 9000g centrifugation of homogenized rat liver that provides enzymes required to activate some environmental chemicals to mutagenic (electrophilic) forms.

Samples were evaluated initially at 9 doses (0.001 to 1 L-equivalents/plate, L-eq/plate), at 1 plate/dose; a replicate experiment was typically done at fewer doses. Selected samples from Site 2 were also evaluated in one experiment (due to limited amounts of these samples) in strain RSJ100, which expresses the rat *GSTT1* gene, and its control strain TPT100. These strains are homologous to TA100, except they do not contain the pKM101 plasmid and either do or do not express *GSTT1*. Increased mutagenicity in strain RSJ100 relative to TPT100 indicates Br-DBPs account for some of the mutagenicity.[52] A positive result in all strains was defined as a dose-related increase in mutant colonies (revertants, rev) per plate that reached or exceeded a 2-fold increase relative to the DMSO control.

Statistical Analyses. We estimated the mutagenic potency (rev/L-eq) by calculating the slope of the best-fit line of rev across dose. We used linear-regression models (SAS/Stat v.9.4 Proc GLM) to estimate slopes for the water extracts and compare these slopes among samples and groups of samples. See SI for further details.

■ RESULTS AND DISCUSSION

DBPs Identified and Quantified. Most of the 27 target DBPs were found at concentrations ranging from 0.9 μg/L for cyanogen chloride in Site 1 Finished Water to 3658 μg/L for

DOI: 10.1021/acs.est.6b00808
Environ. Sci. Technol. 2016, 50, 6652 6662

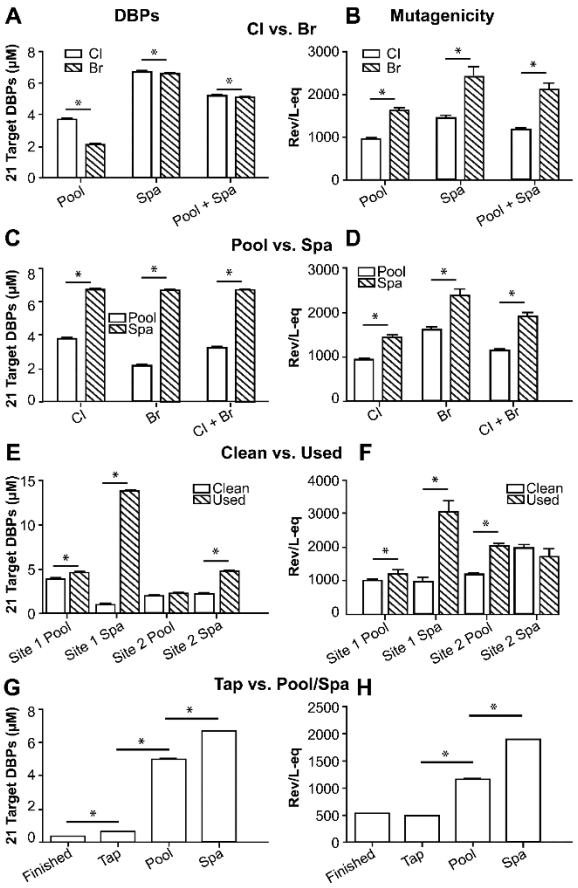

Figure 3. Comparisons of the concentrations (μM) of the sum of the 21 target DBPs and the mutagenic potencies (rev/L-eq) of various categories of water samples. Each bar in the mutagenic potency histograms is the mean ± SE of the average of the slope from the linear regressions for the samples in each category. DBP and mutagenicity data are from SI Table S22. Panels A and B compare the role of chlorination vs bromination relative to DBP concentrations and mutagenic potencies; Panels C and D compare the concentrations of DBPs and mutagenic potencies of pool vs spa samples; Panels E and F compare the role of human inputs on the DBP concentrations and mutagenic potencies of pools and spas at two sites; and Panels G and H compare the DBP concentrations and mutagenic potencies of water samples from Finished to Tap to Pool and Spa. All significant comparisons are $P < 0.04$; nonsignificant comparisons are (E) $P = 0.176$ for DBP concentration for Clean vs Used Pool at Site 2, (F) $P = 0.095$ for mutagenicic potency for Clean vs Used Spa at Site 2, and (H) $P = 0.361$ for mutagenic potency for Finished vs Tap.

dichloromethylamine in Site 1 Heavily Used Spa (SI Tables S2−S15). More than 100 DBPs were identified in the comprehensive analyses, including an iodo-THM, bromoimidazoles, bromoanilines, haloacids, halonitriles, haloamides, halonitromethanes, haloketones, haloaldehydes, halophenols, halobenzenes, halobenzenediols, bromomethanesulfenic acid esters, aldehydes, ketones, and an organic chloramine (SI Tables S10−S18).

Pool and spa samples were highly complex, with numerous chromatographic peaks (SI Figure S1). Due to apparent high concentrations (overloaded chromatographic peaks), most XAD resin extracts were diluted 1:10 to obtain nondistorted mass spectra.

Several DBPs were not in mass spectral library databases, and new ones were identified, including 4,5-dibromo-1-methyl-*1H*-imidazole, 2,4,5-tribromo-1-methylimidazole, 2,3,5-tribromocyclopenta-2,4-dienol, 2-bromopropanedioic acid, 4,4′-diamino-3,5,3′,5′-tetrabromo-benzophenone, 2-(bromo-4-(1,1-dimethylhexyl)phenoxy)ethoxy-acetic acid methyl ester, 2,4-dibromo-1-methoxybenzene, a series of new bromomethanesulfenic acid esters, as well as a homologous series of bromoanilines: dibromo-, tribromo-, tetrabromo-, and pentabromoaniline. The bromoimidazoles (Figure 1), bromoanilines

DOI: 10.1021/acs.est.6b00808
Environ. Sci. Technol. 2016, 50, 6652−6662

(SI Figure S2), and bromomethanesulfenic acid esters (SI Figure S3) represent new classes of DBPs not reported previously. The identities of the two new bromoimidazoles and 2,4,6-tribromoaniline were confirmed by a match of mass spectra and retention times with authentic standards.

High-Resolution MS. High-resolution MS was useful for confirming molecular formulas for new DBPs. Moreover, mass-defect plots using high-resolution MS data enabled the detection of several unknown halogenated DBPs in these complex mixtures. SI Figure S4 illustrates how mass-defect plots can group chemical classes together, enabling detection of halogenated and other chemical groups, such as hydrocarbons and siloxanes. Chemical classes fall along straight lines in these graphs, providing additional structural information.

A Cl−H or Br−H mass-defect plot (Figure 2 and SI Figure S5), which applies a Cl and Br filter to remove ions without M+2 ions and locates peaks occurring within a ±5 ppm Da range, enabled the detection of several halogenated DBPs, including the bromoimidazoles. Specifically, 4,5-dibromo-1-methyl-1*H*-imidazole was identified in brominated spa samples (Figure 1), and 2,4,5-tribromo-1-methylimidazole was identified in brominated pool/spa waters from a large university aquatic center (Site 2). High-resolution MS provided accurate mass information for molecular ions and fragment ions, with empirical formulas matching these assignments. Isotopic patterns also matched with distinctive 2-bromine and 3-bromine patterns in each, respectively.

Neither of these bromoimidazoles was in the NIST mass spectral library; therefore, tentative identifications were confirmed through the analysis of authentic standards. Because there was potential for other isomers, including related bromopyrazoles, we obtained and analyzed several other chemical standards, including 2,5-dibromo-1-methyl-imidazole; 2,4-dibromo-1-methyl-1*H*-imidazole; 2,5-dibromo-4-methylimidazole; 4,5-dibromo-2-methylimidazole; 3,4-dibromo-4-methylpyrazole; and 3,4-dibromo-1-methylpyrazole, which had similar mass spectra but different retention times.

Studies indicate that 2,4,5-tribromoimidazole is the major product from the reaction of imidazole with bromine,[66] consistent with discovery of a similar fully brominated species in brominated spa water. In the public brominated spa and pool (Site 2), the brominated disinfectant, BCDMH, releases chlorine and bromine in the form of HOCl and HOBr, respectively, through the following reaction: $BrClR + 2\ H_2O \rightarrow HOBr + HOCl + RH_2$, in which R is the dimethylhydantoin group (a 5-membered ring containing two nitrogens separated by two carbonyl groups). Both HOBr and HOCl can oxidize and inactivate pathogens; when this occurs for HOBr, Br^- is released back into the water, which subsequently reacts with HOCl through the following reaction to form additional HOBr: $Br^- + HOCl \rightarrow HOBr + Cl^-$.

Consequently, BCDMH is considered a "bromine" disinfectant, and it is not surprising to find predominantly brominated DBP species in these waters. At the same time, some chlorinated DBPs will form due to the presence of chlorine in the BCDMH molecule and release of HOCl. Excess HOBr in brominated pools and spas could explain the formation of the trisubstituted imidazole vs mono- and dibrominated isomers. For example, in the synthesis of 4,5-dibromo-1-methyl-1*H*-imidazole, the formation of the 2,4,5-tribromo-1-methyl-1*H*-imidazole also occurs.[67] Possible sources of imidazole precursors include the amino acid histidine, introduced via urine, and pharmaceuticals and skin-care products containing an imidazole group. Some antibiotics, sedatives, and antifungal drugs contain an imidazole group in their structures.

The use of high-resolution MS and mass-defect plots also enabled the first detection of ibuprofen in Site 2 Average Use Spa sample, discovered in its parent form (carboxylic acid) and as its methyl ester in the methylated sample (SI Figure S6). Notably, ibuprofen was not present in raw, finished, or tap water used to fill the spa. Thus, it clearly resulted from human inputs, most likely urine.

Mutagenicity. The primary mutagenicity data (rev/plate) and mutagenic potencies (rev/L-eq) are shown in SI Tables S19 and S20, and data are plotted in Figure 3A-H. None of the three raw waters was mutagenic either in the absence or presence of S9 (SI Table S19). All waters disinfected with chlorine or bromine were mutagenic, including ozonated-chlorinated pool and tap waters (Site 6, SI Table S19). However, spa water treated by ozonation of groundwater (Site 7) was not mutagenic (SI Table S19). Mutagenic potencies and the sum of the concentrations of the 21 target DBPs for various categories of waters (SI Table S22) are plotted in Figure 3 and discussed further below.

Comparison Across Disinfectants. On average, the concentration of solely chlorinated DBPs was greater than that of solely brominated DBPs in the pool waters (Figure 3A). But, for spas, levels were somewhat similar (SI Tables S6−S9). For example, on a molar basis, the concentration of chloroform (762 nM) in the 1-Cl Heavily Used Pubic Spa was similar to that of bromoform (782 nM) in 2-Br Heavily Used Public Spa. However, MIMS data showed much higher levels, both on a molar and mass basis, for cyanogen bromide vs cyanogen chloride in brominated spas vs chlorinated spas (SI Figure S8, Tables S10−S15).

There was a greater concentration of bromine-containing DBPs (Br-DBPs) in the brominated pool and spas, on both a parts-per-billion (393−2956 μg/L) and a nanomolar (1709−13341 nM) basis, at Sites 2 and 5 than in the chlorinated pools and spas (1.5−283 μg/L; 7.1−1536 nM) (SI Tables S21−S22). Several new brominated DBPs, including the bromoimidazoles and bromoanilines, were also observed in the brominated spas and pools (SI Tables S16−S17). This enhanced formation of Br-DBPs with use of bromine disinfectants was also reflected in the TOX measurements, where concentrations of TOBr in the 2 samples from the brominated pool at Site 2 were 14.7−41.5× those in the sample from the chlorinated pool at Site 1 (Table 2, SI Figure S9A). Likewise, TOBr concentrations in the three samples from the brominated spa at Site 2 were 2.2−5.5× those in the sample from the chlorinated spa from Site 1 (Table 2, SI Figure S9B).

We note that the disinfectant used at Site 2, BCDMH, is itself a brominated organic compound. Thus, before bromine is released to form HOBr, the parent molecule will likely make up a significant proportion of the TOBr. Although we did not quantify BCDMH in the samples, it was identified in GC−MS analyses, with a large peak eluting over 16−18 min (SI Figure S1). On the other hand, the private brominated spa (Site 5), which did not have an organic bromine disinfectant, showed the highest level of TOBr (8093 μg/L as Cl^-), which was 429× that of Site 4 Private Chlorinated Spa (Table 2, SI Figure S9B). This indicates that Br-DBPs were a major contributor to TOBr at Site 5 and likely contributed substantially to the TOBr at Site 2.

DOI: 10.1021/acs.est.6b00808
Environ. Sci. Technol. 2016, 50, 6652−6662

Table 2. Total Organic Chlorine (TOCl) and Total Organic Bromine (TOBr) Measurements (μg/L ± SD)

sampling location	TOCl as Cl^-	TOBr as Br^-	TOBr as Cl^-[a]
1-Cl Clean Public Pool	4791 ± 47	137 ± 34	60.7 ± 15.1
1-Cl Heavily Used Public Pool	4828 ± 28	280 ± 2	124 ± 0.9
1-Cl Heavily Used Public Spa	9197 ± 697	987 ± 29	438 ± 13
2-Cl Finished	672 ± 109	43.2 ± 13.4	19.2 ± 6.0
2-Cl Tap	995 ± 35	39.6 ± 3.1	17.6 ± 1.4
2-Br Clean Public Pool	1511 ± 22	5688 ± 912	2524 ± 405
2-Br Average Use Public Pool	1162 ± 347	4106[b]	1822[b]
2-Br Average Use Public Spa	1394 ± 37	5444 ± 802	2416 ± 356
2-Br Clean Public Spa	950 ± 388	2198 ± 255	975 ± 113
2-Br Heavily Used Public Spa	1294 ± 81	4948 ± 433	2195 ± 192
3-Cl Public Pool	1428[b]	183 ± 18	81.0 ± 7.8
3-Cl Public Spa	7132[b]	483[b]	214[b]
4-Cl Finished	822 ± 119	39.5 ± 1.6	17.5 ± 0.7
4-Cl Tap	1003 ± 239	51.0 ± 0.06	22.6 ± 0.03
4-Cl Private Spa	3846 ± 240	42.5 ± 11.5	18.9 ± 5.1
5-Cl Tap	1495 ± 74	585 ± 21	259 ± 9
5-Br Private Spa	13860 ± 2191	18239 ± 520	8093 ± 231
6-O_3–Cl Tap	1795 ± 117	117 ± 26	52.0 ± 11.7
6-O_3–Cl Public Pool	9512 ± 1259	83.3 ± 16.7	37.0 ± 7.4
7-Tap-Undisinfected Groundwater	285 ± 14	8.8 ± 3.2	3.9 ± 1.4
7-O_3 Private Spa	1081 ± 36	53.1 ± 37.7	23.5 ± 16.7

[a]TOBr normalized as μg/L as Cl^-. [b]No replicate measurement.

The ozonated-chlorinated pool (Site 6) and ozonated spa (Site 7) samples contained several nonhalogenated aldehydes and ketones (SI Table S18), with the ozonated-chlorinated pool having chlorinated aldehydes and ketones (SI Table S17). Aldehydes and ketones are commonly formed in ozonated drinking water,[64,68] and increased levels of chlorinated aldehydes and ketones have been observed in ozonated-postchlorinated drinking water.[64]

Averaging the mutagenic potencies of brominated or chlorinated water samples in the various categories (SI Table S19) led to the following observations. The mutagenic potency of brominated spas (2387.7 rev/L-eq) was 1.7× greater than that of chlorinated spas (1451.7 rev/L-eq) ($P < 0.001$), and the mutagenic potency of brominated pools (1607.3 rev/L-eq) was 1.7× greater than that of chlorinated pools (961.2 rev/L-eq) ($P < 0.001$). The mutagenic potency of brominated pools and spas combined (2117.2 rev/L-eq) was 1.8× greater than that of chlorinated pools and spas combined (1179.0 rev/L-eq) ($P < 0.001$). Although average concentrations of Cl-DBPs were higher than that of Br-DBPs for pools (Figure 3A), average brominated waters were more mutagenic than chlorinated waters (Figure 3B). This is likely due to the fact that Br-DBPs are more mutagenic than Cl-DBPs.[1]

Spas vs Pools. Concentrations of the 21 target DBPs were higher in spas than in pools (Figure 3C). This was possibly due to higher temperatures of spa vs pool water, which increases chemical reaction rates. Although spas are typically drained and cleaned occasionally (Sites 1 and 2 were drained and cleaned every 3 weeks), pools are almost never drained. Thus, different temperatures and the way waters are managed may play a role in the higher DBP and mutagenicity levels found in spas vs pools.

Averaging mutagenic potencies of brominated or chlorinated water samples in the various categories (SI Table S19) led to the following observations. Chlorinated spas (1443.4 rev/L-eq) were 1.5× more mutagenic than chlorinated pools (962.6 rev/L-eq) ($P < 0.001$), and brominated spas (2386.4 rev/L-eq) were 1.5× more mutagenic than the brominated pool (1619.6 rev/L-eq) ($P < 0.001$). The mutagenic potency of all spas combined (1907.7 rev/L-eq) was 1.7× greater than all pools combined (1150.2 rev/L-eq) ($P < 0.001$). Thus, on average, spa water was more mutagenic than pool water, regardless of type of halogen-based disinfectant (Figure 3D). Consistent with a study on ozonated drinking water,[69] spa water prepared from well water and disinfected only by ozone was not mutagenic (Site 7, SI Table S19).

Clean vs Heavily Used. Although HAA9 concentrations increased following a swim meet at Site 1 from 357 to 488 μg/L (2536 to 3332 nM; $P = 0.0045$) (SI Tables S21–S22), THM4 concentrations decreased from 74.6 to 26.2 μg/L (403 to 213 nM; $P < 0.001$) (SI Table S21–S22), likely due to increased splashing and subsequent volatilization, transferring THMs from the aqueous to the gas phase.[39]

Data at Sites 1 and 2 permitted four comparisons of DBP concentrations and mutagenic potencies for waters at 2 pools and 2 spas with low vs high use (SI Table S23; Figure 3E,F). Human inputs increased the concentration of the 21 target DBPs and the mutagenic potencies in three out of the four comparisons (SI Table S23; Figure 3E,F). These data are the first demonstration that human inputs, most likely urine, sweat, skin cells, hair, personal-care products, etc., can increase mutagenic potencies of pool and spa waters and that this is generally associated with an increase in DBP concentrations.

Source to Finished to Tap to Pools and Spas. DBPs continued to form across the continuum from source to finished to tap to pool/spa waters. This was evident in the sum of the 21 DBPs (SI Table S21–S22; Figure 3G) and in TOX data (Table 2, SI Figure S10). NOM likely served as the primary precursor in finished water, where it continued to react to increase DBP levels to the tap, after which, human precursors also contributed to DBP formation in pools and spas. Many DBPs identified were nitrogen-containing (N-DBPs), which are generally more genotoxic and cytotoxic than those without nitrogen;[70] many likely derive their nitrogen from urea in urine.[71]

Brominated pools and spas fed by chlorinated tap water exhibited a change in speciation from chlorinated to brominated analogues upon bromination. At Site 2, the concentration of total Br-DBPs in the chlorinated tap water was 18.2 μg/L (108 nM), which increased to 457 μg/L (1709 nM) in the clean pool and 393 μg/L in the clean spa (1750 nM) (SI Table S21–S22). This was even more evident in Site 5, where the Br-DBP sum was 30.2 μg/L (172 nM) in the incoming chlorinated tap water and 2956 μg/L (13341 nM) for the brominated spa (SI Tables S21–S22). In the chlorinated tap water, Cl-DBPs like chloroform and dichloroacetonitrile were dominant species, whereas Br-DBPs like bromoform and dibromoacetonitrile were dominant in brominated pools/spas (SI Tables S2–S9).

At Site 2, THM speciation shifted from 19.2 μg/L (161 nM) of chloroform in the incoming tap water to 118 and 181 μg/L (467 and 717 nM) for bromoform in the public pool and spa, respectively (SI Tables S3,S7). Haloacetonitrile speciation at Site 2 shifted from 4.7 μg/L (42.5 nM) dichloroacetonitrile in the incoming tap water to 35.3 and 96.3 μg/L (177 and 484

DOI: 10.1021/acs.est.6b00808
Environ. Sci. Technol. 2016, 50, 6652–6662

nM) dibromoacetonitrile in the pool and spa, respectively (SI Tables S3 and S7). A similar trend was found in Site 5, with a shift from 31.4 μg/L (263 nM) chloroform and 2.8 μg/L (25.1 nM) dichloroacetonitrile in the incoming tap water to 253 μg/L (1002 nM) of bromoform and 219 μg/L (1102 nM) of dibromoacetonitrile in the private spa water (SI Tables S5 and S9).

With only a few exceptions, mutagenicity increased across the continuum from source to finished to tap to pool and spa waters. Exceptions were Finished vs Average Use Pool at Site 1, Finished vs Tap at Site 2, and Tap vs Spa at Site 4 (SI Figure S7). However, when these classes of samples were averaged, there was no difference between the average mutagenic potency of Finished (508.1 rev/L-eq) and Tap (477.5 rev/L-eq) water samples ($P = 0.095$). In contrast, average concentrations of the 21 target DBPs among the Tap water samples (86.2 μg/L) were greater than among the Finished water samples (42.3 μg/L) ($P < 0.001$). Average mutagenic potencies of the pools (1149.6 rev/L-eq) and spas (1934.5 rev/L-eq) were 2.4 and 4.1× greater, respectively, than those of the averages for the Tap water (470.6 rev/L-eq) used to fill those pools/spas ($P < 0.001$) (SI Table S19; Figure 3H).

Associations between Mutagenicity and DBP Classes. Mutagenic potencies were correlated with concentrations of several DBP classes based on data for the 21 target DBPs, and some linear regressions are illustrated in SI Figures S11 and S12. Mutagenic potencies of the eight samples at Site 1 correlated most strongly with concentrations of Br-HAAs ($r = 0.98$) and N-DBPs ($r = 0.97$); weakest correlations were with Br-THMs ($r = 0.29$) and Br−N-DBPs ($r = 0.04$) (Table 3).

Table 3. Correlations (Pearson's *r*) between Mutagenic Potency (rev/L-eq) and Concentration (μM) of 21 Target DBPs Grouped by Classes of DBPs[a]

DBP class	site 1 (Cl)	site 2 (Br)	all sites
THM4	0.38	0.61	0.82
THM4+	0.94	0.71	0.79
HAA9	0.69	0.82	0.64
N-DBPs	0.97	0.77	0.73
Br-DBPs	0.90	0.82	0.68
Br-THMs	0.29	0.63	0.64
Br-HAAs	0.98	0.82	0.66
Br−N-DBPs	0.04	0.78	0.66
all 21 target DBPs	0.94	0.82	0.68

[a]Data for correlations from SI Table S22. THM4+ is the sum of the four THMs, four haloacetonitriles, two haloketones, and trichloroacetaldehyde (chloral hydrate).

Mutagenic potencies of the eight samples at Site 2, which were mostly brominated, correlated most strongly ($r = 0.82$) with the HAA9, Br-HAAs, and Br-DBPs (Table 3). Further indication of a role for Br-DBPs in Site 2 samples was indicated by increased mutagenic potency of such samples in a GSTT1-expressing strain of *Salmonella* vs a nonexpressing strain (SI Figure S13).

When all 28 samples were combined, mutagenic potencies correlated best with the sum of the four THMs, four haloacetonitriles, two haloketones, and trichloroacetaldehyde (THM4+) ($r = 0.82$) and moderately ($r = 0.64–0.79$) with other classes of DBPs. Interestingly, mutagenic potencies of all samples combined correlated only moderately with TOCl or TOBr ($r = 0.53$ and 0.60, respectively, SI Figure S14), indicating that these broad measurements were not as informative as specific classes of 21 target DBPs (Table 3).

Implications for Public Health. Previous research has shown dermal and inhalation DBP exposure to be significant. Human studies show that blood concentrations of bromodichloromethane are 40× greater via dermal exposure vs a comparable oral dose.[72] Risk for bladder cancer from chlorinated water is greater via dermal/inhalation exposure (including swimming) than by oral exposure;[34] this risk is increased further depending on genotype.[73] Consistent with studies showing that Br-DBPs are generally more mutagenic and genotoxic than Cl-DBPs,[71] our data show that brominated pool/spa waters are more mutagenic than chlorinated ones. Our data in pools/spas confirm previous work with drinking water showing that ozonated water is less mutagenic than ozonated/chlorinated water, which is less mutagenic than chlorinated water.[69]

Our study shows that mutagenicity of pool/spa waters is generally increased by human inputs. Thus, encouraging practices that reduce these inputs, such as frequent cleaning of spas, more frequent exchange of water in pools, showering before entering pools/spas, and not urinating or wearing personal-care products while in pools/spas, should have a beneficial effect on public health. Positive health effects gained by swimming could be increased, and potential health risks reduced, by implementation of these practices.

■ ASSOCIATED CONTENT

Supporting Information

The Supporting Information is available free of charge on the ACS Publications website at DOI: 10.1021/acs.est.6b00808.

Additional information as noted in the text (PDF)

■ AUTHOR INFORMATION

Corresponding Author

*Phone: 803-777-6932; e-mail: richardson.susan@sc.edu.

Present Addresses

[∇](E.J.D.) Oak Ridge Associated Universities, National Risk Management Research Laboratory, U.S. Environmental Protection Agency, Ada, OK 74820

[○](S.A.R.) PG Assist Services, Ltd. Fourteen Enterprise Ct., Durham, United Kingdom S47 0PS

Notes

The authors declare no competing financial interest.

■ ACKNOWLEDGMENTS

We are honored to be part of this special issue dedicated to Jerry Schnoor, whose incredible vision made the top environmental journal in the world even better. We thank Carla McCord and Ken McMinn at EE&T for THM, HAA, and chloral hydrate measurements; Lidia Samarkina and Caroline Stevens (EPA) and UGA's Soil, Water, and Air Laboratory for TOC analyses; Sarah Riemel and Christina Joseph for assistance with data; Peggy Matthews for mutagenicity experiments; Keith Tarpley and Molly Windsor for their help with the graphics; and finally the aquatic centers, drinking-water plants, and private pool/spa owners who graciously allowed us to collect samples. This article was reviewed by the National Health and Environmental Effects Research Laboratory, U.S. EPA, and approved for publication. Approval does not signify that the contents reflect the views of the agency nor does

mention of trade names or commercial products constitute endorsement or recommendation for use.

REFERENCES

(1) Zwiener, C.; Richardson, S. D.; DeMarini, D. M.; Grummt, T.; Glauner, T.; Frimmel, F. H. Drowning in disinfection byproducts? Assessing swimming pool water. *Environ. Sci. Technol.* **2007**, *41*, 363−372.

(2) Li, J.; Blatchley, E. R., III Volatile disinfection byproduct formation resulting from chlorination of organic-nitrogen precursors in swimming pools. *Environ. Sci. Technol.* **2007**, *41*, 6732−6739.

(3) Walse, S. S.; Mitch, W. A. Nitrosamine carcinogens also swim in chlorinated pools. *Environ. Sci. Technol.* **2008**, *42*, 1032−1037.

(4) Weaver, W. A.; Li, J.; Wen, Y.; Johnston, J.; Blatchley, M. R.; Blatchley, E. R., III Volatile disinfection by-product analysis from chlorinated indoor swimming pools. *Water Res.* **2009**, *43*, 3308−3318.

(5) Aggazzotti, G.; Predieri, G. Survey of volatile halogenated organics (VHO) in Italy: levels of VHO in drinking waters, surface waters and swimming pools. *Water Res.* **1986**, *20*, 959−963.

(6) Aggazzotti, G.; Fantuzzi, G.; Righi, E.; Predieri, G. Environmental and biological monitoring of chloroform in indoor swimming pools. *J. Chromatogr.. A* **1995**, *710*, 181−190.

(7) Aggazzotti, G.; Fantuzzi, G.; Righi, E.; Predieri, G. Blood and breath analyses as biological indicators of exposure to trihalomethanes in indoor swimming pools. *Sci. Total Environ.* **1995**, *217*, 155−163.

(8) Cardador, M.; Gallego, M. Haloacetic acids in swimming pools: swimmer and worker exposure. *Environ. Sci. Technol.* **2011**, *45*, 5783−5790.

(9) Beech, J. A.; Diaz, R.; Ordaz, C.; Palomeque, B. Nitrates, chlorates and trihalomethanes in swimming pool water. *Am. J. Public Health* **1980**, *70*, 79−82.

(10) Bessonneau, V.; Derbez, M.; Clément, M.; Thomas, O. Determinants of chlorination by-products in indoor swimming pools. *Int. J. Hyg. Environ. Health* **2011**, *215*, 76−85.

(11) Catto, C.; Sabrina, S.; Ginette, C. T.; Manuel, R.; Robert, T. Occurrence and spatial and temporal variations of disinfection by-products in the water and air of two indoor swimming pools. *Int. J. Environ. Res. Public Health* **2012**, *9*, 2562−2586.

(12) Chowdhury, S.; Al-Hooshani, K.; Karanfil, T. Disinfection byproducts in swimming pool: occurrences, implications and future needs. *Water Res.* **2014**, *53*, 68−109.

(13) Chu, H.; Nieuwenhuijsen, M. Distribution and determinants of trihalomethane concentrations in indoor swimming pools. *Occup. Environ. Med.* **2002**, *59*, 243−247.

(14) Golfinopoulos, S. K. Volatile halogenated organics in swimming pools. *Toxicol. Environ. Chem.* **2000**, *76*, 219−228.

(15) Judd, S.; Bullock, G. The fate of chlorine and organic materials in swimming pools. *Chemosphere* **2003**, *51*, 869−879.

(16) Kim, H.; Shim, J.; Lee, S. Formation of disinfection by-products in chlorinated swimming pool water. *Chemosphere* **2002**, *46*, 123−130.

(17) Sá, C. S. A.; Boaventura, R. A. R.; Pereira, I. B. Analysis of trihalomethanes in water and air from indoor swimming pools using HS-SPME/GC/ECD. *J. Environ. Sci. Health, Part A: Toxic/Hazard. Subst. Environ. Eng.* **2011**, *46*, 355−363.

(18) Simard, S.; Tardif, R.; Rodriguez, M. J. Variability of chlorination by-product occurrence in water of indoor and outdoor swimming pools. *Water Res.* **2013**, *47*, 1763−1772.

(19) Wang, X.; Leal, M. G.; Zhang, X.; Yang, H.; Xie, Y. Haloacetic acids in swimming pool and spa water in the United States and China. *Front. Environ. Sci. Eng.* **2014**, *8*, 820−824.

(20) Goodman, M.; Hays, S. Asthma and swimming: a meta-analysis. *J. Asthma* **2008**, *45*, 639−649.

(21) Jacobs, J.; Spaan, S.; Van Rooy, G.; Meliefste, C.; Zaat, V.; Rooyackers, J.; Heederik, D. Exposure to trichloramine and respiratory symptoms in indoor swimming pool workers. *Eur. Respir. J.* **2007**, *29*, 690−698.

(22) Stav, D.; Stav, M. Asthma and whirlpool baths. *N. Engl. J. Med.* **2005**, *353*, 1635−1636.

(23) Weisel, C. P.; Richardson, S. D.; Nemery, B.; Aggazzotti, G.; Baraldi, E.; Blatchley, E. R., III; Blount, B. C.; Carlsen, K.-H.; Eggleston, P. A.; Frimmel, F. H.; Goodman, M.; Gordon, G.; Grinshpun, S. A.; Heederik, D.; Kogevinas, M.; LaKind, J. S.; Nieuwenhuijsen, M. J.; Piper, F. C.; Sattar, S. A. Childhood asthma and environmental exposures at swimming pools: state of the science and research recommendations. *Environ. Health Perspect.* **2009**, *117*, 500−507.

(24) Bernard, A.; Carbonnelle, S.; Michel, O.; Higuet, S.; de Burbure, C.; Buchet, J. P.; Hermans, C.; Dumont, X.; Doyle, I. Lung hyperpermeability and asthma prevalence in schoolchildren: unexpected associations with the attendance at indoor chlorinated swimming pools. *Occup. Environ. Med.* **2003**, *60*, 385−394.

(25) Bernard, A.; Carbonnelle, S.; de Burbure, C.; Michel, O.; Nickmilder, M. Chlorinated pool attendance, atopy, and the risk of asthma during childhood. *Environ. Health Perspect.* **2006**, *114*, 1567−1573.

(26) Parrat, J.; Donze, G.; Iseli, C.; Perret, D.; Tomicic, C.; Schenk, O. Assessment of occupational and public exposure of trichloramine in Swiss indoor swimming pools: a proposal for an occupational exposure limit. *Ann. Occup. Hyg.* **2012**, *56*, 264−277.

(27) Fantuzzi, G.; Righi, E.; Predieri, G.; Ceppelli, G.; Gobba, F.; Aggazzotti, G. Occupational exposure to trihalomethanes in indoor swimming pools. *Sci. Total Environ.* **2001**, *264*, 257−265.

(28) Fornander, L.; Ghafouri, B.; Lindahl, M.; Graff, P. Airway irritation among indoor swimming pool personnel: trichloramine exposure, exhaled NO and protein profiling of nasal lavage fluids. *Int. Arch. Occup. Environ. Health* **2013**, *86*, 571−580.

(29) Chu, T.-S.; Cheng, S.-F.; Wang, G.-S.; Tsai, S.-W. Occupational exposures of airborne trichloramine at indoor swimming pools in Taipei. *Sci. Total Environ.* **2013**, *461*−*462*, 317−322.

(30) Font-Ribera, L.; Kogevinas, M.; Zock, J. P.; Gómez, F. P.; Barreiro, E.; Nieuwenhuijsen, M. J.; Fernandez, P.; Lourencetti, C.; Pérez-Olabarría, M.; Bustamante, M. Short-term changes in respiratory biomarkers after swimming in a chlorinated pool. *Environ. Health Perspect.* **2010**, *118*, 1538−1544.

(31) Nickmilder, M.; Bernard, A. Associations between testicular hormones at adolescence and attendance at chlorinated swimming pools during childhood. *Int. J. Androl.* **2011**, *34*, E446−E458.

(32) IARC. *IARC Monographs on the Evaluation of Carcinogenic Risks to Humans. Some Drinking-Water Disinfectants and Contaminants, Including Arsenic*; International Agency for Research on Cancer: Lyon, France, 2004; Vol. *84*.

(33) Villanueva, C. M.; Cantor, K. P.; Cordier, S.; Jaakola, J. J. K.; King, W. D.; Lynch, C. F.; Porru, S.; Kogevinas, M. Disinfection byproducts and bladder cancer. A pooled analysis. *Epidemiology* **2004**, *15*, 357−367.

(34) Villanueva, C. M.; Cantor, K. P.; Grimalt, J. O.; Malats, N.; Silverman, D.; Tardon, A.; Garcia-Closas, R.; Serra, C.; Carrato, A.; Castano-Vinyals, G. Bladder cancer and exposure to water disinfection by-products through ingestion, bathing, showering, and swimming in pools. *Am. J. Epidemiol.* **2007**, *165*, 148−156.

(35) Kogevinas, M.; Villanueva, C. M.; Font-Ribera, L.; Liviac, D.; Bustamante, M.; Espinoza, F.; Nieuwenhuijsen, M. J.; Espinosa, A.; Fernandez, P.; DeMarini, D. M. Genotoxic effects in swimmers exposed to disinfection by-products in indoor swimming pools. *Environ. Health Perspect.* **2010**, *118*, 1531−1537.

(36) Li, J. H.; Wang, Z. H.; Zhu, X. J.; Deng, Z. H.; Cai, C. X.; Qiu, L. Q.; Chen, W.; Lin, Y. J. Health effects from swimming training in chlorinated pools and the corresponding metabolic stress pathways. *PLoS One* **2015**, *10*, e0119241.

(37) Blatchley, E. R., III; Cheng, M. Reaction mechanism for chlorination of urea. *Environ. Sci. Technol.* **2010**, *44*, 8529−8534.

(38) Lian, L.; Yue, E.; Li, J.; Blatchley, E. R., III Volatile disinfection byproducts resulting from chlorination of uric acid: implications for swimming pools. *Environ. Sci. Technol.* **2014**, *48*, 3210−3217.

(39) Weng, S. C.; Weaver, W. A.; Afifi, M. Z.; Blatchley, T. N.; Cramer, J.; Chen, J.; Blatchley, E. R., III Dynamics of gas-phase

DOI: 10.1021/acs.est.6b00808
Environ. Sci. Technol. 2016, 50, 6652−6662

trichloramine (NCl_3) in chlorinated, indoor swimming pool facilities. *Indoor Air* **2011**, *21*, 391−399.
(40) Afifi, M. Z.; Blatchley, E. R., III Seasonal dynamics of water and air chemistry in an indoor chlorinated swimming pool. *Water Res.* **2015**, *68*, 771−783.
(41) Schmalz, C.; Wunderluch, H. G.; Heinze, R.; Frimmel, F. H.; Zwiener, C.; Grummt, T. Application of an optimized system for the well-defined exposure of human lung cells to trichloramine and indoor pool air. *J. Water Health* **2011**, *9*, 586−596.
(42) Jurado-Sánchez, B.; Ballesteros, E.; Gallego, M. Screening of N-nitrosamines in tap and swimming pool waters using fast gas chromatography. *J. Sep. Sci.* **2010**, *33*, 610−616.
(43) Kim, H.; Han, K. Swimmers contribute to additional formation of N-nitrosamines in chlorinated pool water. *Toxicol. Environ. Health Sci.* **2011**, *3*, 168−174.
(44) Lee, J.; Jun, M. J.; Lee, M. H.; Eom, S. W.; Zoh, K. D. Production of various disinfection byproducts in indoor swimming pool waters treated with different disinfection methods. *Int. J. Hyg. Environ. Health* **2010**, *213*, 465−474.
(45) Michalski, R.; Mathews, B. Occurrence of chlorite, chlorate and bromate in disinfected swimming pool water. *Polym. J. Environ. Stud.* **2007**, *16*, 237−241.
(46) Montesinos, I.; Cardador, M.; Gallego, M. Determination of halonitromethanes in treated water. *J. Chromatogr., A* **2011**, *1218*, 2497−2504.
(47) Parinet, J.; Tabaries, S.; Coulomb, B.; Vassalo, L.; Boudenne, J. L. Exposure levels to brominated compounds in seawater swimming pools treated with chlorine. *Water Res.* **2011**, *46*, 828−836.
(48) Pozzi, R.; Bocchini, P.; Pinelli, F.; Galletti, G. C. Determination of nitrosamines in water by gas chromatography/chemical ionization/selective ion trapping mass spectrometry. *J. Chromatogr., A* **2011**, *1218*, 1808−1814.
(49) Manasfi, T.; De Méo, M.; Coulomb, B.; Di Giorgio, C.; Boudenne, J. L. Identification of disinfection by-products in freshwater and seawater swimming pools and evaluation of genotoxicity. *Environ. Int.* **2016**, *88*, 94−102.
(50) German Standard. DIN 19643 *Treatment of Water of Swimming Pools and Baths*; Beuth Verlag: Berlin, 2012.
(51) Agence Nationale de Sécurité Sanitaire de L'alimentation de L'environnement et du Travail (ANSES). *Évaluation des Risques Sanitaires Liés aux Piscines*, 2012.
(52) Richardson, S. D.; DeMarini, D. M.; Kogevinas, M.; Fernandez, P.; Marco, E.; Lourencetti, C.; Ballesté, C.; Heederik, D.; Meliefste, K.; McKague, A. B. What's in the pool? A comprehensive identification of disinfection by-products and assessment of mutagenicity of chlorinated and brominated swimming pool water. *Environ. Health Perspect.* **2010**, *118*, 1523−1530.
(53) Shang, C.; Blatchley, E. R., III Differentiation and quantification of free chlorine and inorganic chloramines in aqueous solution by MIMS. *Environ. Sci. Technol.* **1999**, *33*, 2218−2223.
(54) Xiao, F.; Zhang, X. R.; Zhai, H.; Lo, I. M. C.; Tipoe, G. L.; Yang, M.; Pan, Y.; Chen, G. New halogenated disinfection byproducts in swimming pool water and their permeability across skin. *Environ. Sci. Technol.* **2012**, *46*, 7112−7119.
(55) Kanan, A.; Karanfil, T. Formation of disinfection by-products in indoor swimming pool water: the contribution from filling water natural organic matter and swimmer body fluids. *Water Res.* **2011**, *45*, 926−932.
(56) Benoit, F. M.; Jackson, R. Trihalomethane formation in whirlpool spas. *Water Res.* **1987**, *21*, 353−357.
(57) Teo, T. L. L.; Coleman, H. M.; Khan, S. J. Chemical contaminants in swimming pools: occurrence, implications and control. *Environ. Int.* **2015**, *76*, 16−31.
(58) Liviac, D.; Wagner, E. D.; Mitch, W. A.; Altonji, M. J.; Plewa, M. J. Genotoxicity of water concentrates from recreational pools after various disinfection methods. *Environ. Sci. Technol.* **2010**, *44*, 3527−3532.
(59) Honer, W. G.; Ashwood-Smith, M. J.; Warby, C. Mutagenic activity of swimming-pool water. *Mutat. Res., Genet. Toxicol. Test.* **1980**, *78*, 137−144.
(60) Glauner, T.; Waldmann, P.; Frimmel, F. H.; Zwiener, C. Swimming pool water fractionation and genotoxicological characterization of organic constituents. *Water Res.* **2005**, *39*, 4494−4502.
(61) Yeh, R. Y.; Farré, M. J.; Stalter, D.; Tang, J. Y.; Molendijk, J.; Escher, B. I. Bioanalytical and chemical evaluation of disinfection by-products in swimming pool water. *Water Res.* **2014**, *59*, 172−184.
(62) Plewa, M. J.; Wagner, E. D.; Mitch, W. A. Comparative mammalian cell cytotoxicity of water concentrates from disinfected recreational pools. *Environ. Sci. Technol.* **2011**, *45*, 4159−4165.
(63) Richardson, S. D.; Thruston, A. D., Jr.; Krasner, S. W.; Weinberg, H. S.; Miltner, R. J.; Narotsky, M. G.; Simmons, J. E. Integrated disinfection byproducts mixtures research: comprehensive characterization of water concentrates prepared from chlorinated and ozonated/postchlorinated drinking water. *J. Toxicol. Environ. Health, Part A* **2008**, *71*, 1165−1186.
(64) Richardson, S. D.; Thurston, A. D., Jr.; Caughran, T. V.; Chen, P. H.; Collette, T. W.; Floyd, T. L.; Schlenck, K. M.; Lykins, B. W., Jr.; Sun, R.-R.; Majetich, G. Identification of new ozone disinfection byproducts in drinking water. *Environ. Sci. Technol.* **1999**, *33*, 3368−3377.
(65) Smith, E. M.; Plewa, M. J.; Lindell, C. L.; Richardson, S. D.; Mitch, W. A. Comparison of byproduct formation in waters treated with chlorine and iodine: relevance to point-of-use treatment. *Environ. Sci. Technol.* **2010**, *44*, 8446−8452.
(66) Lutz, A. W.; DeLorenzo, S. *Novel Halogenated Imidazoles. Chloroimidazoles*; Agricultural Division American Cyanamid Company: Princeton, NJ, *976*, pp 399−402.
(67) Noland, W. E.; Cole, K. P.; Britton, D. 4,5-Dibromo-1-methyl-1H-imidazole. *Acta Crystallogr., Sect. E: Struct. Rep. Online* **2003**, *E59*, 458−460.
(68) Glaze, W.; Weinberg, H. *Identification and Occurrence of Ozonation By-products in Drinking Water*; The American Water Works Research Foundation and the American Water Works Association, 1993.
(69) DeMarini, D. M.; Abu-Shakra, A.; Felton, C. F.; Patterson, K. S.; Shelton, M. L. Mutation spectra in Salmonella of chlorinated, chloraminated, or ozonated drinking water extracts: comparison to MX. *Environ. Mol. Mutagen.* **1995**, *26*, 270−285.
(70) Plewa, M. J.; Wagner, E. D.; Muellner, M. G.; Hsu, K. M.; Richardson, S. D. Comparative Mammalian Cell Toxicity of N-DBPs and C-DBPs. In *Disinfection By-Products in Drinking Water: Occurrence, Formation, Health Effects, and Control*; American Chemical Society: Washington, DC, 2008; pp 36−50.
(71) Richardson, S. D.; Plewa, M. J.; Wagner, E. D.; Schoeny, R.; DeMarini, D. M. Occurrence, genotoxicity, and carcinogenicity of regulated and emerging disinfection by-products in drinking water: a review and roadmap for research. *Mutat. Res., Rev. Mutat. Res.* **2007**, *636*, 178−242.
(72) Leavens, T. L.; Blount, B. C.; DeMarini, D. M.; Madden, M. C.; Valentine, J. L.; Case, M. W.; Silva, L. K.; Warren, S. H.; Hanley, N. M.; Pegram, R. A. Disposition of bromodichloromethane in humans following oral and dermal exposure. *Toxicol. Sci.* **2007**, *99*, 432−445.
(73) Cantor, K. P.; Villanueva, C. M.; Silverman, D. T.; Figueroa, J. D.; Real, F. X.; Garcia-Closas, M.; Malats, N.; Chanock, S.; Yeager, M.; Tardon, A.; Garcia-Closas, R.; Serra, C.; Carrato, A.; Castano-Vinyals, G.; Samanic, C.; Rothman, N.; Kovevinas, M. Polymorphisms in *GSTT1, GSTZ1*, and *CYP2E1*, disinfection by-products, and risk of bladder cancer in Spain. *Environ. Health Perspect.* **2010**, *118*, 1545−1550.

DOI: 10.1021/acs.est.6b00808
Environ. Sci. Technol. 2016, 50, 6652−6662